BIOLOGICAL DRIVERS OF VECTOR-PATHOGEN INTERACTIONS

EDITED BY: Ryan Oliver Marino Rego, Job E. Lopez and Alejandro Cabezas-Cruz
PUBLISHED IN: Frontiers in Cellular and Infection Microbiology

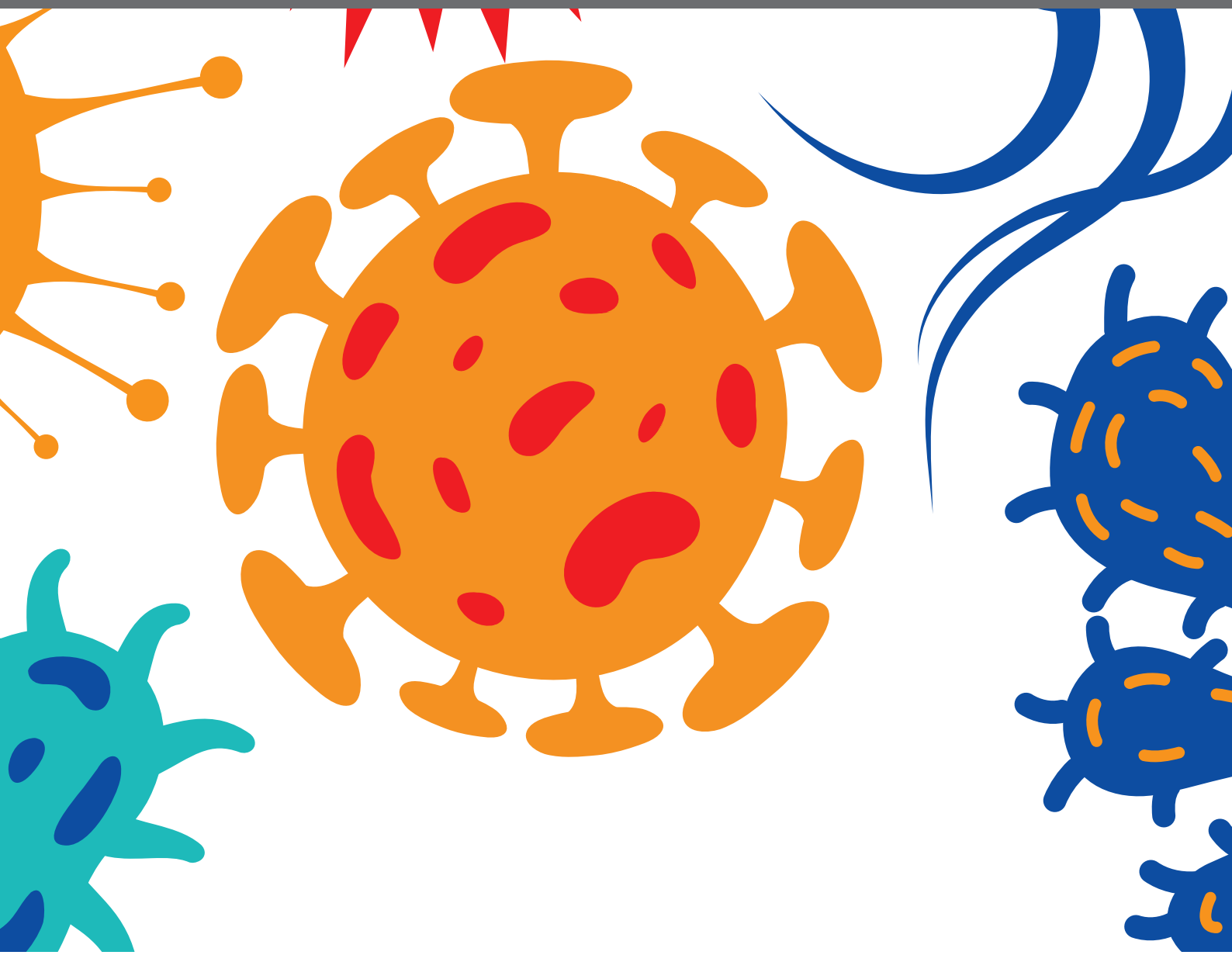

frontiers Research Topics

frontiers

ISSN 1664-8714
ISBN 978-2-88966-243-2
DOI 10.3389/978-2-88966-243-2

About Frontiers

Frontiers is more than just an open-access publisher of scholarly articles: it is a pioneering approach to the world of academia, radically improving the way scholarly research is managed. The grand vision of Frontiers is a world where all people have an equal opportunity to seek, share and generate knowledge. Frontiers provides immediate and permanent online open access to all its publications, but this alone is not enough to realize our grand goals.

Frontiers Journal Series

The Frontiers Journal Series is a multi-tier and interdisciplinary set of open-access, online journals, promising a paradigm shift from the current review, selection and dissemination processes in academic publishing. All Frontiers journals are driven by researchers for researchers; therefore, they constitute a service to the scholarly community. At the same time, the Frontiers Journal Series operates on a revolutionary invention, the tiered publishing system, initially addressing specific communities of scholars, and gradually climbing up to broader public understanding, thus serving the interests of the lay society, too.

Dedication to Quality

Each Frontiers article is a landmark of the highest quality, thanks to genuinely collaborative interactions between authors and review editors, who include some of the world's best academicians. Research must be certified by peers before entering a stream of knowledge that may eventually reach the public - and shape society; therefore, Frontiers only applies the most rigorous and unbiased reviews.
Frontiers revolutionizes research publishing by freely delivering the most outstanding research, evaluated with no bias from both the academic and social point of view. By applying the most advanced information technologies, Frontiers is catapulting scholarly publishing into a new generation.

What are Frontiers Research Topics?

Frontiers Research Topics are very popular trademarks of the Frontiers Journals Series: they are collections of at least ten articles, all centered on a particular subject. With their unique mix of varied contributions from Original Research to Review Articles, Frontiers Research Topics unify the most influential researchers, the latest key findings and historical advances in a hot research area! Find out more on how to host your own Frontiers Research Topic or contribute to one as an author by contacting the Frontiers Editorial Office: researchtopics@frontiersin.org

BIOLOGICAL DRIVERS OF VECTOR-PATHOGEN INTERACTIONS

Topic Editors:
Ryan Oliver Marino Rego, Academy of Sciences of the Czech Republic (ASCR), Czechia
Job E. Lopez, Baylor College of Medicine Houston, United States
Alejandro Cabezas-Cruz, Institut National de Recherche pour l'agriculture, l'alimentation et l'environnement (INRAE), France

Citation: Rego, R. O. M., Lopez, J. E., Cabezas-Cruz, A., eds. (2020). Biological Drivers of Vector-Pathogen Interactions. Lausanne: Frontiers Media SA.
doi: 10.3389/978-2-88966-243-2

Table of Contents

05 ***Editorial: Biological Drivers of Vector–Pathogen Interactions***
Ryan O. M. Rego, Job E. Lopez and Alejandro Cabezas-Cruz

08 ***The Presence of* Acinetobacter baumannii *DNA on the Skin of Homeless People and its Relationship With Body Lice Infestation. Preliminary Results***
Tran Duc Anh Ly, Jad Kerbaj, Sophie Edouard, Van Thuan Hoang, Meriem Louni, Thi Loi Dao, Samir Benkouiten, Sekene Badiaga, Herve Tissot-Dupont, Didier Raoult, Philippe Brouqui, Oleg Mediannikov and Philippe Gautret

14 ***Sex-Specific Linkages Between Taxonomic and Functional Profiles of Tick Gut Microbiomes***
Dasiel Obregón, Emilie Bard, David Abrial, Agustín Estrada-Peña and Alejandro Cabezas-Cruz

30 ***Competition Between Strains of Borrelia* afzelii *in Immature* Ixodes ricinus *Ticks is Not Affected by Season***
Dolores Genné, Anouk Sarr, Olivier Rais and Maarten J. Voordouw

44 ***Where Are We With Human Lice? A Review of the Current State of Knowledge***
Nadia Amanzougaghene, Florence Fenollar, Didier Raoult and Oleg Mediannikov

60 ***New Insights Into CRASP-Mediated Complement Evasion in the Lyme Disease Enzootic Cycle***
Yi-Pin Lin, Amber M. Frye, Tristan A. Nowak and Peter Kraiczy

68 ***Tick-Borne Encephalitis Virus Infection Alters the Sialome of* Ixodes ricinus *Ticks During the Earliest Stages of Feeding***
Charles E. Hart, Jose M. Ribeiro, Maria Kazimirova and Saravanan Thangamani

84 ***Methodological Insight Into Mosquito Microbiome Studies***
Sonia M. Rodríguez-Ruano, Eliška Juhaňáková, Jakub Vávra and Eva Nováková

94 ***Sharing the Ride:* Ixodes scapularis *Symbionts and Their Interactions***
Philip E. Stewart and Marshall E. Bloom

106 ***Differential Expression of Putative* Ornithodoros turicata *Defensins Mediated by Tick Feeding***
Brittany A. Armstrong, Alexander R. Kneubehl, Robert D. Mitchell III, Aparna Krishnavajhala, Pete D. Teel, Adalberto A. Pérez de León and Job E. Lopez

117 ***Corrigendum: Differential Expression of Putative* Ornithodoros turicata *Defensins Mediated by Tick Feeding***
Brittany A. Armstrong, Alexander R. Kneubehl, Robert D. Mitchell III, Aparna Krishnavajhala, Pete D. Teel, Adalberto A. Pérez de León and Job E. Lopez

119 ***Poor Unstable Midgut Microbiome of Hard Ticks Contrasts With Abundant and Stable Monospecific Microbiome in Ovaries***
Melina Garcia Guizzo, Saraswoti Neupane, Matej Kucera, Jan Perner, Helena Frantová, Itabajara da Silva Vaz Junior, Pedro L. de Oliveira, Petr Kopacek and Ludek Zurek

129 ***Tick-Borne Flavivirus Inhibits Sphingomyelinase (IsSMase), a Venomous Spider Ortholog to Increase Sphingomyelin Lipid Levels for its Survival in* Ixodes scapularis *Ticks***
Pravesh Regmi, Supreet Khanal, Girish Neelakanta and Hameeda Sultana

frontiers in Cellular and Infection Microbiology

EDITORIAL
published: 22 October 2020
doi: 10.3389/fcimb.2020.609495

Editorial: Biological Drivers of Vector–Pathogen Interactions

Ryan O. M. Rego[1,2]*, *Job E. Lopez*[3,4] *and Alejandro Cabezas-Cruz*[5]

[1] Biology Centre, Institute of Parasitology, Czech Academy of Sciences, České Budějovice, Czechia, [2] Faculty of Science, University of South Bohemia, České Budějovice, Czechia, [3] Department of Molecular Virology and Microbiology, Baylor College of Medicine, Houston, TX, United States, [4] Department of Pediatrics, National School of Tropical Medicine, Baylor College of Medicine, Houston, TX, United States, [5] UMR BIPAR, INRAE, ANSES, Ecole Nationale Vétérinaire d'Alfort, Université Paris-Est, Maisons-Alfort, France

Keywords: vector, pathogen, immunity, transcriptome, arthropod, microbiome

Editorial on the Research Topic

Biological Drivers of Vector–Pathogen Interactions

Blood feeding arthropods are a highly diverse group of animals that use blood as the main nutrient source. During this process, they transmit various viral, bacterial, and protozoal pathogens that are responsible for some of the worlds' deadliest diseases leading to millions of human deaths as well as that of livestock every year. Understanding the relationships between vectors, pathogens, and the vector microbiota is an area of research, that used to be overlooked and now takes center stage when fighting vector borne diseases. The interactions include those seen at the time of acquisition, dissemination, and persistence of the pathogen within the vector and in the transmission to the vertebrate host. This basic research would help guide investigations into effective methods that would help block pathogen transmission (Shaw and Catteruccia, 2019). We believe the 'biological drivers' highlighted below are important in helping researchers develop tools that would alleviate the disease burden associated with vector-borne pathogens.

OPEN ACCESS

Edited and reviewed by:
Jeroen P. J. Saeij,
University of California, Davis, United States

***Correspondence:**
Ryan O. M. Rego
ryanrego@paru.cas.cz

Specialty section:
This article was submitted to Parasite and Host, a section of the journal Frontiers in Cellular and Infection Microbiology

Received: *23 September 2020*
Accepted: *05 October 2020*
Published: *22 October 2020*

Citation:
Rego ROM, Lopez JE and Cabezas-Cruz A (2020) Editorial: Biological Drivers of Vector–Pathogen Interactions. Front. Cell. Infect. Microbiol. 10:609495. doi: 10.3389/fcimb.2020.609495

VECTOR MICROBIOMES

Vector microbiomes drive key factors of the invertebrate host physiology, development, nutrition, vector competence, and pathogenesis. Since most of the information known regarding pathogen–microbiome interaction in mosquitoes has been conducted in laboratory reared insects, the work by Rodriguez-Ruano et al. compared mosquito sampling methods on microbiome profiles of wild caught mosquitoes. Furthermore, the research team compared the impact of insect preservation methods and pooled *versus* individual samples on the microbiome diversity. The work indicated that microbiome analysis of individual tissues produced little variation compared to whole specimens. Collectively, the study signified the importance of utilizing standardized methods for sample preservation, processing to minimize sampling bias.

Most microbiome studies in ticks are restricted to the taxonomic analysis of the tick microbiota with little insight about the functional roles of the non-pathogenic microbes associated with ticks. Obregón et al. analyzed the gut microbiome metagenomes of three tick species within the family Ixodidae. The results suggest that the tick microbiome forms a complex metabolic network that may increase microbial community resilience and adaptability. For example, the genes for biosynthesis of vitamin B, essential for

tick survival, were present in the genomes of several gut microbiota bacteria. The presence of the same genes and functions in different bacteria of the microbiota implies functional redundancy. Hosting highly diverse and redundant microbiomes may offer ticks a competitive advantage in the environment. Guizzo et al. complement and expand these results by showing that the diversity of tick midgut microbiota is variable. Remarkably, these authors showed that tick midgut microbiota has a very low abundance compared with ovaries. This is a new take on tick microbiota that should be further explored.

VECTOR SYMBIONTS

Stewart and Bloom made an ambitious collection of literature about *Ixodes scapularis* symbionts and microbiome and their microbial interactions with the tick. The authors identified areas where research and conceptual development is needed. Particularly, a distinction between microbes adapted to using *I. scapularis* as a host or vector of transmission, and those that only circumstantially and transiently colonize the tick, is needed. The authors proposed that identifying the microbes that establish a long-term relationship with the tick might provide new insights into tick biology and tick–pathogen interactions. Other generalist microbes, widespread in the environment, may have pleiotropic and non-specific effects on the ticks.

VECTOR IMMUNITY

Argasid ticks are an understudied vector of emerging pathogens including African swine fever virus and relapsing fever spirochetes. Research on immunity in the New World argasid tick *Ornithodoros turicata* led to the identification of four defensin molecules which shared homology to defensins from the Old World tick *Ornithodoros moubata* (Armstrong et al.). The findings indicated that subsets of defensin molecules are produced after blood feeding while others are up-regulated in flat molted ticks. This work sets the foundation to now determine the role of defensins after pathogen acquisition.

VECTOR–PATHOGEN INTERPLAY

Most of the studies on tick–pathogen interactions focus on tick-borne bacteria (de la Fuente et al., 2017; Cabezas-Cruz et al., 2019). In this Research Topic, Hart et al. provide evidence that tick-borne encephalitis virus (TBEV) modifies gene expression in the salivary glands of infected *Ixodes ricinus*. Infected ticks were found to differentially express a number of genes coding for proteins involved in tick–host interactions. The genes include proteases, Kunitz-type serine protease inhibitors, cytotoxins, and lipocalins. Tick saliva components play an essential role in the initial virus transmission during tick feeding. The results suggest that sialome modulation may facilitate virus transmission during the early stages of tick feeding. Going more into the details of molecular mechanisms involved in tick–virus interactions, a different study provided evidence that tick-borne Langat virus (LGTV), related to TBEV, reduces the expression of a tick sphingomyelinase D (*Is*SMase), an enzyme that catalyzes the hydrolytic cleavage of lipids such as sphingomyelin (Regmi et al.). The authors further showed that *I. scapularis* ticks decrease *Is*SMase expression both *in vivo* and *in vitro*, which in turn produced an accumulation of sphingomyelin that supported membrane-associated viral replication and exosome biogenesis in tick cells.

Acinetobacter species have been identified in several insect species including human body lice. However, whether lice can acquire *A. baumannii* from the skin or blood of infected individuals and are able to transmit the bacteria to an uninfected host remain a topic of research. In their study, Ly et al. found a strong association between body lice infestation and the presence of *A. baumannii* DNA in the skin of homeless individuals from Marseille, France. The bacterium was not present in the blood of skin positive and/or lice infested individuals. The results of this study suggest that lice acquire *A. baumannii* while biting the skin of colonized individuals and likely transmit the bacteria in their feces.

Mixed infections within a vector can lead to competitive interactions and change the dynamics of how the pathogenic strains are transmitted or abundant within an ecological area. Dolores et al. showed that when strains of *Borrelia afzelii* were co-infecting the hard tick *I. ricinus*, it led to the reduction in spirochete load for both strains and seasonal treatment of the ticks did not lead to any effect on the intensity of inter-strain competition.

In order to understand how various pathogens are able to establish infection within their mammalian or arthropod host, it is important to determine what factors help them avoid the immune systems. The review by Lin et al. condenses current data studying the roles of various Borrelia associated Complement Regulator Acquiring Surface Proteins (CRASPs) and the importance of these molecules in tick-borne transmission and dissemination of the spirochete in mammalian hosts.

COMPLEXITIES OF A VECTOR

An extremely well timed and extensive review on human head and body lice by Amanzougaghene et al. covers a host of sections connected with phylogenetics, epidemiology, disease–vector interactions as well as insecticide resistance. It certainly is a great resource collection of the current data that is available on one of the world's oldest human parasites. It certainly will help researchers push forward with research that is lacking when it comes to understanding the human louse and its vectorial nature.

Finally, we would like to show our appreciation to all authors who contributed to the Research Topic and have opened more doors in the study of vector–pathogen interactions by providing major insights into these complex relationships.

AUTHOR CONTRIBUTIONS

All authors listed have made a substantial, direct and intellectual contribution to the work, and approved it for publication.

REFERENCES

Cabezas-Cruz, A., Espinosa, P., Alberdi, P., and de la Fuente, J. (2019). Tick-Pathogen Interactions: The Metabolic Perspective. *Trends Parasitol.* 35 (4), 316–328. doi: 10.1016/j.pt.2019.01.006

de la Fuente, J., Antunes, S., Bonnet, S., Cabezas-Cruz, A., Domingos, A. G., Estrada-Peña, A., et al. (2017). Tick-Pathogen Interactions and Vector Competence: Identification of Molecular Drivers for Tick-Borne Diseases. *Front. Cell. Infect. Microbiol.* 7, 114. doi: 10.3389/fcimb.2017.00114

Shaw, W. R., and Catteruccia, F. (2019). Vector biology meets disease control: using basic research to fight vector-borne diseases. *Nat. Microbiol.* 4 (1), 20–34. doi: 10.1038/s41564-018-0214-7

Conflict of Interest: The authors declare that the research was conducted in the absence of any commercial or financial relationships that could be construed as a potential conflict of interest.

frontiers in Cellular and Infection Microbiology

BRIEF RESEARCH REPORT
published: 05 April 2019
doi: 10.3389/fcimb.2019.00086

The Presence of *Acinetobacter baumannii* DNA on the Skin of Homeless People and Its Relationship With Body Lice Infestation. Preliminary Results

Tran Duc Anh Ly[1,2], *Jad Kerbaj*[3], *Sophie Edouard*[2,4], *Van Thuan Hoang*[1,2,5], *Meriem Louni*[1,2], *Thi Loi Dao*[1,2,5], *Samir Benkouiten*[1,2], *Sekene Badiaga*[2,6], *Herve Tissot-Dupont*[2,4], *Didier Raoult*[2,4], *Philippe Brouqui*[1,2], *Oleg Mediannikov*[2,4] and *Philippe Gautret*[1,2]*

[1] Aix Marseille Univ, IRD, AP-HM, SSA, VITROME, Marseille, France, [2] IHU-Méditerranée Infection, Marseille, France, [3] AP-HM, Marseille, France, [4] Aix Marseille Univ, MEPHI, Marseille, France, [5] Department of Pneumology, Thai Binh University of Medicine and Pharmacy, Thai Binh, Vietnam, [6] Aix Marseille Univ, Service des urgences CHU Hôpital Nord, Marseille, France

The presence of *Acinetobacter baumannii* was demonstrated in body lice, however, little is known about the mechanism of natural lice infection. In 2013 and 2014, cross-sectional one-day studies were therefore performed within two Marseille homeless shelters to assess the presence of *A. baumannii* DNA on human skin, blood and in body lice collected from the same homeless individuals. All 332 participants completed questionnaires, were examined for dermatologic signs, and provided four skin samples (hair, neck, armpits, and pelvic belt), blood samples and body lice (if any). We developed a new real-time PCR tool targeting the *ompA/motB* gene for the detection of *A. baumannii* for all collected samples. Blood culture was also performed. Body lice were found in 24/325 (7.4%) of subjects. We showed a prevalence of *A. baumannii* DNA skin-carriage in 33/305 (10.8%) of subjects. No difference was found in *A. baumannii* DNA prevalence according to body sites. A strong association between body lice infestation (OR = 3.07, $p = 0.029$) and *A. baumannii* DNA skin-carriage was noted. In lice, *A. baumannii* DNA was detected in 59/219 arthropods (26.9%). All blood cultures and real-time PCR on blood samples were negative for *A. baumannii.* Lice probably get infected with *A. baumannii* while biting through the colonized skin and likely transmit the bacteria in their feces. We found no evidence that lice facilitate the invasion of *A. baumannii* into the blood stream. Further investigations are needed to compare phenotypic and genotypic features of *A. baumannii* isolates from human skin and lice from the same individuals.

Keywords: body lice, homeless, *Acinetobacter baumannii*, skin, *ompA/motB*

OPEN ACCESS

Edited by:
Alejandro Cabezas-Cruz, Institut National de la Recherche Agronomique (INRA), France

Reviewed by:
Jose Ramos-Vivas, Instituto de Investigación Marques de Valdecilla (IDIVAL), Spain
Raffaele Zarrilli, University of Naples Federico II, Italy

***Correspondence:**
Philippe Gautret
philippe.gautret@club-internet.fr

Specialty section:
This article was submitted to Parasite and Host, a section of the journal Frontiers in Cellular and Infection Microbiology

Received: *14 January 2019*
Accepted: *12 March 2019*
Published: *05 April 2019*

Citation:
Ly TDA, Kerbaj J, Edouard S, Hoang VT, Louni M, Dao TL, Benkouiten S, Badiaga S, Tissot-Dupont H, Raoult D, Brouqui P, Mediannikov O and Gautret P (2019) The Presence of Acinetobacter baumannii DNA on the Skin of Homeless People and Its Relationship With Body Lice Infestation. Preliminary Results. Front. Cell. Infect. Microbiol. 9:86. doi: 10.3389/fcimb.2019.00086

INTRODUCTION

Acinetobacter species are mostly free-living saprophytes found ubiquitously in nature and are considered part of the normal flora of the human skin (Vallenet et al., 2008). Among *Acinetobacter* species, *A. baumannii* is the most important member often associated with hospital-acquired infections worldwide and is responsible for opportunistic infections of the skin, bloodstream, urinary tract, and other soft tissues. Although most *A. baumannii* infections occur in critically ill patients in the intensive care unit setting, the frequency of community-acquired *A. baumannii* infections has been increasing gradually. Furthermore, *A. baumannii* has been showed to rapidly develop resistance to antimicrobials (Lee et al., 2017).

Acinetobacter species are hosted by several insect species (Dillon and Dillon, 2004) but the occurrence of *A. baumannii* in hematophagous groups is poorly documented. It has been isolated from *Aedes albopictus* in Madagascar (Minard et al., 2013), moth fly species *Clogmia albipunctata* with colonization rates of 0–17.5% in several German hospitals (Faulde and Spiesberger, 2013) or Brazilian phlebotomine sand flies *Lutzomyia longipalpis* (Gouveia et al., 2008). *A. baumannii* DNA have also been detected in human body lice, suggesting that lice can possibly transmit this pathogen. It was first isolated from body lice collected from homeless people in Marseille (La-Scola et al., 2001). A 21% prevalence of *A. baumannii* DNA was then found in a large collection of 622 body lice collected in France, Burundi, Rwanda, Peru, Algeria, Portugal, and the Netherlands (La-Scola and Raoult, 2004). It has also been isolated at high rates from body lice collected from Ethiopian subjects (Kempf et al., 2012) and finally from body lice collected from Algerian homeless people (Louni et al., 2018a). *A. baumannii* DNA was detected in head lice from French children (Bouvresse et al., 2011), and from infested people in Thailand (Sunantaraporn et al., 2015), Republic of Congo, Niger, and Algeria (Amanzougaghene et al., 2016; Mana et al., 2017; Louni et al., 2018b). Phenotypic and genotypic features of *A. baumannii* isolates from body lice differ significantly from *A. baumannii* clinical isolate from humans (Vallenet et al., 2008). Experimental infection of lice by feeding on infected rabbits demonstrated that they were able to acquire and maintain a persistent life-long infection with *A. baumannii*. Moreover, infected body lice excreted living *A. baumannii* within their feces and did not transmit their infection to their nurse host during feeding or transovarially (Houhamdi and Raoult, 2006).

Natural lice infection may result from the ingestion of infective blood meals from patients with ongoing bacteremia, or from the penetration of colonized human skin by lice mouth parts during feeding. To challenge this hypothesis, we conducted an epidemiological study among Marseille homeless individuals addressing the presence of *A. baumannii* DNA on human skin and blood and in body lice collected from the same individuals.

METHODS

Cohorts

In our one-shot studies, all adult homeless people residing in two Marseille emergency shelters were enrolled on a voluntary basis in winter in 2013 and 2014. The participants completed a specially designed questionnaire providing information on demographics, chronic medical conditions, substance abuse, cutaneous symptoms (pruritus, scratch lesions), and were physically examined by the medical doctor.

Samples

Body lice were removed from the clothes and body of the infested participants, transferred to sterile plastic tubes and were subsequently processed for molecular analysis (**Supplementary Table 1**). Four skin (hair, neck, armpits, and pelvic belt) swabs and one blood sample (collected in EDTA tube) were obtained from each participant. In the laboratory, each louse was washed with 200 µl of sterile water and then decontaminated by immersion in 70% ethanol and 0.2% eosin for 5 min as previously described (La-Scola et al., 2001). After being crushed, lice were placed in tubes containing 180 µl tampon G2 and 20 µl proteinase K (QIAGEN, Hilden, Germany) and the samples were incubated at 56°C overnight. The skin swabs were resuspended in 1 ml of HBSS (Hank's balanced salt solution). The blood samples were incubated in the BACTEC 9240 system (Reisner and Woods, 1999) and were considered negative for *A. baumannii* if no bacterial growth was detected after 5 days.

DNA Extraction

The automated DNA extraction was performed on 190 µl collected samples from skin swabs, blood, lice-washing liquid, crushed lice using a BioRobot®EZ1 Advanced XL instrument (QIAGEN, Hilden, Germany) and DNeasy® Blood & Tissue according to the manufacturer's instructions. The quality of all DNA extracts was assessed by real-time PCR (qPCR) targeting internal control TISS phage that was added to each extraction (Sow et al., 2017).

Real-Time PCR

The ready-to-use reaction mix Light-Cycler® 480 Probes Master (Roche Diagnostics, Meylan, France) was used for PCR assay performed in the C1000 Touch™ Thermal Cycle (Bio-Rad, USA) according to the manufacturer's recommendations. Positive control (Plasmid DNA) and negative control template (PCR mix + sterile H_2O or *A. spp.* other than *A. baumannii*) were incorporated in each experimental run. For homeless samples, results were considered positive accepted when the cycle threshold value of real-time PCR was $\leq$35.

Specific Identification of *Acinetobacter baumannii*

We designed a novel qPCR system by choosing *A. baumannii*-specific gene encoding for Type VI secretion system *OmpA/MotB* (accession number CP019034.1, GenBank) because of its presence in all sequenced genomes of *A. baumannii* available in the public domain (Hassan et al., 2016). Our detailed experimental procedures are described in supplementary material (**Technical Appendix**).

Statistical Analysis

Collected data were statistically treated using SPSS 23.0 software. Missing data and unidentified samples were not analyzed. Statistical differences in baseline characteristics were evaluated by Pearson's chi-square or Fisher's exact tests as categorical variables. A two-tailed p-value < 0.05 was considered as statistically significant. We performed a binomial logistic regression with *A. baumannii* DNA carriage on the skin as a dependent variable. Univariate analysis based on only variables with a prevalence $\geq 5.0\%$ by descriptive analysis was used to examine associations between multiple factors (demographic, chronic medical condition) and cutaneous clinical presentations toward prevalence of *A. baumannii* DNA skin-carriage. The initial model, therefore, included variables presenting a p-value < 0.2. The step-wise regression procedure and likelihood-ratio tests were applied to determine the final model.

RESULTS

Participant Characteristics (Table 1)

At enrolment, the population of 332 homeless people (shelter A [56%] and B [44%]) was mainly men with a mean age of 41 ± 14.1 years old (range, 19–84 years). About 16% were French while the rest (84%) were migrants, originating mostly from African countries and having settled in France ∼9 years before the survey was conducted. Overall, the average duration of homelessness was about 3 years and chronic homelessness, defined as an episode of homelessness ≥1 year, accounted for 42.8% of cases. A 22.3% prevalence of pruritus was recorded, in line with 17.5% individuals presenting with scratch lesions. Body lice were observed on 24 participants (7.4%); however, only 15 among them allowed our team to collect their lice.

Acinetobacter baumannii DNA on Human Skin (Table 2)

A total of 1,266 skin swabs were obtained from 332 participants and of these, 33 individuals (of 305, [10.8%]) had *A. baumannii* DNA on at least 1 swab. We found that 9/319 (2.8%) hair swabs, 16/319 (5.0%) neck swabs, 6/317 (1.9%) armpit swabs, and 12/311 (3.9%) pelvic belt swabs were positive for *A. baumannii* DNA. There was no statically significant difference in the prevalence of *A. baumannii* DNA according to sampling site ($p = 0.2$).

Factor Associated With *Acinetobacter baumannii* DNA Skin-Carriage: Multivariate Model (Table 1)

The prevalence of *A. baumannii* DNA skin-carriage was lower in migrants, compared to French individuals, but was significantly higher in those infested by lice compared to others in univariate. In the multivariate analysis, only individuals infested by lice OR = 3.07 (1.13–8.4), $p = 0.029$ remained associated with an increased prevalence of *A. baumannii* DNA skin-carriage.

Acinetobacter baumannii DNA in Lice

We collected 1,780 lice from 15 participants. The most infested individual had 560 lice on his clothes (**Supplementary Table 4**). Of the 219 lice analyzed, 59 (23.9%) were positive for *A. baumannii* DNA in the crushed lice, 40 (18.3%) were positive in the lice-washing liquid (**Table 2**) and 38 (17.4%) were also positive in both crushed lice and the same lice-washing liquid. Overall, among 15 individuals whose lice were tested, 9 (60%) had at least one louse positive for *A. baumannii* DNA, 4 (26.7%) had *A. baumannii* DNA in both lice and skin samples.

Acinetobacter baumannii in Blood

All bacterial qPCRs and cultures performed on the 298 homeless blood samples were negative.

DISCUSSION

Acinetobacter has gained increasing attention in recent decades due to its ability to develop resistance on a large scale to almost all major classes of antibiotics and its capacity to survive for a long period in the environment (Peleg et al., 2008). While routine clinical diagnostic laboratories often have difficulties in differentiating *A. baumannii* from other *Acinetobacter spp*. (from the same genetic group but less implicated as human pathogens), herein, we established a specific real-time PCR for *A. baumannii* designed from the virulence gene encoding for Type VI secretion system *OmpA/MotB*, which showed 100% conservation pattern among all strains of *A. baumannii*.

A 10.8% prevalence of *A. baumannii* DNA skin-carriage was detected in our cohorts and no significant difference in *A. baumannii* DNA prevalence was observed between body sites. In previous studies, the prevalence of bacterium has been reported to be rare on the surface of the skin, about 3% in different human populations (Seifert et al., 1997; Aucken et al., 1999). Nevertheless, *A. baumannii* hand-carriage rates up to 23% were reported in healthcare workers (Almasaudi, 2018). The *A. baumannii* strains that cause nosocomial infections are common and highly resistant to antimicrobials (Peleg et al., 2008). Conversely, *A. baumannii* causing community-acquired infections are rare and highly susceptible to antimicrobial treatment (Farrugia et al., 2013).

A. baumannii DNA was present in 26.9% of lice, and the positive association between the presence of body lice and *A. baumannii* skin-carriage was highly significant in this work. An experimental study conducted in 2004 showed that lice that ingest the blood of infected rabbits become infected with *A. baumannii* but do not transmit the bacterium to healthy rabbits or to their offspring; however, they excreted the living bacteria in their feces (Houhamdi and Raoult, 2006). Our preliminary results suggest that lice ingest *A. baumannii* while penetrating the colonized skin. Then, as soon as lice excrete viable *A. baumannii* through lice feces that are deposed directly on the skin, the transmission may occur when the subjects scratch their skin. Lice can move from one subject to another and, as a result, epidemic transmissions of *A. baumannii* strains may occur. The bacterial transmission by lice via the ingestion of *A. baumannii* from blood could not be documented here because no subject had *A. baumannii* bacteremia in our study. *A. baumannii* bacteremia has only been reported in two homeless in our previous surveys, making this event very unlikely (Brouqui et al., 2005). Consequently, as in studies on *Bartonella quintana* endocarditis,

TABLE 1 | Univariate analysis and multivariate analysis with *Acinetobacter baumannii* DNA-carriage on the skin as a dependent variable.

Characteristics	Total *N*	*Acinetobacter baumannii* on the skin *N* (%)	No *Acinetobacter baumannii* on the skin *N* (%)	Univariate analysis Odds ratio (95%CI), *p*-value	Multivariate analysis Odds ratio (95%CI), *p*-value
Total	**332**	**33 (10.8)**	**272 (89.2)**		
YEAR OF STUDY					
2014	144 (43.4)	15 (12.8)	102 (87.2)	REF[a]	
2013	188 (56.6)	18 (9.6)	170 (90.4)	0.72 (0.35–.49), $p = 0.38$	
SHELTER					
B	146 (44.0)	18(12.9)	122 (87.1)	REF[a]	
A	186 (56.0)	15 (9.1)	150 (90.9)	0.68 (0.33–1.40), $p = 0.29$	
GENRE					
Female	11 (3.3)	0 (0)	5 (100)	N/A	
Male	321 (96.7)	33 (11.0)	267 (89.0)		
AGE					
Mean age (SD) (years)	41 ± 14.1	N/A			
Age range (years)	19–84	N/A			
≤40 years of age[c]	170 (52.1)	15 (9.7)	139 (90.3)	REF[a]	
>40 years of age	156 (47.9)	18 (12.2)	129 (87.8)	1.29 (0.63–2.67), $p = 0.5$	
Unknown[b]	6 (–)				
BIRTHPLACE					
France (mainland)	52 (15.9)	9 (20.5)	35 (79.5)	REF[a]	
Migrants	**275 (84.1)**	**24 (9.3)**	**234 (90.7)**	**0.40 (0.17–0.93), $p = 0.03$**	**–**
Africa	214 (62.1)	18 (8.9)	185 (91.1)		
Europe	36 (11.0)	2 (5.8)	32 (94.2)		
Asia	16 (5.0)	2 (14.3)	12 (85.7)		
Other	9(2.8)	2(28.6)	5(71.4)		
Unknown[b]	5 (–)				
Mean duration of residence in France for migrants (SD) (years)	8.9 (0–24.4)				
Range of duration of residence in France for migrants (years)	0–66				
≤1.5 years[c]	134 (50)	6 (4.9)	117 (95.1)	N/A	
>1.5 years	134 (50)	14 (10.9)	114 (89.1)		
Unknown[b]	12 (–)				
No visits to country of origin since immigration	191 (71.8)	15 (8.4)	164 (91.6)	REF[a]	
Visit to country of origin since immigration	75 (28.2)	8 (11.8)	60 (88.2)	1.45 (0.59–3.61), $p = 0.41$	
Unknown[b]	14 (–)				
Mean duration of homelessness (SD), min, max (years)	2.8 (0–7.0)				
Range of duration of homelessness	1 month−48 years				
<1 year[c]	172 (51.8)	14 (8.9)	143 (91.1)	REF[a]	
≥1 year	142 (42.8)	17(12.9)	115 (87.1)	1.6 (0.8–3.42), $p = 0.21$	
Unknown[b]	18 (–)				
ALCOHOL CONSUMPTION					
Rare or never	274 (85.1)	28 (11.2)	233 (88.8)	REF[a]	
Frequent	48 (14.9)	5 (10.9)	41 (89.1)	0.97 (0.35–2.66), $p = 0.96$	
Unknown[b]	10 (–)				

(Continued)

TABLE 1 | Continued

Characteristics	Total *N*	*Acinetobacter baumannii* on the skin *N* (%)	No *Acinetobacter baumannii* on the skin *N* (%)	Univariate analysis Odds ratio (95%CI), *p*-value	Multivariate analysis Odds ratio (95%CI), *p*-value
SMOKING CIGARETTES					
Never	123 (38.1)	13 (11.8)	97 (88.2)	REF[a]	
Yes	200 (61.9)	20 (10.6)	168 (89.4)	0.89 (0.42–1.87), $p = 0.75$	
Unknown[b]	9 (–)				
Cannabis	72 (22.3)	9 (13.4)	58 (86.8)	1.34 (0.59–3.04), $p = 0.49$	
Intravenous drug use	3 (0.9)	0 (0)	2 (100)		
Snorted drug use	6 (1.9)	1 (0.2)	4 (80)		
Drug substitutes	1 (0.3)	0 (0)	1 (100)		
CHRONIC DISEASES					
Chronic respiratory diseases	41 (12.3)	5 (13.9)	31 (86.1)	1.39 (0.5–3.9), $p = 0.53$	
Diabetes mellitus	11 (3.3)	0 (0)	11(0)		
BMI					
Mean BMI (SD) (kg/m^2)	23.6 ± 5.2				
Range of BMI (kg/m^2)	15.1–40.2				
Normal weight	190 (61.3)	2 (12.4)	155 (87.6)	REF[a]	
Underweight	20 (6.5)	1 (5.3)	18 (94.7)	0.39 (0.50–3.08), $p = 0.36$	
Overweight	84 (27.1)	8 (9.9)	73 (90.1)	0.77 (0.39–1.82), $p = 0.55$	
Obesity	16 (5.2)	1 (7.7)	12 (92.3)	0.59 (0.07–4.74), $p = 1.00$	
Unknown[b]	22 (–)				
CLINICAL PRESENTATIONS					
Pruritus	72 (22.3)	7 (10.8)	58 (89.2)	0.96 (0.39–2.32), $p = 0.93$	
Scratch lesions	55 (17.5)	7 (14.3)	42 (85.7)	1.5 (0.62–3.76), $p = 0.36$	
No body lice	301 (92.6)	27 (9.8)	249 (90.2)	REF[a]	
Body lice infestation	**24 (7.4)**	**6 (25)**	**18 (75)**	**3.07 (1.13–8.4), $p = 0.022$**	**3.07 (1.13–8.4), $p = 0.029$**
Unknown[b]	7 (–)				

SD, standard deviation; BMI, Body mass index; N/A, not applicable. [a]REF: Reference category. [b]Unknown: missing data or unidentified samples. [c]Median of the variable is used for analysis. Bold lines indicate the variables recruited in the initial multivariate model.

TABLE 2 | Prevalence of *Acinetobacter baumannii* DNA-carriage of various body sites and body lice.

	Acinetobacter baumannii N (%)
BODY LICE	
Crushed lice (*N* = 219 samples)	59 (26.9)
Lice-washing liquid (*N* = 219 samples)	40 (18.3)
HUMAN SKIN	
Total (*N* = 1,266 samples)	43 (3.4)
Hair (*N* = 319 samples)	9 (2.8)
Neck (*N* = 319 samples)	16 (5.0)
Arm pits (*N* = 317 samples)	6 (1.9)
Pelvic belt (*N* = 311 samples)	12 (3.9)

it would be very difficult to establish a causal link between *A. baumannii* infected lice and bacteremia. Further clonal investigations are needed to better assess both antimicrobial susceptibilities of isolates and genotypic profiles to challenge our hypothesis. This would directly demonstrate if viable *A. baumannii* isolates from body-lice are identical or different from those isolated from human skin.

ETHICS STATEMENT

This protocol was approved by the Marseille Institutional Review Board/Ethics Committee (Protocol: 2010-A01406-33). Signed informed consent was signed by all individuals.

AUTHOR CONTRIBUTIONS

TL, JK, PB, OM, and PG contributed to experimental design, data analysis, statistics, interpretation, and writing. JK, VH, TD, SaB, SeB, and HT-D administered questionnaires, examined patients, and collected samples. SE and ML provided technical

assistance. DR, PB, and OM contributed to critically reviewing the manuscript. PG coordinated the work.

FUNDING

This study was supported by the Institut Hospitalo-Universitaire (IHU) Méditerranée Infection, the National Research Agency under the program Investissements d'avenir, reference ANR-10-IAHU-03, the Région Provence Alpes Côte d'Azur, and European funding FEDER PRIMI.

ACKNOWLEDGMENTS

We are grateful to our colleagues Younes Laidoudi and Hacene Medkour for their technical assistance.

SUPPLEMENTARY MATERIAL

The Supplementary Material for this article can be found online at: https://www.frontiersin.org/articles/10.3389/fcimb.2019.00086/full#supplementary-material

REFERENCES

Almasaudi, S. B. (2018). *Acinetobacter* spp. as nosocomial pathogens: Epidemiology and resistance features. *Saudi J Biol Sci*. 25, 586–596. doi: 10.1016/j.sjbs.2016.02.009

Amanzougaghene, N., Akiana, J., Mongo-Ndombe, G., Davoust, B., Nsana, N. S., Parra, H. J., et al. (2016). Head lice of pygmies reveal the presence of relapsing fever borrelia in the republic of Congo. *PLoS Negl. Trop. Dis*. 10:0005142. doi: 10.1371/journal.pntd.0005142

Aucken, H., Berlau, J., Malnick, H., and Pitt, T. (1999). Distribution of *Acinetobacter* species on skin of healthy humans. *Eur. J. Clin. Microbiol. Infect. Dis*. 18,179–183.

Bouvresse, S., Socolovschi, C., Berdjane, Z., Durand, R., Izri, A., Raoult, D., et al. (2011). No evidence of *Bartonella quintana* but detection of *Acinetobacter baumannii* in head lice from elementary schoolchildren in Paris. *Comp. Immunol. Microbiol. Infect. Dis*. 34, 475–477. doi: 10.1016/j.cimid.2011.08.007

Brouqui, P., Stein, A., Dupont, H. T., Gallian, P., Badiaga, S., Rolain, J. M., et al. (2005). Ectoparasitism and vector-borne diseases in 930 homeless people from Marseilles. *Medicine* 84, 61–68. doi: 10.1097/01.md.0000152373.07500.6e

Dillon, R. J., and Dillon, V. M. (2004). The gut bacteria of insects: nonpathogenic interactions. *Annu. Rev. Entomol*. 49, 71–92. doi: 10.1146/annurev.ento.49.061802.123416

Farrugia, D. N., Elbourne, L. D., Hassan, K. A., Eijkelkamp, B. A., Tetu, S. G., Brown, M. H., et al. (2013). The complete genome and phenome of a community-acquired Acinetobacter baumannii. *PLoS ONE*. 8:58628. doi: 10.1371/journal.pone.0058628

Faulde, M., and Spiesberger, M. (2013). Role of the moth fly *Clogmia albipunctata* (*Diptera*: *Psychodinae*) as a mechanical vector of bacterial pathogens in German hospitals. *J. Hosp. Infect*. 83, 51–60. doi: 10.1016/j.jhin.2012.09.019

Gouveia, C., Asensi, M. D., Zahner, V., Rangel, E. F., and Oliveira, S. M. (2008). Study on the bacterial midgut microbiota associated to different Brazilian populations of *Lutzomyia longipalpis* (Lutz and Neiva) (Diptera: Psychodidae). *Neotrop. Entomol*. 37, 597–601. doi: 10.1590/S1519-566X2008000500016

Hassan, A., Naz, A., Obaid, A., Paracha, R. Z., Naz, K., Awan, F. M., et al. (2016). Pangenome and immuno-proteomics analysis of *Acinetobacter baumannii* strains revealed the core peptide vaccine targets. *BMC Genomics*. 17:732. doi: 10.5061/dryad.k44f0

Houhamdi, L., and Raoult, D. (2006). Experimental infection of human body lice with *Acinetobacter baumannii*. *Am. J. Trop. Med. Hyg*. 74, 526–531. doi: 10.4269/ajtmh.2006.74.526

Kempf, M., Abdissa, A., Diatta, G., Trape, J. F., Angelakis, E., Mediannikov, O., et al. (2012). Detection of *Acinetobacter baumannii* in human head and body lice from Ethiopia and identification of new genotypes. *Int. J. Infect. Dis*. 16, 680–683. doi: 10.1016/j.ijid.2012.05.1024

La-Scola, B., Fournier, P. E., Brouqui, P., and Raoult, D. (2001). Detection and culture of *Bartonella quintana*, *Serratia marcescens*, and *Acinetobacter* spp. from decontaminated human body lice. *J. Clin. Microbiol*. 39,1707–1709. doi: 10.1128/JCM.39.5.1707-1709.2001

La-Scola, B., and Raoult, D. (2004). *Acinetobacter baumannii* in human body louse. *Emerg. Infect. Dis*. 10,1671–1673. doi: 10.3201/eid1009.040242

Lee, C. R., Lee, J. H., Park, M., Park, K. S., Bae, I. K., Kim, Y. B., et al. (2017). Biology of *Acinetobacter baumannii*: pathogenesis, antibiotic resistance mechanisms, and prospective treatment options. *Front. Cell. Infect. Microbiol*. 7:55. doi: 10.3389/fcimb.2017.00055

Louni, M., Amanzougaghene, N., Mana, N., Fenollar, F., Raoult, D., Bitam, I., et al. (2018a). Detection of bacterial pathogens in clade E head lice collected from Niger's refugees in Algeria. *Parasit. Vectors*. 11:348. doi: 10.1186/s13071-018-2930-5

Louni, M., Mana, N., Bitam, I., Dahmani, M., Parola, P., Fenollar, F., et al. (2018b). Body lice of homeless people reveal the presence of several emerging bacterial pathogens in northern Algeria. *PLoS Negl. Trop. Dis*. 12:0006397. doi: 10.1371/journal.pntd.0006397

Mana, N., Louni, M., Parola, P., and Bitam, I. (2017). Human head lice and pubic lice reveal the presence of several *Acinetobacter* species in Algiers, Algeria. *Comp. Immunol Microbiol. Infect*. 53:33–39. doi: 10.1016/j.cimid.2017.06.003

Minard, G., Tran, F. H., Raharimalala, F. N., Hellard, E., Ravelonandro, et al. (2013). Prevalence, genomic and metabolic profiles of *Acinetobacter* and Asaia associated with field-caught Aedes albopictus from Madagascar. *FEMS. Microbiol. Ecol*. 83, 63–73. doi: 10.1111/j.1574-6941.2012.01455.x

Peleg, A. Y., Seifert, H., and Paterson, D. L. (2008). *Acinetobacter baumannii*: emergence of a successful pathogen. *Clin. Microbiol. Rev*. 21, 538–582. doi: 10.1128/CMR.00058-07

Reisner, B. S., and Woods, G. L. (1999). Times to detection of bacteria and yeasts in BACTEC 9240 blood culture bottles. *J. Clin. Microbiol*. 37, 2024–2026.

Seifert, H., Dijkshoorn, L., Gerner-Smidt, P., Pelzer, N., Tjernberg, I., and Vaneechoutte, M. (1997). Distribution of *Acinetobacter* species on human skin: comparison of phenotypic and genotypic identification methods. *J. Clin. Microbiol*. 35, 2819–2825.

Sow, D., Parola, P., Sylla, K., Ndiaye, M., Delaunay, P., Halfon, P., et al. (2017). Performance of real-time polymerase chain reaction assays for the detection of 20 gastrointestinal parasites in clinical samples from senegal. *Am. J. Trop. Med. Hyg*. 97,173–182. doi: 10.4269/ajtmh.16-0781

Sunantaraporn, S., Sanprasert, V., Pengsakul, T., Phumee, A., Boonserm, R., Tawatsin, A., et al. (2015). Molecular survey of the head louse *Pediculus humanus* capitis in Thailand and its potential role for transmitting *Acinetobacter* spp. *Parasit Vectors*. 8:127. doi: 10.1186/s13071-015-0742-4

Vallenet, D., Nordmann, P., Barbe, V., Poirel, L., Mangenot, S., Bataille, E., et al. (2008). Comparative analysis of acinetobacters: three genomes for three lifestyles. *PLoS ONE*. 3:1805. doi: 10.1371/journal.pone.0001805

Conflict of Interest Statement: The authors declare that the research was conducted in the absence of any commercial or financial relationships that could be construed as a potential conflict of interest.

frontiers in Cellular and Infection Microbiology

ORIGINAL RESEARCH
published: 14 August 2019
doi: 10.3389/fcimb.2019.00298

Sex-Specific Linkages Between Taxonomic and Functional Profiles of Tick Gut Microbiomes

Dasiel Obregón[1,2], Emilie Bard[3], David Abrial[3], Agustín Estrada-Peña[4] and Alejandro Cabezas-Cruz[5]**

[1] Center for Nuclear Energy in Agriculture, University of São Paulo, Piracicaba, Brazil, [2] School of Environmental Sciences, University of Guelph, Guelph, ON, Canada, [3] EPIA, INRA, VetAgro Sup, Saint Genès Champanelle, France, [4] Faculty of Veterinary Medicine, University of Zaragoza, Zaragoza, Spain, [5] UMR BIPAR, INRA, ANSES, Ecole Nationale Vétérinaire d'Alfort, Université Paris-Est, Maisons-Alfort, France

Ticks transmit the most diverse array of disease agents and harbor one of the most diverse microbial communities. Major progress has been made in the characterization of the taxonomic profiles of tick microbiota. However, the functional profiles of tick microbiome have been comparatively less studied. In this proof of concept we used state-of-the-art functional metagenomics analytical tools to explore previously reported datasets of bacteria found in male and female *Ixodes ovatus*, *Ixodes persulcatus,* and *Amblyomma variegatum*. Results showed that both taxonomic and functional profiles have differences between sexes of the same species. KEGG pathway analysis revealed that male and female of the same species had major differences in the abundance of genes involved in different metabolic pathways including vitamin B, amino acids, carbohydrates, nucleotides, and antibiotics among others. Partial reconstruction of metabolic pathways using KEGG enzymes suggests that tick microbiome form a complex metabolic network that may increase microbial community resilience and adaptability. Linkage analysis between taxonomic and functional profiles showed that among the KEGG enzymes with differential abundance in male and female ticks only 12% were present in single bacterial genera. The rest of these enzymes were found in more than two bacterial genera, and 27% of them were found in five up to ten bacterial genera. Comparison of bacterial genera contributing to the differences in the taxonomic and functional profiles of males and females revealed that while a small group of bacteria has a dual-role, most of the bacteria contribute only to functional or taxonomic differentiation between sexes. Results suggest that the different life styles of male and female ticks exert sex-specific evolutionary pressures that act independently on the phenomes (set of phenotypes) and genomes of bacteria in tick gut microbiota. We conclude that functional redundancy is a fundamental property of male and female tick microbiota and propose that functional metagenomics should be combined with taxonomic profiling of microbiota because both analyses are complementary.

Keywords: functional metagenomics, ticks, taxonomic-funtional linkages, microbiota, microbiome, sex-specific differentiation, functional redundancy

OPEN ACCESS

Edited by:
Angel Angelov, Tübingen University Hospital, Germany

Reviewed by:
Huiluo Cao, The University of Hong Kong, Hong Kong
Gergely Maroti, Biological Research Centre (MTA), Hungary

****Correspondence:***
Dasiel Obregón
dasielogv@gmail.com
Alejandro Cabezas-Cruz
cabezasalejandrocruz@gmail.com

Specialty section:
This article was submitted to Parasite and Host, a section of the journal Frontiers in Cellular and Infection Microbiology

Received: *01 April 2019*
Accepted: *31 July 2019*
Published: *14 August 2019*

Citation:
Obregón D, Bard E, Abrial D, Estrada-Peña A and Cabezas-Cruz A (2019) Sex-Specific Linkages Between Taxonomic and Functional Profiles of Tick Gut Microbiomes. Front. Cell. Infect. Microbiol. 9:298. doi: 10.3389/fcimb.2019.00298

INTRODUCTION

Research on host-microbe interactions have brought us to the realization that organisms are colonized by commensal, symbiotic, and pathogenic microorganisms (Byrd et al., 2018; Cani, 2018; Pasolli et al., 2019), ticks are not the exception (Cabezas-Cruz et al., 2018). However, although there is abundant information regarding the taxonomic composition of different host microbiomes, the functional significance of bacterial communities composition and diversity remains largely unknown (Greay et al., 2018; Pasolli et al., 2019). Recent studies have begun to close the information gap between taxonomy and functional profiling in microbiome research, revealing that the distribution of functional groups is strongly influenced environmental conditions by shaping metabolic niches, while the taxonomic composition is weakly affected. Therefore, functional structure and composition within functional groups constitute independent and complementary variation axes (Louca et al., 2016; Heintz-Buschart and Wilmes, 2018). The study of gene function in complex microbial communities, known as functional metagenomics, has been extensively applied to environmental research (Mendes et al., 2014; Jung et al., 2016) and studies in model organisms (Pasolli et al., 2019) enabling higher-resolution descriptions of microbiomes (Pasolli et al., 2019; Zou et al., 2019).

From a functional point of view, it is now irrefutable that host microbiota shape almost every aspect of host biology (Hall et al., 2017; Tang et al., 2018; Canfora et al., 2019). Computational modeling studies suggested that microbiome diversity is strongly influenced by selection acting on microbes, increasing microbial fitness, whereas selection acting on hosts only influences microbiome diversity when there is parental contribution to the microbiomes of offspring (Zeng et al., 2017). Furthermore, a recent meta-analysis of arthropod microbiomes combined taxa clustering with functional profiles and highlighted the presence of conserved functional groups with redundant metabolic capacities. The functional groups were distributed across different classes of proteobacteria suggesting that environmental filtering shapes the structure of arthropod's microbiota (Degli Esposti and Martinez Romero, 2017).

Available reports are conclusive about the high diversity of bacterial taxa harbored by ticks (Cabezas-Cruz et al., 2018), likely as part of the evolutionary strategy of ticks to cope with their complex life cycle and metabolic deficiencies. Recently, Duron et al. (2018) demonstrated that a symbiont of the genus *Francisella*, F-Om, complements a nutritional deficiency of vitamin B in the blood meal of soft ticks *Ornithodoros moubata*. The genome of F-Om exhibits a substantial level of genome reduction and pseudogenization events were identified in around half of protein-coding sequences (Duron et al., 2018). However, the pathways for synthesis of biotin (B7), riboflavin (B2), and folic acid (B9) are conserved and intact in the F-Om genome (Duron et al., 2018). The presence of vitamin B synthesis pathway genes in *Francisella* is fundamental for tick survival and elimination of these bacteria in tick offspring produced anomalies in tick development (Duron et al., 2018). Similarly, despite massive genome reduction in the *Coxiella*-like symbiont of the hard tick *Amblyomma americanum*, the bacterial genome encodes most major vitamin and cofactor biosynthesis pathways, implicating *Coxiella*-like symbiont (CLEAA) as a vitamin provisioning symbiont (Smith et al., 2015). These studies highlight the functional importance of the catalog of genes encoded in tick metagenomes. Considering the microbial diversity of tick microbiota, we hypothesized that functional contributions of tick microbiome could go beyond vitamin B biosynthesis and that unique gene-encoded functions can be harbored by more than one bacteria species or genera.

A holistic view of the functional contribution of tick microbiome is, however, missing, since available analyses offer little insights into the functional profiles of arthropod-associated microbiota. This study is a proof of concept aimed to evaluate the relation between taxonomic and functional differences in male and female ticks of three species, *Ixodes ovatus*, *Ixodes persulcatus,* and *Amblyomma variegatum*.

MATERIALS AND METHODS

Data Source

We used a metagenomic dataset described previously (Nakao et al., 2013) containing the metagenomes of tick gut (hereafter samples) obtained from ticks of different species, such as *Amblyomma testudinarium*, *Haemaphysalis formosensis*, *Haemaphysalis longicornis*, *I. ovatus*, *I. persulcatus*, *Ixodes ricinus*, and *A. variegatum*, collected in the field in different regions. The tick samples were classified as nymph and adult, and these according to sex, then were pooled (+20 ticks per pool) and the DNA corresponding to bacteria/archaea cells was extracted and filtered. Subsequently, shotgun sequencing of the microbiome was performed by pyrosequencing strategy, on a Roche/454 Genome Sequencer FLX Titanium (Roche Applied Science/454 Life Science, Branford, CT), for more detailed information on the sequencing strategy we refer the reader to Nakao et al. (2013).

The raw metagenomic sequences are available in the DNA Data Bank of Japan (DDBJ) (http://www.ddbj.nig.ac.jp), Sequence Read Archive (SRA) under the accession no. DRA000590. For comparative purposes only species represented by adult stages of both sexes were included in the analysis, using only the metagenomes corresponding to adult male (m) and female (f) *A. variegatum* (AVf, DRX001659 and AVm, DRX001660), *I. ovatus* (IOf, DRX001661 and IOm, DRX001662) and *I. persulcatus* (IPf, DRX001663 and IPm, DRX001664).

Metagenomics Data Preprocessing, Annotation, and Analysis

Single-end DNA sequences were pre-processed and annotated with the web application server Metagenomic Rapid Annotations using Subsystems Technology (MG-RAST), pipeline version 4 (Meyer et al., 2008). Briefly, the raw sequences were processed by quality control (QC) using SolexaQA software package by removing low-quality segments using the "Dynamic Trim" method (Cox et al., 2010), according to the lowest Phred score of 15 and a maximum of 5 bases below the Phred score.

In another stage, the artificial replicate sequences formed by sequencing artifacts were removed (Gomez-Alvarez et al., 2009) and the reads passed a screening step to remove sequences with near-exact matches to human genome using Bowtie software (Langmead et al., 2009).

The features (protein coding regions) identification was based on the protein database M5nr which provides non-redundant integration of many protein databases (Wilke et al., 2012). The taxonomic origin of the features was determinate using the RefSeq database (O'Leary et al., 2016). The functional profiles were analyzed according the three data sources that provide hierarchical arrangements of genes and pathways: SEED subsystem (Aziz et al., 2008), KEGG orthologs (Kanehisa and Goto, 2000) and COG database (Tatusov et al., 2000), however we focused our analyses on SEED database. On the annotation parameters we follow the recommendations of Randle-boggis et al. (2016), using the default values in the MG-RAST which maximize sensibility: maximum *e*-value cut-off of 1e-5, and minimum alignment length of 15 bp, hence, the minimal identity cutoff of 60 and 80% were used for the taxonomical and functional profiling, respectively, allowing trade-off between sensitivity and precision. The abundance profiles were determined using the "Best Hit Classification" method.

During the analysis process, features annotated as bacteria domain were filtered (eukaryote and virus sequences removed), and the dataset was normalized based on negative binomial distribution approach, using "DESeq" method (Anders and Huber, 2010) implemented in the MG-RAST Web server. The metagenome dataset resulting from our QC and feature annotation are publicly available in the MG-RAST database under projects number mgp88242 (IO and IP), and mgp88326 (AV).

Phylogenomic Analysis

Phylogenetic trees were built using NCBI Taxonomy Browser (Benson et al., 2009; Sayers et al., 2009). The taxonomic ID of all genus identified in previous step were collected using the Taxonomy name/id tool. In order to improve graphical readability, the bacteria were then split in six groups according to phylum or class. Phylogenetic trees were built by submitting the taxonomic ID list of each group to the NCBI Common Tree tool. The graphical output was obtained using "ggtree" R package (Yu et al., 2017), providing tools to build custom phylogenetic trees and associated heatmap.

Statistical Analysis

The Statistical Analysis of Metagenomic Profiles (STAMP) software package (Parks and Beiko, 2010) was used to compare the relative abundance of the taxonomical and functional features, at all organizational levels, between male and female ticks. Analysis considering all the samples were performed using ANOVA test with Tukey-Kramer *post-hoc* method (IC 95%). Two-side Fisher's Exact Test (IC 95%) was used for comparing the relative abundance of bacteria between sexes within each tick species. Multiple test correction was applied in all the analysis, using the Benjamini–Hochberg FDR (false discovery) method. The selection of features included in the charts was made according to the statistical significance of the differences (q-corrected <0.05).

RESULTS

Data Filtering and Sequence Annotation

To achieve a quality functional annotation, raw sequences were submitted to a completely new analysis workflow. A high proportion of raw sequence data failed to pass the stringent data cleansing process as performed QC pipeline using MG-RAST (**Table 1**). In the samples of AV, 64.3% of sequences in AVf and 33.6% in AVm were discarded, while in *Ixodes* spp. the highest proportion of eliminated sequences were in male tick samples, with 79.4% in IPm and 62% in IOm, compared to 15.5 and 12.1% in IPf and IOf, respectively. After QC and features annotation, we found differences among the samples from males and females, including but not limited to higher GC content in the microbiome of male ticks of every species to **Table 1**. The Bacteria domain was predominant in all samples, although a comparatively minor proportion of sequences were annotated in other domains, including Eukaryote, Archaea, and Virus. Only bacterial sequences were included in further analyses.

Sex-Specific Taxonomic Profiles in the Microbiota of AV, IO, and IP

Although included in the study by Nakao et al. (2013), we performed our own bacterial composition analysis workflow. The results of the rarefaction curves indicate that sampling effort in the samples was sufficient to ensure a comprehensive comparison of their microbiota composition (**Supplementary Figure 1A**). The rarefaction curves and α-diversity analysis also indicate a higher microbial richness in the microbiota of female ticks compared to males of the same species (**Supplementary Figure 1B**). However, the α-diversity analysis also showed similar values among ticks from the same species, with the higher α-diversity in IO (**Supplementary Figure 1B**).

The overall bacterial composition of the different samples resulted in 28 phyla, of which Chlamydiae, Proteobacteria, Actinobacteria, and Firmicutes were the four most dominant phyla, accounting for >90% of the bacteria present in the samples (**Supplementary Figure 2**). However, the distribution of each phylum varied between tick species. The Proteobacteria encompassed >95% of members of the microbial communities of IP, while it only represented 20% in the microbial communities of IO, which were in turn composed mainly (>50%) by representatives of Chlamydiae. In the case of AV, differences were also observed between sexes, wherein Actinobacteria and Proteobacteria were the dominant phyla in AVm and AVf, respectively. The variability of microbial taxa profiles between sex and tick species was also observed analyzing lower taxonomic levels (i.e., family) (**Supplementary Figure 2**). Furthermore, a pattern of differentiated predominance of related genera in

TABLE 1 | Statistical summary of the process of submission, QC, and features annotation in the MG-RAST web server of metagenomic sequences retrieved from tick gut microbiomes.

Stages	Statistical parameter	AVf	AVm	IPf	IPm	IOf	IOm
Upload	Base pair count (bp)	10 973 277	14 010 027	20 941 861	17 030 492	20 108 476	8 450 898
	Sequences count	42 258	27 582	37 667	35 544	37 136	33 789
	Sequence Length (bp)	260 ± 184	508 ± 81	556 ± 68	479 ± 114	541 ± 73	250 ± 173
	GC proportion (%)	43 ± 7	55 ± 6	31 ± 8	54 ± 8	36 ± 4	47 ± 7
Post QC	Base pair count (bp)	4 888 443	8 729 399	15 985 228	3 002 495	15 920 721	3 833 115
	Sequences count	15 089	18 303	31 826	7 316	32 659	12 786
	Sequence length (bp)	324 ± 198	477 ± 87	502 ± 73	410 ± 148	487 ± 75	300 ± 181
	GC proportion (%)	41 ± 9	54 ± 6	31 ± 8	47 ± 13	36 ± 4	44 ± 9
Annoted	Protein features	8 730	9 294	25 583	6 759	28 676	8 707
	rRNA features	310	37	345	68	275	82
	Bacteria domain (%)*	90.6	82.6	94.6	92.5	97.6	87.4

**Proportion of features annotated as Bacteria domain, the rest corresponds to Eukaryote, Archaea, and Virus.*

the microbiota according to tick species was observed (i.e., the genera *Actinobacillus, Haemophilus, Lonepinella, Pasteurella, Mannheimia, Aggregatibacter, Histophilus,* and *Basfia,* all belonging to the family *Pasteurellaceae* were mostly present in AV; while the genera *Mycoplasma, Ureaplasma, Mesoplasma, Spiroplasma,* and *Acholeplasma* from the Mollicutes class were predominant in IP) (**Supplementary Figure 3**).

Venn diagrams of bacterial genera found in the gut microbiota of female and male AV, IP, and IO revealed that the three tick species share only a small proportion of bacterial genera, 6.2% in females and 2.8% in males (**Figure 1A**). More common bacterial genera were found between *Ixodes* (35.1% in females and 12.6% in males) ticks than between *Ixodes* and *Amblyomma* (5% in females and 4.7% in males). Likewise, the proportion of genera shared between females and males of the same tick species was lower in AV (14.5%) and IP (17.9%) than in IO (35.7%) (**Figure 1B**). The dissimilarity in gut microbiota composition between tick species was confirmed by principal component analysis (PCA) comparing genera-level abundance profiles in samples from the three tick species and both sexes (**Figure 2A**). Relative abundance comparison of the microbiota of male and female ticks revealed that several bacterial genera are more abundant in female ticks, regardless of the tick species (**Figure 2B**). To further explore this clustering; two-side Fisher's exact test was used to compare the relative abundance of bacterial genera in male and female within the same tick species. Results revealed that the abundance of some bacterial genera was significantly different between male and female AV (**Figure 2C**), IO (**Figure 2D**), and IP (**Figure 2E**). The differences in bacterial genera composition between sex were higher in AV than in IO and IP. In addition, the distribution of genera varied between tick species. For example, while AVf has a higher proportion of *Staphylococcus* and *Aggregatibacter*, IOf, and IPf have higher proportion of *Rickettsia* and *Rickettsia* and *Wolbachia*, respectively. IOm, IPm, and AVm have greater abundance of the genera *Rickettsiella, Pseudomonas,* and *Corynebacterium,* respectively.

Sex-Specific Functional Profiles in the Microbiomes of AV, IO, and IP

The functional metagenomic profiling was based on the SEED database because (i) the functional categories of SEED and KEGG are equivalent and (ii) SEED provides the most consistent and accurate microbial genome annotations of any publicly available source (Meyer et al., 2008; Wilke et al., 2017). Nevertheless, in a first stage, the abundance profiles was also analyzed according to the COG database in order to compare with previous results by Nakao et al. (2013), revealing uniformity in the abundance of functional traits (**Supplementary Figures 4A,B**). The analysis of functional profiles based on SEED subsystem resulted in 863 functional features (SEED level 4, **Supplementary Table 1**) identified across all the samples, and these functions were grouped in 26 SEED level 1 categories (**Supplementary Figure 4C**).

In the first stage of the analysis, we explored the similarities between ticks of the same sex, regardless of the tick species. The analysis of similarities ANOSIM based on Bray–Curtis dissimilarity index revealed no differences on averages of rank similarity within groups and between groups ($R = -0.074$; $p = 0.5$). Consequently, no difference ($p > 0.05$) was found for any of the 863 individual functions when the microbiomes of ticks of the same sex were compared (**Supplementary Table 1**). Then, we observed that similar to taxonomical composition, the PCA on the abundance of functional traits indicated that the sex separated the samples of the same tick species, being the differences between sexes more striking in AV (**Figure 3A**). Clustering analysis using effect size ANOVA confirmed that the sex influence microbiome composition in functional traits associated with respiration, virulence, and stress response among others (**Figure 3B**). Therefore, we compared the functional traits of the microbiomes of each tick species, and a detailed analysis of the metabolic profile of these microbiomes revealed significant differences between male and female ticks (**Figures 3C–E**). In agreement with the PCA analysis, AV have the highest number of categories (i.e., 14) for which significant differences were found

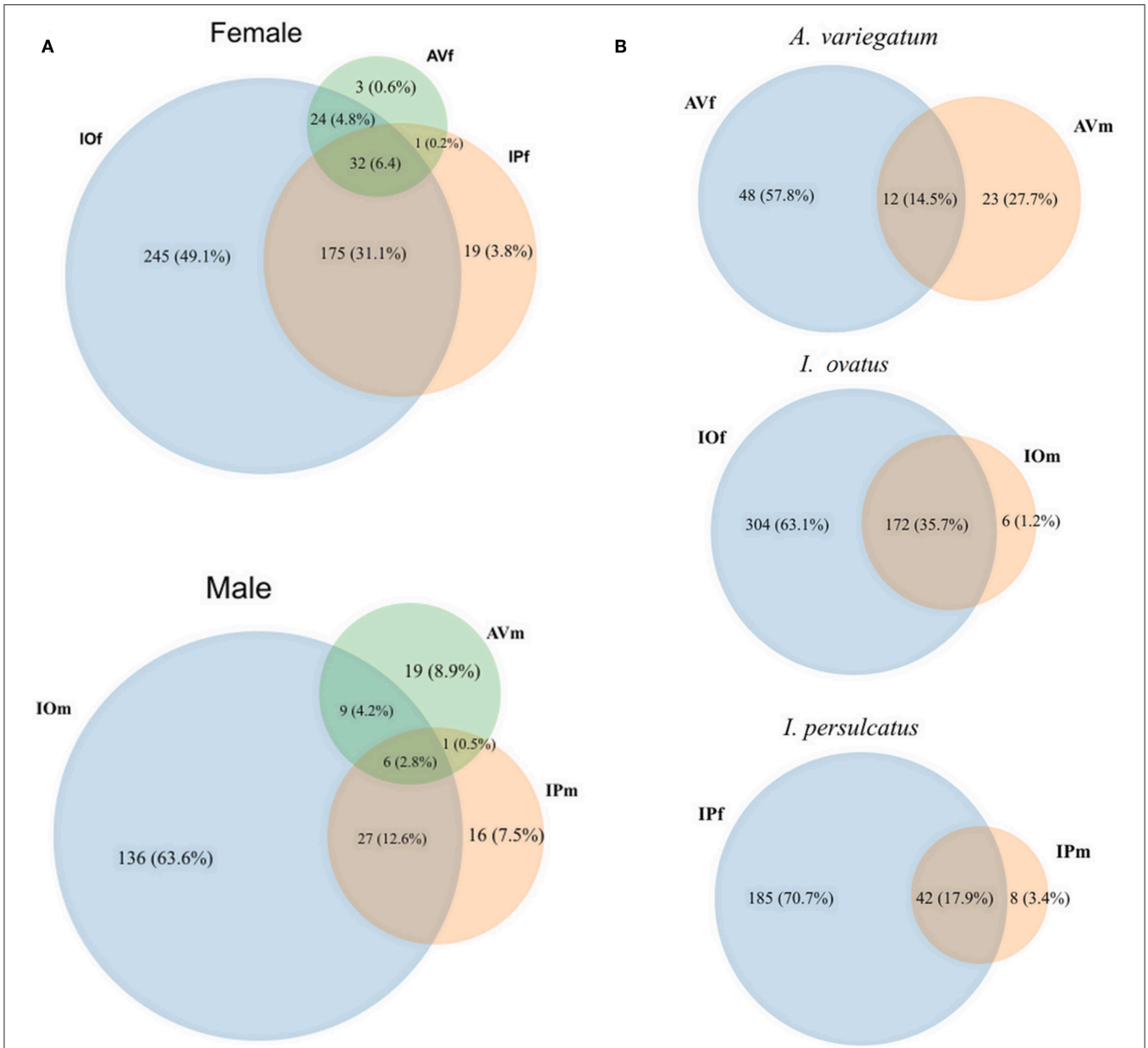

FIGURE 1 | Venn diagrams of bacterial genera composition of the gut microbiota of female and male ticks. **(A)** Comparison of the bacterial genera composition in AV, IP, and IO according to sex. **(B)** Comparisons between female and male in each tick species. The numbers represent the number of genera found in each tick species and those shared by two or all three tick species. The percentage represents their proportionality among the entire set of genera found. Taxonomical features annotated on MG-TAST, based on RefSeq database at minimal identity cut-off of 60%. Graphical representation of Venn diagrams was achieved in BioVinci version 1.1.5 (BioTuring Inc., San Diego, California USA, www.bioturing.com).

between males and females (**Figure 3C**). A comparatively lower number of categories were found to differentiate the microbiome of males and females of IO (i.e., 6, **Figure 3D**) and IP (i.e., 5, **Figure 3E**). Among all the categories only Stress Response was common and showed a significant increase in males of the three species. No other single category was shared in the microbiomes of male and female within each tick species. These results suggest a sex-dependent selection of the microbiome in AV, IO and IP ticks.

Differences in Carbohydrate and Amino Acid Metabolism Genes in the Microbiomes of Female and Male AV, IO, and IP

Analysis of bacterial genes composition and abundance between sexes revealed major differences in the metabolism of amino acids, proteins, carbohydrates, respiration, nucleic acids, and chemical elements among others (**Figure 4**). An analysis of metabolic genes with KEGG annotation shows high

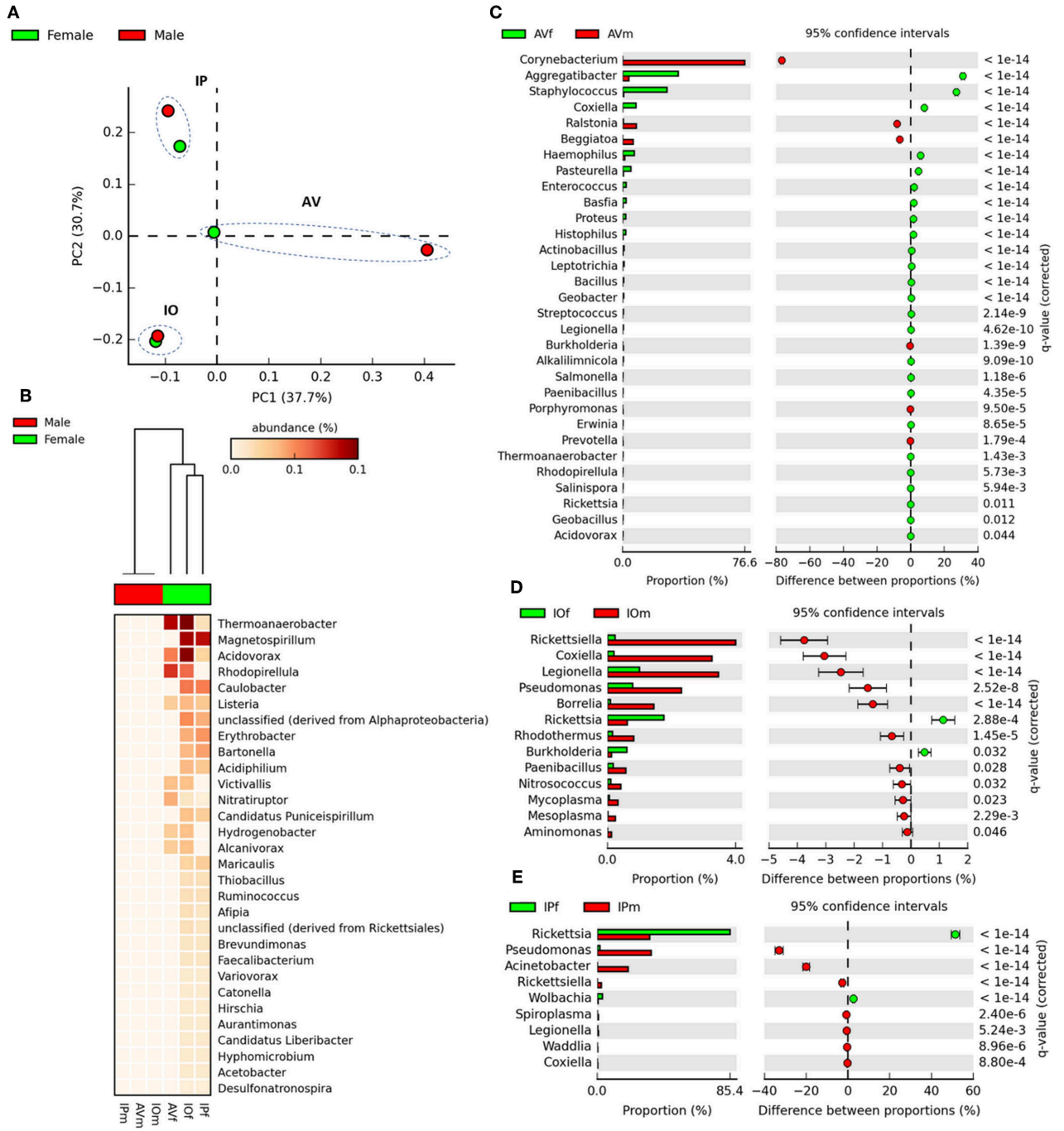

FIGURE 2 | Comparison of taxonomical profiles in the gut microbiota of AVf, AVm, IPf, IPm, IOf, and IOm. **(A)** First axis PCA plot showing the variance of taxonomical profile at level of genera between samples according to tick species and sex, arbitrary ellipses (dashed lines) were drawn to facilitate the interpretation of the figure. **(B)** Heatmap plot showing differences in relative abundance of bacterial genera's in tick gut microbiota between sex. The differences in the abundance of bacterial genera between gut microbiomes from male and female ticks are shown in extended error bars plot for AV **(C)**, IP **(D)**, and IO **(E)**. Only genera with significantly different abundances between males and females are shown ($q < 0.05$).

representation of genes involved in metabolic interconnections between amino acid and carbohydrate metabolism in the three tick species (**Figure 5**). Compared to female ticks, AV males show a diverse array of genes involve in the synthesis of metabolic precursors of the glycolysis intermediates fructose-6-phosphate (Fru-6P) and pyruvate. Three key enzymes (EC 4.1.3.3, EC 2.7.1.60, and EC 5.1.3.9) involved in the transformation of N-acetylneuraminic acid (Neu5Ac) in N-acetyl-D-glucosamine

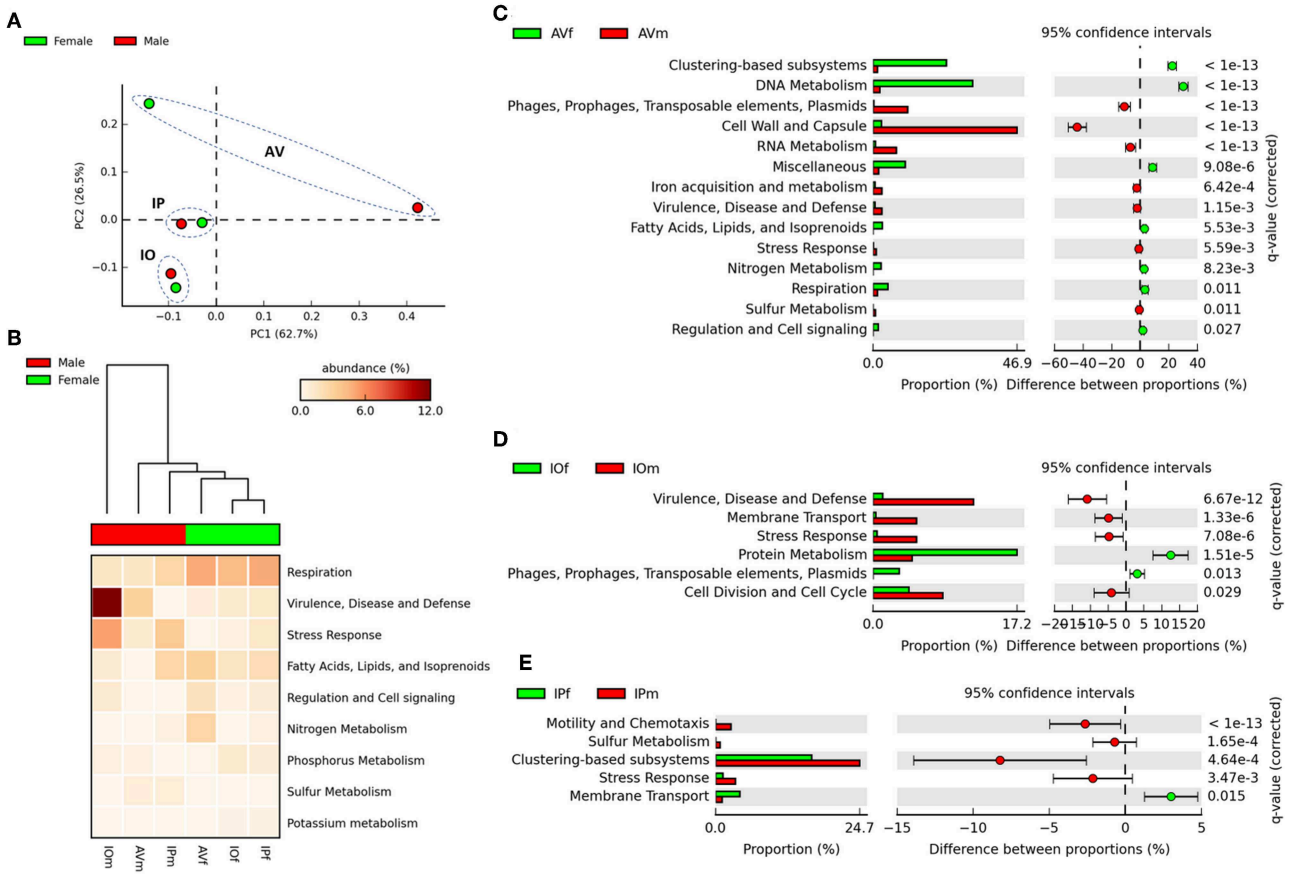

FIGURE 3 | Comparison of functional profiles in the gut microbiota of AVf, AVm, IPf, IPm, IOf, and IOm. **(A)** The first axis PCA plot showing the variance on functional profiling, based on SEED subsystem collapsed at the higher categorical level (level 1), between samples according sex and tick species, arbitrary ellipses (dashed lines) were drawn to facilitate the interpretation of the figure. **(B)** Heatmap plot showing differences between sex of tick on functional traits collapsed at the highest level (SEED, level 1), the functional categories are ranked acordid the effect size, only categories with significant effect in the differences are shown ($\eta^2 > 0.01$). Comparison between sexes is shown as extended error bar plot for AV **(C)**, IP **(D)**, and IO **(E)**. Only the functional categories significantly different in abundances are shown ($q < 0.05$).

6-phosphate (GlcNAc-6P) were more abundant in AVm than in AVf (**Figures 4**, **5**). The monosaccharide derivative of glucose, GlcNAc-6P, is the main component of the peptidoglycan cell wall in bacteria and can be further metabolized to Fru-6P by two additional enzymatic reactions catalyzed by N-acetylglucosamine-6-phosphate deacetylase (EC 3.5.1.25) and glucosamine-6-phosphate deaminase (EC 3.5.99.6). Of these two enzymes, EC 3.5.99.6 was also most abundant in AVm compared to AVf. The beta-galactosidase (EC 3.2.1.23) that catalyzes the transformation of galactan and lactose in galactose which can then enter glycolysis as glucose-6P (Glu-6P) was also more abundant in AVm. Both metabolites, Glu-6P and Fru-6P, can enter in successive steps of glycolysis to be transformed in phosphoenolpyruvate (PEP) which can be also synthesized from oxaloacetate by the gluconeogenesis enzyme phosphoenolpyruvate carboxykinase (PEPCK, EC 4.1.1.49), another of the enzymes with higher abundance in AVm. Depending on the origin of PEP, catalyzed by PEPCK or enolase, this metabolite has different metabolic fates: rapid transformation to pyruvate, when produced by enolase, or participate in various metabolic processes including gluconeogenesis, glyceroneogenesis, *de novo* serine synthesis pathway, shikimate pathway among others. DAHP synthase (EC 2.5.1.54), highly abundant in AVm, is the first enzyme in the shikimate pathway, which is responsible for the biosynthesis of the amino acids phenylalanine, tyrosine, and tryptophan. DAHP synthase catalyzes the condensation of phosphoenolpyruvate and erythrose 4-phosphate to form 3-deoxy-D-arabino-heptulosonate 7-phosphate and inorganic phosphate. Since DAHP synthase is the first enzyme in the shikimate pathway, it controls the amount of carbon entering the pathway. An additional amino acid aminotransferase (EC 2.6.1.21) involved in phenylalanine, arginine and alanine synthesis, as well as lysine degradation, has higher abundance in AVm.

Only three metabolic enzymes were more abundant in AVf compared with AVm (**Figure 4**), prephenate dehydratase (EC 4.2.1.51), succinyl-diaminopimelate desuccinylase (EC 3.5.1.18),

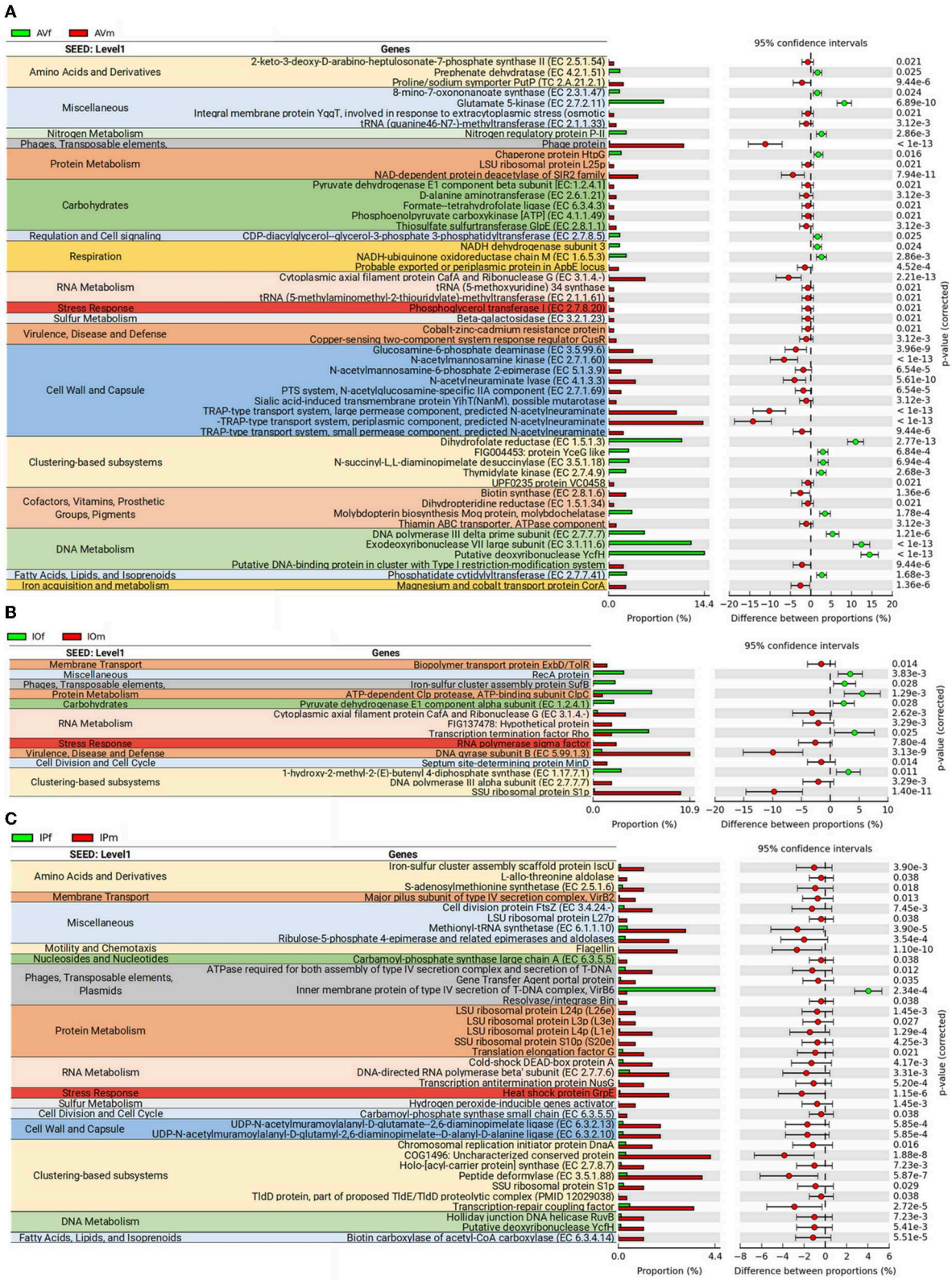

FIGURE 4 | Differences in metabolic functions of tick gut microbiome of AVf, AVm, IPf, IPm, IOf, and IOm. Extended error bar plot showing the more abundant features acording sexes in AV **(A)**, IP **(B)**, and IO **(C)**. Only features with significant differences in relative abundance are shown ($q < 0.05$).

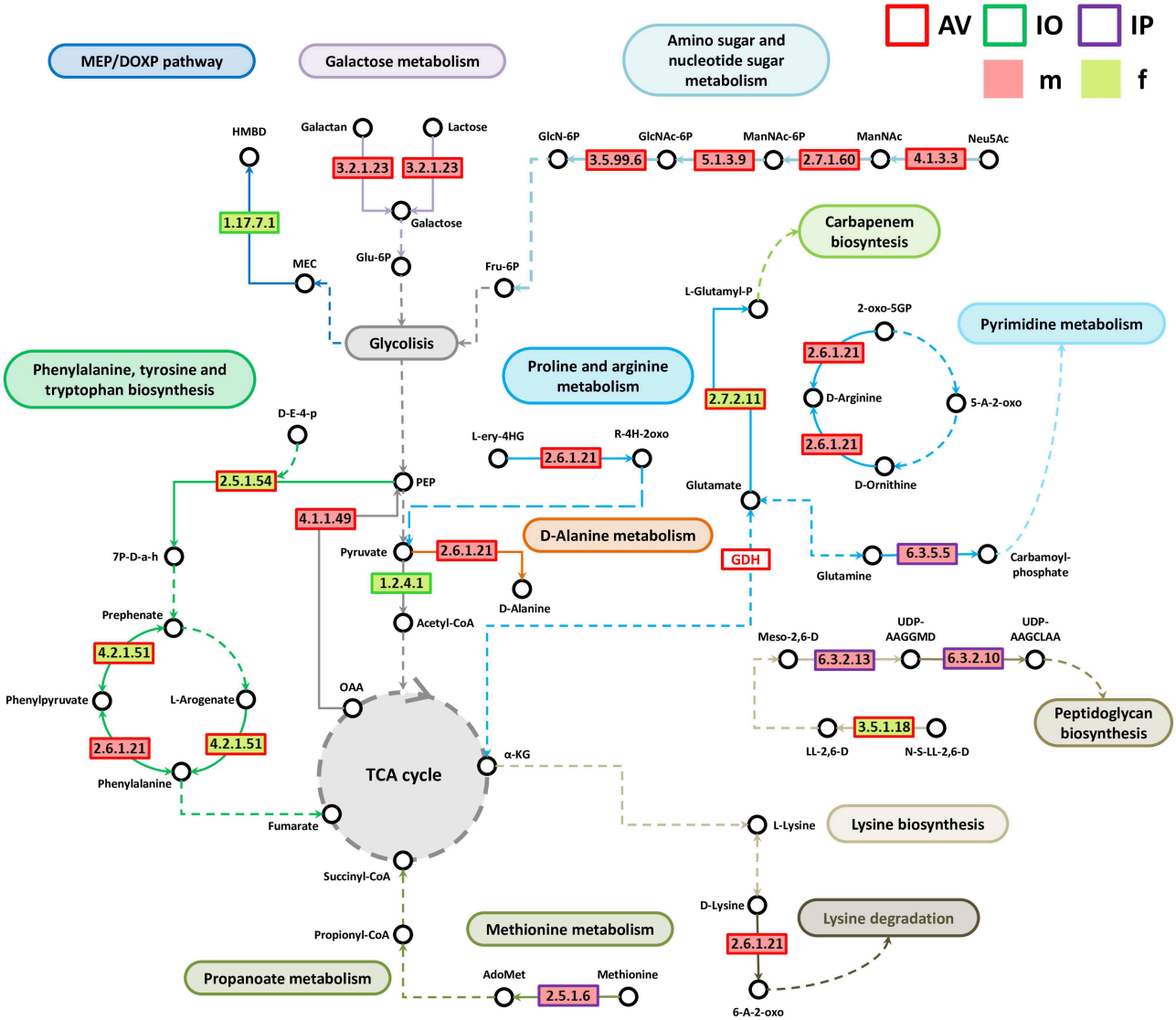

FIGURE 5 | Partial pathway reconstruction of genes involved in amino acid and carbohydrate metabolism. Only metabolic enzymes with significant differences in relative abundance ($q < 0.05$) between male and female ticks and KEGG annotation were included in this analysis. Continuous lines represent reactions catalyzed by the enzymes with significant differences in relative abundance between male and female ticks. Dashed lines represent pathway reconstruction based in KEGG. Fru-6P, Fructose 6-phosphate; GlcNAc-6P, N-acetyl-D-glucosamine 6-phosphate; GlcN-6P, Glucosamine 6-phosphate; Neu5Ac, N-acetylneuraminic acid; ManNAc, N-acetyl-D-mannosamine; ManNAc-6P, N-acetyl-D-mannosamine 6-phosphate; Glu-6P, Glucose-6P; PEP, phosphoenolpyruvate; L-Glutamyl-P, L-glutamate 5-phosphate; HMBPP, (E)-4-hydroxy-3-methyl-but-2-enyl diphosphate; HMBD, 1-hydroxy-2-methyl-2-butenyl 4-diphosphate; MEC, 2-C-Methyl-D-erythritol 2, 4-cyclodiphosphate; UDP-AAGGMD, UDP-N-acetylmuramoyl-L-alanyl-gamma-D-glutamyl-meso-2,6-diaminopimelate; UDP-AAGCLAA, UDP-N-acetylmuramoyl-L-alanyl-D-glutamyl-6-carboxy-L-lysyl-D-alanyl-D-alanine; AdoMet, S-adenosylmethionine; a-KG, a-ketoglutarate; L-ery-4HG, L-erythro-4-hydroxy-glutamate; R-4H-2oxo, (R)-4-Hydroxy-2-oxoglutarate; Meso-2,6-D, Mseso-2,6-Diaminopimelate; LL-2,6-D, LL-2,6-Diaminopimelate; N-S-LL-2,6-D, N-Succinyl-LL-2, 6-diaminopimelate; 6-A-2-oxo, 6-Amino-2-oxohexanoate; 7P-D-a-h, 7P-2-Dehydro-3-deoxy-D-arabino-heptonate; OAA, Oxaloacetate; GDH, Glutamate dehydrogenase; 5-A-2-oxo, 5-Amino-2-oxopentanoate; 2-oxo-5GP, 2-Oxo-5-guanidino-pentanoate; D-E-4-p, D-Erythose 4-phosphate.

and glutamate kinase (EC 2.7.2.11). Prephenate dehydratase is involved in two reactions of phenylalanine biosynthesis pathway, the conversion of L-Arogenate and prephenate in phenylalanine and phenylpyruvate, respectively. In contrast to AVm in which one enzyme of lysine degradation pathway was highly abundant, succinyl-diaminopimelate desuccinylase, highly abundant in AVf, is involved lysine biosynthesis. The transformation catalyzed by glutamate kinase, the transfer of a phosphate group to glutamate to form L-glutamate 5-phosphate, is involved in the biosynthesis of proline and, interestingly, the carbapenem antibiotics northienamycin and thienamycin.

The abundance of only two enzymes was significatively different between IOm [(E)-4-hydroxy-3-methylbut-2-enyl-diphosphate synthase, IspG, EC 1.17.7.1] and IOf (pyruvate dehydrogenase, EC 1.2.4.1). IspG catalyzes one of the terminal steps of the MEP/DOXP pathway where it converts 2-C-Methyl-D-erythritol 2,4-cyclodiphosphate in 1-hydroxy-2-methyl-2-butenyl 4-diphosphate which is later transformed in terpenoid backbones. In the mitochondrial matrix, pyruvate is decarboxylated by pyruvate dehydrogenase which is the first step of a series of enzymatic reactions that transform pyruvate into acetyl coenzyme A (Acetyl-CoA).

Four enzymes related with amino acid metabolism were more abundant in IPm than in IPf. In addition to its role in protein synthesis, large amounts of methionine are used for the synthesis of S-adenosylmethionine (AdoMet) by methionine adenosyltransferases (MAT, EC 2.5.1.6) in a reaction that is the rate-limiting step of the methionine cycle. AdoMet participates in a large number of reactions, notably the 5′-deoxyadenosyl moiety of AdoMet participates in biotin synthesis, and thought propanoate metabolism AdoMet can enter to TCA cycle. Other two enzymes, MurE synthetase (EC 6.3.2.13) and MurF synthetase (EC 6.3.2.10), are involve in lysine and peptidoglycan biosynthesis. The first catalyzes the addition of an amino acid to the nucleotide precursor UDP-N-acetylmuramoyl-L-alanyl-D-glutamate (UMAG) in the biosynthesis of bacterial cell-wall peptidoglycan and the second catalyzes the final step in the synthesis of UDP-N-acetylmuramoyl-pentapeptide, the precursor of murein, a polymer that forms a mesh-like layer outside the plasma membrane of most bacteria. The last enzyme (EC 6.3.5.5), carbamoyl-phosphate synthase, uses glutamine to synthesize carbamoyl phosphate, an anion involved in pyrimidines metabolism and arginine biosynthesis.

Differences in Lipid and Vitamin B Metabolism Genes in the Microbiomes of Female and Male AV, IO, and IP

Most of the genes associated with lipid, vitamin B, nucleotide, and Pterin metabolisms were identified in AV (**Figure 6**). Only one enzyme, biotin carboxylase (EC 6.3.4.14), was found in IP and it was more abundant in IPm compared to IPf (**Figure 6**). Biotin carboxylase carboxylates the biotin of the biotin carboxyl carrier protein (BCCP) and these two enzymes are part of the acetyl-CoA carboxylase complex (ACC) that catalyzes the irreversible carboxylation of acetyl-CoA to produce malonyl-CoA which provides 2-carbon units to fatty acids and commits them to fatty acid chain synthesis. Two other enzymes involved in biotin synthesis, EC 2.3.1.47 and EC 2.8.1.6, were more abundant in AVf and AVm, respectively. While EC 2.3.1.47 synthesizes the intermediate 8-Amino-7-oxononanoate, biotin synthase (EC 2.8.1.6) catalyzes the final step in the biotin biosynthetic pathway. Biotin plays an important role as a cofactor of several enzymes including pyruvate carboxylase, propionyl-CoA carboxylase and, as mentioned before, ACC (**Figure 6**).

Enzymes involved in pyrimidine (EC 2.7.4.9) and purine and folate metabolism (EC 1.5.1.3 and EC 6.3.4.3) were more abundant in AVf (EC 2.7.4.9 and EC 1.5.1.3) and AVm (EC 6.3.4.3). Dihydrofolate reductase (EC 1.5.1.3) converts dihydrofolate into folate or tetrahydrofolate which contains methyl groups required for the *de novo* synthesis of purines, thymidylic acid, and certain amino acids. Tetrahydrofolate is then transformed by formate–tetrahydrofolate ligase (EC 6.3.4.3) to 10-formyltetrahydrofolate, a donor of formyl groups in purine biosynthesis and formylation of methionyl-tRNA formyltransferase to give fMet-tRNA.

Pterins are heterocyclic compounds composed of a pteridine ring system with a keto and amino groups. Among them, tetrahydrobiopterin (BH_4) is an essential cofactor for phenylalanine, tyrosine, and tryptophan hydroxylases. BH_4 is the product of the dihydropteridine reductase (EC 1.5.1.34), that uses quinonoid dihydrobiopterin (qBH_2) as substrate, and this enzyme was more abundant in AVm than in AVf. Two other enzymes, EC 3.2.1.23 and EC 2.7.8.20 were also more abundant in AVm than in AVf. The first enzyme EC 3.2.1.23 is a beta-galactosidase that in addition to be involved in galactose synthesis (**Figure 5**), participates in keratan sulfate degradation (**Figure 6**). Keratan sulfate is a glycosaminoglycan that plays role as a structural carbohydrate and is widely distributed in the extracellular matrices of animal tissues. The second enzyme EC 2.7.8.20, a phosphoglycerol transferase, may be involved in the synthesis of two glycosyldiacylglycerols (i.e., 1,2-Diacyl-3-(sn-glycerol-1-P-6Glcα1-2Glcα1)-sn-glycerol,1,2-Diacyl-3-(sn-glycerol-1-P-6Glcβ1-6Glcβ1)-sn-glycerol) that may be building blocks for lipoteichoic acid (LTA) synthesis (**Figure 6**). LTA are major constituents of the cell wall of gram-positive bacteria. Finally, AVf have more abundance of the enzymes phosphatidate cytidylyltransferase (EC 2.7.7.41) and phosphatidylglycerophosphate synthase (EC 2.7.8.5) compared with AVm. These two enzymes catalyze the two final steps in the synthesis of phosphatidyl glycerophosphate that is then transformed into phosphatidylglycerol, a step necessary for the *de novo* biosynthesis of cardiolipin, the major anionic phospholipids in bacteria that functionally interacts with membrane proteins that are involved in energy metabolism and cellular division.

Linkages Between Taxonomic and Functional Profiles in the Microbiomes of Male and Female AV, IO, and IP

In an attempt to identify possible links between taxonomic and functional profiles, sex-specific functional categories (**Figure 4**) were linked with the bacterial genera where those genes were annotated. In AV, 23 bacterial genera contain all the genes of interest. Notably, five bacterial genera contained 89.9% of the genes: *Haemophilus* (29.3%), *Aggregatibacter* (22.8%), *Proteus* (16.7%), *Pasteurella* (11.7%), and *Coxiella* (9.4%) (**Figure 7A** and **Supplementary Table 2**). Linkage analysis in AV revealed two types of patterns: (i) several enzyme-encoding genes were harbored by the same bacterial genus; (ii) a single enzyme was found in several bacterial genera. About 50% of the genes analyzed in AV were found in four or more

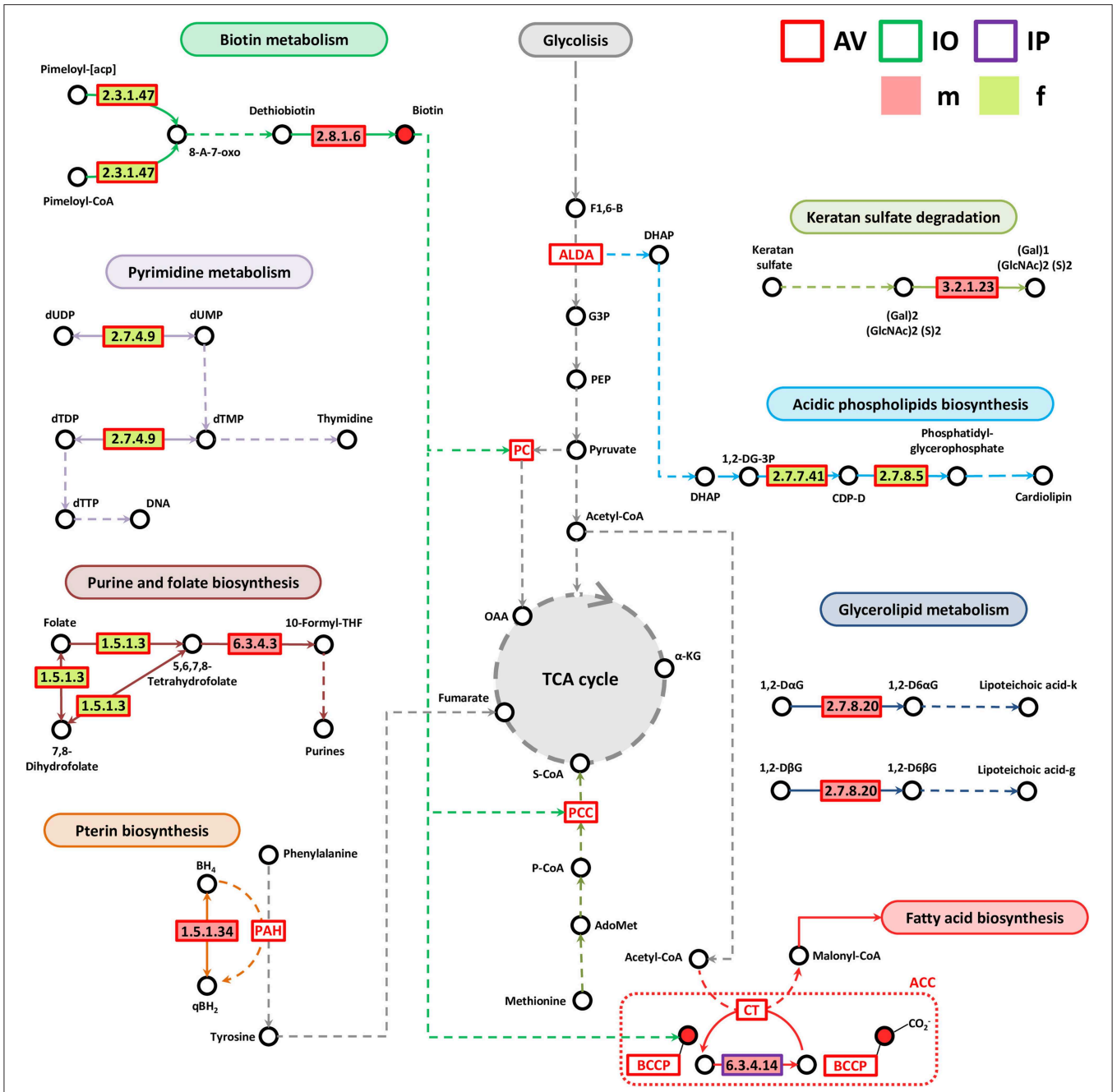

FIGURE 6 | Partial pathway reconstruction of genes involved in lipids, nucleotides and vitamins metabolism. Only metabolic enzymes with significant differences in relative abundance ($q < 0.05$) between male and female ticks and KEGG annotation were included in this analysis. Continuous lines represent reactions catalyzed by the enzymes with significant differences in relative abundance between male and female ticks. Dashed lines represent pathway reconstruction based in KEGG. DHAP, Dihydroxyacetone phosphate; ALDA, Fructose-bisphosphate aldolase; G3P, Glyceraldehyde 3-phosphate; F1,6-B, Fructose 1,6-bisphosphate; 8-A-7-oxo, 8-Amino-7-oxononanoate; PCC, Propionyl-CoA carboxylase; S-CoA, Succinyl-CoA, P-CoA, Propionyl-CoA; LacCer, lactosylceramide; SPH, Sphingomyelin; GlcCer, Glucosylceramide; α-KG, α-ketoglutarate; qBH2, quinoid dihydrobiopterin; PAH, phenylalanine-4-hydroxylase, 1,2-DG-3P, 1,2-Diacyl-sn-glycerol-3P; CDP-D, CDP-Diacylglycerol; 1,2-DaG, 1,2-Diacyl-3-(Glca1-2Glca1)-sn-glycerol; 1,2-DbG, 1,2-Diacyl-3-(Glcb1-6Glcb1)-sn-glycerol; 1,2-D6aG, 1,2-Diacyl-3-(sn-glycerol-1-P-6Glca1-2Glca1)-sn-glycerol; 1,2-D6bG, 1,2-Diacyl-3-(sn-glycerol-1-P-6Glcb1-6Glcb1)-sn-glycerol; Lipoteichoic acid-k, Lipoteichoic acid (kojibiose-containing); Lipoteichoic acid-g, Lipoteichoic acid (gentiobiose-containing); BCCP, biotin carboxyl carrier protein; ACC, Acetyl-CoA carboxylase complex; OAA, Oxaloacetate; PC, pyruvate carboxylase; BH4, Tetrahydrobiopterin; qBH2, quinonoid dihydrobiopterin.

bacterial genera. The top enzyme, exodeoxyribonuclease VII large subunit (EC 3.1.11.6), was found in 10 genera (**Figure 7B**). This enzyme, EC 3.1.11.6, is a bacterial nuclease involved in DNA repair and recombination that hydrolyses single-stranded DNA into large acid-insoluble oligonucleotides, which are then degraded further into small acid-soluble oligonucleotides. Other

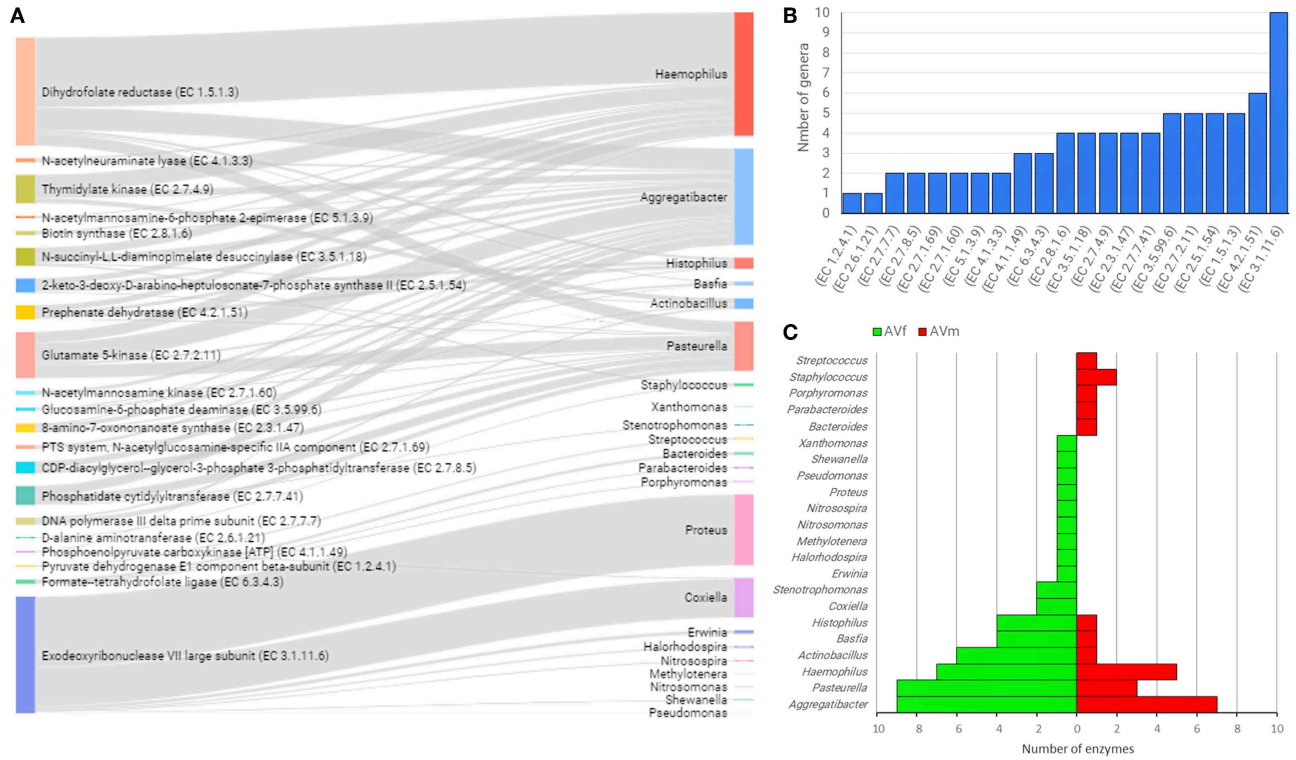

FIGURE 7 | Linkage of enzyme-encoding genes with bacterial genera harboring them into the gut microbiome of AV ticks. Only enzyme-encoding genes with significant differences in relative abundance ($q < 0.05$) between male and female ticks and KEGG annotation were included in this analysis **(A)**. Sankey graph showing the connectivity between functional genes (left) and bacterial genera (right) wherein those were annotated. The edges link genes and source (bacterial genera). The node size is proportional to the number of hits (number of sequences containing the annotation), and consequently the edges size is proportional to the hit's distribution among bacterial genera. **(B)** Bar plot indicating the number of bacterial genera harboring every enzyme-encoding gene. **(C)** Mirror bar plot showing the distribution of enzyme-encoding genes across the bacterial genera in female (AVf) and male (AVm) ticks. A detailed list of enzymes and bacterial source can be found in **Supplementary Table 2**.

enzyme-encoding genes widespread among bacterial genera (i.e., found in four or more genera), were associated with amino acids and carbohydrates metabolism (EC 4.2.1.51, EC 2.5.1.54, EC 2.7.2.11, EC 3.5.99.6, and EC 3.5.1.18) and lipid and vitamin B metabolism (EC 2.3.1.47, EC 1.5.1.3, EC 2.7.4.9, EC 2.8.1.6, and EC 2.7.7.41) (**Figure 7B**). The genera *Aggregatibacter*, *Pasteurella*, *Haemophilus*, *Actinobacillus*, *Basfia,* and *Histophilus* were found to harbor four or more of the enzyme-encoding genes included in this analysis (**Figure 7C**). The same genera *Aggregatibacter*, *Pasteurella*, *Haemophilus*, *Actinobacillus*, *Basfia,* and *Histophilus* contributed to a higher number of enzyme-encoding genes in AVf than in AVm. In addition, other bacterial genera harboring at least one of these genes were found only in AVf or AVm (**Figure 7C**).

The linkage analysis between the taxonomic and functional profiles in the two *Ixodes* species revealed that the genes of interest were found across 35 bacterial genera and only five genera accounted for 87.8% of hits: *Rickettsia* (39.1%), *Candidatus Protochlamydia* (16.3%), *Chlamydophila* (11.7%), *Waddlia* (10.9%), and *Chlamy*dia (9.8%) (**Figure 8A** and **Supplementary Table 3**). The enzyme found in the highest number of genera (i.e., 10) was associated to DNA metabolism, in this case, the enzyme DNA polymerase III (EC 2.7.7.7), which constitute the primary enzyme complex involved in prokaryotic DNA replication. Other enzymes present the genome of four or more bacterial genera include EC 1.17.7.1, EC 2.5.1.6, EC 6.3.4.14, and EC 6.3.5.5 (**Figure 8B**) for which the function was described above. Differences were also found in the bacterial genera that contributed to the different functional profiles of female and male *Ixodes* ticks (**Figure 8C**). The genus *Rickettsia* harbored seven enzyme-encoding genes in both female and male ticks, while *Candidatus Protochlamydia* also contributed with three and two enzymes on the microbiome of females and males *Ixodes* ticks, respectively. Nevertheless, 83% (26/31) of the genera contributed with a single functional gene on *Ixodes* tick microbiomes, and this proportion was higher when compared to 56.5% (13/23) in AV.

The bacterial genera of the sex-specific taxonomic and functional profiles of the three tick species were compared (**Figure 9**). Results showed that only a small group of bacterial genera contribute to differentiate males and females metagenomes at both functional and taxonomic levels. Most of the bacterial genera were found to contribute to either the functional or the taxonomic profiles.

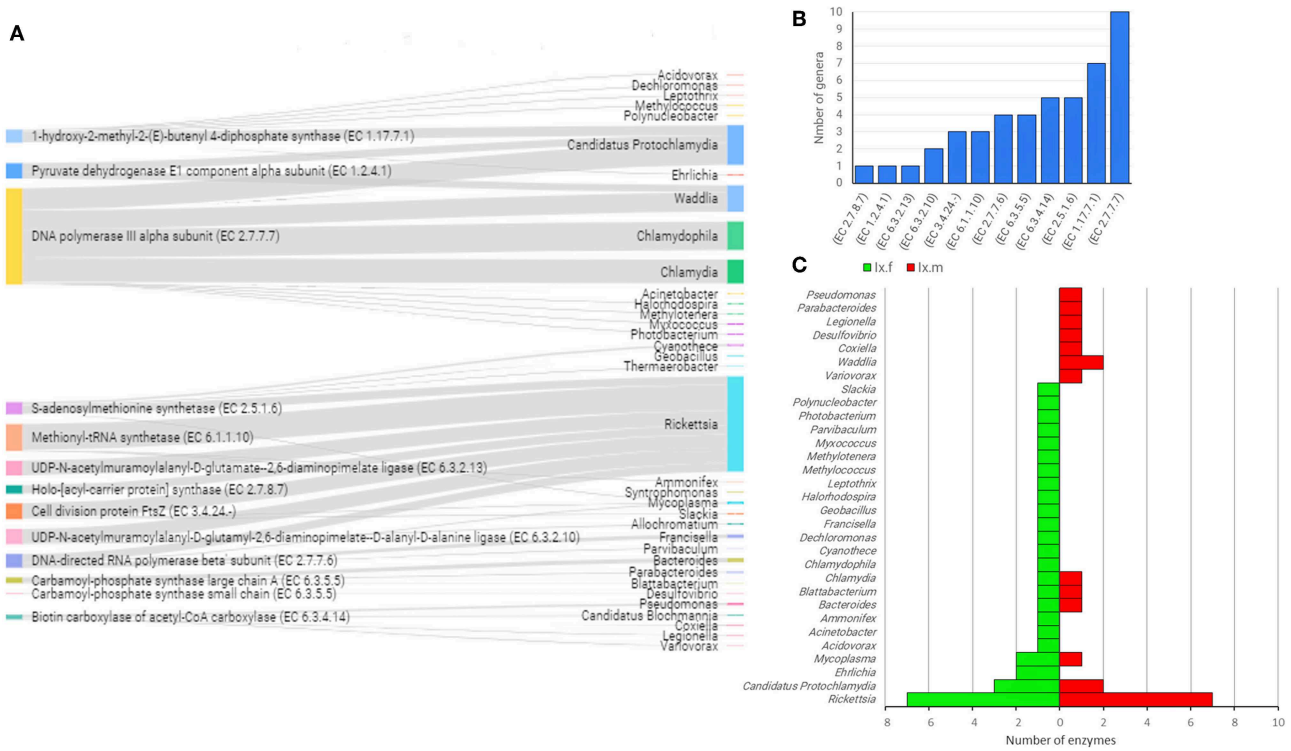

FIGURE 8 | Linkage of enzyme-encoding genes with bacterial genera harboring them into the gut microbiome of both IO and IP ticks. Only enzyme-encoding genes with significant differences in relative abundance ($q < 0.05$) between male and female ticks and KEGG annotation were included in this analysis **(A)**. Sankey graph showing the connectivity between functional genes (left) and bacterial genera (right) wherein those were annotated. The edges link genes and source (bacterial genera). The node size is proportional to the number of hits (number of sequences containing the annotation), and consequently the edges size is proportional to the hit's distribution among bacterial genera. **(B)** Bar plot indicating the number of bacterial genera harboring every enzyme-encoding gene. **(C)** Mirror bar plot showing the distribution of enzyme-encoding genes across the bacterial genera in female (Ix.f) and male (Ix.m) *Ixodes* ticks (data on both ticks species, IO and IP, was merged). A detailed list of enzymes and bacterial source can be found in **Supplementary Table 3**.

DISCUSSION

The dataset reported by Nakao et al. (2013) is one of the few studies, in addition to Carpi et al. (2011), that used whole-metagenome sequencing to study the taxonomic composition of tick microbiota. Most of the studies are based on the NGS approach using amplicon sequencing of marker genes (Greay et al., 2018). Yet, the functional traits of the microbial communities living in body compartments of ticks, as well as the pattern of the functional diversity remain largely unexplored. The trait-based approaches in microbial ecology research enable a deeper understanding of the role of biodiversity in maintaining multiple ecosystem functioning (Krause et al., 2014; Louca et al., 2016). Such approach has a direct application to tick vectors, for which the debate about the relevance of "*differences in taxonomic profiles only*" is open (Estrada-Peña and Cabezas-Cruz, 2019). Here we used the MG-RAST pipeline (Meyer et al., 2008) version 4 (Meyer et al., 2017) to achieved a workflow substantially different to that followed by Nakao et al. (2013). Using MG-RAST we were able to perform taxonomic and functional feature annotation and profiling of the gut microbiota of males and females of three tick species IO, IP, and AV. Despite the original dataset has the weakness of the reduced number of biological replicates and the limited coverage resulting from a 454 pyrosequencing technology (Liu et al., 2012; Goodwin et al., 2016), the results of this study are meaningful.

The rationale behind our study is rooted on the experiences about the role of *Coxiella* (Smith et al., 2015) and *Francisella* (Duron et al., 2018), proposed to complement some nutritional deficiencies in the tick diet, which was proposed to be one of the functional implications of the tick microbiome (Estrada-Peña and Cabezas-Cruz, 2019). Despite massive genome reduction compared to pathogenic *Francisella* and *Coxiella* species, the genes for biosynthesis of vitamin B were conspicuously intact in the genome of the F-Om and CLEAA symbionts of soft and hard ticks (Smith et al., 2015; Duron et al., 2018). In this study, in addition to bacteria of the genus *Coxiella*, B vitamins biosynthesis genes were also found in *Actinobacillus*, *Aggregatibacter*, *Basfia*, *Ehrlichia*, *Haemophilus*, *Histophilus*, *Neorickettsia*, *Pasteurella*, and *Rickettsia* in AV, IO, and IP (**Figures 6–8**). Despite we performed only a partial reconstruction of metabolic pathways and therefore it is not known whether B vitamins biosynthesis pathways are completed; the presence of B vitamins biosynthesis genes in several bacterial genera suggests

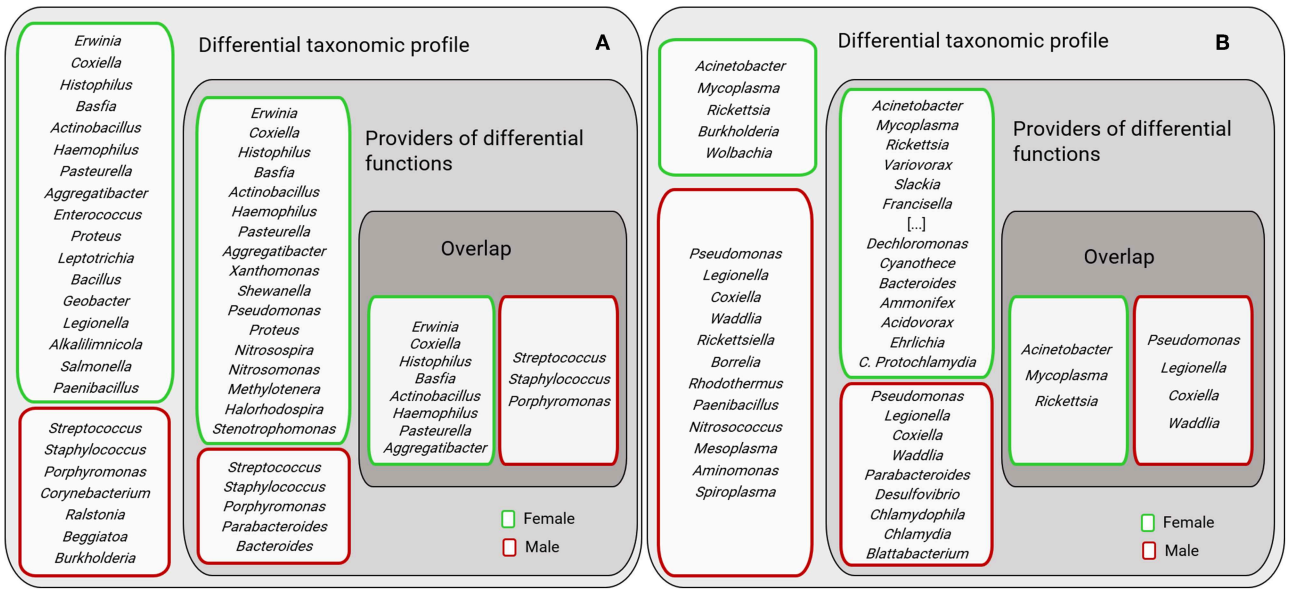

FIGURE 9 | Comparison of bacterial genera identified in the sex-specific taxonomic and functional profiles. The figure displays female and male AV **(A)** and *Ixodes* spp. **(B)**. "Differential taxonomic profiles" include those genera with differential abundance between AVf and AVm (as shown in **Figure 2C**) and female (Ix.f) and male (Ix.m) *Ixodes* ticks (data on both ticks species, IO and IP, was merged) (as shown in **Figures 2D,E**). "Providers of differential functions" were described in **Figures 7**, **8** for AV and Ix, respectively. "Overlap" displays the genera found in both groups "Differential taxonomic profiles" and "Providers of differential functions." For figure display purposes the following genera were not included: *Polynucleobacter*, *Photobacterium*, *Parvibaculum*, *Myxococcus*, *Methylotenera*, *Methylococcus*, *Leptothrix*, *Halorhodospira*, *Geobacillus,* and their position is labeled as "[…]".

that bacteria other than *Francisella* and *Coxiella* may also complement the nutritional deficiency of vitamin B in the tick blood meal.

Several other enzyme-encoding genes not related with B vitamins metabolism were also present in four or more bacteria genera of the gut microbiota of AV (**Figure 7**). The metabolic pathways of these genes were as diverse as amino acid, antibiotics, pyrimidine, lipids, and amino sugars metabolism suggesting that the contribution of tick gut microbiota can go beyond B vitamins supplementation. Highly redundant enzymes (i.e., present in four or more bacteria genera) were also found in *Ixodes* tick microbiomes (**Figure 8**) and these enzymes are also involved in very disparate pathways including MEP/DOXP, amino acid degradation, DNA replication, fatty acid biosynthesis, and pyrimidines biosynthesis. The presence of the same genes and functions in different bacteria of the microbiota implies functional redundancy, a property of microbiota reported in other species, for example humans (Heintz-Buschart and Wilmes, 2018), but poorly studied in arthropod vectors. Functional redundancy can increase tick resilience in case of perturbations affecting the taxonomic composition of the bacterial community within the tick microbiota (Estrada-Peña et al., 2018). In contrast to the long-term mutualism of *Francisella* with ticks (Duron et al., 2018), the capacity of ticks to harbor a variable bacterial composition according to the life stage and the changing environmental conditions may contribute to tick survival in extreme environments and stressful conditions.

The presence of stress response genes in the metagenome of male, compared to female ticks, of the three species included in this study (**Figure 3**), suggests that male ticks may maximize the presence of bacteria containing this gene category to cope with specific conditions to which they are exposed. While the sole presence of genes in the metagenome does not guaranty a role in tick physiology, the differences in the life cycle of males and females could help explaining why all males have more stress response genes than females. For example in *Ixodes* spp., they quest for a host, but mate females commonly before or while feeding. The need for a prolonged survival of males even under adverse conditions is even more evident in the case of some *Amblyomma* spp., males being the first stages reaching a suitable host and then emitting a "call pheromone" to stimulate the females to climb on the host already occupied by males (Sonenshine and Mather, 1994). In both cases, male ticks should be better prepared to cope with environmental stress (e.g., exhaustion of hydric resources (Sonenshine and Mather, 1994) than females.

Surprisingly, the bacterial genera providing major functional differences between males and females did not match completely the most abundant bacterial genera in males and females, respectively (**Figure 9**). We hypothesized that this could result from sex-specific selective pressures that act independently on the phenomes (set of phenotypes) and the genomes of bacteria in the tick gut microbiota. In a simple model, "one genome-one phenome," the genome of a single bacterium could easily predict its phenome. For example, genome-phenome correspondence

analysis of *Burkholderia cenocepacia* during long-term chronic infection identified a number of candidate genes that were highly associated with the motility and biofilm phenotypes of these bacteria (Lee et al., 2017) and the specific inhibition of one of these genes may affect one trait and not the other. However, the simultaneous evolution of hundreds of bacteria within a host allows a playground for evolution where a high number of trait complementation could emerge from trait-by-trait phenomena, including horizontal gene transfer, epistasis (Zeng et al., 2017) and metabolic networks resulting from community-based phenomes. For example, fitness traits of *Drosophila melanogaster* could not be tracked to specific bacteria of the fly microbiota, but instead microbiota bacteria interactions were shown to shape both microbiome abundance and host fitness traits (Gould et al., 2018). In this framework, it can be hypothesized that bacteria in the group "Providers of differential functions" (**Figure 9**) may be selected based on community-dependent phenomes that are influenced by sexual traits of the ticks. Other bacteria in the group "Differential taxonomic profiles" (**Figure 9**) may be "independent players" selected for their individual phenome. Finally, bacteria genera in the groups "Overlap" may be selected based on both individual and community-dependent phenomes.

CONCLUSION

Functional metagenomics is a powerful analytical tool that complements microbiota composition studies. The high diversity of tick microbiome and the rich functionality of tick metagenomes suggest that these arthropods evolved mechanisms to maximize the genetic diversity of the microorganisms they harbor, which in turn may increase the functional capabilities of the ticks. Hosting highly diverse and redundant microbiomes may offer ticks a competitive advantage in the environment. Differences in taxonomical and functional microbiomes between tick species, and even more between females and males of the same species, suggest the specialization of tick gut microbiota in response to peculiarities of the life cycle and fitness of the tick hosts. In agreement with this hypothesis, a strong phylosymbiotic signal revealed that phylosymbiosis may be a widespread phenomenon in tick-microbiota evolution (Díaz-Sánchez et al., 2019). This finding, together with the results of the current study, supports the existence of a species-specific and sex-specific tick hologenome with a largely unexplored influence on tick biology and pathogen transmission. We proposed that the characterization of tick gut microbiome should be undertaken in terms of functional and taxonomic diversity instead of only taxonomic diversity.

DATA AVAILABILITY

Publicly available datasets were analyzed in this study. This data can be found here: https://www.nature.com/articles/ismej2012171.

AUTHOR CONTRIBUTIONS

AC-C, AE-P, and DO conceived the study. DO, AC-C, EB, and DA analyzed the data. AC-C and DO drafted the manuscript. All authors read the manuscript and made critical revisions.

SUPPLEMENTARY MATERIAL

The Supplementary Material for this article can be found online at: https://www.frontiersin.org/articles/10.3389/fcimb.2019.00298/full#supplementary-material

Supplementary Figure 1 | Species richness in the gut microbiota of AVf, AVm, IPf, IPm, IOf, and IOm. **(A)** Rarefaction curve of annotated species represented the total number of distinct species as a function of the number of sequences sampled. **(B)** α-diversity values summarize the species richness in each sample. The species-level annotations were performed in MG-RAST and species richness calculated as the antilog of the Shannon diversity.

Supplementary Figure 2 | Phylum-level and Family-level taxonomic profiles of gut microbiota of AVf, AVm, IPf, IPm, IOf, and IOm. Taxonomical features annotated on MG-TAST, based on RefSeq database at minimal identity cutoff of 60%. Only the most abundant phyla are shown in the legend.

Supplementary Figure 3 | Phylogenetic tree and relative abundance of bacterial genera found in the gut microbiota of AVf, AVm, IPf, IPm, IOf, and IOm. The relative abundance of each genus is indicated by the scale bar, and bars are pattern-coded for each tick species and sex. Phylogenetic trees were built using NCBI Taxonomy Browser. For this purpose the taxonomic ID of all genus identified in the taxonomic profiling in MG-RAST pipeline (based on RefSeq database at minimal identity cutoff of 60%) were collected using the Taxonomy name/id tool. The bacteria were then split in six groups according to phylum or class, and the phylogenetic trees were built by submitting the taxonomic ID list of each group to the NCBI Common Tree tool.

Supplementary Figure 4 | The functional profile of AVf, AVm, IPf, IPm, IOf, and IOm based on COG database. **(A)** Abundance profiles of functions clustered at Level 1 **(B)** and Level 2. Protein features annotated following the MG-RAST pipeline, profiles acording representative hit method, with maximum e-value cut-off of 1e-5, minimal identity cut off of 80%; and minimum alignment length of 15 bp. **(C)** The functional profile of gut microbiome of AVf, AVm, IPf, IPm, IOf, and IOm based on the SEED subsystem database at categorical Level 1, with minimal identity cutoff of 80%.

Supplementary Table 1 | Comparison of all the functional features annotated in the metagenomes of female and males AV, IO, and IP. Annotation based on SEED at level 4.

Supplementary Table 2 | Linkage list of enzymes and their bacterial sources in AV.

Supplementary Table 3 | Linkage list of enzymes and their bacterial sources in IP and IO.

REFERENCES

Anders, S., and Huber, W. (2010). Differential expression analysis for sequence count data. *Genome Biol.* 11, 1–12. doi: 10.1186/gb-2010-11-10-r106

Aziz, R. K., Bartels, D., Best, A. A., Dejongh, M., Disz, T., Edwards, R. A., et al. (2008). The RAST server: rapid annotations using subsystems technology. *BMC Genomics* 9:75. doi: 10.1186/1471-2164-9-75

Benson, D. A., Karsch-Mizrachi, I., Lipman, D. J., Ostell, J., and Sayers, E. W. (2009). GenBank. *Nucleic Acids Res.* 37, D26–D31. doi: 10.1093/nar/gkn723

Byrd, A. L., Belkaid, Y., and Segre, J. A. (2018). The human skin microbiome. *Nat. Rev. Microbiol.* 16, 143–155. doi: 10.1038/nrmicro.2017.157

Cabezas-Cruz, A., Pollet, T., Estrada-Peña, A., Allain, E., Bonnet, S. I., and Moutailler, S. (2018). "Handling the microbial complexity associated to ticks," in *Ticks and Tick-Borne Pathogens*, ed D. M. Abubakar (London: IntechOpen), 1–36. doi: 10.5772/intechopen.80511

Canfora, E. E., Meex, R. C. R., Venema, K., and Blaak, E. E. (2019). Gut microbial metabolites in obesity, NAFLD and T2DM. *Nat. Rev. Endocrinol.* 15, 261–273. doi: 10.1038/s41574-019-0156-z

Cani, P. D. (2018). Microbiota and metabolites in metabolic. *Nat. Rev. Endocrinol.* 15, 69–70. doi: 10.1038/s41574-018-0143-9

Carpi, G., Cagnacci, F., Wittekindt, N. E., Zhao, F., Qi, J., Tomsho L, P., et al. (2011). Metagenomic profile of the bacterial communities associated with *Ixodes ricinus* ticks. *PLoS ONE* 6:e25604. doi: 10.1371/journal.pone.0025604

Cox, M. P., Peterson, D. A., and Biggs, P. J. (2010). SolexaQA: at-a-glance quality assessment of Illumina second-generation sequencing data. *BMC Bioinformatics* 11:485. doi: 10.1186/1471-2105-11-485

Degli Esposti, M., and Martinez Romero, E. (2017). The functional microbiome of arthropods. *PLoS ONE* 12:e0176573. doi: 10.1371/journal.pone.0176573

Díaz-Sánchez, S., Estrada-Peña, A., Cabezas-Cruz, A., and de la Fuente, J. (2019). Evolutionary insights into the tick hologenome. *Trends Parasitol.* doi: 10.1016/j.pt.2019.06.014. [Epub ahead of print].

Duron, O., Morel, O., and Bouchez, O. (2018). Tick-bacteria mutualism depends on B vitamin article tick-bacteria mutualism depends on B vitamin synthesis pathways. *Curr. Biol.* 28, 1896–1902. doi: 10.1016/j.cub.2018.04.038

Estrada-Peña, A., and Cabezas-Cruz, A. (2019). Ticks and tick-borne diseases. *Ticks Tick. Borne. Dis.* 10, 34–35. doi: 10.1016/j.ttbdis.2018.08.017

Estrada-Peña, A., Cabezas-Cruz, A., Pollet, T., Vayssier-Taussat, M., and Cosson, J. F. (2018). High throughput sequencing and network analysis disentangle the microbial communities of ticks and hosts within and between ecosystems. *Front. Cell. Infect. Microbiol.* 8:236. doi: 10.3389/fcimb.2018.00236

Gomez-Alvarez, V., Teal, T. K., and Schmidt, T. M. (2009). Systematic artifacts in metagenomes from complex microbial communities. *ISME J.* 3, 1314–1317. doi: 10.1038/ismej.2009.72

Goodwin, S., McPherson, J. D., and McCombie, W. R. (2016). Coming of age: ten years of next-generation sequencing technologies. *Nat. Rev. Genet.* 17, 333–351. doi: 10.1038/nrg.2016.49

Gould, A. L., Zhang, V., Lamberti, L., Jones, E. W., Obadia, B., Korasidis, N., et al. (2018). Microbiome interactions shape host fitness. *Proc. Natl. Acad. Sci. U.S.A.* 115, E11951–E11960. doi: 10.1073/pnas.1809349115

Greay, T. L., Gofton, A. W., Paparini, A., Ryan, U. M., Oskam, C. L., and Irwin, P. J. (2018). Recent insights into the tick microbiome gained through next-generation sequencing. *Parasites Vectors* 11, 1–14. doi: 10.1186/s13071-017-2550-5

Hall, A. B., Tolonen, A. C., and Xavier, R. J. (2017). Human genetic variation and the gut microbiome in disease. *Nat. Publ. Gr.* 18, 690–699. doi: 10.1038/nrg.2017.63

Heintz-Buschart, A., and Wilmes, P. (2018). Human gut microbiome: function matters. *Trends Microbiol.* 26, 563–574. doi: 10.1016/j.tim.2017.11.002

Jung, J., Philippot, L., and Park, W. (2016). Metagenomic and functional analyses of the consequences of reduction of bacterial diversity on soil functions and bioremediation in diesel-contaminated microcosms. *Sci. Rep.* 6, 1–10. doi: 10.1038/srep23012

Kanehisa, M., and Goto, S. (2000). KEGG : Kyoto encyclopedia of genes and genomes. *Nucleic Acids Res.* 28, 27–30. doi: 10.1093/nar/28.1.27

Krause, S., Le Roux, X., Niklaus, P. A., Van Bodegom, P. M., Lennon, J. T., Bertilsson, S., et al. (2014). Trait-based approaches for understanding microbial biodiversity and ecosystem functioning. *Front. Microbiol.* 5:251. doi: 10.3389/fmicb.2014.00251

Langmead, B., Trapnell, C., Pop, M., and Salzberg, S. L. (2009). Ultrafast and memory-efficient alignment of short DNA sequences to the human genome. *Genome Biol.* 10:R25. doi: 10.1186/gb-2009-10-3-r25

Lee, A. H., Flibotte, S., Sinha, S., Paiero, A., Ehrlich, R, L., Balashov, S., et al. (2017). Phenotypic diversity and genotypic flexibility of *Burkholderia cenocepacia* during long-Term chronic infection of cystic fibrosis lungs. *Genome Res.* 27, 650–662. doi: 10.1101/gr.213363.116

Liu, L., Li, Y., Li, S., Hu, N., He, Y., Pong, R., et al. (2012). Comparison of next-generation sequencing systems. *J. Biomed. Biotechnol.* 2012, 1–11. doi: 10.1155/2012/251364

Louca, S., Parfrey, L. W., and Doebeli, M. (2016). Decoupling function and taxonomy in the global ocean microbiome. *Science* 353, 1272–1277. doi: 10.1126/science.aaf4507

Mendes, L. W., Kuramae, E. E., Navarrete, A. A., van Veen, J. A., and Tsai, S. M. (2014). Taxonomical and functional microbial community selection in soybean rhizosphere. *Isme J.* 8, 1577–1587. doi: 10.1038/ismej.2014.17

Meyer, F., Bagchi, S., Chaterji, S., Gerlach, W., Grama, A., Harrison, T., et al. (2017). MG-RAST version 4 — lessons learned from a decade of low-budget ultra-high-throughput metagenome analysis. *Brief. Bioinform.* doi: 10.1093/bib/bbx105. [Epub ahead of print].

Meyer, F., Paarmann, D., D'Souza, M. D., Olson, R., Glass, E. M., Kubal, M., et al. (2008). The metagenomics RAST server – a public resource for the automatic phylogenetic and functional analysis of metagenomes. *BMC Bioinformatics* 9:386. doi: 10.1186/1471-2105-9-386

Nakao, R., Abe, T., Nijhof, A. M., Yamamoto, S., Jongejan, F., Ikemura, T., et al. (2013). A novel approach, based on BLSOMs (Batch Learning Self-Organizing Maps), to the microbiome analysis of ticks. *ISME J.* 7, 1003–1015. doi: 10.1038/ismej.2012.171

O'Leary, N. A., Wright, M. W., Brister, J. R., Ciufo, S., Haddad, D., Mcveigh, R., et al. (2016). Reference sequence (RefSeq) database at NCBI : current status, taxonomic expansion, and functional annotation. *Nucleic Acids Res.* 44, 733–745. doi: 10.1093/nar/gkv1189

Parks, D. H., and Beiko, R. G. (2010). Identifying biologically relevant differences between metagenomic communities. *Bioinformatics* 26, 715–721. doi: 10.1093/bioinformatics/btq041

Pasolli, E., Asnicar, F., Manara, S., Zolfo, M., Karcher, N., Armanini, F., et al. (2019). Extensive unexplored human microbiome diversity resource extensive unexplored human microbiome diversity revealed by over 150 000 genomes from metagenomes spanning age, geography, and lifestyle. *Cell* 176, 649–662. doi: 10.1016/j.cell.2019.01.001

Randle-boggis, R. J., Helgason, T., Sapp, M., and Ashton, P. D. (2016). Evaluating techniques for metagenome annotation using simulated sequence data. *FEMS Microbiol. Ecol.* 92, 1–15. doi: 10.1093/femsec/fiw095

Sayers, E. W., Barrett, T., Benson, D. A., Bryant, S. H., Canese, K., Chetvernin, V., et al. (2009). Database resources of the National Center for Biotechnology Information. *Nucleic Acids Res.* 37, D5–D15. doi: 10.1093/nar/gkp382

Smith, T. A., Driscoll, T., Gillespie, J. J., and Raghavan, R. (2015). A Coxiella-like endosymbiont is a potential vitamin source for the lone star tick. *Genome Biol. Evol.* 7, 831–838. doi: 10.1093/gbe/evv016

Sonenshine, D. E., and Mather, T. N. (1994). *Ecological Dynamics of Tick-Borne Zoonoses*. Oxford: Oxford University Press.

Tang, W. H. W., Li, D. Y., and Hazen, S. L. (2018). Dietary metabolism, the gut microbiome, and heart failure. *Nat. Rev. Cardiol.* 16, 137–154. doi: 10.1038/s41569-018-0108-7

Tatusov, R. L., Galperin, M. Y., Natale, D. A., and Koonin, E. V. (2000). The COG database : a tool for genome-scale analysis of protein functions and evolution. *Nucleic Acids Res.* 28, 33–36. doi: 10.1093/nar/28.1.33

Wilke, A., Gerlach, W., Harrison, T., Paczian, T., Trimble, W. L., and Meyer, F. (2017). *MG-RAST Manual for Version 4*, *Revision* 3. Available online at: ftp://ftp.metagenomics.anl.gov/data/manual/mg-rast-manual.pdf

Wilke, A., Harrison, T., Wilkening, J., Field, D., Glass, E. M., Kyrpides, N., et al. (2012). The M5nr: a novel non-redundant database containing protein sequences and annotations from multiple sources and associated tools. *BMC Bioinformatics* 13:141. doi: 10.1186/1471-2105-13-141

Yu, G., Smith, D. K., Zhu, H., Guan, Y., and Lam, T. T.-Y. (2017). ggtree: an r package for visualization and annotation of phylogenetic trees with their covariates and other associated data. *Methods Ecol. Evol.* 8, 28–36. doi: 10.1111/2041-210X.12628

Zeng, Q., Wu, S., Sukumaran, J., and Rodrigo, A. (2017). Models of microbiome evolution incorporating host and microbial selection. *Microbiome* 5:127. doi: 10.1186/s40168-017-0343-x

Zou, Y., Xue, W., Luo, G., Deng, Z., Qin, P., Guo, R., et al. (2019). 1,520 reference genomes from cultivated human gut bacteria enable functional microbiome analyses. *Nat. Biotechnol.* 37, 179–185. doi: 10.1038/s41587-018-0008-8

Conflict of Interest Statement: The authors declare that the research was conducted in the absence of any commercial or financial relationships that could be construed as a potential conflict of interest.

frontiers in Cellular and Infection Microbiology

ORIGINAL RESEARCH
published: 19 December 2019
doi: 10.3389/fcimb.2019.00431

Competition Between Strains of *Borrelia afzelii* in Immature *Ixodes ricinus* Ticks Is Not Affected by Season

Dolores Genné[1]*, *Anouk Sarr*[1], *Olivier Rais*[2] and *Maarten J. Voordouw*[1,3]

[1] Laboratory of Ecology and Evolution of Parasites, Institute of Biology, University of Neuchâtel, Neuchâtel, Switzerland,
[2] Laboratory of Ecology and Epidemiology of Parasites, Institute of Biology, University of Neuchâtel, Neuchâtel, Switzerland,
[3] Department of Veterinary Microbiology, Western College of Veterinary Medicine, University of Saskatchewan, Saskatoon, SK, Canada

Vector-borne pathogens often consist of genetically distinct strains that can establish co-infections in the vertebrate host and the arthropod vector. Co-infections (or mixed infections) can result in competitive interactions between strains with important consequences for strain abundance and transmission. Here we used the spirochete bacterium, *Borrelia afzelii*, as a model system to investigate the interactions between strains inside its tick vector, *Ixodes ricinus*. Larvae were fed on mice infected with either one or two strains of *B. afzelii*. Engorged larvae were allowed to molt into nymphs that were subsequently exposed to three seasonal treatments (artificial summer, artificial winter, and natural winter), which differed in temperature and light conditions. We used strain-specific qPCRs to quantify the presence and abundance of each strain in the immature ticks. Co-infection in the mice reduced host-to-tick transmission to larval ticks and this effect was maintained in the resultant nymphs at 1 and 4 months after the larva-to-nymph molt. Competition between strains in co-infected ticks reduced the abundance of both strains. This inter-strain competition occurred in the three life stages that we investigated: engorged larvae, recently molted nymphs, and overwintered nymphs. The abundance of *B. afzelii* in the nymphs declined by 40.5% over a period of 3 months, but this phenomenon was not influenced by the seasonal treatment. Future studies should investigate whether inter-strain competition in the tick influences the subsequent strain-specific transmission success from the tick to the vertebrate host.

Keywords: *Borrelia afzelii*, co-infection, inter-strain competition, *Ixodes ricinus*, transmission, vector-borne pathogen, Lyme disease

OPEN ACCESS

Edited by:
Ryan Oliver Marino Rego, Institute of Parasitology (ASCR), Czechia

Reviewed by:
Andrei Daniel Mihalca, University of Agricultural Sciences and Veterinary Medicine of Cluj-Napoca, Romania
Yi-Pin Lin, Wadsworth Center, United States

***Correspondence:**
Dolores Genné
dolores.genne@unine.ch

Specialty section:
This article was submitted to Parasite and Host, a section of the journal Frontiers in Cellular and Infection Microbiology

Received: *01 October 2019*
Accepted: *04 December 2019*
Published: *19 December 2019*

Citation:
Genné D, Sarr A, Rais O and Voordouw MJ (2019) Competition Between Strains of Borrelia afzelii in Immature Ixodes ricinus Ticks Is Not Affected by Season. Front. Cell. Infect. Microbiol. 9:431. doi: 10.3389/fcimb.2019.00431

INTRODUCTION

Many infections consist of multiple strains or genotypes of the same pathogen, which are called co-infections (Read and Taylor, 2001; Balmer and Tanner, 2011; Alizon et al., 2013). Co-infections (also referred to as mixed infections or multiple-strain infections) will result in positive or negative interactions between co-infecting strains that result in facilitation (Taylor et al., 1997; de Roode et al., 2004; Abkallo et al., 2015) or competition (Bruce et al., 2000; de Roode et al., 2005a,b; Bell et al., 2006; Harrison et al., 2006; Mideo, 2009; Pollitt et al., 2011; Khan et al., 2019), respectively.

In facilitation (positive interaction), the performance (e.g., transmission, fitness, abundance) of a particular strain in a mixed infection is enhanced compared to when this strain infects the host by itself. In competition (negative interaction), the performance of a particular strain in a mixed infection is reduced compared to the single-strain infection. Multiple-strain infections are important because interactions between strains in their host shape the optimal life history strategies of pathogen transmission and virulence, which is the level of harm that the pathogen causes in its host (Mideo, 2009; Alizon et al., 2013).

In the case of vector-borne pathogens, mixed infections can occur in both the vertebrate host and the arthropod vector. Numerous studies have investigated interactions between pathogen strains in the vertebrate host (Bruce et al., 2000; de Roode et al., 2005a; Bell et al., 2006; Harrison et al., 2006; Pollitt et al., 2011; Reif et al., 2014). In contrast, studies on inter-strain interactions in the arthropod vector are rare (Reif et al., 2014; Pollitt et al., 2015; Genné et al., 2018), but these studies have shown that these interactions exist and that they influence the performance of the pathogen strains inside the arthropod vector. The population dynamics of vector-borne pathogens inside their arthropod vectors are also highly dependent on abiotic factors, such as temperature (Sternberg and Thomas, 2014). For example, warmer temperatures reduce the vectorial capacity of malaria mosquitoes (Paaijmans et al., 2011) and high temperatures can clear the Lyme disease pathogen from ticks so that they are no longer infectious to mice (Shih et al., 1995). Taken together, these observations suggest that temperature (and other abiotic variables) could influence the outcome of the interactions between strains in mixed infections in the arthropod vector, but to date there are no studies on this subject.

In the present study, we used the tick-borne spirochete, *Borrelia afzelii*, to test whether season (temperature and light) influences the competition between strains in mixed infections inside its long-lived tick vector. *B. afzelii* is the most common cause of Lyme borreliosis in Europe and is transmitted among small mammal reservoir hosts by the hard tick *Ixodes ricinus* (van Duijvendijk et al., 2015). Larvae acquire *B. afzelii* when they feed on an infected host [there is no transovarial transmission (Richter et al., 2012; Rollend et al., 2013)] and the engorged larvae molt into flat (unfed) nymphs by early fall. These flat nymphs overwinter in the soil (Dusbabek et al., 1971; Daniel et al., 1972) and enter a diapause phase (Belozerov, 1982; Dautel et al., 2008; Gray et al., 2016). The nymphs become active the following spring and search for new hosts (Belozerov, 2009; Gray et al., 2016). From a life history perspective, the nymphs are the most important stage for tick-to-host transmission because they feed on competent reservoir hosts and because their density is an order of magnitude greater than adult ticks (Kurtenbach et al., 2006; Tsao, 2009).

In areas where Lyme borreliosis is endemic, mixed infections in the nymph are common (Qiu et al., 2002; Pérez et al., 2011; Durand et al., 2015, 2017). A recent experimental infection study found that strains of *B. afzelii* experience competition inside *I. ricinus* nymphs (Genné et al., 2018). The population size of *B. afzelii* inside the unfed nymph decreases over time suggesting that competition between strains could intensify with increasing nymphal age (Jacquet et al., 2017; Pospisilova et al., 2019). There is indirect evidence that spirochete load in the nymph is an important phenotype for nymph-to-host transmission: *B. afzelii* strains with higher population sizes in nymphs are more common in the field (Durand et al., 2017). In summary, Lyme disease is an interesting system for studying whether inter-strain competition changes over the life cycle of a long-lived arthropod vector and whether this competition is influenced by abiotic factors like temperature.

We recently used an experimental infection approach to show that strains of *B. afzelii* experience competition inside *I. ricinus* nymphs that were 1 month old (Genné et al., 2018). As part of that study, we also collected engorged larvae, and we allowed a subset of nymphs to age under different seasonal treatments (i.e., different temperature and light conditions that represented summer vs. winter), but these ticks were not analyzed until now. The aim of the present study was to investigate whether competition between strains of *B. afzelii* occurs at different stages of the life cycle of immature *I. ricinus* ticks, and whether this competition is influenced by seasonal treatment. We made three predictions with respect to the interactions between interstrain competition, life cycle stage, and seasonal treatment. First, competition between strains would occur at each of the three life cycle stages: engorged larvae, 1-month-old nymphs, and 4-month-old nymphs. Second, the nymphal spirochete load would decrease with nymphal age and that competition between strains would be more intense in the older nymphs. Third, the nymphal spirochete load would decrease quickly under summer conditions but remain static under winter conditions.

MATERIALS AND METHODS

General

In a previous study, we investigated competition between two strains of *B. afzelii* (Fin-Jyv-A3 and NE4049) in the rodent host *Mus musculus* and in the tick vector *I. ricinus* (Genné et al., 2018). We tested the effects of interstrain competition on two phenotypes of *B. afzelii*: strain-specific host-to-tick transmission and strain-specific spirochete load in ticks. Both of these phenotypes were measured in 1-month-old nymphs ($n = 301$) that had fed as larvae on experimentally infected mice, and that had been killed 1 month after the larva-to-nymph molt. What is new in the present study is that we investigated competition in the engorged larvae immediately following drop-off ($n = 142$), and in 4-month-old nymphs that were allowed to age under different seasonal treatments ($n = 357$). These two additional tick age classes allowed us to investigate competition between strains of *B. afzelii* at three different time points of the tick life cycle.

Strains of *B. afzelii* and Mice

Borrelia afzelii strains NE4049 and Fin-Jyv-A3 were chosen for this study because both strains are highly infectious to rodent hosts (Genné et al., 2018). Strains NE4049 and Fin-Jyv-A3 were obtained from an *I. ricinus* nymph in Neuchatel, Switzerland and from a bank vole (*Myodes glareolus*) in Jyväskylä, Finland, respectively. Both strains were passaged fewer than five times

to avoid the loss of the plasmids that carry the virulence genes that are critical for infection (Tonetti et al., 2015; Cayol et al., 2018). These strains have strain ID numbers 1961 and 1887 in the *Borrelia* multi-locus sequence type (MLST) database. Strain NE4049 has MLST 679 and *ospC* allele A10 and strain Fin-Jyv-A3 has MSLT 676 and *ospC* allele A3. The two *ospC* alleles used in this study (A3 and A10) have a genetic distance of 23.19% and an amino acid distance of 62.57%. The concatenated sequences of these two MLSTs differ at 9 base pairs over 4,785 bp (i.e., they are 99.81% similar).

The details of this experimental infection study were described in Genné et al. (2018) and are shown in **Figure 1**. Briefly, we performed two independent experiments to test whether the presence of a competitor strain influenced the performance of the focal strain. In experiments 1 and 2, the focal strain was Fin-Jyv-A3 and NE4049, respectively. Each experiment contained two infection treatments: single infection with the focal strain and co-infection with both strains. Thus, 40 female *Mus musculus* BALB/c mice aged 5 weeks were randomly assigned to four different experimental infection groups ($n = 10$

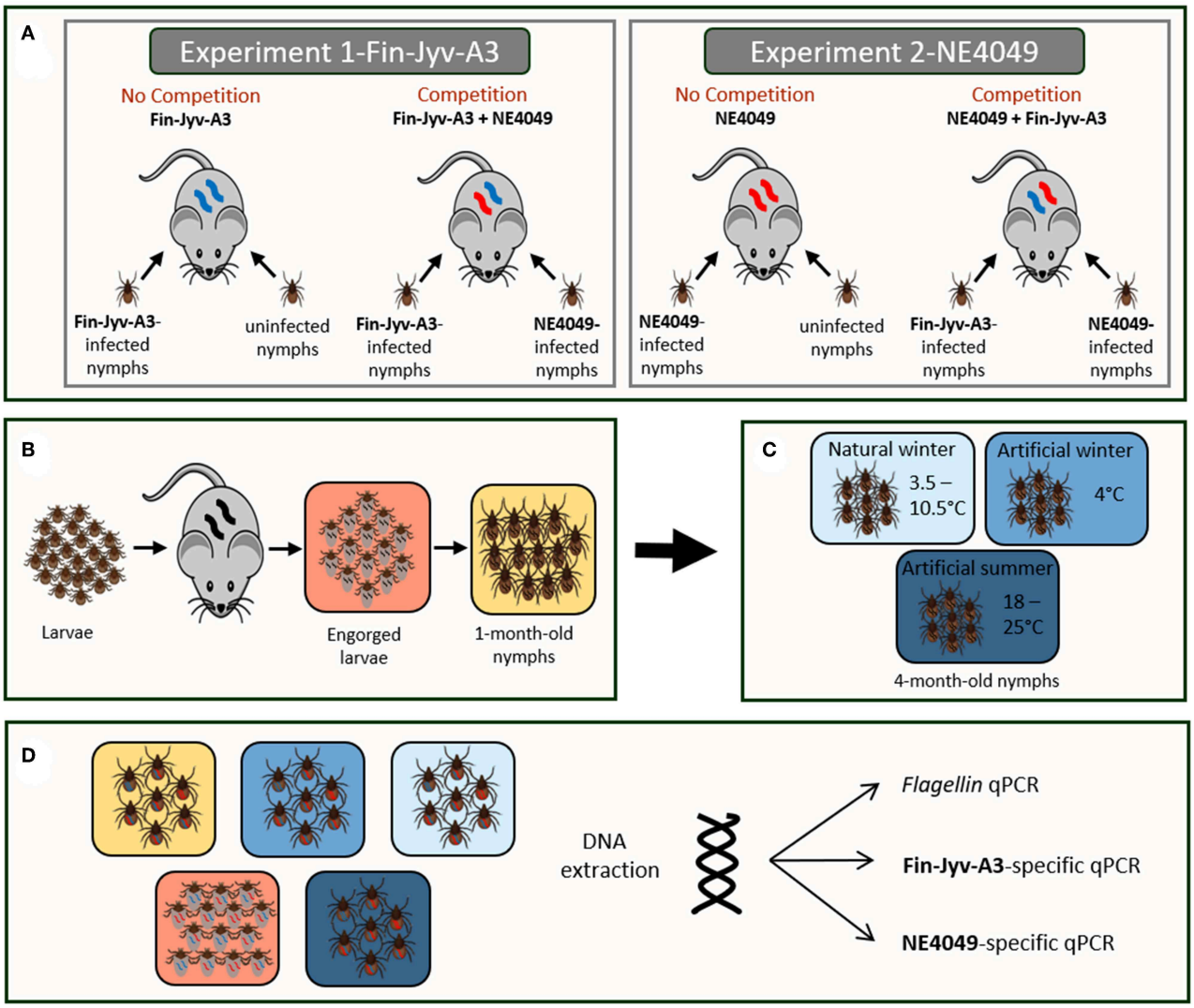

FIGURE 1 | (A) The study was divided into two competition experiments that differed in the focal strain. In experiments 1 and 2, the focal strain was Fin-Jyv-A3 and NE4049, respectively. Each experiment was divided into two groups: no competition (infection with the focal strain only) and competition (infection with both strains). The sample size of each group was 10 mice. In the no competition treatment, each mouse was infected with 5 nymphs infected with the focal strain and 5 uninfected nymphs. In the competition treatment, each mouse was infected with 5 nymphs infected with strain Fin-Jyv-A3 and 5 nymphs infected with strain NE4049. **(B)** At 34 days post-infection, the mice were infested with ∼100 larvae. Engorged larvae were allowed to molt into nymphs under laboratory conditions. **(C)** One month after the larva-to-nymph molt, the 1-month-old nymphs were exposed for 3 months to one of the three seasonal treatments: natural winter, artificial winter, and artificial summer. **(D)** Ticks were sacrificed at three different ages: engorged larvae, 1-month-old nymphs, and 4-month old nymphs. Only the 4-month old nymphs had been exposed to three different seasonal treatments (natural winter, artificial winter, and artificial summer). DNA was extracted from all ticks and the total number of spirochetes in each tick was estimated using *flagellin* qPCR. For the co-infected ticks, the abundance of strain Fin-Jyv-A3 and strain NE4049 was estimated using a strain-specific qPCR that targeted the *ospC* A3 allele and the *ospC* A10 allele, respectively.

per group): Fin-Jyv-A3 (Single infection), Fin-Jyv-A3 + NE4049 (Co-infection), NE4049 (Single infection), and NE4049 + Fin-Jyv-A3 (Co-infection). Mice were infected with the appropriate strains of *B. afzelii* via the bite of experimentally infected *I. ricinus* nymphs.

Mice in the co-infection treatment (**Figure 1A**), were infested with 5 nymphs putatively infected with strain Fin-Jyv-A3 and 5 nymphs putatively infected with strain NE4049 (total of 10 nymphs). Mice in the single strain infection treatments were infested with 5 nymphs putatively infected with the focal strain and 5 uninfected nymphs (total of 10 nymphs). Prior to the nymphal infestation, we determined the prevalence of infection by testing a random sample of Fin-Jyv-A3 nymphs ($n = 10$) and NE4049 nymphs ($n = 14$) using the *flagellin* qPCR. The prevalence of infection was 70.0% (7/10) for the Fin-Jyv-A3 nymphs and 71.4% (10/14) for the NE4049 nymphs. Thus, the expected number of infected nymphs to which the mice were exposed was 3.50 for strain Fin-Jyv-A3 and 3.57 for strain NE4049. The mean spirochete load in the subset of infected nymphs was ∼380 for the Fin-Jyv-A3 nymphs and ∼198 for the NE4049 nymphs. Assuming that the number of spirochetes inoculated by a nymph into a mouse is linearly related to the product of the number of infected nymphs and the mean spirochete load per infected nymph, we calculate that the infectious dose for strain Fin-Jyv-A3 (3.57 infected nymphs*380 spirochetes/nymph = 1,356) was almost two times larger than the infectious dose for strain NE4049 (3.50 infected nymphs*198 spirochetes/nymph = 694 spirochetes).

Age Classes of the Ticks

At 34 days post-infection, each infected mouse was infested with ∼100 pathogen-free *I. ricinus* larvae (**Figure 1B**). Following drop-off, ∼50 engorged larvae were collected from each mouse and stored in individual Eppendorf tubes to facilitate random sampling. Each Eppendorf tube contained a piece of moistened paper towel to maintain high humidity. The engorged larvae were randomly assigned to be sacrificed at one of three ages: engorged larvae, 1-month-old nymphs, and 4-month-old nymphs. Immediately following drop-off, up to 6 engorged larvae per mouse were frozen at −20°C for the engorged larva age class. The remaining engorged larvae were allowed to molt into nymphs under standard laboratory conditions. At 1 month after the larva-to-nymph molt (22 January 2016), up to 10 nymphs per mouse were frozen at −20°C for the 1-month-old nymph age class. The remaining nymphs were randomly assigned to three different seasonal treatments (see below). At 4 months after the larva-to-nymph molt (16 April 2016), up to 15 nymphs per mouse were frozen at −20°C for the 4-month-old nymph age class. The tick age classes, mouse sample sizes, and tick sample sizes are shown in **Table 1**.

Seasonal Treatment of the 4-Month-Old Nymphs

When the 4-month-old nymphs were 1 month old, they were randomly assigned to one of three seasonal treatments: artificial summer, artificial winter, and natural winter (**Figure 1C**), hereafter referred to as phytotron, fridge, and underground, respectively. These three treatments were chosen to simulate summer conditions (warm temperature and long photoperiod) and winter conditions (cold temperature and no light) that are experienced by *I. ricinus* ticks in the natural environment. We chose to have no light in both winter treatments to simulate the natural situation. *Ixodes* ticks encounter very little light during the winter because they hide in the soil and under the leaf litter to protect themselves from cold temperatures (Dusbabek et al., 1971; Daniel et al., 1972; Gray et al., 2016). The nymphs spent a total of 3 months in these three seasonal treatments (22 January 2016–15 April 2016).

In the artificial summer treatment, the nymphs were kept in a phytotron [4–5 h: 1 lumen (lm), 21.5°C; 5–19 h: 2 lm, 25°C; 19–20 h: 1 lm, 21.5°C; 20–4 h; 0 lm, 18°C] with a relative humidity of 85%. In the artificial winter treatment, the nymphs were kept in a fridge at a temperature of 4°C and with no light. For the natural winter treatment, the nymphs were kept in a plastic box (30 cm × 23 cm × 10 cm) that was buried in the soil at a depth of 10 cm in a forest in the botanical garden of Neuchâtel. The box contained three button logs that measured the temperature every 30 min. The mean daily average temperature in the natural winter treatment was 6.44°C (range = 3.72–10.50°C; for details see Section 1 in the **Supplementary Material**). In each of the three seasonal treatments, the nymphs were kept in their individual Eppendorf tubes.

Four months after the larva-to-nymph molt (15 April 2016), the 4-month-old nymphs were checked to determine whether they were alive or dead. The survival was very high, only 4 of the 444 nymphs had died (3, 0, and 1 in the artificial summer, artificial winter, and natural winter, respectively). The next day (16 April 2016), all live 4-month-old nymphs were frozen at −20°C. The seasonal treatments, mouse sample sizes, and tick sample sizes are shown in **Table 1**.

TABLE 1 | Sample sizes are shown for immature *I. ricinus* ticks that were collected in our previous study (1-month-old nymphs) and the present study (larvae and 4-month-old nymphs).

Stage	Age	Seasonal treatment	Infected mice	Ticks per mouse	Total ticks
Larva	2 days	NA	33	5–6	142
Nymph	1 month	NA	33	10	301
Nymph	4 months	Combined	26	15	357
Nymph	4 months	Phytotron	26	5	119
Nymph	4 months	Fridge	26	5	120
Nymph	4 months	Underground	26	5	118

Ticks that had fed as larvae on mice infected with one or two strains of B. afzelii were sacrificed at three different ages: 2 days after drop-off, 1 month after the larva-to-nymph molt, and 4 months after the larva-to-nymph molt, which corresponds to two different stages: larva and nymph. The 4-month-old nymphs had been exposed to three different seasonal treatments: artificial summer (phytotron), artificial winter (fridge), and natural winter (underground). For each tick stage, tick age, and seasonal treatment, the number of infected mice, the number of ticks per mouse, and the total number of ticks are shown.

DNA Extraction

The engorged larvae, 1-month-old nymphs, and 4-month-old nymphs were crushed in a TissueLyser II (**Figure 1D**) using

a previously described protocol (Jacquet et al., 2015; Genné et al., 2018). The crushed ticks were digested with proteinase K at 56°C overnight. Tick DNA was extracted using QIAGEN DNeasy 96 Blood and Tissue kit well-plates and following the QIAGEN protocol. Each plate contained two *Anopheles gambiae* mosquitoes as negative *B. afzelii* DNA extraction controls. For each sample, the DNA was eluted into 65 μl of water.

General and Strain-Specific qPCR Assays

The *B. afzelii* infection status of the ticks was assessed with a qPCR assay that targets a 132-bp fragment of the *flagellin* gene (**Figure 1D**), as described previously (Genné et al., 2018). The identities of the strains in the nymphs were determined using two strain-specific qPCRs (**Figure 1D**). These qPCR assays amplify the same 143-bp fragment of the *ospC* gene but use different probes that are specific for *ospC* alleles A3 and A10, as described previously (Genné et al., 2018). For each qPCR reaction, 3 μl of DNA template was used. The qPCRs were done using a LightCycler® 96 Multiwell Plate white (Roche). All the plates contained 80 tick DNA samples, 2 negative *B. afzelii* DNA extraction controls (mosquitoes), 2 negative controls for the qPCR (PCR-grade water), and 12 positive controls. For each of the three different qPCR assays (*flagellin*, *ospC* A3, and *ospC* A10), a sample of 81 ticks was tested twice to determine the repeatability of the assay (Genné et al., 2018). For the *flagellin, ospC* A3, and *ospC* A10 qPCR, the repeatability of the log10-transformed spirochete loads was 98.3%, 97.8%, and 97.0%, respectively (Genné et al., 2018).

Statistical Analyses

B. afzelii Infection Status of Immature *I. ricinus* Ticks

The *flagellin* qPCR and the *ospC* qPCRs were used to determine the *B. afzelii* infection status of the ticks. Samples were excluded from the analysis whenever the *ospC* qPCR and the *flagellin* qPCR differed with respect to the infection status of the tick. Generalized linear mixed effects models (GLMMs) with binomial errors were used to analyse the infection status of the ticks (0 = uninfected, 1 = infected). The fixed factor that combined tick age class and seasonal treatment had 5 levels: engorged larvae, 1-month-old nymphs, phytotron 4-month-old nymphs, fridge 4-month-old nymphs, and underground 4-month-old nymphs. These levels were combined to create new factors with fewer levels: tick age (3 levels: larvae, 1-month-old nymphs, and 4-month-old nymphs), and tick stage (2 levels: larvae and nymphs). Mouse ID was modeled as a random factor. To determine the statistical significance of the fixed factors, models that differed with respect to the fixed factor of interest were compared using log-likelihood ratio (LLR) tests. Similarly, comparing a model that includes the 5 levels of tick age class and seasonal treatment with a model that contains 3 levels of tick age, tests whether the seasonal treatment had a significant effect on the phenotype of the 4-month-old nymphs.

B. afzelii Spirochete in Immature *I. ricinus* Ticks

The total spirochete abundance inside the ticks (hereafter referred to as total spirochete load) was analyzed for the subset of ticks infected with *B. afzelii*. The total estimate of the spirochete load inside each tick was estimated by correcting the spirochete load in 3 μl of DNA template to the total DNA extraction elution volume (i.e., multiplied by a factor of 21.67 = 65 μl/3 μl). The *flagellin* qPCR was used to estimate the total spirochete load in the ticks. In co-infected ticks, the strain-specific spirochete loads estimated by the *ospC* qPCRs were constrained to sum to the total spirochete load estimated by the *flagellin* qPCR (Genné et al., 2018). Linear mixed effects models (LMMs) were used to analyse the spirochete loads, which were $\log_{10}$-transformed to normalize the residuals. The fixed factors were the same as for the GLMM of infection status. Mouse ID was modeled as a random factor.

Competition Between Strains Over the Life Cycle of the Immature Tick

GLMMs with binomial errors and LMMs with normal errors were used to analyse the strain-specific prevalence and the strain-specific spirochete load, respectively. The fixed factor that combined tick age class and seasonal treatment (5 levels: engorged larvae, 1-month-old nymphs, phytotron 4-month-old nymphs, fridge 4-month-old nymphs, and underground 4-month-old nymphs), the strain (2 levels: Fin-Jyv-A3, NE4049), competition (2 levels: no, yes), and their interactions were fixed factors. Mouse identity was included as a random factor. As before, we tested whether the 5-level factor of tick age class and seasonal treatment could be reduced to tick age (3 levels: larvae, 1-month-old nymphs, and 4-month-old nymphs), or tick stage (2 levels: larvae and nymphs). To determine the statistical significance of the fixed factors, models that differed with respect to the fixed factor of interest were compared using LLR tests. The results from this stepwise model simplification approach were compared with a model selection approach based on the Akaike information criterion (AIC).

Statistical Software

The statistical analyses were done in R v. 1.1.463 and using the following R packages: base, lme4, emmeans, and MuMIn. The "lmer" and "glmer" functions (lme4 package) were used to create the GLMMs and LMMs. The "anova" function (base package) was used to perform the log-likelihood ratio tests. The "model.sel" function (MuMIn package) was used to perform the AIC-based model selection. The "emmeans," "contrast," and "pairs" functions (emmeans package) were used for the *post-hoc* analyses of the GLMMs and LMMs (details of the *post-hoc* tests are shown in Section 8 of the **Supplementary Material**).

RESULTS

Mice

Of the 40 mice used in this study, 2 mice died (S5 and S12), 1 mouse did not become infected (S37), and 4 mice in the co-infected treatments acquired only one strain (S17, S20, S25, S29). Ticks produced by these 7 mice were excluded from the study. For the engorged larvae and the 1-month-old nymphs, the final sample size was 33 infected mice that were distributed across the four infection treatments as follows: Fin-Jyv-A3 ($n = 9$), Fin-Jyv-A3 + NE4049 ($n = 7$), NE4049 ($n = 9$), and NE4049 + Fin-Jyv-A3 ($n = 8$). For the 4-month-old nymphs, the final sample size

was 26 infected mice because some mice did not produce enough ticks to be included in this tick age group (**Table 1**).

Ticks

Of the 849 ticks in this study, 49 were excluded because the *flagellin* qPCR and the *ospC* qPCR disagreed with respect to tick infection status. Specifically, this criterion excluded 13.9% (23/165) of the larvae, 5.3% (17/318) of the 1-month-old nymphs, and 2.5% (9/366) of the 4-month-old nymphs. The final sample sizes for each of the five groups were as follows: engorged larvae ($n = 142$), 1-month-old nymphs ($n = 301$), 4-month-old phytotron nymphs ($n = 119$), 4-month-old fridge nymphs ($n = 120$), and 4-month-old underground nymphs ($n = 118$).

Prevalence of *B. afzelii* in Immature Ticks

The infection prevalence is defined as the percentage of ticks that tested positive for *B. afzelii* (ignoring strain identity). The infection prevalence for the different tick ages (**Table 2**) was as follows: larvae (37.3% = 53/142), 1-month-old-nymphs (87.7% = 264/301), and 4-month-old nymphs (82.6% = 295/357). After combining all the nymphs, the prevalence of *B. afzelii* infection in the nymphs (85.0% = 559/658) was 2.3 times higher compared to the larvae (37.3% = 53/142). The statistical analysis of these infection prevalences is presented in the next section.

Effect of Tick Age and Tick Seasonal Treatment on the Prevalence of *B. afzelii* Infection

We analyzed the prevalence of *B. afzelii* infection in the immature *I. ricinus* ticks (ignoring strain identity) as a function of tick age and seasonal treatment. The seasonal treatment had no effect on the infection prevalence and we therefore combined all the 4-month-old nymphs into a single group (see Section 2 in the **Supplementary Material**).

TABLE 2 | The prevalence of *B. afzelii* infection in *I. ricinus* ticks and the *B. afzelii* spirochete loads in the subset of infected *I. ricinus* ticks are shown separately for the seasonal treatment, tick age, and tick stage.

Factor	Level	Inf/Total	Prev (%)	Mean	95% CI
Treatment	Larva	53/142	37.3%	429	286–644
Treatment	1-month-old nymph	264/301	82.6%	5,055	4,215–6,063
Treatment	4-month-old phytotron nymph	95/119	79.8%	2,651	1,959–3,589
Treatment	4-month-old fridge nymph	98/120	81.7%	2,928	2,173–3,945
Treatment	4-month-old underground nymph	102/118	86.4%	3,477	2,596–4,657
Tick age	Larva	53/142	37.3%	429	286–644
Tick age	1-month-old nymph	264/301	87.7%	5,055	4,216–6,062
Tick age	4-month-old nymph	295/357	82.6%	3,009	2,534–3,574
Tick stage	Larva	53/142	37.3%	429	285–647
Tick stage	Nymph	559/658	85.0%	3,845	3,388–4,363

The spirochete load is the total number of spirochetes in the tick and is based on the flagellin qPCR. Shown are the geometric mean of the spirochete loads and the 95% confidence intervals (95% CI).

There was a significant effect of age on infection prevalence (LLR test of age vs. null: Δ df = 2, Δ dev = 146.16 $p < 0.0001$). The infection prevalence in the larvae was significantly lower compared to the 1-month-old nymphs (emmeans: $p < 0.0001$) and compared to the 4-month-old nymphs (emmeans: $p < 0.0001$). The infection prevalence was not significantly different between the 1-month-old nymphs and the 4-month-old nymphs (emmeans: $p = 0.249$).

Spirochete Load of *B. afzelii* in Immature Ticks

The spirochete load is defined as the total number of spirochetes in an infected tick (ignoring strain identity). The geometric mean spirochete loads were calculated for the subset of infected ticks (**Table 2**) and were as follows: larvae ($n = 53$; mean = 429; range = 28–269,154), 1-month-old nymphs ($n = 264$; mean = 5,055; range = 34–218,776), and 4-month-old nymphs ($n = 295$; mean = 3,009; range = 36–275,423). The spirochete load in the 1-month-old nymphs was 11.8 times higher compared to the larvae and 1.7 times higher compared to the 4-month-old nymphs. Over the 3-month overwintering period, the nymphs lost spirochetes at a rate of 22.7 spirochetes per day. The statistical analysis of these spirochete loads is presented in the next section.

Effect of Tick Age and Tick Seasonal Treatment on the *B. afzelii* Spirochete Load

We analyzed the total *B. afzelii* spirochete load in the immature *I. ricinus* ticks (ignoring strain identity) as a function of tick age and seasonal treatment. The seasonal treatment had no effect on the nymphal spirochete load and we therefore combined all the 4-month-old nymphs into a single group (see Section 3 in the **Supplementary Material**).

There was a significant effect of tick age on the tick spirochete load (LLR test of age vs. null: Δ df = 2, Δ dev = 124.65, $p < 0.0001$; **Table 2**, **Figure 2**). The spirochete loads in the engorged larvae were significantly lower compared to the 1-month-old nymphs (emmeans: $p < 0.0001$) and compared to the 4-month-old nymphs (emmeans: $p < 0.0001$). The 1-month-old nymphs had a significantly higher spirochete load than the 4-month-old nymphs (emmeans: $p = 0.0002$). In summary, the spirochete load was lowest in the larvae, highest in the 1-month-old nymphs, and intermediate in the 4-month-old nymphs (**Table 2**, **Figure 2**).

Effect of Competition Between Strains on the Strain-Specific Transmission to Immature *I. ricinus* Ticks

Here the response variable is the strain-specific infection prevalence in the immature ticks, as estimated by the *ospC* qPCR. To be conservative, the competition factor (two levels: no, yes) was based on the co-infection status of the mice rather than the co-infection status of the ticks (see Section 4 in the **Supplementary Material**). Model comparison found justification for combining all of the nymphs into a single group (see Section 5 in the **Supplementary Material**). Thus, the strain-specific prevalence was analyzed as a function of three fixed factors: strain, competition, tick stage, and their interactions.

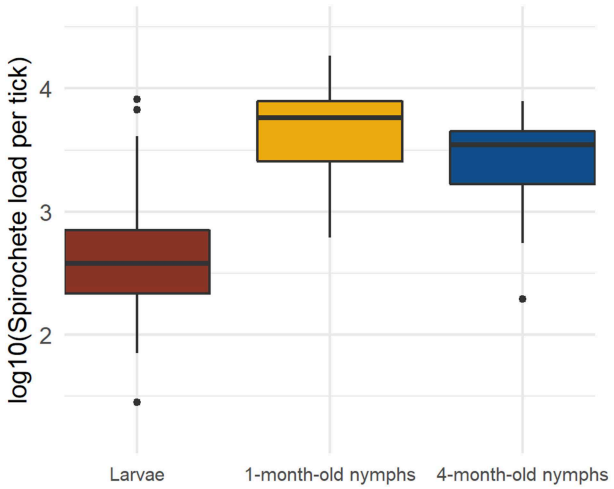

FIGURE 2 | The *B. afzelii* spirochete loads in immature *I. ricinus* ticks change with the age of the tick. The spirochete load is lowest in the engorged larvae, highest in 1-month-old nymphs, and intermediate in 4-month-old nymphs. Each data point represents the mean for ticks sampled from the same mouse. The total numbers of ticks for each of the three tick ages are as follows: engorged larvae ($n = 142$), 1-month-old nymphs ($n = 301$), and 4-month-old nymphs ($n = 357$). The boxplot shows the medians (black line), the 25th and 75th percentiles (edges of the box), the minimum and maximum values (whiskers), and the outliers (solid circles).

TABLE 3 | The strain-specific infection prevalences in the immature *I. ricinus* ticks are shown for each of the eight unique combinations of tick stage, *B. afzelii* strain, and competition.

Stage	Strain	Competition	% Infected
Larvae	Fin-Jyv-A3	No	20/44 (45.5%)
Larvae	Fin-Jyv-A3	Yes	4/27 (15.8%)
Larvae	NE4049	No	6/40 (15.0%)
Larvae	NE4049	Yes	11/31 (35.5%)
Nymphs	Fin-Jyv-A3	No	127/147 (86.4%)
Nymphs	Fin-Jyv-A3	Yes	79/157 (50.3%)
Nymphs	NE4049	No	152/194 (78.4%)
Nymphs	NE4049	Yes	109/160 (68.1%)

A classic step-wise model simplification approach using LLR tests found that the best model included strain, competition, tick stage, the competition: tick stage interaction, and the strain:competition interaction (see Section 5 in the **Supplementary Material**). The AIC-based model selection approach converged on the same model (see Section 7 in the **Supplementary Material**). The presence of two significant two-way interactions complicates the interpretation of the main effects and requires splitting the statistical analyses. We ran separate analyses for larvae and nymphs; this approach allowed us to independently test the effects of competition and strain for each tick stage.

In the larvae, the interaction between strain and competition was significant (GLME LLR: Δ df = 1, Δ dev = 8.228, $p = 0.004$), the effect of competition was therefore tested separately for each strain. For strain Fin-Jyv-A3, its prevalence was higher in larvae that fed on singly infected mice (45.5% = 20/44) compared to larvae that fed on co-infected (14.8% = 4/27) mice, and this difference was significant (GLME LLR: Δ df = 1, Δ dev = 5.173, $p = 0.023$). For strain NE4049, its prevalence was lower in larvae that fed on singly infected mice (15.0% = 6/40) compared to larvae that fed on co-infected mice (35.5% = 11/31), but this difference was not significant (GLME LLR: Δ df = 1, Δ dev = 3.16, $p = 0.075$). In summary, competition between strains significantly reduced transmission to engorged larval ticks for strain Fin-Jyv-A3 but not strain NE4049 (**Table 3**, **Figure 3**, **Figure S3**).

In the nymphs, the interaction between strain and competition was not significant (GLME LLR: Δ df = 1, Δ dev = 2.724, $p = 0.091$) and was removed from the model. Competition was significant (GLME LLR: Δ df = 1, Δ dev = 8.683, $p = 0.003$), but strain was not (GLME LLR: Δ df = 1, Δ dev = 0.024, $p = 0.877$). The prevalence of both strains was higher in nymphs that had fed as larvae on singly infected mice (81.8% = 279/341) compared to nymphs that had fed as larvae on co-infected mice (59.3% = 188/317; **Table 3**, **Figure 3**, **Figure S3**).

Effect of Competition Between Strains on the Strain-Specific Spirochete Load in Immature *I. ricinus* Ticks

Here the response variable is the strain-specific spirochete load in the immature ticks, as estimated by combining the *ospC* qPCR and the *flagellin* qPCR. Model comparison showed that we could combine all of the 4-month-old nymphs into a single group (see Section 6 in the **Supplementary Material**). Thus, the strain-specific spirochete load was analyzed as a function of three fixed factors: strain, competition, tick age and their interactions.

A classic stepwise model simplification approach using LLR tests found that none of the interactions were significant and that the best model contained the three fixed factors of strain, competition, and tick age (see Section 6 in the **Supplementary Material**). The AIC-based model selection approach converged on the same model (see Section 7 in the **Supplementary Material**).

The three fixed factors all had significant effects on the spirochete load: tick age (LLR test: Δ df = 2, Δ dev = 86.393, $p = < 0.001$), strain (LLR test: Δ df = 1, Δ dev = 3.948, $p = 0.047$), and competition (LLR test: Δ df = 1, Δ dev = 10.589, $p = 0.011$) (**Figure 4**, **Figure S4**). The spirochete load in the engorged larvae was significantly lower compared to the 1-month-old nymphs (emmeans: $p < 0.0001$) and the 4-month-old nymphs (emmeans: $p < 0.0001$) (**Table 3**, **Figure 4**, **Figure S4A**). The 1-month-old nymphs had a higher spirochete load than the 4-month-old nymphs (emmeans: $p < 0.0046$; **Table 3**, **Figure 4**, **Figure S4A**). According to our parameter estimates, strain Fin-Jyv-A3 always had a higher spirochete load in the tick than strain NE4049 (raw data in **Figure 4**, parameter estimates in **Figure S4B**, **Table S3**). Competition reduced the spirochete load of each strain and this effect was the same for engorged larvae,

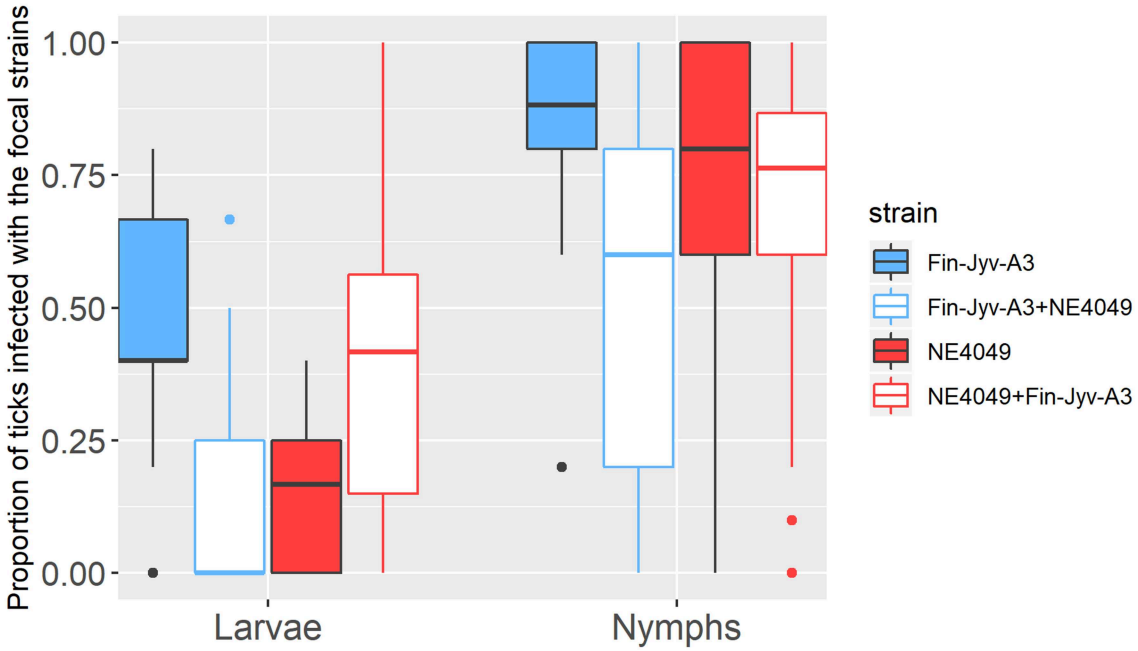

FIGURE 3 | The proportion of immature *I. ricinus* ticks infected with *B. afzelii* is shown as a function of three factors: (1) tick age (engorged larvae, 1-month-old nymphs, and 4-month-old nymphs), (2) strain (Fin-Jyv-A3 in blue and NE4049 in red), and (3) competition (competition absent in solid colors vs. competition present in white). The proportion of ticks infected with the focal strain is an estimate of strain-specific host-to-tick transmission. The graph shows the raw data and not all observable differences are statistically significant. According to the parameter estimates of our statistical analysis, competition between strains in co-infected mice reduced host-to-tick transmission of strain Fin-Jyv-A3 to engorged larvae and nymphs and reduced the host-to-tick transmission of strain NE4049 to nymphs. In contrast, competition between strains in co-infected mice did not influence the host-to-tick transmission of strain NE4049 to engorged larvae. Each data point represents the mean for a single mouse. The boxplots show the medians (black line), the 25th and 75th percentiles (edges of the box), the minimum and maximum values (whiskers), and the outliers (solid circles).

1-month-old nymphs, and 4-month-old nymphs (raw data in **Figure 4**, parameter estimates in **Figure S4C**). In all three of these tick ages, the spirochete load of each strain was reduced in ticks that had fed on co-infected mice compared to ticks that had fed on mice infected with single strains (raw data in **Figure 4**, **Table 4**, parameter estimates in **Figure S4A**, **Table S3**).

DISCUSSION

Competition in the Rodent Host Reduces Host-to-Tick Transmission

Our study found that co-infection in the rodent host reduced host-to-tick transmission success of both strains of *B. afzelii* to *I. ricinus* nymphs. This result is in agreement with other studies that have investigated how mixed strain infections of *B. burgdorferi* sl in the rodent host influence strain-specific transmission to *Ixodes* ticks (Derdáková et al., 2004; Rynkiewicz et al., 2017; Genné et al., 2018). Studies on other vector-borne pathogens have also shown that competition between strains in the vertebrate host reduces strain-specific transmission to the arthropod vector (de Roode et al., 2005b; Reif et al., 2014), suggesting that this result is a general phenomenon in these systems. To date, all *B. burgdorferi* sl studies on the relationship between co-infection and host-to-tick transmission have measured the latter phenotype in young nymphs (i.e., sacrificed shortly after the larva-to-nymph molt) that have not overwintered (Derdáková et al., 2004; Rynkiewicz et al., 2017; Genné et al., 2018). In nature, the majority of *Ixodes* nymphs overwinter and search for a host the following spring when they are much older (Gray, 1984, 1991; Gray et al., 2016). Hence, a new contribution of our study was to show that the effects of inter-strain competition in the rodent host persist in *I. ricinus* nymphs that were allowed to overwinter and age. We found that co-infection reduced the host-to-nymph transmission of both strains, which is different from previous studies (including ours) that found asymmetric competition (Rynkiewicz et al., 2017; Genné et al., 2018).

Interestingly, our study shows that reduced host-to-tick transmission can be detected in engorged larval ticks immediately following drop-off. This observation reinforces the idea that competition between strains in the tissues of the rodent host (Strandh and Råberg, 2015) reduces the probability that a given strain will colonize a feeding larval tick. The much lower infection prevalence in the engorged larvae compared to the nymphs is due to their much lower spirochete load, which the qPCR then fails to detect. However, an alternative explanation for the observation that the infection prevalence and spirochete load in engorged larvae are lower compared to the nymphs is that mouse blood interferes with the efficacy of the qPCR assays (Schrader et al., 2012; Buckwalter et al., 2014; Sidstedt et al.,

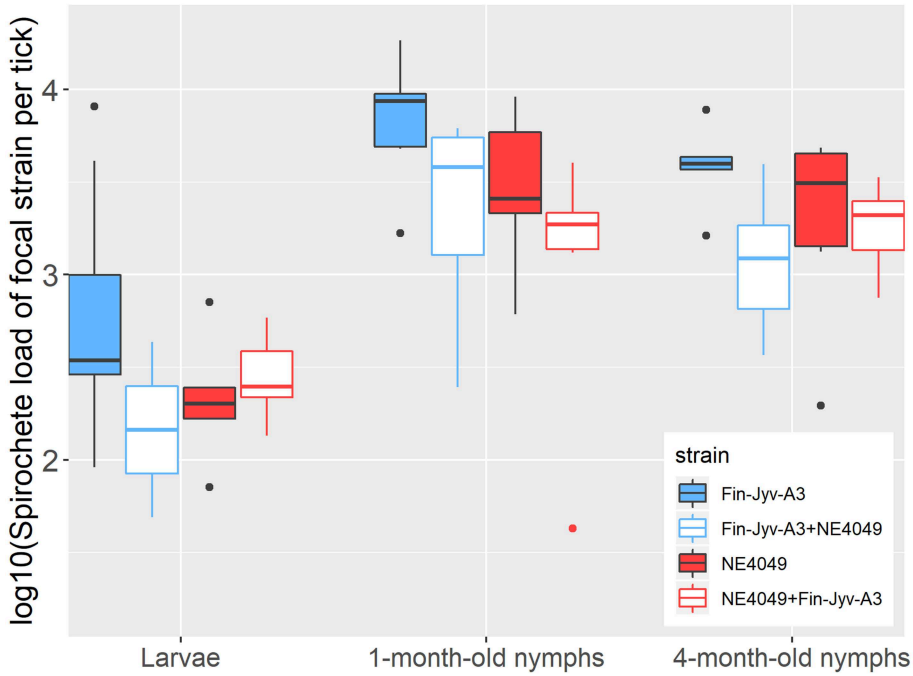

FIGURE 4 | The *B. afzelii* spirochete loads in immature *I. ricinus* ticks are shown as a function of three factors: (1) tick age (engorged larvae, 1-month-old nymphs, and 4-month-old nymphs), (2) strain (Fin-Jyv-A3 in blue and NE4049 in red), and (3) competition (competition absent in solid colors vs. competition present in white). The strain-specific spirochete loads were log10-transformed to normalize the residuals. The graph shows the raw data and not all observable differences are statistically significant. According to the parameter estimates of our statistical analysis, competition between strains reduced the spirochete loads of both strains in all three age classes of ticks. Our statistical analysis also found that strain Fin-Jyv-A3 had a higher spirochete load in immature *I. ricinus* ticks compared to strain NE4049. Each data point represents the mean for a single mouse. The boxplots show the medians (black line), the 25th and 75th percentiles (edges of the box), the minimum and maximum values (whiskers), and the outliers (solid circles).

2018). We consider this explanation unlikely because an early study that used immunofluorescence microscopy also showed that *Ixodes scapularis* larvae acquire a small inoculum of *B. burgdorferi* sensu stricto (ss) spirochetes, which subsequently expands during the period of larva-to-nymph development (Piesman et al., 1990). Similarly, a recent study on the population dynamics of *B. afzelii* in immature *I. ricinus* ticks showed that qPCR and immunofluorescence microscopy gave the same results (Pospisilova et al., 2019). In summary, there is a general consensus that *Ixodes* larvae acquire a small inoculum of *B. burgdorferi* sl spirochetes, which grows to a larger size in the tick midgut during the period of larva-to-nymph development (Piesman et al., 1990; Soares et al., 2006; Jacquet et al., 2017; Pospisilova et al., 2019).

Competition in the Arthropod Vector

To date, very few studies have investigated interactions between pathogen strains in the arthropod vector (Reif et al., 2014; Pollitt et al., 2015; Genné et al., 2018). Inter-strain facilitation has been shown for malaria parasites in Anopheline mosquitoes (Pollitt et al., 2015), whereas inter-strain competition has been shown for *Francisella novicida* in *Dermacentor andersoni* ticks (Reif et al., 2014), and for *Borrelia afzelii* in *Ixodes ricinus* ticks (Genné et al., 2018). Our study found that competition resulted in decreased spirochete loads for both strains and in all three tick age classes in this study: engorged larvae, 1-month-old nymphs, and 4-month-old nymphs. This result is in agreement with our previous study, which was restricted to the 1-month-old nymphs (Genné et al., 2018). The present study is an improvement on our previous

TABLE 4 | The strain-specific spirochete loads in the subset of infected *I. ricinus* ticks are shown for each of the 12 unique combinations of tick age, *B. afzelii* strain, and competition.

Tick age	Strain	Competition	Mean	95% CI
Larva	Fin-Jyv-A3	No	513	241–1,090
Larva	Fin-Jyv-A3	Yes	146	27–786
Larva	NE4049	No	209	53–829
Larva	NE4049	Yes	338	122–934
1-month-old nymph	Fin-Jyv-A3	No	7,111	4,873–10,376
1-month-old nymph	Fin-Jyv-A3	Yes	3,352	1,972–5,697
1-month-old nymph	NE4049	No	3,493	2,394–5,098
1-month-old nymph	NE4049	Yes	1,875	1,216–2,892
4-month-old nymph	Fin-Jyv-A3	No	3,951	2,738–5,703
4-month-old nymph	Fin-Jyv-A3	Yes	1,410	923–2,154
4-month-old nymph	NE4049	No	2,520	1,851–3,429
4-month-old nymph	NE4049	Yes	1,960	1,350–2,847

Mean is the geometric mean of the strain-specific spirochete loads on the original scale. The 95% confidence interval (95% CI) for the geometric mean is also shown.

study because it is based on a larger sample size (800 ticks vs. 301 ticks) and because the results are more general; i.e., we show here that inter-strain competition occurs at three different time points over the first 5 months of the life cycle of immature *I. ricinus* ticks compared to only one time point (Genné et al., 2018). An important remaining question is whether competition between strains of *B. burgdorferi* sl in the nymph influences subsequent nymph-to-host transmission of the bacterium.

Dynamics of *B. burgdorferi* sl Spirochete Populations in Immature *Ixodes* Ticks

The population size of *B. burgdorferi* sl spirochetes is highly dynamic over the life cycle of immature *Ixodes* ticks (Piesman et al., 1990, 2001; De Silva and Fikrig, 1995; Soares et al., 2006; Jacquet et al., 2017; Pospisilova et al., 2019). A recent study on the spirochete population dynamics of *B. afzelii* in *I. ricinus* found that engorged larvae acquired a small inoculum (∼600 spirochetes), which subsequently expanded 34-fold to reach a peak spirochete population size (21,005 spirochetes) in 2-week-old nymphs (Pospisilova et al., 2019). The results of our study were very similar; the engorged larvae acquired a small inoculum of *B. afzelii* (∼400 spirochetes), which expanded and was 12 times higher in the 1-month-old nymphs (5,005 spirochetes). Numerous studies on *B. burgdorferi* ss in *I. scapularis* have likewise shown that the spirochete population size increases dramatically after a blood meal in both larvae and nymphs (Piesman et al., 1990, 2001; De Silva and Fikrig, 1995; Soares et al., 2006).

The ability of *B. burgdorferi* sl to persist inside the nymph over long periods of time (8–12 months) is critical for the maintenance of Lyme disease in nature (Fazzino et al., 2015). A recent study on the spirochete population dynamics of *B. afzelii* in *I. ricinus* nymphs found that the spirochete population size decreased by 71.3% between 2 and 6 weeks post-molt but reached a stable plateau after this period (Pospisilova et al., 2019). We have observed a similar decrease in spirochete population size between 1-month-old and 4-month-old nymphs in the present study (decrease of 40.5%), and in a previous study (85.8% decrease) (Jacquet et al., 2017). As we only measured the nymphal spirochete population size at two time points, we do not know whether it plateaued, as was shown in the other study (Pospisilova et al., 2019). A recent study on the genetic mechanisms underlying persistence of *B. burgdorferi* ss in *I. scapularis* found no evidence that the spirochete population size declined over time (Fazzino et al., 2015).

One explanation for the observed decrease in the spirochete population over time is bloodmeal digestion, which is a slow process in ixodid ticks that occurs in the gut epithelium rather than the gut lumen (Sonenshine, 1991; Horn et al., 2009; Sojka et al., 2013). Proteomics studies have shown that digestion of the larval blood meal causes host proteins to decrease slowly over time, and some can be identified 10 months after the larva-to-nymph molt (Wickramasekara et al., 2008; Laskay et al., 2013). The slow digestion of the blood meal could explain the gradual decrease of the spirochetes over time in the tick midgut (Kung et al., 2013). We expected that the intensity of inter-strain competition would increase with this age-related decline in the spirochete population, but we found no evidence that competition was stronger in the 4-month-old nymphs compared to the 1-month-old nymphs. One limitation of our qPCR-based approach is that it allows us to estimate spirochete abundance but not spirochete viability, which may decline with advanced nymphal age.

Mechanisms of Competition Inside the Tick Vector

The mechanisms underlying the competition between *B. afzelii* strains in the tick remain unknown. Competition between parasite strains is classified into three different types: interference, exploitation, and apparent competition (Mideo, 2009). Interference competition is unlikely in *B. burgdorferi* sl, because spirochetes are not known to produce toxic substances (Tilly et al., 2008). In exploitation competition, strains compete over limited resources like space or nutrients. This type of competition is expected because nutrients in the tick midgut will disappear over time as the tick digests its bloodmeal (Laskay et al., 2013). Furthermore, studies have shown that ticks contain a relatively small number of spirochetes, suggesting that strains compete over space as well (Durand et al., 2017; Genné et al., 2018). In apparent competition, interactions between strains are mediated by the host immune system. The innate immune system of ticks uses antimicrobial peptides (e.g., lysozymes and defensins) as defense against microbial pathogens (Kopáček et al., 2010; Hajdušek et al., 2013). Spirochetes in the tick hemolymph are cleared by hemocytes using phagocytosis (Rittig et al., 1996; Coleman et al., 1997; Johns et al., 2001). However, we are not aware of any experimental evidence demonstrating that the tick immune system mediates competition between strains of *B. burgdorferi* sl.

Inter-strain Competition and Nymph-to-Host Transmission

Our study found that competition between strains reduced the strain-specific spirochete loads in *I. ricinus* nymphs. An important question is whether this inter-strain competition influences the subsequent nymph-to-host transmission success of the strains. Most *B. afzelii* spirochetes spend 8 months or more in the nymph midgut before achieving nymph-to-host transmission (Gray et al., 2016). We expect that the temporal decline in quantity or viability of the nymphal spirochete population could eventually result in the loss of the less abundant strains from the co-infected nymph (i.e., competitive exclusion). Studies on *B. burgdorferi* ss and *F. novicida* have found that ticks can limit the number of strains that are transmitted to the vertebrate host (Rego et al., 2014; Reif et al., 2014). The biology of spirochetes in blood-feeding nymphs further suggests that inter-strain competition could reduce strain-specific nymph-to-host transmission. During the nymphal blood meal, spirochetes migrate from the midgut to the salivary glands (Spielman et al., 1987; Zung et al., 1989), where their abundance is surprisingly low (Piesman et al., 2001). One study suggested that nymphs

inoculate only ∼100 spirochetes into the vertebrate host (Kern et al., 2011). These observations suggest that *B. burgdorferi* sl strains that are the most abundant in co-infected nymphs are more likely to be transmitted to the reservoir host during the nymphal blood meal (Durand et al., 2017). Future experimental infection studies should test whether co-infection in the nymph reduces strain-specific nymph-to-host transmission.

Relevance of Our Study to the Situation in Nature

The results of our laboratory experiment are relevant to understanding what happens in nature. Studies on wild *I. ricinus* nymphs found that 77–79% of the nymphs are co-infected with multiple strains of *B. afzelii* and that nymphs carry an average of 2.4–2.9 strains (Durand et al., 2015, 2017). Numerous studies in North America have found that wild *I. scapularis* ticks are commonly infected with multiple strains of *B. burgdorferi* ss (Wang et al., 1999; Qiu et al., 2002; Brisson and Dykhuizen, 2004; Walter et al., 2016; Di et al., 2018). Thus, co-infected nymphs are the norm rather than the exception in areas where Lyme disease is endemic. A field study on *B. afzelii* in wild *I. ricinus* nymphs found indirect evidence that competition between strains in nymphs reduces the strain-specific abundance and strain-specific nymph-to-host transmission (Durand et al., 2017). First, this study found the same pattern that we found in the present study: co-infection in the nymph reduced the abundance of the constituent strains (Durand et al., 2017). Second, this study found a positive correlation between the strain-specific spirochete load and the strain-specific prevalence suggesting that *B. afzelii* strains with higher nymphal abundance have higher nymph-to-host transmission (Durand et al., 2017). In summary, our controlled experiments found patterns of co-infection and competition that we have also found in surveys of wild *I. ricinus* populations.

No Effect of Seasonal Treatment on Spirochete Load

We found no effect of seasonal treatment on the *B. afzelii* spirochete load in the 4-month-old nymphs. The seasonal treatments were chosen to simulate summer conditions (mean temperature of 22.4°C and 16 h light: 8 h darkness) and winter conditions (mean temperature of 4 and 6.44°C and 24 h darkness) that are experienced by *I. ricinus* ticks in the natural environment (Dusbabek et al., 1971; Daniel et al., 1972; Gray et al., 2016). We expected that the nymphs exposed to summer conditions would have higher metabolism, faster digestion, and therefore lower spirochete population sizes in their midguts than nymphs exposed to winter conditions. We were surprised that the seasonal treatment had no effect on the spirochete population size in the nymphal midgut. This result suggests that the large differences in temperature and light conditions between the summer and winter conditions over a period of 3 months was not enough to influence tick metabolism, tick digestion of spirochetes, and the dynamics of the *B. afzelii* spirochete population inside the nymphs. Future studies should investigate whether more extreme conditions (e.g., hotter and colder temperatures) would influence the spirochete population dynamics and inter-strain competition inside the nymph vector. We had previously suggested that the temporal decline in nymphal spirochete load following the larva-to-nymph molt could be an artifact of housing our ticks under unnatural "summer-like" conditions in the lab (Jacquet et al., 2017). Thus, the present study demonstrates that the nymphal spirochete load also decreases over time when nymphs are housed under more natural "winter-like" conditions. The survival of the nymphs over the 3-month winter treatments was very high (99.1%) due to the mild temperatures (6.44°C in natural winter and 4.00°C in artificial winter). Storing ticks in separate Eppendorf tubes and burying them underground is a promising approach for measuring individual tick survival under natural winter conditions.

The Infectious Dose and the Importance of Using Ticks Instead of Needles

In studies that investigate competition between pathogen strains, it is critical to control the infectious dose (ID) with which the vertebrate host is infected (de Roode et al., 2005b). If the ID was consistently larger for one strain, we would expect this strain to have higher competitive success (all else being equal). There is evidence that when mice are infected with *B. burgdorferi* ss using artificial needle inoculation, a 10-fold difference in the ID can influence the spirochete load in the mouse tissues (Ma et al., 1998), and presumably the efficiency of host-to-tick transmission. In the Methods, we assumed that the ID delivered by the nymphs is proportional to the product of the number of infected nymphs and the mean spirochete load per infected nymph, and we estimated that the ID for strain Fin-Jyv-A3 was two times higher than strain NE4049. Despite having a (theoretical) 2-fold disadvantage in abundance during the nymphal tick bite (**Figure 1A**), strain NE4049 was still able to reduce the performance of strain Fin-Jyv-A3. This observation suggests that competitive interactions would remain even if both strains had the exact same ID.

Alternatively, one could infect mice via needle inoculation of spirochete cultures, which can be more easily quantified, but this artificial approach creates other problems. Tick saliva enhances the ability of *B. burgdorferi* sl pathogens to infect their vertebrate host (Kazimírová and Stibraniova, 2013). For example, cultured spirochetes are an order of magnitude less infectious than the spirochetes in tick salivary glands (Xu et al., 1996; Lima et al., 2005). Tick saliva also increases the spirochete load of *B. burgdorferi* sl in rodent tissues (Zeidner et al., 2002). A recent study found that the mode of inoculation (needle vs. tick) influenced tissue tropism of *B. burgdorferi* sl (Sertour et al., 2018). In summary, there is lots of evidence that the mode of inoculation influences the infection phenotype. *B. burgdorferi* sl spirochetes have co-evolved with ticks and not needles. Using ticks will generally give a better reflection of what occurs in nature.

CONCLUSION

This study found that co-infection in the mice reduced the strain-specific host-to-tick transmission success to larval ticks

and that this effect was maintained for both strains in the resultant nymphs at 1 and 4 months after the larva-to-nymph molt. This study also demonstrates that competition between strains of *B. afzelii* occurs in co-infected immature *I. ricinus* ticks. Inter-strain competition resulted in decreased spirochete loads for both strains in all three ages of immature ticks investigated in our study. The 3-month-long seasonal treatments did not affect the strain-specific spirochete load nor the intensity of inter-strain competition in the 4-month-old nymphs. Future studies should investigate whether inter-strain competition in the nymph influences the strain-specific nymph-to-host transmission success.

DATA AVAILABILITY STATEMENT

The raw data for this study are stored on Zenodo (https://doi.org/10.5281/zenodo.3569759) in an Excel file titled "Raw data.xlsx."

ETHICS STATEMENT

The commission that is part of the "Service de la Consommation et des Affaires Vétérinaires (SCAV)" of Canton Vaud, Switzerland evaluated and approved the ethics of this study. The Veterinary Service of the Canton of Neuchâtel, Switzerland issued the animal experimentation permit used in this study (NE04/2016).

AUTHOR CONTRIBUTIONS

DG and MV conceived and designed the study, and wrote the manuscript. DG and AS conducted the experiment and performed the molecular work. OR helped with the experimental infections. DG conducted the statistical analyses. All authors read and approved the final version of the manuscript.

FUNDING

This work was supported by a Swiss National Science Foundation grant to MV (FN 31003A_141153).

ACKNOWLEDGMENTS

The authors sincerely thank Alessandro Belli, Kheirie Kabalan, and Gäel Hauser for their help during the study. We would also like to thank Andrei Daniel Mihalca, Yi-Pin Lin, and Ryan Rego for reviewing our manuscript. This study was part of the Ph.D. thesis of DG.

SUPPLEMENTARY MATERIAL

The Supplementary Material for this article can be found online at: https://www.frontiersin.org/articles/10.3389/fcimb.2019.00431/full#supplementary-material

REFERENCES

Abkallo, H. M., Tangena, J.-A., Tang, J., Kobayashi, N., Inoue, M., Zoungrana, A., et al. (2015). Within-host competition does not select for virulence in malaria parasites; studies with *Plasmodium yoelii*. *PLoS Pathog.* 11:e1004628. doi: 10.1371/journal.ppat.1004628

Alizon, S., de Roode, J. C., and Michalakis, Y. (2013). Multiple infections and the evolution of virulence. *Ecol. Lett.* 16, 556–567. doi: 10.1111/ele.12076

Balmer, O., and Tanner, M. (2011). Prevalence and implications of multiple-strain infections. *Lancet Infect. Dis.* 11, 868–878. doi: 10.1016/S1473-3099(11)70241-9

Bell, A. S., De Roode, J. C., Sim, D., and Read, A. F. (2006). Within-host competition in genetically diverse malaria infections: parasite virulence and competitive success. *Evolution* 60, 1358–1371. doi: 10.1111/j.0014-3820.2006.tb01215.x

Belozerov, V. (1982). "Diapause and biological rhythms in ticks," in *Physiology of Ticks,* eds F. D. Obenchain and R. Galun (Oxford: Pergamon Press), 469–500. doi: 10.1016/B978-0-08-024937-7.50018-4

Belozerov, V. (2009). Diapause and quiescence as two main kinds of dormancy and their significance in life cycles of mites and ticks (Chelicerata: Arachnida: Acari). Part 2. Parasitiformes. *Acarina* 17, 3–32.

Brisson, D., and Dykhuizen, D. E. (2004). ospC diversity in *Borrelia burgdorferi*: different hosts are different niches. *Genetics* 168, 713–722. doi: 10.1534/genetics.104.028738

Bruce, M. C., Donnelly, C. A., Alpers, M. P., Galinski, M. R., Barnwell, J. W., Walliker, D., et al. (2000). Cross-species interactions between malaria parasites in humans. *Science* 287, 845–848. doi: 10.1126/science.287.5454.845

Buckwalter, S., Sloan, L., Cunningham, S., Espy, M., Uhl, J., Jones, M., et al. (2014). Inhibition controls for qualitative real-time PCR assays: are they necessary for all specimen matrices? *J. Clin. Microbiol.* 52, 2139–2143. doi: 10.1128/JCM.03389-13

Cayol, C., Giermek, A., Gomez-Chamorro, A., Hytönen, J., Kallio, E. R., Mappes, T., et al. (2018). *Borrelia afzelii* alters reproductive success in a rodent host. *Proc. R. Soc. B* 285:20181056. doi: 10.1098/rspb.2018.1056

Coleman, J. L., Gebbia, J. A., Piesman, J., Degen, J. L., Bugge, T. H., and Benach, J. L. (1997). Plasminogen is required for efficient dissemination of *B. burgdorferi* in ticks and for enhancement of spirochetemia in mice. *Cell* 89, 1111–1119. doi: 10.1016/S0092-8674(00)80298-6

Daniel, M., Honzakova, E., and Cerný, V. (1972). Overwintering of the tick *Ixodes ricinus* (L.) under conditions of a field experiment. *Folia Parasitol.* 19, 305–14.

Dautel, H., Dippel, C., Kämmer, D., Werkhausen, A., and Kahl, O. (2008). Winter activity of *Ixodes ricinus* in a Berlin forest. *Int. J. Med. Microbiol.* 298, 50–54. doi: 10.1016/j.ijmm.2008.01.010

de Roode, J. C., Culleton, R., Cheesman, S. J., Carter, R., and Read, A. F. (2004). Host heterogeneity is a determinant of competitive exclusion or coexistence in genetically diverse malaria infections. *Proc. R. Soc. B* 271, 1073–1080. doi: 10.1098/rspb.2004.2695

de Roode, J. C., Helinski, M. E., Anwar, M. A., and Read, A. F. (2005a). Dynamics of multiple infection and within-host competition in genetically diverse malaria infections. *Am. Nat.* 166, 531–542. doi: 10.1086/491659

de Roode, J. C., Pansini, R., Cheesman, S. J., Helinski, M. E., Huijben, S., Wargo, A. R., et al. (2005b). Virulence and competitive ability in genetically diverse malaria infections. *Proc. Natl. Acad. Sci. U.S.A.* 102, 7624–7628. doi: 10.1073/pnas.0500078102

De Silva, A. M., and Fikrig, E. (1995). Growth and migration of *Borrelia burgdorferi* in *Ixodes* ticks during blood feeding. *Am. J. Trop. Med. Hyg.* 53, 397–404. doi: 10.4269/ajtmh.1995.53.397

Derdáková, M., Dudiòák, V., Brei, B., Brownstein, J. S., Schwartz, I., and Fish, D. (2004). Interaction and transmission of two *Borrelia burgdorferi* sensu stricto strains in a tick-rodent maintenance system. *Appl. Environ. Microbiol.* 70, 6783–6788. doi: 10.1128/AEM.70.11.6783-6788.2004

Di, L., Wan, Z., Akther, S., Ying, C., Larracuente, A., Li, L., et al. (2018). Genotyping and quantifying Lyme pathogen strains by deep sequencing of the outer surface protein C (ospC) locus. *J. Clin. Microbiol.* 56, e00940–e00918. doi: 10.1128/JCM.00940-18

Durand, J., Herrmann, C., Genné, D., Sarr, A., Gern, L., and Voordouw, M. J. (2017). Multistrain infections with Lyme borreliosis pathogens

in the tick vector. *Appl. Environ. Microbiol.* 83, e02552–e02516. doi: 10.1128/AEM.02552-16

Durand, J., Jacquet, M., Paillard, L., Rais, O., Gern, L., and Voordouw, M. J. (2015). Cross-immunity and community structure of a multiple-strain pathogen in the tick vector. *Appl. Environ. Microbiol.* 81, 7740–7752. doi: 10.1128/AEM.02296-15

Dusbabek, F., Daniel, M., and Cerný, V. (1971). Stratification of engorged *Ixodes ricinus* larvae overwintering in soil. *Folia Parasitol.* 18, 261–266.

Fazzino, L., Tilly, K., Dulebohn, D. P., and Rosa, P. A. (2015). Long-term survival of *Borrelia burgdorferi* lacking the hibernation promotion factor homolog in the unfed tick vector. *Infect. Immun.* 83, 4800–4810. doi: 10.1128/IAI.00925-15

Genné, D., Sarr, A., Gomez-Chamorro, A., Durand, J., Cayol, C., Rais, O., et al. (2018). Competition between strains of *Borrelia afzelii* inside the rodent host and the tick vector. *Proc. R. Soc. B* 285:20181804. doi: 10.1098/rspb.2018.1804

Gray, J. (1984). Studies on the dynamics of active populations of the sheep tick, *Ixodes ricinus* L. in Co. Wicklow, Ireland. *Acarologia* 25, 167–178.

Gray, J. (1991). The development and seasonal activity of the tick *Ixodes ricinus*: a vector of Lyme borreliosis. *Rev. Med. Vet. Entomol.* 79, 323–333.

Gray, J. S., Kahl, O., Lane, R. S., Levin, M. L., and Tsao, J. I. (2016). Diapause in ticks of the medically important *Ixodes ricinus* species complex. *Ticks Tick Borne Dis.* 7, 992–1003. doi: 10.1016/j.ttbdis.2016.05.006

Hajdušek, O., Šíma, R., Ayllón, N., Jalovecká, M., Perner, J., De La Fuente, J., et al. (2013). Interaction of the tick immune system with transmitted pathogens. *Front. Cell. Infect. Microbiol.* 3:26. doi: 10.3389/fcimb.2013.00026

Harrison, F., Browning, L. E., Vos, M., and Buckling, A. (2006). Cooperation and virulence in acute *Pseudomonas aeruginosa* infections. *BMC Biol.* 4:21. doi: 10.1186/1741-7007-4-21

Horn, M., Nussbaumerová, M., Šanda, M., Kovárová, Z., Srba, J., Franta, Z., et al. (2009). Hemoglobin digestion in blood-feeding ticks: mapping a multipeptidase pathway by functional proteomics. *Chem. Biol.* 16, 1053–1063. doi: 10.1016/j.chembiol.2009.09.009

Jacquet, M., Durand, J., Rais, O., and Voordouw, M. J. (2015). Cross-reactive acquired immunity influences transmission success of the Lyme disease pathogen, *Borrelia afzelii*. *Infect. Genet. Evol.* 36, 131–140. doi: 10.1016/j.meegid.2015.09.012

Jacquet, M., Genné, D., Belli, A., Maluenda, E., Sarr, A., and Voordouw, M. J. (2017). The abundance of the Lyme disease pathogen *Borrelia afzelii* declines over time in the tick vector *Ixodes ricinus*. *Parasit. Vectors* 10:257. doi: 10.1186/s13071-017-2187-4

Johns, R., Ohnishi, J., Broadwater, A., Sonenshine, D. E., De Silva, A. M., and Hynes, W. L. (2001). Contrasts in tick innate immune responses to *Borrelia burgdorferi* challenge: immunotolerance in *Ixodes scapularis* versus immunocompetence in *Dermacentor variabilis* (Acari: Ixodidae). *J. Med. Entomol.* 38, 99–107. doi: 10.1603/0022-2585-38.1.99

Kazimírová, M., and Stibraniova, I. (2013). Tick salivary compounds: their role in modulation of host defences and pathogen transmission. *Front. Cell. Infect. Microbiol.* 3:43. doi: 10.3389/fcimb.2013.00043

Kern, A., Collin, E., Barthel, C., Michel, C., Jaulhac, B., and Boulanger, N. (2011). Tick saliva represses innate immunity and cutaneous inflammation in a murine model of Lyme disease. *Vector Borne Zoonotic Dis.* 11, 1343–1350. doi: 10.1089/vbz.2010.0197

Khan, S., Voordouw, M. J., and Hill, J. E. (2019). Competition among Gardnerella subgroups from the human vaginal microbiome. *Front. Cell. Infect. Microbiol.* 9:374. doi: 10.3389/fcimb.2019.00374

Kopáček, P., Hajdušek, O., Burešová, V., and Daffre, S. (2010). Tick innate immunity. *Adv. Exp. Med. Biol.* 708, 137–162. doi: 10.1007/978-1-4419-8059-5_8

Kung, F., Anguita, J., and Pal, U. (2013). *Borrelia burgdorferi* and tick proteins supporting pathogen persistence in the vector. *Future Microbiol.* 8, 41–56. doi: 10.2217/fmb.12.121

Kurtenbach, K., Hanincová, K., Tsao, J. I., Margos, G., Fish, D., and Ogden, N. H. (2006). Fundamental processes in the evolutionary ecology of Lyme borreliosis. *Nat. Rev. Microbiol.* 4, 660–669. doi: 10.1038/nrmicro1475

Laskay, Ü. A., Breci, L., Vilcins, I.-M. E., Dietrich, G., Barbour, A. G., Piesman, J., et al. (2013). Survival of host blood proteins in *Ixodes scapularis* (Acari: Ixodidae) ticks: a time course study. *J. Med. Entomol.* 50, 1282–1290. doi: 10.1603/ME12125

Lima, C., Zeidner, N., Beard, C., Soares, C., Dolan, M., Dietrich, G., et al. (2005). Differential infectivity of the Lyme disease spirochete *Borrelia burgdorferi* derived from *Ixodes scapularis* salivary glands and midgut. *J. Med. Entomol.* 42, 506–510. doi: 10.1603/0022-2585(2005)042[0506:DIOTLD]2.0.CO;2

Ma, Y., Seiler, K. P., Eichwald, E. J., Weis, J. H., Teuscher, C., and Weis, J. J. (1998). Distinct characteristics of resistance to *Borrelia burgdorferi*-induced arthritis in C57BL/6N mice. *Infect. Immun.* 66, 161–168.

Mideo, N. (2009). Parasite adaptations to within-host competition. *Trends Parasitol.* 25, 261–268. doi: 10.1016/j.pt.2009.03.001

Paaijmans, K. P., Blanford, S., Chan, B. H., and Thomas, M. B. (2011). Warmer temperatures reduce the vectorial capacity of malaria mosquitoes. *Biol. Lett.* 8, 465–468. doi: 10.1098/rsbl.2011.1075

Pérez, D., Kneubühler, Y., Rais, O., Jouda, F., and Gern, L. (2011). *Borrelia afzelii* ospC genotype diversity in *Ixodes ricinus* questing ticks and ticks from rodents in two Lyme borreliosis endemic areas: contribution of co-feeding ticks. *Ticks Tick Borne Dis.* 2, 137–142. doi: 10.1016/j.ttbdis.2011.06.003

Piesman, J., Oliver, J. R., and Sinsky, R. J. (1990). Growth kinetics of the Lyme disease spirochete (*Borrelia burgdorferi*) in vector ticks (*Ixodes dammini*). *Am. J. Trop. Med. Hyg.* 42, 352–357. doi: 10.4269/ajtmh.1990.42.352

Piesman, J., Schneider, B. S., and Zeidner, N. S. (2001). Use of quantitative PCR to measure density of *Borrelia burgdorferi* in the midgut and salivary glands of feeding tick vectors. *J. Clin. Microbiol.* 39, 4145–4148. doi: 10.1128/JCM.39.11.4145-4148.2001

Pollitt, L. C., Bram, J. T., Blanford, S., Jones, M. J., and Read, A. F. (2015). Existing infection facilitates establishment and density of malaria parasites in their mosquito vector. *PLoS Pathog.* 11:e1005003. doi: 10.1371/journal.ppat.1005003

Pollitt, L. C., Mideo, N., Drew, D. R., Schneider, P., Colegrave, N., and Reece, S. E. (2011). Competition and the evolution of reproductive restraint in malaria parasites. *Am. Nat.* 177, 358–367. doi: 10.1086/658175

Pospisilova, T., Urbanova, V., Hes, O., Kopacek, P., Hajdusek, O., and Sima, R. (2019). Tracking of *Borrelia afzelii* transmission from infected *Ixodes ricinus* nymphs to mice. *Infect. Immun.* 87, e00896–18. doi: 10.1128/IAI.00896-18

Qiu, W.-G., Dykhuizen, D. E., Acosta, M. S., and Luft, B. J. (2002). Geographic uniformity of the Lyme disease spirochete (*Borrelia burgdorferi*) and its shared history with tick vector (*Ixodes scapularis*) in the northeastern United States. *Genetics* 160, 833–849.

Read, A. F., and Taylor, L. H. (2001). The ecology of genetically diverse infections. *Science* 292, 1099–1102. doi: 10.1126/science.1059410

Rego, R. O., Bestor, A., Štefka, J., and Rosa, P. A. (2014). Population bottlenecks during the infectious cycle of the Lyme disease spirochete *Borrelia burgdorferi*. *PLoS ONE* 9:e101009. doi: 10.1371/journal.pone.0101009

Reif, K. E., Palmer, G. H., Crowder, D. W., Ueti, M. W., and Noh, S. M. (2014). Restriction of *Francisella novicida* genetic diversity during infection of the vector midgut. *PLoS Pathog.* 10:e1004499. doi: 10.1371/journal.ppat.1004499

Richter, D., Debski, A., Hubalek, Z., and Matuschka, F.-R. (2012). Absence of Lyme disease spirochetes in larval *Ixodes ricinus* ticks. *Vector Borne Zoonotic Dis.* 12, 21–27. doi: 10.1089/vbz.2011.0668

Rittig, M. G., Kuhn, K.-H., Dechant, C. A., Gauckler, A., Modolell, M., Ricciardi-Castagnoli, P., et al. (1996). Phagocytes from both vertebrate and invertebrate species use "coiling" phagocytosis. *Dev. Comp. Immunol.* 20, 393–406. doi: 10.1016/S0145-305X(96)00023-7

Rollend, L., Fish, D., and Childs, J. E. (2013). Transovarial transmission of *Borrelia* spirochetes by *Ixodes scapularis*: a summary of the literature and recent observations. *Ticks Tick Borne Dis.* 4, 46–51. doi: 10.1016/j.ttbdis.2012.06.008

Rynkiewicz, E. C., Brown, J., Tufts, D. M., Huang, C.-I., Kampen, H., Bent, S. J., et al. (2017). Closely-related *Borrelia burgdorferi* (sensu stricto) strains exhibit similar fitness in single infections and asymmetric competition in multiple infections. *Parasit. Vectors* 10:64. doi: 10.1186/s13071-016-1964-9

Schrader, C., Schielke, A., Ellerbroek, L., and Johne, R. (2012). PCR inhibitors–occurrence, properties and removal. *J. Appl. Microbiol.* 113, 1014–1026. doi: 10.1111/j.1365-2672.2012.05384.x

Sertour, N., Cotte, V., Garnier, M., Malandrin, L., Ferquel, E., and Choumet, V. (2018). Infection kinetics and tropism of *Borrelia burgdorferi* sensu lato in mouse after natural (via ticks) or artificial (needle) infection depends on the bacterial strain. *Front. Microbiol.* 9:1722. doi: 10.3389/fmicb.2018.01722

Shih, C.-M., Telford, S., and Spielman, A. (1995). Effect of ambient temperature on competence of deer ticks as hosts for Lyme disease spirochetes. *J. Clin. Microbiol.* 33, 958–961.

Sidstedt, M., Hedman, J., Romsos, E. L., Waitara, L., Wadsö, L., Steffen, C. R., et al. (2018). Inhibition mechanisms of hemoglobin, immunoglobulin G, and whole blood in digital and real-time PCR. *Anal. Bioanal. Chem.* 410, 2569–2583. doi: 10.1007/s00216-018-0931-z

Soares, C., Zeidner, N., Beard, C., Dolan, M., Dietrich, G., and Piesman, J. (2006). Kinetics of *Borrelia burgdorferi* infection in larvae of refractory and competent tick vectors. *J. Med. Entomol.* 43, 61–67. doi: 10.1093/jmedent/43.1.61

Sojka, D., Franta, Z., Horn, M., Caffrey, C. R., Mareš, M., and Kopáček, P. (2013). New insights into the machinery of blood digestion by ticks. *Trends Parasitol.* 29, 276–285. doi: 10.1016/j.pt.2013.04.002

Sonenshine, D. E. (1991). *Biology of Ticks.* New York, NY: Oxford University Press.

Spielman, A., Ribeiro, J., Mather, T., and Piesman, J. (1987). Dissemination and salivary delivery of Lyme disease spirochetes in vector ticks (Acari: Ixodidae). *J. Med. Entomol.* 24, 201–205. doi: 10.1093/jmedent/24.2.201

Sternberg, E. D., and Thomas, M. B. (2014). Local adaptation to temperature and the implications for vector-borne diseases. *Trends Parasitol.* 30, 115–122. doi: 10.1016/j.pt.2013.12.010

Strandh, M., and Råberg, L. (2015). Within-host competition between *Borrelia afzelii* ospC strains in wild hosts as revealed by massively parallel amplicon sequencing. *Philos. Trans. R. Soc. B* 370:20140293. doi: 10.1098/rstb.2014.0293

Taylor, L. H., Walliker, D., and Read, A. F. (1997). Mixed–genotype infections of malaria parasites: within–host dynamics and transmission success of competing clones. *Proc. R. Soc. Lond. Ser. B: Biol. Sci.* 264, 927–935. doi: 10.1098/rspb.1997.0128

Tilly, K., Rosa, P. A., and Stewart, P. E. (2008). Biology of infection with *Borrelia burgdorferi*. *Infect. Dis. Clin. North Am.* 22, 217–234. doi: 10.1016/j.idc.2007.12.013

Tonetti, N., Voordouw, M. J., Durand, J., Monnier, S., and Gern, L. (2015). Genetic variation in transmission success of the Lyme borreliosis pathogen *Borrelia afzelii*. *Ticks Tick Borne Dis.* 6, 334–343. doi: 10.1016/j.ttbdis.2015.02.007

Tsao, J. I. (2009). Reviewing molecular adaptations of Lyme borreliosis spirochetes in the context of reproductive fitness in natural transmission cycles. *Vet. Res.* 40:36. doi: 10.1051/vetres/2009019

van Duijvendijk, G., Sprong, H., and Takken, W. (2015). Multi-trophic interactions driving the transmission cycle of *Borrelia afzelii* between *Ixodes ricinus* and rodents: a review. *Parasit. Vectors* 8:643. doi: 10.1186/s13071-015-1257-8

Walter, K. S., Carpi, G., Evans, B. R., Caccone, A., and Diuk-Wasser, M. A. (2016). Vectors as epidemiological sentinels: patterns of within-tick *Borrelia burgdorferi* diversity. *PLoS Pathog.* 12:e1005759. doi: 10.1371/journal.ppat.1005759

Wang, N., Dykhuizen, D. E., Qiu, W., Dunn, J. J., Bosler, E. M., and Luft, B. J. (1999). Genetic diversity of ospC in a local population of *Borrelia burgdorferi* sensu stricto. *Genetics* 151, 15–30.

Wickramasekara, S., Bunikis, J., Wysocki, V., and Barbour, A. G. (2008). Identification of residual blood proteins in ticks by mass spectrometry proteomics. *Emerging Infect. Dis.* 14:1273–5. doi: 10.3201/eid1408.080227

Xu, Y., Kodner, C., Coleman, L., and Johnson, R. C. (1996). Correlation of plasmids with infectivity of *Borrelia burgdorferi* sensu stricto type strain B31. *Infect. Immun.* 64, 3870–3876.

Zeidner, N., Schneider, B., Nuncio, M., Gern, L., and Piesman, J. (2002). Coinoculation of *Borrelia* spp. with tick salivary gland lysate enhances spirochete load in mice and is tick species–specific. *J. Parasitol.* 88, 1276–1278. doi: 10.1645/0022-3395(2002)088[1276:COBSWT]2.0.CO;2

Zung, J., Lewengrub, S., Rudzinska, M., Spielman, A., Telford, S., and Piesman, J. (1989). Fine structural evidence for the penetration of the Lyme disease spirochete *Borrelia burgdorferi* through the gut and salivary tissues of *Ixodes dammini*. *Can. J. Zool.* 67, 1737–1748. doi: 10.1139/z89-249

Conflict of Interest: The authors declare that the research was conducted in the absence of any commercial or financial relationships that could be construed as a potential conflict of interest.

frontiers in Cellular and Infection Microbiology

REVIEW
published: 21 January 2020
doi: 10.3389/fcimb.2019.00474

Where Are We With Human Lice? A Review of the Current State of Knowledge

Nadia Amanzougaghene[1,2]*, *Florence Fenollar*[2,3], *Didier Raoult*[1,2] and *Oleg Mediannikov*[1,2]*

[1] Aix Marseille Univ, IRD, AP-HM, SSA, VITROME, Marseille, France, [2] IHU-Méditerranée Infection, Marseille, France, [3] Aix Marseille Univ, IRD, AP-HM, MEPHI, Marseille, France

Pediculus humanus is an obligate bloodsucking ectoparasite of human that includes two ecotypes, head louse and body louse, which differ slightly in morphology and biology, but have distinct ecologies. Phylogenetically, they are classified on six mitochondrial clades (A, B, C, D, E, and F), head louse encompasses the full genetic diversity of clades, while body louse belongs to clades A and D. Recent studies suggested that not only body louse, but also head louse can transmit disease, which warrants greater attention as a serious public health problem. The recent sequencing of body louse genome confirmed that *P. humanus* has the smallest genome of any hemimetabolous insect reported to date, and also revealed numerous interesting characteristics in the nuclear and mitochondrial genomes. The transcriptome analyses showed that body and head lice were almost genetically identical. Indeed, the phenotypic flexibility associated with the emergence of body lice, is probably a result of regulatory changes, perhaps epigenetic in origin, triggered by environmental signals. Current lice control strategies have proven unsuccessful. For instance, ivermectin represents a relatively new and very promising pediculicide. However, ivermectin resistance in the field has begun to be reported. Therefore, novel opportunities for pest control strategies are needed. Our objective here is to review the current state of knowledge on the biology, epidemiology, phylogeny, disease-vector and control of this fascinating and very intimate human parasite.

Keywords: *Pediculus humanus*, biology, epidemiology, phylogeny, disease-vector, control

OPEN ACCESS

Edited by:
Ryan Oliver Marino Rego, Institute of Parasitology (ASCR), Czechia

Reviewed by:
Carlo José Freire Oliveira, Universidade Federal Do Triângulo Mineiro, Brazil
Sally Jane Cutler, University of East London, United Kingdom

***Correspondence:**
Nadia Amanzougaghene
amanzougaghene_nadia@yahoo.fr
Oleg Mediannikov
olegusss1@gmail.com

Specialty section:
This article was submitted to Parasite and Host, a section of the journal Frontiers in Cellular and Infection Microbiology

Received: *15 May 2019*
Accepted: *24 December 2019*
Published: *21 January 2020*

Citation:
Amanzougaghene N, Fenollar F, Raoult D and Mediannikov O (2020) Where Are We With Human Lice? A Review of the Current State of Knowledge. Front. Cell. Infect. Microbiol. 9:474. doi: 10.3389/fcimb.2019.00474

BIOLOGY, EPIDEMIOLOGY AND GENOMIC OF LICE

Human lice, commonly known as sucking lice, are hemimetabolous insects that belong to the suborder *Anoplura* (order: *Phthiraptera).* They pierce the skin of their human hosts and feed on their blood, which is their only diet (Durden and Musser, 1994). More than 530 species have been described and each species parasitizes one or more closely related placental mammalian host species (Durden and Musser, 1994). Two louse species are known to parasite humans, *Pediculus humanus* and *Pthirus pubis* (Reed et al., 2007). *Pthirus pubis,* found in the pubic area and known as the pubic or crab louse (not considered further in this review) belongs to the genus *Pthirus,* which is shared with gorillas (*Pt. gorilla*) (Durden and Musser, 1994; Reed et al., 2007). *Pediculus humanus* belongs to the genus of *Pediculus*, which is shared with chimpanzees (*P. schaeffi*) and New World monkey (*P. mjobergi*) (Durden and Musser, 1994; Reed et al., 2007; Drali et al., 2016a).

Pediculus humanus comprises two ecotypes, which are body lice (*P. h. humanus*) and head lice (*P. h. capitis*). These two ecotypes have almost the same morphology but differ in their ecology and have distinct nutritional patterns (Veracx and Raoult, 2012). The head louse lives, breeds, and lays its eggs (nits) at the base of hair shafts and frequently feed on human blood every 4–6 h (Light et al., 2008b; Veracx and Raoult, 2012). Body louse lives and lays eggs in clothing, feeds less frequently and ingests greater quantities compared with head louse (Light et al., 2008b; Li et al., 2010; Brouqui, 2011). In addition, it lays more eggs and grows faster than head louse (Light et al., 2008b; Li et al., 2010). Furthermore, body louse is more resistant to environmental conditions, can withstand lower humidity and survives longer outside the host (more than 72 h for the off-host survival) (Veracx and Raoult, 2012).

Head louse infestation is very common worldwide, especially among schoolchildren, whatever their hygiene status, and the transmission occurs mainly by head-to-head contact (Chosidow, 2000). Adults with poor personal hygiene are also commonly affected (Chosidow, 2000). Body louse infestation is less prevalent and is related with poor hygiene and a lack of sanitation, overcrowding, damp, and cold weather conditions (Raoult and Roux, 1999). For that reason, homeless, jail, and refugee populations are predominantly affected (Raoult and Roux, 1999; Brouqui, 2011). In addition to their role as a dangerous disease vector (we will discuss this point in greater detail later in the review), louse infestations cause itching that may lead to intense irritation (Chosidow, 2000; Veracx and Raoult, 2012). Severe itching can lead to excoriations in which a secondary bacterial infection is likely to occur (Chosidow, 2000). Post inflammatory pigmentation is also common in chronically infested persons (Chosidow, 2000).

The recent sequencing and annotation of body louse genome confirmed that *P. humanus* harbor the smallest known holometabolic insect genome sequenced to date, and revealed interesting information and characteristics on nuclear and mitochondrial genomes. Thus, body louse genome holds great potential for the understanding of the coevolution among lice population, symbionts and pathogens (Kirkness et al., 2010). Its genome about 108 Mb contains 10,773 predicted protein-coding genes and 57 microRNAs (Kirkness et al., 2010). Interestingly, the number of genes related to sensing and responding to the environmental factors were significantly reduced in body louse genome compared to other insect genomes (Kirkness et al., 2010; Pittendrigh et al., 2013). Thus, reflecting its simple life cycle, whereby humans serve as the sole host and human blood as the only diet (Kirkness et al., 2010; Pittendrigh et al., 2013).

Unlike bilateral animals from which the 37 mitochondrial genes are typically arranged on a single circular chromosome, the body and head lice have their genes organized in an unusual architecture of 20 minichromosomes, each minichromosome has a size of 3–4 kb and has 1–3 genes and a control region (Shao et al., 2012). Notably, this extensively fragmented mitochondrial genome of *P. humanus* is a fascinating phenomenon and represents the most radical departure to date in bilateral animals, and may be associated with the loss of the gene involved in mitochondrial genome replication which encodes the mitochondrial single-stranded DNA binding protein (Kirkness et al., 2010; Shao et al., 2012). However, why and how exactly mitochondrial genome became fragmented, are still poorly understood.

Body and head lice host the same primary endosymbiotic bacteria (*Candidatus* Riesia pediculicola) that supply the lice with B-vitamins, absent in the human blood (Kirkness et al., 2010; Boyd and Reed, 2012). *Candidatus* Riesia pediculicola has a small genome that encodes <600 genes distributed between a short linear chromosome (∼0.57 Mb) and a circular plasmid (∼8 kb) including genes required for the synthesis of essential B vitamins (Kirkness et al., 2010; Boyd et al., 2017). The bacterium is housed in specialized structures known as mycetomes, localized on the ventral side of the midgut, and is vertically transmitted from the female louse to its progeny (Perotti et al., 2007). It belongs to the family of *Enterobacteriaceae* within the *Candidatus* Riesia genus, which is shared with lice that parasitize chimpanzees and gorillas (Perotti et al., 2007; Boyd et al., 2017). Phylogenetic studies have shown that the symbiont co-evolved with head and body lice and shared a common ancestor with *P. schaeffi* endosymbiont (*Candidatus* Riesa pediculischaeffi) roughly 5.4 Mya ago (Boyd et al., 2017). Lice endosymbionts might also support investigations on human evolution (Boyd et al., 2017).

Moreover, in addition to being fundamental to lice development and survival, which makes it an interesting target for the development of an alternative lice control strategy (we will discuss this point in detail later in the review), the question of whether this symbiont has an influence on lice behavior or competence as a disease vector merits further study.

PHYLOGENY AND PHYLOGEOGRAPHY OF LICE

Phylogeny Relationships Between Head and Body Lice

The body and head lice have a morphology and biological characteristics almost similar, but differ in their ecological niches (Veracx and Raoult, 2012). Although the taxonomic status of these two types of lice has been debated for more than a century, they are now considered as ecotypes of a single species as opposed to distinct species (Light et al., 2008b; Veracx and Raoult, 2012; Tovar-Corona et al., 2015). Despite numerous studies, the genetic basis and evolutionary relationships among body and head lice remain obscure.

Until recently, the most predominant opinion was that body louse descended from head louse in nature (Veracx and Raoult, 2012). Indeed, as the body louse lives and lays eggs on the clothing of the host (Raoult and Roux, 1999; Light et al., 2008b; Veracx and Raoult, 2012), it was thought that body lice had only recently appeared when modern humans started wearing clothes (Kittler et al., 2003; Light et al., 2008b). However, the most recent data available do not share the same view. Indeed, a novel theory for the emergence of body lice has been reported recently, suggesting that under certain conditions of poor hygiene, an infestation of head lice can turn into a massive infestation, which has allowed variants (genetic or phenotypic) of head lice able

of ingesting a large amount of blood, a typical characteristic of body lice, to colonize clothing (Li et al., 2010; Brouqui, 2011; Veracx and Raoult, 2012). This assumption was based on the genotypic and phylogenetic analyses using highly variable intergenic spacers showing that head and body lice are not indistinguishable (Li et al., 2010). In addition, several researchers pointed that when head lice raised under appropriate conditions, they could develop into body louse ecotypes (Keilin and Nuttall, 1919; Alpatov and Nastukova, 1955). Thus, the divergence of head and body lice is obviously not the result of a single event, but probably takes place constantly among the two shared louse clades A and D (see below for louse mitochondrial clades), this transformation being facilitated by mass infestations (Li et al., 2010; Veracx and Raoult, 2012).

Moreover, the comparison of head and body louse transcriptomes has revealed that among the 14 genes with differential expression, only one gene was thought to be missing in head louse, which is the PHUM540560 gene that encodes a hypothetical 69-amino acids protein of unknown function (Olds et al., 2012). A thorough analysis conducted by Drali et al. (2013) revealed that this gene was also present in the head louse but with a rearranged sequence compared to body louse. Notably, based on the variation of this gene, a molecular tool based on real-time PCR has been developed and allows for the first time to differentiate between the two ecotypes (Drali et al., 2013). These findings indicate that head and body lice have almost the same genomic content; therefore, their phenotypic difference is likely to be associated with a variation in gene expression (Olds et al., 2012; Veracx and Raoult, 2012).

Indeed, a recent study analyzed alternative splicing using previously reported transcriptome data for both head and body lice, and reported evidence of differences between transcription pools (Tovar-Corona et al., 2015). Interestingly, while no genes functional categories associated with louse-specific alternative splicing events were found to be overexpressed, genes containing body louse-specific alternative splicing events were found to be significantly enriched for functional categories associated with development of the nervous system and feeding, and ovarian follicle cells, as well as regulation of transcription (Tovar-Corona et al., 2015). For example, the observed enrichment of functional categories related to feeding, in particular the development of salivary gland and open tracheal system, may reflect the adaptation of body lice to more sporadic dietary habits in the clothing environment compared with the more continuous feeding of head lice (Tovar-Corona et al., 2015). Alternative splicing is through to be a major contributor to proteome diversification (Nakka et al., 2018). Indeed, several studies have strongly associated alternative splicing with phenotypic plasticity in eusocial insects, where distinct regulatory programs and phenotypes derive from a single genome (Lyko et al., 2010; Terrapon et al., 2014). Thus, the changes in the development program observed in body lice compared to head lice, may underpin some of the phenotypic flexibility observed in body lice allowing them to colonize clothing (Tovar-Corona et al., 2015).

Taken together, these data evidence that the phenotypic shifts associated with the emergence of body lice are likely to be a consequence of regulatory changes, possibly epigenetic in origin, triggered by environmental cues. Such phenotypic modification has been reported to occur in other insects, such as in honey bees, termites, and migratory locusts (Simpson et al., 2001; Hayashi et al., 2007; Lyko et al., 2010). For example, in honey bees, the development of queens and workers is strictly controlled by the differential feeding of royal jelly and their adult behaviors are accompanied by epigenomic changes (Lyko et al., 2010). Certainly, further efforts on the genetic studies of head and body lice are needed to link their genetic difference with phenotypic differences. Whole genome sequencing of head lice and comparative genomics combined with transcriptomic, proteomic, and epigenomic studies between head and body lice would be useful to better understand lice and address these questions.

Louse Mitochondrial Clades

Genetic studies based on mitochondrial genes have inferred to *Pediculus* lice a robust phylogenetic classification into several divergent clades or haplogroups, exhibiting some geographic differences (**Figure 1**) (Light et al., 2008b; Ashfaq et al., 2015; Drali et al., 2015b; Amanzougaghene et al., 2017). Six mitochondrial clades were described (A, D, B, F, C, and E) (Ashfaq et al., 2015; Drali et al., 2015b; Amanzougaghene et al., 2016b, 2017, 2019). In addition to the inter clade diversity, human lice also display intra clade diversity, as illustrated by the multiple distinct haplotypes for each clade (**Figure 1B**) (Ascunce et al., 2013; Ashfaq et al., 2015; Amanzougaghene et al., 2016a; Drali et al., 2016a). Head lice encompass all clades diversity, while body lice belong to clades A and D only (Amanzougaghene et al., 2017).

Clade A is widely and globally distributed, while clade D has so far only been reported in sub-Saharan African countries, including the Democratic Republic of Congo (DRC) and the Republic of Congo (Congo-Brazzaville), where it was characterized for the first time among the Pygmy populations (Ascunce et al., 2013; Ashfaq et al., 2015; Drali et al., 2015b; Amanzougaghene et al., 2016a). The clade D was also found in Zimbabwe and Ethiopia (Amanzougaghene et al., 2016a, 2019). Clade B is mainly found in America, where it exhibits a high diversification (Reed et al., 2004; Light et al., 2008a; Ascunce et al., 2013). This clade is also found in Western Europe, Australia, North Algeria, South Africa, Saudi Arabia, and in Israel among head lice remains dating back to the Roman period (Raoult et al., 2008; Ascunce et al., 2013; Ashfaq et al., 2015; Boutellis et al., 2015; Al-Shahrani et al., 2017). Clade F is the sister group of clade B. This clade was first described in head lice recovered from members of the Wayampi community living in a remote Trois-Sauts village, located in French Guiana. This clade was also found in Argentina and Mexico (Amanzougaghene et al., 2019). *Pediculus mjobergi*, the lice of South American monkeys of *Cebidae* family, also belong to this clade. These lice are supposed to be acquired by their monkey's hosts from the first peoples who penetrated the New World across the Bering straits thousands of years ago (Drali et al., 2016a; Amanzougaghene et al., 2019).

Clade C has been reported mainly from two continents, Africa (from Ethiopia and the Republic of Congo) and Asia (Nepal, Pakistan, and Thailand) (Sunantaraporn et al., 2015; Amanzougaghene et al., 2016a, 2017). Lastly, clade E was chiefly

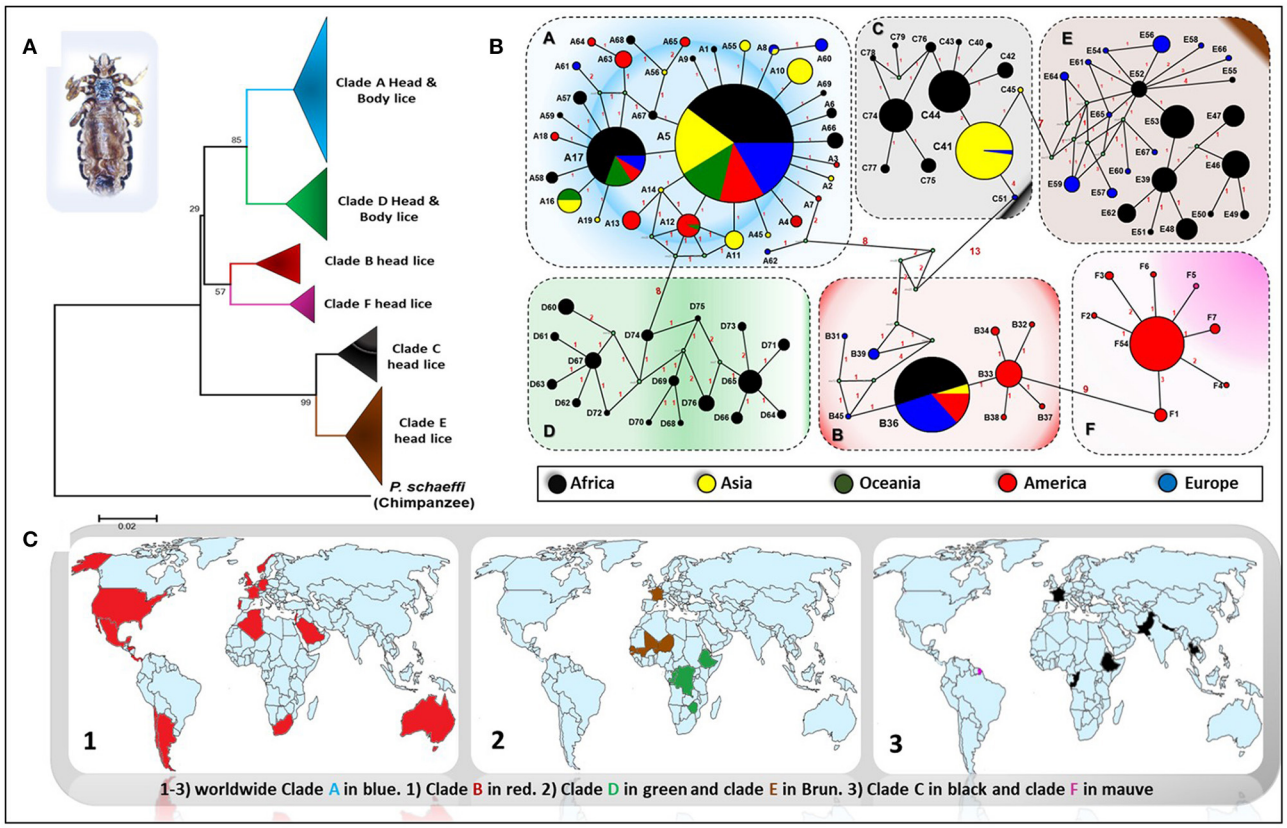

FIGURE 1 | Phylogeography of body and head lice haplogroups. **(A)** Neighbor-joining tree based on Cytb haplotypes. **(B)** Median Joining Network representing the existing relationships between different haplotypes. Pie colors and sizes in circles represent the continents and the number of their sequence for a haplotype. **(C)** Maps of the world showing the distribution of louse clades.

found in head lice from West African countries (in Senegal and Mali) (Amanzougaghene et al., 2017, 2019). This clade was also frequently recovered from migrants communities coming mainly from West African countries, as is the case of its detection among Nigerian refugees in Algeria and from migrant communities living in Bobigny, France (Candy et al., 2018a; Louni et al., 2018). Taken together, these data support the idea that all these louse clades accompanied our hominid ancestors since their migrations out of Africa (Li et al., 2010; Amanzougaghene et al., 2017).

Lice as Marker of Human Evolution

Because human lice are highly host specific and have been evolving in tandem with their primate hosts for a thousand of years, they offer a unique feature to reconstruct human migration and human evolutionary history, thereby complementing the hominin fossil records (Reed et al., 2004; Boutellis et al., 2014; Perry, 2014). Studies to date have only started to exploit this invaluable source of precious information (Perry, 2014). Indeed, phylogenetic analyses of *Pediculus* lice have confirmed some events in the human evolution. For instance, lice of human (*P. humanus*) and those of chimpanzee (*P. schaeffi*) have shared a common ancestor about 6 million years ago, which appears to be meeting to the estimated date for the divergence of their respective hosts (Reed et al., 2004, 2007). The lice population presents the genetic signature of a recent demographic expansion that occurred roughly 100,000 years ago, coinciding with the out-of-Africa expansion of modern human hosts, allowing us to use lice to learn about human migration, such as the travel itinerary and the timing of peopling the New Word (Reed et al., 2004; Ascunce et al., 2013). Reed et al. (2004) suggested that two ancient head louse clades (B and C), which originated before modern *Homo sapiens*, were from archaic hominins (Reed et al., 2004). They found that clade B head lice diverged from clade A between 0.7 and 1.2 Mya, and may have evolved on Neanderthals populated the Eurasian continent, whereas clade C is even more ancient (ca. 2 Mya) and may have evolved on *H. erectus* (Reed et al., 2004). Because head lice are primarily transmitted horizontally through a physical contact host-to-host, these data support the view of the existence of a direct contact of modern humans with archaic hominin species, and from which they have acquired a distinct lineages of head lice (Reed et al., 2004).

Lice have also helped to elucidating events in the history of human evolution that are absent or uncertain from host fossil or host DNA (Raoult et al., 2008), such as the date on which *H. sapiens* started wearing clothing by estimating the age of onset of the body louse, which would have evolved only after humans had worn these clothes since this louse lives exclusively in clothing

(Kittler et al., 2003). As recently suggested by Toups et al. (2011), based on the molecular dating of body louse, the use of clothing would have started between 83,000 and 170,000 years previous to what was expected (anywhere from 40 Ka to 3 Ma based on the emergence of eyed needles and the loss of body hair), and the use of clothing by *H. sapiens* probably originated in Africa and may have made it easier for them to move during frosty weathers as they traveled outside Africa and possibly around the planet earth (Toups et al., 2011).

All these studies demonstrate how lice can provide us with information about the mysteries of our evolution. Further studies on lice and other specific human host parasites, which carry a written record of our past in their DNA, will clarify other events of the human history, while extinct hominid species no longer exist to give us clues about our origins.

Paleoentomology

Paleoentomological investigations can provide relevant information on the antiquity of lice and their relationship with humans, ancient human migrations across the world and their sanitary conditions (Amanzougaghene et al., 2016b; Drali et al., 2016b). Human lice are most likely among the oldest permanent ectoparasites of humans (Mumcuoglu, 2008; Boutellis et al., 2014). In the Bible, louse infestations are described as the third plague (Mumcuoglu, 2008). Louse infestations of the ancient inhabitants of the Middle East have also been evidenced from the Sumerian, Akkadian, and Egyptian sources (Mumcuoglu, 2008). Moreover, the fossil record of lice and nits from different archaeological sites around the world has expanded greatly over the last 20 years (Drali et al., 2016b).

The oldest head louse nits were found on hair sample collected from an archaic human skeleton found in an archeological site in northeastern Brazil (Araújo et al., 2000). These samples were dated approximately to more than 10,000 years old, demonstrating that the lice were introduced into the New World through the earliest peoples (Araújo et al., 2000). In the Old World, the oldest head louse remains were recovered from an individual who lived in the Nahal Hemar cave near the Dead Sea in Israel during the Neolithic era, 9,000 years ago (Mumcuoglu, 2008). Head lice and their eggs have been recovered on mummified remains in Egypt, China, the Aleutian Islands, Greenland and South America (Drali et al., 2016b). Head lice combs from about 6,500 years ago, very similar to modern lice combs, were already used for delousing in the Pharaonic era in Egypt (Mumcuoglu, 2008). Head lice and their nits have been recovered in combs from different archaeological excavations sites in Egypt and Israel (Mumcuoglu, 2008; Drali et al., 2015a, 2016b; Amanzougaghene et al., 2016b).

The DNA analysis conducted on ancient louse samples provided valuable information to record past genetic structure and diversity of *Pediculus* lice that can be exploited to reconstruct ancient human evolutionary events (Amanzougaghene et al., 2016b; Drali et al., 2016b). However, so far, only a few genetic studies have focused on the remains of ancient lice. Thus, phylogenetic analysis of the remains of head lice eggs dating from the Chalcolithic and early Islamic periods found in Israel has shown that these remains can be associated with people from West Africa because they belonged to the mitochondrial subclade C (now known as clade E) specific to this region (Drali et al., 2015a). The analysis of pre-Columbian mummies' lice revealed that head lice belonged to clade A, had a pre-Columbian presence in the America, and would therefore be linked to the Old World (Raoult et al., 2008). Subsequent study conducted by Boutellis et al. (2013a) endorsed this finding and further reported that the presence of clade B head lice on the American continent dates back more than 4,000 years, before the arrival of European settlers, which support an American origin for this clade (Boutellis et al., 2013a). However, this hypothesis has been challenged by its recent discovery among the remains of head lice from 2,000 years ago, found in Israel, supporting a Middle Eastern origin for this clade, followed by its introduction to the American continent with the first people who set up there (Amanzougaghene et al., 2016b).

LICE-BORNE BACTERIAL DISEASE

Body Louse Associated Pathogens

Body louse is the major vector of three humans pathogenic bacteria, which are: *Rickettsia prowazekii, Borrelia recurrentis,* and *Bartonella quintana* (**Figure 2**) (Raoult and Roux, 1999; Brouqui, 2011). All these three bacterial pathogens have genomes that are smaller in size than their free-living close relatives (Veracx and Raoult, 2012). Body lice acquire infection during blood meals from an infected patient, carrying this infection for the remainder of their short life (Raoult and Roux, 1999). The transmission of these infections to uninfected people occurs through the feces or crushed bodies of infected lice, that contaminate the bite sites, conjunctiva, mucous membranes or microlesions of the skin (Raoult and Roux, 1999).

Rickettsia prowazekii is the causative agent of epidemic typhus, which caused significant health problems in times of war and social disorder (Raoult and Roux, 1999; Bechah et al., 2008). Despite the effectiveness of antibiotic treatment, the disease remains a serious health threat because it can reoccur at any time (Bechah et al., 2008; Brouqui, 2011). Indeed, healed patients can keep the infection from it for life and, under stressful conditions, the outbreak can occur as milder typhus, Brill-Zinsser's disease, which could be a source of new outbreaks if lice reappear (Bechah et al., 2008; Brouqui, 2011). Furthermore, since the infection with *R. prowazekii* can occur by inhalation, the bacterium is also classified as a biological selective agent (Bechah et al., 2008).

Borrelia recurrentis is a spirochete that causes relapsing fever (Raoult and Roux, 1999). In the past, massive epidemics have affected Africa and Eurasia, but nowadays the disease has persisted, particularly in Ethiopia and in other surrounding countries, and has recently emerged among travelers returning from endemic areas in Europe and North America (Bonilla et al., 2013; Antinori et al., 2016a,b).

Bartonella quintana, is well-known as the causative agent of trench fever, but it may also cause clinical manifestations, including chronic bacteremia, bacillary angiomatosis and endocarditis (Raoult and Roux, 1999; Brouqui, 2011). The disease was widespread in France during the Napoleonic Wars (1803–1815) and the two world wars (Raoult and Roux, 1999;

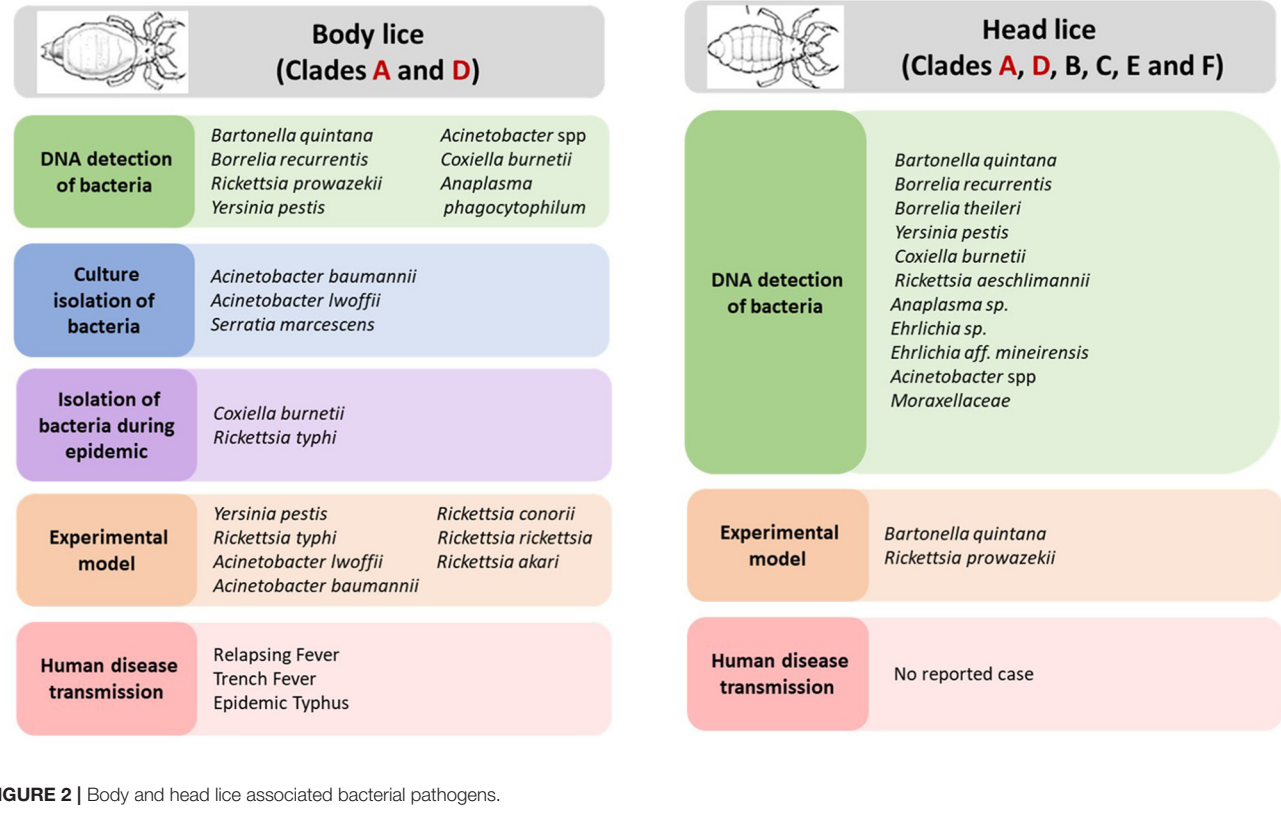

FIGURE 2 | Body and head lice associated bacterial pathogens.

Raoult et al., 2006). Currently, it is considered as a re-emerging pathogen in poor countries, and among homeless populations in the developed countries (Brouqui, 2011). It has long been agreed that *B. quintana* was transmitted only by body louse on humans, which is thought to be the sole reservoir. However, some human cases of *B. quintana* infection have been associated with kittens and flea-infested kittens (Raoult et al., 1994; Drancourt et al., 1996). The bacterium was also recovered from a cat's dental pulp (La et al., 2005) and in cat fleas collected in France (Rolain et al., 2003). These data suggest that cats may serve as reservoir hosts for *B. quintana* and may follow a transmission mode similar to that described for *B. henselae* in cat-scratch disease. In addition, *Pedicinus obtusus* lice and their macaque host have also been implicated in the transmission cycle of *B. quintana* (Li et al., 2013; Sato et al., 2015). The role of head louse as additional vector was also raised and discussed thereafter.

The combined evidence from laboratory and epidemiological studies strongly implicates body lice as a vector of *Yersinia pestis*, the causal agent of plague (Houhamdi et al., 2006; Piarroux et al., 2013). Body lice could be involved in plague pandemics that would better match the epidemiology of louse borne infections, this hypothesis has been established by paleomicrobiological studies (Raoult, 2016).

Moreover, the potential role of body louse as vectors for other pathogenic bacteria has also been suspected (**Figure 2**). Indeed, studies showed that experimentally infected body lice have the potential to acquire, to sustain and to transmit *R. conorii* (Mediterranean spotted fever, Indian tick typhus), *R. rickettsii* (Rocky Mountain spotted fever), which are both transmitted by ticks, and *R. akari* (rickettsial pox) and *R. typhi* (endemic or murine typhus), which are typically transmitted, respectively, by acari mites and insect fleas (Weyer, 1952; Houhamdi et al., 2003; Houhamdi and Raoult, 2006b). Furthermore, during an outbreak of murine typhus that occurred in northern China and India (Kashmir State), *R. typhi* has been isolated from body lice infesting the sick patients (Liu, 1944; Kalra and Rao, 1951). Initial field observations in East Africa reported that body lice recovered from an area where a Q fever outbreak that had took place 3 months before had been able to transmit *Coxiella burnetii* to guinea pigs (Giroud and Jadin, 1954; Babudieri, 1959). Subsequently, it was reported that *C. burnetii* infection of body lice could occur under experimental conditions (Babudieri, 1959). Other bacteria species, such as *Serratia marcescens Acinetobacter baumannii* and *A. lwoffii* have been linked with body lice, assuming that body lice may also transmit these agents (La Scola et al., 2001; Houhamdi and Raoult, 2006a).

Together, these studies suggested that body lice may carry a broad spectrum of pathogens bacteria. In addition, as blood-feeder insect lice are predisposed to absorb many other types of microorganisms, including viruses and hemoparasites, when they feed on their human host (such as *Babesia* or *Plasmodium*). Theoretically, it is possible that lice can transmit any of these agents, if they are ingested with blood meal and if they are able to survive in the insect's midgut (Raoult and Roux, 1999).

Moreover, the very reduced genome of human lice lacks many genes associated with immune response, odorant and gustatory receptors and detoxifying enzymes (Kirkness et al., 2010; Lee et al., 2010; Previte et al., 2014). The reduced number of defense mechanisms may facilitate the louse infection by different microorganisms. Furthermore, a recent study suggested that body louse phagocytes might host microbes and could be reservoirs for several unidentified pathogens (Coulaud et al., 2015). Therefore, the role of body lice as vectors of these microorganisms is an interesting research topic that deserves to be addressed in future studies.

Head Louse Associated Pathogens

In recent decades, there has been a growing recognition that head lice are vectors of pathogens, which has changed the long-established paradigm that only body lice are vectors of disease. Although it is currently agreed that body lice are the most powerful vectors of pathogens, the potential of head lice as disease vector is not yet fully understood.

Recently, several studies have performed comparative analyses in the immune responses following the bacterial challenge using *in vitro*-rearing system and have shown that body lice relative to head lice show a significant reduction in immune responses, particularly at the onset of the immune challenge (Kim et al., 2011, 2012, 2017; Previte et al., 2014). In one study in particular, Kim et al. (2017) demonstrated that, as in the case of body lice, head lice can withstand a persistent charge of *B. quintana* infection for several days following the acquisition in a bloodmeal and spread in their feces viable bacteria. However, the rates of proliferation in the gut and numbers of viable *B. quintana* in the feces were significantly lower in head lice compared to body lice (Kim et al., 2017). For example, in body lice, the *B. quintana* proliferation rate in the gut was significantly higher (2.0–12.1-fold) over time when compared with head lice until 12 days post-challenge. The viability index of *B. quintana* in the feces over the entire 11 days post-challenge was 6.4–10.6-fold higher in body lice compared to head lice (Kim et al., 2017). The reduction of the immune response in body lice may be partly the consequence for their increased competence as a vector, compared to head lice (Kim et al., 2011, 2012, 2017; Previte et al., 2014), which develop a more effective immune response to restrict bacterial replication.

Indeed, following *B. quintana* oral challenge, the transcriptional analysis of the immune response of the alimentary tract of body lice, revealed a reduction in the level of transcription of the main immune genes, including peptidoglycan recognition protein, defensins, and defensin 1, when compared to head lice. How this transcription repression occurs in body lice remains currently unknown (Kim et al., 2012, 2017). Kim et al. (2017) suggested that this regulation may be a consequence of regulatory changes in the epigenetic pathways and in the post-transcriptional miRNA-mediated factors (Kim et al., 2017). The level of reactive oxygen species, which is thought to be one of the key mediators of antimicrobial innate immunity defense in the insect gut (Molina-Cruz et al., 2008), was also reduced in body lice compared to head lice (Kim et al., 2017). Moreover, the role of endosymbiotic bacteria in the modulation of the host immune responses to pathogenic infections should be investigated (Kim et al., 2017). The impact of endosymbionts to insect antibacterial immune responses was already described in several insects (Eleftherianos et al., 2013). For example, the flies carrying the *Spiroplasma* endosymbiont have been shown to be more susceptible to septic injury with some Gram-negative bacteria, compared to flies lacking the endosymbiont. These results suggest that *Spiroplasma* endosymbionts are able to confer antibacterial immunity against certain bacterial pathogens in flies (Herren and Lemaitre, 2011).

Moreover, the fact that body and head lice have distinct ecological niches and have distinctly different feeding patterns, are additional factors that might influence the transmission of pathogens by lice. Body lice live in clothing where they must face the movements of the host's body to access blood, so they are under increased stress compared to head lice (Raoult and Roux, 1999; Veracx and Raoult, 2012). The effects of stress on immunity are well-known in insect vectors (Muturi et al., 2011) and may cause alterations that may lead to the reduced innate immune response observed in body lice against pathogenic bacteria. Similarly, the body lice are known to ingest large blood meal as compared to head lice (Brouqui, 2011; Veracx and Raoult, 2012). Absorption of larger meals of infectious blood may result in more bacteria entering the louse midgut, and therefore, a possible increase in infection.

Under laboratory conditions, head lice can also transmit *R. prowazekii*. The first evidence was reported by Goldberger and Anderson, who have successfully transmitted typhus to naïve rhesus macaques by subcutaneous inoculation of infected crushed head lice, recovered from patients with epidemic typhus (Goldberger and Anderson, 1912). Subsequently, this finding was confirmed by Murray and Torrey (1975) who showed that head lice feeding on rabbits infected with *R. prowazekii* can be easily infected and spread virulent organisms in their feces, thus demonstrating that head lice have the potential to transmit pathogenic bacteria when placed under favorable epidemiological conditions (Murray and Torrey, 1975). In addition, it has been proposed that this louse could also be implicated in the transmission and maintenance of this pathogen in the nature (Robinson et al., 2003).

In recent years, several pathogenic bacteria DNA have been increasingly reported in head lice in many parts of the world (**Figure 2**). Detailed results on the epidemiological studies are reported in **Table 1**. For instance, *B. quintana* was the most frequently found in head lice belonging to clades A, D, E, and C. Furthermore, it is important to underline that, except one reported case of its detection in lice collected from school children (Eremeeva et al., 2017), all other cases occurred on lice infesting deprived populations living in poverty and lacking standard medications (**Table 1**). An interesting study of head lice collected from the rural population of Senegal, where several cases of trench fever have occurred, showed that several head lice were positive for *B. quintana*. These findings, together with the absence of body lice from this area for more than 30 years, strongly implicate head lice as the principal acting in maintaining the cycle of transmission of *B. quintana* among the population concerned (Diatta et al., 2014).

TABLE 1 | Bacteria species found in head lice using molecular methods.

Pathogen	Lice tested (% positive)	Louse-clade	Collection year	Population	Country	Co-occurrence of body louse	Comment	References
B. quintana	21 (9.5%)	–	2002	Homeless and school children	Nepal	Yes	All lice collected from school children were *B. quintana* negatives	Sasaki et al., 2006
	15 pools (20%)	–	2007–2008	Homeless persons	California-USA	Not all	–	Bonilla et al., 2009
	16 pools (37.5%)	–	2008–2010, 2012	Homeless persons	California-USA	Not all	–	Bonilla et al., 2014
	3 pools nits (100%)	–	–	Homeless persons	France	No	Attempt to cultivate *B. quintana* from these nits was failed	Angelakis et al., 2011b
	35 (17.1%)	A and D	2010	Persons living in a highly plague-endemic area	Congo RDC	Yes	–	Piarroux et al., 2013; Drali et al., 2015b
	35 (2.85%)	–	2011	Patients with louse-borne relapsing fever	Ethiopia	Yes	–	Boutellis et al., 2013b
	65 pools (9.2%)	–	2010	Street beggars (in poorer regions)	Ethiopia	–	More pools of head lice were found positive than body lice	Cutler et al., 2012
	271 (7%)	C	–	Persons living at locations at different altitudes	Ethiopia	Not all	*B. quintana* in head lice was positively linked to altitude (>2,121 m). At this altitude all body lice were *B. quintana* negatives	Angelakis et al., 2011a
	274 (6.93%)	A and E	2010–2011	Persons living in poor conditions	Senegal	No	–	Boutellis et al., 2012
	381 (0.52)	A	2011	Rural community	Senegal	–	–	Sangaré et al., 2014
	148 (1.3%)	A	2011	Rural villagers living in poor conditions	Senegal	No	Co-occurrence of trench fever cases with absence of body lice for more than 30 years in the studied area	Diatta et al., 2014
	75 (2.66)	A	2010–2011	Rural community with low income	Madagascar	–	–	Sangaré et al., 2014
	600 (0.5%)	E	2013	Rural villagers living in poor conditions	Mali	No	Apparently healthy individuals, low socioeconomic level	Amanzougaghene et al., 2017
	168 (10.3%)		2013–2015	School children	Georgia-USA	No	The *kdr*-permethrin resistance (T917I mutation) was detected in 99.9% of 168 lice tested	Eremeeva et al., 2017
B. recurrentis	35 (22.8%)	–	2011	Patients with louse-borne relapsing fever	Ethiopia	Not all	4 of 5 patients were co-infested with body louse	Boutellis et al., 2013b
	630 (1.6%)	A	2015	Pygmy populations, living in poor conditions	Republic of Congo	No	–	Amanzougaghene et al., 2016a
Y. pestis	35 (2.86%)	A	2010	Persons living in a highly plague-endemic area	Congo RDC	Yes	–	Piarroux et al., 2013; Drali et al., 2015b

(Continued)

TABLE 1 | Continued

Pathogen	Lice tested (% positive)	Louse-clade	Collection year	Population	Country	Co-occurrence of body louse	Comment	References
B. theileri	630 (0.16%)	A	2015	Pygmy populations, living in poor conditions	Republic of Congo	No	–	Amanzougaghene et al., 2016a
C. burnetii	600 (1.16%)	E	2013	Rural villagers living in poor conditions	Mali	No	MST genotype 35 and new genotype (genotype 59)	Amanzougaghene et al., 2017
	37 (8.10%)	E	2016	Niger's refugees arriving in Algeria, living in poor conditions	Algeria	No	–	Louni et al., 2018
R. aeschlimannii	600 (0.6%)	E	2013	Rural villagers living in poor conditions	Mali	No	Apparently healthy individuals, low socioeconomic level	Amanzougaghene et al., 2017
Anaplasma	600 (0.3%)	E	2013	Rural villagers living in poor conditions	Mali	No	Potential new species	Amanzougaghene et al., 2017
Ehrlichia	600 (2.3%)	E	2013	Rural villagers living in poor conditions	Mali	No	*E. aff. mineirensis* and potential new species	Amanzougaghene et al., 2017
Acinetobacter	288 (33%)	–	2008–2009	School children	France	–	–	Bouvresse et al., 2011
	115 (47%)	A and C	–	Healthy individuals	Ethiopia	Yes	13 of 23 lice sequenced were *A. baumannii*	Kempf et al., 2012
	275 (3.62%)	A and C	2013–2014	School children	Thailand	No	Species: *A. baumannii, A. radioresistens,* and *A. schindleri*	Sunantaraporn et al., 2015
	630 (31.1%)	A, C, and D	2015	Pygmy populations, living in poor conditions	Republic of Congo	No	Species: *A. junii, A. ursingii, A. baumannii, A. johnsonii, A. schindleri, A. lwoffii, A. nosocomialis,* and *A. towneri*	Amanzougaghene et al., 2016a
	52 (80.8%)	–	2013–2015	School children	Georgia-USA	No	–	Eremeeva et al., 2017
	235 (11.5%)	A, B, and E	2015–2016	Middle-class suburban families	France	No	*A. baumannii*, *A. calcoaceticus, A. nosocomialis*, *A. junii,* and 2 potential new species (*Candidatus* Acinetobacter Bobigny-1 and 2)	Candy et al., 2018a
	64 (27%)	A and B	2014	School children	Algeria	No	*A. baumannii, A. johnsonii,* and *A. variabilis*	Mana et al., 2017
	37 (46.94%)	E	2016	Niger's refugees arriving in Algeria	Algeria	No	*A. baumannii*	Louni et al., 2018
Moraxellaceae	630 (0.95%)	A	2015	Pygmy populations, living in poor conditions	Republic of Congo	No	New species	Amanzougaghene et al., 2016a

The DNA of this bacterium was also recovered in head louse nits from homeless individuals in Marseille. This funding strongly support a possible vertical transmission of this pathogen in lice (Angelakis et al., 2011b). A study performed on lice from persons at various locations in Ethiopia revealed that head lice infection by *B. quintana* was linked to high altitude (Angelakis et al., 2011a). Interestingly, the head lice collected from persons living at higher altitudes (>2,121 m) were *B. quintana* positive (24% of 79), while at these altitudes, none of the 63 tested body lice were found to be infected with *B. quintana* (Angelakis et al., 2011a). This finding raises important question about the possible relationship of the head lice vectorial capacity and environmental-ecological factors that may drive force underpinning the transmission potential in some geographic areas.

Borrelia recurrentis was detected in clade C head lice from patients suffering with louse-borne relapsing fever living in poor regions from Ethiopia, and more recently in head lice clade A from hunter-gatherer pygmy individuals in the Republic of the Congo (Boutellis et al., 2013b; Amanzougaghene et al., 2016a). The *Y. pestis* DNA was also found in clade A head lice infesting individuals from a highly endemic plague area in the eastern Congo (Piarroux et al., 2013; Drali et al., 2015b). Other human pathogenic bacteria, which are not usually associated with lice transmission, such as *C. burnetii, R. aeschlimannii,* and potential new species from the *Anaplasma* and *Ehrlichia* genera were also detected in head lice (Amanzougaghene et al., 2017). Moreover, the DNA of Ixodid hard tick-associated *B. theileri*, which is not known to infect humans, was also detected in one head louse infesting an African pygmy from the Republic of Congo (Amanzougaghene et al., 2016a). As head lice feed only on human blood, the authors suggested that the acquired louse infection would be from the blood of patients with ongoing bacteremia (Amanzougaghene et al., 2016a). However, whether this spirochete is able to infect human is currently not known and requires further investigation.

Head louse infection with all of the above pathogenic bacteria most likely occurs among the most vulnerable and poor populations living in poverty and poor hygiene, the same conditions that usually lead to the proliferation of body louse ecotype and the emergence of louse-borne diseases (Raoult and Roux, 1999; Brouqui, 2011). This point of view is also supported by the fact that most studies on head lice infesting schoolchildren and populations living in more hygienic conditions have failed to detect these pathogenic bacteria (Fournier et al., 2002; Bouvresse et al., 2011; Sunantaraporn et al., 2015; Candy et al., 2018a).

However, head lice infection with *Acinetobacter* is an exception, as several species have been detected with high prevalence in head lice, as well as in body lice everywhere they have been sought, reflecting the ubiquitous occurrence of these bacterial species (Bouvresse et al., 2011; Sunantaraporn et al., 2015; Amanzougaghene et al., 2016a; Candy et al., 2018a). This widespread infection of human lice suggests that they could be a preferential host for these bacteria. Nevertheless, it remains to be determined whether these strains of *Acinetobacter* found in lice are the same as those causing infections in humans (Amanzougaghene et al., 2016a; Candy et al., 2018a). In addition, the susceptibility of these isolates to antibiotics is currently unknown. In one study, Vallenet et al. (2008) showed that phenotypic and genotypic characteristics of the human multidrug resistant isolate *A. baumannii* AYE significantly differ from the SDF strain isolated from body lice (Vallenet et al., 2008). Further studies are warranted to compare both phenotypic and genotypic characteristics, as well as antimicrobial susceptibility of louse derived *Acinetobacter* isolates. Greater attention is given to extra-hospital reservoirs of these opportunistic bacteria and their potential involvement in emerging human community-acquired infections, as drug-resistant strains worldwide are increasingly being identified (Eveillard et al., 2013).

Based on the combined evidence of both epidemiological and laboratory studies, we believe that head lice can transmit disease to their human host under favorable epidemiological conditions, although its vectorial capacity is weaker compared to body lice. Therefore, given the scale of head louse infestations around the world and the emergence and spread of insecticides resistance, this pest is warranting more attention as a serious public health problem. For instance, epidemiological studies on louse specimens collected worldwide to investigate the diversity of pathogenic bacteria associated with head lice, but also for body lice, are missing. Regarding experimental models, the vectorial competence of lice should be investigated for pathogenic bacteria, such as *C. burnetii*, and other pathogenic bacteria, which are not usually associated with lice.

CONTROL OF LICE INFESTATIONS AND EVOLUTION OF INSECTICIDE RESISTANCE

Therapeutic Options for Pediculosis Treatment

There are many therapeutic options for pediculosis, including chemical insecticides, topically applied physical agents (**Table 2**), herbal formulations and mechanical methods (combs and heating devices) (Bonilla et al., 2013; Feldmeier, 2014; Sangaré et al., 2016a). However, the recourse to chemical insecticides with an insect neurotoxic mode of action is still the method of choice and the most extensively used approach (Durand et al., 2012; Clark et al., 2013). These include organochloride (lindane), organophosphates (malathion), carbamates (carbaryl), pyrethrins (extract of chrysanthemum), and pyrethroids (synthetic derivates of pyrethrins: permethrin, phenothrin, and deltamethrin) (**Table 2**) (Durand et al., 2012; Bonilla et al., 2013; Clark et al., 2013). Among them, malathion and permethrin remain the most widely used pediculicides since their introduction on the market in 1971 and 1992, respectively (Durand et al., 2012; Clark et al., 2013).

Unfortunately, the wider use of conventional pediculicides has resulted in the emergence and rapid propagation of resistant lice populations in many regions of the world (Durand et al., 2012; Clark et al., 2013). This has prompted research into the development of compounds with other modes of action. Ivermectin and spinosad seem to be the most hopeful new pediculicides. They have generated interest in their new

TABLE 2 | Main Therapeutic options for pediculosis treatment.

Pediculicide	Class	Mechanism of action	Adulticide/ovicidal activities	Documented adverse health effect	Documented resistance in lice	References
PEDICULICIDE WITH A NEUROTOXIC MODE OF ACTION						
DDT, dichlorodiphenyltrichloroethane	Organochloride	Opening of sodium ion channels in neurons	Yes/yes	Toxic	Yes	Durand et al., 2012; Bonilla et al., 2013
Lindane	Organochloride	Inhibition of c-aminobutyric acid- gated chloride channel	Yes/yes	Toxic	Yes	Durand et al., 2012; Bonilla et al., 2013
Natural pyrethrins	Chrysanthemum extract	Delayed repolarization of voltage-gated	Yes/no	Minor	Yes	Bonilla et al., 2013
Permethrin, synthetic pyrethrin	(+)-3-phenoxybenzyl 3-(2,2-dichlorovinyl)-2,2, dimethyl cyclopropan carboxylate	The same as natural pyrethrins	Yes/no	Minor	Yes	Durand et al., 2012; Bonilla et al., 2013; Clark et al., 2013
Malathion	Organophosphate	Irreversible inhibition of acetylcholinesterase	Yes/no	Minor	Yes	Durand et al., 2012; Bonilla et al., 2013; Kwon et al., 2014
Carbaryl	Carbamate	Irreversible inhibition of acetylcholinesterase	Yes/no	Moderate to very toxic	Yes	Durand et al., 2012; Bonilla et al., 2013
Ivermectin*	Macrocyclic lactone	Binding to glutamate-gated chloride ion channels	Yes/no	None to minimal	Yes	Chosidow et al., 2010; Clark et al., 2013; Diatta et al., 2016
Spinosad	Macrocyclic lactone	Overstimulates nerve cells by acting like acetylcholine	Yes/yes	Minor	No	Aditya and Rattan, 2012; Feldmeier, 2014
PEDICULICIDE WITH PHYSICAL MODE OF ACTION						
Dimeticone	Synthetic silicone oils	Work by occlusion	Yes/yes	Low	No	Durand et al., 2012; Burgess et al., 2013; Feldmeier, 2014
Isopropyl myristate	Ester	Work by occlusion or by dissolving cuticle wax	Only head lice tested	Minimal	No	Feldmeier, 2014
1,2-octanediol	Detergent	Dehydration by reducing the ability of louse to prevent water loss through the cuticle	Yes/no	Minimal	No	Burgess et al., 2012; Feldmeier, 2014; Burgess and Silverston, 2015
Benzyl alcohol	Aromatic alcohol	Asphyxiates lice by "stunning" the spiracles open	Yes/no	Minimal	No	Meinking et al., 2010

**Ivermectin is the only pediculicide used on topical and oral administrations whereas the other pediculicides are only available through topical applications.*

neurotoxic modes of action; have low mammalian toxicity and relatively low cross-resistance with commonly used conventional pediculicides (Chosidow et al., 2010; Aditya and Rattan, 2012; Bonilla et al., 2013; Clark et al., 2015). In addition, ivermectin is the only drug currently used for oral treatment, and its highly effectiveness was clinically approved for both louse ecotypes treatment (Foucault et al., 2006; Chosidow et al., 2010), although empirically noted ivermectin resistance has started to be reported in the field in Senegal (Diatta et al., 2016).

There is also growing interest in the use of natural products such as pediculicides based on plant-derived essential oils (eucalyptus oil and tea tree oil) or with a purely physical mode of action, such as dimeticone and benzyl alcohol (Meinking et al., 2010; Burgess et al., 2013; Candy et al., 2018b), but little attention has been given to their clinical evaluation for effectiveness, even though some of them are already commercialized.

Insecticide Resistance

Insecticide resistance leading to treatment failure is considered a crucial factor in the increasing incidence of head lice infestations (Durand et al., 2012; Bonilla et al., 2013). Resistance is an established trait that an insect pest acquires over time through selective pressure from continuous or inappropriate insecticide use (Durand et al., 2012). The recently sequenced body louse genome provides a unique opportunity to address fundamental issues related to the molecular mechanisms that determine the insecticides resistances, which is fundamental to ensure the longest possible active lifespan of existing insecticides and to accelerate the achievement of sustainable, new, and effective strategies to control pest infestations (Kirkness et al., 2010; Clark et al., 2015).

Possible resistance mechanisms include knockdown-resistance in the case of permethrin, which is the result of three-point mutations (M815I, T917I, and L920) within the α-subunit gene of the voltage-gated sodium channel, and enhanced activity of a carboxylesterase enzyme was found to be chiefly responsible for the resistance to malathion (Clark, 2009; Kwon et al., 2014). Recently, a researcher from our team documented the first field resistance to ivermectin observed in head lice recovered in rural populations from Senegal (Diatta et al., 2016).

Genetic analysis of these lice by targeting GluCl gene, which is the primary target-site of ivermectin and already known to be implicated in resistance of arthropods and nematodes, revealed the presence of three relevant non-synonymous mutations (A251V, H272R, and S46P) that may be responsible for the treatment failure (Amanzougaghene et al., 2018a).

In addition, in another study, a proteomic comparison of laboratory-sensitive lice (wild type) and ivermectin-selected resistant lice found that a complexin was most significatively suppressed in resistant lice. A complexin is a neuronal protein that is known to be one of the main regulators of neurotransmitter release. DNA-mutation analysis revealed that some complexin transcripts from resistant lice gained a premature stop codon. The association between complexin and ivermectin-resistance was further confirmed by RNA-interfering and found that the knocking down complexin expression induces resistance to ivermectin in the susceptible lice. All together, these results provide a convincing evidence that complexin plays a significant role in regulating ivermectin resistance in the body louse and represents the first evidence that links complexin to insecticide resistance (Amanzougaghene et al., 2018b). Although, how this resistance effect is mediated requires further elucidation.

New Therapeutic Approaches

Symbiotic Therapy

This approach incited great interest for potential applications in public health entomology (Sassera et al., 2013) and has the advantage to target the bacteria susceptible to antibiotics (Sassera et al., 2013). Since the *Pediculus* lice' primary endosymbiont, *Candidatus* Riesia pediculicola, is essential to the metabolism of their louse host, related to its ability of synthesizing B-group vitamins, the harmful effect exerted by the antibiotic treatment should have repercussions on the host (Kirkness et al., 2010; Sangaré et al., 2016a). A first case report showed that antibiotic treatment (trimethoprim and sulfamethoxazole), administered to treat a respiratory infection in a 12-year-old girl, had the side effect of head lice death (Shashindran et al., 1978). Subsequently, studies conducted by Sangaré et al. (2015) demonstrated the effectiveness of this therapy under laboratory conditions and showed that antibiotics (such as doxycycline, erythromycin, rifampicin, and azithromycin) kill lice via their direct activity on their symbiotic bacteria. In addition, the combination of this antibiotic with ivermectin has proven to be very effective compared to ivermectin alone in the treatment and prevention of body lice (Sangaré et al., 2016b). This approach could be employed to eradicate lice and could potentially retard the apparition of resistance to ivermectin (Sangaré et al., 2016b). This approach is a promising therapy but has not yet been the subject of field studies.

RNAi-Based Insecticides

RNA interference (RNAi) is a promising and safe environmentally friendly method for insect control (Das et al., 2015). This technology is initiated by the presence of a small interfering RNA (siRNA) or double-stranded RNA (dsRNA) to trigger post-transcriptional gene silencing (Das et al., 2015). RNAi can induce mortality, create phenotypes that are beneficial for insect control and prevent insecticide resistance in insect pests (Gordon and Waterhouse, 2007; Airs and Bartholomay, 2017). Currently, the greater potential of this technology for successful future management of pest insects is widely recognized and holds great promise (Baum et al., 2007; Airs and Bartholomay, 2017). Therefore, it is exciting to consider its role in lice control as a promising alternative to chemical insecticides, to specifically to suppress the expression of essential genes that lead to death (Scott et al., 2013). Two lines of evidence support its potential use as control strategy in lice. First, the analysis of body louse genome has been shown to contain the necessary genes for RNAi machinery (Pittendrigh et al., 2013). Subsequently, the studies conducted on both body and head lice confirmed that the injection of dsRNA to these two ecotypes can efficiently repress the expression of target genes (Yoon et al., 2011; Kwon et al., 2014). A second beneficial of using this technology in *Pediculus* lice is the lack of gene redundancy in its small genome. Thus, a smaller set of genes can be investigated to identify which one is essential for a given biological process (Pittendrigh et al., 2013). A priority for the future should focus on the identification of effective target genes for RNAi and, subsequently, on the exploration of delivery methods using field-proven applications (Pittendrigh et al., 2013). Finally, although technically realizable, it remains to be defined whether such strategies could comply with the requirements of regulatory authorities and whether an economically attractive strategy can be implemented to use RNAi approach to fight against lice (Pittendrigh et al., 2013).

CONCLUDING REMARKS AND FUTURE PERSPECTIVES

In the twenty-first century, human lice infestation remains widespread all over the world. Surprising new discoveries into the biology, epidemiology, and the evolutionary history of lice, their bacterial disease agents and control strategies have further stimulated a renewal of interest in this bloodsucking insect. In recent years, knowledge about lice has evolved, with the sequencing of the body lice genome and the development of transcriptomes of body and head lice. However, functional and comparative genomics of the fundamental aspects of lice biology is still in its infancy and many aspects are not yet well-understood and remain to be discovered.

Additional efforts will be necessary to shed the light on lice biology. Whole genome sequencing of head lice belonging to different clades with integration of high-throughput technologies to study global changes in mRNA transcription, translation and computational approaches, will accelerate the addressing of important biological questions, identification, and exploitation of new target genes of this insect vector, insecticide discovery, as well as to develop novel therapies. Although our knowledge of the vector competence of head lice is increasing, there is still a need to explore factors that can influence the difference observed between body and head lice, such as the influence of the immune response and microbiota (especially the

role of endosymbiotic bacteria). Such factors, once addressed, will provide us with a better understanding of effective lice control and prevention strategies for re-emerging diseases. Finally, because *P. humanus* is one of the oldest parasites of human which carries a written record of our past in its DNA, integrating phylogenomic and genomic population patterns in lice will provide a more complete picture of the evolution of this parasite and clarify additional events in our evolutionary history.

AUTHOR CONTRIBUTIONS

NA, OM, FF, and DR conceived the paper. NA wrote the paper.

FUNDING

This work was supported by the Fondation Méditerranée Infection and the French National Research Agency under the Investissements d'avenir program, reference ANR-10-IAHU-03.

REFERENCES

Aditya, S., and Rattan, A. (2012). Spinosad: an effective and safe pediculicide. *Indian Dermatol. Online J.* 3, 213–214. doi: 10.4103/2229-5178.101825

Airs, P. M., and Bartholomay, L. C. (2017). RNA interference for mosquito and mosquito-borne disease control. *Insects* 8:E4. doi: 10.3390/insects8010004

Alpatov, V., and Nastukova, O. (1955). Transformation of the head form of *Pediculus humanus* into the body form under changed conditions of existence. *Bull Mosc. Nat Hist Res Soc*. 60, 79–92.

Al-Shahrani, S. A., Alajmi, R. A., Ayaad, T. H., Al-Shahrani, M. A., and Shaurub, E.-S. H. (2017). Genetic diversity of the human head lice, *Pediculus humanus capitis*, among primary school girls in Saudi Arabia, with reference to their prevalence. *Parasitol. Res.* 116, 2637–2643. doi: 10.1007/s00436-017-5570-3

Amanzougaghene, N., Akiana, J., Mongo Ndombe, G., Davoust, B., Nsana, N. S., Parra, H.-J., et al. (2016a). Head lice of pygmies reveal the presence of relapsing fever borreliae in the Republic of Congo. *PLoS Negl. Trop. Dis.* 10:e0005142. doi: 10.1371/journal.pntd.0005142

Amanzougaghene, N., Fenollar, F., Davoust, B., Djossou, F., Ashfaq, M., Bitam, I., et al. (2019). Mitochondrial diversity and phylogeographic analysis of *Pediculus humanus* reveals a new Amazonian clade "F." *Infect. Genet. Evol.* 70, 1–8. doi: 10.1016/j.meegid.2019.02.006

Amanzougaghene, N., Fenollar, F., Diatta, G., Sokhna, C., Raoult, D., and Mediannikov, O. (2018a). Mutations in GluCl associated with field ivermectin-resistant head lice from Senegal. *Int. J. Antimicrob. Agents*. 52, 593–598. doi: 10.1016/j.ijantimicag.2018.07.005

Amanzougaghene, N., Fenollar, F., Nappez, C., Ben-Amara, A., Decloquement, P., Azza, S., et al. (2018b). Complexin in ivermectin resistance in body lice. *PLoS Genet.* 14:e1007569. doi: 10.1371/journal.pgen.1007569

Amanzougaghene, N., Fenollar, F., Sangaré, A. K., Sissoko, M. S., Doumbo, O. K., Raoult, D., et al. (2017). Detection of bacterial pathogens including potential new species in human head lice from Mali. *PLoS ONE* 12:e0184621. doi: 10.1371/journal.pone.0184621

Amanzougaghene, N., Mumcuoglu, K. Y., Fenollar, F., Alfi, S., Yesilyurt, G., Raoult, D., et al. (2016b). High ancient genetic diversity of human lice, *Pediculus humanus*, from Israel reveals new insights into the origin of clade B lice. *PLoS ONE* 11:e0164659. doi: 10.1371/journal.pone.0164659

Angelakis, E., Diatta, G., Abdissa, A., Trape, J.-F., Mediannikov, O., Richet, H., et al. (2011a). Altitude-dependent *Bartonella quintana* genotype C in head lice, Ethiopia. *Emerg. Infect. Dis.* 17, 2357–2359. doi: 10.3201/eid1712.110453

Angelakis, E., Rolain, J.-M., Raoult, D., and Brouqui, P. (2011b). *Bartonella quintana* in head louse nits. *FEMS Immunol. Med. Microbiol.* 62, 244–246. doi: 10.1111/j.1574-695X.2011.00804.x

Antinori, S., Mediannikov, O., Corbellino, M., Grande, R., Parravicini, C., Bestetti, G., et al. (2016a). Louse-borne relapsing fever (*Borrelia recurrentis*) in a Somali refugee arriving in Italy: a re-emerging Infection in Europe? *PLoS Negl. Trop. Dis.* 10:e0004522. doi: 10.1371/journal.pntd.0004522

Antinori, S., Mediannikov, O., Corbellino, M., and Raoult, D. (2016b). Louse-borne relapsing fever among East African refugees in Europe. *Travel Med. Infect. Dis.* 14, 110–114. doi: 10.1016/j.tmaid.2016.01.004

Araújo, A., Ferreira, L. F., Guidon, N., Maues da Serra Freire, N., Reinhard, K. J., and Dittmar, K. (2000). Ten thousand years of head lice infection. *Parasitol. Today* 16:269. doi: 10.1016/S0169-4758(00)01694-X

Ascunce, M. S., Fane, J., Kassu, G., Toloza, A. C., Picollo, M. I., González-Oliver, A., et al. (2013). Mitochondrial diversity in human head louse populations across the Americas. *Am. J. Phys. Anthropol.* 152, 118–129. doi: 10.1002/ajpa.22336

Ashfaq, M., Prosser, S., Nasir, S., Masood, M., Ratnasingham, S., and Hebert, P. D. N. (2015). High diversity and rapid diversification in the head louse, *Pediculus humanus* (*Pediculidae*: *Phthiraptera*). *Sci. Rep.* 5:14188. doi: 10.1038/srep14188

Babudieri, B. (1959). Q fever: a zoonosis. *Adv. Vet. Sci.* 5, 82–182.

Baum, J. A., Bogaert, T., Clinton, W., Heck, G. R., Feldmann, P., Ilagan, O., et al. (2007). Control of coleopteran insect pests through RNA interference. *Nat. Biotechnol.* 25, 1322–1326. doi: 10.1038/nbt1359

Bechah, Y., Capo, C., Mege, J.-L., and Raoult, D. (2008). Epidemic typhus. *Lancet Infect. Dis.* 8, 417–426. doi: 10.1016/S1473-3099(08)70150-6

Bonilla, D. L., Cole-Porse, C., Kjemtrup, A., Osikowicz, L., and Kosoy, M. (2014). Risk factors for human lice and bartonellosis among the homeless, San Francisco, California, USA. *Emerg. Infect. Dis.* 20, 1645–1651. doi: 10.3201/eid2010.131655

Bonilla, D. L., Durden, L. A., Eremeeva, M. E., and Dasch, G. A. (2013). The biology and taxonomy of head and body lice–implications for louse-borne disease prevention. *PLoS Pathog.* 9:e1003724. doi: 10.1371/journal.ppat.1003724

Bonilla, D. L., Kabeya, H., Henn, J., Kramer, V. L., and Kosoy, M. Y. (2009). *Bartonella quintana* in body lice and head lice from homeless persons, San Francisco, California, USA. *Emerg. Infect. Dis.* 15, 912–915. doi: 10.3201/eid1506.090054

Boutellis, A., Abi-Rached, L., and Raoult, D. (2014). The origin and distribution of human lice in the world. *Infect. Genet. Evol.* 23, 209–217. doi: 10.1016/j.meegid.2014.01.017

Boutellis, A., Bitam, I., Fekir, K., Mana, N., and Raoult, D. (2015). Evidence that clade A and clade B head lice live in sympatry and recombine in Algeria. *Med. Vet. Entomol.* 29, 94–98. doi: 10.1111/mve.12058

Boutellis, A., Drali, R., Rivera, M. A., Mumcuoglu, K. Y., and Raoult, D. (2013a). Evidence of sympatry of clade a and clade B head lice in a pre-Columbian Chilean mummy from Camarones. *PLoS ONE* 8:e76818. doi: 10.1371/journal.pone.0076818

Boutellis, A., Mediannikov, O., Bilcha, K. D., Ali, J., Campelo, D., Barker, S. C., et al. (2013b). *Borrelia recurrentis* in head lice, Ethiopia. *Emerg. Infect. Dis.* 19, 796–798. doi: 10.3201/eid1905.121480

Boutellis, A., Veracx, A., Angelakis, E., Diatta, G., Mediannikov, O., Trape, J.-F., et al. (2012). *Bartonella quintana* in head lice from Sénégal. *Vector Borne Zoonotic Dis.* 12, 564–567. doi: 10.1089/vbz.2011.0845

Bouvresse, S., Socolovshi, C., Berdjane, Z., Durand, R., Izri, A., Raoult, D., et al. (2011). No evidence of *Bartonella quintana* but detection of *Acinetobacter baumannii* in head lice from elementary schoolchildren in Paris. *Comp. Immunol. Microbiol. Infect. Dis.* 34, 475–477. doi: 10.1016/j.cimid.2011.08.007

Boyd, B. M., Allen, J. M., Nguyen, N.-P., Vachaspati, P., Quicksall, Z. S., Warnow, T., et al. (2017). Primates, lice and bacteria: speciation and genome evolution in the symbionts of hominid lice. *Mol. Biol. Evol.* 34, 1743–1757. doi: 10.1093/molbev/msx117

Boyd, B. M., and Reed, D. L. (2012). Taxonomy of lice and their endosymbiotic bacteria in the post-genomic era. *Clin. Microbiol. Infect.* 18, 324–331. doi: 10.1111/j.1469-0691.2012.03782.x

Brouqui, P. (2011). Arthropod-borne diseases associated with political and social disorder. *Annu. Rev. Entomol.* 56, 357–374. doi: 10.1146/annurev-ento-120709-144739

Burgess, I. F., Brunton, E. R., and Burgess, N. A. (2013). Single application of 4% dimeticone liquid gel versus two applications of 1% permethrin creme rinse for treatment of head louse infestation: a randomised controlled trial. *BMC Dermatol.* 13:5. doi: 10.1186/1471-5945-13-5

Burgess, I. F., Lee, P. N., Kay, K., Jones, R., and Brunton, E. R. (2012). 1,2-Octanediol, a novel surfactant, for treating head louse infestation: identification of activity, formulation, and randomised, controlled trials. *PLoS ONE* 7:e35419. doi: 10.1371/journal.pone.0035419

Burgess, I. F., and Silverston, P. (2015). Head lice. *BMJ Clin. Evid.* 2015:1703.

Candy, K., Amanzougaghene, N., Izri, A., Brun, S., Durand, R., Louni, M., et al. (2018a). Molecular survey of head and body lice, *Pediculus humanus*, in France. *Vector Borne Zoonotic Dis.* 18, 243–251. doi: 10.1089/vbz.2017.2206

Candy, K., Nicolas, P., Andriantsoanirina, V., Izri, A., and Durand, R. (2018b). *In vitro* efficacy of five essential oils against *Pediculus humanus capitis*. *Parasitol. Res.* 117, 603–609. doi: 10.1007/s00436-017-5722-5

Chosidow, O. (2000). Scabies and pediculosis. *Lancet* 355, 819–826. doi: 10.1016/S0140-6736(99)09458-1

Chosidow, O., Giraudeau, B., Cottrell, J., Izri, A., Hofmann, R., Mann, S. G., et al. (2010). Oral ivermectin versus malathion lotion for difficult-to-treat head lice. *N. Engl. J. Med.* 362, 896–905. doi: 10.1056/NEJMoa0905471

Clark, J. M. (2009). Determination, mechanism and monitoring of knockdown resistance in permethrin-resistant human head lice, *Pediculus humanus capitis*. *J. Asia Pac. Entomol.* 12, 1–7. doi: 10.1016/j.aspen.2008.10.007

Clark, J. M., Yoon, K. S., Kim, J. H., Lee, S. H., and Pittendrigh, B. R. (2015). Utilization of the human louse genome to study insecticide resistance and innate immune response. *Pestic. Biochem. Physiol.* 120, 125–132. doi: 10.1016/j.pestbp.2014.11.008

Clark, J. M., Yoon, K. S., Lee, S. H., and Pittendrigh, B. R. (2013). Human lice: past, present and future control. *Pestic. Biochem. Physiol.* 3, 162–171. doi: 10.1016/j.pestbp.2013.03.008

Coulaud, P.-J., Lepolard, C., Bechah, Y., Berenger, J.-M., Raoult, D., and Ghigo, E. (2015). Hemocytes from *Pediculus humanus humanus* are hosts for human bacterial pathogens. *Front. Cell. Infect. Microbiol.* 4:183. doi: 10.3389/fcimb.2014.00183

Cutler, S., Abdissa, A., Adamu, H., Tolosa, T., and Gashaw, A. (2012). *Bartonella quintana* in Ethiopian lice. *Comp. Immunol. Microbiol. Infect. Dis.* 35, 17–21. doi: 10.1016/j.cimid.2011.09.007

Das, S., Debnath, N., Cui, Y., Unrine, J., and Palli, S. R. (2015). Chitosan, carbon quantum dot, and silica nanoparticle mediated dsRNA delivery for gene silencing in *Aedes aegypti*: a comparative analysis. *ACS Appl. Mater. Interfaces* 7, 19530–19535. doi: 10.1021/acsami.5b05232

Diatta, G., Abat, C., Sokhna, C., Tissot-Dupont, H., Rolain, J.-M., and Raoult, D. (2016). Head lice probably resistant to ivermectin recovered from two rural girls in Dielmo, a village in Sine-Saloum, Senegal. *Int. J. Antimicrob. Agents* 47, 501–502. doi: 10.1016/j.ijantimicag.2016.03.013

Diatta, G., Mediannikov, O., Sokhna, C., Bassene, H., Socolovschi, C., Ratmanov, P., et al. (2014). Prevalence of *Bartonella quintana* in patients with fever and head lice from rural areas of Sine-Saloum, Senegal. *Am. J. Trop. Med. Hyg.* 91, 291–293. doi: 10.4269/ajtmh.13-0685

Drali, R., Abi-Rached, L., Boutellis, A., Djossou, F., Barker, S. C., and Raoult, D. (2016a). Host switching of human lice to new world monkeys in South America. *Infect. Genet. Evol.* 39, 225–231. doi: 10.1016/j.meegid.2016.02.008

Drali, R., Boutellis, A., Raoult, D., Rolain, J. M., and Brouqui, P. (2013). Distinguishing body lice from head lice by multiplex real-time PCR analysis of the Phum_PHUM540560 gene. *PLoS ONE* 8:e58088. doi: 10.1371/journal.pone.0058088

Drali, R., Mumcuoglu, K., and Raoult, D. (2016b). Human lice in paleoentomology and paleomicrobiology. *Microbiol. Spectr.* 4:PoH-0005-2014. doi: 10.1128/microbiolspec.PoH-0005-2014

Drali, R., Mumcuoglu, K. Y., Yesilyurt, G., and Raoult, D. (2015a). Studies of ancient lice reveal unsuspected past migrations of vectors. *Am. J. Trop. Med. Hyg.* 93, 623–625. doi: 10.4269/ajtmh.14-0552

Drali, R., Shako, J.-C., Davoust, B., Diatta, G., and Raoult, D. (2015b). A new clade of african body and head lice infected by *Bartonella quintana* and *Yersinia pestis*-Democratic Republic of the Congo. *Am. J. Trop. Med. Hyg.* 93, 990–993. doi: 10.4269/ajtmh.14-0686

Drancourt, M., Moal, V., Brunet, P., Dussol, B., Berland, Y., and Raoult, D. (1996). *Bartonella (Rochalimaea) quintana* infection in a seronegative hemodialyzed patient. *J. Clin. Microbiol.* 34, 1158–1160.

Durand, R., Bouvresse, S., Berdjane, Z., Izri, A., Chosidow, O., and Clark, J. M. (2012). Insecticide resistance in head lice: clinical, parasitological and genetic aspects. *Clin. Microbiol. Infect.* 18, 338–344. doi: 10.1111/j.1469-0691.2012.03806.x

Durden, L. A., and Musser, G. G. (1994). "The sucking lice (Insecta, Anoplura) of the world: a taxonomic checklist with records of mammalian hosts and geographical distributions. Bulletin of the AMNH; no. 218," in *Sucking Lice and Hosts*. Available online at: http://digitallibrary.amnh.org/handle/2246/825 (accessed April 15, 2018).

Eleftherianos, I., Atri, J., Accetta, J., and Castillo, J. (2013). Endosymbiotic bacteria in insects: guardians of the immune system? *Front. Physiol.* 4:46. doi: 10.3389/fphys.2013.00046

Eremeeva, M. E., Capps, D., Winful, E. B., Warang, S. S., Braswell, S. E., Tokarevich, N. K., et al. (2017). Molecular markers of pesticide resistance and pathogens in human head lice (*Phthiraptera*: *Pediculidae*) from rural Georgia, USA. *J. Med. Entomol.* 54, 1067–1072. doi: 10.1093/jme/tjx039

Eveillard, M., Kempf, M., Belmonte, O., Pailhoriès, H., and Joly-Guillou, M.-L. (2013). Reservoirs of *Acinetobacter baumannii* outside the hospital and potential involvement in emerging human community-acquired infections. *Int. J. Infect. Dis.* 17, e802–805. doi: 10.1016/j.ijid.2013.03.021

Feldmeier, H. (2014). Treatment of pediculosis capitis: a critical appraisal of the current literature. *Am. J. Clin. Dermatol.* 15, 401–412. doi: 10.1007/s40257-014-0094-4

Foucault, C., Ranque, S., Badiaga, S., Rovery, C., Raoult, D., and Brouqui, P. (2006). Oral ivermectin in the treatment of body lice. *J. Infect. Dis.* 193, 474–476. doi: 10.1086/499279

Fournier, P.-E., Ndihokubwayo, J.-B., Guidran, J., Kelly, P. J., and Raoult, D. (2002). Human pathogens in body and head lice. *Emerg. Infect. Dis.* 8, 1515–1518. doi: 10.3201/eid0812.020111

Giroud, P., and Jadin, J. (1954). Infection latente et conservation de "*Rickettsia burnetii*" chez l'homme, le rôle du pou. *Bull Soc. Pathol. Exotique* 47, 764–765.

Goldberger, J., and Anderson, J. F. (1912). "The transmission of typhus fever, with especial reference to transmission by the head louse (*Pediculus capitis*)," in *Public Health Report 1896-1970*, Vol. 27 (Washington, DC), 297–307.

Gordon, K. H. J., and Waterhouse, P. M. (2007). RNAi for insect-proof plants. *Nat. Biotechnol.* 25, 1231–1232. doi: 10.1038/nbt1107-1231

Hayashi, Y., Lo, N., Miyata, H., and Kitade, O. (2007). Sex-linked genetic influence on caste determination in a termite. *Science* 318, 985–987. doi: 10.1126/science.1146711

Herren, J. K., and Lemaitre, B. (2011). Spiroplasma and host immunity: activation of humoral immune responses increases endosymbiont load and susceptibility to certain Gram-negative bacterial pathogens in *Drosophila melanogaster*. *Cell. Microbiol.* 13, 1385–1396. doi: 10.1111/j.1462-5822.2011.01627.x

Houhamdi, L., Fournier, P.-E., Fang, R., and Raoult, D. (2003). An experimental model of human body louse infection with *Rickettsia typhi*. *Ann. N.Y. Acad. Sci.* 990, 617–627. doi: 10.1111/j.1749-6632.2003.tb07436.x

Houhamdi, L., Lepidi, H., Drancourt, M., and Raoult, D. (2006). Experimental model to evaluate the human body louse as a vector of plague. *J. Infect. Dis.* 194, 1589–1596. doi: 10.1086/508995

Houhamdi, L., and Raoult, D. (2006a). Experimental infection of human body lice with *Acinetobacter baumannii*. *Am. J. Trop. Med. Hyg.* 74, 526–531. doi: 10.4269/ajtmh.2006.74.526

Houhamdi, L., and Raoult, D. (2006b). Experimentally infected human body lice (*Pediculus humanus humanus*) as vectors of *Rickettsia rickettsii* and *Rickettsia conorii* in a rabbit model. *Am. J. Trop. Med. Hyg.* 74, 521–525. doi: 10.4269/ajtmh.2006.74.521

Kalra, S. L., and Rao, K. N. A. (1951). Typhus fevers in kashmir state. Part II. Murine Typhus. *Indian J. Med. Res.* 39, 297–302.

Keilin, D., and Nuttall, G. H. F. (1919). Hermaphroditism and other Abnormalities in *Pediculus humanus*. *Parasitology* 11, 279–328. doi: 10.1017/S0031182000004285

Kempf, M., Abdissa, A., Diatta, G., Trape, J.-F., Angelakis, E., Mediannikov, O., et al. (2012). Detection of *Acinetobacter baumannii* in human head and body lice from Ethiopia and identification of new genotypes. *Int. J. Infect. Dis.* 16, e680–683. doi: 10.1016/j.ijid.2012.05.1024

Kim, J. H., Min, J. S., Kang, J. S., Kwon, D. H., Yoon, K. S., Strycharz, J., et al. (2011). Comparison of the humoral and cellular immune responses between body and head lice following bacterial challenge. *Insect Biochem. Mol. Biol.* 41, 332–339. doi: 10.1016/j.ibmb.2011.01.011

Kim, J. H., Previte, D. J., Yoon, K. S., Murenzi, E., Koehler, J. E., Pittendrigh, B. R., et al. (2017). Comparison of the proliferation and excretion of *Bartonella quintana* between body and head lice following oral challenge. *Insect Mol. Biol.* 26, 266–276. doi: 10.1111/imb.12292

Kim, J. H., Yoon, K. S., Previte, D. J., Pittendrigh, B. R., Clark, J. M., and Lee, S. H. (2012). Comparison of the immune response in alimentary tract tissues from body versus head lice following *Escherichia coli* oral infection. *J. Asia Pac. Entomol.* 15, 409–412. doi: 10.1016/j.aspen.2012.05.010

Kirkness, E. F., Haas, B. J., Sun, W., Braig, H. R., Perotti, M. A., Clark, J. M., et al. (2010). Genome sequences of the human body louse and its primary endosymbiont provide insights into the permanent parasitic lifestyle. *Proc. Natl. Acad. Sci. U.S.A.* 107, 12168–12173. doi: 10.1073/pnas.1003379107

Kittler, R., Kayser, M., and Stoneking, M. (2003). Molecular evolution of *Pediculus humanus* and the origin of clothing. *Curr. Biol.* 13, 1414–1417. doi: 10.1016/S0960-9822(03)00507-4

Kwon, D. H., Kim, J. H., Kim, Y. H., Yoon, K. S., Clark, J. M., and Lee, S. H. (2014). Identification and characterization of an esterase involved in malathion resistance in the head louse *Pediculus humanus capitis*. *Pestic. Biochem. Physiol.* 112, 13–18. doi: 10.1016/j.pestbp.2014.05.006

La Scola, B., Fournier, P.-E., Brouqui, P., and Raoult, D. (2001). Detection and culture of *Bartonella quintana*, *Serratia marcescens*, and *Acinetobacter* spp. from decontaminated human body lice. *J. Clin. Microbiol.* 39, 1707–1709. doi: 10.1128/JCM.39.5.1707-1709.2001

La, V. D., Tran-Hung, L., Aboudharam, G., Raoult, D., and Drancourt, M. (2005). *Bartonella quintana* in domestic cat. *Emerg. Infect. Dis.* 11, 1287–1289. doi: 10.3201/eid1108.050101

Lee, S. H., Kang, J. S., Min, J. S., Yoon, K. S., Strycharz, J. P., Johnson, R., et al. (2010). Decreased detoxification genes and genome size make the human body louse an efficient model to study xenobiotic metabolism. *Insect Mol. Biol.* 19, 599–615. doi: 10.1111/j.1365-2583.2010.01024.x

Li, H., Liu, W., Zhang, G.-Z., Sun, Z.-Z., Bai, J.-Y., Jiang, B.-G., et al. (2013). Transmission and maintenance cycle of *Bartonella quintana* among Rhesus Macaques, China. *Emerg. Infect. Dis.* 19, 297–300. doi: 10.3201/eid1902.120816

Li, W., Ortiz, G., Fournier, P.-E., Gimenez, G., Reed, D. L., Pittendrigh, B., et al. (2010). Genotyping of human lice suggests multiple emergencies of body lice from local head louse populations. *PLoS Negl. Trop. Dis.* 4:e641. doi: 10.1371/journal.pntd.0000641

Light, J. E., Allen, J. M., Long, L. M., Carter, T. E., Barrow, L., Suren, G., et al. (2008a). Geographic distributions and origins of human head lice (*Pediculus humanus capitis*) based on mitochondrial data. *J. Parasitol.* 94, 1275–1281. doi: 10.1645/GE-1618.1

Light, J. E., Toups, M. A., and Reed, D. L. (2008b). What's in a name: the taxonomic status of human head and body lice. *Mol. Phylogenet. Evol.* 47, 1203–1216. doi: 10.1016/j.ympev.2008.03.014

Liu, W. T. (1944). Studies on the murine origin of typhus epidemics in North China. 3. Isolation of murine typhus *Rickettsia* from rats, rat-fleas and body-lice of patients during an epidemic in a poor house. *Chin. Med. J.* 62, 119–39.

Louni, M., Amanzougaghene, N., Mana, N., Fenollar, F., Raoult, D., Bitam, I., et al. (2018). Detection of bacterial pathogens in clade E head lice collected from Niger's refugees in Algeria. *Parasit. Vectors* 11:348. doi: 10.1186/s13071-018-2930-5

Lyko, F., Foret, S., Kucharski, R., Wolf, S., Falckenhayn, C., and Maleszka, R. (2010). The honey bee epigenomes: differential methylation of brain DNA in queens and workers. *PLoS Biol.* 8:e1000506. doi: 10.1371/journal.pbio.1000506

Mana, N., Louni, M., Parola, P., and Bitam, I. (2017). Human head lice and pubic lice reveal the presence of several *Acinetobacter* species in Algiers, Algeria. *Comp. Immunol. Microbiol. Infect. Dis.* 53, 33–39. doi: 10.1016/j.cimid.2017.06.003

Meinking, T. L., Villar, M. E., Vicaria, M., Eyerdam, D. H., Paquet, D., Mertz-Rivera, K., et al. (2010). The clinical trials supporting benzyl alcohol lotion 5% (Ulesfia): a safe and effective topical treatment for head lice (*Pediculosis humanus capitis*). *Pediatr. Dermatol.* 27, 19–24. doi: 10.1111/j.1525-1470.2009.01059.x

Molina-Cruz, A., DeJong, R. J., Charles, B., Gupta, L., Kumar, S., Jaramillo-Gutierrez, G., et al. (2008). Reactive oxygen species modulate *Anopheles gambiae* immunity against bacteria and Plasmodium. *J. Biol. Chem.* 283, 3217–3223. doi: 10.1074/jbc.M705873200

Mumcuoglu, K. Y. (2008). "Human lice: *Pediculus* and *Pthirus*," in *Paleomicrobiology*, eds D. Raoult and M. Drancourt (Berlin: Springer), 215–222. doi: 10.1007/978-3-540-75855-6_13

Murray, E. S., and Torrey, S. B. (1975). Virulence of *Rickettsia prowazeki* for head lice. *Ann. N.Y. Acad. Sci.* 266, 25–34. doi: 10.1111/j.1749-6632.1975.tb35086.x

Muturi, E. J., Kim, C.-H., Alto, B. W., Berenbaum, M. R., and Schuler, M. A. (2011). Larval environmental stress alters *Aedes aegypti* competence for Sindbis virus. *Trop. Med. Int. Health* 16, 955–964. doi: 10.1111/j.1365-3156.2011.02796.x

Nakka, K., Ghigna, C., Gabellini, D., and Dilworth, F. J. (2018). Diversification of the muscle proteome through alternative splicing. *Skelet. Muscle* 8:8. doi: 10.1186/s13395-018-0152-3

Olds, B. P., Coates, B. S., Steele, L. D., Sun, W., Agunbiade, T. A., Yoon, K. S., et al. (2012). Comparison of the transcriptional profiles of head and body lice. *Insect Mol. Biol.* 21, 257–268. doi: 10.1111/j.1365-2583.2012.01132.x

Perotti, M. A., Allen, J. M., Reed, D. L., and Braig, H. R. (2007). Host-symbiont interactions of the primary endosymbiont of human head and body lice. *FASEB J.* 21, 1058–1066. doi: 10.1096/fj.06-6808com

Perry, G. H. (2014). Parasites and human evolution. *Evol. Anthropol. Issues News Rev.* 23, 218–228. doi: 10.1002/evan.21427

Piarroux, R., Abedi, A. A., Shako, J.-C., Kebela, B., Karhemere, S., Diatta, G., et al. (2013). Plague epidemics and lice, Democratic Republic of the Congo. *Emerg. Infect. Dis.* 19, 505–506. doi: 10.3201/eid1903.121542

Pittendrigh, B. R., Olds, B. P., Yoon, K. S., Lee, S. H., Sun, W., and Clark, J. M. (2013). The genomics of human lice: from the genome to the potential for future control strategies. *Pestic. Biochem. Physiol.* 106, 172–176. doi: 10.1016/j.pestbp.2013.03.010

Previte, D., Olds, B. P., Yoon, K., Sun, W., Muir, W., Paige, K. N., et al. (2014). Differential gene expression in laboratory strains of human head and body lice when challenged with *Bartonella quintana*, a pathogenic bacterium. *Insect Mol. Biol.* 23, 244–254. doi: 10.1111/imb.12077

Raoult, D. (2016). A personal view of how paleomicrobiology aids our understanding of the role of lice in plague pandemics. *Microbiol. Spectr.* 4:PoH-0001-2014. doi: 10.1128/microbiolspec.PoH-0001-2014

Raoult, D., Drancourt, M., Carta, A., and Gastaut, J. A. (1994). *Bartonella (Rochalimaea) quintana* isolation in patient with chronic adenopathy, lymphopenia, and a cat. *Lancet Lond. Engl.* 343:977. doi: 10.1016/S0140-6736(94)90102-3

Raoult, D., Dutour, O., Houhamdi, L., Jankauskas, R., Fournier, P.-E., Ardagna, Y., et al. (2006). Evidence for louse-transmitted diseases in soldiers of Napoleon's Grand Army in Vilnius. *J. Infect. Dis.* 193, 112–120. doi: 10.1086/498534

Raoult, D., Reed, D. L., Dittmar, K., Kirchman, J. J., Rolain, J.-M., Guillen, S., et al. (2008). Molecular identification of lice from pre-Columbian mummies. *J. Infect. Dis.* 197, 535–543. doi: 10.1086/526520

Raoult, D., and Roux, V. (1999). The body louse as a vector of reemerging human diseases. *Clin. Infect. Dis.* 29, 888–911. doi: 10.1086/520454

Reed, D. L., Light, J. E., Allen, J. M., and Kirchman, J. J. (2007). Pair of lice lost or parasites regained: the evolutionary history of anthropoid primate lice. *BMC Biol.* 5:7. doi: 10.1186/1741-7007-5-7

Reed, D. L., Smith, V. S., Hammond, S. L., Rogers, A. R., and Clayton, D. H. (2004). Genetic analysis of lice supports direct contact between modern and archaic humans. *PLoS Biol.* 2:e340. doi: 10.1371/journal.pbio.0020340

Robinson, D., Leo, N., Prociv, P., and Barker, S. C. (2003). Potential role of head lice, *Pediculus humanus capitis*, as vectors of *Rickettsia prowazekii*. *Parasitol. Res.* 90, 209–211. doi: 10.1007/s00436-003-0842-5

Rolain, J.-M., Franc, M., Davoust, B., and Raoult, D. (2003). Molecular detection of *Bartonella quintana, B. koehlerae, B. henselae, B. clarridgeiae, Rickettsia felis*, and *Wolbachia pipientis* in cat fleas, France. *Emerg. Infect. Dis.* 9, 338–342. doi: 10.3201/eid0903.020278

Sangaré, A. K., Boutellis, A., Drali, R., Audoly, G., Weber, P., Rolain, J. M., et al. (2015). Doxycycline kills human lice through its activity on their bacterial symbiont. *Int. J. Antimicrob. Agents* 45, 675–676. doi: 10.1016/j.ijantimicag.2015.02.008

Sangaré, A. K., Boutellis, A., Drali, R., Socolovschi, C., Barker, S. C., Diatta, G., et al. (2014). Detection of *Bartonella quintana* in African body and

head lice. *Am. J. Trop. Med. Hyg.* 91, 294–301. doi: 10.4269/ajtmh.13-0707

Sangaré, A. K., Doumbo, O. K., and Raoult, D. (2016a). Management and treatment of human lice. *BioMed Res. Int.* 2016:8962685. doi: 10.1155/2016/8962685

Sangaré, A. K., Rolain, J. M., Gaudart, J., Weber, P., and Raoult, D. (2016b). Synergistic activity of antibiotics combined with ivermectin to kill body lice. *Int. J. Antimicrob. Agents* 47, 217–223. doi: 10.1016/j.ijantimicag.2016.01.001

Sasaki, T., Poudel, S. K. S., Isawa, H., Hayashi, T., Seki, N., Tomita, T., et al. (2006). First molecular evidence of *Bartonella quintana* in *Pediculus humanus capitis* (*Phthiraptera*: *Pediculidae*), collected from Nepalese children. *J. Med. Entomol.* 43, 110–112. doi: 10.1603/0022-2585(2006)043[0110:FMEOBQ]2.0.CO;2

Sassera, D., Epis, S., Pajoro, M., and Bandi, C. (2013). Microbial symbiosis and the control of vector-borne pathogens in tsetse flies, human lice, and triatomine bugs. *Pathog. Glob. Health* 107, 285–292. doi: 10.1179/2047773213Y.0000000109

Sato, S., Kabeya, H., Yoshino, A., Sekine, W., Suzuki, K., Tamate, H. B., et al. (2015). Japanese Macaques (*Macaca fuscata*) as natural reservoir of *Bartonella quintana*. *Emerg. Infect. Dis.* 21, 2168–2170. doi: 10.3201/eid2112.150632

Scott, J. G., Michel, K., Bartholomay, L., Siegfried, B. D., Hunter, W. B., Smagghe, G., et al. (2013). Towards the elements of successful insect RNAi. *J. Insect Physiol.* 59, 1212–1221. doi: 10.1016/j.jinsphys.2013.08.014

Shao, R., Zhu, X.-Q., Barker, S. C., and Herd, K. (2012). Evolution of extensively fragmented mitochondrial genomes in the lice of humans. *Genome Biol. Evol.* 4, 1088–1101. doi: 10.1093/gbe/evs088

Shashindran, C. H., Gandhi, I. S., Krishnasamy, S., and Ghosh, M. N. (1978). Oral therapy of pediculosis capitis with cotrimoxazole. *Br. J. Dermatol.* 98, 699–700. doi: 10.1111/j.1365-2133.1978.tb03591.x

Simpson, S. J., Despland, E., Hägele, B. F., and Dodgson, T. (2001). Gregarious behavior in desert locusts is evoked by touching their back legs. *Proc. Natl. Acad. Sci. U.S.A.* 98, 3895–3897. doi: 10.1073/pnas.071527998

Sunantaraporn, S., Sanprasert, V., Pengsakul, T., Phumee, A., Boonserm, R., Tawatsin, A., et al. (2015). Molecular survey of the head louse *Pediculus humanus capitis* in Thailand and its potential role for transmitting *Acinetobacter* spp. *Parasit. Vectors* 8:127. doi: 10.1186/s13071-015-0742-4

Terrapon, N., Li, C., Robertson, H. M., Ji, L., Meng, X., Booth, W., et al. (2014). Molecular traces of alternative social organization in a termite genome. *Nat. Commun.* 5:3636. doi: 10.1038/ncomms4636

Toups, M. A., Kitchen, A., Light, J. E., and Reed, D. L. (2011). Origin of clothing lice indicates early clothing use by anatomically modern humans in Africa. *Mol. Biol. Evol.* 28, 29–32. doi: 10.1093/molbev/msq234

Tovar-Corona, J. M., Castillo-Morales, A., Chen, L., Olds, B. P., Clark, J. M., Reynolds, S. E., et al. (2015). Alternative splice in alternative lice. *Mol. Biol. Evol.* 32, 2749–2759. doi: 10.1093/molbev/msv151

Vallenet, D., Nordmann, P., Barbe, V., Poirel, L., Mangenot, S., Bataille, E., et al. (2008). Comparative analysis of *Acinetobacters*: three genomes for three lifestyles. *PLoS ONE* 3:e1805. doi: 10.1371/journal.pone.0001805

Veracx, A., and Raoult, D. (2012). Biology and genetics of human head and body lice. *Trends Parasitol.* 28, 563–571. doi: 10.1016/j.pt.2012.09.003

Weyer, F. (1952). The behavior of *Rickettsia akari* in the body louse after artificial infection. *Am. J. Trop. Med. Hyg.* 1, 809–820. doi: 10.4269/ajtmh.1952.1.809

Yoon, K. S., Strycharz, J. P., Baek, J. H., Sun, W., Kim, J. H., Kang, J. S., et al. (2011). Brief exposures of human body lice to sub-lethal amounts of ivermectin over transcribes detoxification genes involved in tolerance. *Insect Mol. Biol.* 20, 687–699. doi: 10.1111/j.1365-2583.2011.01097.x

Conflict of Interest: The authors declare that the research was conducted in the absence of any commercial or financial relationships that could be construed as a potential conflict of interest.

frontiers in Cellular and Infection Microbiology

MINI REVIEW
published: 30 January 2020
doi: 10.3389/fcimb.2020.00001

New Insights Into CRASP-Mediated Complement Evasion in the Lyme Disease Enzootic Cycle

Yi-Pin Lin[1,2]*, *Amber M. Frye*[1,2], *Tristan A. Nowak*[1,2] and *Peter Kraiczy*[3]*

[1] Department of Biomedical Sciences, State University of New York at Albany, Albany, NY, United States, [2] Division of Infectious Diseases, New York State Department of Health, Wadsworth Center, Albany, NY, United States, [3] Institute of Medical Microbiology and Infection Control, University Hospital, Goethe University Frankfurt, Frankfurt, Germany

Lyme disease (LD), which is caused by genospecies of the *Borrelia burgdorferi* sensu lato complex, is the most common vector-borne disease in the Northern hemisphere. Spirochetes are transmitted by *Ixodes* ticks and maintained in diverse vertebrate animal hosts. Following tick bite, spirochetes initially establish a localized infection in the skin. However, they may also disseminate hematogenously to several distal sites, including heart, joints, or the CNS. Because they need to survive in diverse microenvironments, from tick vector to mammalian hosts, spirochetes have developed multiple strategies to combat the numerous host defense mechanisms. One of these strategies includes the production of a number of complement-regulator acquiring surface proteins (CRASPs) which encompass CspA, CspZ, and OspE paralogs to blunt the complement pathway. These proteins are capable of preventing complement activation on the spirochete surface by binding to complement regulator Factor H. The genes encoding these CRASPs differ in their expression patterns during the tick-to-host infection cycle, implying that these proteins may exhibit different functions during infection. This review summarizes the recent published reports which investigated the roles that each of these molecules plays in conferring tick-borne transmission and dissemination in vertebrate hosts. These findings offer novel mechanistic insights into LD pathobiology and may facilitate the identification of new targets for preventive strategies against Lyme borreliosis.

Keywords: *Borrelia*, complement, Factor H, CspA, CspZ, OspE, tick, host-pathogen interaction

OPEN ACCESS

Edited by:
Ryan Oliver Marino Rego, Institute of Parasitology (ASCR), Czechia

Reviewed by:
Juan Anguita, Center for Cooperative Research in Biosciences, Spain
Jon Blevins, University of Arkansas for Medical Sciences, United States

***Correspondence:**
Yi-Pin Lin
Yi-Pin.Lin@health.ny.gov
Peter Kraiczy
Kraiczy@em.uni-frankfurt.de

Specialty section:
This article was submitted to Bacteria and Host, a section of the journal Frontiers in Cellular and Infection Microbiology

Received: *29 November 2019*
Accepted: *06 January 2020*
Published: *30 January 2020*

Citation:
Lin Y-P, Frye AM, Nowak TA and Kraiczy P (2020) New Insights Into CRASP-Mediated Complement Evasion in the Lyme Disease Enzootic Cycle. Front. Cell. Infect. Microbiol. 10:1. doi: 10.3389/fcimb.2020.00001

LYME DISEASE SPIROCHETES EVADE THE VERTEBRATE HOSTS' COMPLEMENT

Lyme disease (LD) is the most common vector-borne disease in the northern hemisphere (Steere et al., 2016). A recent report from the CDC categorizes LD as one of the zoonotic diseases of the greatest concern in the United States. The disease is caused by spirochetes of the *Borrelia burgdorferi* sensu lato complex (Rosa et al., 2005; Brisson et al., 2012; Radolf et al., 2012). Among the ∼20 *Borrelia* species that comprise the sensu lato complex, at least six have been confirmed to cause LD in humans including *Borrelia (B.) burgdorferi* sensu stricto (hereafter referred as *B. burgdorferi*), *B. afzelii, B. garinii, B. spielmanii, B. bavariensis,* and *B. mayonii*, all of which are transmitted by *Ixodes* ticks and maintained in diverse reservoir hosts (mainly small mammals and birds) (Tufts et al., 2019). Upon tick feeding, spirochetes are exposed to host blood and the first line of innate immunity which they must overcome to survive (Hovius et al., 2007; Steere et al., 2016; **Figure 1**).

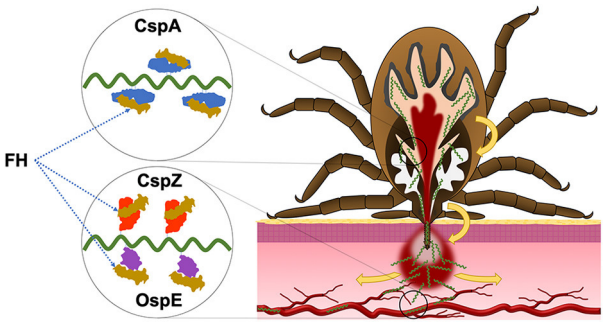

FIGURE 1 | The roles of CRASP proteins in the enzootic cycle of LD spirochetes. During the infection, LD spirochetes require the ability to evade the complement in the vertebrate blood. CspA facilitates spirochete survival in the blood meal of fed ticks and thereby enabling spirochetes to be transmitted to the host. CspZ promotes spirochete survival in the bloodstream of vertebrate animals, allowing in dissemination to distal tissues. While the role that OspE paralogs (OspE) play in enzootic cycle remain unclear, the current evidence supports that these proteins confer spirochete dissemination in the vertebrate animals.

Spirochetes then migrate through the tick midgut epithelium and the salivary glands and are transmitted to the host skin to establish the infection (Hovius et al., 2007; Steere et al., 2016; **Figure 1**). In untreated humans, the spirochetes may disseminate hematogenously to distal tissues and organs (Coburn et al., 2013; Hyde, 2017; Bernard et al., 2019; **Figure 1**).

Complement is a central component of the host innate immune system and the first line of defense against bacterial infection. Evasion of the host complement system is essential for *Borrelia* to successfully establish infection (Caine and Coburn, 2016; Kraiczy, 2016; Marcinkiewicz et al., 2017) (see Sjoberg et al., 2009; Zipfel and Skerka, 2009; Meri, 2016 for more thorough reviews). The complement system is composed of more than 30 proteins and inactive precursors (Zipfel and Skerka, 2009). Activation of complement cascades on the microbial surface is initiated via three distinct pathways (Meri, 2016). Antibody-antigen complexes trigger activation of the classical pathway (CP) whereas the mannose-binding lectin pathway (LP) is activated by recognition of carbohydrate complexes (collectins and ficolins) on microbial surfaces. The alternative pathway (AP) is activated when C3b is bound to the surface of invading microbes. Activation of all three pathways leads to the formation and deposition of C3 and C5 convertases on the microbial surface. This results in the insertion of the pore-forming membrane attack complex (MAC), leading to bacterial cell lysis.

In the absence of invading microbes or cell/tissue damage, vertebrate hosts produce complement regulatory proteins (CRPs) which are deposited on host cells/tissues to avoid non-specific damage by the complement cascade (Sjoberg et al., 2009; Zipfel and Skerka, 2009; Meri, 2016). Factor H (FH) is a CRP that binds to C3b by recruiting the serum protease, factor I. This complex leads to the degradation of C3b and coincidently terminates activation of AP (Zipfel and Skerka, 2009; Zipfel et al., 2013).

LD spirochetes produce several outer surface proteins that facilitate host complement evasion (de Taeye et al., 2013; Caine and Coburn, 2016; Kraiczy, 2016; Marcinkiewicz et al., 2017). These proteins include five complement-regulator acquiring surface proteins (BbCRASPs or CRASPs) (Kraiczy and Stevenson, 2013): CspA (CRASP-1, BBA68), CspZ (CRASP-2, BBH06), and OspE paralogs [i.e., ErpP (CRASP-3, BBN38), ErpC (CRASP-4), and ErpA/I/N (CRASP-5, BBP38, BBL39)] (**Table 1**). While all these proteins bind to FH to inactivate human complement, CspA and CspZ also bind to FH-like protein 1 (FHL-1), the truncated form of FH (Zipfel and Skerka, 1999; Kraiczy and Stevenson, 2013). Additionally, ErpP, ErpC, and ErpA bind to different FH-related proteins (CFHR), a family of CRPs with similar sequence identity and high-resolution structures to that of FH (Zipfel et al., 2002; Kraiczy and Stevenson, 2013). The expression of the genes encoding these outer surface proteins varies at different stages of the infection cycle, e.g., during spirochete transmission and dissemination (Miller et al., 2003; von Lackum et al., 2005; Bykowski et al., 2007; Brissette et al., 2008). These findings suggest that CRASPs play distinct roles in facilitating spirochete survival in ticks and/or vertebrate hosts. However, until recently, the role of these CRASPs in the spirochete infection cycle in vertebrate hosts is still unclear.

In this review, we summarize previous findings regarding the role of CRASPs in the pathobiology and provide mechanistic insights into transmission and dissemination of LD spirochetes in ticks and different vertebrate animals.

CspA FACILITATES SPIROCHETE SURVIVAL IN TICKS' BLOOD MEAL AND DURING TRANSMISSION FROM TICKS TO HOSTS

During feeding, ticks are vulnerable to the attack by complement present in the blood meal. To neutralize complement and other dangerous constituents, ticks generate a cocktail of diverse immunomodulatory proteins with immunosuppressive, anti-inflammatory, and anti-complement activity in their saliva (Tyson et al., 2007, 2008; Schuijt et al., 2008, 2011; Wagemakers et al., 2016) (see de Taeye et al., 2013 for the review). These proteins shield spirochetes from complement-mediated killing in the ticks' midgut. However, ticks devoid of any one of these anti-complement proteins can still transmit spirochetes to vertebrate animals (Schuijt et al., 2011; Wagemakers et al., 2016). Additionally, LD spirochetes survive at similar levels in the ticks feeding on wild-type or complement-deficient mice (Rathinavelu et al., 2003; Hart et al., 2018). These results suggest that spirochetes have developed

Abbreviations: CRASPs, Complement regulator acquiring surface proteins; OspE, OspE paralogs; CP, Classical Pathway; LP, Mannose-binding lectin pathway; AP, Alternative pathway; TP, Terminal pathway; MAC, Membrane attacking complex; CRPs, Complement regulatory proteins; FH, Factor H; BbCRASPs, *Borrelia burgdorferi* sensu lato complement regulator acquiring surface proteins; FHL-1, Factor H like protein 1; CFHR, Factor H related protein; lp54, Linear plasmid 54; lp28-3, Linear plasmid 28-3; cp32, Circular plasmid 32; UHB, Upstream homology box; LD, Lyme diseases.

TABLE 1 | *In vitro* and *in vivo* characteristics of CRASPs[a,b].

		CspA	CspZ	OspE paralogs		
Synonyms and other designations		CRASP-1 BbCRASP-1 BBA68 FHBP	CRASP-2 BbCRASP-2 BBH06	CRASP-3 BbCRASP-3 BBN38	CRASP-4 BbCRASP-4 ErpC	CRASP-5 BbCRASP-5 ErpI ErpN ErpA BBP38 BBL39
Gene name		*cspA*	*cspZ*	*erpP*	*erpC*	*erpA*
Gene location in *B. burgdorferi* strain B31		lp54	lp28-3	cp32-9	cp32-2	cp32-1 cp32-5 cp32-8
Gene expression in enzootic cycle	Fed larvae	+	+ (low expression)	+ (high expression)	+ (high expression)	+ (high expression)
	Unfed nymphs	+ (high expression)	–	–	–	–
	Fed nymphs	+ (low expression)	+ (low expression)	+	+	+
	Tick biting sites	+	+ (high expression)	+ (high expression)	+ (high expression)	+ (high expression)
	Dissemination	–	+ (high expression)	+ (high expression)	+ (high expression)	+ (high expression)
FH binding	Purified proteins	+	+	+	-	+
	GOF[c]	+	+	+	–	+
	LOF[d]	+	+[e]	ND[f]	ND	ND
Additional non-FH ligands related to complement inactivation		C7, C9, FHL-1	FHL-1	CFHR1 CFHR2 CFHR5	CFHR1 CFHR2	CFHR1 CFHR2 CFHR5
Serum resistance	GOF[c]	+	+	–	–	–
	LOF[d]	+	+[e]	+[g]	–	+[g]
Infection phenotype	Spirochetes transmission by ticks	Mutant showed defects in surviving at fed nymphs and transmission to hosts	ND	ND	ND	ND
	Spirochete acquisition by ticks	–	–	ND	ND	ND
	Intradermal inoculation	–	Mutant showed defects in bloodstream survival and tissue colonization[c]	ND	ND	Mutant showed defects in tissue colonization[h]

[a] *Table adapted from Kraiczy and Stevenson (2013).*
[b] *Different information may be shown because of different strains used to define that information. The information here is derived from B. burgdorferi strain B31.*
[c] *Produced in a gain-of-function background (GOF).*
[d] *Produced in a loss-of-function background (LOF).*
[e] *Only in blood treated condition.*
[f] *Not determined.*
[g] *Only when ErpP and ErpA are expressed under flaB promoter in a cspA-deficient B. burgdorferi in the infectious background.*
[h] *Performed using a transposon-inserted erpA mutant in an infectious B. burgdorferi background.*

additional means to evade complement when residing in fed ticks.

The *cspA* gene is located on a linear plasmid 54 (lp54) which is essential for LD spirochetes survival in the infection cycle (Purser and Norris, 2000; **Table 1**). This gene is uniquely expressed in spirochetes residing in ticks, suggesting that CspA plays a role during spirochetal colonization of ticks (von Lackum et al., 2005; Bykowski et al., 2007; Hart et al., 2018; **Table 1**). Ectopically producing CspA into a non-infectious, serum-sensitive, and *cspA*-deficient *B. burgdorferi* strain enables this strain to inactivate complement and survive when exposed to sera from various vertebrate animals *in vitro* (Kraiczy et al., 2004b; Brooks et al., 2005; Hammerschmidt et al., 2014; Muhleip et al., 2018; **Table 1**). Conversely, deleting *cspA* from a low passage and fully infectious *B. burgdorferi* strain results in the inability of this strain to survive in presence of serum from vertebrate animals and enhances complement activation on spirochete surface (Kenedy et al., 2009; **Table 1**). These results demonstrate the role of CspA in conferring spirochetal evasion from complement.

Moreover, a previous study demonstrates that CspA also confers protection when spirochetes are exposed to complement components in blood acquired during tick feeding. A recent study shows that a LD *Borrelia* strain deficient in *cspA* is eliminated in nymphs after the nymphs feed on wild-type mice (Hart et al., 2018). However, this strain survives in the nymphs

feeding on complement deficient mice, indicating that CspA promotes spirochetal evasion of complement in ticks' blood meal (Hart et al., 2018). The CspA-mediated blood meal survival has been attributed to the ability of CspA to bind FH (Hart et al., 2018; **Figure 1** and **Table 1**). CspA orthologs from different LD species differ in their ability to bind to FH from other vertebrate animals including birds, mice, and humans (Bhide et al., 2009; Hart et al., 2018; Muhleip et al., 2018). CspA of *B. burgdorferi* displays <50% of sequence identity compared to other LD *Borrelia* species but >95% identity on the intra-species level (von Lackum et al., 2005; Wywial et al., 2009). Further, the sequence variability of CspA orthologs correlates with their ability to interact with FH from humans and other hosts (von Lackum et al., 2005; Bhide et al., 2009; Hammerschmidt et al., 2014; Hart et al., 2018; Muhleip et al., 2018). Of note, one previous study showed that recombinant CspA from *B. burgdorferi* B31 does not bind to non-human FH in the sera applied on a Far-Western blot (McDowell et al., 2006). This result suggests that those non-human FH variants are required to be maintained as a native form in order to display their ability to bind to CspA. Consistent with the allelic differences in FH-binding activity of CspA, a *cspA*-deficient *B. burgdorferi* strain producing CspA from *B. garinii* was incapable of surviving in nymphs upon feeding on wild-type mice (Hart et al., 2018). That isogenic strains survived in nymphs feeding on the complement-deficient mice, similar to the isogenic strain producing CspA from *B. burgdorferi* strain B31 (Hart et al., 2018). These findings imply an allelic variation of CspA-mediated FH-binding activity. Such results also lead to an intriguing possibility that CspA determines spirochete host tropism by driving the transmission from ticks to specific hosts (Kurtenbach et al., 2002; Kraiczy, 2016; Tufts et al., 2019).

Recent investigations also revealed that CspA acts in multiple ways to inactivate complement. CspA was shown to inactivate the AP by binding to FH and FHL-1 as well as by binding to complement proteins C7 and C9 to block MAC formation (Hallstrom et al., 2013; **Table 1**). The presence of CspA on the bacterial surface prevents the formation of MAC, suggesting a FH-independent mechanism to confer complement evasion. However, compared to the high affinity binding to FH (K_D < 100 nM), CspA binds only moderately to C7 and C9 (K_D > 5 μM). These results raise questions regarding the physiological relevance of CspA-mediated C7- and C9-binding activity (Kraiczy et al., 2004a; Hallstrom et al., 2013; Hart et al., 2018).

THE ROLE OF CspZ IN PROMOTING SPIROCHETE DISSEMINATION AFTER INVADING VERTEBRATE HOSTS

A previous finding indicates that a *B. burgdorferi* strain deficient in *cspA* is capable of surviving at the inoculation site in skin at similar levels to the wild-type parental strain introduced by needle infection (Hart et al., 2018). This suggests that additional proteins confer this phenotype and/or work collaboratively with CspA to facilitate the establishment of infection. In fact, CspZ has been identified as an additional FH/FHL-1-binding protein which is encoded on the linear plasmid 28-3 (lp28-3) of *B. burgdorferi* B31 (**Table 1**). During tick-to-host transmission, the expression of *cspZ* is undetectable when spirochetes reside in ticks, but up-regulated when spirochetes reach the bite site in host skin (Bykowski et al., 2007). Further investigation reveals that *cspZ* is expressed throughout different infection stages in vertebrate animals (Bykowski et al., 2007; Marcinkiewicz et al., 2019), suggesting that the expression of CspZ and its role in the infection are restricted to the host (**Table 1**). Similar to CspA, introduction of CspZ into a *cspZ*-deficient, serum-sensitive borrelial strain allows the transformed strains to survive *in vitro* in presence of serum from various vertebrate animals by preventing complement activation (Hartmann et al., 2006; Siegel et al., 2008; **Table 1**). However, a *cspZ*-deficient strain in the infectious background of *B. burgdorferi* also survived in sera and colonized mouse tissues at similar levels as the parental strain (Coleman et al., 2008; Marcinkiewicz et al., 2019; **Table 1**). These findings support the following notions that such indistinguishable phenotypes could be attributed to low expression levels of *cspZ* in *B. burgdorferi* (Bykowski et al., 2007; Rogers and Marconi, 2007; Marcinkiewicz et al., 2019). As LD spirochetes produce additional complement interacting proteins that confer evasion during dissemination, delineating CspZ's phenotype can be cumbersome (Kraiczy et al., 2003, 2004a; Alitalo et al., 2004, 2005; Pietikainen et al., 2010; Bhattacharjee et al., 2013; Garcia et al., 2016; Caine et al., 2017).

To amplify the phenotype conferred by these genes, vertebrate blood has been used to cultivate spirochetes as cue to mimic *in vivo* conditions, possibly due to host-specific nutrients and ions in blood (Tokarz et al., 2004). Several borrelial genes upregulated during transmission can be triggered *in vitro* by incubation of the spirochetes with host blood (Tokarz et al., 2004). These genes include *cspZ*. These findings are consistent with additional data showing that a *cspZ*-deficient strain in an infectious background of *B. burgdorferi* displays reduced ability to survive when incubated with vertebrate sera (Marcinkiewicz et al., 2019; **Table 1**). Furthermore, this *cspZ* mutant strain when pre-treated with blood shows a delayed onset of dissemination and lower burdens in distal tissues, compared to wild-type *B. burgdorferi* strain, demonstrating CspZ' role in promoting spirochete dissemination (Marcinkiewicz et al., 2019; **Figure 1** and **Table 1**).

Further, several studies examined the role of CspZ (or the plasmid encoding *cspZ*) in infection cycle. CspZ was shown not essential for spirochetes acquisition from mammalian hosts to ticks (Coleman et al., 2008). However, fewer mice develop antibody reactivity against whole spirochete cell lysates after being fed on by the ticks carrying a *B. burgdorferi* strain missing lp28-3 plasmid which encodes *cspZ*, compared to wild-type parental spirochete strain (Dulebohn et al., 2013). These findings suggest that the proteins encoded by lp28-3 (e.g., CspZ) facilitate spirochete to establish an infection and disseminate to distal sites after tick bites. A previous study revealed that LD patients with manifestations (e.g., acrodermatitis, neuroborreliosis, erythema migran) and/or positivity in two-tier LD serological tests elicited

antibodies to CspZ, indicating that spirochetes produce this protein during the infection process (Kraiczy et al., 2008; Rogers et al., 2009).

Rogers et al. observed that CspZ shows allelically different ability in binding to human FH (Rogers and Marconi, 2007; Rogers et al., 2009). As CspZ is highly conserved (nearly 98% identical among *B. burgdorferi* strains and ∼70% identical among LD spirochetes), the difference of these variants may convey the observed strain-to-strain variation in binding activity to human FH (Rogers et al., 2009; Brangulis et al., 2014). Several sequence diverse regions in CspZ have been identified (Brangulis et al., 2014). According to a recently reported high-resolution co-crystal structure of CspZ-FH binding complex (Protein Data Bank #6ATG) some of these variable regions are located in the binding site/interface with human FH. These results support the possibility that these variable regions of CspZ mediate the different levels of FH-binding activity and spirochete survival in the infection cycle (**Table 1**).

THE ROLE OF OspE PARALOGS IN SPIROCHETE SURVIVAL DURING THE INFECTION CYCLE REMAINS UNCLEAR

Not every spirochete strain isolated from ticks feeding on LD spirochetes-infected vertebrate hosts encodes CspZ (Rogers and Marconi, 2007; Kraiczy et al., 2008), supporting that additional FH-binding proteins confer dissemination during infection. In fact, LD spirochetes produce multiple copies of OspE proteins, encoded by several circular plasmids 32 (cp32) (Marconi et al., 1996; Stevenson et al., 1996; Akins et al., 1999; Caimano et al., 2000; Kraiczy and Stevenson, 2013; **Table 1**). Most of these OspE paralogs bind to FH *in vitro* and share similar promoter sequences (as known as upstream homology box or "UHB") to other outer surface proteins on cp32, such as OspF (Marconi et al., 1996; Akins et al., 1999; Caimano et al., 2000; Brissette et al., 2008). Because of these similarities, these Osp*E*/F-related proteins were grouped under the term as Erps (Brissette et al., 2008).

Although some Erps have been shown to bind FH and confer complement evasion, their role in spirochete survival during the infection remains less clear. A serum-sensitive *B. burgdorferi* strain which expresses *erpP* or *erpA* (the genes encoding OspE paralogs in *B. burgdorferi* B31) driven by the endogenous promoters, remains susceptible to complement-mediated killing in human serum (Siegel et al., 2010; Hammerschmidt et al., 2012; **Table 1**). This result is consistent with other *B. burgdorferi* strains (i.e., the *cspA*-deficient strain) encoding *erpP* and *erpA* under the control by the endogenous promoters which remain susceptible to human serum. However, when those genes are expressed ectopically in a serum-sensitive *B. burgdorferi* strain using a strong and constitutive promoter, these spirochetes inactivate complement and survive when incubated with human serum (Kenedy and Akins, 2011; **Table 1**). These results imply that high expression levels of OspE are needed for complement inactivation and serum resistance.

The genes encoding OspE paralogs are not expressed when spirochetes are in post-molting flat nymphs whereas they are upregulated immediately after blood meals (Hefty et al., 2001; Miller et al., 2003). Additionally, the expression of *ospE* is maintained throughout different stages of infection after spirochete transmission from ticks to hosts (Hefty et al., 2001; Miller et al., 2003, 2005; **Table 1**). Consistent with the expression profiles of these *ospE* genes, spirochete burdens are reduced in nymphs feeding on mice passively immunized with anti-OspE IgG, but remain unaffected when feeding on mice inoculated with Ig isotype control (Nguyen et al., 1994). Further, the transposon-inserted *erpA* mutant in an infectious *B. burgdorferi* strain causes a 2-week delay in dissemination to distal tissues when co-infected with a library of other transposon-inserted mutants (Lin et al., 2012; **Table 1**). These findings suggest that OspE paralogs may play a role in conferring tick-to-host transmission of spirochetes as well as facilitating rapid dissemination to distal tissues (**Figure 1**). However, the off-target silencing by antibody-dependent deletion or transposon insertion methodologies may be the confounding effects of these results. Generating the deletion mutant of *ospE* paralogs could be the favorable approach to address this caveat, but multiple copies of OspE present in LD spirochetes could be cumbersome. Thus, the gain-of-function approach such as producing these OspE paralogs in a serum-sensitive strain and evaluating bloodstream survival during a short-term infection may be a suitable approach to address these technical hurdles (Caine and Coburn, 2015).

OspE paralogs among different strains have highly variable sequences (Marconi et al., 1996; Sung et al., 1998; Akins et al., 1999; Caimano et al., 2000; Stevenson and Miller, 2003; Brissette et al., 2008). These variants differ in their ability to bind to vertebrate animals' FH (Stevenson et al., 2002; McDowell et al., 2003; Hovis et al., 2006). These results imply potential roles of OspE paralogs in promoting LD spirochetes complement evasion in a host-specific manner. Besides FH, OspE also binds to different isotypes of CFHR (Zipfel et al., 2002; Siegel et al., 2010; Kraiczy and Stevenson, 2013; Skerka et al., 2013; Jozsi et al., 2015). However, the physiological importance of CFHR-binding activity of OspE proteins is unclear and warrants further investigation.

CONCLUSION

To survive their complex life cycle, LD spirochetes have developed several strategies to evade the host immune system that they encounter in ticks during feeding (blood meal) and in the bloodstream of vertebrate animals. A key evasion mechanism is to circumvent the complement components by producing complement- or CRP-binding proteins, including CRASPs, which facilitate complement inactivation. These CRASPs have been shown to confer spirochete transmission from ticks to hosts and promote infection and dissemination in vertebrate hosts. However, the concurrent production of CRASPs increases the complexity in delineating the contribution of these proteins individually in each of the stages within the infection cycle.

Elucidating such mechanisms will provide new insights into how spirochetes survive in two distinct environments, ticks, and vertebrate hosts. Such information will provide foundation for the development of preventions through targeting CRASPs to block these infection mechanisms, which will ultimately reduce LD burdens in humans.

AUTHOR CONTRIBUTIONS

Y-PL, AF, TN, and PK wrote the manuscript. TN and Y-PL prepared the figures.

FUNDING

This work was supported by NSF IOS1755286 (to Y-PL, AF, and TN), DoD TB170111 (to Y-PL, AF, and TN), NIAID 75N93019C00040 (to Y-PL, AF, and TN), New York State Department of Health Wadsworth Center Start-Up Grant (to Y-PL, AF, and TN), and NIH R01AI121401 (to PK).

ACKNOWLEDGMENTS

We thank Klemen Strle, Ashley Marcinkiewicz, and Thomas Hart for critical reading of the manuscript.

REFERENCES

Akins, D. R., Caimano, M. J., Yang, X., Cerna, F., Norgard, M. V., and Radolf, J. D. (1999). Molecular and evolutionary analysis of *Borrelia burgdorferi* 297 circular plasmid-encoded lipoproteins with OspE- and OspF-like leader peptides. *Infect. Immun.* 67, 1526–1532. doi: 10.1128/IAI.67.3.1526-1532.1999

Alitalo, A., Meri, T., Chen, T., Lankinen, H., Cheng, Z. Z., Jokiranta, T. S., et al. (2004). Lysine-dependent multipoint binding of the *Borrelia burgdorferi* virulence factor outer surface protein E to the C terminus of factor H. *J. Immunol.* 172, 6195–6201. doi: 10.4049/jimmunol.172.10.6195

Alitalo, A., Meri, T., Comstedt, P., Jeffery, L., Tornberg, J., Strandin, T., et al. (2005). Expression of complement factor H binding immunoevasion proteins in *Borrelia garinii* isolated from patients with neuroborreliosis. *Eur. J. Immunol.* 35, 3043–3053. doi: 10.1002/eji.200526354

Bernard, Q., Thakur, M., Smith, A. A., Kitsou, C., Yang, X., and Pal, U. (2019). *Borrelia burgdorferi* protein interactions critical for microbial persistence in mammals. *Cell Microbiol.* 21:e12885. doi: 10.1111/cmi.12885

Bhattacharjee, A., Oeemig, J. S., Kolodziejczyk, R., Meri, T., Kajander, T., Lehtinen, M. J., et al. (2013). Structural basis for complement evasion by Lyme disease pathogen *Borrelia burgdorferi*. *J. Biol. Chem.* 288, 18685–18695. doi: 10.1074/jbc.M113.459040

Bhide, M. R., Escudero, R., Camafeita, E., Gil, H., Jado, I., and Anda, P. (2009). Complement factor H binding by different Lyme disease and relapsing fever *Borrelia* in animals and human. *BMC Res. Notes* 2:134. doi: 10.1186/1756-0500-2-134

Brangulis, K., Petrovskis, I., Kazaks, A., Bogans, J., Otikovs, M., Jaudzems, K., et al. (2014). Structural characterization of CspZ, a complement regulator factor H and FHL-1 binding protein from *Borrelia burgdorferi*. *FEBS J.* 281, 2613–2622. doi: 10.1111/febs.12808

Brissette, C. A., Cooley, A. E., Burns, L. H., Riley, S. P., Verma, A., Woodman, M. E., et al. (2008). Lyme borreliosis spirochete Erp proteins, their known host ligands, and potential roles in mammalian infection. *Int. J. Med. Microbiol.* 298(Suppl. 1), 257–267. doi: 10.1016/j.ijmm.2007.09.004

Brisson, D., Drecktrah, D., Eggers, C. H., and Samuels, D. S. (2012). Genetics of *Borrelia burgdorferi*. *Annu. Rev. Genet.* 46, 515–536. doi: 10.1146/annurev-genet-011112-112140

Brooks, C. S., Vuppala, S. R., Jett, A. M., Alitalo, A., Meri, S., and Akins, D. R. (2005). Complement regulator-acquiring surface protein 1 imparts resistance to human serum in *Borrelia burgdorferi*. *J. Immunol.* 175, 3299–3308. doi: 10.4049/jimmunol.175.5.3299

Bykowski, T., Woodman, M. E., Cooley, A. E., Brissette, C. A., Brade, V., Wallich, R., et al. (2007). Coordinated expression of *Borrelia burgdorferi* complement regulator-acquiring surface proteins during the Lyme disease spirochete's mammal-tick infection cycle. *Infect. Immun.* 75, 4227–4236. doi: 10.1128/IAI.00604-07

Caimano, M. J., Yang, X., Popova, T. G., Clawson, M. L., Akins, D. R., Norgard, M. V., et al. (2000). Molecular and evolutionary characterization of the cp32/18 family of supercoiled plasmids in *Borrelia burgdorferi* 297. *Infect. Immun.* 68, 1574–1586. doi: 10.1128/IAI.68.3.1574-1586.2000

Caine, J. A., and Coburn, J. (2015). A short-term *Borrelia burgdorferi* infection model identifies tissue tropisms and bloodstream survival conferred by adhesion proteins. *Infect. Immun.* 83, 3184–3194. doi: 10.1128/IAI.00349-15

Caine, J. A., and Coburn, J. (2016). Multifunctional and redundant roles of *Borrelia burgdorferi* outer surface proteins in tissue adhesion, colonization, and complement evasion. *Front. Immunol.* 7:442. doi: 10.3389/fimmu.2016.00442

Caine, J. A., Lin, Y. P., Kessler, J. R., Sato, H., Leong, J. M., and Coburn, J. (2017). *Borrelia burgdorferi* outer surface protein C (OspC) binds complement component C4b and confers bloodstream survival. *Cell Microbiol.* 12:e12786. doi: 10.1111/cmi.12786

Coburn, J., Leong, J., and Chaconas, G. (2013). Illuminating the roles of the *Borrelia burgdorferi* adhesins. *Trends Microbiol.* 21, 372–379. doi: 10.1016/j.tim.2013.06.005

Coleman, A. S., Yang, X., Kumar, M., Zhang, X., Promnares, K., Shroder, D., et al. (2008). *Borrelia burgdorferi* complement regulator-acquiring surface protein 2 does not contribute to complement resistance or host infectivity. *PLoS ONE* 3:3010e. doi: 10.1371/journal.pone.0003010

de Taeye, S. W., Kreuk, L., Van Dam, A. P., Hovius, J. W., and Schuijt, T. J. (2013). Complement evasion by *Borrelia burgdorferi*: it takes three to tango. *Trends Parasitol.* 29, 119–128. doi: 10.1016/j.pt.2012.12.001

Dulebohn, D. P., Bestor, A., and Rosa, P. A. (2013). *Borrelia burgdorferi* linear plasmid 28–3 confers a selective advantage in an experimental mouse-tick infection model. *Infect. Immun.* 81, 2986–2996. doi: 10.1128/IAI.00219-13

Garcia, B. L., Zhi, H., Wager, B., Hook, M., and Skare, J. T. (2016). *Borrelia burgdorferi* BBK32 inhibits the classical pathway by blocking activation of the C1 complement complex. *PLoS Pathog.* 12:e1005404. doi: 10.1371/journal.ppat.1005404

Hallstrom, T., Siegel, C., Morgelin, M., Kraiczy, P., Skerka, C., and Zipfel, P. F. (2013). CspA from *Borrelia burgdorferi* inhibits the terminal complement pathway. *MBio* 4:e00481-13. doi: 10.1128/mBio.00481-13

Hammerschmidt, C., Hallstrom, T., Skerka, C., Wallich, R., Stevenson, B., Zipfel, P. F., et al. (2012). Contribution of the infection-associated complement regulator-acquiring surface protein 4 (ErpC) to complement resistance of *Borrelia burgdorferi*. *Clin. Dev. Immunol.* 2012:349657. doi: 10.1155/2012/349657

Hammerschmidt, C., Koenigs, A., Siegel, C., Hallstrom, T., Skerka, C., Wallich, R., et al. (2014). Versatile roles of CspA orthologs in complement inactivation of serum-resistant Lyme disease spirochetes. *Infect. Immun.* 82, 380–392. doi: 10.1128/IAI.01094-13

Hart, T., Nguyen, N. T. T., Nowak, N. A., Zhang, F., Linhardt, R. J., Diuk-Wasser, M., et al. (2018). Polymorphic factor H-binding activity of CspA protects Lyme borreliae from the host complement in feeding ticks to facilitate tick-to-host transmission. *PLoS Pathog.* 14:e1007106. doi: 10.1371/journal.ppat.1007106

Hartmann, K., Corvey, C., Skerka, C., Kirschfink, M., Karas, M., Brade, V., et al. (2006). Functional characterization of BbCRASP-2, a distinct outer membrane protein of *Borrelia burgdorferi* that binds host complement regulators factor H and FHL-1. *Mol. Microbiol.* 61, 1220–1236. doi: 10.1111/j.1365-2958.2006.05318.x

Hefty, P. S., Jolliff, S. E., Caimano, M. J., Wikel, S. K., Radolf, J. D., and Akins, D. R. (2001). Regulation of OspE-related, OspF-related, and Elp lipoproteins of *Borrelia burgdorferi* strain 297 by mammalian host-specific signals. *Infect. Immun.* 69, 3618–3627. doi: 10.1128/IAI.69.6.3618-3627.2001

Hovis, K. M., Tran, E., Sundy, C. M., Buckles, E., McDowell, J. V., and Marconi, R. T. (2006). Selective binding of *Borrelia burgdorferi* OspE paralogs to

factor H and serum proteins from diverse animals: possible expansion of the role of OspE in Lyme disease pathogenesis. *Infect. Immun.* 74, 1967–1972. doi: 10.1128/IAI.74.3.1967-1972.2006

Hovius, J. W., Van Dam, A. P., and Fikrig, E. (2007). Tick-host-pathogen interactions in Lyme borreliosis. *Trends Parasitol.* 23, 434–438. doi: 10.1016/j.pt.2007.07.001

Hyde, J. A. (2017). *Borrelia burgdorferi* keeps moving and carries on: a review of borrelial dissemination and invasion. *Front. Immunol.* 8:114. doi: 10.3389/fimmu.2017.00114

Jozsi, M., Tortajada, A., Uzonyi, B., Goicoechea De Jorge, E., and Rodriguez De Cordoba, S. (2015). Factor H-related proteins determine complement-activating surfaces. *Trends Immunol.* 36, 374–384. doi: 10.1016/j.it.2015.04.008

Kenedy, M. R., and Akins, D. R. (2011). The OspE-related proteins inhibit complement deposition and enhance serum resistance of *Borrelia burgdorferi*, the lyme disease spirochete. *Infect. Immun.* 79, 1451–1457. doi: 10.1128/IAI.01274-10

Kenedy, M. R., Vuppala, S. R., Siegel, C., Kraiczy, P., and Akins, D. R. (2009). CspA-mediated binding of human factor H inhibits complement deposition and confers serum resistance in *Borrelia burgdorferi*. *Infect. Immun.* 77, 2773–2782. doi: 10.1128/IAI.00318-09

Kraiczy, P. (2016). Hide and seek: how lyme disease spirochetes overcome complement attack. *Front. Immunol.* 7:385. doi: 10.3389/fimmu.2016.00385

Kraiczy, P., Hartmann, K., Hellwage, J., Skerka, C., Kirschfink, M., Brade, V., et al. (2004a). Immunological characterization of the complement regulator factor H-binding CRASP and Erp proteins of *Borrelia burgdorferi*. *Int. J. Med. Microbiol.* 293(Suppl. 37), 152–157. doi: 10.1016/S1433-1128(04)80029-9

Kraiczy, P., Hellwage, J., Skerka, C., Becker, H., Kirschfink, M., Simon, M. M., et al. (2004b). Complement resistance of *Borrelia burgdorferi* correlates with the expression of BbCRASP-1, a novel linear plasmid-encoded surface protein that interacts with human factor H and FHL-1 and is unrelated to Erp proteins. *J. Biol. Chem.* 279, 2421–2429. doi: 10.1074/jbc.M308343200

Kraiczy, P., Hellwage, J., Skerka, C., Kirschfink, M., Brade, V., Zipfel, P. F., et al. (2003). Immune evasion of *Borrelia burgdorferi*: mapping of a complement-inhibitor factor H-binding site of BbCRASP-3, a novel member of the Erp protein family. *Eur. J. Immunol.* 33, 697–707. doi: 10.1002/eji.200323571

Kraiczy, P., Seling, A., Brissette, C. A., Rossmann, E., Hunfeld, K. P., Bykowski, T., et al. (2008). *Borrelia burgdorferi* complement regulator-acquiring surface protein 2 (CspZ) as a serological marker of human Lyme disease. *Clin. Vaccine Immunol.* 15, 484–491. doi: 10.1128/CVI.00415-07

Kraiczy, P., and Stevenson, B. (2013). Complement regulator-acquiring surface proteins of *Borrelia burgdorferi*: structure, function and regulation of gene expression. *Ticks Tick Borne Dis.* 4, 26–34. doi: 10.1016/j.ttbdis.2012.10.039

Kurtenbach, K., De Michelis, S., Etti, S., Schafer, S. M., Sewell, H. S., Brade, V., et al. (2002). Host association of *Borrelia burgdorferi* sensu lato–the key role of host complement. *Trends Microbiol.* 10, 74–79. doi: 10.1016/S0966-842X(01)02298-3

Lin, T., Gao, L., Zhang, C., Odeh, E., Jacobs, M. B., Coutte, L., et al. (2012). Analysis of an ordered, comprehensive STM mutant library in infectious *Borrelia burgdorferi*: insights into the genes required for mouse infectivity. *PLoS ONE* 7:e47532. doi: 10.1371/journal.pone.0047532

Marcinkiewicz, A., Kraiczy, P., and Lin, Y.-P. (2017). There is a method to the madness: strategies to study host complement evasion by Lyme disease and relapsing fever spirochetes. *Front. Microbiol.* 8:328. doi: 10.3389/fmicb.2017.00328

Marcinkiewicz, A. L., Dupuis, A. P. II, Zamba-Campero, M., Nowak, N., Kraiczy, P., Ram, S., Kramer, L. D., et al. (2019). Blood treatment of Lyme borreliae demonstrates the mechanism of CspZ-mediated complement evasion to promote systemic infection in vertebrate hosts. *Cell Microbiol.* 21:e12998. doi: 10.1111/cmi.12998

Marconi, R. T., Sung, S. Y., Hughes, C. A., and Carlyon, J. A. (1996). Molecular and evolutionary analyses of a variable series of genes in *Borrelia burgdorferi* that are related to ospE and ospF, constitute a gene family, and share a common upstream homology box. *J. Bacteriol.* 178, 5615–5626. doi: 10.1128/JB.178.19.5615-5626.1996

McDowell, J. V., Hovis, K. M., Zhang, H., Tran, E., Lankford, J., and Marconi, R. T. (2006). Evidence that the BBA68 protein (BbCRASP-1) of the Lyme disease spirochetes does not contribute to factor H-mediated immune evasion in humans and other animals. *Infect. Immun.* 74, 3030–3034. doi: 10.1128/IAI.74.5.3030-3034.2006

McDowell, J. V., Wolfgang, J., Tran, E., Metts, M. S., Hamilton, D., and Marconi, R. T. (2003). Comprehensive analysis of the factor h binding capabilities of borrelia species associated with lyme disease: delineation of two distinct classes of factor h binding proteins. *Infect. Immun.* 71, 3597–3602. doi: 10.1128/IAI.71.6.3597-3602.2003

Meri, S. (2016). Self-nonself discrimination by the complement system. *FEBS Lett.* 590, 2418–2434. doi: 10.1002/1873-3468.12284

Miller, J. C., Narayan, K., Stevenson, B., and Pachner, A. R. (2005). Expression of *Borrelia burgdorferi erp* genes during infection of non-human primates. *Microb. Pathog.* 39, 27–33. doi: 10.1016/j.micpath.2005.04.001

Miller, J. C., von Lackum, K., Babb, K., Mcalister, J. D., and Stevenson, B. (2003). Temporal analysis of *Borrelia burgdorferi* Erp protein expression throughout the mammal-tick infectious cycle. *Infect. Immun.* 71, 6943–6952. doi: 10.1128/IAI.71.12.6943-6952.2003

Muhleip, J. J., Lin, Y. P., and Kraiczy, P. (2018). Further insights into the interaction of human and animal complement regulator factor H with viable lyme disease spirochetes. *Front. Vet. Sci.* 5:346. doi: 10.3389/fvets.2018.00346

Nguyen, T. P., Lam, T. T., Barthold, S. W., Telford, S. R. III, Flavell, R. A., and Fikrig, E. (1994). Partial destruction of *Borrelia burgdorferi* within ticks that engorged on OspE- or OspF-immunized mice. *Infect. Immun.* 62, 2079–2084. doi: 10.1128/IAI.62.5.2079-2084.1994

Pietikainen, J., Meri, T., Blom, A. M., and Meri, S. (2010). Binding of the complement inhibitor C4b-binding protein to Lyme disease Borreliae. *Mol. Immunol.* 47, 1299–1305. doi: 10.1016/j.molimm.2009.11.028

Purser, J. E., and Norris, S. J. (2000). Correlation between plasmid content and infectivity in *Borrelia burgdorferi*. *Proc. Natl. Acad. Sci. U.S.A.* 97, 13865–13870. doi: 10.1073/pnas.97.25.13865

Radolf, J. D., Caimano, M. J., Stevenson, B., and Hu, L. T. (2012). Of ticks, mice and men: understanding the dual-host lifestyle of Lyme disease spirochaetes. *Nat. Rev. Microbiol.* 10, 87–99. doi: 10.1038/nrmicro2714

Rathinavelu, S., Broadwater, A., and De Silva, A. M. (2003). Does host complement kill *Borrelia burgdorferi* within ticks? *Infect. Immun.* 71, 822–829. doi: 10.1128/IAI.71.2.822-829.2003

Rogers, E. A., Abdunnur, S. V., McDowell, J. V., and Marconi, R. T. (2009). Comparative analysis of the properties and ligand binding characteristics of CspZ, a factor H binding protein, derived from *Borrelia burgdorferi* isolates of human origin. *Infect. Immun.* 77, 4396–4405. doi: 10.1128/IAI.00393-09

Rogers, E. A., and Marconi, R. T. (2007). Delineation of species-specific binding properties of the CspZ protein (BBH06) of Lyme disease spirochetes: evidence for new contributions to the pathogenesis of *Borrelia* spp. *Infect. Immun.* 75, 5272–5281. doi: 10.1128/IAI.00850-07

Rosa, P. A., Tilly, K., and Stewart, P. E. (2005). The burgeoning molecular genetics of the Lyme disease spirochaete. *Nat. Rev. Microbiol.* 3, 129–143. doi: 10.1038/nrmicro1086

Schuijt, T. J., Coumou, J., Narasimhan, S., Dai, J., Deponte, K., Wouters, D., et al. (2011). A tick mannose-binding lectin inhibitor interferes with the vertebrate complement cascade to enhance transmission of the lyme disease agent. *Cell Host Microbe* 10, 136–146. doi: 10.1016/j.chom.2011.06.010

Schuijt, T. J., Hovius, J. W., Van Burgel, N. D., Ramamoorthi, N., Fikrig, E., and Van Dam, A. P. (2008). The tick salivary protein Salp15 inhibits the killing of serum-sensitive *Borrelia burgdorferi* sensu lato isolates. *Infect. Immun.* 76, 2888–2894. doi: 10.1128/IAI.00232-08

Siegel, C., Hallstrom, T., Skerka, C., Eberhardt, H., Uzonyi, B., Beckhaus, T., et al. (2010). Complement factor H-related proteins CFHR2 and CFHR5 represent novel ligands for the infection-associated CRASP proteins of *Borrelia burgdorferi*. *PLoS ONE* 5:e13519. doi: 10.1371/journal.pone.0013519

Siegel, C., Schreiber, J., Haupt, K., Skerka, C., Brade, V., Simon, M. M., et al. (2008). Deciphering the ligand-binding sites in the *Borrelia burgdorferi* complement regulator-acquiring surface protein 2 required for interactions with the human immune regulators factor H and factor H-like protein 1. *J. Biol. Chem.* 283, 34855–34863. doi: 10.1074/jbc.M805844200

Sjoberg, A. P., Trouw, L. A., and Blom, A. M. (2009). Complement activation and inhibition: a delicate balance. *Trends Immunol.* 30, 83–90. doi: 10.1016/j.it.2008.11.003

Skerka, C., Chen, Q., Fremeaux-Bacchi, V., and Roumenina, L. T. (2013). Complement factor H related proteins (CFHRs). *Mol. Immunol.* 56, 170–180. doi: 10.1016/j.molimm.2013.06.001

Steere, A. C., Strle, F., Wormser, G. P., Hu, L. T., Branda, J. A., Hovius, J. W., et al. (2016). Lyme borreliosis. *Nat. Rev. Dis. Primers* 2:16090. doi: 10.1038/nrdp.2016.90

Stevenson, B., El-Hage, N., Hines, M. A., Miller, J. C., and Babb, K. (2002). Differential binding of host complement inhibitor factor H by *Borrelia burgdorferi* Erp surface proteins: a possible mechanism underlying the expansive host range of Lyme disease spirochetes. *Infect. Immun.* 70, 491–497. doi: 10.1128/IAI.70.2.491-497.2002

Stevenson, B., and Miller, J. C. (2003). Intra- and interbacterial genetic exchange of Lyme disease spirochete erp genes generates sequence identity amidst diversity. *J. Mol. Evol.* 57, 309–324. doi: 10.1007/s00239-003-2482-x

Stevenson, B., Tilly, K., and Rosa, P. A. (1996). A family of genes located on four separate 32-kilobase circular plasmids in *Borrelia burgdorferi* B31. *J. Bacteriol.* 178, 3508–3516. doi: 10.1128/JB.178.12.3508-3516.1996

Sung, S. Y., Lavoie, C. P., Carlyon, J. A., and Marconi, R. T. (1998). Genetic divergence and evolutionary instability in *ospE*-related members of the upstream homology box gene family in *Borrelia burgdorferi* sensu lato complex isolates. *Infect. Immun.* 66, 4656–4668. doi: 10.1128/IAI.66.10.4656-4668.1998

Tokarz, R., Anderton, J. M., Katona, L. I., and Benach, J. L. (2004). Combined effects of blood and temperature shift on *Borrelia burgdorferi* gene expression as determined by whole genome DNA array. *Infect. Immun.* 72, 5419–5432. doi: 10.1128/IAI.72.9.5419-5432.2004

Tufts, D. M., Hart, T. M., Chen, G. F., Kolokotronis, S. O., Diuk-Wasser, M. A., and Lin, Y. P. (2019). Outer surface protein polymorphisms linked to host-spirochete association in Lyme borreliae. *Mol. Microbiol.* 111, 868–882. doi: 10.1111/mmi.14209

Tyson, K., Elkins, C., Patterson, H., Fikrig, E., and De Silva, A. (2007). Biochemical and functional characterization of Salp20, an *Ixodes scapularis* tick salivary protein that inhibits the complement pathway. *Insect Mol. Biol.* 16, 469–479. doi: 10.1111/j.1365-2583.2007.00742.x

Tyson, K. R., Elkins, C., and De Silva, A. M. (2008). A novel mechanism of complement inhibition unmasked by a tick salivary protein that binds to properdin. *J. Immunol.* 180, 3964–3968. doi: 10.4049/jimmunol.180.6.3964

von Lackum, K., Miller, J. C., Bykowski, T., Riley, S. P., Woodman, M. E., Brade, V., et al. (2005). *Borrelia burgdorferi* regulates expression of complement regulator-acquiring surface protein 1 during the mammal-tick infection cycle. *Infect. Immun.* 73, 7398–7405. doi: 10.1128/IAI.73.11.7398-7405.2005

Wagemakers, A., Coumou, J., Schuijt, T. J., Oei, A., Nijhof, A. M., Van 'T Veer, C., et al. (2016). An *Ixodes ricinus* tick salivary lectin pathway inhibitor protects *Borrelia burgdorferi* sensu lato from human complement. *Vector Borne Zoonotic Dis.* 16, 223–228. doi: 10.1089/vbz.2015.1901

Wywial, E., Haven, J., Casjens, S. R., Hernandez, Y. A., Singh, S., Mongodin, E. F., et al. (2009). Fast, adaptive evolution at a bacterial host-resistance locus: the PFam54 gene array in *Borrelia burgdorferi*. *Gene* 445, 26–37. doi: 10.1016/j.gene.2009.05.017

Zipfel, P. F., Hallstrom, T., and Riesbeck, K. (2013). Human complement control and complement evasion by pathogenic microbes–tipping the balance. *Mol. Immunol.* 56, 152–160. doi: 10.1016/j.molimm.2013.05.222

Zipfel, P. F., and Skerka, C. (1999). FHL-1/reconectin: a human complement and immune regulator with cell-adhesive function. *Immunol. Today* 20, 135–140. doi: 10.1016/S0167-5699(98)01432-7

Zipfel, P. F., and Skerka, C. (2009). Complement regulators and inhibitory proteins. *Nat. Rev. Immunol.* 9, 729–740. doi: 10.1038/nri2620

Zipfel, P. F., Skerka, C., Hellwage, J., Jokiranta, S. T., Meri, S., Brade, V., et al. (2002). Factor H family proteins: on complement, microbes and human diseases. *Biochem. Soc. Trans.* 30, 971–978. doi: 10.1042/bst0300971

Conflict of Interest: The authors declare that the research was conducted in the absence of any commercial or financial relationships that could be construed as a potential conflict of interest.

frontiers in Cellular and Infection Microbiology

ORIGINAL RESEARCH
published: 18 February 2020
doi: 10.3389/fcimb.2020.00041

Tick-Borne Encephalitis Virus Infection Alters the Sialome of *Ixodes ricinus* Ticks During the Earliest Stages of Feeding

Charles E. Hart[1,2,3], *Jose M. Ribeiro*[4], *Maria Kazimirova*[5] *and Saravanan Thangamani*[1,2,6*]

[1] SUNY Center for Environmental Health and Medicine, SUNY Upstate Medical University, Syracuse, NY, United States, [2] Institute for Global Health and Translational Science, SUNY Upstate Medical University, Syracuse, NY, United States, [3] The Institute for Translational Science, University of Texas Medical Branch, Galveston, TX, United States, [4] Laboratory of Malaria and Vector Research, National Institute of Allergy and Infectious Diseases, Bethesda, MD, United States, [5] Institute of Zoology, Slovak Academy of Sciences, Bratislava, Slovakia, [6] Department of Microbiology and Immunology, SUNY Upstate Medical University, Syracuse, NY, United States

OPEN ACCESS

Edited by:
Alejandro Cabezas-Cruz, Institut National de la Recherche Agronomique (INRA), France

Reviewed by:
Sara Moutailler, Agence Nationale de Sécurité Sanitaire de l'Alimentation, de l'Environnement et du Travail (ANSES), France
Jan Kopecky, University of South Bohemia, Czechia
Jennifer Patricia Richardson, Institut National de la Recherche Agronomique (INRA), France

***Correspondence:**
Saravanan Thangamani
ThangamS@upstate.edu

Specialty section:
This article was submitted to Virus and Host, a section of the journal Frontiers in Cellular and Infection Microbiology

Received: 25 October 2019
Accepted: 21 January 2020
Published: 18 February 2020

Citation:
Hart CE, Ribeiro JM, Kazimirova M and Thangamani S (2020) Tick-Borne Encephalitis Virus Infection Alters the Sialome of Ixodes ricinus Ticks During the Earliest Stages of Feeding. Front. Cell. Infect. Microbiol. 10:41. doi: 10.3389/fcimb.2020.00041

Ticks are hematophagous arthropods that transmit a number of pathogens while feeding. Among these is tick-borne encephalitis virus (TBEV), a flavivirus transmitted by *Ixodes ricinus* ticks in the temperate zone of Europe. The infection results in febrile illness progressing to encephalitis and meningitis with a possibility of fatality or long-term neurological sequelae. The composition of tick saliva plays an essential role in the initial virus transmission during tick feeding. Ticks secrete a diverse range of salivary proteins to modulate the host response, such as lipocalins to control the itch and inflammatory response, and both proteases and protease inhibitors to prevent blood coagulation. Here, the effect of viral infection of adult females of *Ixodes ricinus* was studied with the goal of determining how the virus alters the tick sialome to modulate host tissue response at the site of infection. Uninfected ticks or those infected with TBEV were fed on mice and removed and dissected one- and 3-h post-attachment. RNA from the salivary glands of these ticks, as well as from unfed ticks, was extracted and subjected to next-generation sequencing to determine the expression of key secreted proteins at each timepoint. Genes showing statistically significant up- or down-regulation between infected and control ticks were selected and compared to published literature to ascertain their function. From this, the effect of tick viral infection on the modulation of the tick-host interface was determined. Infected ticks were found to differentially express a number of uncategorized genes, proteases, Kunitz-type serine protease inhibitors, cytotoxins, and lipocalins at different timepoints. These virus-induced changes to the tick sialome may play a significant role in facilitating virus transmission during the early stages of tick feeding.

Keywords: vector-skin interface, tick-borne encephalitis virus, tick sialome, tick feeding, immunomodulation

INTRODUCTION

Ticks are obligate hematophagous arthropods of the order Ixodida that transmit a variety of disease agents to humans and animals. In Europe, Russia, and Northern Asia, tick-borne viral diseases are a major public health concern. Of particular concern is tick-borne encephalitis virus (TBEV), a flavivirus endemic to Europe and northern Asia which is vectored by *Ixodes ricinus* in Europe and *Ixodes persulcatus* in parts of Eastern Europe and Asiatic Russia. Upon TBEV-infected tick feeding, the virus initially replicates in host skin fibroblasts (Hermance et al., 2016) and macrophages (Labuda et al., 1996). The virus is then transported by these macrophages to the draining lymph nodes, where it replicates before entering the blood and progressing to the remainder of the body. This results in febrile illness that may progress to neuroinvasive disease with meningitis or in more severe cases to encephalitis or myeloencephalitis (Zavadska et al., 2018). Tick-borne encephalitis (TBE) is diagnosed in about 12,000 people per year (World Health Organization, 2011), although the rate of exposure is thought to be substantially higher. The fatality rate of the European subtype of TBE (transmitted by *I. ricinus*) is 1–3%, with over 40% of neuroinvasive cases resulting in long-term neurological sequelae.

Ticks are pool-feeders. To facilitate the feeding process, ticks secrete to the feeding pool a complex mixture of compounds in their saliva, containing hundreds of proteinaceous, and non-proteinaceous molecules that modulate host hemostasis, inflammation, immune reactions, and wound healing. The expression of the tick salivary factors undergoes significant and dynamic temporal regulation, where different factors are expressed and secreted throughout the feeding process (Francischetti et al., 2009; Šimo et al., 2017). These complex processes allow the ticks to remain attached for a prolonged period and compensate for different host defense mechanisms and requirements of the tick feeding cycle. Tick salivary molecules can be grouped into major categories based on their function, such as lipocalins (acting as kratagonists of biogenic amines and prostanoids), metalloproteases (having fibrinolytic activity), Kunitz-domain containing peptides (having putative sodium channel blocking or anticlotting activities), basic tail polypeptides (a unique protein family having anti-thrombin or plasminogen-activating activities), the salp-15 family (having immunosuppressive activity), the Isac family (having anti-complement activity), glycine-rich peptides (immunogenic components of the tick cement) (Francischetti et al., 2009; Blisnick et al., 2017; Chmelar et al., 2017; Šimo et al., 2017). Interestingly, not all molecules are secreted simultaneously (Kotsyfakis et al., 2015). This indicates that ticks adapt the composition of their sialomes (from the Greek, sialo = saliva) to the time of feeding, to their hosts, to the presence of pathogens, or to stress signals (Liu et al., 2014; Chmelar et al., 2016; Šimo et al., 2017; Tirloni et al., 2019). However, the mechanism of this adaptation is unknown.

In addition to creating a favorable microenvironment to acquire blood, the immunomodulatory functions of tick salivary molecules have been demonstrated to facilitate pathogen transmission. Tick saliva initially alters the inflammatory state of the inoculation site by altering the expression of cytokines (Thangamani et al., 2017) to increase neutrophil and monocyte (Hermance et al., 2016) influx. This results in an inflammatory environment that is conducive to viral invasion and macrophage-driven replication and dissemination (Labuda et al., 1996; Hermance et al., 2016). Elements of the tick saliva can also alter the behavior of dendritic cells to increase the replication of TBEV, in turn accelerating viral dissemination through the lymphatic system (Fialova et al., 2010; Lieskovska et al., 2018). Part of this effect appears to be due to lipocalins which target dendritic cells by binding to surface cholesterol (Roversi et al., 2017). Other affected cells include leukocytes (Rodriguez-Valle et al., 2013), natural killer cells, and other skin residents. Additional salivary factors can alter inflammation by targeting pro-inflammatory signaling molecules such as histamine, serotonin, leukotrienes, and complement (Francischetti et al., 2009; Šimo et al., 2017; Štibrániová et al., 2019).

The presence of tick saliva has been shown to increase both the acquisition and transmission of viruses. For example, ticks fed on animals inoculated with Thogoto virus have been shown to acquire infection at a higher rate when the inoculate also contained tick salivary gland extract (SGE) (Jones et al., 1989); the same has been observed with TBEV (Labuda et al., 1993). Experiments with Powassan virus (POWV), which is closely related to TBEV, had demonstrated that the amount of virus required to produce lethal animal infection was significantly lower when tick SGE was present (Hermance and Thangamani, 2015). This suggests that tick-borne viruses have evolved to exploit immunological events in the vertebrate hosts evoked by ticks to facilitate their feeding (Kazimírová et al., 2017). It is also plausible that the infection and replication of viruses in tick salivary glands induce alterations that enhance the transmission properties of tick saliva. For example, in contrast to uninfected ticks, the presence of POWV has been shown to increase skin inflammation during tick feeding (Hermance et al., 2016), which in turn increased the influx of macrophages and may potentially accelerate early viral infection and dissemination through the lymphatic system.

The potential of tick-borne viruses to alter the immunomodulatory properties of tick saliva to further enhance their own pathogenicity has not previously been accounted for in experiments involving the effect of tick saliva on viral transmission. This information is of great importance to understand the processes at the tick-host-virus interface and how these factors interact to produce early infection and systemic disease. In this manuscript, we describe for the first time the dynamic expression of tick salivary factors during the early stages of TBEV transmission and the implications of the components of the saliva of infected ticks in creating an immunomodulated feeding site.

MATERIALS AND METHODS

Ticks and Animals

Ixodes ricinus ticks were obtained from a laboratory colony maintained at the Institute of Zoology, Slovak Academy of

Sciences (Bratislava, Slovakia). BALB/c mice (females, 5-weeks-old) were purchased from Dobrá Voda Breeding Station (Institute of Experimental Pharmacology and Toxicology, Slovak Academy of Sciences). The mice were housed at the Institute of Virology (BMC SAS) under standard conditions. Food and water were provided *ad libitum*. Mice were 6 weeks old at the start of the experiments, and at the end of the experiments they were euthanized by cervical dislocation under anesthesia induced by carbon dioxide.

Ethics Statement

The experiments involving laboratory mice were performed in accordance with the animal use protocol approved by the State Veterinary and Food Administration of the Slovak Republic (permit number 1335/12-221) and the Institute of Virology, Biomedical Research Center of the Slovak Academy of Sciences (BMC SAS).

Tick Infection With TBEV, Feeding, and Dissection

F1 generation of laboratory-bred *I. ricinus* females were used for virus inoculation. TBEV (Hypr strain prepared as a 10% mouse brain suspension of 1.1×10^9 PFU/ml in Leibovitz's L-15 medium) was provided by the Institute of Virology BMC SAS. Unfed *I. ricinus* females were inoculated with TBEV (5.5×10^4 PFU per tick) through the coxal plate of the second pair of legs by a digital microinjector TM system (MINJ-D-CE; Tritech Research, Inc., USA) (for details see Thangamani et al., 2017) and subsequently kept at room temperature and 85% relative humidity in a desiccator for 21 days. The infection rate achieved by this procedure is ∼100% (Slovák et al., 2014).

Two groups of BALB/c mice ($n = 6$ each) were infested with TBEV-infected or uninfected (control) *I. ricinus* females, respectively. The ticks were placed in small neoprene capsules glued on the shaved backs of the mice (two capsules per mouse, four tick females per capsule) (Thangamani et al., 2017). Ticks in each capsule were allowed to feed for either 1 or 3 h. After the allotted feeding time, mice ($n = 3$ per group and timepoint) were euthanized, and the attached ticks from one of the capsules were removed from the skin. The ticks and skin from the other capsules were used for the study by Thangamani et al. (2017). Ticks were dissected in chilled sterile PBS, pH 7.2, and their salivary glands were stored individually in either RNALater (uninfected ticks) or Tri Reagent (TBEV-infected ticks). Along with feeding ticks, salivary glands of unfed ticks (both TBEV-infected and uninfected) were prepared as described above. Samples in RNALater and TriReagent were stored at −80°C.

Next Generation Sequencing

Three ticks (one tick per mouse) for each treatment condition (infected or non-infected) and each of the feeding timepoints were used in this study. RNA from the salivary glands of these ticks were extracted as described by us earlier (Hermance and Thangamani, 2015), and pooled prior to Illumina Next Generation Sequencing analysis. Illumina TruSeq v2 sample preparation kits were used for the RNA-Seq library construction. Each sample library was uniquely indexed to allow combining libraries during sequencing, and subsequent separation post-sequencing. Next generation sequencing (NGS) was performed at the UTMB NGS core facility. Sample libraries were analyzed by the Illumina HiSeq 1,500 using a 2×50 base paired end run protocol, with TruSeq v3 sequencing-by-synthesis chemistry.

Bioinformatic Analysis

Bioinformatic analyses were conducted following the methods described previously (Chagas et al., 2013; Ribeiro et al., 2014), with some modifications. Briefly, the fastq files were trimmed of low-quality reads (<20), removed from contaminating primer sequences and concatenated for single-ended assembly using the Abyss (using k parameters from 25 to 95 in 10 fold increments) (Birol et al., 2009) and Trinity (Grabherr et al., 2011) assemblers. The combined fasta files were further assembled together with previous assemblies from *I. ricinus* (Schwarz et al., 2013; Kotsyfakis et al., 2015) using an iterative blast and CAP3 pipeline as previously described Karim et al. (2011). Coding sequences (CDS) were extracted based on the existence of a signal peptide in the longer open reading frame (ORF) and by similarities to other proteins found in the Refseq invertebrate database from the National Center for Biotechnology Information (NCBI), proteins from Acari deposited at NCBI's GenBank and from SwissProt. Reads for each library were mapped on the deducted CDS using the program blastn with a word size of 25, minimum identity of 97% and only one gap allowed. Functional classification of the transcripts was achieved by scanning the output of the different blast and rpsblast results using a vocabulary of ∼400 words, the e value of the result and a result coverage > 75%. The classification of "unknown" was given if no informative match could be found. Read counts for each CDS were transformed to FPKM values. FPKM is a measure proportional to the relative molar abundance of each transcript.

Pairwise statistical comparisons between infected and uninfected libraries at the three different physiological states were assessed by a chi-squared test. The Bonferroni and FDR correction (Benjamini and Hochberg, 1995) were applied using the *P*-value package version 3.3.0 from the R software package (Team R. C., 2013). The normalized reads rate was determined by the expressions $r1 \times R2/[R1 \times (r2 + 1)]$ e $r2 \times R1/[R2 \times (r1 + 1)]$, in which r1 and r2 are the reads for each library (T– and T+) mapping to a particular transcript and R1 and R2 the number of total reads from each library mapped over all the CDS. One unit was added to the denominator to avoid division by zero. The Kruskall-Wallis statistical test (within the R package) was used to test for significant differences in FPKM values between transcripts within the different functional classes.

Class Organization and Categorization

The list of identified transcripts was narrowed based on several parameters. Firstly, contigs with RPKM values of <10 were excluded. Transcripts were then selected based on having a p-value smaller than 0.05 for at least one timepoint (unfed ticks, 1 h post-attachment, and 3 h post attachment). The list was further narrowed to only proteins that were likely to be secreted as defined by the presence of secretion-related sequences or the

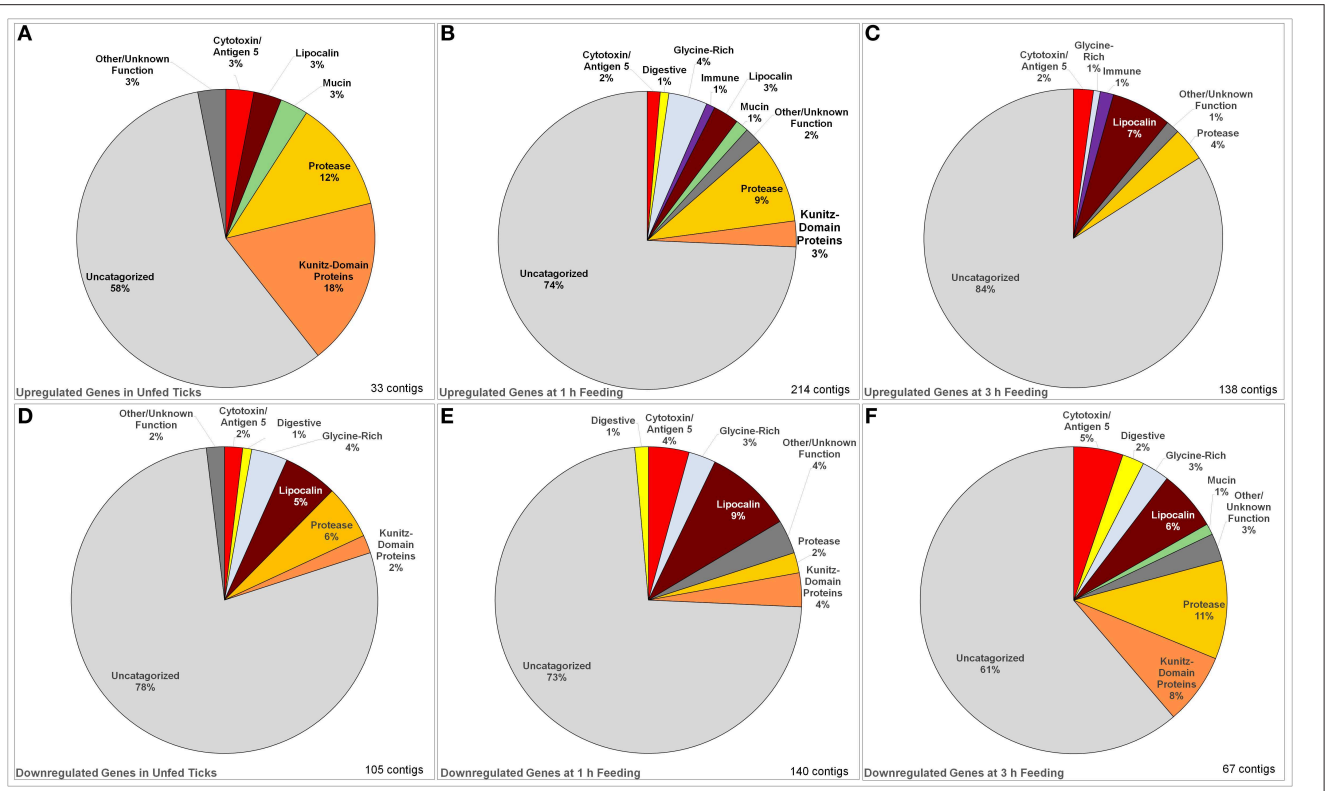

FIGURE 1 | Identified categories of saliva-associated genes in *Ixodes ricinus* ticks upregulated and downregulated in response to tick infection with TBEV. Upregulation was observed in unfed ticks **(A)**, ticks after 1 h of feeding **(B)**, and ticks after 3 h of feeding **(C)** showing an overall increase in the number of genes upregulated. The dominant change in upregulation is in uncategorized genes, with the proportion of proteases and serine protease inhibitors decreasing with feeding while upregulation of lipocalins increase. Downregulation was also observed in unfed ticks **(D)** as well as those at 1 h **(E)** and 3 h **(F)** of feeding. In downregulated genes, the proportion of uncharacterized genes decreased while the downregulation of proteases, lipocalins, serine protease inhibitors, and cytotoxins became dominant.

predicted function of the protein being identified as salivary in nature (i.e., lipocalins or cystatins).

These genes were then organized based on functional class, the results of which are presented in **Figure 1**, with a specific focus only on those components that are transferred to the host via saliva to modulate the host response to tick feeding (as opposed to metabolic or signaling genes within the salivary gland itself). Genes were identified as upregulated if expression in infected ticks was at least 10-fold higher than in uninfected ticks for at least one timepoint. Downregulated genes were defined as any that were downregulated below 0.1-fold during active tick feeding at 1 and 3-h timepoints as well as in cases where a gene was downregulated at any timepoint and upregulated at another. This relatively high 10-fold threshold was used to avoid false positives. This list was compiled into **Tables 1**, **2**.

Comparisons were derived from comparing expression changes of each functional class of predicted secreted salivary proteins at each timepoint.

Evolutionary Relationships of *Ixodes ricinus* Lipocalins

The evolutionary history was inferred using the Neighbor-Joining method (Saitou and Nei, 1987). The bootstrap consensus tree inferred from 1000 replicates is taken to represent the evolutionary history of the taxa analyzed (Felsenstein, 1985). The percentage of replicate trees in which the associated taxa clustered together in the bootstrap test (1,000 replicates) are shown next to the branches. The evolutionary distances were computed using the Poisson correction method (Zuckerkandl et al., 1965) and are in the units of the number of amino acid substitutions per site. The analysis involved 106 amino acid sequences. All positions with <50% site coverage were eliminated. That is, fewer than 50% alignment gaps, missing data, and ambiguous bases were allowed at any position. There were a total of 196 positions in the final dataset. Evolutionary analyses were conducted in MEGA7 (Kumar et al., 2016). Clades with strong bootstrap support are numbered I–XXVII (**Figure S2**). Clades with red colored branches contain lipocalins detected in adult ticks feeding for 5 days (Beaufays et al., 2008a); these are marked with a red symbol. Branches of green color contain sequences that are upregulated at time zero when ticks are infected with TBEV; these are marked with a green square. Branches of turquoise color contain sequences that are upregulated at 1 h in TBEV-infected ticks; these are marked with a turquoise triangle.

PCR Validation

Pooled tick RNA was converted into cDNA using a REPLI-g WTA Single Cell kit (Qiagen) in accordance with the kit

TABLE 1 | Regulation of individual contigs and associated proteins in response to TBEV infection in salivary glands of unfed *Ixodes ricinus* ticks and at one and three hours of feeding organized by category, showing proteases and miscellaneous genes.

Contig name	Miscallaneous	Unfed fold change	1 h fold change	3 h fold change	Specific type	Regulation pattern
IrSigP-350116_FR2_1-200	scp gapr-1 like scp-like extracellular protein	0.59	0.00	0.00	Antigen 5	DOWN
IrSigP-120441_FR3_1-213	scp gapr-1 like scp-like extracellular protein	0.55	0.00	0.04	Antigen 6	DOWN
IrSigP-375532_FR3_1-137	U33-theraphotoxin-Cg1b	3.25	0.00	0.00	Cytotoxin	DOWN
IrSigP-257748_FR6_1-97	Cytotoxin-like protein	0.04	0.00	0.00	Cytotoxin	DOWN
Ir-343968	Cytotoxin-like protein	0.03	0.00	0.00	Cytotoxin	DOWN
IrSigP-228420_FR6_1-201	Antigen 5 protein	1.77	57.93	0.00	Antigen 5	UP
IrSigP-335607_FR3_98-231	Cytotoxin-like protein	3.54	18.25	0.00	Cytotoxin	UP
IrSigP-335605_FR1_100-362	Salivary secreted cytotoxin	2.47	22.11	0.01	Cytotoxin	UP
IrSigP-78898_FR3_6-103	Cytotoxin-like protein	0.20	0.39	23.10	Cytotoxin	UP
IrSigP-214219_FR3_66-354	Cytotoxin-like protein	0.37	0.04	19.57	Cytotoxin	UP
Ir-157968	Cytotoxin-like protein	0.17	0.23	19.25	Cytotoxin	UP
IrSigP-340386_FR3_43-459	Lipase	0.00	72.66	7.20	Lipase	UP
IrSigP-333694_FR2_33-438	Phospholipase	0.34	38.01	0.03	Lipase	UP
IrSigP-18398_FR2_13-108	5'-nucleotidase/apyrase	2.36	0.00	0.00	Nucleotidase	DOWN
Ir-389310	DDE superfamily endonuclease	1.03	0.06	0.00	Nucleotidase	DOWN
IrSigP-329586_FR4_1-305	Ficolin/ixoderin	1.54	11.74	0.05	Anticomplement	UP
IrSigP-270098_FR3_1-159	Microplusin preprotein	0.82	36.53	0.05	Antimicrobial	UP
IrSigP-72234_FR5_4-108	Defensin	1.77	0.31	27.60	Antimicrobial	UP
IrSigP-320485_FR1_6-333	Toll-like receptor 4	0.35	0.22	17.80	Unlnown	UP
IrSigP-229351_FR2_27-108	Salivary mucin	41.79	0.60	0.01	Mucous	UP
IrSigP-191860_FR2_160-436	Mucin-5ac	1.64	15.27	0.24	Mucous	UP
IrSigP-13558_FR4_1-129	Tick_mucins_17	0.43	16.99	0.03	Mucous	UP
IrSigP-355603_FR2_12-166	Tick_mucins_5	0.16	23.63	0.11	Mucous	UP
IrSigP-219752_FR5_71-232	Anticomplement protein ixac-b4 precusor	0.77	24.75	0.00	Anticomplement	UP
IrSigP-228937_FR5_31-448	Calreticulin	2.10	10.45	0.06	Calcium-Binding	UP
IrSigP-236871_FR5_46-121	5.3 kda protein	0.14	0.08	26.31	Antimicrobial	UP
Ir-230276	18.3_1–18.3 kda subfamily of the Basic tail superfamily	10.49	1.00	0.38	Unknown Function	UP
IrSigP-230278_FR2_12-166	18.3_1–18.3 kda subfamily of the Basic tail superfamily	0.02	264.75	0.46	Unknown Function	UP
IrSigP-4606_FR5_4-39-239	18.3_1–18.3 kda subfamily of the Basic tail superfamily	0.00	19.83	0.00	Unknown Function	UP
IrSigP-334686_FR1_85-367	23 kDa_1	0.51	0.03	32.41	Unknown Function	UP
IrSigP-384913_FR5_1-97	Secreted collagen-like peptide	1.18	0.00	0.00	Unknown Function	DOWN
IrSigP-344272_FR2_13-85	8.9 kda protein	3.08	0.00	0.00	Unknown Function	DOWN
IrSigP-5395_FR3_16-98	8.9 kda protein	1.19	0.00	0.00	Unknown Function	DOWN
Contig name	**Proteases**	**Unfed fold change**	**1 h fold change**	**3 h fold change**	**Specific type**	**Regulation pattern**
IrSigP-362100_FR2_36-293	Secreted metalloprotease	14.06	2.04	0.08	Metalloprotease	UP
IrSigP-256258_FR3_58-190	Secreted metalloprotease	61.09	12.59	0.00	Metalloprotease	UP
IrSigP-251827_FR3_33-213	Secreted metalloprotease	67.12	23.60	0.06	Metalloprotease	UP
IrSigP-362063_FR6_63-177	Dipeptidyl peptidase/kininase	16.11	4.64	0.00	Kininase	UP
Ir-364555	Secreted metalloprotease	0.00	10.24	0.00	Metalloprotease	UP
IrSigP-213551_FR6_1-495	Secreted metalloprotease	0.00	17.64	0.00	Metalloprotease	UP
IrSigP-230279_FR6_218-463	Secreted metalloprotease	0.41	18.78	0.64	Metalloprotease	UP

(Continued)

TABLE 1 | Continued

Contig name	Proteases	Unfed fold change	1 h fold change	3 h fold change	Specific type	Regulation pattern
IrSigP-317111_FR6_39-280	Secreted metalloprotease	0.15	27.38	0.00	Metalloprotease	UP
IrSigP-213340_FR5_1-177	Secreted metalloprotease	2.05	27.28	0.08	Metalloprotease	UP
IrSigP-7165_FR5_1-150	Secreted metalloprotease	0.08	42.47	0.00	Metalloprotease	UP
IrSigP-213336_FR3_28-166	Secreted metalloprotease	3.03	42.20	0.00	Metalloprotease	UP
IrSigP-317110_FR2_1-150	Secreted metalloprotease	0.02	86.16	0.01	Metalloprotease	UP
IrSigP-218287_FR3_180-401	Secreted metalloprotease	0.00	110.78	0.43	Metalloprotease	UP
IrSigP-195061_FR1_23-118	Metalloprotease	0.90	11.21	0.01	Metalloprotease	UP
IrSigP-349107_FR2_284-526	Metalloprotease	1.69	14.64	0.10	Metalloprotease	UP
IrSigP-251870_FR1_13-811	M13 family peptidase	0.83	23.95	0.00	Neprilysin-Like Protease	UP
IrSigP-364331_FR3_106-370	Cathepsin B-like cysteine protease form 1	0.06	18.88	0.00	Cysteine Protease	UP
Ir-240260	Neutral endopeptidase-like protein	2.30	13.22	0.03	Neprilysin-Like Protease	UP
IrSigP-343497_FR6_11-110	Serin protease	0.30	10.81	0.00	Serine Protease	UP
IrSigP-371761_FR5_22-194	Typsin-like serin protease	1.18	32.41	0.15	Serine Protease	UP
IrSigP-305695_FR2_95-261	Typsin-like serin protease	1.79	67.28	2.19	Serine Protease	UP
IrSigP-365277_FR5_14-279	Typsin-like serin protease	1.90	11.94	0.03	Serine Protease	UP
IrSigP-305694_FR4_27-296	Typsin-like serin protease	1.69	49.62	0.64	Serine Protease	UP
IrSigP-371762_FR1_7-330	Typsin-like serin protease	1.61	102.54	0.45	Serine Protease	UP
IrSigP-299712_FR2_1-282	Secreted metalloprotease	0.45	0.95	18.61	Metalloprotease	UP
IrSigP-212742_FR1_38-533	Secreted metalloprotease	0.50	0.24	10.11	Metalloprotease	UP
Ir-263403	Peptidase family M28	0.35	0.03	11.55	Metalloprotease	UP
IrSigP-321314_FR5_72-813	M13 family peptidase	0.75	0.11	11.56	Neprilysin-Like Protease	UP
Ir-66057	Peptidase family m13	0.26	0.06	13.96	Neprilysin-Like Protease	UP
IrSigP-9195_FR5_47-292	Secreted metalloprotease	6.44	0.06	0.02	Metalloprotease	DOWN

The dominant regulation pattern is determined to be "up" if at least one timepoint shows >10-fold increase or "down" if at least one timepoint shows a 10-fold decrease but no significant upregulation is observed.

instructions for purified total RNA. In brief, the kit generates cDNA from the RNA template, ligates the resulting cDNA into high molecular weight DNA molecules, and finally copies the ligated DNA using a proofreading DNA polymerase. This type of kit is more efficient than others and generates a larger quantity of cDNA for qPCR. The product of the kit was diluted 1:100 with molecular-grade water.

Targets of interest were identified based on the NGS data. The targets were required to be statistically significant at all three timepoints, to have an FPKM of ten or greater, and a change in expression of at least ten in at least one timepoint. Nineteen genes were selected from this group based on number of reads and the presence of sequence indicators representing secretion into the saliva.

Primers were designed based on sequencing data and ordered from Integrated DNA technologies. The sequences of these primers are listed in **Table S1**. They were reconstituted with molecular grade water and diluted to 10 μM. These samples were run in duplicate on a Biorad IQ5 machine using 10 μL Biorad iTaq Universal SYBR Green Mix, 0.6 μL of forward primer, 0.6 μL of reverse primer, 3.3 μL molecular grade water, and 2 μL diluted cDNA per sample. The thermal cycle included 50°C for 10 min, 95°C for 3 min, and then 45 cycles of 95°C for 15 s and 60°C for 30 s during which the samples were observed by the machine. After completion, melt curves were automatically generated, beginning with treatment at 95°C for 1 min followed by 55°C for 1 min and 81 observation cycles beginning at 55°C. The final results were baseline-normalized at an absorbance 100.

The Ct values between the technical duplicates were averaged, and changes in expression were calculated (**Figure S1**) using the ΔΔCt method, normalizing against the tick ribosomal S4 signal (Cabezas-Cruz et al., 2016).

RESULTS AND DISCUSSION

To understand the differential response of the *I. ricinus* salivary gland transcriptome during early stages of TBEV transmission, ticks were inoculated with TBEV by coxal microinjection 21 days prior to being fed on mice. This technique for infection is allowed for the generation of infected ticks with a high rate of success and has been widely accepted (Labuda et al., 2006; Slovák et al., 2014;

TABLE 2 | Regulation of individual contigs and associated proteins in response to TBEV infection in salivary glands of unfed *Ixodes ricinus* ticks and at one and three hours of feeding organized by category, showing lipocalins, Kunitz-domain proteins, and glycine-rich family proteins.

Contig name	Lipocalins	Unfed fold change	1 h fold change	3 h fold change	Regulation pattern
IrSigP-221462_FR1_8-375	Salivary lipocalin	12.43	2.57	0.05	UP
IrSigP-220271_FR6_65-192	Lipocalin-1 1	0.00	20.17	0.00	UP
IrSigP-276153_FR6_14-222	Licpodalin-4_1 lipocalin	0.00	43.64	0.00	UP
IrSigP-183760_FR5_1-83	Lipocalin	0.64	16.63	0.76	UP
IrSigP-20975_FR4_21-174	Salivary lipocalin	0.00	39.02	0.00	UP
IrSigP-219616_FR4_1-149	Salivary lipocalin	10.14	14.18	0.00	UP
IrSigP-210096_FR5_1-211	Salivary lipocalin	0.00	78.32	0.43	UP
IrSigP-364550_FR2_70-334	Lipocal-1_37 lipocalin	1.41	0.04	47.83	UP
IrSigP-364548_FR2_70-353	Lipocal-1_37 lipocalin	2.01	0.00	17.35	UP
IrSigP-364544_FR2_70-350	Lipocal-1_37 lipocalin	0.14	0.09	13.01	UP
IrSigP-364543_FR5_1-246	Lipocal-1_37 lipocalin	0.30	0.45	10.52	UP
IrSigP-222396_FR3_1-106	Lipocalin-2 1	0.14	0.03	20.90	UP
IrSigP-288978_FR2_1-151	Lipocalin-2_1 lipocalin	0.37	0.00	78.29	UP
IrSigP-221393_FR4_1-262	Lipocalin-2_1 lipocalin	0.84	0.00	17.39	UP
IrSigP-318325_FR1_1-248	Lipocalin-2_1 lipocalin	1.05	0.07	13.28	UP
IrSigP-359698_FR2_22-253	Salivary lipocalin	0.17	0.14	111.28	UP
IrSigP-219614_FR6_1-112	Salivary lipocalin	8.69	0.00	0.00	DOWN
IrSigP-308104_FR5_9-217	Salivary lipocalin	5.61	0.00	0.00	DOWN
IrSigP-215089_FR1_281-606	Lipocalin	4.54	0.00	0.00	DOWN
IrSigP-333450_FR6_60-167	Salivary lipocalin	1.45	0.08	0.07	DOWN
IrSigP-231826_FR4_21-269	Lipocalin-2_1 Lipocalin	0.01	0.05	0.00	DOWN
IrSigP-232013_FR2_1-136	Lipocalin-2_1 lipocalin	0.00	0.00	0.00	DOWN
Contig name	**Kunitz-Domain proteins**	**Unfed fold change**	**1 h fold change**	**3 h fold change**	**Regulation pattern**
IrSigP-196594_FR3_14-286	BPTI/Kunitz family of serine protease inhibitors	16.33	2.64	0.03	UP
IrSigP-233783_FR4_27-108	Salivary kunitz domain protein	12.26	1.89	0.02	UP
IrSigP-194429_FR6_23-125	Salivary kunitz domain protein	16.16	0.24	0.00	UP
IrSigP-267369_FR6_1-92	Salivary kunitz domain protein	54.15	0.00	0.00	UP
IrSigP-247833_FR5_76-171	Tick kunitz 46	13.40	1.16	0.03	UP
IrSigP-138775_FR4_1-100	Tick_Kunitz_56	12.02	0.00	0.00	UP
IrSigP-226572_FR5_1-141	u3-aranetoxin-ce1a	10.98	0.28	0.00	UP
IrSigP-353563_FR5_1-97	Serine proteinase inhibitor (KU family)	0.00	61.68	0.00	UP
IrSigP-5685_FR5_27-338	Salivary kunitz domain protein	0.59	138.37	0.43	UP
IrSigP-300370_FR3_1-184	Tick kunitz 38	1.80	10.64	0.03	UP
IrSigP-286607_FR3_15-359	Tick_Kunitz_134	1.67	13.77	0.05	UP
IrSigP-389808_FR1_1-86	Tick_Kunitz_44	0.80	48.52	0.04	UP
IrSigP-362807_FR3_68-283	Tick_Kunitz_88	1.09	18.18	0.22	UP
IrSigP-292668_FR3_1-93	Tick_Kunitz_43	4.60	0.01	0.03	DOWN
IrSigP-249585_FR2_1-123	Tick_Kunitz_53	0.02	0.00	0.00	DOWN
IrSigP-257404_FR5_1-105	Salivary kunitz domain protein	2.49	0.03	0.01	DOWN
Contig name	**Glycine-Rick (Cement) proteins**	**Unfed fold change**	**1 h fold change**	**3 h fold change**	**Regulation pattern**
Ir-12879	GRP-2_441 Glycine rich family	0.00	14.03	0.00	UP
Ir-216707	GRP-2_441 Glycine rich family	2.28	19.63	0.02	UP
IrSigP-8569_FR6_25-160	GRP-2_441 Glycine rich family	2.26	46.52	0.02	UP
Ir-357614	GRP-2_441 Glycine rich family	3.54	63.88	0.00	UP
IrSigP-345293_FR5_35-172	GRP-2_441 Glycine rich family	0.00	83.52	0.46	UP
IrSigP-361126_FR6_1-133	GRP-2_441 Glycine rich family	1.80	105.26	0.00	UP
IrSigP-363306_FR5_53-179	GRP-2_441 Glycine rich family	0.18	151.07	0.47	UP

(Continued)

TABLE 2 | Continued

Contig name	Glycine-Rick (Cement) proteins	Unfed fold change	1 h fold change	3 h fold change	Regulation pattern
IrSigP-347965_FR2_15-168	GRP-2_441 Glycine rich family	0.02	168.29	0.11	UP
IrSigP-209173_FR2_40-179	GRP-2_449 Glycine rich family	0.00	20.34	0.64	UP
IrSigP-20709_FR3_56-211	GRP-2_590 Glycine rich family	0.49	0.05	23.37	UP
IrSigP-354603_FR4_25-133	GRP-2_471 Glycine rich family	1.91	0.00	0.00	DOWN

The dominant regulation pattern is determined to be "up" if at least one timepoint shows >10-fold increase or "down" if at least one timepoint shows a 10-fold decrease but no significant upregulation is observed.

Thangamani et al., 2017). Cohorts of infected and non-infected ticks were then allowed to feed on mice. At times 1 h and 3 h post attachment, ticks were removed from the mice for salivary gland dissection followed by RNA extraction. The RNAs were then sequenced and analyzed.

Distribution of Changes in Gene Expression

Several classes of transcripts with significant salivary functions were identified as either up- or down-regulated in response to infection with TBEV. The numbers of genes with significant changes in regulation in each class in unfed, 1 h fed, and 3 h fed ticks are summarized in **Table 3**. In unfed ticks, only 33 genes were observed to be significantly upregulated in response to infection, as opposed to 214 after 1 h of tick attachment and 138 after 3 h. Comparing infected ticks to uninfected ticks, the number of downregulated genes in unfed infected ticks was 104, as opposed to 138 after 1 h of feeding and 174 after 3 h. This suggests that the strongest viral-induced changes to salivary expression occur after 1 h of feeding. This ability to modulate expression at a specific temporal point suggests that the virus has a direct and specific effect on gene regulation during the feeding process as opposed to a generic, global change in response to infection.

The changes in expression skew heavily toward uncharacterized genes whose function is unknown (**Figure 1**), which make up between 58 and 84% of up- or down-regulated genes in each category. Proteases, serine protease inhibitors, and lipocalins tended to be the dominant functionally identifiable classes of genes, although their proportion of the total of up- or down-regulated genes varies substantially by timepoint. This was especially notable in unfed ticks, where 18% of the upregulated genes were identified as serpins or Kunitz-domain proteins, and 12% were proteases and metalloproteases. This proportion decreased during feeding so that after 3 h, lipocalins were more prevalently upregulated (7%) while serine protease inhibitors were not altered, and protease involvement had dropped to 4% of the genes. The opposite pattern is observed in downregulated genes: although a group of lipocalins was observed to be downregulated relatively consistently (5, 9, and 6% at unfed, 1 and 3 h timepoint, respectively), the proportion of downregulated proteases and serpin/Kunitz-domain proteins increased.

The expression of individual genes was also found to be remarkably inconstant across the three timepoints. None of the identified genes were found to be significantly upregulated at more than one timepoint. Many genes would often be upregulated at some points and downregulated at others (**Tables 1**, **2** and **Figures 2**, **3**). These results indicate that viral interaction with the transcriptional regulation of salivary proteins is a highly dynamic process. Different sets of proteins are expressed at each individual timepoint in accordance with the stage of tick feeding; these, in turn, have different effects on the host immune response to both the tick and the virus it introduces.

IMPLICATIONS OF INDIVIDUAL PROTEIN CLASSES ON VIRAL BEHAVIOR AND TRANSMISSION

Serine Protease Inhibitors

Serine protease inhibitors of the Kunitz family comprise a broad class of enzyme inhibitors that generally serve a regulatory purpose. In some animals, however, these inhibitors evolved to serve as venom (Mourao and Schwartz, 2013). For arachnids, Kunitz-domain-containing proteins either interfere with ion channel activity (Chen et al., 2012; Dai et al., 2012; Valdes and Moal, 2014; Santibañez-Lopez et al., 2018) or inhibit critical host proteins (Decrem et al., 2008; Bronsoms et al., 2011; Andreotti et al., 2012; Louw et al., 2013; Zhang et al., 2017). Tick saliva is essentially a form of venom evolved to facilitate blood-feeding, and although *Ixodes* spp. ticks retain some of their ion channel-manipulating Kunitz-domain peptides (Dai et al., 2012; Valdes and Moal, 2014), they largely fall within the enzyme inhibitor group.

Kunitz-domain serine protease inhibitors are known to inhibit coagulation (Dai et al., 2012; Chen et al., 2013; Louw et al., 2013; Assumpção et al., 2015; Zhang et al., 2017), angiogenesis (Drewes et al., 2012; Soares et al., 2016), and may reduce inflammation (Bronsoms et al., 2011). Their primary purpose is to ensure successful feeding by inhibiting blood coagulation. Multiple inhibitors are expressed to target several proteins involved in the coagulation cascade.

A steady supply of blood is required for a tick to continuously salivate. Unlike spiders, ticks have no equivalent to a venom sack and cannot synthesize and store substantial quantities of saliva in advance. It is instead produced in real-time during feeding, with the necessary fluid being provided as the bloodmeal is concentrated in the midgut. Viral transmission requires this continuous flow of outgoing fluid both as a vehicle for entry into the host and because the immunomodulatory portion of

TABLE 3 | Numbers of genes up and downregulated in response to TBEV infection in salivary glands of unfed *Ixodes ricinus* ticks and at one and three hours of feeding, categorized by predicted functional class.

Class	Number of genes					
	Upregulated (Unfed)	Downregulated (Unfed)	Upregulated (1 h feeding)	Downregulated (1 h feeding)	Upregulated (3 h feeding)	Downregulated (3 h feeding)
Cytotoxin/Antigen 5	1	2	3	6	3	9
Digestive	0	1	2	2	0	3
Glycine-Rich	0	4	9	2	1	6
Immune	0	0	2	0	2	2
Lipocalin	1	5	6	13	9	9
Mucin	1	0	3	0	0	2
Other/Unknown	1	2	4	5	2	6
Protease	4	6	20	3	5	18
Kunitz-Domain	6	2	6	5	0	13
Uncategorized	19	82	159	102	116	106
Total	33	104	214	138	138	174

the saliva generates a microenvironment within the host that enhances viral infection (Thangamani et al., 2017).

As such, viral infection benefits from maintenance and enhancement of the anticoagulation system during the early stages of infection. Six Kunitz-type inhibitors and an arenetoxin analog (a probable trypsin inhibitor) were found to be upregulated in unfed ticks, with an average fold change of twenty and including one transcript that demonstrated a 54-fold increase. These represent a small amount of initial saliva prepared for an immediate and robust anticoagulant effect to facilitate more rapid early feeding. This group is not substantially upregulated at 1 h of feeding but shows downregulation when detected by 3 h with a fold change of 0.02–0.03.

Six additional Kunitz-type inhibitors were upregulated by infection after 1 h of feeding. The level of upregulation was more diverse at this timepoint than in unfed ticks, with three values having a fold change between 10 and 20, one having a change of 49-fold, one with a change of 62-fold, and one with a change of 138-fold. These contigs were not found upregulated at any other timepoint, and several were reduced at 3 h of feeding, including a change from 11 to 0.03 fold, 14 to 0.05 fold, and 49 to 0.04 fold.

At 3 h of feeding, the overall trend was a decreased expression of Kunitz-like inhibitors in response to viral infection, with no upregulated genes observed. Downregulation was not observed at any timepoint apart from 3 h in all but three genes, two of which were downregulated at 1 (0.008 and 0.03 fold) and one downregulated in uninfected ticks (0.02 fold). This downregulation continued for 3 h.

By 3 h, the ticks have already transmitted the infectious dose of the virus (Hermance and Thangamani, 2018) and have already imbibed a small supply of fluid from the host. Forced downregulation of the anticoagulant response interferes with feeding and may serve as a mechanism to trigger additional salivation (using already-consumed blood as a fluid source) as the tick attempts to compensate for increasingly poor fluidity of its bloodmeal. This process, in turn, forces the tick to inject more virus and immune-modulatory factors into the host. It may also lead to tick dislodgement of the host.

Lipocalins

Lipocalins are proteins that bind to small organic molecules. Within the context of tick saliva, lipocalins are used to sequester histamine (Paesen et al., 1999; Sangamnatdej et al., 2002; Diaz-Martin et al., 2011; Valdes et al., 2016; Wang et al., 2016; Neelakanta et al., 2018), serotonin (Xu et al., 2013), leukotrienes (Beaufays et al., 2008a,b; Mans and Ribeiro, 2009), and other signaling molecules to reduce the anti-tick inflammatory response. A critical role of salivary lipocalins is to reduce itch and pain response resulting from histamine and serotonin signaling. This prevents from a scratching response of the host that could potentially damage the tick. Additionally, some salivary lipocalins have also often evolved secondary functions including anticoagulant activity (Mans and Ribeiro, 2008), as well as the ability to modulate the behavior of leukocytes (Rodriguez-Valle et al., 2013) and dendritic cells (Preston et al., 2013).

Our data show that lipocalins are differentially expressed at different timepoints during early phases of tick feeding, and the presence of TBEV causes both upregulation and downregulation of particular lipocalins. Unlike Kunitz-domain inhibitors, which tended toward early upregulation and later downregulation, lipocalins were more heavily upregulated at later timepoints but showed less significant changes in unfed ticks. Only two contigs showed upregulation in unfed, infected ticks with fold-changes of 12 and 10 compared to uninfected controls. By 1 h of feeding, six genes were upregulated in infected ticks vs. controls. This includes one of the genes that was upregulated in unfed ticks, which changed from 10- to a 14-fold increase. Other genes showed fold changes of 17, 20, 44, and 78, which represents a substantial change in several lipocalins.

At 3 h, nine genes were upregulated in infected ticks compared to uninfected ones. Six of these were between 10 and 21-fold. The remaining three showed fold changes of 48, 78, and 111. Although this trend is similar to what was observed at 1 h, the

Contig Name	Miscellaneous Proteins	Unfed	1 h	3 h
IrSigP-350116_FR2_1-200	scp gapr-1 like scp-like extracellular protein			
IrSigP-120441_FR3_1-213	scp gapr-1 like scp-like extracellular protein			
IrSigP-375532_FR3_1-137	U33-theraphotoxin-Cg1b			
IrSigP-257748_FR6_1-97	cytotoxin-like protein			
Ir-343968	cytotoxin-like protein			
IrSigP-228420_FR6_1-201	antigen 5 protein			
IrSigP-335607_FR3_98-231	cytotoxin-like protein			
IrSigP-335605_FR1_100-362	salivary secreted cytotoxin			
IrSigP-78898_FR3_6-103	cytotoxin-like protein			
IrSigP-214219_FR3_66-354	cytotoxin-like protein			
Ir-157968	cytotoxin-like protein			
IrSigP-340386_FR3_43-459	lipase			
IrSigP-333694_FR2_33-438	phospholipase			
IrSigP-18398_FR2_13-108	5'-nucleotidase/apyrase			
Ir-389310	DDE superfamily endonuclease			
IrSigP-329586_FR4_1-305	ficolin/ixoderin			
IrSigP-270098_FR3_1-159	microplusin preprotein			
IrSigP-72234_FR5_4-108	defensin			
IrSigP-320485_FR1_6-333	toll-like receptor 4			
IrSigP-229351_FR2_27-180	salivary mucin			
IrSigP-191860_FR2_160-436	mucin-5ac			
IrSigP-13558_FR4_1-129	Tick_mucins_17			
IrSigP-355603_FR2_12-166	Tick_mucins_2			
IrSigP-219752_FR5_71-232	anticomplement protein ixac-b4 precursor			
IrSigP-228937_FR5_31-448	Calreticulin			
IrSigP-236871_FR5_46-121	5.3 kda protein			
Ir-230276	18.3_1 - 18.3 kda subfamily of the Basic tail superfamily			
IrSigP-230278_FR2_12-166	18.3_1 - 18.3 kda subfamily of the Basic tail superfamily			
IrSigP-4606_FR4_39-239	18.3_1 - 18.3 kda subfamily of the Basic tail superfamily			
IrSigP-334686_FR1_85-367	23kDa_1			
IrSigP-384913_FR5_1-97	secreted collagen-like peptide			
IrSigP-344272_FR2_13-85	8.9 kda protein			
IrSigP-5395_FR3_16-98	8.9 kda protein			

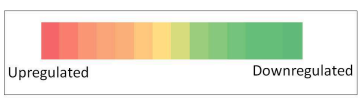

FIGURE 2 | Heatmaps of several categories of genes identified in salivary glands of *Ixodes ricinus* ticks as up or down regulated in response to TBEV infection, including miscellaneous genes (cytotoxins, anti-microbial genes, and mucins). Regulation is generally most influenced at a single timepoint, often as the inverse of the pattern seen in other timepoints. Expression in each category is also not consistent between proteins, indicating that expression of each individual gene is not equivalent, and under complex regulatory control.

genes expressed are different at 3 h. Many of these 3-h genes were actually downregulated at 1 h, including 0.04 (48 at 3 h), 0.08 (13 at 3 h), 0.03 (21 at 3 h), 0.07 (13 at 3 h), and one as low as 0.0004 which became 17 at 3 h.

Additionally, six lipocalins were not found to be upregulated in infected ticks, but significantly downregulated compared to control ticks in at least one group.

Since *I. ricinus* lipocalins have been segregated into distinct phylogenetic groups (Beaufays et al., 2008a), we constructed a phylogram using the lipocalin sequences found in this study plus the lipocalin sequences described in Beaufays et al. (2008a), which were derived from transcripts of adult ticks feeding for 5 days. The resulting phylogram, made from 106 sequences, is complex, producing 27 clades with strong bootstrap support (**Figure S2**). Interestingly, the sequences that were upregulated at zero or 1 h are in different clades. All the sequences derived from 5 day feeding ticks inhabit clades that are not shared by those upregulated by TBEV. This is not surprising, since ticks switch their sialomes with time (Karim and Ribeiro, 2015; Perner et al., 2018), possibly as an immune evasion mechanism. Thus, the different clades may represent proteins with different functions, or with different antigenic character. Whether the different clades containing TBEV upregulated lipocalins at zero and 1 h represent different lipocalin functions or different antigenicity cannot be resolved.

From the perspective of viral infection, these results are complex. It has been previously demonstrated that the presence of TBEV causes an increased inflammatory reaction during a tick-bite (Thangamani et al., 2017). Viral transmission benefits from a pro-inflammatory

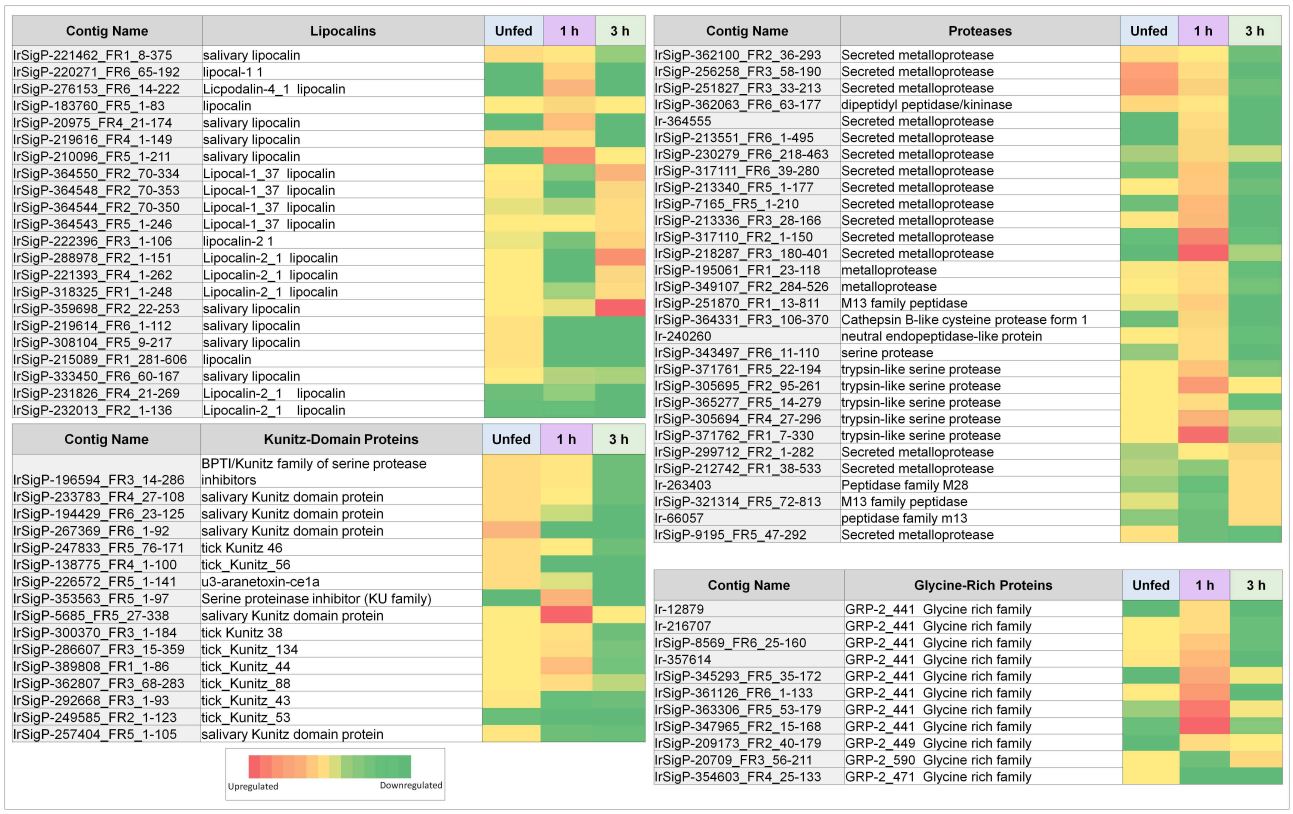

FIGURE 3 | Heatmaps of several categories of genes identified in salivary glands of *Ixodes ricinus* ticks as up or down regulated in response to TBEV infection, including lipocalins, proteases, and protease inhibitors (largely Kunitz-type). Regulation is generally most influenced at a single timepoint, often as the inverse of the pattern seen in other timepoints. Expression in each category is also not consistent between proteins, indicating that expression of each individual gene is not equivalent and under complex regulatory control.

response (Hermance and Thangamani, 2018) by summoning macrophages that can subsequently be infected and used to disseminate the virus to other tissues. By reducing histamine- and leukotriene-binding lipocalins, the host response to the saliva becomes more conducive to inflammation and consequently macrophage and neutrophil invasion. Additionally, modulating the behavior of dendritic cells and leukocytes by upregulated lipocalin expression has the overall effect of making the tissue less responsive to the presence of virus and thereby directing the brunt of the response against the tick. This altered expression increases the itch response, risking tick damage by host scratching. Since transmission of TBEV starts within a few minutes after tick attachment (Hermance and Thangamani, 2018), destruction of the tick does not outright prevent the transmission of virus, and in addition, pressure on the tick may in fact force the tick to partially regurgitate into the skin. Ticks that are unable to feed properly can dislodge themselves (Piesman, 1991) and attach to new hosts to attempt to complete the feeding, thus increasing virus transmission.

Lectins

Lectins are carbohydrate-binding proteins found in tick saliva. Their exact role is poorly understood (Vechtova et al., 2018). Their function is thought to be immunomodulatory or antimicrobial (Sterba et al., 2011; Smith and Pal, 2014), although their agglutination property has also been linked to blood digestion in the midgut (Vechtova et al., 2018). It is possible that, as in the case of spiders, ticks begin some of their digestion process externally through saliva; in ticks, this would specifically occur within the blood-pool before ingestion. Ticks also actively modulate the lectin-mediated complement system, for example by the tick salivary lectin pathway inhibitor (TSLP1) (Hajdušek et al., 2013); the simultaneous production of ficolin-like lectins in tick saliva therefore appears counterintuitive unless it either fails to initiate the host complement cascade or acts as a direct competitor to host ficolin on lectin receptors.

Ixoderin, an analog of ficolin, was found to be upregulated in infected ticks at 1 h feeding (with a fold-change of 12) but downregulated compared to controls at the 3 h timepoint (fold-change 0.05). It is difficult to determine the exact function of this particular lectin within the context of TBEV infection, as it could either modulate the host response or be produced as a reaction to viral infection of the salivary gland. If the latter is true and the lectin targets glycosylated amino acids on the viral particles, it may serve as an adaptor to protect the virus from mammalian host response or to facilitate phagocytosis and

infection of macrophages. Functional studies will be required to confirm if this viral/lectin interaction is common.

Cystatins

Cystatins serve several functions within ticks, mainly with regard to hemoglobin digestion (Chmelar et al., 2017). Like tick lectins, they are present in tick saliva and also modulate host responses. Some inhibit TNF-α and IL12 production from dendritic cells and decrease CD4+ proliferation (Chmelar et al., 2017). TBEV replication in dendritic cells is enhanced by suppression of IFN signaling induced by cystatin exposure (Lieskovska et al., 2015). Cystatins have been shown to interfere with IL1β and IL18 in macrophages during *Anaplasma* infection and promote TBEV infection by further altering signaling in the dendritic cells. Cystatins bias the immune reaction away from the Th1 type that would be most effective against viral or intracellular pathogens (Schonenmeyer et al., 2017).

In our experiments, only one cystatin was observed with altered expression, although it is not listed in the presented tables and figures due to being down-regulated at only one of the required two exclusion points. It showed a fold-change of 0 (indicating that it was not detected in infected ticks) in unfed ticks and at 1 h, and then it showed a non-significant fold-change of 3 at 3 h.

This is unexpected, as the presence of cystatin is thought to enhance TBEV infection, yet is reduced here. The cystatin detected may be one of a more diverse group, may serve an alternate function and experience different regulation, as the sequencing data cannot positively identify it as cystatin 2, the salivary version. In this case, it probably serves a regulatory function in the way cystatin 3 does in human cells.

Glycine-Rich Proteins

Upon attaching to a host, ticks begin to secrete a thick proteinaceous cement to better secure their mouthparts to the host skin. This cement is immunogenic, and though largely structural it has an impact on modulating host responses. Glycine-rich proteins are one of the cement's characteristic constituents (Hollmann et al., 2018).

The presence of glycine-rich proteins is critical to the transmission of TBEV (Labuda et al., 2006). Mice vaccinated against a particular glycine-rich protein proved resistant to TBEV transmitted by ticks. This vaccine was derived from a cement protein from *Rhipicephalus appendiculatus*, but proved cross-protective against proteins from *I. ricinus*, suggesting strong evolutionary conservation between the proteins as well as high homology of their respective immunogenic sites.

Our data show that most of the glycine-rich proteins identified were upregulated substantially at 1 h feeding in TBEV infected ticks. Of eleven genes detected, nine were upregulated. Three were found upregulated between 10 and 20 fold, three between 45 and 85 fold, and three higher than 100 fold. Only one gene was upregulated at 3 h with a fold change of 23, and the genes that were upregulated at 1 h were either not significantly changed or slightly downregulated. This most likely corresponds to a shift in the stage of cement deposition, with the viral-altered portion of the cement being applied early in the feeding and therefore of high early immunological relevance. These results imply that the production of cement has either increased or its composition has been altered in favor of its glycine-rich component. This corresponds with our observation that the production of tick mucin, another component of tick cement, was upregulated in response to infection at the 1-h timepoint. Of four mucin genes detected, three were upregulated 15, 17, and 24-fold, respectively in infected ticks compared to controls. The additional expression of glycine-rich proteins in the tick cement suggests a direct benefit to TBEV transmission.

Proteases

The presence of proteases in tick saliva allows the tick to actively degrade host proteins that would otherwise impede its feeding activity. Ticks primarily employ reprolysin-like metalloproteases that directly degrade fibrinogen and the extracellular matrix (Francischetti et al., 2003; Mans et al., 2003; Harnoi et al., 2007; Barnard et al., 2012; Ali et al., 2014, 2015), though they also employ dipeptidyl carboxypeptidase to inactivate bradykinin (Ribeiro and Mather, 1998; Bastiani et al., 2002), a pain-inducing peptide. Metalloproteases are required for tick feeding; when animals are vaccinated against them, ticks feed poorly or die during the feeding process, usually in the later stages (post 24-h) (Decrem et al., 2008; Ali et al., 2015).

Similar to serine protease inhibitors, upregulation of metalloproteases increases the potency of the tick saliva's anticoagulant effect. Tick-borne viruses benefit when the tick consumes greater amounts of blood faster and is able to salivate more. Although these salivary compounds are usually associated with long-term (24 h or longer) tick feeding, the presence of TBEV causes their marked downregulation in infected ticks. These included a change of 61, 67, 14, and 16-fold, with the latter being the only definitive kininase detected. Of these four, those with the fold changes of 61 and 67 were still upregulated at 1 h of feeding, though to a lower extent (13 and 24-fold, respectively). Two genes were found downregulated (0.02 and 0.06-fold).

More infection-upregulated genes were identified at the 1-h timepoint. Of these 22 genes, fourteen had fold changes between 10 and 30, six had fold-changes between 30 and 90, and two had fold-changes of >100. Only three genes were found downregulated at this timepoint, with fold changes of 0.03, 0.06, and 0.05.

In contrast, nine protease contigs were found decreased in the presence of TBEV at the 3 h timepoint (0.01–0.08). Five were found upregulated, with four between 10 and 15-fold and one at 19-fold.

The expression of proteases mirrors our observations with serine protease inhibitors, where the presence of virus increases anticoagulant activity in the first two timepoints but downregulates it in the third. Likewise, this will cause the ticks to struggle to feed and force them to salivate more, thereby introducing more immunomodulatory compounds and virus as they attempt to continue feeding. They may also detach from the host without a blood meal, and may reattach to another, thus increasing virus transmission.

It should also be noted that while reprolysin-like or even astrolycin-like metalloproteases have been studied in ticks, these

data have additionally identified several neprilysin-like proteases, a cysteine protease, and several serine proteases. The presence of serine proteases was largely upregulated at the 1 h timepoint and may correspond with the production of Kunitz-domain serine proteinase inhibitors. In this context the Kunitz proteins may serve to inhibit the serine proteases prior to saliva release to prevent damage to the tick salivary gland, with both assuming separate functions after release into the host.

Other Tick Genes

Several miscellaneous genes of immunological and secretory importance have also been observed in this study. Calreticulin was found to be upregulated in infected ticks during the 1 h timepoint. In tick saliva, calreticulin has been shown to act as an immune signaling compound in addition to its normal calcium-binding function. It was found to contribute to the transmission of *Babesia* (Hajdušek et al., 2013) and may be of benefit to TBEV as well.

Several antimicrobial compounds also showed changes in expression. These include defensin, which was upregulated in infected ticks at the 3 h timepoint (fold change of 28), as well as a 5.3 kDa protein, which was also upregulated at 3 h (fold-change of 26) despite being slightly downregulated at 1 h feeding (fold-change 0.08). Microplusin was highly upregulated in infected ticks vs. controls (fold-change of 37), but then downregulated at 3 h (fold-change of 0.05), suggesting a decrease in tick response to the pathogen. Microplusin, however, is considered to be an antifungal and antibacterial compound (Silva et al., 2009) whereas defensin and possibly the 5.3 kDa protein can interact with viruses. Its role, therefore, may be part of a generic tick immune response to TBEV. These antimicrobial responses are probably not meant to interact with the host during feeding, but rather the result of the salivary glands reacting to their own infection. The temporal aspects are the result of changing gene expression during feeding.

Another category of molecules that is associated with cytotoxicity is represented by antigen-5. Antigen-5 is a compound of unknown function in insect venoms that results in potent allergenic response. Here, antigen-5 was found to be upregulated at the 1-h timepoint in infected ticks and then downregulated at 3 h feeding, resulting in a more powerful inflammatory response, as has been observed due to TBEV-infected ticks (Thangamani et al., 2017). This may serve to drive macrophages to the site of inoculation for infection and pathogen dissemination. Contributing to this effect are several cytotoxins found to be upregulated at 1 (3 genes) and 3 h (three genes) in infected ticks. These imply increased toxicity of the saliva, and the possibility of pro-inflammatory molecules being released from damaged or necrotic cells. Upregulation of this process may serve a direct benefit to the virus through increased inflammation. However, it will be necessary to perform deeper analysis of this gene and the structure and function of its product to fully understand what role this protein has in tick feeding, and what effect its upregulation may have on the transmission of TBEV.

One additional gene of interest was a member of the 18.3 kDa subfamily. The role of this type of protein in tick/host interaction is not fully understood and further specificities of this protein could not be identified immediately from the sequencing data. While its function is unknown, it showed the highest upregulation of any identified gene with a fold-change of 265 at the 1-h timepoint in infected ticks vs. uninfected ticks. It was downregulated in unfed infected ticks with a fold-change of 0.02, while its regulation was not significantly altered at the 3 h timepoint.

Uncategorized Genes

A substantial number (>75%) of the genes recovered could not be identified. All of those listed possess signals that identify them as secreted compounds, and they all show differential expression at one or more timepoint. Their role cannot be ascertained at present.

CONCLUSION

Tick saliva is essential to the tick's ability to modulate host hemostasis and inflammatory and immune responses against a tick during feeding and pathogen transmission. Our study clearly indicates a temporal variation in the tick salivary transcriptome expression during the first 3 h of feeding. Further, the pattern of expression is significantly impacted by infection of the tick with TBEV. The resulting changes to salivary transcriptome create an environment that is favorable to early viral infection and dissemination by altering compounds which affect the host immune system and hemostatic pathways. The early downregulation of lipocalins, metalloproteases and Kunitz-domain containing proteins by TBEV infection suggests that the tick will struggle to counteract host hemostatic and inflammatory responses and may be dislodged. Reattachment to another host would increase virus transmission. This strategy appears to be similar in effect to the method employed by *Yersinia pestis* where the bacillus impairs the ingestion of blood by infected fleas, leading them to bite multiple hosts in an attempt to feed (Hinnebusch et al., 2017). Tick saliva additionally contains compounds that facilitate tick infection, as determined by previously observed experimental evidence that tick saliva has pro-viral effect on infection; accordingly, this suggests that the virus has adapted in such a way as to not only take advantage of the immunomodulatory properties of the vector's saliva but to adjust the composition of the saliva in a way that benefits its own transmission. The exact mechanism of how the virus interacts with the vector's cellular machinery to alter transcription in this way is still unknown and it will be the subject of future investigations.

DATA AVAILABILITY STATEMENT

The raw reads used in this article were deposited at the Sequence Read Archive (SRA) of the National Center for Biotechnology Information (NCBI) under bioproject PRJNA576167, Biosample SAMN12956709, and runs SRR10240055, SRR10240054, SRR10240053, SRR10240052, SRR10240051, and SRR10240050. Seventy-three novel coding sequences have been deposited to DDBJ/EMBL/GenBank through the Transcriptome Shotgun Annotation portal under the accession GHXN00000000.

The version described in this paper is the first version, GHXN01000000. The hyperlinked spreadsheet mapping the coding sequences, their annotation and statistical analysis can be downloaded from https://proj-bip-prod-publicread.s3.amazonaws.com/transcriptome/Ixric-TBEV-2019/Ir-tbev.zip.

ETHICS STATEMENT

The experiments involving laboratory mice were performed in accordance with the animal use protocol approved by the State Veterinary and Food Administration of the Slovak Republic (permit number 1335/12-221) and the Institute of Virology, Biomedical Research Center of the Slovak Academy of Sciences (BMC SAS).

AUTHOR CONTRIBUTIONS

ST and MK designed the experiments, provided reagents, and materials and performed the experiments. JR, CH, and ST analyzed the data. CH and ST drafted the manuscript. All authors critically read and revised the manuscript.

FUNDING

This study was financially supported in part by Departmental start-up funds to ST. MK was supported by the Slovak Research and Development Agency (Contract No. APVV-18-0201) and grant VEGA 2/0047/18. JR was supported by the Intramural Research Program of the National Institute of Allergy and Infectious Diseases (Vector-Borne Diseases: Biology of Vector Host Relationship, Z01 AI000810-18).

ACKNOWLEDGMENTS

The authors wish to thank Dr. Boris Klempa and Marta Siebenstichova from the Institute of Virology, Biomedical Research Center, Slovak Academy of Sciences (SAS) for providing TBEV MBS for tick inoculations and Dr. Mirko Slovák from the Institute of Zoology SAS for tick inoculations. This work utilized the computational resources of the NIH HPC Biowulf cluster (http://hpc.nih.gov).

SUPPLEMENTARY MATERIAL

The Supplementary Material for this article can be found online at: https://www.frontiersin.org/articles/10.3389/fcimb.2020.00041/full#supplementary-material

Table S1 | A list of primers utilized for PCR validation for this experiment.

Figure S1 | Expression changes as determined by qPCR and the ΔΔCt method for ten genes showing a change in expression of >10 or <0.1-fold for at least one timepoint.

Figure S2 | Evolutionary relationships of *Ixodes ricinus* lipocalins.

REFERENCES

Ali, A., Parizi, L. F., Guizzo, M. G., Tirloni, L., Seixas, A., Vaz, I. S. Jr., et al. (2015). Immunoprotective potential of a *Rhipicephalus (Boophilus) microplus metalloprotease. Vet. Parasitol.* 207, 107–114. doi: 10.1016/j.vetpar.2014.11.007

Ali, A., Triloni, L., Isezaki, M., Seixas, A., Konnai, S., Ohashi, K., et al. (2014). Reprolysin metalloproteases from *Ixodes persculatus*, *Rhipicephalus sanguineus* and *Rhipicephalus microplus* ticks. *Exp. Appl. Acarol.* 63, 559–578. doi: 10.1007/s10493-014-9796-9

Andreotti, R., Cunha, R. C., Soares, M. A., Guerrero, F. D., Leite, F. P. L., and de Leon, A. A. P. (2012). Protective immunity against tick infestation in cattle vaccinated with recombinant typsin inhibitor of *Rhipicephalus microplus. Vaccine* 30, 6678–6685. doi: 10.1016/j.vaccine.2012.08.066

Assumpção, T. C., Ma, D., Mizurini, D. M., Kini, R. M., Ribeiro, J. M. C., Kotsyfakis, M., et al. (2015). *In vitro* mode of action and anti-thrombotic activity of boophilin, a multifunctional Kunitz protease inhibitor from the midgut of a tick vector of babesiosis, *Rhipicephalus microplus*. *PLoS Negl. Trop. Dis.* 10:e0004298. doi: 10.1371/journal.pntd.0004298

Barnard, A. C., Nijhof, A. M., Gaspar, A. R. M., Neitz, A. W. H., Jongejan, F., and Maritz-Olivier, C. (2012). Expression profiling, gene silencing and transcriptional networking of metzincin metalloproteases in the cattle tick. *Vet. Parasitol.* 186, 403–414. doi: 10.1016/j.vetpar.2011.11.026

Bastiani, M., Hillebrand, S., Horn, F., Kist, T. B. L., Guimaraes, J. A., and Termingnoni, C. (2002). Cattle tick *Boophilus microplus* salivary gland contains a thiol-activated metalloendopeptidase displaying kininase activity. *Insect Biochem. Mol. Biol.* 32, 1439–1446. doi: 10.1016/S0965-1748(02)00064-4

Beaufays, J., Adam, B., Decrem, Y., Prevot, P., Santinin, S., Brasseur, R., et al. (2008a). *Ixodes ricinus* tick lipocalins: identification, cloning, phylogenetic analysis and biochemical characterization. *PLoS ONE* 3:e3941. doi: 10.1371/journal.pone.0003941

Beaufays, J., Adam, B., Menten-Dedoyart, C., Fievez, L., Grosjean, A., Decrem, Y., et al. (2008b). Ir-LBP, and *Ixodes ricinus* tick salivary LTB4-binding lipocalin, interferes with host neutrophil function. *PLoS ONE* 3:e3987. doi: 10.1371/journal.pone.0003987

Benjamini, Y., and Hochberg, Y. (1995). Controlling the false discovery rate: a practical and powerful approach to multiple testing. *J. R. Statist. Soc. B* 57, 289–300. doi: 10.1111/j.2517-6161.1995.tb02031.x

Birol, I., Jackman, S. D., Nielsen, C. B., Qian, J. Q., Varhol, R., Stazyk, G., et al. (2009). *De novo* transcriptome assembly with ABySS. *Bioinformatics* 25, 2872–2877. doi: 10.1093/bioinformatics/btp367

Blisnick, A. A., Foulon, T., and Bonnet, S. I. (2017). Serine protease inhibitors in ticks: an overview of their role in tick biology and tick-borne pathogen transmission. *Front. Cell Infect. Microbiol.* 7:199. doi: 10.3389/fcimb.2017.00199

Bronsoms, S., Pantoja-Uceda, D., Gabrijelcic-Geiger, D., Sanglas, L., Aviles, F. X., Santoro, J., et al. (2011). Oxidative folding and structural analyses of a Kunitz-related inhibitor and its disulfide intermediates: functional implications. *J. Mol. Biol.* 414, 427–441. doi: 10.1016/j.jmb.2011.10.018

Cabezas-Cruz, A., Alberdi, P., Alyllon, N., Valdes, J. J., Pierce, R., Villar, M., et al. (2016). *Anaplasma phagocytophilum* increases the levels of histone modifying enzymes to inhibit cell apoptosis and facilitate pathogen infection in the tick vector *Ixodes scapularis*. *Epigenetics* 11, 303–319. doi: 10.1080/15592294.2016.1163460

Chagas, A. C., Calvo, E., Rios-Velasquez, C. M., Pessoa, F. A., Medeiros, J. F., and Ribeiro, J. M. (2013). A deep insight into the sialotranscriptome of the mosquito, *Psorophora albipes*. *BMC Genom.* 14:875. doi: 10.1186/1471-2164-14-875

Chen, Z., Wang, B., Hu, J., Yang, W., Cao, Z., Zhuo, R., et al. (2013). SjAPI, the first functionally characterized Ascaris type protease inhibitor from animal venoms. *PLoS ONE* 8:e57529. doi: 10.1371/journal.pone.0057529

Chen, Z. Y., Hu, Y. T., Yang, W. S., He, Y. W., Feng, J., Wang, B., et al. (2012). Hg1, novel peptide inhibitor specific for Kv1.3 channels from first scorpion Kunitz-type potassium channel toxin family. *J. Biol. Chem.* 287, 13819–13821. doi: 10.1074/jbc.M112.343996

Chmelar, J., Kotál, J., Kopecký, J., Pedra, J. H. F., and Kotsyfakis, M. (2016). All for one and one for all on the tick-host battlefield. *Trends Parasitol.* 32, 368–377. doi: 10.1016/j.pt.2016.01.004

Chmelar, J., Kotál, J., Langhansová, H., and Kotsyfakis, M. (2017). Protease inhibitors in tick saliva: the role of serpins and cystatins in tick-host-pathogen interaction. *Front. Cell. Infect. Microbiol.* 7:2016. doi: 10.3389/fcimb.2017.00216

Dai, S. X., Zhang, A. D., and Huang, J. F. (2012). Evolution, expansion and expression of the Kunitz/BPTI gene family associated with long-term blood feeding in *Ixodes scapularis*. *BMC Evol. Biol.* 12:4. doi: 10.1186/1471-2148-12-4

Decrem, Y., Beaufays, J., Blasioli, V., Lahaye, K., Brossard, M., Vanhamme, L., et al. (2008). A family of putative metalloproteases in the salivary glands of the tick *Ixodes ricinus*. *FEBS J.* 275, 1485–1499. doi: 10.1111/j.1742-4658.2008.06308.x

Diaz-Martin, V., Manzano-Roman, R., Siles-Lucas, M., Oleaga, A., and Perez-Sanchez, R. (2011). Cloning, characterization and diagnostic performance of the salivary lipocalin protein TSGP1 from *Ornithodoros moubata*. *Vet. Parasitol.* 171, 163–172. doi: 10.1016/j.vetpar.2010.12.014

Drewes, C. C., Dias, R. Y. S., Hebeda, C. B., Simons, S. M., Barreto, S. A., Ferreira, J. M. Jr., et al. (2012). Actions of the Kunitz-type serine protease inhibitor Amblyomin-X on VEGF-A-induced angiogenesis. *Toxicon* 60, 333–340. doi: 10.1016/j.toxicon.2012.04.349

Felsenstein, J. (1985). Confidence-limits on phylogenies - an approach using the bootstrap. *Evolution* 39, 783–791. doi: 10.1111/j.1558-5646.1985.tb00420.x

Fialova, A., Cimburek, Z., Iezzi, G., and Kopecky, J. (2010). *Ixodes ricinus* tick saliva modulates tick-borne encephalitis virus infection of dendritic cells. *Microbes Infect.* 12, 580–585. doi: 10.1016/j.micinf.2010.03.015

Francischetti, I. M. B., Mather, R. N., and Ribeiro, J. M. C. (2003). Cloning of a salivary gland metalloprotease and characterization of gelatinase and fibrin(ogen)lytic activities in the saliva of the Lyme disease tick vector *Ixodes scapularis*. *Biochem. Biophys. Res. Commun.* 305, 869–875. doi: 10.1016/S0006-291X(03)00857-X

Francischetti, I. M. B., Sa-Nunes, A., Mans, B. J., Santos, I. M., and Ribeiro, J. M. C. (2009). The role of saliva in tick feeding. *Front. Biosci.* 14, 2051–2088. doi: 10.2741/3363

Grabherr, M. G., Haas, B. J., Yassour, M., Levin, J. Z., Thompson, D. A., Amit, I., et al. (2011). Full-length transcriptome assembly from RNA-Seq data without a reference genome. *Nat. Biotechnol.* 29, 644–652. doi: 10.1038/nbt.1883

Hajdušek, O., Šíma, R., Ayllón, N., Jalovecká, M., Perner, J., de la Fuente, J., and Kopáček, P. (2013). Interactions of the tick immune system with transmitted pathogens. *Front. Cell. Infect. Microbiol.* 3:26. doi: 10.3389/fcimb.2013.00026

Harnoi, T., Sakaguchi, T., Nishikawa, Y., Xuan, X., and Fujisaki, K. (2007). Molecular characterization and comparative study of 6 salivary glands metalloproteases from the hard tick, *Haemaphysalis longicornis*. *Comp. Biochem. Physiol.* 147, 93–101. doi: 10.1016/j.cbpb.2006.12.008

Hermance, M. E., Santos, R. I., Kelly, B. C., Valbuena, G., and Thangamani, S. (2016). Immune cell targets of infection at the tick-skin interface during Powassan virus transmission. *PLoS ONE* 11:e0155889. doi: 10.1371/journal.pone.0155889

Hermance, M. E., and Thangamani, S. (2015). Tick saliva enhances Powassan virus transmission to the host, influencing its dissemination and the course of disease. *J. Virol.* 89, 7852–7860. doi: 10.1128/JVI.01056-15

Hermance, M. E., and Thangamani, S. (2018). Tick-virus-host interactions at the cutaneous interface: the nidus of flavivirus transmission" *Viruses* 10:362. doi: 10.3390/v10070362

Hinnebusch, B. J., Jarrett, C. O., and Bland, D. M. (2017). "Fleaing' the plague: Adaptations of *Yersinia pestis* to its insect vector that lead to transmission. *Annu. Rev. Microbiol.* 71, 215–232. doi: 10.1146/annurev-micro-090816-093521

Hollmann, T., Kim, T. K., Tirloni, L., Radulovic, Z. M., Pinto, A. F. M., Diedrich, J. K., et al. (2018). Identification and characterization of proteins in the *Amblyomma americanum* tick cement cone. *Int. J. Parasitol.* 48, 211–224. doi: 10.1016/j.ijpara.2017.08.018

Jones, L. D., Hodgson, E., and Nuttall, P. A. (1989). Enhancement of virus transmission by tick salivary glands. *J. Gen Virol.* 70, 1895–1898. doi: 10.1099/0022-1317-70-7-1895

Karim, S., and Ribeiro, J. M. (2015). An insight into the sialome of the Lone Star tick, *Amblyomma americanum*, with a glimpse on its time dependent gene expression. *PLoS One*. 10:e0131292.

Karim, S., Singh, P., and Ribeiro, J. M. (2011). A deep insight into the sialotranscriptome of the gulf coast tick, *Amblyomma maculatum*" *PLoS ONE* 6:e28525. doi: 10.1371/journal.pone.0028525

Kazimírová, M., Thangamani, S., Bartíková, P., Hermance, M., Holíková, V., Štibrániová, I., et al. (2017). Tick-borne viruses and biological processes at the tick-host-virus interface. *Front. Cell. Infect. Microbiol.* 7:339. doi: 10.3389/fcimb.2017.00339

Kotsyfakis, M., Schwarz, A., Erhart, J., and Ribeiro, J. M. (2015). Tissue- and time-dependent transcription in *Ixodes ricinus* salivary glands and midguts when blood feeding on the vertebrate host. *Sci. Rep.* 5:9103. doi: 10.1038/srep09103

Kumar, S., Stecher, G., and Tamura, K. (2016). MEGA7: molecular evolutionary genetics analysis version 7.0 for bigger datasets. *Mol. Biol. Evol.* 33, 1870–1874. doi: 10.1093/molbev/msw054

Labuda, M., Austyn, J. M., Zuffova, E., Kozuch, O., Fuchsberger, N., Lysy, J., et al. (1996). Importance of localized skin infection in tick-borne encephalitis virus transmission. *Virology* 219, 357–366. doi: 10.1006/viro.1996.0261

Labuda, M., Jones, L. D., Williams, T., and Nuttall, P. A. (1993). Enhancement of tick-borne encephalitis virus by tick salivary gland extracts. *Med. Vet. Entomol.* 7, 193–196. doi: 10.1111/j.1365-2915.1993.tb00674.x

Labuda, M., Trimnell, A. R., Lickova, M., Kazimirova, M., Davies, G. M., Lissina, O., et al. (2006). An antivector vaccine protects against a lethal vector-borne pathogen. *PLoS Pathog.* 2:e27. doi: 10.1371/journal.ppat.0020027

Lieskovska, J., Palenikova, J., Langhansova, H., Chmelar, J., and Kopecky, J. (2018). Saliva of *Ixodes ricinus* enhances TBE virus replication in dendritic cells by modulation of pro-survival Akt pathway. *Virology* 514, 98–105. doi: 10.1016/j.virol.2017.11.008

Lieskovska, J., Palenikova, J., Širmarova, J., Elsterova, J., Kotsyfakis, M., Campos Chagas A, Calvo, E., et al. (2015). Tick salivary cystatin sialostatin L2 supresses IFN responses in mouse dendritic cells. *Parasite Immunol.* 37, 70–78. doi: 10.1111/pim.12162

Liu, X. Y., de la Fuente, J., Cote, M., Galindo, R. C., Moutailler, S., Vayssier-Taussat, M., et al. (2014). IrSPI, a tick serine protease inhibitor involved in tick feeding and *Bartonella henselae* infection. *PLoS Negl. Trop. Dis.* 8:e2993. doi: 10.1371/journal.pntd.0002993

Louw, E., van der Merwe, N., Neitz, A. W. H., and Maritz-Olivier, C. (2013). Evolution of the tissue factor pathway inhibitor-like Kunitz domain-containing protein family in *Rhipicephalus microplus*. *Int. J. Parasitol.* 43, 81–94. doi: 10.1016/j.ijpara.2012.11.006

Mans, B. J., Louw, A. I., and Neitz, A. W. H. (2003). "The major tick salivary gland proteins and toxins from the soft tick, *Ornithodoros savignyi*, are part of the tick lipocalin family: implications for the origins of tick toxicosis". *Mol. Biol. Evol.* 10, 1158–1167. doi: 10.1093/molbev/msg126

Mans, B. J., and Ribeiro, J. M. C. (2008). Function, mechanism and evolution of the moubatin-clade of soft tick lipocalins. *Insect Biochem. Mol. Biol.* 38, 841–852. doi: 10.1016/j.ibmb.2008.06.007

Mans, B. J., and Ribeiro, J. M. C. (2009). A novel clade of cysteinyl leukotriene scavengers in soft ticks. *Insect Biochem. Mol. Biol.* 38, 862–870. doi: 10.1016/j.ibmb.2008.06.002

Mourao, C. B. F., and Schwartz, E. F. (2013). Protease inhibitors from marine venomous animals and their counterparts in terrestrial venomous animals. *Mar. Drugs.* 11, 2069–2112. doi: 10.3390/md11062069

Neelakanta, G., Sultanah, H., Sonenshine, D. E., and Andersen, J. F. (2018). Identification and characterization of a histamine-binding lipocalin-like molecule from the relapsing fever tick *Ornithodoros turicata*. *Insect Mol. Biol.* 27, 177–187. doi: 10.1111/imb.12362

Paesen, G. C., Adams, P. L., Harlos, K., Nuttall, P. A., and Stuart, D. I. (1999). Tick histamine-binding proteins: isolation, cloning, and three-dimensional structure. *Mol. Cell.* 3, 661–671. doi: 10.1016/S1097-2765(00)80359-7

Perner, J., Kropáčková, S., Kopáček, P., and Ribeiro, J. M. C. (2018). Sialome diversity of ticks revealed by RNAseq of single tick salivary glands. *PLoS Negl. Trop. Dis.* 12:e0006410. doi: 10.1371/journal.pntd.0006410

Piesman, J. (1991). Experimental acquisition of the Lyme disease spirochete, *Borrelia burgdorferi*, by larval *Ixodes dammini* (Acari: Ixodidae) during partial blood meals. *J. Med. Entomol.* 28, 259–262. doi: 10.1093/jmedent/28.2.259

Preston, S. G., Majtán, J., Kouremenou, C., Rysnik, O., Burger, L. F., Cabezas Cruz, A., et al. (2013). Novel immunomodulators from hard ticks selectively reprogramme human dendritic cell responses. *PLoS Pathog.* 9:e1003450. doi: 10.1371/journal.ppat.1003450

Ribeiro, J. M., Chagas, A. C., Pham, V. M., Lounibos, L. P., and Calvo, E. (2014). An insight into the sialome of the frog-biting fly, *Corethrella appendiculata*. *Insect. Biochem. Mol. Biol.* 44, 23–32. doi: 10.1016/j.ibmb.2013.10.006

Ribeiro, J. M. C., and Mather, T. N. (1998). *Ixodes scapularis*: salivary kinase activity is a metallo dipeptidyl carboxypeptidase. *Exp. Parasitol.* 89, 213–221. doi: 10.1006/expr.1998.4296

Rodriguez-Valle, M., Moolhuijzen, P., Piper, E. K., Weiss, O., Vance, M., Bellgard, M., et al. (2013). *Rhipicephalus microplus* lipocalins (LRMs): genomic identification and analysis of the bovine immune response using in silico predicted B and T cell epitopes. *Int. J. Parasitol.* 43, 739–752. doi: 10.1016/j.ijpara.2013.04.005

Roversi, P., Johnson, S., Preston, S. G., Nunn, M. A., Paesen, G. C., Austyn, J. M., et al. (2017). Structural basis of cholesterol binding by a novel clade of dendritic cell modulators from ticks. *Sci. Rep.* 7:16057. doi: 10.1038/s41598-017-16413-2

Saitou, N., and Nei, M. (1987). The neighbor-joining method: a new method for reconstructing phylogenetic trees. *Mol. Biol. Evol.* 4, 406–425.

Sangamnatdej, S., Paesen, G. C., Slovak, M., and Nuttall, P. A. (2002). A high affinity serotonin- and histamine-binding lipocalin from tick saliva. *Insect Mol. Biol.* 11, 79–86. doi: 10.1046/j.0962-1075.2001.00311.x

Santibañez-Lopez, C. E., Ontano, A. Z., Harvey, M. S., and Sharma, P. P. (2018). Transcriptomic analysis of pseudoscorpion venom reveals a unique cocktail dominated by enzymes and protease inhibitors. *Toxins* 10:207. doi: 10.3390/toxins10050207

Schonenmeyer, A., Lucius, R., Sonnenburg, B., Brattig, N., Sabat, R., Schilling, K., et al. (2017). Modulation of human T cell responses and macrophage functions by onchosystatin, a secreted protein of the filarial nematode *Ochocerca volvulus*. *J. Immunol.* 167, 3207–3215. doi: 10.4049/jimmunol.167.6.3207

Schwarz, A., von Reumont, B. M., Erhart, J., Chagas, A. C., Ribeiro, J. M., and Kotsyfakis, M. (2013). *De novo Ixodes ricinus* salivary gland transcriptome analysis using two next-generation sequencing methodologies. *FASEB J.* 27, 4745–4756. doi: 10.1096/fj.13-232140

Silva, F. D., Rezende, C. A., Rossi, D. C. P., Esteves, E., Dyszy, F. H., Schreier, S., et al. (2009). Structure and mode of action of microplusin, a copper II-chelating antimicrobial peptide from the catle tick Ripicephalus (Boophilus) microplus. *J. Biol. Chem.* 284, 34735–34746. doi: 10.1074/jbc.M109.016410

Šimo, L., Kazimirova, M., Richardson, J., and Bonnet, S. I. (2017). The essential role of tick salivary glands and saliva in tick feeding and pathogen transmission. *Front. Cell. Infect. Microbiol.* 7:281. doi: 10.3389/fcimb.2017.00281

Slovák, M., Kazimírová, M., Siebenstichová, M., Ustaniková, K., Klempa, B., Gristun, T., et al. (2014). Survival dynamics of tick-borne encephalitis virus in *Ixodes ricinus* ticks. *Ticks Tick Borne Dis.* 4, 962–969. doi: 10.1016/j.ttbdis.2014.07.019

Smith, A. A., and Pal, U. (2014). Immunity-related genus in *Ixodes scapularis*-perspectives from genome information. *Front. Cell. Infect. Microbiol.* 4:116. doi: 10.3389/fcimb.2014.00116

Soares, T. S., Oliveira, F., Torquato, R. J. S., Sasaki, S. D., Araujo, M. S., Paschoalin, T., et al. (2016). BmTI-A, a Kunitz type inhibitor from *Rhipicephalus microplus* able to interfere in vessel formation. *Vet. Parasitol.* 219, 44–52. doi: 10.1016/j.vetpar.2016.01.021

Sterba, J., Dupejova, J., Fiser, M., Vancova, M., and Grubhoffer, L. (2011). Fibrinogen-related proteins in ixodid ticks. *Parasit. Vectors.* 4:127. doi: 10.1186/1756-3305-4-127

Štibrániová, I., Bartíková, P., Holíková, V., and Kazimírová, M. (2019). Deciphering biological processes at the tick-host interface opens new strategies for treatment of human diseases. *Front. Physiol.* 10:830. doi: 10.3389/fphys.2019.00830

Team R. C. (2013). *R: A Language and Environment for Statistical Computing. R Foundation for Statistical Computing*, Vienna, Austria.

Thangamani, S., Hermance, M. E., Santos, R. I., Slovak, M., Heinze, D., Widen, S. G., et al. (2017). Transcriptional immunoprofiling at the tick-virus-host interface during early stages of tick-borne encephalitis virus transmission. *Front. Cell. Infect. Microbiol.* 7:494. doi: 10.3389/fcimb.2017.00494

Tirloni, L., Kim, T. K., Berger, M., Termignoni, C., da Silva Vaz, I. Jr., and Mulenga, A. (2019). *Amblyomma americanum* serpin 27 (AAS27) is a tick salivary anti-inflammatory protein secreted into the host during feeding. *PLoS Negl. Trop. Dis.* 13:e0007660. doi: 10.1371/journal.pntd.0007660

Valdes, J. J., Cabezas-Cruz, A., Sima, R., Butterill, P. T., Ruzek, D., and Nuttall, P. A. (2016). Substrate prediction of *Ixodes ricinus* salivary lipocalins differentially expressed during *Borrelia afzelii* infection. *Sci. Rep.* 6:32372. doi: 10.1038/srep32372

Valdes, J. J., and Moal, I. H. (2014). Prediction of Kunitz ion channel effectors and protease inhibitors from the *Ixodes ricinus* sialome. *Ticks Tick Borne Dis.* 5, 947–950. doi: 10.1016/j.ttbdis.2014.07.016

Vechtova, P., Sterbova, J., Sterba, J., Vancova, M., Rego, R. O. M., Selinger, M., et al. (2018). A bite so sweet: the glycobiology interface of tick-host-pathogen interactions. *Parasit. Vectors.* 11:594. doi: 10.1186/s13071-018-3062-7

Wang, Y., Li, Z., Zhou, Y., Cao, J., Zhang, H., Gong, H., et al. (2016). Specific histamine binding activity of a new lipocalin from *Hyalomma asiaticum* (Ixodidae) and therapeutic effects on allergic asthma in mice. *Parasit. Vec.* 9:506. doi: 10.1186/s13071-016-1790-0

World Health Organization (2011). *Weekly Epidemiological Record (2011)*. No. 24, 86, 241–256.

Xu, X., Chang, B. W., Mans, B. J., Ribeiro, J. M. C., and Andersen, J. F. (2013). Structure and ligand-binding properties of the biogenic amin-binding protein from the saliva of a blood-feeding insect vector of Trypanosoma cruzi. *Acta Crystallograph. D*69, 105–113. doi: 10.1107/S0907444912043326

Zavadska, D., Odzelevica, Z., Karelis, G., Liepina, L., Litaurniece, Z. A., Bormane, A., et al. (2018). Tick-borne encephalitis: a 43-year summary of epidemiological and clinical data from Latvia (1973 to 2016). *PLoS ONE* 13:e0204844. doi: 10.1371/journal.pone.0204844

Zhang, H., Qiao, R., Gong, H., Cao, J., Zhou, Y., and Zhou, J. (2017). Identification and anticoagulant activity of a novel Kunitz-type protein HA11 from the salivary gland of the tick *Hyalomma asiaticum*. *Exp. Appl. Acarol.* 71, 71–85. doi: 10.1007/s10493-017-0106-1

Zuckerkandl, E., and Pauling, L. (1965). Molecules as documents of evolutionary history. *J. Theor. Biol.* 8, 357–366. doi: 10.1016/0022-5193(65)90083-4

Conflict of Interest: The authors declare that the research was conducted in the absence of any commercial or financial relationships that could be construed as a potential conflict of interest.

The reviewer JR declared a past co-authorship with one of the authors MK to the handling editor.

frontiers in Cellular and Infection Microbiology

ORIGINAL RESEARCH
published: 17 March 2020
doi: 10.3389/fcimb.2020.00086

Methodological Insight Into Mosquito Microbiome Studies

Sonia M. Rodríguez-Ruano[1]*, *Eliška Juhaňáková*[1], *Jakub Vávra*[1] and *Eva Nováková*[1,2]

[1] Department of Parasitology, Faculty of Science, University of South Bohemia, Ceske Budejovice, Czechia, [2] Institute of Parasitology, Biology Centre of ASCR, Ceske Budejovice, Czechia

Symbiotic bacteria affect competence for pathogen transmission in insect vectors, including mosquitoes. However, knowledge on mosquito-microbiome-pathogen interactions remains limited, largely due to methodological reasons. The current, cost-effective practice of sample pooling used in mosquito surveillance and epidemiology prevents correlation of individual traits (i.e., microbiome profile) and infection status. Moreover, many mosquito studies employ laboratory-reared colonies that do not necessarily reflect the natural microbiome composition and variation in wild populations. As a consequence, epidemiological and microbiome studies in mosquitoes are to some extent uncoupled, and the interactions among pathogens, microbiomes, and natural mosquito populations remain poorly understood. This study focuses on the effect the pooling practice poses on mosquito microbiome profiles, and tests different approaches to find an optimized low-cost methodology for extensive sampling while allowing for accurate, individual-level microbiome studies. We tested the effect of pooling by comparing wild-caught, individually processed mosquitoes with pooled samples. With individual mosquitoes, we also tested two methodological aspects that directly affect the cost and feasibility of broad-scale molecular studies: sample preservation and tissue dissection. Pooling affected both alpha- and beta-diversity measures of the microbiome, highlighting the importance of using individual samples when possible. Both RNA and DNA yields were higher when using inexpensive reagents such as NAP (nucleic acid preservation) buffer or absolute ethanol, without freezing for short-term storage. Microbiome alpha- and beta-diversity did not show overall significant differences between the tested treatments compared to the controls (freshly extracted samples or dissected guts). However, the use of standardized protocols is highly recommended to avoid methodological bias in the data.

Keywords: dissection, epidemiology, microbiome, mosquito, pooling, preservation, vector

OPEN ACCESS

Edited by:
Job E. Lopez,
Baylor College of Medicine,
United States

Reviewed by:
Fred David Mast,
Seattle Children's Research Institute,
United States
Iris Bruchhaus,
Bernhard Nocht Institute for Tropical Medicine (BMITM), Germany

***Correspondence:**
Sonia M. Rodríguez-Ruano
soniamrr@ugr.es

Specialty section:
This article was submitted to Parasite and Host, a section of the journal Frontiers in Cellular and Infection Microbiology

Received: *14 October 2019*
Accepted: *19 February 2020*
Published: *17 March 2020*

Citation:
Rodríguez-Ruano SM, Juhaňáková E, Vávra J and Nováková E (2020) Methodological Insight Into Mosquito Microbiome Studies. Front. Cell. Infect. Microbiol. 10:86. doi: 10.3389/fcimb.2020.00086

INTRODUCTION

The spread of vector-borne diseases, particularly those vectored by mosquitoes, is one of the main problems humanity has faced (Johnson et al., 2018). The relevance of the topic to human health has encouraged a great number of epidemiological studies in this field. However, most of the research has been focused on mosquito population distribution, early detection of invasive species, and disease agent surveillance (Kampen et al., 2015). This information is essential for keeping track of mosquito-vectored diseases, but lacks any further insight into the processes that underlie or affect the mosquito-pathogen interactions. For this reason, research focuses are shifting to the

mechanisms involved in vectors' infection by pathogens and the development of new vector control strategies (Niang et al., 2018).

Microbiomes have arisen as a key factor driving many aspects of host physiology (i.e., the holobiont theory: Bordenstein and Theis, 2015; Guégan et al., 2018), including development, nutrition, survival, and competence for pathogen transmission in insect vectors (Saldaña et al., 2017). Particularly, the extent to which the microbiome can interact with arboviruses (i.e., arthropod-borne RNA viruses of the families Flaviviridae, Togaviridae, Bunyaviridae, Reoviridae, and Rhabdoviridae) has received great attention due to their epidemiological relevance (reviewed in Palmer et al., 2018). Nevertheless, most of the knowledge on microbiome-pathogen interactions in mosquitoes lacks validation from field-collected data, as it is often based on laboratory-reared mosquitoes (Minard et al., 2013; Guégan et al., 2018). In addition, large numbers of field-collected mosquitoes are processed by sample pooling to decrease research time and expenses in epidemiological studies (for a review see Engler et al., 2013).

Pooled samples allow us to track microbiome dynamics at the population level and to examine general species-specific patterns. However, pooling fails to capture the inter-individual diversity found in populations, which can be substantial and variable across vector species (Nováková et al., 2017). The resolution of inter-individual variation and individual diversity of vector-associated microbiomes has principal implications for epidemiology. The microbiome, being the more dynamic component of a holobiont, can promptly react to changing environmental conditions and drive vector adaptation and evolution. The inter-individual variation among host microbiomes is fertile ground for evolutionary novelties to arise in vector populations. The current quest to develop novel microbe-based vector control strategies thus goes through the exploration of natural microbiome variability. Understanding its role in host evolution, adaptation and physiology, including pathogen acquisition, resistance, and transmission, are key for efficient and sustainable biocontrol (Guégan et al., 2018). Although *Wolbachia*-based strategies have been successfully applied in several tropical areas as part of the World Mosquito Program (reviewed in O'Neill, 2018), consideration of the epidemiological, ecological, and evolutionary aspects of the holobiont is missing in current approaches.

The aim of this study is to demonstrate how sample pooling affects the microbiome profile obtained from wild mosquito samples, and to test different methodologies that could be applied in epidemiological studies to reduce processing costs whilst simultaneously allowing for individual specimen data collection and analysis. Particularly, we compare the microbiome alpha- and beta- diversity at different levels of pooling in two cosmopolitan species of mosquitoes, *Aedes vexans* and *Culex pipiens*. We test how different preservation methods and the use of dissected versus whole mosquitoes affects the nucleic acid yields and the diversity of the microbiome sequenced from the extracted DNA of *Aedes vexans*. Our results allow researchers in the field of vector epidemiology to choose between the proposed cost-effective methods for handling vector samples as individuals on which rigorous microbiome studies can be performed.

MATERIALS AND METHODS

Mosquito Collection

Mosquitoes were collected in forest areas of south west part of Czech Republic (48°58′52.6″N, 14°47′56.3″E) in summer 2016 (July 20 and August 17, under similar weather conditions) using an entomological aspirator. After morphological identification, 53 female mosquitoes of *Aedes vexans* species complex were selected and divided into the different methodological categories tested (for preservation and dissection) as shown in **Table 1**.

In order to assess the pooling effect, we used already sequenced data from a previously published study in which adult female mosquitoes of 11 species were collected from 9 locations in Ontario, Canada between 2011 and 2013 (Nováková et al., 2017). Briefly, CDC ultraviolet light traps were set in urban areas from June to September each year. The collected individuals were morphologically identified to species. Individuals from each trap and date were pooled into samples containing 1–50 mosquitoes according to their taxonomy. The details of the specific data subset used are described below.

Sample Preservation

Prior to DNA/RNA extraction (see below), the 53 mosquitoes were individually processed according to different methodologies. Whole mosquitoes were surface sterilized with absolute ethanol and then divided into different experimental groups (**Table 1**). The procedures used were as follows: (1) extraction the same day of capture without preservation (fresh), either (1a) processed as a whole, or (1b) dissected in sterile PBS under the stereo microscope to obtain the gut and the rest of the body separately; (2) individual preservation, without dissection, in microfuge tubes with (2a) AllProtect reagent (Qiagen), (2b) molecular grade absolute ethanol (VWR Life Sciences), or (2c) nucleic acid preservation (NAP) buffer (Camacho-Sanchez et al., 2013). Samples preserved in each reagent were stored for one week, either at 4°C or at −20°C. See **Table 1** for a detailed list of the samples used in each treatment. Some samples were damaged during dissection and had to be discarded, resulting in uneven numbers for gut and rest of the body.

TABLE 1 | List of processing treatments and number of samples used in the experiment.

Dissected tissue	Preservation method	*Ae. vexans* samples
Gut	None (Fresh)	7
Rest of body	None (Fresh)	10
Whole mosquito	None (Fresh)	11
	All Protect 4°C	6
	All Protect −20°C	5
	Ethanol 4°C	4
	Ethanol −20°C	6
	NAP 4°C	6
	NAP −20°C	5

DNA/RNA Extraction and Yield Assessment

After the different procedures were applied, a total of 60 samples were individually homogenized in Buffer RLT Plus (Qiagen) using sterile 1.5 mL microfuge tubes and pestles. To ensure maximum extraction yields for both DNA and RNA from the same sample, we used the gDNA Eliminator spin column from the RNA protocol (Qiagen) to separate RNA and DNA content. Subsequently, total RNA and DNA were extracted using the RNeasy Plus Micro Kit (Qiagen) and the QIAamp DNA Micro Kit (Qiagen) respectively, following manufacturer instructions. Both DNA and RNA were eluted in PCR-grade, RNase-free ultrapure water (Qiagen), and their concentrations in nanograms per microliter were measured using a NanoPhotometer (Implen GmbH), following the manufacturer's instructions for each nucleic acid.

Microbiome Analysis

DNA from whole specimens and dissected guts was amplified according to the EMP protocol (http://www.earthmicrobiome.org/protocols-and-standards/16s/). The 16S rRNA gene amplicons were purified using AMPure XP magnetic beads (Beckman Coulter), and pooled equimolarly based on concentrations quantified using a Synergy H1 microplate reader (Biotek). One negative control for the extraction and three blanks for the reagents were included in the library preparation, as recommended by Knight et al. (2018). The raw, demultiplexed sequences produced in this work (Illumina MiSeq run, 300 cycles with v2 chemistry) are available under the ENA (European Nucleotide Archive) project number PRJEB35477.

Paired-end reads were merged using fastq_mergepairs with fastq_minovlen set to 20 from USEARCH v7.0.1001 (Edgar, 2013). Demultiplexing and quality filtering were performed in QIIME 1.9 using split_libraries_fastq.py with phred_quality_threshold set to 19 (Caporaso et al., 2010b). The resulting high-quality sequences were aligned using the QIIME implementation of Pynast (Caporaso et al., 2010a) and trimmed to an equal length of 251 bp with USEARCH. Finally, the dataset was clustered at 100% identity and this representative set of sequences was used for de novo OTU picking with the USEARCH global alignment option set to 97% identity. Each OTU was assigned to different taxonomic levels using the BLAST+ algorithm (Camacho et al., 2009) against the release 123 of the SILVA database (Pruesse et al., 2007). Singletons, very low abundant OTUs (as recommended in Bokulich et al., 2013), and all non-bacterial, chloroplast, and mitochondrial OTUs were filtered out using QIIME 1.9.

One of the blanks showed a high number of reads from a *Staphylococcus* OTU, which was absent in the other blanks and could be a specific contamination of this particular control. The second blank and the extraction negative control showed 4 OTUs and 9 OTUs, respectively. None of these OTUs represented more than 2% of the sequences in the analyzed mosquito samples. All the OTUs detected in these controls were considered contaminants, and were thus filtered out for our analyses. We also found *Spiroplasma* in the third blank, suggesting a cross-sample contamination. In fact, insect pathogens (i.e., Entomoplasmatales and Spirochaetales) were present in 28% of the samples ($N = 50$), showing high abundance (above 10%) in six of them. Since the presence of these groups may distort the profile of the affected individuals and thus any further comparisons, these OTUs were also removed from our analyses.

After this filtering step, we filtered the OTU table at a minimum of 1250 sequences per sample and rarefied at 1,000 sequences per sample to allow for resampling, even in the samples with the fewest reads, while normalizing the dataset (as recommended in Weiss et al., 2017). However, many samples from different treatments did not pass this threshold. We therefore lowered the filtering and rarefaction to 200 and 150 sequences per sample, respectively, to retain the maximum number of samples in each experimental treatment. A comparison of the microbiome profile at both rarefaction levels is shown in **Supplementary Figure 1**. Since all samples showed a very similar profile at both rarefaction levels, the analyses of the data set rarefied at the lower level (40 samples) are presented in the main text. When possible, the equivalent analyses for the rarefaction at 1,000 sequences per sample (23 samples) are available in **Supplementary Material**.

The evaluation of the pooling effect was performed on 16S rRNA data from *A. vexans* ($N = 59$) and *C. pipiens* ($N = 67$) collected in Toronto, Canada in 2012. The data used here are a subset of a previously published data set (Nováková et al., 2017) available at the European Bioinformatics Institute database (accession number ERP021438) and at https://qiita.ucsd.edu/ (ID 10815). Briefly, following the EMP protocol, the sequences were obtained in a HiSeq 2000 Illumina run (2×125 bp), demultiplexed using QIIME1.9, stitched and quality filtered using USEARCH software, and clustered to obtain the OTU table as described above. Taxonomic assignments for this study were performed using BLAST against the SILVA 123 database, and OTU table filtering followed the same steps as described above, with a rarefaction depth of 5,000 sequences per sample in this case. According to our previous results (Nováková et al., 2017) no contaminants needed to be filtered out from the data set. In addition to the individually processed mosquitoes (*Aedes* $N = 32$; *Culex* $N = 12$), the pooling levels used were: pools of 10 mosquitoes (*Aedes* $N = 7$; *Culex* $N = 12$), pools including between 20 and 25 mosquitoes (*Aedes* $N = 12$; *Culex* $N = 23$), and pools of 50 mosquitoes (*Aedes* $N = 8$; *Culex* $N = 20$).

Alpha-diversity indexes were calculated using QIIME 1.9. The richness of the samples (i.e., number of OTUs present) was estimated by Chao1 index, and OTU abundance and evenness in the samples was measured by Shannon index. Beta diversity analyses were performed in R (R Development Core Team, 2014) with the "biomformat" package (McMurdie and Paulson, 2019). The distance matrices were calculated using Bray-Curtis dissimilarities with the vegdist function of the "vegan" package (Oksanen et al., 2013). Core microbiomes at 100% were computed in QIIME 1.9, and Venn and Euler charts obtained using the online tool available at http://bioinformatics.psb.ugent.be/webtools/Venn/ and the upset function of "UpSetR" package (Conway et al., 2017), respectively. Additionally, these analyses were repeated using 10 random sub-samplings of our data set ($n = 10$ for each group), to check for sample size effects in our results (see **Supplementary Material**).

Statistical Analyses

All statistical tests were performed in R (R Development Core Team, 2014), including outlier detection and removal (see a report of number of outliers for each analysis in **Supplementary Table 1**). We used the Kruskal-Wallis rank sum test (R "stats" package) to compare the yields (i.e., concentration values) and the alpha-diversity indexes among treatments. We used the adonis function in the "vegan" package (Oksanen et al., 2013) to compare the beta-diversity of the samples according to the different treatments, and performed NMDS analyses with the metaMDS function of the same package. Plots were obtained using the "ggplot2" package (Wickham, 2009).

RESULTS

DNA and RNA Yields

After removing the detected outliers, the only significant differences among treatments were found according to the preservation method used when considering RNA yields ($X^2 = 18.93$, $p = 0.004$). RNA yields did not significantly differ regardless of the body part used, including the rest of the body after dissection ($X^2 = 2.36$, $p = 0.307$). The preservation method did not significantly affect DNA yields ($X^2 = 7.85$, $p = 0.249$). DNA concentration differences were significant at 95% but not at 99% confidence interval when evaluating the body part used ($X^2 = 7.81$, $p = 0.020$). See **Supplementary Table 1** for a complete overview of the data and the results of the statistical tests.

Alpha-Diversity

The comparison of the different levels of pooling revealed significant differences both for *A. vexans* and *C. pipiens*. In the first case, the richness of the samples measured by Chao1 index was significantly different among pooling levels after removing outliers ($X^2 = 18.935$, $p < 0.001$; **Figure 1A**), but not Shannon index, which accounts for both OTU abundance and evenness in the samples ($X^2 = 2.326$, $p = 0.508$; **Figure 1B**). In the second case, both Chao1 ($X^2 = 14.997$, $p = 0.002$; **Figure 1C**) and Shannon ($X^2 = 10.769$, $p = 0.013$; **Figure 1D**) indices were significantly different, at 99 and 95% confidence interval respectively, regarding the pooling levels compared. See **Supplementary Table 2** for a complete overview of the data and the results of the statistical tests.

The different treatments did not affect alpha-diversity found in *A. vexans* (**Supplementary Table 1**). Specifically, no significant differences were found among Chao1 indices for samples preserved in different ways ($X^2 = 4.01$, $p = 0.676$; **Figure 2A**), or those that originated from guts of whole specimens ($X^2 = 2.83$, $p = 0.093$; **Figure 2B**; see also **Supplementary Figure 2A**). Shannon index did not show significant differences among treatments either regarding preservation method ($X^2 = 1.52$, $p = 0.958$; **Figure 2C**) or dissection ($X^2 = 1.07$, $p = 0.302$; **Figure 2D**; see also **Supplementary Figure 2B**). See **Supplementary Table 1** for a complete overview of the data and the results of the statistical tests.

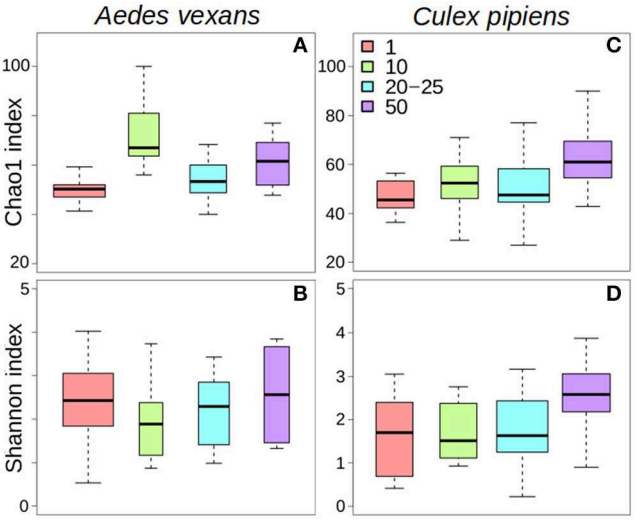

FIGURE 1 | Box-plots showing the alpha-diversity of *Aedes vexans* and *Culex pipiens* microbiomes according to the number of mosquitoes pooled per sample: **(A)** Chao1 index and **(B)** Shannon index for *Aedes vexans*; **(C)** Chao1 index, and **(D)** Shannon index for *Culex pipiens*.

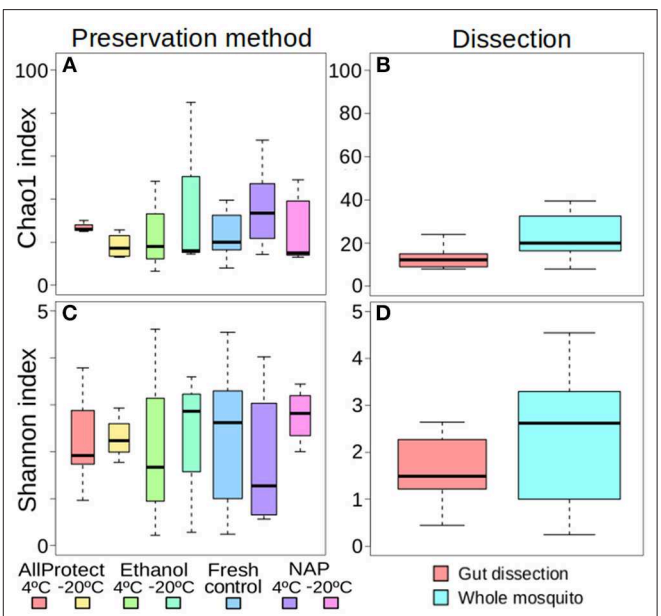

FIGURE 2 | Box-plots showing the alpha-diversity of *Aedes vexans* microbiomes with the different processing treatments of this study: Chao1 index according to **(A)** preservation method and **(B)** dissection; Shannon index according to **(C)** preservation method and **(D)** dissection.

Beta-Diversity

When the beta-diversity was assessed for the different pooling levels compared, the differences were statistically significant for both *A. vexans* ($R^2 = 0.125$, $p < 0.001$; **Figure 3A**, NMDS stress = 0.180) and *C. pipiens* ($R^2 = 0.131$, $p < 0.001$; **Figure 3B**, NMDS stress = 0.200). Since individual

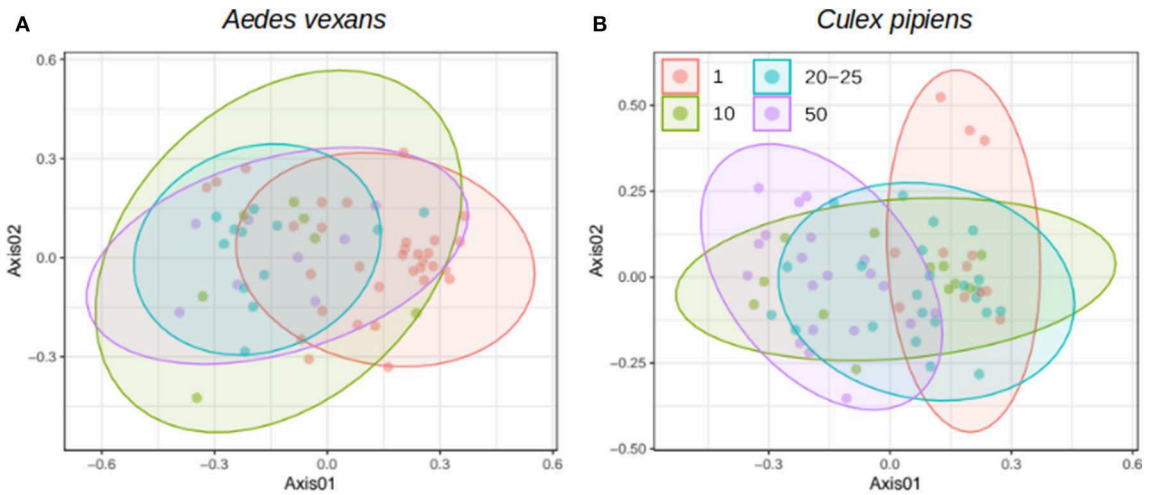

FIGURE 3 | NMDS showing the beta-diversity of **(A)** *Aedes vexans* and **(B)** *Culex pipiens* microbiomes according to the number of mosquitoes pooled per sample. Confidence ellipses are shown for each group.

samples were the functional control for pooling levels, additional pairwise comparisons between all groups and the control were performed. All the pooling levels differed significantly from the individual samples at 95% confidence interval, with the higher pooling levels (i.e., 20–25 and 50 individuals per pool) showing significant differences compared to the control at 99% confidence interval. The detailed results are shown in **Table 2**. To further explore the extent of the pooling effect on beta-diversity, we compared individual and pooled samples for both species together (**Figure 4**, NMDS stress = 0.218). The results showed significant differences between species ($R^2 = 0.121$, $p < 0.001$) and between individual and pooled samples ($R^2 = 0.051$, $p < 0.001$). The interaction of both factors was not statistically significant ($R^2 = 0.008$, $p = 0.302$). The results for the randomly sub-sampled data sets can be found in **Supplementary Figure 3**.

On the other hand, no significant differences in beta-diversity were found when assessing preservation method effect ($R^2 = 0.214$, $p = 0.070$; NMDS stress = 0.244), nor dissection ($R^2 = 0.103$, $p = 0.156$; NMDS stress = 0.170) in *A. vexans*. When the preservation analysis was repeated, taking into account preservation buffer and storage temperature separately, temperature had a significant effect at 99% confidence interval ($R^2 = 0.118$, $p < 0.001$), while the different buffers had none ($R^2 = 0.056$, $p = 0.525$). The interaction of the two variables was not statistically significant ($R^2 = 0.040$, $p = 0.942$). Since fresh samples were considered the control for preservation method, additional pairwise comparisons between all treatments and the control were performed. None of the preservation methods significantly differed from the control, and the detailed results are shown in **Table 3**.

Core Microbiomes

The specific effect of pooling on the retrieval of total OTUs and core microbiome components was assessed for *A. vexans* and *C. pipiens*. The core microbiomes (i.e., OTUs present in all samples)

TABLE 2 | Pairwise comparisons between all pooling levels and the control (i.e., individual samples).

	Aedes vexans		*Culex pipiens*	
Mosquitoes in pool vs. individuals	R^2	*p*	R^2	*p*
10	0.06	0.0112*	0.08	0.0497*
20–25	0.1	0.0001**	0.07	0.0081**
50	0.07	0.0030**	0.19	0.0001**

Results are shown for Aedes vexans and Culex pipiens samples. Statistically significant results are indicated at 95% (*) and 99% (**) confidence.

were plotted against the total number of OTUs for both the individual samples and the pooled ones, to show the amount of unique microbiome members as well as the representation of the core microbiome retrieved by each group (**Figure 5**). The results for the randomly sub-sampled data sets can be found in **Supplementary Figure 4**.

In *A. vexans* individuals, the total number of OTUs found was 174, compared to the 186 OTUs found in pooled samples. Out of those, 12 (6.9%) and 24 (12.9%) were unique to individual and pooled samples, respectively, and 157 were common to both groups. The core microbiome of individual samples comprised two (1.1%) OTUs, *Pseudomonas* sp. and an unclassified Methylophilaceae, while the core microbiome of pooled samples comprised up to five (2.7%), including the previous two plus *Enterobacter* sp., *Serratia* sp. and a second *Pseudomonas* sp. (see **Figures 5A–B**; for an overview of the sub-sampled data sets average results, see **Figure 5C**).

In *C. pipiens* individuals, the total number of OTUs found was 137, compared to the 200 OTUs found in pooled samples. Out of those, 63 (31.5%) were unique to pooled samples, while all the 137 OTUs from individual samples were also found in the pools. The core microbiome of individual samples comprised five

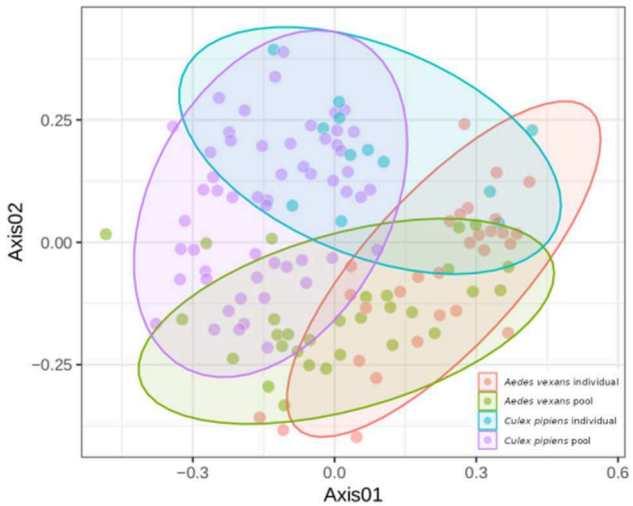

FIGURE 4 | NMDS showing the beta-diversity of *Aedes vexans* and *Culex pipiens* microbiomes both from individuals and pools. Confidence ellipses are shown for each group.

TABLE 3 | Pairwise comparisons of beta-diversity between all preservation treatments and the control.

Preservation method vs. fresh samples	R^2	*p*
All Protect 4°C	0.13	0.05
All Protect −20°C	0.11	0.15
Ethanol 4°C	0.08	0.64
Ethanol −20°C	0.09	0.52
NAP 4°C	0.1	0.2
NAP −20°C	0.12	0.06

Control includes whole Aedes vexans mosquitoes extracted upon collection without any preservation step (i.e., freshly extracted).

(3.6%) OTUs: *Wolbachia*, *Enterobacter* sp., two *Pseudomonas* sp., and an unclassified Methylophilaceae. The core microbiome of pooled samples included also five (2.5%) OTUs: four present in the individual samples core and another unique: *Tumebacillus* sp. (see **Figures 5D–E**; for an overview of the sub-sampled data sets average results, see **Figure 5F**).

DISCUSSION

Pooling is expected to bias the observed diversity of the microbiome, particularly when inter-individual variability is high in the analyzed populations. This is the case in mosquitoes, for which previous studies identified several eco-physiological factors affecting the microbial community composition (Minard et al., 2013). Microbiome data is *per se* highly dimensional (i.e., many categories), sparse (i.e., dominated by zero values) and compositional (i.e., absolute abundances are unknown) (Tsilimigras and Fodor, 2016). These complex microbiome characteristics pose a general challenge to microbiome data analysis that is only deepened with sample pooling. Each individual pooled adds on categories (e.g., infrequent taxa) and skews the relative abundances in different, unknown directions (either toward dominance of particular OTUs or evenness). This may cause, for instance, an increase of richness due to additive occurrence of rare taxa as previously discussed for tick microbiomes (Clow et al., 2018). It can also affect the beta-diversity metrics (i.e., pool inter-variability) when alpha-diversity variance increases due to differential pool intra-variability. Our results show a clear shift between the microbiome of mosquitoes processed as individuals and samples coming from pools of variable number. Along with other studies revealing microbiome differences between individual and pooled samples (e.g., in humans: Aguirre et al., 2014; and chigger mites: Chaisiri et al., 2019), this emphasizes the need for careful interpretation of results. Both the microbiome alpha- and beta-diversity of the mosquitoes used here, *Aedes vexans* and *Culex pipiens*, were significantly different between individual and pooled samples. These differences occurred independently of the species considered, and were comparable to those found between samples of the different species, suggesting the effect of pooling is considerable. We also show that the core microbiome is overestimated when using pools. For example, OTUs that may be abundant in only a few individuals could be retrieved in all pools and be included in the core microbiome of the study group. This would alter the conclusions made about potentially interesting (i.e., functionally relevant) members of the microbiome and their interactions.

Whole specimens are usually pooled in surveillance studies to screen mosquito samples for viruses using RNA and RT-PCR techniques (e.g., Čabanová et al., 2019). However, individual dissection of particular tissues (i.e., guts) is the reference methodology to study site/organ specific microbiomes (e.g., Muturi et al., 2019). This approach is, in many cases, technically complicated (i.e., when working with very small organisms) and/or logistically limiting (i.e., when large numbers of individuals have to be processed in a limited amount of time and/or with restricted resources). Since the main aim of this study was to find a feasible way to simultaneously conduct disease surveillance and obtain individual microbiomes in disease vectors, the number of individuals to dissect is the main limiting factor in this context. Our results show that, although the use of whole specimens causes an increase in the overall microbiome alpha-diversity compared to the dissected guts, the differences are not significant. The increase in diversity is most likely due to the detection of bacteria present in other parts of the body. However, the non-gut bacteria should be relatively much less abundant, and in fact, we did not find significant differences when assessing the bacterial composition of the mosquito microbiome (i.e., beta-diversity) in dissected guts and whole body samples. Such an assumption does not apply to systems in which endosymbionts associated with specific tissues like *Asaia, Rickettsia*, *Wolbachia*, *Spiroplasma*, or other reproductive manipulators are found (Duron et al., 2008; Segata et al., 2016). Nonetheless, these endosymbionts can be easily identified in the data and filtered out if necessary (e.g., *Wolbachia*: Nováková et al., 2017; Hegde et al., 2018). For insects lacking more specialized symbionts gut bacteria amplify preferentially

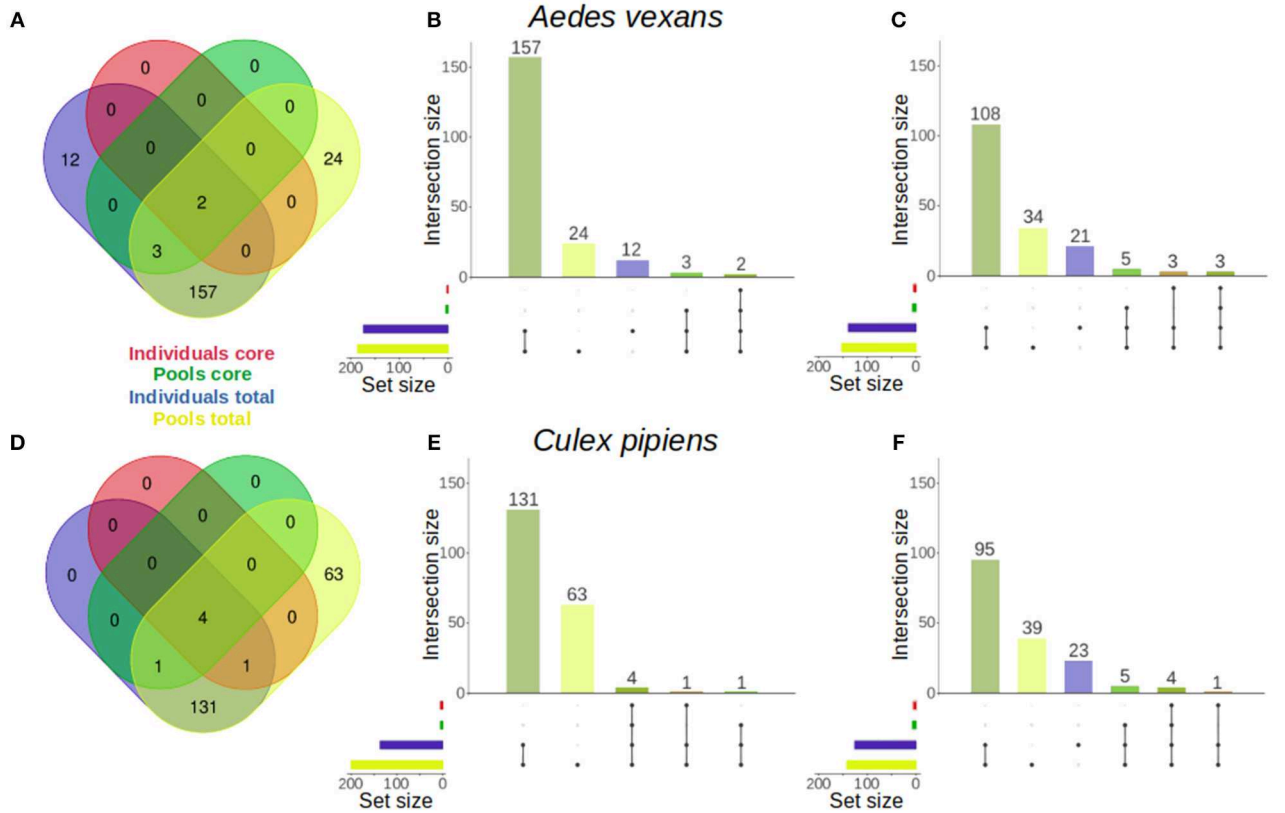

FIGURE 5 | Venn diagrams comparing the number of OTUs present in individual and pooled samples, both in total and in the core microbiome of **(A)** *Aedes vexans* and **(D)** *Culex pipiens* full data sets. Proportional representations ("Euler grids") of the same information are given for the full data set **(B,E)** and the average values of the randomly sub-sampled data sets **(C,F)** of each species.

as shown in *Drosophila* gut microbiomes, successfully described using whole specimens (Wong et al., 2013). Similarly, Whitaker et al. (2016) found no differences for two particular OTUs of interest when comparing whole specimens and dissected guts of lycaenid butterflies. Among blood-feeding vectors, comparable results were previously obtained for kissing bugs (Rodríguez-Ruano et al., 2018) and *Anopheles* mosquitoes (Coon et al., 2014), for which the microbiome profiles of dissected guts and whole bodies/abdomens did not differ significantly. Along with the results presented here, these findings collectively support the use of whole specimens in epidemiological-microbiome studies, saving the difficulties and costs of dissecting every individual prior to DNA/RNA extraction. Particular attention should be payed to the washing and surface sterilization steps prior to the extraction to avoid as much as possible external contaminants. Even though the effect of surface microbes in the whole microbiome assessment may be minimal as well (Hammer et al., 2015), the method used for surface sterilization can impact the microbiome diversity retrieved (Binetruy et al., 2019).

Methodology optimization also involves sample preservation. All methods evaluated here were able to preserve DNA (i.e., needed for microbiome profiling) and RNA (i.e., needed for virus screening), in agreement with previous studies performed with different kinds of samples (e.g., freshwater insects: Astrid et al., 2016; and mammalian blood and tissues: Camacho-Sanchez et al., 2013). Significant differences among treatments were found for RNA yields, but not for DNA. The highest extraction yields were obtained using preservation in NAP buffer at 4°C for both DNA and RNA, followed by All Protect at 4°C and absolute ethanol at 4°C, respectively. The better performance of non-freezing storage conditions may be a result of avoiding freezing-thaw cycles during sample manipulation. The finding of absolute ethanol as an efficient RNA preservative may seem surprising, but it has previously been shown for insect larvae and nymphs (Astrid et al., 2016). In general, our results agree with previous studies where NAP buffer was found as an efficient nucleic acid preservative for various samples (e.g., rat tissues: Camacho-Sanchez et al., 2018; and frog tissues Montero-Mendieta et al., 2017), including those for microbiome studies (e.g., fecal samples: Menke et al., 2017). Nevertheless, we faced difficulties fully submerging the mosquito specimens in NAP buffer. Different concentrations of glycerol (25–50%) added during preparation resulted in salt precipitation of the solution. We thus encourage future attempts on the development of efficient laboratory-made buffers that would overcome this issue and facilitate their massive usage, being an easy to prepare and more economic alternative to commercial buffers.

Almost all preservation treatments produced a slight increase in the OTU richness found in the samples compared to the control (i.e., specimens freshly extracted upon collection), with the exception of All Protect combined with freezing at −20°C. These results are contrary to those obtained by Menke et al. (2017), yet the differences found in our study are not significant. In addition, the control treatment they used involved sample freezing. Here we consider freezing as a preservation method itself, which our results show has a strong effect. Additionally, we found the OTU abundance and evenness to be lower overall with all the preservation methods when compared to the control, with the exception of NAP buffer at −20°C. These differences were non-significant in all cases, allowing us to conclude that specimen preservation method does not strongly affect the retrieved alpha-diversity of bacterial communities in the conditions tested in our study. On the other hand, preservation method did affect the beta-diversity observations. The storage temperature was more important in determining the significant differences found than the preservation buffer used. Menke et al. (2017) found a similar effect of their different preservation treatments, with a strong effect of storage temperature irrespective of the preservation buffer used. Nevertheless, none of the preservation buffers combined with storage at 4°C or freezing at −20°C significantly differed from the freshly extracted controls in our beta-diversity analyses. The differences found in the global test (i.e., when comparing all treatments) occurred among preservation treatments. This means that each method can quite accurately reflect the actual diversity of the samples, but different preservation methods can act as a confounding factor in the analyses performed. Our results highlight the importance of using the same preservation technique throughout a study, in order to avoid the bias in beta-diversity observed when different preservation methods are employed.

In summary, we confirm that sample pooling distorts the real picture of the mosquito microbiome. An accurate description of the microbiome requires, thus, the use of individual samples. Furthermore, the inter-individual variations and direct interactions between different microbiome components and transmitted pathogens, as well as their effect on host ecophysiology, can only be clarified at the individual level. We propose alternatives to optimize the cost-efficiency of the protocols to assess the microbiome of epidemiologically relevant vectors (such as mosquitoes). In general, the OTUs we observe in the mosquito microbiome are congruent with previous reports (Muturi et al., 2017; Nováková et al., 2017). Our analyses show there are no major effects on the diversity and composition of the microbiome posed by the use of whole specimens vs. dissected guts, or when combining any of the preservation buffers tested with short-term storage at 4°C or −20°C. However, the lack of a priori power analysis and the small sample size remaining after data processing combined with the high variability found in the mosquito microbiome limits the extent of our conclusions. Based on the obtained results we recommend the use of whole specimens and inexpensive preservative reagents like NAP or absolute ethanol, which do not require the samples to be stored in the freezer in the short term (i.e., during field sampling). This methodology allows for valid assessments of the bacterial microbiome alpha- and beta-diversity, while providing enough material for pathogen screening both using DNA (e.g., for nematodes and protists) and RNA (e.g., for arboviruses). In addition, it allows for the assessment of other components of the microbiome (i.e., DNA-based mycobiome and RNA-based viriome). Finally, we highlight the particular importance of using standardized methodology for sample processing and preservation when possible, in order to minimize methodological bias in microbiome studies.

DATA AVAILABILITY STATEMENT

The datasets generated for this study can be found in the European Nucleotide Archive (ENA) under project number PRJEB35477 (https://www.ebi.ac.uk/ena/browser/view/PRJEB35477).

AUTHOR CONTRIBUTIONS

SR-R and EN designed the study and drafted the manuscript. SR-R, EJ, and JV managed the field collections and performed the experiments. SR-R generated the data and performed the data analyses. All authors read and contributed to the final text.

FUNDING

SR-R was funded by the Czech Ministry of Education, Youth and Sports (MSMT) and European Structural and Investment Funds through the project: Rozvoj JU - Mezinárodní mobility - MSCA-IF - CZ.02.2.69/0.0/0.0/17_050/0008486.

ACKNOWLEDGMENTS

We thank František Vácha for his contribution to test collection methods and Joel Brown for the revision of the English text. We also thank the two reviewers whose comments helped to improve and clarify this manuscript.

SUPPLEMENTARY MATERIAL

The Supplementary Material for this article can be found online at: https://www.frontiersin.org/articles/10.3389/fcimb.2020.00086/full#supplementary-material

REFERENCES

Aguirre, M., Ramiro-Garcia, J., Koenen, M. E., and Venema, K. (2014). To pool or not to pool? Impact of the use of individual and pooled fecal samples for *in vitro* fermentation studies. *J. Microbiol. Methods* 107, 1–7. doi: 10.1016/j.mimet.2014.08.022

Astrid, T., Margit, E., and Leopold, F. (2016). Ethanol: a simple and effective RNA-preservation for freshwater insects living in remote habitats. *Limnol. Oceanogr. Methods* 14, 186–195. doi: 10.1002/lom3.10079

Binetruy, F., Dupraz, M., Buysse, M., and Duron, O. (2019). Surface sterilization methods impact measures of internal microbial diversity in ticks. *Parasit. Vectors* 12:268. doi: 10.1186/s13071-019-3517-5

Bokulich, N. A., Subramanian, S., Faith, J. J., Gevers, D., Gordon, J. I., Knight, R., et al. (2013). Quality-filtering vastly improves diversity estimates from Illumina amplicon sequencing. *Nat. Methods* 10, 57–59. doi: 10.1038/nmeth.2276

Bordenstein, S. R., and Theis, K. R. (2015). Host biology in light of the microbiome: ten principles of holobionts and hologenomes. *PLoS Biol.* 13:e1002226. doi: 10.1371/journal.pbio.1002226

Čabanová, V., Šikutová, S., Straková, P., Šebesta, O.,Vichová, B., Zubríková, D., et al. (2019). Co-circulation of West Nile and Usutu flaviviruses in mosquitoes in slovakia, 2018. *Viruses* 11:639. doi: 10.3390/v11070639

Camacho, C., Coulouris, G., Avagyan, V., Ma, N., Papadopoulos, J., Bealer, K., et al. (2009). BLAST+: architecture and applications. *BMC Bioinform.* 10:421. doi: 10.1186/1471-2105-10-421

Camacho-Sanchez, M., Burraco, P., Gomez-Mestre, I., and Leonard, J. A. (2013). Preservation of RNA and DNA from mammal samples under field conditions. *Mol. Ecol. Resour.* 13, 663–673. doi: 10.1111/1755-0998.12108

Camacho-Sanchez, M., Quintanilla, I., Hawkins, M. T. R., Tuh, F. Y. Y., Wells, K., Maldonado, J. E., et al. (2018). Interglacial refugia on tropical mountains: novel insights from the summit rat (*Rattus baluensis*), a Borneo mountain endemic. *Divers. Distrib.* 24, 1252–1266. doi: 10.1111/ddi.12761

Caporaso, J. G., Bittinger, K., Bushman, F. D., deSantis, T. Z., Andersen, G. L., and Knight, R. (2010a). PyNAST: a flexible tool for aligning sequences to a template alignment. *Bioinformatics* 26, 266–267. doi: 10.1093/bioinformatics/btp636

Caporaso, J. G., Kuczynski, J., Stombaugh, J., Bittinger, K., Bushman, F. D., Costello, E. K., et al. (2010b). QIIME allows analysis of high-throughput community sequencing data. *Nat. Methods* 7, 335–336. doi: 10.1038/nmeth.f.303

Chaisiri, K., Gill, A. C., Stekolnikov, A. A., Hinjoy, S., McGarry, J. W., Darby, A. C., et al. (2019). Ecological and microbiological diversity of chigger mites, including vectors of scrub typhus, on small mammals across stratified habitats in Thailand. *Animal Microbiome* 1:18. doi: 10.1101/523845

Clow, K. M., Weese, J. S., Rousseau, J., and Jardine, C. M. (2018). Microbiota of field-collected *Ixodes scapularis* and *Dermacentor variabilis* from eastern and southern Ontario, Canada. *Ticks Tick-Borne Dis.* 9, 235–244. doi: 10.1016/j.ttbdis.2017.09.009

Conway, J. R., Lex, A., and Gehlenborg, N. (2017). UpSetR: an R package for the visualization of intersecting sets and their properties. *Bioinformatics* 33, 2938–2940. doi: 10.1093/bioinformatics/btx364

Coon, K. L., Vogel, K. J., Brown, M. R., and Strand, M. R. (2014). Mosquitoes rely on their gut microbiota for development. *Mol. Ecol.* 23, 2727–2739. doi: 10.1111/mec.12771

Duron, O., Bouchon, D., Boutin, S., Bellamy, L., Zhou, L., Engelstädter, J., et al. (2008). The diversity of reproductive parasites among arthropods: *Wolbachia* do not walk alone. *BMC Biol.* 6:27. doi: 10.1186/1741-7007-6-27

Edgar, R. C. (2013). UPARSE: highly accurate OTU sequences from microbial amplicon reads. *Nat. Methods* 10, 996–998. doi: 10.1038/nmeth.2604

Engler, O., Savini, G., Papa, A., Figuerola, J., Groschup, M. H., Kampen, H., et al. (2013). European surveillance for West nile virus in mosquito populations. *Int. J. Environ. Res. Public. Health* 10, 4869–4895. doi: 10.3390/ijerph10104869

Guégan, M., Zouache, K., Démichel, C., Minard, G., Tran van, V., Potier, P., et al. (2018). The mosquito holobiont: fresh insight into mosquito-microbiota interactions. *Microbiome* 6:49. doi: 10.1186/s40168-018-0435-2

Hammer, T. J., Dickerson, J. C., and Fierer, N. (2015). Evidence-based recommendations on storing and handling specimens for analyses of insect microbiota. *PeerJ* 3:e1190. doi: 10.7717/peerj.1190

Hegde, S., Khanipov, K., Albayrak, L., Golovko, G., Pimenova, M., Saldaña, M. A., et al. (2018). Microbiome interaction networks and community structure from laboratory-reared and field-collected *Aedes aegypti, Aedes albopictus,* and *Culex quinquefasciatus* mosquito vectors. *Front. Microbiol.* 9:2160. doi: 10.3389/fmicb.2018.02160

Johnson, N., Fernández de Marco, M., Giovannini, A., Ippoliti, C., Danzetta, M. L., Svartz, G., et al. (2018). Emerging mosquito-borne threats and the response from European and eastern Mediterranean countries. *Int. J. Environ. Res. Public. Health* 15:2775. doi: 10.3390/ijerph15122775

Kampen, H., Medlock, J. M., Vaux, A. G., Koenraadt, C. J., van Vliet, A. J., Bartumeus, F., et al. (2015). Approaches to passive mosquito surveillance in the EU. *Parasit. Vectors* 8:9. doi: 10.1186/s13071-014-0604-5

Knight, R., Vrbanac, A., Taylor, B. C., Aksenov, A., Callewaert, C., Debelius, J., et al. (2018). Best practices for analysing microbiomes. *Nat. Rev. Microbiol.* 16, 410–422. doi: 10.1038/s41579-018-0029-9

McMurdie, P., and Paulson, J. (2019). *Biomformat: An Interface Package for the Biom File Format*. Available online at: http://biom-format.org/.

Menke, S., Gillingham, M. A. F., Wilhelm, K., and Sommer, S. (2017). Home-made cost effective preservation buffer is a better alternative to commercial preservation methods for microbiome research. *Front. Microbiol.* 8:102. doi: 10.3389/fmicb.2017.00102

Minard, G., Mavingui, P., and Moro, C. V. (2013). Diversity and function of bacterial microbiota in the mosquito holobiont. *Parasit. Vectors* 6:146. doi: 10.1186/1756-3305-6-146

Montero-Mendieta, S., Grabherr, M., Lantz, H., la Riva, I. D., Leonard, J. A., Webster, M. T., et al. (2017). A practical guide to build *de-novo* assemblies for single tissues of non-model organisms: the example of a neotropical frog. *PeerJ.* 5:e3702. doi: 10.7717/peerj.3702

Muturi, E. J., Dunlap, C., Ramirez, J. L., Rooney, A. P., and Kim, C.-H. (2019). Host blood-meal source has a strong impact on gut microbiota of *Aedes aegypti*. *FEMS Microbiol. Ecol.* 95, 1–9. doi: 10.1093/femsec/fiy213

Muturi, E. J., Ramirez, J. L., Rooney, A. P., and Kim, C.-H. (2017). Comparative analysis of gut microbiota of mosquito communities in central Illinois. *PLoS Negl. Trop. Dis.* 11:e0005377. doi: 10.1371/journal.pntd.0005377

Niang, E. H. A., Bassene, H., Fenollar, F., and Mediannikov, O. (2018). Biological control of mosquito-borne diseases: the potential of *Wolbachia*-based interventions in an IVM framework. *J. Trop. Med.* 2018:1470459. doi: 10.1155/2018/1470459

Nováková, E., Woodhams, D. C., Rodríguez-Ruano, S. M., Brucker, R. M., Leff, J. W., Maharaj, A., et al. (2017). Mosquito microbiome dynamics, a background for prevalence and seasonality of West Nile Virus. *Front. Microbiol.* 8:526. doi: 10.3389/fmicb.2017.00526

Oksanen, J., Blanchet, F. G., Kindt, R., Legendre, P., Minchin, P. R., O'Hara, R. B., et al. (2013). *Vegan: Community Ecology Package.* The Comprehensive R Archive Network (CRAN). Available online at: http://CRAN.R-project.org/package=vegan (accessed June 27, 2014).

O'Neill, S. L. (2018). "The use of *Wolbachia* by the world mosquito Program to interrupt transmission of *Aedes aegypti* transmitted viruses," in *Dengue and Zika: Control and Antiviral Treatment Strategies*, eds R. Hilgenfeld and S. G. Vasudevan (Singapore: Springer Singapore), 355–360. doi: 10.1007/978-981-10-8727-1_24

Palmer, W. H., Varghese, F. S., and van Rij, R. P. (2018). Natural variation in resistance to virus infection in dipteran insects. *Viruses* 10:118. doi: 10.3390/v10030118

Pruesse, E., Quast, C., Knittel, K., Fuchs, B. M., Ludwig, W., Peplies, J., et al. (2007). SILVA: a comprehensive online resource for quality checked and aligned ribosomal RNA sequence data compatible with ARB. *Nucleic Acids Res.* 35, 7188–7196. doi: 10.1093/nar/gkm864

R Development Core Team (2014). *R: A Language and Environment for Statistical Computing*. R Foundation for Statistical Computing Vienna, Austria. Available online at: http://www.R-project.org/ (accessed June 27, 2014).

Rodríguez-Ruano, S. M., Škochová, V., Rego, R. O. M., Schmidt, J. O., Roachell, W., Hypša, V., et al. (2018). Microbiomes of North American Triatominae: the grounds for Chagas disease epidemiology. *Front. Microbiol.* 9:1167. doi: 10.3389/fmicb.2018.01167

Saldaña, M. A., Hegde, S., and Hughes, G. L. (2017). Microbial control of arthropod-borne disease. *Mem. Inst. Oswaldo Cruz.* 112, 81–93. doi: 10.1590/0074-02760160373

Segata, N., Baldini, F., Pompon, J., Garrett, W. S., Truong, D. T., Dabiré, R. K., et al. (2016). The reproductive tracts of two malaria vectors are populated by a core microbiome and by gender- and swarm-enriched microbial biomarkers. *Sci. Rep.* 6:24207. doi: 10.1038/srep24207

Tsilimigras, M. C. B., and Fodor, A. A. (2016). Compositional data analysis of the microbiome: fundamentals, tools, and challenges. *Ann. Epidemiol.* 26, 330–335. doi: 10.1016/j.annepidem.2016.03.002

Weiss, S., Xu, Z. Z., Peddada, S., Amir, A., Bittinger, K., Gonzalez, A., et al. (2017). Normalization and microbial differential abundance strategies depend upon data characteristics. *Microbiome* 5:27. doi: 10.1186/s40168-017-0237-y

Whitaker, M. R. L., Salzman, S., Sanders, J., Kaltenpoth, M., and Pierce, N. E. (2016). Microbial communities of *Lycaenid butterflies* do not correlate with larval diet. *Front. Microbiol.* 7:1920. doi: 10.3389/fmicb.2016.01920

Wickham, H. (2009). *Ggplot2: Elegant Graphics for Data Analysis*. New York, NY: Springer-Verlag.

Wong, A. C.-N., Chaston, J. M., and Douglas, A. E. (2013). The inconstant gut microbiota of *Drosophila* species revealed by 16S rRNA gene analysis. *ISME J.* 7, 1922–1932. doi: 10.1038/ismej.2013.86

Conflict of Interest: The authors declare that the research was conducted in the absence of any commercial or financial relationships that could be construed as a potential conflict of interest.

frontiers in Cellular and Infection Microbiology

REVIEW
published: 08 April 2020
doi: 10.3389/fcimb.2020.00142

Sharing the Ride: *Ixodes scapularis* Symbionts and Their Interactions

Philip E. Stewart and Marshall E. Bloom*

Biology of Vector-Borne Viruses Section, Laboratory of Virology, Rocky Mountain Laboratories, National Institute of Allergy and Infectious Diseases, National Institutes of Health, Hamilton, MT, United States

The deer tick *Ixodes scapularis* transmits a variety of disease agents in the United States, spreading the bacteria that causes Lyme borreliosis, the protozoan agent of babesiosis, and viruses such as Powassan. However, a variety of other organisms have also evolved symbiotic relationships with this tick species, and it seems likely that some of these microbes have simultaneously coevolved mechanisms to impact each other and their tick host. The number of organisms identified as *I. scapularis* symbionts has increased seemingly exponentially with the advent of PCR and next generation sequencing technologies, but convincing arguments have proposed that some of these are of environmental origin, unadapted to surviving the physiological conditions of the tick or that they are artifacts of ultrasensitive detection methods. In this review, we examine the diversity of the known microbes occurring within the *I. scapularis* microbiome, the evidence for interactions between microbes, and discuss whether some organisms reported to be symbionts of *I. scapularis* are experimental artifacts.

Keywords: *Babesia*, *Ehrlichia*, *Rickettsia*, deer tick virus, *Borrelia burgdorferi*, microbiome

OPEN ACCESS

Edited by:
Alejandro Cabezas-Cruz, Institut National de la Recherche Agronomique, France

Reviewed by:
Sukanya Narasimhan, Yale University, United States
Jianmin Zhong, Humboldt State University, United States
Aleksandra Krawczyk, National Institute for Public Health and the Environment, Netherlands

****Correspondence:***
Philip E. Stewart
pestewart@niaid.nih.gov

Specialty section:
This article was submitted to Virus and Host, a section of the journal Frontiers in Cellular and Infection Microbiology

Received: *18 November 2019*
Accepted: *18 March 2020*
Published: *08 April 2020*

Citation:
Stewart PE and Bloom ME (2020) Sharing the Ride: Ixodes scapularis Symbionts and Their Interactions. Front. Cell. Infect. Microbiol. 10:142. doi: 10.3389/fcimb.2020.00142

INTRODUCTION

The interactions of microbial symbionts with each other and with their hosts can be viewed analogously to passengers sharing a ride—they may or may not interact directly with each other; they may contribute to the cost or ride at the expense of another; they might help each other, ignore each other, or be antagonistic; they may sit together or segregate to different parts of the car; and they may get out at different destinations or stay in for the long haul. Symbiotic examples of these ride-sharing characteristics have been well-documented among arthropods and their microbiota. Specific instructive examples of beneficial interactions include two bacterial endosymbionts of the glassy-winged sharpshooter (*Homalodisca coagulata*) each of which synthesizes different essential metabolites for the host and possibly for each other (Wu et al., 2006) and a gut commensal bacterium of the *Aedes aegypti* mosquito that facilitates arboviral infection by altering the gut epithelial layer (Wu et al., 2019). An example of an antagonistic interaction in arthropods includes the inhibition of *Plasmodium falciparum* development within the midgut of *Anopheles gambiae* mosquitos resulting from generation of reactive oxygen species by an endogenous *Enterobacter* strain (Cirimotich et al., 2011).

While there has been intensive study of some arthropods' microbiota, these have typically focused on mosquitos (because of their role in pathogen transmission) or on agricultural pests, such as aphids. However, similar studies on tick microbiomes have only recently accelerated and still lag behind that of insects. *Ixodes scapularis*, commonly known as the black-legged or deer tick, is a major vector of human disease agents in the United States. In New York state, 22% of surveyed *I. scapularis* carried more than one human pathogen (Sanchez-Vicente et al., 2019). In some regions of North America, these polymicrobial infections occur at a higher prevalence than

previously thought and may complicate both proper diagnoses and treatments. Identifying the full range of microorganisms that inhabit this tick species has practical implications for medical and veterinary health by helping to improve diagnosis, treatment and recovery. Characterizing the biological interactions between symbionts and the host tick may illuminate new strategies to prevent tick-borne diseases by inhibiting pathogen colonization of *I. scapularis* or for engineering paratransgenic organisms antagonistic to pathogens. Studies suggest that some microbes may be excluded from *I. scapularis* by the presence of others (Steiner et al., 2008; Narasimhan et al., 2014; Ross et al., 2018) and acquisition of a paratransgenic bacterium has been demonstrated for the hard tick *Hyalomma dromedarii* (Koosha et al., 2019).

A diversity of microbes is known to inhabit *I. scapularis*, either as a vehicle for transport or for permanent residence. This microbiome includes extracellular and intracellular bacteria, viruses, and eukaryotes. Bacteria infecting *I. scapularis* include the human pathogens *Borrelia burgdorferi* (agent of Lyme borreliosis) (Burgdorfer et al., 1982), *B. miyamotoi* (relapsing fever) (Scoles et al., 2001), and *Anaplasma phagocytophilum* (anaplasmosis) (Telford et al., 1996), while non-pathogenic, intracellular bacteria such as *Rickettsia buchneri* also inhabit this tick (Kurtti et al., 2015). The Deer tick virus (Powassan virus lineage II), a human viral pathogen, is also vectored by *I. scapularis* (Telford et al., 1997), as are viruses predicted to be symbionts (Tokarz et al., 2018). Eukaryotes identified within this tick species include protozoans, nematodes, and fungi. Here, we define "symbionts" as those organisms (mutualistic, commensal, parasitic, etc…) that require *I. scapularis* for their survival in nature. Similarly, we follow the definition of "microbiome" as set forth by Whipps et al. in 1988: "This may be defined as a characteristic microbial community occupying a reasonably well-defined habitat which has distinct physio-chemical properties. The term thus not only refers to the microorganisms involved but also encompasses their theater of activity" (Whipps et al., 1988). Therefore, we propose the microbiome of *I. scapularis* to be composed of both symbionts and free-living, environmentally acquired microbes that likely do not survive transstadially but persist while the bloodmeal nutrients are accessible. These relatively transient passengers may not be dependent on the tick for their survival in nature but may impact the tick or its symbionts and therefore may be viewed as potentially influential components of the microbiome. Some microbes are important human pathogens, but in this review we are focused on all the microbes and their relationships with the tick, though we do highlight human health impacts where relevant.

Less clear than the diversity of organisms, is the extent, if any, to which some of these microbes may interact with each other, either directly or indirectly. The published studies in this area are largely limited to predicted interactions based on co-occurrences of two or more organisms in the same tick (Cross et al., 2018; Ross et al., 2018). This review will focus on both the composition of the *I. scapularis* microbiome and the potential microbial interactions occurring within this tick species. Many of the organisms detected in microbiome studies are free-living environmental bacteria, and we discuss the reasons why some of these may artificially inflate the microbial diversity estimates. A further emphasis of this review is placed on interactions associated with *B. burgdorferi*, as this bacterium is perhaps the most studied symbiont of *I. scapularis* and an agent of Lyme borreliosis in the U.S. First, though, descriptions of the life cycle and the physiological environment that the internal anatomy of *I. scapularis* presents to its microbial inhabitants are both critical to understanding the composition of the microbiome and the interactions that may occur between its constituents.

I. scapularis LIFE CYCLE AND PHYSIOLOGY

After hatching from the egg, *I. scapularis* undergoes three developmental stages: larval, nymphal, and adult (**Figure 1**, left panel), with an average life span of ∼2 years. A bloodmeal is required at each developmental stage to progress through the life cycle. The white-footed mouse, *Peromyscus leucopus*, is a primary host species for both the larvae and nymphs, while white-tailed deer (*Odocoileus virginianus*) are the maintenance host for adults (Piesman and Spielman, 1979; Piesman et al., 1979; Carey et al., 1980). However, *I. scapularis* feeds upon a variety of vertebrates including birds, lizards, and mammals. Once feeding is complete, the tick detaches and returns to the environment to digest the bloodmeal and molt to the next life stage. The molting process allows the tick to increase in size and produces acute physiological changes in the tick that must be tolerated by any symbionts. *I. scapularis* sexually develops during the nymphal molt, and the female requires a bloodmeal for fecundity although males do not need to feed. After mating the female deposits her egg mass (consisting of thousands of eggs) and dies, while the male may mate repeatedly.

Although blood feeding (hematophagy) is a characteristic of many arthropod species, ticks evolved a unique feeding style that merits description and has a significant impact on those microbiota that seek to infect the tick via ingestion of the blood into the midgut (**Figure 1**, middle) or that require the nutrients and signals from the blood. Lacking mandibles to bite with, *I. scapularis* instead use their saw-like chelicerae (**Figure 1**, right panel) to tear through the host skin and sever blood vessels, allowing the blood to pool into the bite site. While imbibing blood, the tick is also discharging saliva into the lesion, which has a profound effect on the host at the bite site as salivary components include immunomodulatory proteins and compounds that inhibit coagulation, pain and inflammation and may aid in the transmission of microbes from the tick to the host. The feeding process can last from several days to over a week, depending on the life stage, and this extended timeframe provides ample opportunity for microbes to be acquired by *I. scapularis*. Within the midgut lumen, the erythrocytes are lysed, but the remaining components are absorbed and digested intracellularly over an extended time period.

This mode of digestion makes the midgut lumen a relatively hospitable environment for microbes due to a neutral pH and the absence of digestive enzymes (Hajdusek et al., 2013), although hemoglobin moieties released during digestion of the bloodmeal have antimicrobial activity (Sonenshine et al., 2005). The brevity

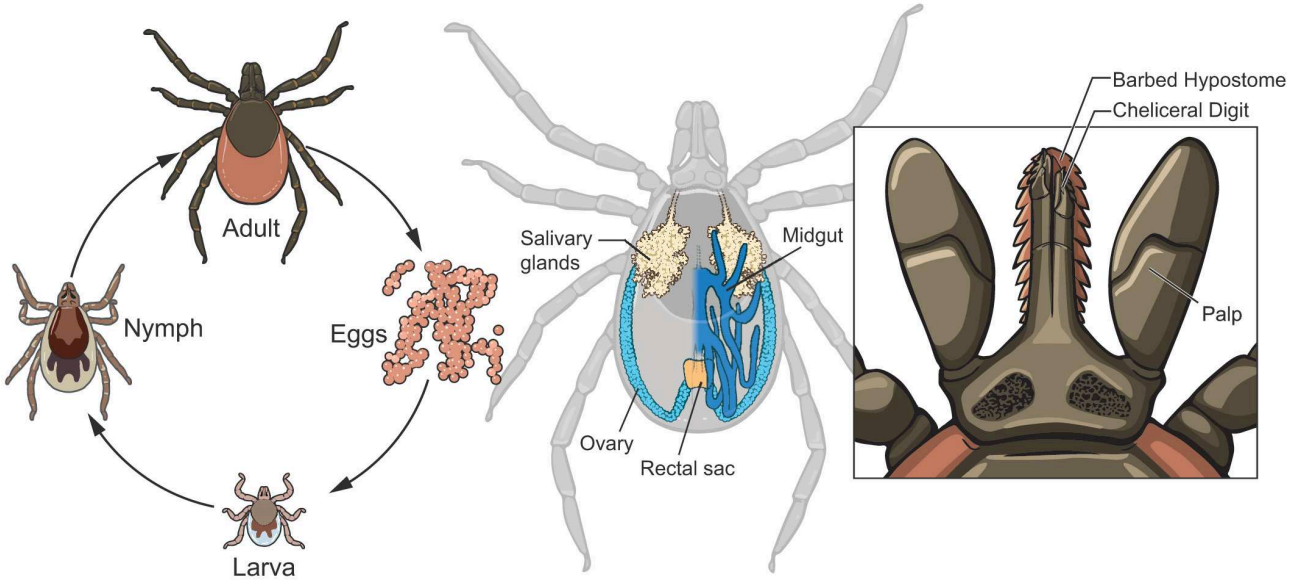

FIGURE 1 | Life cycle and anatomical features of *Ixodes scapularis*. After hatching from eggs, *I. scapularis* progresses through 3 developmental stages: larval, nymphal and adult (left panel). Note the morphological differences that occur during each molt (see text for additional details): size successively increases and the larval-nymphal molt produces an additional pair of legs while sexual development occurs during the nymphal-adult molt. The midgut (dark blue with only the right half depicted, middle panel) is the site of digestion of the bloodmeal and is a significant entry route for microbes. The salivary glands (beige) are the exit ramps for transmission of infectious microbes to vertebrate hosts. Ovaries (light blue) are also organs of transmission for those symbionts transmitted to the progeny. The anatomy of the tick mouthparts (right panel) facilitates the feeding of *I. scapularis*, with the saw-like chelicerae cutting through host tissues and vessels to gain access to the blood.

of tick feeding compared to its life span, and therefore infrequent access to nutrients, presents a limitation that organisms must overcome to establish a stable symbiotic relationship with *I. scapularis.* The peritrophic membrane is another limitation. Many arthropod species form a peritrophic membrane to separate the ingested blood from the epithelial cells of the midgut. This membrane may function to protect midgut cells from abrasive food particles and to limit dissemination of parasitic organisms that enter during feeding, preventing or reducing the number of microbes that escape to infect distal organs of the tick. Observed in all life stages of both *I. scapularis* and *Ixodes ricinus* (European species), initial formation of the peritrophic membrane is detected within 24 h after the onset of feeding (Rudzinska et al., 1982; Zhu et al., 1991; Sojka et al., 2007; Yang et al., 2014). Presumably, those microbes that seek to disperse throughout the tick body must do so either before the peritrophic membrane has fully solidified or after it breaks down. *Babesia microti*, the agent of human babesiosis and a symbiont of *I. scapularis*, is the only organism with the demonstrated capability to traverse the fully formed barrier (Rudzinska et al., 1982). Using a highly specialized organelle, termed the arrowhead, *B. microti* appears to cleave through the membrane and penetrate the epithelial lining of the midgut. Recent studies suggest that both *B. burgdorferi* and *A. phagocytophilum* may also penetrate the peritrophic membrane by unknown mechanisms (Abraham et al., 2017; Narasimhan et al., 2017).

Microbes that have evolved to establish residency within the tick must be tolerated by the host's innate immune defenses or have a mechanism to avoid or cope with it. The immune system of *I. scapularis* includes hemocyte cells (some of which are capable of phagocytosis), antimicrobial peptides and compounds, reactive oxygen and nitrogen species, lysozyme, peptidoglycan-recognition proteins, and small interfering RNAs (Johns et al., 2001; Schnettler et al., 2014; Bourret et al., 2016; Gulia-Nuss et al., 2016). The densities of some microorganisms are known to be controlled by factors of the immune system but still establish residency. *A. phagocytophilum*, an intracellular symbiont of *I. scapularis*, is limited by a member of the 5.3 kDa family of antimicrobial peptides expressed in the salivary glands (Liu et al., 2012). The extracellular spirochete *B. burgdorferi* can be phagocytosed by tick hemocytes (Johns et al., 2001), and is believed to be cleared by this mechanism from the hemocoel of the tick after feeding. However, *I. scapularis* hemocytes are less effective at killing *B. burgdorferi* than those of *Dermacenter variabilis* (which is not a competent vector for this bacterium), suggesting that the former tick may have evolved a level of immunotolerance to *B. burgdorferi*.

In addition to the barriers presented by the midgut and the innate immune system, feeding and molting produce substantial changes in *I. scapularis* anatomy. Passive oxygen diffusion from the surface of the tick is sufficient for the physiologic needs of the larval tick but occurs too slowly for the increased size of the nymph. Therefore, spiracles and the associated tracheal system (a branched, air-filled tubular network) develops during the larval molt and facilitates gas exchange to all tissues and organs. An additional pair of legs also develop during the larval

molt. During the nymphal molt, gender development occurs. Shedding of the old cuticle and generation of a "new" exoskeleton occurs in every molt. The salivary gland acini (responsible for secretion during feeding) are a microbial transmission route from the tick and degenerate after feeding. These secretory acini reform before *I. scapularis* feeds again. From a microbial viewpoint, disintegration of the salivary gland acini means that permanent residency for symbionts seeking transmission from the tick cannot be maintained at this site but must be established elsewhere and reinfect these acini prior to or during feeding.

The successful transmission cycle of the spirochete *B. burgdorferi* is illustrative of the adaptations required for a symbiont to overcome the difficult and changing environment of *I. scapularis*. *B. burgdorferi* may be acquired by larval *I. scapularis* when it feeds on an infected vertebrate, and the bacterium will then establish residency in the midgut. Because *B. burgdorferi* lacks cellular biosynthetic pathways (Fraser et al., 1997), the bacterium appears to be dependent on the tick or the bloodmeal components to acquire certain nutrients and metabolic intermediates for survival. Using gas chromatography coupled to mass spectrometry, Hoxmeier et al. identified reductions in levels of compounds in the tick that correlate to the presence of *B. burgdorferi*, including purine metabolites, hydrophobic and aliphatic amino acids, galactose, glycerol and maltose, and specific fatty acids (Hoxmeier et al., 2017). With the depletion of the bloodmeal and the physiological changes that occur during the molt, *B. burgdorferi* densities decline (Piesman et al., 1990). To maintain required metabolic activities when the bloodmeal is depleted, *B. burgdorferi* may switch from using glucose as a carbon source to glycerol, which is present in the hemolymph (Pappas et al., 2011). When the nymphal tick begins to feed, the spirochete populations increase and *B. burgdorferi* evades entrapment by the peritrophic membrane and escapes the midgut, migrates into the hemocoel and from there penetrates the regenerated salivary glands for transmission to the vertebrate host. After the tick has completed its feeding, those *B. burgdorferi* that remain outside the midgut are eventually destroyed, likely by the hemocyte immune cells (Johns et al., 2001). However, the spirochetes remaining in the midgut act as a seed population during the next *I. scapularis* bloodmeal and can outgrow and again infect the salivary glands for potential transmission. Like *B. burgdorferi*, other microbes have adapted to these barriers present by *I. scapularis* physiology and established a symbiotic relationship with this tick species.

MICROBIOTA OF *I. scapularis*

Although the composition and dynamics of the *I. scapularis* microbiome is still being defined, it is clearly diverse, with intra- and extra-cellular bacteria, viruses, fungi, nematodes, and protozoa having been identified by various methods (**Table 1**). We have included microbes that were detected in >1% of the ticks in each study and that have been corroborated by multiple studies or by more than one technique. However, we have excluded common environmental microbes demonstrated to be artifacts from contaminated reagents, such as *Delftia*, *Comamonas*, *Acidovorax*, and others (Salter et al., 2014). Sequence-based studies indicate a larger variety of bacterial residents may temporarily survive in this tick species (Benson et al., 2004; Narasimhan et al., 2014; Rynkiewicz et al., 2015; Van Treuren et al., 2015; Zolnik et al., 2016, 2018; Abraham et al., 2017; Cross et al., 2018; Landesman et al., 2019; Tokarz et al., 2019), but other reports suggest that many of the detectable bacteria from such studies may have been of environmental origin or introduced from contaminated reagents (Martin and Schmidtmann, 1998; Salter et al., 2014; Ross et al., 2018; Zolnik et al., 2018).

The bacterial diversity of *I. scapularis* diminishes as the tick matures to the adult stage, with females having less diversity than males (Zolnik et al., 2016; Thapa et al., 2019). While many of these microbes are either stably maintained in *I. scapularis* and others are acquired from the environment and subsequently eliminated when the nutrients are depleted, it is likely that some microbes were erroneously attributed to the microbiome. Ross et al. concluded that *I. scapularis* lacks a stable bacterial microbiome, and those that are long-term residents are mostly intracellular (Ross et al., 2018). Microbiome studies using low biomass samples that are subjected to amplification and high-throughput sequencing often overestimate microbial diversity as a result of contaminating DNA present in reagents or from human skin (Salter et al., 2014), and this may provide an alternative explanation for the detection of some of the environmental bacteria. Further, sequencing errors and limited database sequences has led to the misidentification of at least one species in a microbiome study (Tijsse-Klasen et al., 2010). Likewise, Tokarz et al. disputed the identification of *Bartonella* as a component of the *I. scapularis* microbiome, attributing the mistake to a lack of specificity in primer design (Tokarz et al., 2019). Another factor that can inflate bacterial diversity estimates is the method of tick sterilization employed prior to sequencing, where ethanol-based surface sterilization of *Amblyomma cajennense* ticks correlated with reports of higher internal bacterial diversity than studies that used bleach-based methods, likely due to cuticular contaminants that were not removed by ethanol (Binetruy et al., 2019). Finally, detection of microbial DNA does not in and of itself prove that a specific species is a component of the microbiome. Organisms may be acquired with a bloodmeal but not survive, whereas their DNA may still be detectable. Due to the variety of issues that can arise in identifying microbiome members, it seems prudent that multiple techniques should be used to verify the members of any microbiome.

Most studies concur that *Rickettsia buchneri* is the predominant prokaryotic *I. scapularis* symbiont, and its relationship to the tick is significantly different from that of *B. burgdorferi*. An obligate intracellular bacteria, it appears to be able to establish itself in a variety of tissues including the salivary glands, midgut tissues, and ovaries (Noda et al., 1997; Kurtti et al., 2015; Zolnik et al., 2016; Al-Khafaji et al., 2020). *R. buchneri* is not known to infect vertebrate hosts but is an obligate symbiont of *I. scapularis* and transmitted transovarially from the mother to the progeny. All life stages of the tick can harbor *R. buchneri*, though it can reach exclusive levels in the adult

TABLE 1 | Microbes detected in *I. scapularis*.

Organism	Identification methods*	Infection prevalence (developmental stage)**	References
Bacteria, extracellular			
Acinetobacter spp.	p	22% (L, N, A)	Narasimhan et al., 2014, 2017; Abraham et al., 2017; Thapa et al., 2019
Borrelia burgdorferi	i, d, v, p	30–72% (N, A)	Burgdorfer et al., 1982; Steiner et al., 2008; Aliota et al., 2014; Tokarz et al., 2019
Borrelia mayonii	i, v, p	0.65–2.9% (N, A)	Pritt et al., 2016; Cross et al., 2018; Johnson et al., 2018
Borrelia miyamotoi	p, d	1–5% (N, A)	Scoles et al., 2001; Tokarz et al., 2010, 2019; Cross et al., 2018; Johnson et al., 2018
Corneybacterium spp.	p	2% (L, N, A)	Narasimhan et al., 2014, 2017; Abraham et al., 2017; Thapa et al., 2019
Enterobacteriaceae	p	100% (N, A)	Van Treuren et al., 2015; Ross et al., 2018; Zolnik et al., 2018
Enteroccocus spp.	p	ND (L, N)	Narasimhan et al., 2014, 2017; Abraham et al., 2017
Rhizobium spp.	p	1% (L, N, A)	Zolnik et al., 2016; Thapa et al., 2019
Rhodococcus spp.	p	ND (N)	Rynkiewicz et al., 2015; Landesman et al., 2019
Pseudomonas spp.	p	1–100% (L, N, A)	Benson et al., 2004; Narasimhan et al., 2014, 2017; Zolnik et al., 2016, 2018; Abraham et al., 2017; Ross et al., 2018; Landesman et al., 2019; Thapa et al., 2019
Sphingomonadaceae	p	5% (L, N, A)	Benson et al., 2004; Zolnik et al., 2016, 2018; Abraham et al., 2017; Ross et al., 2018; Landesman et al., 2019; Thapa et al., 2019
Staphylococcus spp.	p	2% (L, N, A)	Narasimhan et al., 2014, 2017; Abraham et al., 2017; Zolnik et al., 2018; Thapa et al., 2019
Streptococcus spp.	p	ND (L, N)	Benson et al., 2004; Narasimhan et al., 2014
Bacteria, intracellular			
Anaplasma phagocytophilum	i, p	1.9–18% (N, A)	Adelson et al., 2004; Aliota et al., 2014; Cross et al., 2018; Tokarz et al., 2019
Bartonella spp.	p	13–90% (L, N)	Adelson et al., 2004; Rynkiewicz et al., 2015
Ehrlichia spp.	i, p	1.3–3.6% (N, A)	Aliota et al., 2014; Cross et al., 2018; Johnson et al., 2018
Rickettsia buchneri	i, v, p	46–100% (L, N, A)	Adelson et al., 2004; Narasimhan et al., 2014, 2017; Kurtti et al., 2015; Rynkiewicz et al., 2015; Zolnik et al., 2016; Cross et al., 2018; Tokarz et al., 2019
Wolbachia spp.	p	8–28% (A)	Zolnik et al., 2016; Cross et al., 2018
Viruses			
Blacklegged tick phleboviruses+	p	11–78% (A)	Tokarz et al., 2014a, 2018, 2019; Cross et al., 2018
Deer tick virus (Powassan virus lineage II)	i, p	0.4–4.7% (N, A)	Thomas et al., 1960; Telford et al., 1997; Dupuis et al., 2013; Aliota et al., 2014; Knox et al., 2017; Campagnolo et al., 2018; Johnson et al., 2018; Tokarz et al., 2019
I. scapularis-associated viruses+	p	0.5–4.5% (A)	Cross et al., 2018; Tokarz et al., 2018
Laurel Lake virus	p	ND (A)	Tokarz et al., 2018
Mononegavirus-like viruses+	p	2% (A)	Tokarz et al., 2014b; Cross et al., 2018
South Bay virus	p	20–52 (A) %	Tokarz et al., 2014b, 2018, 2019; Cross et al., 2018
Suffolk virus	p	10–17% (A)	Cross et al., 2018; Tokarz et al., 2018, 2019
Fungi			
Beauveria sp.	i	ND (N)	Ginsberg and LeBrun, 1996; Tuininga et al., 2009
Cladosporium sp.	i, p	ND (A)	Tuininga et al., 2009
Colletotrichum spp.	i, p	ND (A)	Tuininga et al., 2009
Discostroma tricellulare	i, p	ND (N)	Tuininga et al., 2009
Hypocrea koningii	i, p	ND (N)	Tuininga et al., 2009
Metarhizium sp.	i	ND (A)	Benoit et al., 2005; Tuininga et al., 2009
Myrothecium verrucaria	i, p	ND (N)	Tuininga et al., 2009
Paecilomyces spp.	i, p	ND (A)	Tuininga et al., 2009
Penicillium spp.	i	ND (A)	Tuininga et al., 2009; Greengarten et al., 2011
Pestalotiopsis caudata	i	ND (N)	Tuininga et al., 2009
Phoma sp.	i, p	ND (N)	Tuininga et al., 2009
Verticillium fungicola	i, p	ND (N)	Tuininga et al., 2009
Verticillium lecanii	i	4% (A)	Ginsberg and LeBrun, 1996; Zhioua et al., 1999
Nematodes			
Acanthocheilonema spp.	d, p	22–30% (N, A)	Namrata et al., 2014; Tokarz et al., 2019
Onchocercidae sp.	p	18% (A)	Cross et al., 2018
Unidentified microfilari	i, v	0.4% (A)	Beaver and Burgdorfer, 1984

(Continued)

TABLE 1 | Continued

Organism	Identification Methods*	Infection Prevalence (developmental stage)**	References
Protozoans			
Babesia microti	p	3–20% (N, A)	Steiner et al., 2008; Tokarz et al., 2010, 2019; Aliota et al., 2014; Cross et al., 2018
Babesia odocoilei	p	1–15% (A)	Steiner et al., 2008; Hamer et al., 2014; Tokarz et al., 2019

*i, isolation from I. scapularis; v, microscopic visualization; d, FISH, IFA or other method of indirect detection; p, PCR and sequence-based methods.

**Infection prevalence of individual ticks varied widely depending on the developmental stage of the tick (L = larva, N = nymph, A = adult) and the geographic location from which samples were collected. Confounding these factors was the method of calculating infection rates, some studies examined individual ticks while others pooled ticks and estimated individual infection rates.

+Multiple viruses present within this grouping.

ND, not determined.

female (Zolnik et al., 2016; Thapa et al., 2019). Its abundance in *I. scapularis* may relate to the ability of this prokaryote to provide folate (vitamin B9) to the tick, as animals are unable to synthesize this essential vitamin (Hunter et al., 2015). However, this does not appear to be an obligatory symbiotic relationship as *I. scapularis* ticks devoid of *R. buchneri* have been reported (Steiner et al., 2008; Tokarz et al., 2019).

A few human pathogenic bacteria are also well-documented symbionts of *I. scapularis* but with a wide variation in infection rates. *B. burgdorferi*, for example, is present in 30–64% of the ticks examined in areas endemic for Lyme borreliosis, while *Ehrlichia* species occurs in 1–3% of the ticks in the same geographic region (**Table 1**). Because of the potential overestimates of bacteria in the tick midgut due to the technical issues previously described (contaminated reagents and/or inefficient removal of DNA from the tick cuticle), further studies demonstrating interactions between *I. scapularis* and putative symbionts are required. Free-living, environmentally acquired bacteria may flourish within the fed midgut while nutrients from the bloodmeal are available. Although they may not persist transstadially, they may still impact the existing microbiota by competing for nutrients, altering the midgut environment (e.g., changing the pH), stimulating tick immune defenses, or by secreting toxic compounds (such as proteases or oxidative radicals).

Some bacterial symbionts may directly affect the fitness or behavior of their tick host. *A. phagocytophilum* was reported to induce an antifreeze glycoprotein of *I. scapularis*, thereby increasing the tick's cold tolerance (Neelakanta et al., 2010). Adult ticks infected with *B. burgdorferi* were less active and quested at lower heights compared to uninfected ticks, while infected nymphs had an increased phototaxis response and were more attracted to vertical surfaces than control nymphs (Lefcort and Durden, 1996). The effect on tick fitness of these altered behaviors remain unclear. As mentioned previously, *R. buchneri* may synthesize the essential vitamin B9, providing the tick with an essential nutrient that is scarce in the bloodmeal (Hunter et al., 2015). Although intriguing, such studies need further elaboration and are not likely to be the only interactions between the microbes and their tick host.

Although viruses associated with arthropods are common and collectively referred to as arboviruses (arthropod-borne viruses), few have been isolated and characterized from *I. scapularis*. Several PCR- and sequence-based studies have identified the *Bunyaviridae* South Bay virus and the Black-legged tick phlebovirus as putative symbionts of *I. scapularis* (Tokarz et al., 2014b, 2018; Sakamoto et al., 2016; Cross et al., 2018). Further research is needed to confirm the specific roles of these viruses in *I. scapularis*, but Tokarz and coworkers indicate a 3-fold greater viral diversity in *I. scapularis* relative to *Amblyomma americanum* (Tokarz et al., 2018). Deer tick virus (DTV), also known as Powassan virus lineage II, is a human pathogen and is the most well-characterized virus of *I. scapularis*. DTV, a flavivirus, was reported and named by Telford et al. in 1997 (Telford et al., 1997), but had previously been described in 1960 (Thomas et al., 1960). DTV is thought to display an interesting mechanism of tick acquisition in addition to being directly acquired from a viremic host. As demonstrated for other arboviruses, DTV may be acquired by cofeeding between uninfected and infected ticks (Jones et al., 1987; Labuda et al., 1993a,b). This, non-viremic mechanism occurs when multiple ticks are simultaneously feeding in proximity to each other, allowing the infected ticks to transmit the virus into the same blood pool that naïve ticks are also feeding from. Because DTV can be delivered into the host by an infected tick as early as 15 min after attachment (Ebel and Kramer, 2004), and the feeding period of *I. scapularis* takes days to over a week, the virus can amplify within the feeding lesion during this timeframe and be acquired by cofeeding naïve ticks. Transovarial transmission of DTV occurs at a relatively low rate (Costero and Grayson, 1996), but transstadial transmission (maintenance of the virus through the molt) is relatively inefficient, with only 20% of the newly molted ticks retaining the infection (Ebel and Kramer, 2004), indicating that DTV requires a vertebrate reservoir to be maintained.

Fungi and nematodes have been isolated from *I. scapularis* and these interactions are of some interest as entomopathogenic agents (Zhioua et al., 1995, 1997; Hill, 1998; Greengarten et al., 2011). Since the majority of the *I. scapularis* life cycle is spent on the ground in the same environment as many fungi and nematodes, it is not surprising that a variety of these species infect this tick. The invasive fungi produce proteases and chitinases that allow the hyphae to penetrate the exoskeleton and colonize the internal anatomy of the tick while nematodes may infect through the genital or anal openings. Some nematodes, though,

are thought to be acquired by *I. scapularis* through the bloodmeal from infected animals (Namrata et al., 2014). Because nematodes and fungi may have their own microbiome, it is possible that some of the bacteria and viruses detected in the *I. scapularis* microbiome high-throughput sequencing studies might have originated from these parasites (Cross et al., 2018; Tokarz et al., 2019).

As shown in **Table 1**, the microbes that have adapted to infect *I. scapularis* are diverse and little is known about their ability to interact with each other. The bacterial symbionts and endosymbionts of *I. scapularis* (*Borrelia*, *Ehrlichia*, *Anaplasma*, and *Rickettsia*) lack most of the genes for mediating interbacterial interactions (Ross et al., 2018), suggesting they have evolved in an environment where these interfaces are unnecessary. However, potential microbe-microbe interactions may be indirect, where one organism modifies its environment (i.e., tick tissues) to the benefit or to the detriment of others.

I. scapularis can harbor multiple pathogens simultaneously (**Table 2**), raising the possibility of humans acquiring multiple microbial infections from a single tick bite. In a large serosurvey cohort study, patients with concurrent babesiosis and Lyme borreliosis had a greater number of symptoms and a longer duration of illness than patients with either infection alone (Kraiczy et al., 2001). For matters of human health, more research is needed to elucidate key aspects of polymicrobial infections and symbiont interactions within the tick.

EVIDENCE FOR MICROBIAL INTERACTIONS

No direct mechanistic interactions have been experimentally defined among the microbiota of *I. scapularis*, but several studies have detected correlations between various organisms. The likelihood of *I. scapularis* being coinfected with both *B. microti* and *B. burgdorferi* was found to be higher than expected based on single infection rates (Dunn et al., 2014; Hersh et al., 2014; Edwards et al., 2019). This co-occurrence rate may potentially be explained by the existence of a host competent for both microbes, allowing acquisition of *B. microti* and *B. burgdorferi* in a single bloodmeal. In contrast, an interference effect was observed in ticks acquiring *A. phagocytophilum* and *B. burgdorferi* from infected *P. leucopus* (Levin and Fish, 2001). In these experiments, the primary agent inoculated into mice lowered tick acquisition rates of the second agent. However, in field-collected ticks from midwestern states, Hamer et al. found a higher than expected co-infection prevalence with *B. burgdorferi* and *A. phagocytophilum* (Hamer et al., 2014). This apparent discrepancy may relate to the former study examining the rate of both organisms being acquired simultaneously from an infected mammal while the latter report surveyed field-collected adults, which may have acquired the microbes in separate bloodmeals. Ross et al. reported that ticks highly colonized by species of the environmental bacteria *Bacillus*, *Pseudomonas*, and members of the Enterobacteriaceae had a lower frequency of infection with *B. burgdorferi* (Ross et al., 2018). In a multi-state study, Steiner and colleagues found that co-infections with *B. burgdorferi* and the endosymbiont *R. buchneri* were lower than predicted for male ticks based on individual infection prevalences (Steiner et al., 2008). Cross et al. collected individual ticks from Wisconsin and identified positive correlations (i.e., the presence of one microbe might predispose *I. scapularis* to infection by the other) between the presence of South Bay virus RNA levels and *B. burgdorferi*, South Bay virus and Blacklegged tick phlebovirus-1, and the *Onchocercidae* filarial worm and *Wolbachia* spp. (Cross et al., 2018). The correlation between *Wolbachia* and the filarial worm, though, may have been due to this bacterium being a natural component of the worm's fauna, and not as part of the tick microbiota (Cross et al., 2018; Tokarz et al., 2019). Analogously, *Wolbachia pipientis*, previously thought to be an endosymbiont of *I. ricinus*, actually derives from the endoparasitoid wasp *Ixodiphagus hookeri* which lays its eggs in the tick (Plantard et al., 2012). Cross et al. also detected a negative co-occurrence

TABLE 2 | Coinfection of *I. scapularis* with human pathogens*.

Pathogens	% of ticks coinfected	References
Dual infections		
B. burgdorferi – A. phagocytophilum	1–26	Schwartz et al., 1997; Steiner et al., 2008; Tokarz et al., 2010, 2017, 2019; Aliota et al., 2014; Johnson et al., 2018; Sanchez-Vicente et al., 2019
B. burgdorferi – Babesia microti	1–22	Adelson et al., 2004; Steiner et al., 2008; Tokarz et al., 2010, 2017, 2019; Aliota et al., 2014; Johnson et al., 2018; Sanchez-Vicente et al., 2019
B. burgdorferi – Bartonella spp.	8	Adelson et al., 2004
B. burgdorferi – B. miyamotoi	1–3.5	Tokarz et al., 2017, 2019; Sanchez-Vicente et al., 2019
B. burgdorferi – DTV	0.4–2.5	Aliota et al., 2014; Tokarz et al., 2017, 2019
A. phagocytophilum – B. microti	1–2	Steiner et al., 2008; Tokarz et al., 2017
Triple infections		
B. burgdorferi – A. phagocytophilum – B. microti	1–8	Tokarz et al., 2010, 2017, 2019; Aliota et al., 2014; Sanchez-Vicente et al., 2019
B. burgdorferi – B. microti – B. miyamotoi	1–2	Tokarz et al., 2017

**Only infections ≥ 1% are shown.*

between Blacklegged tick phlebovirus-1 and−2, perhaps due to superinfection exclusion between closely related viruses (Cross et al., 2018). Tokarz et al. identified two positive correlations in ticks collected from New York and Connecticut: between *B. microti* and Blacklegged tick virus 1, and between Blacklegged tick phlebovirus and *B. burgdorferi* (Tokarz et al., 2019).

Experimental studies with *I. scapularis* produced interesting observations on the tick microbiome. Rearing *I. scapularis* in a sterile environment altered the tick microbiome compared to those reared in non-sterile conditions. These ticks with a perturbed microbiota were less efficiently colonized by *B. burgdorferi*, suggesting that the normal microbiome facilitates *B. burgdorferi* infection by an unknown mechanism (Narasimhan et al., 2014). Abraham et al. reported that *A. phagocytophilum* infection both weakens the peritrophic membrane of *I. scapularis* and inhibits bacterial biofilm formation, consequently altering the microbiome, but enhancing colonization of the tick by *A. phagocytophilum* (Abraham et al., 2017).

All of these lines of evidence suggest a rich interaction network among *I. scapularis* symbionts. In contrast to a wide variety of experimentally confirmed interfaces between microbes in insects, such interactions have not been demonstrated among the microbiota of *I. scapularis*. Partly this is due to the emphasis placed on vectors that have a greater impact on human health, such as mosquitos, and on agriculturally important pests. Additionally, development of biological tools has lagged behind those available in some insects, largely due to the relatively prolonged life span of ticks and their extended feeding period. Recent technical achievements, though, are producing rapid advances in our basic knowledge of tick physiology and its microbiome.

NEW DIMENSIONS FOR THE STUDY OF TICK BIOLOGY

Four recent developments provide the groundworks for rapidly advancing our understanding of *I. scapularis* biology and microbial interactions. These are: (1) application of RNA interference (RNAi) gene silencing methods for functional analysis of tick proteins; (2) the release of the annotated *I. scapularis* genome (Gulia-Nuss et al., 2016); (3) a contained, artificial feeding system for nymphal and adult *I. scapularis* (Oliver et al., 2016); and (4) *ex vivo* organ culture of midgut and salivary glands (Grabowski et al., 2017, 2019).

RNAi temporarily down-regulates gene expression through an incompletely understood pathway. Essentially, introduction of a double-stranded RNA template homologous to a target sequence will complex with endogenous proteins (including RNAseIII) that lead to degradation of the target RNA. As efficient targeted gene deletion techniques are not currently feasible in *I. scapularis*, RNAi gene silencing allows analysis of gene-product function in tick physiology and in microbial interactions. However, RNAi has limitations that need to be considered as the target transcript is only temporarily reduced and the existence of redundant proteins can mask the phenotype.

In conjunction with RNAi, the release of the annotated *I. scapularis* genome provides the sequence information necessary to design double-stranded RNA molecules for gene silencing experiments. The genome data also provide the complete sequence (introns/exons) of genes involved in pathogen acquisition, persistence and transmission by the tick, and allows identification of differentially regulated proteins in response to microbial infection using quantitative proteomic approaches (Gulia-Nuss et al., 2016). This assembly, although encompassing 1.8 Gb of sequence, does not close the 2.1 Gb genome, leaving about 14% of the genome yet to be completed.

Moving from the molecular to the organismal level, the development of an artificial feeding system opens up new avenues of research in tick biology. The lengthy feeding period of *I. scapularis* was problematic in obtaining fully engorged ticks from artificial feeding systems, as opposed to the long-standing success achieved with fast-feeding arthropods such as soft ticks, sandflies, fleas, and mosquitos (Hindle and Merriman, 1912; Adler and Theodor, 1927; Woke, 1937; Cerwonka and Castillo, 1958). Recently, a silicone-based membrane feeding system has been successfully adapted for *I. scapularis* to feed to repletion (Krober and Guerin, 2007; Oliver et al., 2016). After engorgement, nymphal ticks molted to adults and females mated and laid viable egg masses. Such membrane feeding systems have been useful for introducing specific pathogens into *I. scapularis* and to test different acaricides effectiveness on *I. ricinus* (Krober and Guerin, 2007; Oliver et al., 2016). Several recent studies have used these systems to elucidate the contribution of *B. burgdorferi* proteins in acquisition and transmission of mutant strains and to assess nutritional requirements for tick reproduction (Perner et al., 2016; Bernard et al., 2018; Hart et al., 2018; Koci et al., 2018). Larval ticks, though, did not successfully feed with this technique, likely due to the inability of the smaller mouthparts of larvae to penetrate through the thickness of the silicone membrane (Oliver et al., 2016). However, larvae can be infected with bacteria and viruses using the immersion technique first described by Policastro and Schwan (2003) (Mitzel et al., 2007; Policastro et al., 2011). The ability to acquire arboviruses has not been tested with this system, indicating a potential limitation in symbiont studies. Overall, the advantages of the artificial feeding system outweighs its disadvantages and opens new avenues to explore, including quantitation of pathogen transmission during feeding and effects on tick development of reducing the bacterial microbiota (dysbiosis) by addition of antibiotics in the bloodmeal. Symbionts can be reintroduced sequentially to dysbiosed ticks to study the individual contributions of each to the physiology of *I. scapularis* and to assess potential microbial interactions.

Symbiont—tick interactions can also be studied in specific tissues using the recently described *ex vivo* organ culture system described by Grabowski et al. (2017, 2019). Dissected midgut, salivary glands, and synganglion were maintained in a metabolically active state for 9–10 days. Powassan virus and Langat virus were able to infect and replicate in these artificially maintained organ cultures, indicating that this system can be used to study microbial infection and persistence in isolated tissues. These studies also demonstrated that RNAi could be used effectively in *ex vivo* organs to perturb virus replication. Although useful for the study of endosymbionts, it is not apparent how the

ex vivo system might mimic the interactions between tick organs and extracellular bacteria with the influence of culture medium.

A MODEL SYSTEM FOR STUDYING MICROBIAL INTERACTIONS WITHIN *I. scapularis*

Together, these resources open new avenues of investigation that were previously daunting to study. For example, DTV is designated as a BSL3-level agent in the U.S. and therefore feeding cohorts of infected ticks on animals becomes cumbersome and requires additional levels of containment. However, artificial membrane feeding chambers have been developed for safely containing and feeding infected ticks to repletion (Krober and Guerin, 2007; Oliver et al., 2016). DTV is the only native virus of *I. scapularis* that has been extensively studied *in vitro* and for which laboratory mouse and tick infectious models exist, making it an attractive candidate to study as a viral symbiont. *B. burgdorferi* represents an excellent model bacterium because it can be cultured *in vitro*, efficient molecular genetic tools exist to construct mutations, it is also efficiently transmitted in a laboratory mouse-tick infectious cycle, and it is a significant agent of disease in the United States. Although other bacteria listed in **Table 1** would also be suitable, none possess all of the characteristics described above for *B. burgdorferi*.

Little evidence exists as to whether these two microbes interact within the tick. Because of the low rate of DTV circulating within wild *I. scapularis* populations, tick capture studies have not produced significant numbers of single or coinfections to compare prevalences. The question of whether *B. burgdorferi* impacts the ability of DTV or other microbial species to infect the same tick remains open. Attempts to address this question by examining European coinfection data is confounded by multiple factors: (1) different tick species transmit these microbial infections: *I. ricinus* in Europe and western Asia and *I. persulcatus* in Asia; (2) POWV is restricted to specific geographic regions in eastern Russia, whereas tick-borne encephalitis virus is more widely disseminated throughout Eurasia but is a distinct and separate flavivirus that has evolved in different tick species; and (3) multiple *Borrelia* species cause Lyme borreliosis in Eurasia. Therefore, *B. burgdorferi*—DTV—*I. scapularis* present a tantalizing combination for laboratory coinfection studies that permit characterization of symbiont interactions with each other and with the tick.

PERSPECTIVE AND CONCLUSIONS

Ticks transmit the largest variety of pathogens of any arthropod vector, many of which are significant causes of medical and veterinary disease. In human health, dual infections transmitted by ticks may not only complicate accurate diagnosis and proper treatment but may potentially alter the symptoms (Krause et al., 1996; Djokic et al., 2019). The lack of licensed human vaccines in the U.S. for any tick-borne illness makes the study of *I. scapularis* and its microbiome imperative from a One Health perspective. Understanding the different components of the microbiome, their strategies for persistence within the tick, and their effects on each other and their host provide potential roadmaps in preventing tick-borne illnesses. However, this requires a more detailed knowledge of the microbial ecology existing within *I. scapularis*. First, we must distinguish between organisms adapted to using *I. scapularis* as a host or vector of transmission vs. those that only circumstantially and transiently interact with the tick. Focusing on the long-term passengers is more likely to be profitable because these microbes are adapted to and specific for *I. scapularis*, whereas generalists are widespread in the environment and may have pleiotropic effects on non-target organisms. Symbionts may be useful tools in themselves for disrupting the infectious cycle of pathogens, as they may be used as antagonistic symbionts, to engineer as paratransgenic microbes, or some may possess entomopathogenic properties. Further, the natural microbiota has identified vulnerabilities in *I. scapularis* physiology and evolved mechanisms to exploit these weaknesses to colonize and persist in the tick. These weaknesses in tick fitness may highlight pathways we can also exploit to design countermeasures (e.g., vaccines or therapeutics) against tick-borne diseases.

AUTHOR CONTRIBUTIONS

PS prepared the manuscript. MB critically reviewed the manuscript and provided thoughtful insights.

FUNDING

This manuscript was supported by the Division of Intramural Research of the National Institute of Allergy and Infectious Diseases, National Institutes of Health.

ACKNOWLEDGMENTS

We thank Ryan Kissinger for his talents and expertise in construction of **Figure 1** and Tom Schwan for critical reading of the manuscript and insightful discussions. This manuscript was supported by the Division of Intramural Research of the National Institute of Allergy and Infectious Diseases, National Institutes of Health.

REFERENCES

Abraham, N. M., Liu, L., Jutras, B. L., Yadav, A. K., Narasimhan, S., Gopalakrishnan, V., et al. (2017). Pathogen-mediated manipulation of arthropod microbiota to promote infection. *Proc. Natl. Acad. Sci. U.S.A.* 114, E781–E790. doi: 10.1073/pnas.1613422114

Adelson, M. E., Rao, R. V., Tilton, R. C., Cabets, K., Eskow, E., Fein, L., et al. (2004). Prevalence of *Borrelia burgdorferi, Bartonella* spp., *Babesia microti*, and

Anaplasma phagocytophila in *Ixodes scapularis* ticks collected in northern New Jersey. *J. Clin. Microbiol.* 42, 2799–2801. doi: 10.1128/JCM.42.6.2799-2801.2004

Adler, S., and Theodor, O. (1927). The behaviour of cultures of *Leishmania tropica, L. infantum, and L. braziliense* in the sandfly, *Phlebotomus papatasii. Nature* 119, 48–49. doi: 10.1038/119048b0

Aliota, M. T., Dupuis, A. P. II, Wilczek, M. P., Peters, R. J., Ostfeld, R. S., and Kramer, L. D. (2014). The prevalence of zoonotic tick-borne pathogens in *Ixodes scapularis* collected in the Hudson Valley, New York State. *Vector Borne Zoonot. Dis.* 14, 245–250. doi: 10.1089/vbz.2013.1475

Al-Khafaji, A. M., Armstrong, S. D., Varotto Boccazzi, I., Gaiarsa, S., Sinha, A., Li, Z., et al. (2020). Rickettsia buchneri, symbiont of the deer tick ixodes scapularis, can colonise the salivary glands of its host. *Ticks Tick Borne Dis.* 11:101299. doi: 10.1016/j.ttbdis.2019.101299

Beaver, P. C., and Burgdorfer, W. (1984). A microfilaria of exceptional size from the ixodid tick, *Ixodes dammini*, from Shelter Island, New York. *J. Parasitol.* 70, 963–966. doi: 10.2307/3281647

Benoit, J. B., Yoder, J. A., Ark, J. T., and Rellinger, E. J. (2005). Fungal fauna of *Ixodes scapularis* say and *Rhipicephalus sanguineus* (Latreille) (*Acari : Ixodida*) with special reference to species-associated internal mycoflora. *Int. J. Acarol.* 31, 417–422. doi: 10.1080/01647950508683683

Benson, M. J., Gawronski, J. D., Eveleigh, D. E., and Benson, D. R. (2004). Intracellular symbionts and other bacteria associated with deer ticks (*Ixodes scapularis*) from nantucket and wellfleet, cape cod, massachusetts. *Appl. Environ. Microbiol.* 70, 616–620. doi: 10.1128/AEM.70.1.616-620.2004

Bernard, Q., Smith, A. A., Yang, X., Koci, J., Foor, S. D., Cramer, S. D., et al. (2018). Plasticity in early immune evasion strategies of a bacterial pathogen. *Proc. Natl. Acad. Sci. U.S.A.* 115, E3788–E3797. doi: 10.1073/pnas.1718595115

Binetruy, F., Dupraz, M., Buysse, M., and Duron, O. (2019). Surface sterilization methods impact measures of internal microbial diversity in ticks. *Parasit. Vectors* 12:268. doi: 10.1186/s13071-019-3517-5

Bourret, T. J., Lawrence, K. A., Shaw, J. A., Lin, T., Norris, S. J., and Gherardini, F. C. (2016). The nucleotide excision repair pathway protects *Borrelia burgdorferi* from nitrosative stress in *Ixodes scapularis* ticks. *Front. Microbiol.* 7:1397. doi: 10.3389/fmicb.2016.01397

Burgdorfer, W., Barbour, A. G., Hayes, S. F., Benach, J. L., Grunwaldt, E., and Davis, J. P. (1982). Lyme disease - a tick-borne spirochetosis? *Science* 216, 1317–1319. doi: 10.1126/science.7043737

Campagnolo, E. R., Tewari, D., Farone, T. S., Livengood, J. L., and Mason, K. L. (2018). Evidence of powassan/deer tick virus in adult black-legged ticks (*Ixodes scapularis*) recovered from hunter-harvested white-tailed deer (*Odocoileus virginianus*) in Pennsylvania: a public health perspective. *Zoonoses Public Health* 65, 589–594. doi: 10.1111/zph.12476

Carey, A. B., Krinsky, W. L., and Main, A. J. (1980). *Ixodes dammini* (acari: ixodidae) and associated ixodid ticks in South-central Connecticut, USA. *J. Med. Entomol.* 17, 89–99. doi: 10.1093/jmedent/17.1.89

Cerwonka, R. H., and Castillo, R. A. (1958). An apparatus for artificial feeding of *Siphonaptera. J. Parasitol.* 44, 565–566. doi: 10.2307/3274432

Cirimotich, C. M., Dong, Y., Clayton, A. M., Sandiford, S. L., Souza-Neto, J. A., Mulenga, M., et al. (2011). Natural microbe-mediated refractoriness to *Plasmodium* infection in *Anopheles gambiae*. *Science* 332, 855–858. doi: 10.1126/science.1201618

Costero, A., and Grayson, M. A. (1996). Experimental transmission of powassan virus (flaviviridae) by *Ixodes scapularis* ticks (acari:ixodidae). *Am. J. Trop. Med. Hyg.* 55, 536–546. doi: 10.4269/ajtmh.1996.55.536

Cross, S. T., Kapuscinski, M. L., Perino, J., Maertens, B. L., Weger-Lucarelli, J., Ebel, G. D., et al. (2018). Co-Infection patterns in individual *Ixodes scapularis* ticks reveal associations between viral, eukaryotic and bacterial microorganisms. *Viruses* 10:388. doi: 10.3390/v10070388

Djokic, V., Akoolo, L., Primus, S., Schlachter, S., Kelly, K., Bhanot, P., et al. (2019). Protozoan parasite *Babesia microti* subverts adaptive immunity and enhances lyme disease severity. *Front. Microbiol.* 10:1596. doi: 10.3389/fmicb.2019.01596

Dunn, J. M., Krause, P. J., Davis, S., Vannier, E. G., Fitzpatrick, M. C., Rollend, L., et al. (2014). *Borrelia burgdorferi* promotes the establishment of *Babesia microti* in the northeastern United States. *PLoS ONE* 9:e115494. doi: 10.1371/journal.pone.0115494

Dupuis, A. P. II, Peters, R. J., Prusinski, M. A., Falco, R. C., Ostfeld, R. S., and Kramer, L. D. (2013). Isolation of deer tick virus (powassan virus, lineage II) from *Ixodes scapularis* and detection of antibody in vertebrate hosts sampled in the Hudson Valley, New York State. *Parasit. Vectors* 6:185. doi: 10.1186/1756-3305-6-185

Ebel, G. D., and Kramer, L. D. (2004). Short report: duration of tick attachment required for transmission of powassan virus by deer ticks. *Am. J. Trop. Med. Hyg.* 71, 268–271. doi: 10.4269/ajtmh.2004.71.3.0700268

Edwards, M. J., Russell, J. C., Davidson, E. N., Yanushefski, T. J., Fleischman, B. L., Heist, R. O., et al. (2019). A 4-yr survey of the range of ticks and tick-borne pathogens in the Lehigh Valley region of eastern Pennsylvania. *J. Med. Entomol.* 56, 1122–1134. doi: 10.1093/jme/tjz043

Fraser, C. M., Casjens, S., Huang, W. M., Sutton, G. G., Clayton, R., Lathigra, R., et al. (1997). Genomic sequence of a lyme disease spirochaete, *Borrelia burgdorferi*. *Nature* 390, 580–586. doi: 10.1038/37551

Ginsberg, H. S., and LeBrun, R. A. (1996). "*Population regulation, natural enemies, and host-seeking patterns of deer ticks, Ixodes scapularis (Acari: Ixodidae)," in NEFA Regional Publications Series* (Boston, MA: National Park Service).

Grabowski, J. M., Nilsson, O. R., Fischer, E. R., Long, D., Offerdahl, D. K., Park, Y., et al. (2019). Dissecting flavivirus biology in salivary gland cultures from fed and unfed *Ixodes scapularis* (black-legged tick). *MBio* 10:e02628-18. doi: 10.1128/mBio.02628-18

Grabowski, J. M., Tsetsarkin, K. A., Long, D., Scott, D. P., Rosenke, R., Schwan, T. G., et al. (2017). Flavivirus infection of *Ixodes scapularis* (black-legged tick) *ex vivo* organotypic cultures and applications for disease control. *MBio* 8:e01255-17. doi: 10.1128/mBio.01255-17

Greengarten, P. J., Tuininga, A. R., Morath, S. U., Falco, R. C., Norelus, H., and Daniels, T. J. (2011). Occurrence of soil- and tick-borne fungi and related virulence tests for pathogenicity to *Ixodes scapularis* (acari: ixodidae). *J. Med. Entomol.* 48, 337–344. doi: 10.1603/ME09116

Gulia-Nuss, M., Nuss, A. B., Meyer, J. M., Sonenshine, D. E., Roe, R. M., Waterhouse, R. M., et al. (2016). Genomic insights into the *Ixodes scapularis* tick vector of Lyme disease. *Nat. Commun.* 7:10507. doi: 10.1038/ncomms10507

Hajdusek, O., Sima, R., Ayllon, N., Jalovecka, M., Perner, J., de la Fuente, J., et al. (2013). Interaction of the tick immune system with transmitted pathogens. *Front. Cell. Infect. Microbiol.* 3:26. doi: 10.3389/fcimb.2013.00026

Hamer, S. A., Hickling, G. J., Walker, E. D., and Tsao, J. I. (2014). Increased diversity of zoonotic pathogens and *Borrelia burgdorferi* strains in established versus incipient *Ixodes scapularis* populations across the Midwestern United States. *Infect. Genet. Evol.* 27, 531–542. doi: 10.1016/j.meegid.2014.06.003

Hart, T., Yang, X., Pal, U., and Lin, Y. P. (2018). Identification of lyme borreliae proteins promoting vertebrate host blood-specific spirochete survival in *Ixodes scapularis* nymphs using artificial feeding chambers. *Ticks Tick Borne Dis.* 9, 1057–1063. doi: 10.1016/j.ttbdis.2018.03.033

Hersh, M. H., Ostfeld, R. S., McHenry, D. J., Tibbetts, M., Brunner, J. L., Killilea, M. E., et al. (2014). Co-infection of blacklegged ticks with *Babesia microti* and *Borrelia burgdorferi* is higher than expected and acquired from small mammal hosts. *PLoS ONE* 9:e99348. doi: 10.1371/journal.pone.0099348

Hill, D. E. (1998). Entomopathogenic nematodes as control agents of developmental stages of the black-legged tick, *Ixodes scapularis*. *J. Parasitol.* 84, 1124–1127. doi: 10.2307/3284660

Hindle, E., and Merriman, G. (1912). The sensory perceptions of *Argas persicus* (oken). *Parasitology* 5, 203–216. doi: 10.1017/S0031182000000305

Hoxmeier, J. C., Fleshman, A. C., Broeckling, C. D., Prenni, J. E., Dolan, M. C., Gage, K. L., et al. (2017). Metabolomics of the tick-borrelia interaction during the nymphal tick blood meal. *Sci. Rep.* 7:44394. doi: 10.1038/srep44394

Hunter, D. J., Torkelson, J. L., Bodnar, J., Mortazavi, B., Laurent, T., Deason, J., et al. (2015). The *Rickettsia* endosymbiont of *Ixodes pacificus* contains all the genes of *de novo* folate biosynthesis. *PLoS ONE* 10:e0144552. doi: 10.1371/journal.pone.0144552

Johns, R., Ohnishi, J., Broadwater, A., Sonenshine, D. E., De Silva, A. M., and Hynes, W. L. (2001). Contrasts in tick innate immune responses to *Borrelia burgdorferi* challenge: immunotolerance in *Ixodes scapularis* versus immunocompetence in *Dermacentor variabilis* (Acari: Ixodidae). *J. Med. Entomol.* 38, 99–107. doi: 10.1603/0022-2585-38.1.99

Johnson, T. L., Graham, C. B., Maes, S. E., Hojgaard, A., Fleshman, A., Boegler, K. A., et al. (2018). Prevalence and distribution of seven human pathogens in host-seeking *Ixodes scapularis* (Acari: Ixodidae) nymphs in Minnesota, USA. *Ticks Tick Borne Dis.* 9, 1499–1507. doi: 10.1016/j.ttbdis.2018.07.009

Jones, L. D., Davies, C. R., Steele, G. M., and Nuttall, P. A. (1987). A novel mode of arbovirus transmission involving a nonviremic host. *Science* 237, 775–777. doi: 10.1126/science.3616608

Knox, K. K., Thomm, A. M., Harrington, Y. A., Ketter, E., Patitucci, J. M., and Carrigan, D. R. (2017). Powassan/deer tick virus and *borrelia burgdorferi* infection in wisconsin tick populations. *Vector Borne Zoonotic Dis.* 17, 463–466. doi: 10.1089/vbz.2016.2082

Koci, J., Bernard, Q., Yang, X., and Pal, U. (2018). *Borrelia burgdorferi* surface protein Lmp1 facilitates pathogen dissemination through ticks as studied by an artificial membrane feeding system. *Sci. Rep.* 8:1910. doi: 10.1038/s41598-018-20208-4

Koosha, M., Vatandoost, H., Karimian, F., Choubdar, N., and Oshaghi, M. A. (2019). Delivery of a genetically marked *Serratia* AS1 to medically important arthropods for use in RNAi and paratransgenic control Strategies. *Microb. Ecol.* 78, 185–194. doi: 10.1007/s00248-018-1289-7

Kraiczy, P., Skerka, C., Brade, V., and Zipfel, P. F. (2001). Further characterization of complement regulator-acquiring surface proteins of *Borrelia burgdorferi*. *Infect. Immun.* 69, 7800–7809. doi: 10.1128/IAI.69.12.7800-7809.2001

Krause, P. J., Telford, S. R. III, Spielman, A., Sikand, V., Ryan, R., Christianson, D., et al. (1996). Concurrent lyme disease and babesiosis. Evidence for increased severity and duration of illness. *JAMA* 275, 1657–1660. doi: 10.1001/jama.1996.03530450047031

Krober, T., and Guerin, P. M. (2007). An *in vitro* feeding assay to test acaricides for control of hard ticks. *Pest Manag. Sci.* 63, 17–22. doi: 10.1002/ps.1293

Kurtti, T. J., Felsheim, R. F., Burkhardt, N. Y., Oliver, J. D., Heu, C. C., and Munderloh, U. G. (2015). *Rickettsia buchneri* sp. nov., a rickettsial endosymbiont of the blacklegged tick *Ixodes scapularis*. *Int. J. Syst. Evol. Microbiol.* 65, 965–970. doi: 10.1099/ijs.0.000047

Labuda, M., Danielova, V., Jones, L. D., and Nuttall, P. A. (1993a). Amplification of tick-borne encephalitis virus infection during co-feeding of ticks. *Med. Vet. Entomol.* 7, 339–342. doi: 10.1111/j.1365-2915.1993.tb00702.x

Labuda, M., Jones, L. D., Williams, T., Danielova, V., and Nuttall, P. A. (1993b). Efficient transmission of tick-borne encephalitis virus between cofeeding ticks. *J. Med. Entomol.* 30, 295–299. doi: 10.1093/jmedent/30.1.295

Landesman, W. J., Mulder, K., Allan, B. F., Bashor, L. A., Keesing, F., LoGiudice, K., et al. (2019). Potential effects of blood meal host on bacterial community composition in *Ixodes scapularis* nymphs. *Ticks Tick Borne Dis.* 10, 523–527. doi: 10.1016/j.ttbdis.2019.01.002

Lefcort, H., and Durden, L. A. (1996). The effect of infection with Lyme disease spirochetes (*Borrelia burgdorferi*) on the phototaxis, activity, and questing height of the tick vector *Ixodes scapularis*. *Parasitology* 113, 97–103. doi: 10.1017/S0031182000066336

Levin, M. L., and Fish, D. (2001). Interference between the agents of Lyme disease and human granulocytic ehrlichiosis in a natural reservoir host. *Vector Borne Zoonotic Dis.* 1, 139–148. doi: 10.1089/153036601316977741

Liu, L., Dai, J., Zhao, Y. O., Narasimhan, S., Yang, Y., Zhang, L., et al. (2012). *Ixodes scapularis* JAK-STAT pathway regulates tick antimicrobial peptides, thereby controlling the agent of human granulocytic anaplasmosis. *J. Infect. Dis.* 206, 1233–1241. doi: 10.1093/infdis/jis484

Martin, P. A., and Schmidtmann, E. T. (1998). Isolation of aerobic microbes from *Ixodes scapularis* (Acari: Ixodidae), the vector of lyme disease in the eastern United States. *J. Econ. Entomol.* 91, 864–868. doi: 10.1093/jee/91.4.864

Mitzel, D. N., Wolfinbarger, J. B., Long, R. D., Masnick, M., Best, S. M., and Bloom, M. E. (2007). Tick-borne flavivirus infection in *Ixodes scapularis* larvae: development of a novel method for synchronous viral infection of ticks. *Virology* 365, 410–418. doi: 10.1016/j.virol.2007.03.057

Namrata, P., Miller, J. M., Shilpa, M., Reddy, P. R., Bandoski, C., Rossi, M. J., et al. (2014). Filarial nematode infection in *Ixodes scapularis* ticks collected from southern connecticut. *Vet. Sci.* 1, 5–15. doi: 10.3390/vetsci1010005

Narasimhan, S., Rajeevan, N., Liu, L., Zhao, Y. O., Heisig, J., Pan, J., et al. (2014). Gut microbiota of the tick vector *Ixodes scapularis* modulate colonization of the lyme disease spirochete. *Cell Host Microbe.* 15, 58–71. doi: 10.1016/j.chom.2013.12.001

Narasimhan, S., Schuijt, T. J., Abraham, N. M., Rajeevan, N., Coumou, J., Graham, M., et al. (2017). Modulation of the tick gut milieu by a secreted tick protein favors *Borrelia burgdorferi* colonization. *Nat. Commun.* 8:184. doi: 10.1038/s41467-017-00208-0

Neelakanta, G., Sultana, H., Fish, D., Anderson, J. F., and Fikrig, E. (2010). *Anaplasma phagocytophilum* induces *Ixodes scapularis* ticks to express an antifreeze glycoprotein gene that enhances their survival in the cold. *J. Clin. Invest.* 120, 3179–3190. doi: 10.1172/JCI42868

Noda, H., Munderloh, U. G., and Kurtti, T. J. (1997). Endosymbionts of ticks and their relationship to *Wolbachia* spp. and tick-borne pathogens of humans and animals. *Appl. Environ. Microbiol.* 63, 3926–3932. doi: 10.1128/AEM.63.10.3926-3932.1997

Oliver, J. D., Lynn, G. E., Burkhardt, N. Y., Price, L. D., Nelson, C. M., Kurtti, T. J., et al. (2016). Infection of immature *Ixodes scapularis* (Acari: Ixodidae) by membrane feeding. *J. Med. Entomol.* 53, 409–415. doi: 10.1093/jme/tjv241

Pappas, C. J., Iyer, R., Petzke, M. M., Caimano, M. J., Radolf, J. D., and Schwartz, I. (2011). *Borrelia burgdorferi* requires glycerol for maximum fitness during the tick phase of the enzootic cycle. *PLoS Pathog.* 7:e1002102. doi: 10.1371/journal.ppat.1002102

Perner, J., Sobotka, R., Sima, R., Konvickova, J., Sojka, D., Oliveira, P. L., et al. (2016). Acquisition of exogenous haem is essential for tick reproduction. *Elife* 5:e14166. doi: 10.7554/eLife.12318.031

Piesman, J., Oliver, J. R., and Sinsky, R. J. (1990). Growth kinetics of the lyme disease spirochete (*Borrelia burgdorferi*) in vector ticks (*Ixodes dammini*). *Am. J. Trop. Med. Hyg.* 42, 352–357. doi: 10.4269/ajtmh.1990.42.352

Piesman, J., and Spielman, A. (1979). Host-associations and seasonal abundance of immature *Ixodes dammini* in southeastern massachusetts. *Ann. Entomol. Soc. Am.* 72, 829–832. doi: 10.1093/aesa/72.6.829

Piesman, J., Spielman, A., Etkind, P., Ruebush, T. K. II, and Juranek, D. D. (1979). Role of deer in the epizootiology of b*abesia microti* in massachusetts, USA. *J. Med. Entomol.* 15, 537–540. doi: 10.1093/jmedent/15.5-6.537

Plantard, O., Bouju-Albert, A., Malard, M. A., Hermouet, A., Capron, G., and Verheyden, H. (2012). Detection of *Wolbachia* in the tick *Ixodes ricinus* is due to the presence of the hymenoptera endoparasitoid *Ixodiphagus hookeri*. *PLoS ONE* 7:e30692. doi: 10.1371/journal.pone.0030692

Policastro, P. F., Raffel, S. J., and Schwan, T. G. (2011). Cotransmission of divergent relapsing fever spirochetes by artificially infected *Ornithodoros hermsi*. *Appl. Environ. Microbiol.* 77, 8494–8499. doi: 10.1128/AEM.05830-11

Policastro, P. F., and Schwan, T. G. (2003). Experimental infection of *Ixodes scapularis* larvae (Acari: Ixodidae) by immersion in low passage cultures of *Borrelia burgdorferi*. *J. Med. Entomol.* 40, 364–370. doi: 10.1603/0022-2585-40.3.364

Pritt, B. S., Mead, P. S., Johnson, D. K., Neitzel, D. F., Respicio-Kingry, L. B., Davis, J. P., et al. (2016). Identification of a novel pathogenic *Borrelia* species causing lyme borreliosis with unusually high spirochaetaemia: a descriptive study. *Lancet Infect. Dis.* 16, 556–564. doi: 10.1016/S1473-3099(15)00464-8

Ross, B. D., Hayes, B., Radey, M. C., Lee, X., Josek, T., Bjork, J., et al. (2018). *Ixodes scapularis* does not harbor a stable midgut microbiome. *ISME J.* 12, 2596–2607. doi: 10.1038/s41396-018-0161-6

Rudzinska, M. A., Spielman, A., Lewengrub, S., Piesman, J., and Karakashian, S. (1982). Penetration of the peritrophic membrane of the tick by *Babesia microti*. *Cell Tissue Res.* 221, 471–481. doi: 10.1007/BF00215696

Rynkiewicz, E. C., Hemmerich, C., Rusch, D. B., Fuqua, C., and Clay, K. (2015). Concordance of bacterial communities of two tick species and blood of their shared rodent host. *Mol. Ecol.* 24, 2566–2579. doi: 10.1111/mec.13187

Sakamoto, J. M., Ng, T. F. F., Suzuki, Y., Tsujimoto, H., Deng, X., Delwart, E., et al. (2016). Bunyaviruses are common in male and female *Ixodes scapularis* ticks in central Pennsylvania. *PeerJ* 4:e2324. doi: 10.7717/peerj.2324

Salter, S. J., Cox, M. J., Turek, E. M., Calus, S. T., Cookson, W. O., Moffatt, M. F., et al. (2014). Reagent and laboratory contamination can critically impact sequence-based microbiome analyses. *BMC Biol.* 12:87. doi: 10.1186/s12915-014-0087-z

Sanchez-Vicente, S., Tagliafierro, T., Coleman, J. L., Benach, J. L., and Tokarz, R. (2019). Polymicrobial nature of tick-borne diseases. *MBio* 10:e02055-19. doi: 10.1128/mBio.02055-19

Schnettler, E., Tykalova, H., Watson, M., Sharma, M., Sterken, M. G., Obbard, D. J., et al. (2014). Induction and suppression of tick cell antiviral RNAi responses by tick-borne flaviviruses. *Nucleic Acids Res.* 42, 9436–9446. doi: 10.1093/nar/gku657

Schwartz, I., Fish, D., and Daniels, T. J. (1997). Prevalence of the rickettsial agent of human granulocytic ehrlichiosis in ticks from a hyperendemic focus of Lyme disease. *N. Engl. J. Med.* 337, 49–50. doi: 10.1056/NEJM199707033370111

Scoles, G. A., Papero, M., Beati, L., and Fish, D. (2001). A relapsing fever group spirochete transmitted by *Ixodes scapularis* ticks. *Vector Borne Zoonotic Dis.* 1, 21–34. doi: 10.1089/153036601750137624

Sojka, D., Hajdusek, O., Dvorak, J., Sajid, M., Franta, Z., Schneider, E. L., et al. (2007). IrAE: an asparaginyl endopeptidase (legumain) in the gut of the hard tick *Ixodes ricinus*. *Int. J. Parasitol.* 37, 713–724. doi: 10.1016/j.ijpara.2006.12.020

Sonenshine, D. E., Hynes, W. L., Ceraul, S. M., Mitchell, R., and Benzine, T. (2005). Host blood proteins and peptides in the midgut of the tick *Dermacentor variabilis* contribute to bacterial control. *Exp. Appl. Acarol.* 36, 207–223. doi: 10.1007/s10493-005-2564-0

Steiner, F. E., Pinger, R. R., Vann, C. N., Grindle, N., Civitello, D., Clay, K., et al. (2008). Infection and co-infection rates of *Anaplasma phagocytophilum* variants, *Babesia* spp., *Borrelia burgdorferi*, and the rickettsial endosymbiont in *Ixodes scapularis* (Acari: Ixodidae) from sites in Indiana, Maine, Pennsylvania, and Wisconsin. *J. Med. Entomol.* 45, 289–297. doi: 10.1093/jmedent/45.2.289

Telford, S. R. III, Armstrong, P. M., Katavolos, P., Foppa, I., Garcia, A. S., Wilson, M. L., et al. (1997). A new tick-borne encephalitis-like virus infecting New England deer ticks, *Ixodes dammini*. *Emerg. Infect. Dis.* 3, 165–170. doi: 10.3201/eid0302.970209

Telford, S. R. III, Dawson, J. E., Katavolos, P., Warner, C. K., Kolbert, C. P., and Persing, D. H. (1996). Perpetuation of the agent of human granulocytic ehrlichiosis in a deer tick-rodent cycle. *Proc. Natl Acad. Sci. U.S.A.* 93, 6209–6214. doi: 10.1073/pnas.93.12.6209

Thapa, S., Zhang, Y., and Allen, M. S. (2019). Bacterial microbiomes of *Ixodes scapularis* ticks collected from Massachusetts and Texas, USA. *BMC Microbiol.* 19:138. doi: 10.1186/s12866-019-1514-7

Thomas, L. A., Kennedy, R. C., and Eklund, C. M. (1960). Isolation of a virus closely related to Powassan virus from *Dermacentor andersoni* collected along North Cache la Poudre River, Colo. *Proc. Soc. Exp. Biol. Med.* 104, 355–359. doi: 10.3181/00379727-104-25836

Tijsse-Klasen, E., Fonville, M., van Overbeek, L., Reimerink, J. H., and Sprong, H. (2010). Exotic Rickettsiae in *Ixodes ricinus*: fact or artifact? *Parasit. Vectors* 3:54. doi: 10.1186/1756-3305-3-54

Tokarz, R., Jain, K., Bennett, A., Briese, T., and Lipkin, W. I. (2010). Assessment of polymicrobial infections in ticks in New York state. *Vector Borne Zoonotic Dis.* 10, 217–221. doi: 10.1089/vbz.2009.0036

Tokarz, R., Sameroff, S., Leon, M. S., Jain, K., and Lipkin, W. I. (2014a). Genome characterization of Long Island tick rhabdovirus, a new virus identified in *Amblyomma americanum* ticks. *Virol. J.* 11:26. doi: 10.1186/1743-422X-11-26

Tokarz, R., Sameroff, S., Tagliafierro, T., Jain, K., Williams, S. H., Cucura, D. M., et al. (2018). Identification of novel viruses in *Amblyomma americanum, Dermacentor variabilis*, and *Ixodes scapularis* ticks. *mSphere* 3:e00614-1. doi: 10.1128/mSphere.00614-17

Tokarz, R., Tagliafierro, T., Cucura, D. M., Rochlin, I., Sameroff, S., and Lipkin, W. I. (2017). Detection of *Anaplasma phagocytophilum, Babesia microti, Borrelia burgdorferi, Borrelia miyamotoi*, and powassan virus in ticks by a multiplex real-time reverse transcription-PCR assay. *mSphere* 2:e00151-17. doi: 10.1128/mSphere.00151-17

Tokarz, R., Tagliafierro, T., Sameroff, S., Cucura, D. M., Oleynik, A., Che, X., et al. (2019). Microbiome analysis of *Ixodes scapularis* ticks from New York and Connecticut. *Ticks Tick Borne Dis.* 10, 894–900. doi: 10.1016/j.ttbdis.2019.04.011

Tokarz, R., Williams, S. H., Sameroff, S., Sanchez Leon, M., Jain, K., and Lipkin, W. I. (2014b). Virome analysis of *Amblyomma americanum, Dermacentor variabilis*, and *Ixodes scapularis* ticks reveals novel highly divergent vertebrate and invertebrate viruses. *J. Virol.* 88, 11480–11492. doi: 10.1128/JVI.01858-14

Tuininga, A. R., Miller, J. L., Morath, S. U., Daniels, T. J., Falco, R. C., Marchese, M., et al. (2009). Isolation of entomopathogenic fungi from soils and *Ixodes scapularis* (Acari: Ixodidae) ticks: prevalence and methods. *J. Med. Entomol.* 46, 557–565. doi: 10.1603/033.046.0321

Van Treuren, W., Ponnusamy, L., Brinkerhoff, R. J., Gonzalez, A., Parobek, C. M., Juliano, J. J., et al. (2015). Variation in the microbiota of *Ixodes* ticks with regard to geography, species, and sex. *Appl. Environ. Microbiol.* 81, 6200–6209. doi: 10.1128/AEM.01562-15

Whipps, J. M., Lewis, K., and Cooke, R. C. (1988). "Mycoparasitism and plant disease control," in *Fungi in Biological Control Systems,* ed M.N. Burge (Manchester: Manchester University Press), 161–187.

Woke, P. A. (1937). Effects of various blood fractions on egg production of *Aedes aegypti* Linn. *Am. J. Hyg.* 25, 372–380. doi: 10.1093/oxfordjournals.aje.a118313

Wu, D., Daugherty, S. C., Van Aken, S. E., Pai, G. H., Watkins, K. L., Khouri, H., et al. (2006). Metabolic complementarity and genomics of the dual bacterial symbiosis of sharpshooters. *PLoS Biol.* 4:e188. doi: 10.1371/journal.pbio.0040188

Wu, P., Sun, P., Nie, K., Zhu, Y., Shi, M., Xiao, C., et al. (2019). A gut commensal bacterium promotes mosquito permissiveness to arboviruses. *Cell Host Microbe. 25*, 101–112.e105. doi: 10.1016/j.chom.2018.11.004

Yang, X., Smith, A. A., Williams, M. S., and Pal, U. (2014). A dityrosine network mediated by dual oxidase and peroxidase influences the persistence of Lyme disease pathogens within the vector. *J. Biol. Chem.* 289, 12813–12822. doi: 10.1074/jbc.M113.538272

Zhioua, E., Browning, M., Johnson, P. W., Ginsberg, H. S., and LeBrun, R. A. (1997). Pathogenicity of the entomopathogenic fungus *Metarhizium anisopliae* (Deuteromycetes) to *Ixodes scapularis* (Acari: Ixodidae). *J. Parasitol.* 83, 815–818. doi: 10.2307/3284273

Zhioua, E., Ginsberg, H. S., Humber, R. A., and Lebrun, R. A. (1999). Preliminary survey for entomopathogenic fungi associated with *Ixodes scapularis* (Acari: Ixodidae) in southern New York and New England, USA. *J. Med. Entomol.* 36, 635–637. doi: 10.1093/jmedent/36.5.635

Zhioua, E., Lebrun, R. A., Ginsberg, H. S., and Aeschlimann, A. (1995). Pathogenicity of *Steinernema carpocapsae* and *S. glaseri* (nematoda: steinernematidae) to *Ixodes scapularis* (Acari: Ixodidae). *J. Med. Entomol.* 32, 900–905. doi: 10.1093/jmedent/32.6.900

Zhu, Z., Gern, L., and Aeschlimann, A. (1991). The peritrophic membrane of *Ixodes ricinus*. *Parasitol. Res.* 77, 635–641. doi: 10.1007/BF00931028

Zolnik, C. P., Falco, R. C., Daniels, T. J., and Kolokotronis, S. O. (2018). Transient influence of blood meal and natural environment on blacklegged tick bacterial communities. *Ticks Tick Borne Dis.* 9, 563–572. doi: 10.1016/j.ttbdis.2018.01.007

Zolnik, C. P., Prill, R. J., Falco, R. C., Daniels, T. J., and Kolokotronis, S. O. (2016). Microbiome changes through ontogeny of a tick pathogen vector. *Mol. Ecol.* 25, 4963–4977. doi: 10.1111/mec.13832

Conflict of Interest: The authors declare that the research was conducted in the absence of any commercial or financial relationships that could be construed as a potential conflict of interest.

frontiers in Cellular and Infection Microbiology

ORIGINAL RESEARCH
published: 05 May 2020
doi: 10.3389/fcimb.2020.00152

Differential Expression of Putative *Ornithodoros turicata* Defensins Mediated by Tick Feeding

Brittany A. Armstrong[1,2], *Alexander R. Kneubehl*[1,2], *Robert D. Mitchell III*[3], *Aparna Krishnavajhala*[2], *Pete D. Teel*[4], *Adalberto A. Pérez de León*[3] *and Job E. Lopez*[1,2]*

[1] Department of Molecular Virology and Microbiology, Baylor College of Medicine, Houston, TX, United States, [2] Department of Pediatrics, National School of Tropical Medicine, Baylor College of Medicine, Houston, TX, United States, [3] Knipling-Bushland U.S. Livestock Insects Research Laboratory, Veterinary Pest Genomics Center, Department of Agriculture—Agricultural Research Service, Kerrville, TX, United States, [4] Department of Entomology, Texas A&M AgriLife Research, College Station, TX, United States

OPEN ACCESS

Edited by:
Emily Derbyshire,
Duke University, United States

Reviewed by:
Iris Bruchhaus,
Bernhard Nocht Institute for Tropical Medicine (BMITM), Germany
Galadriel Hovel-Miner,
George Washington University, United States

***Correspondence:**
Job E. Lopez
job.lopez@bcm.edu

Specialty section:
This article was submitted to Parasite and Host, a section of the journal Frontiers in Cellular and Infection Microbiology

Received: 10 December 2019
Accepted: 23 March 2020
Published: 05 May 2020

Citation:
Armstrong BA, Kneubehl AR, Mitchell RD III, Krishnavajhala A, Teel PD, Pérez de León AA and Lopez JE (2020) Differential Expression of Putative Ornithodoros turicata Defensins Mediated by Tick Feeding. Front. Cell. Infect. Microbiol. 10:152. doi: 10.3389/fcimb.2020.00152

Additional research on soft ticks in the family Argasidae is needed to bridge the knowledge gap relative to hard ticks of the family Ixodidae; especially, the molecular mechanisms of *Ornithodoros* biology. *Ornithodoros* species are vectors of human and animal pathogens that include tick-borne relapsing fever spirochetes and African swine fever virus. Soft tick vector-pathogen interactions involving components of the tick immune response are not understood. Ticks utilize a basic innate immune system consisting of recognition factors and cellular and humoral responses to produce antimicrobial peptides, like defensins. In the present study, we identified and characterized the first putative defensins of *Ornithodoros turicata*, an argasid tick found primarily in the southwestern United States and regions of Latin America. Four genes (*otdA*, *otdB*, *otdC*, and *otdD*) were identified through sequencing and their predicted amino acid sequences contained motifs characteristic of arthropod defensins. A phylogenetic analysis grouped these four genes with arthropod defensins, and computational structural analyses further supported the identification. Since pathogens transmitted by *O. turicata* colonize both the midgut and salivary glands, expression patterns of the putative defensins were determined in these tissues 1 week post engorgement and after molting. Defensin genes up-regulated in the tick midgut 1 week post blood feeding were *otdA* and *otdC,* while *otdD* was up-regulated in the midgut of post-molt ticks. Moreover, *otdB* and *otdD* were also up-regulated in the salivary glands of flat post-molt ticks, while *otdC* was up-regulated within 1 week post blood-feeding. This work is foundational toward additional studies to determine mechanisms of vector competence and pathogen transmission from *O. turicata.*

Keywords: *Ornithdoros turicata*, antimicrobial peptide (AMP), gene expression, defensins, argasid (soft) ticks, immune response

INTRODUCTION

Ornithodoros (argasid) species are vectors of veterinary and medically significant pathogens. The primary species in the United States that transmit pathogens include *Ornithodoros turicata*, *Ornithodoros hermsi*, *Ornithodoros parkeri*, *Ornithodoros talaje*, and *Ornithodoros coriaceus* (Davis, 1939; Cooley and Kohls, 1944; Hess et al., 1987; Donaldson et al., 2016; Lopez et al., 2016; Sage et al., 2017). These species have been implicated in the transmission of tick-borne relapsing fever spirochetes (Lane et al., 1985; Dworkin et al., 2002; Nieto et al., 2012; Lopez et al., 2016; Christensen et al., 2017; Bissett et al., 2018). Moreover, *O. turicata* and *O. coriaceus* were experimentally shown to be competent vectors of African swine fever virus (ASFV) (Hess et al., 1987), an emerging pathogen in Europe and Asia. *O. parkeri* was able to be infected with ASFV, but unable to transmit the pathogen via tick bite (Hess et al., 1987). *Ornithodoros* ticks play a significant role in pathogen maintenance, yet very little is known regarding vector competence.

The life cycles of *Ornithodoros* ticks and their pathogens has been predominantly characterized utilizing *O. hermsi* and *O. turicata* models, and these studies identified significant challenges when attempting to elucidate mechanisms of vector competence. *Ornithodoros* species are rapid feeders, completing the bloodmeal within 5–60 min (Balashov, 1972). As ticks blood feed, pathogens initially colonize the midgut (Schwan, 1996; Schwan and Hinnebusch, 1998; Krishnavajhala et al., 2017). Given that transmission can occur within seconds of tick attachment, pathogens must also colonize the salivary glands to ensure entrance into a vertebrate host (Schwan and Hinnebusch, 1998; Boyle et al., 2014; Krishnavajhala et al., 2017). *Ornithodoros* species are also unique from other tick genera because they live for 10–20 years and can endure over 5 years of starvation and still remain competent vectors (Davis, 1943; Assous and Wilamowski, 2009). Recently, physiological differences were detected between the midgut and salivary glands of *O. turicata*, which revealed selective pressures that pathogens encounter in the argasid tick including reactive nitrogen and oxygen species (ROS and RNS) (Bourret et al., 2019). However, it remains vague what other immunological pressures exist in these two disparate environments.

Three identified branches of tick immunity are currently recognized: immune regulation components (recognition factors and signaling pathways), cellular, and humoral (Kopáček et al., 2010; Hynes, 2014). In argasid ticks, identified recognition factors include lectins, which are important for self and non-self-recognition (Grubhoffer et al., 2004; Kopáček et al., 2010). Cellular responses have primarily been found in the hemocoel and include hemocyte responses and phagocytosis of pathogens (Sonenshine et al., 2002; Nakajima et al., 2003b; Oliva Chavez et al., 2017; Sonenshine and Macaluso, 2017). The most characterized portion of soft tick immunity, though still significantly understudied, is humoral immunity. Within this branch of immunity are proteases, protease inhibitors, and antimicrobial peptides (AMPs) (Sonenshine and Hynes, 2008; Hajdusek et al., 2013; Oliva Chavez et al., 2017).

AMPs are a broad category of immune molecules that function to protect the vector from pathogens (Sonenshine et al., 2002; Boulanger et al., 2006; Hajdusek et al., 2013; Tonk et al., 2014). AMPs include lysozymes, hebraein, microplusin, ixodidin, ixosin, *Ixodes scapularis* AMP (isAMP), hemoglobin fragments, and defensins (Grunclová et al., 2003; Lai et al., 2004; Sonenshine et al., 2005; Fogaça et al., 2006; Liu et al., 2008; Silva et al., 2009; Chrudimska et al., 2010; Hajdusek et al., 2013). A key component of tick and other arthropod immunity are defensins. These are cationic molecules that disrupt the cell membrane of pathogens by binding to the negatively charged membrane and forming a pore leading to cell depolarization and ultimately cell death (Nakajima et al., 2003a; Bulet and Stöcklin, 2005). Tick defensins consist of a signal peptide, pro-segment containing a furin cleavage site (RVRR) (Chrudimska et al., 2014), and the mature peptide (Hosaka et al., 1991; Nakajima et al., 2001). The mature peptide is characterized with six cysteine residues that form three disulfide bonds resulting in a cysteine-stabilized αβ (CSαβ) motif (Bulet and Stöcklin, 2005). Proper cysteine pairing through disulfide bonds is crucial for antimicrobial activity (Isogai et al., 2011).

In this study, we focused on identifying immunological pressures produced in the tick midgut and salivary glands. Since genomic and transcriptomic resources are limited for *O. turicata*, we utilized a salivary gland transcriptome to identify putative defensins (Bourret et al., 2019). These candidates had the characteristic six cysteine residues observed in known defensin molecules of insects and arthropods. Transcripts were further evaluated by rapid amplification of cDNA ends (RACE) to obtain full-length sequences. We performed computational analyses at the protein level to generate predictive structures, which further supported the characterization of theses transcripts as defensins. A phylogenetic analysis was also performed with defensins from numerous arthropod species. Lastly, we investigated expression patterns of these putative defensins in the midgut and salivary gland tissues 1 week after *O. turicata* fed and after the molt. These time points were chosen because of their importance in early and post-molt pathogen colonization. Our initial findings suggest that in *Ornithodoros* species defensins may have a role directly after blood feeding, while others are utilized in post-molt ticks. Our findings provide a foundation to further investigate the molecular mechanisms of vector competence in a rapid feeding, long-lived tick.

MATERIALS AND METHODS

Identification of Defensins and RACE Sequencing

O. turicata defensins were identified from our previously reported salivary gland transcriptome (Bourret et al., 2019). The transcriptome was analyzed to select transcripts that were annotated as defensins. Putative defensins were evaluated in National Center for Biotechnology Information (NCBI) using Basic Local Alignment Search Tool (BLAST) to confirm the transcriptome results by assessing amino acid sequence homology with other arthropod defensins (Altschul et al., 1990).

Rapid amplification of cDNA ends (RACE) was performed with mRNA extracted from a pool of 9 ticks 9 days post blood feeding, using the Nucleotrap mRNA MiniKit (Takara Bio Inc, Kusatsu, Japan) and following the manufacturer's instructions. Purified mRNA was used with the SMARTer RACE 5'/3' kit (Takara Bio Inc, Kusatsu, Japan) and for both the 5' and 3' ends of the defensin transcripts. Gene-specific oligos for 5' and 3' RACE (**Table 1**) were designed according to manufacturer's instructions based on sequences identified as defensins in the RNA-seq dataset and were manufactured by Sigma-Aldrich (St. Louis, MO). The 5' and 3' RACE reactions were performed following the manufacturer's instructions using the Touchdown PCR protocol. The only modification was the extension times throughout the protocol were shortened to 1 min. RACE PCR reactions were analyzed by agarose gel electrophoresis (0.8% agarose tris-acetate EDTA buffer) and positive PCR reactions were purified using the QIAquick PCR purification kit (Qiagen, Hilden, Germany). Following manufacturers' instructions, purified PCR products were cloned using the Zero Blunt TOPO PCR Cloning Kit for Sequencing (ThermoFisher, Waltham, MA) and used to transform NEB10-beta chemically competent cells (New England BioLabs, Ipswich, MA). Transformants were plated on LB-Miller agar (BD Biosciences, San Jose, CA) containing 50 ug/mL of kanamycin (Sigma-Aldrich, St. Louis, MO) overnight at 37°C. Colonies were screened by PCR with universal M13F/R primers (Sigma-Aldrich, St. Louis, MO) at a final concentration of 200 nM and using OneTaq 2x PCR mastermix with standard buffer (New England BioLabs, Ipswich, MA) using the following colony PCR protocol: 94°C for 5 min: 1 cycle; 94°C 30 s, 50°C 30 s, 68°C 40 s: 25 cycles; 68°C 5 min: 1 cycle; 10°C hold. Colony PCR was analyzed by agarose gel electrophoresis and the colonies with the largest products were selected for sequencing. Selected colonies were cultured overnight in 5 mL of LB-Miller with 50 ug/mL of kanamycin and plasmid isolated the following day with the QiaPrep Spin Miniprep Kit (Qiagen). Purified RACE product plasmids were sent to GeneWiz (Plainfield, NJ) for Sanger sequencing using M13F/R sequencing primers. Sequencing results were analyzed using FinchTV (v1.4.0, Digital World Biology) and the predicted amino acid sequences were BLASTed (Blastp) against representative non-redundant protein sequences on NCBI to confirm their identity (Altschul et al., 1990). Complete coding sequences were submitted to Genbank under the names *otdA* (MN725028), *otdB* (MN725029), *otdC* (MN725030), and *otdD* (MN725031).

TABLE 1 | Oligonucleotides and probes used for qPCR and RACE.

Gene	Primer sequences (5′-3′)
qPCR primer sets	
OtdA F	AGGACGGTACGGGGAAT
OtdA R	CGCACTTCTGGTCCAGC
OtdA Probe	YAK-ACCAGTACCAGTGCCACAGCCACTG-BBQ
OtdB F	AGGACGGTACGGGGAAT
OtdB R	CGCACTTCTGGTCCAGC
OtdB Probe	YAK-AGCCCGGTGCATCTTCCATATGC-BBQ
OtdC F	TGTTCTGAGTGCCGTTGTTAC
OtdC R	TGCTTCCGACACATAGCG
OtdC Probe	YAK-AGGCGTGCTCCGTGTTATGCAC-BBQ
OtdD F	TTTCGGTGTGCATTGTAGC
OtdD R	GGCAATGCTGATTGCACT
OtdD Probe	YAK-TGCAGATGGTGGCAGCGGCT-BBQ
BA F	TATCCACGAGACCACCTACAA
BA R	TCTGCATACGATCGGCAATAC
BA Probe	FAM-AAGGACCTGTACGCCAACACTGTC-IBFQ
RACE primers	
M13 F	GTAAAACGACGGCCAG
M13 R	CAGGAAACAGCTATGAC
OtdA 5′	AGTGGCTGTGGCACTGGTACTGG
OtdA 3′	AAGAGTCATCAGCCGTCCGAGTTCGT
OtdB 5′	CCTTTCGCACTTGAAGGTACAGGCAA
OtdB 3′	TGCTGCTTCTTACTGGGCTTCTCACTTC
OtdC 5′	AAGTCTCTACGCAGTGCTTCCGACACAT
OtdC 3′	CCCAGCAATGACTCCTCTCCGTTT
OtdD 5′	TCTGGTGTCGAGGCAATGCTGATT
OtdD 3′	CGGTGTGCATTCTAGCCCTCCTGC

F, forward; R, reverse; YAK, Yakima dye; BBQ, blackberry quencher; FAM, fluorescein amide; IBFQ, Iowa Black FQ quencher.

Defensin Sequence Alignment and Protein Structure Prediction

The amino acid sequences of the identified *O. turicata* defensins were aligned with defensins published in Genbank from *Ornithodoros moubata* (BAB41028.1), *Carios puertoricensis* (ACJ04430.1), *I. scapularis* (XP_029834656.1), *Haemaphysalis longicornis* (ATN39848.1), *Dermacentor variabilis* (AAO24323.1), *Amblyomma americanum* (ABI74752.1), and *Argas monolakensis* (ABI52686.1). Mature peptide sequences were aligned using ClustalW in MEGAX 10.0.5 (Kumar et al., 2018). The signal peptide and propeptide cleavage sites were predicted using the ProP 1.0 Server (Duckert et al., 2004).

The structure of the defensins was predicted as described by Rodríguez-García et al. (2016). Briefly, protein model templates were identified based on sequence alignments generated with the Hhpred server (https://toolkit.tuebingen.mpg.de/tools/hhpred). The top three sequences were selected from tertiary structure prediction using MODELLER (https://toolkit.tuebingen.mpg.de/tools/modeller) (Webb and Sali, 2016; Zimmermann et al., 2018). The predicted structure was analyzed with ProSA-web (https://prosa.services.came.sbg.ac.at/prosa.php) to assess the Z-score (Wiederstein and Sippl, 2007). The final structure was generated using the Swiss-PDB Viewer 4.1.0 (Guex and Peitsch, 1997).

Phylogenetic Analysis of Arthropod Defensins

All reported analyses were performed using NGPhylogeny.fr (Lemoine et al., 2018). Analyses with the same input data were also performed using MEGAX for comparison (data not shown) (Kumar et al., 2018). Alignments of the mature peptide sequence were performed using MUSLCE v3.8.31 under the "most accurate, maxiters = 16" run option setting and "UPGMB" under the clustering setting (Edgar, 2004). Noisy v1.5.12.1 was used for alignment curation with a cut-off threshold of 0.8 and the Hamming distance method via the Neighbor-Net ordering

method (Dress et al., 2008). FastTree v2.1.10_1 was used to infer the phylogenetic tree with the WAG evolutionary model using Gamma distribution and 1,000 bootstraps (Price et al., 2009, 2010).

Tick Colony Maintenance, Feedings, and Dissections

The present study used laboratory reared mid to late nymphal stage *O. turicata* ticks descendent of ticks originally collected in Travis County, Texas (Kim et al., 2017). The ticks were maintained in colony at 25°C and 80–85% humidity, as previously described (Lopez et al., 2013). Ticks were fed on an Institute of Cancer Research (ICR) mouse and dissected 1 week later (fed) or allowed to molt (post-molt). Each biological replicate consisted of 10 pooled midguts or salivary gland pairs from post-molt or fed ticks.

Midguts and salivary glands were extracted using an Axio Stemi dissection microscope (Zeiss, Munich, Germany). An individual tick was placed on a microscope slide in 10 to 20 μl of 1x Dulbecco's Phosphate Buffered Saline (DPBS) (Life Technologies, Grand Island, NY). The cuticle was removed, and the midgut extracted and placed in 100 μl of RNAlater (Qiagen, Hilden, Germany). The tick was then rinsed with 10 μl of 1x DPBS, the salivary glands removed and placed in 15 μl of 1x DPBS, rinsed, and placed in a tube containing 100 μl of RNAlater. Each sample consisted of 10 pooled midguts or salivary gland pairs. Samples were stored at −80°C until RNA was extracted.

RNA Extraction, cDNA Synthesis, and RT-qPCR Analysis

Tissues were homogenized using a pestle (Argos Technologies, Elgin, IL) and were spun through a QIAshredder column per manufacturer's instructions (Qiagen, Hilden, Germany). RNA was extracted using the RNeasy mini kit (Qiagen, Hilden, Germany) following manufacturer's instructions. Samples were DNase treated (Qiagen, Hilden, Germany) and eluted in 30 μl of nuclease free water (Ambion, Inc, Austin, TX). RNA was quantified using a NanoDrop 2000 spectrophotometer (software v1.6.198, ThermoFisher Scientific, Waltham, MA).

RNA was converted to cDNA using the iScript cDNA synthesis kit (Bio-Rad, Hercules, CA) per the manufacturer's instructions. Gene expression was assessed using the cDNA to perform duplex qPCR. Primers against the defensins for qPCR (**Table 1**) were designed using the sequences from RACE sequencing and were synthesized by Integrated DNA Technologies (Coralville, IA). Defensins were run in duplex with *O. turicata β-actin* (Krishnavajhala et al., 2018), using the SsoAdvanced Universal Probes Supermix (Bio-Rad, Hercules, CA). Assays were performed with primers and probes at a concentration of 400 and 300 nM, respectively. The conditions for the assay were 50°C for 2 min (hold), 95°C for 3 min (polymerase activation), 95°C for 15 s (DNA denaturation), 60°C for 30 s (annealing and extension), repeating steps three (DNA denaturation) and four (annealing and extension) for 40 cycles on a CFX384 Touch Real-Time PCR Detection System (Bio-Rad, Hercules, CA). Each defensin was run with at least four biological replicates per tissue, with each replicate being run in technical triplicate.

Statistical Analyses

The RT-qPCR data were statistically evaluated using Prism (Graphpad 8.2.1, San Diego, CA). Data were analyzed by normalizing the defensin genes to *β-actin* (ΔCt) and calculating the $2^{-\Delta Ct}$ of each reaction and performing a Student's *t*-test with Welch's correction to determine significance. In order to perform a statistical analysis, any gene that we could not detect expression in a given condition, the Ct value was set to 40 (the cutoff number of cycles). This was done for *otdC* in post-molt midguts and *otdD* in fed midguts. To determine the $\log_2$ fold change, the average fold change was calculating by dividing the $2^{-\Delta Ct}$ value by the average of the post-molt reactions $2^{-\Delta Ct}$ for that defensin and tissue. Subsequently, the $\log_2$ fold change for each reaction was determined and the mean and standard deviation calculated for fed and post-molt samples. Expression was significantly different if there was a $\log_2$ fold change of at least 1 (equivalent to a fold change of 2) and the *p*-value for the *t*-test was ≤ 0.05.

RESULTS

Molecular Analysis of *O. turicata* Defensins

We evaluated the *O. turicata* salivary gland transcriptome (Bourret et al., 2019) with the goal of identifying defensin transcripts. Through this analysis we identified five candidates. RACE and Sanger sequencing validated the transcriptome results and confirm the full coding sequence of each defensin. We analyzed the full coding sequences by BLASTp and one candidate was omitted because the full-length cDNA failed to align to known arthropod defensins. The remaining four defensin genes were designated putative *O. turicata defensin A* (*otdA*), *B* (*otdB*), *C* (*otdC*), and *D* (*otdD*), and their sequences are in **Table 2**.

We used the ProP 1.0 server to predict potential cleavage sites within the defensin sequences and to identify the signal, pro-, and mature peptides (**Table 2**). OtdA was predicted to have both a signal peptide and propeptide, as indicated by the presence of a furin motif (RVRR), while OtdB, OtdC, and OtdD only had predicted signal peptides. No other *O. turicata* putative defensins contained the furin motif. The amino acid

TABLE 2 | Predicted cleavage sites of putative *O. turicata* defensins.

Defensin	Amino acid sequence
OtdA	MKTVFVIALVFALAVASMA*QDVDDVEESSAVRVRR ∧ GYGC PFNQYQCHSHCSGIRGYKGGYCKGLFKQTCTCY
OtdB	MKVLCFLLLLLLTGLLTSRA*AVLDTRRDPEDGT‡GNDCPHN EIACTLKCERDGFAYGRCTGLVLDQKCECIA
OtdC	MTPLRFSLVCFLVLSAVVTATA*FQLRSVHNTEH‡AYGCPGY RAMCRKHCVETFGFEGYCGGAHRNECKCRG
OtdD	MKIVLVLLVCVMAFGVHS*SPPAADGGSGY‡GNGCPSNPAQ CNQHCLDTRDLTGHCKGYQMTFCDCGW

**Signal peptide cleavage site; ∧ propeptide cleavage site; ‡ predicted mature peptide start site if there is no propeptide.*

sequences of the mature putative defensins also were aligned to the sequences of 10 tick defensins from ixodids and argasids (**Figure 1**). Importantly, all four putative *O. turicata* defensins had six cysteines that aligned with the cysteines of other tick defensins (**Figure 1**). OtdA also had the most conserved amino acids (67.6%) of any of the *O. turicata* defensins when compared to the other proteins. OtdB had the fewest conserved amino acids (25.5%), while OtdC and OtdD had 27.1 and 31.3% amino acid identity, respectively. Except for *A. monolakensis*, all other tick defensin sequences had at least 46.2% of their amino acids identical, and 7 of 10 sequences had more than 50% amino acid identity.

Using protein modeling templates, tertiary structures of the putative *O. turicata* defensins were predicted. Included in the analyses were the tertiary structures for *O. moubata* defensin A and *A. monolakensis* defensin because they were the most similar to the *O. turicata* defensins (**Figures 2A,B**). All the evaluated defensins had an alpha helix followed by two beta

Tick Species	Defensin name	1	2	3	4	5	6	7	8	9	10	11	12	13	14	15	16	17	18	19
																				*
O. turicata	OtdA	-	-	-	-	-	-	-	-	-	-	-	-	G	Y	G	-	-	C	
O. turicata	OtdB	A	V	L	D	T	R	R	D	P	E	D	G	T	G	N	D	-	-	C
O. turicata	OtdC	-	F	Q	L	R	S	V	H	-	N	T	E	H	A	Y	G	-	-	C
O. turicata	OtdD	-	-	-	-	S	P	P	A	A	D	G	G	S	G	Y	G	N	G	C
O. moubata	defensin A	-	-	-	-	-	-	-	-	-	-	-	-	-	G	Y	G	-	-	C
O. papillipes	defensin B	-	-	-	-	-	-	-	-	-	-	-	-	-	G	Y	G	-	-	C
O. coriaceus	defensin	-	-	-	-	-	-	-	-	-	-	-	-	-	G	C	G	-	-	C
C. puertoricensis	defensin B	-	-	-	-	-	-	-	-	-	-	-	-	-	G	Y	G	-	-	C
I. ricinus	defensin	-	-	-	-	-	-	-	-	-	-	-	-	G	G	Y	Y	-	-	C
I. scapularis	defensin	-	-	-	-	-	-	-	-	-	-	-	-	S	G	Y	Y	-	-	C
H. longicornis	defensin DFS2	-	-	-	-	-	-	-	-	-	-	-	-	-	G	F	G	-	-	C
D. variabilis	varisin A1	-	-	-	-	-	-	-	-	-	-	-	-	-	G	F	G	-	-	C
A. americanum	amercin	-	-	-	-	-	-	-	-	-	-	-	-	-	G	F	G	-	-	C
A. monolakensis	defensin	-	L	P	P	R	I	I	H	H	N	T	G	H	A	Y	G	-	-	C

Tick Species	Defensin name	20	21	22	23	24	25	26	27	28	29	30	31	32	33	34	35	36	37
								*				*							
O. turicata	OtdA	P	F	N	Q	Y	Q	C	H	S	H	C	S	G	I	R	G	Y	K
O. turicata	OtdB	P	H	N	E	I	A	C	T	L	K	C	E	R	D	-	G	F	A
O. turicata	OtdC	P	G	Y	R	A	M	C	R	K	H	C	V	E	T	F	G	F	E
O. turicata	OtdD	P	S	N	P	A	Q	C	N	Q	H	C	L	D	T	-	R	D	L
O. moubata	defensin A	P	F	N	Q	Y	Q	C	H	S	H	C	S	G	I	R	G	Y	K
O. papillipes	defensin B	P	F	N	Q	Y	Q	C	H	S	H	C	R	G	I	R	G	Y	K
O. coriaceus	defensin	P	L	N	Q	G	A	C	H	R	H	C	K	S	I	-	G	R	R
C. puertoricensis	defensin B	P	F	N	Q	Y	Q	C	H	S	H	C	R	G	I	R	G	Y	K
I. ricinus	defensin	P	F	F	Q	D	K	C	H	R	H	C	R	S	F	-	G	R	K
I. scapularis	defensin	P	F	Q	Q	D	K	C	H	L	H	C	I	S	I	-	G	R	K
H. longicornis	defensin DFS2	P	L	N	Q	G	A	C	H	R	H	C	R	S	I	-	R	R	R
D. variabilis	varisin A1	P	L	N	Q	G	A	C	H	N	H	C	R	S	I	-	R	R	R
A. americanum	amercin	P	F	N	Q	Y	Q	C	H	S	H	C	L	S	I	-	G	R	R
A. monolakensis	defensin	P	D	D	Y	S	R	C	Q	Q	H	C	S	A	T	F	G	W	T

Tick Species	Defensin name	38	39	40	41	42	43	44	45	46	47	48	49	50	51	52	53	54	55
				*									*		*				
O. turicata	OtdA	G	G	Y	C	K	G	-	L	F	K	Q	T	C	T	C	Y	-	-
O. turicata	OtdB	Y	G	R	C	T	G	L	V	L	D	Q	K	C	E	C	I	A	-
O. turicata	OtdC	-	G	Y	C	G	G	-	A	H	R	N	E	C	K	C	R	G	-
O. turicata	OtdD	T	G	H	C	K	G	-	Y	Q	M	T	F	C	D	C	G	W	-
O. moubata	defensin A	G	G	Y	C	K	G	-	T	F	K	Q	T	C	K	C	Y	-	-
O. papillipes	defensin B	G	G	Y	C	T	G	-	R	F	K	Q	T	C	K	C	Y	-	-
O. coriaceus	defensin	G	G	Y	C	A	G	-	F	L	K	Q	T	C	T	C	Y	R	N
C. puertoricensis	defensin B	G	G	Y	C	T	G	-	R	F	K	Q	T	C	K	C	Y	-	-
I. ricinus	defensin	A	G	Y	C	G	G	-	F	L	K	K	T	C	I	C	V	-	-
I. scapularis	defensin	A	G	Y	C	G	N	-	F	L	K	R	T	C	I	C	V	M	K
H. longicornis	defensin DFS2	G	G	Y	C	S	G	-	I	I	K	Q	T	C	T	C	Y	R	N
D. variabilis	varisin A1	G	G	Y	C	S	G	-	I	I	K	Q	T	C	T	C	Y	R	N
A. americanum	amercin	G	G	Y	C	G	G	-	S	F	K	T	T	C	T	C	Y	N	-
A. monolakensis	defensin	-	G	W	C	G	G	-	V	T	R	G	E	C	K	C	R	E	-

FIGURE 1 | Alignment of mature tick defensin amino acid sequences. Amino acid sequences for the mature peptide of 10 tick defensins and our four putative defensins were obtained from NCBI and RACE sequencing, respectively. Alignment was performed using ClustalW in MEGAX 10.0.5. Shaded amino acids indicate amino acids that are shared among at least 50% of the sequences. Asterisks indicated the cysteines common to defensins. Numbers indicate the position of amino acids.

sheets held together by three disulfide bridges. As is characteristic of arthropod defensins, it is predicted that the disulfide bridges form between C1–C4, C2–C5, and C3–C6. From the prediction, OtdA and *O. moubata* defensin A had longer alpha helices (11 amino acids) and shorter beta sheets (three amino acids) (**Figure 2A**). OtdB had a longer alpha helix (10 amino acids) and longer beta sheets (five amino acids) (**Figure 2A**). OtdC and OtdD had shorter alpha helices (nine amino acids) and longer beta sheets (five amino acids), which was similar to *A. monolakensis* defensin (alpha helix: eight amino acids, beta sheets: five amino acids) (**Figure 2B**).

Phylogenetic Analysis of Arthropod Defensins

A maximum likelihood (ML) analysis of tick, insect, and scorpion mature defensins and defensin-like toxins was generated to assess the evolutionary relationship between our novel putative *O. turicata* defensins and other arthropod defensins (**Figure 3**). The ML analysis showed a distinct clade for scorpion defensin-like toxins (orange), insect defensins (green), and four clades for tick defensins. OtdA was within a clade made up of *Ornithodoros* and *Argas* defensins. OtdB, OtdC, and OtdD clustered together in one clade with *Argas* and *Amblyomma* defensins.

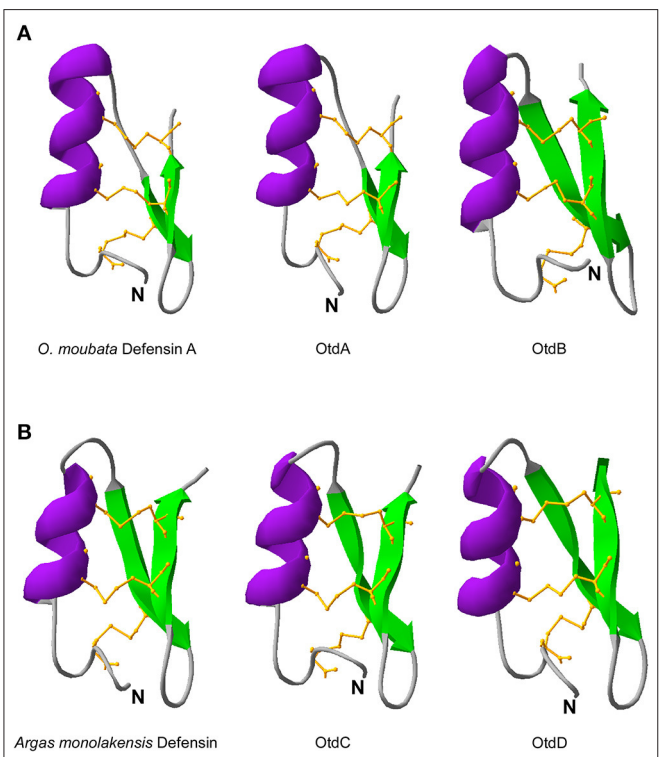

FIGURE 2 | Predicted protein structure of defensins. In **(A)** are the protein structure of soft tick defensins *O. moubata* and the two most structurally similar *O. turicata* defensins, OtdA, OtdB. In **(B)** *A. monolakensis* defensin is shown with the most similar *O. turicata* defensins, OtdC and OtdD. Structures were predicted using MODELLER and visualized using SWISS-PDB viewer. Purple represents the alpha helix, green are the beta sheets, and the orange ball and stick regions are the disulfide bridges between cysteines C1–C4, C2–C5, and C3–C6. *N* represents the *N* terminus of the model.

Expression of *O. turicata* Defensins in the Midgut and Salivary Glands of Post-molt and Fed Ticks

Previous studies indicate midgut and salivary gland colonization is essential for pathogen transmission from *Ornithodoros* species (Hess et al., 1987; Lopez et al., 2011; Boyle et al., 2014; Krishnavajhala et al., 2017). Therefore, expression of the four putative defensins was further evaluated in pooled midguts and salivary glands 1 week after ticks fed and after they molted. Expression was considered significantly different if there was a $\log_2$ fold change of at least 1 and the $p \leq 0.05$. In fed ticks (**Figure 4A**), *otdA* and *otdC* were up-regulated compared to post-molt *O. turicata*. *otdA* was expressed in the midgut of post-molt ticks and significantly up-regulated in the midgut within a week after feeding ($\log_2$ fold change $= 2.26 \pm 0.29$) (**Figure 4A**). *otdA* was expressed in the salivary glands of fed and post-molt ticks and there was not a significant change in expression between the conditions. Also, we did not detect transcripts of *otdC* within 40 cycles in the midgut of post-molt ticks, but the gene was significantly up-regulated in fed ticks ($\log_2$ fold change $= 3.46 \pm 1.18$) (**Figure 4A**). *otdC* was expressed in the salivary glands of post-molt ticks and was significantly up-regulated within 1 week after ticks fed ($\log_2$ fold change $= 4.14 \pm 0.35$) (**Figure 4A**).

We also detected defensin genes to be up-regulated in post-molt ticks (**Figure 4B**). Transcripts of *otdD* were not detected in the midgut of fed ticks but the gene was up-regulated after ticks molted ($\log_2$ fold change $= 7.32 \pm 1.59$) (**Figure 4B**). Moreover, this gene was expressed in the salivary glands of fed ticks and significantly up-regulated in post-molt *O. turicata* ($\log_2$ fold change $= 2.52 \pm 1.31$) (**Figure 4B**). While there was no significant difference in *otdB* expression in the midgut between fed and post-molt ticks, the gene was significantly up-regulated in the salivary glands of post-molt ticks relative to fed ticks ($\log_2$ fold change $= 3.82 \pm 2.02$) (**Figure 4B**).

DISCUSSION

The present study identified transcripts coding for annotated defensins from *O. turicata* and assessed their expression in the midgut and salivary glands of fed and post-molted ticks. Since the four putative defensin genes (*otdA*, *otdB*, *otdC*, and *otdD*) were initially identified in a salivary gland transcriptome from *O. turicata* (Bourret et al., 2019), we determined and validated their full sequences. Additionally, a computational analysis identified conserved motifs and the six cysteines characteristic of defensins. The expression patterns of these defensins in the midgut and salivary glands suggested they may have differing functional roles dependent upon whether the tick is fed or in the post-molted state. Collectively, these findings set the framework to further define soft tick immunity, an understudied aspect of vector biology.

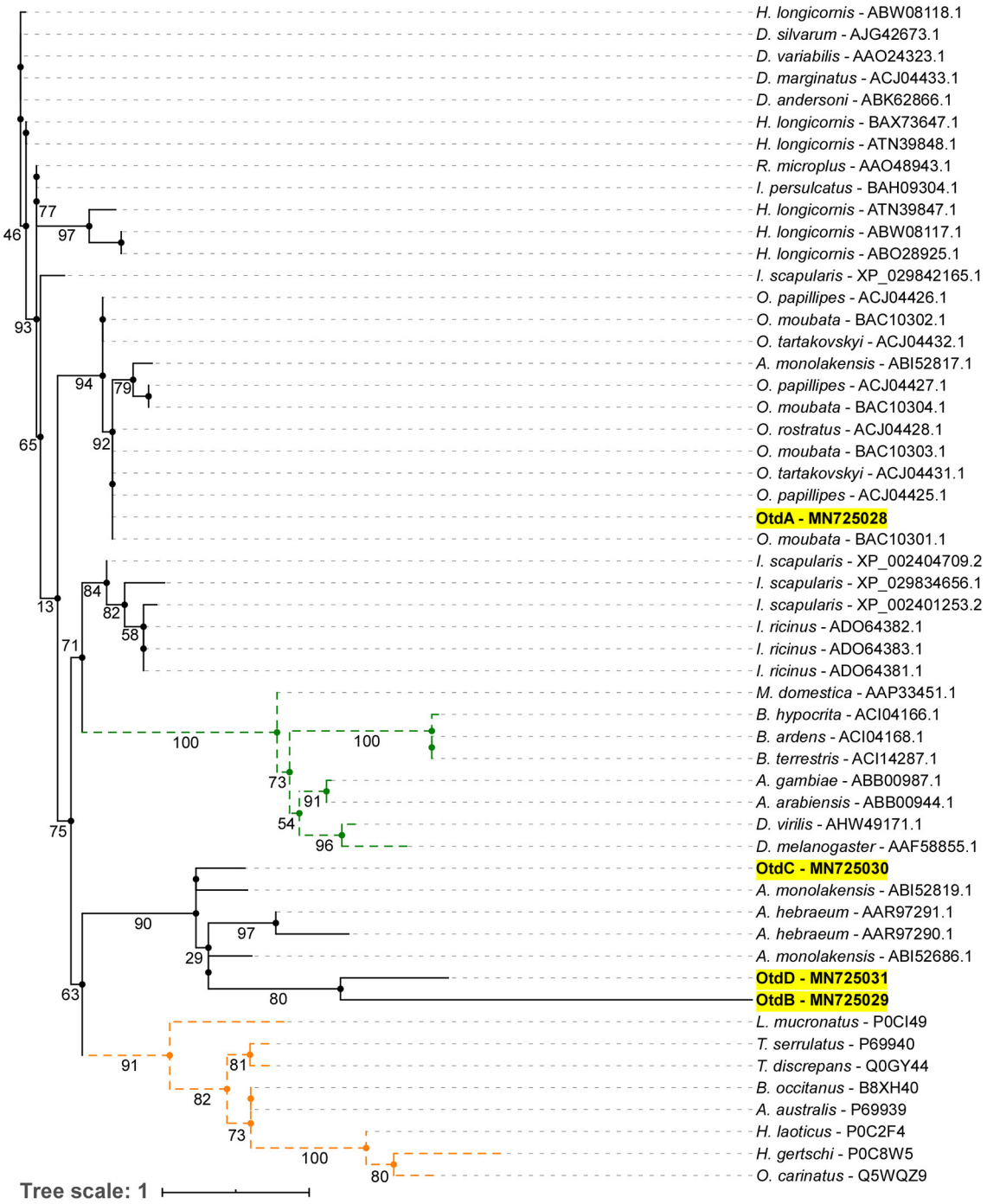

FIGURE 3 | Phylogenetic tree of mature arthropod defensins. Maximum likelihood tree showing mature protein region of defensins from ticks and insects, and defensin-like scorpion toxins. Bootstrap values (1,000 bootstraps) are shown at the nodes. Names highlighted in yellow represent the *O. turicata* defensins (OtdA, OtdB, OtdC, and OtdD) introduced in this manuscript. Dotted orange lines represent scorpion toxin, defensin-like sequences, and dotted green lines represent insect defensin sequences.

Seminal work in *Ornithodoros* defensins was performed in the Old World species *O. moubata.* Van der Goes van Naters-Yasui and colleagues purified and determined the partial amino acid sequence of a small peptide (4 kDa) with homology to a scorpion defensin (Van Der Goes Van Naters-Yasui et al., 1999). Subsequently, Nakajima and co-workers identified four isoforms of this defensin that were over 78% homologous, constitutively produced in the midgut lumen of *O. moubata,* and up-regulated after ticks blood fed (Nakajima et al., 2001, 2002a,b). In *O. turicata,* OtdA was most homologous to *O.*

moubata defensin isoform A. While additional isoforms of OtdA were not identified in our study, our transcriptional findings were consistent with the work performed in *O. moubata*. We detected *otdA* transcript in post-molt ticks, and upon feeding the gene was up-regulated in the midgut. Moreover, we expanded our investigation to assess *otdA* expression in the salivary glands, which is another tissue typically colonized by pathogens (Boyle et al., 2014; Krishnavajhala et al., 2017). Within the salivary glands *otdA* was expressed, but we failed to detect a change in transcript levels in response to blood feeding.

Our computational analyses indicated differences in amino acid motifs between the four identified defensins. Typically, arthropod defensin motifs include a signal peptide, a propeptide, and a mature peptide that consists of six cysteine residues that form three disulfide bonds (Bulet and Stöcklin, 2005). Furthermore, the propeptide is characterized by a furin motif that serves as a cleavage site. OtdA was most similar to other known tick defensins because it contained the signal peptide and propeptide. OtdB, OtdC, and OtdD lacked the propetide but retained the signal peptide. Furthermore, these proteins contain the necessary cysteines for disulfide bridge formation in the mature peptide, which is critical for microbicidal activity (Bulet and Stöcklin, 2005). Our findings suggest that not all defensins require the furin cleavage site for functionality, and that OtdB, OtdC, and OtdD likely form a mature peptide after the signal peptide is cleaved. In support of this, production of synthetic defensins only consists of the mature peptides, and they retain their functional activity (Nakajima et al., 2002b; Prinsloo et al., 2013; Malan et al., 2016).

While defensins are important in tick immunity, studies indicate that they possess a dual-function role in homeostasis. OsDef2, a defensin identified in *Ornithodoros savignyi,* was shown to have immune function and antioxidant properties acting as a scavenger for ROS and RNS, respectively) (Prinsloo et al., 2013; Malan et al., 2016). Previous work indicated that the midgut and salivary glands of *O. turicata* are nitrosative and oxidative environments, respectively (Bourret et al., 2019). Expression of two putative dual oxidase (*duox1* and *duox2*) genes in midgut tissue from *O. turicata,* and a single nitric oxide synthase (*nos*) gene, was expressed in salivary glands (Bourret et al., 2019). Immunofluorescent staining of *O. turicata* further validated transcriptional findings and determined the production of RNS in midguts and ROS in salivary glands (Bourret et al., 2019). Given these findings, determining a dual role of tick defensins in homeostasis and immunity is important for the development of control measures for these vectors and their respective pathogenic microbes.

Pathogens transmitted by *Ornithodoros* ticks have evolved to colonize this long-lived vector that completes blood feeding within minutes of attachment to the host. Vector competence studies in relapsing fever spirochete and ASFV models demonstrated persistent colonization of *Ornithodoros* midguts, and within ∼10–20 days the pathogens colonize the salivary glands (Hess et al., 1987; Schwan and Hinnebusch, 1998; Boyle et al., 2014; Krishnavajhala et al., 2017). Once colonized, the tick remains infected for years (Davis, 1943; Hess et al., 1987). Consequently, the tick immune response likely plays a role in early pathogen colonization after blood feeding and during persistent infection in post-molt ticks.

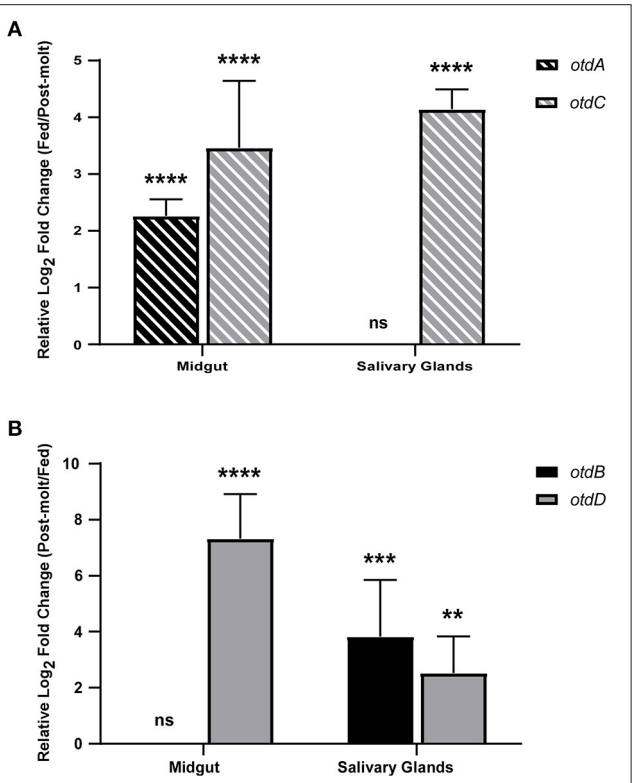

FIGURE 4 | Expression analysis of putative *O. turicata* defensins in post-molt and fed midguts and salivary glands. Putative *O. turicata* defensins **(A,B)** expression was assessed in the fed and post-molt midguts and salivary glands. Defensin expression was normalized to *β-actin* expression and the relative $\log_2$ fold change was calculated using the $2^{-\Delta Ct}$ method with post-molt **(A)** or fed **(B)** tissues as the control. Statistical significance was calculated between post-molt and fed tissue using the Student's *t*-test with Welch's correction. (*P*-value: **≤0.01, ***≤0.001, ****≤0.0001).

The expression kinetics of *otdA, otdB, otdC,* and *otdD* suggest functional roles of the proteins in early and persistent colonization, and our hypothesized model is shown in **Figure 5**. For example, *otdA* and *otdC* were significantly up-regulated in the midgut within a week after blood feeding, which suggests the proteins function in homeostasis and during early pathogen colonization. In the midgut of post-molt ticks, the up-regulation of *otdD* suggests the protein may function in maintaining pathogen load during persistent colonization.

Our study also evaluated defensin expression in salivary glands, which is an important tissue for pathogen maintenance and transmission. In these tissues, *otdC* was expressed in post-molt ticks and up-regulated within a week after blood feeding. We hypothesize that this gene may function in tick immunity during early microbe colonization of the salivary glands (**Figure 5**). Furthermore, persistent infection may be characterized by the up-regulation of *otdB* and *otdD*. While these genes were expressed 1 week after blood feeding, they were up-regulated after *O. turicata* molted.

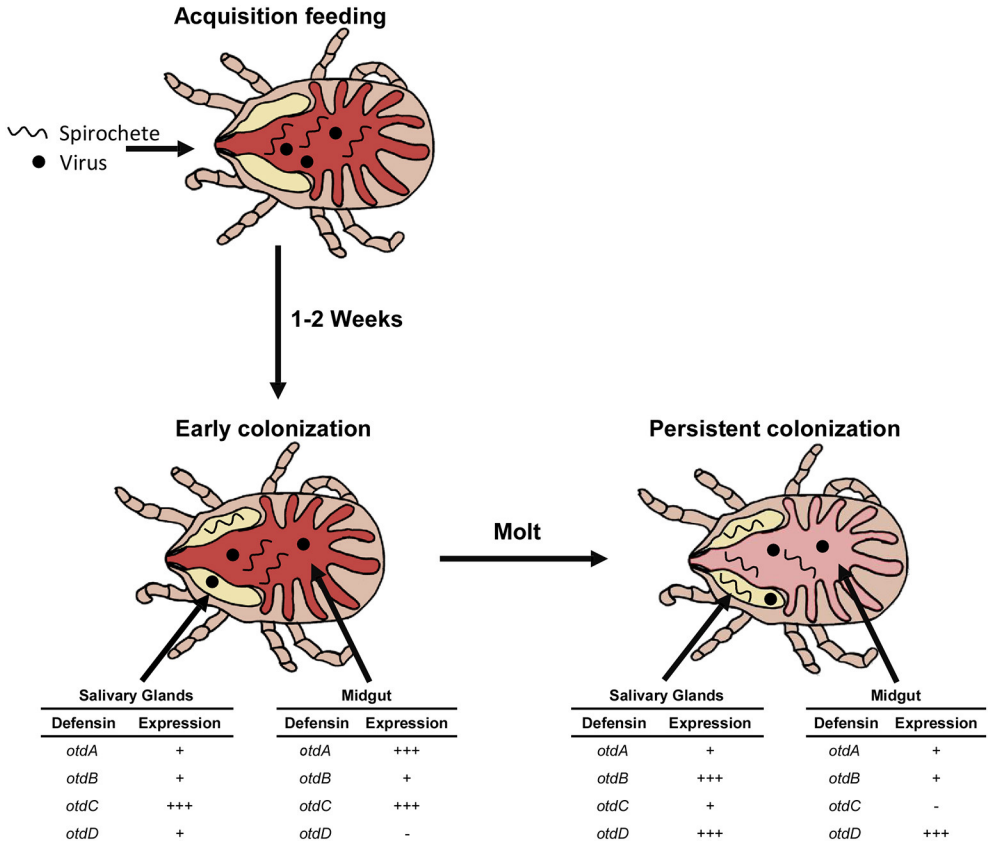

Salivary Glands		Midgut	
Defensin	Expression	Defensin	Expression
otdA	+	*otdA*	+++
otdB	+	*otdB*	+
otdC	+++	*otdC*	+++
otdD	+	*otdD*	-

Salivary Glands		Midgut	
Defensin	Expression	Defensin	Expression
otdA	+	*otdA*	+
otdB	+++	*otdB*	+
otdC	+	*otdC*	-
otdD	+++	*otdD*	+++

FIGURE 5 | Model of pathogen colonization and defensin expression. Spirochetes and viruses are imbibed during the acquisition blood feeding and enter the midgut (red). Over the next 1–2 weeks a subset of the population migrates out of the midgut to colonize the salivary glands (yellow). At this time there is an upregulation (+ + +) of *otdA* and *otdC* in the midgut and *otdC* in the salivary glands. *otdB* is expressed (+) in the midgut. *otdD* is not expressed in the midgut (-) but transcript detected in the salivary glands with *otdA* and *otdB*. This characterizes early pathogen colonization of the tick. Persistent colonization occurs after the tick has molted and the pathogen remain in both the midgut (light red) and salivary glands. In the midgut *otdA* and *otdB* are expressed (+), *otdC* is not expressed (-), and *otdD* is upregulated (+ + +). In the salivary glands *otdA* and *otdC* are expressed (+), while *otdB* and *otdD* are upregulated (+ + +).

With very little work focused on soft tick immunity and defensins, our study provides a basis to further define the molecular mechanisms of vector competence. While we assessed expression kinetics of four novel defensins in late stage *O. turicata* nymphs, additional studies should confirm expression at different tick life stages. Additionally, given that relapsing fever spirochetes and ASFV are transmitted transovarially, assessment of defensin expression in reproductive organs is an important aspect of vector biology and pathogenesis. Future work will also focus on the validation of our transcriptional findings at the protein level. We will also assess the bactericidal properties of the identified putative defensins on relapsing fever spirochetes and determine whether the pathogens have evolved mechanisms to modulate tick immunity. These studies will provide critical insight into the maintenance of pathogens in an understudied tick vector.

DATA AVAILABILITY STATEMENT

The datasets generated for this study can be found in the Genbank database with the following accession numbers: otdA (MN725028), otdB (MN725029), otdC (MN725030), and otdD (MN725031).

ETHICS STATEMENT

Tick feedings were performed with mice in accordance with the Institutional Care and Use Committee (IACUC) at Baylor College of Medicine under protocol number AN-6563. The animal program at Baylor College of Medicine is compliant with standards and guidance established by the Association for the Assessment and Accreditation of Laboratory Animal Care and the Nation Institution of Health of Laboratory Animal Welfare. The animal husbandry team at Baylor College of Medicine provided all veterinary staff and animal care.

AUTHOR CONTRIBUTIONS

BA designed the study, performed experiments, analyzed data, and wrote the manuscript. ARK performed the experiments and data analysis. RM performed the phylogenetic analysis and wrote the phylogenetic analysis. AK performed experiments

and assisted in data analysis. PT provided samples and provided experimental critique. AP contributed to phylogenetic analysis. JL designed the study, analyzed the data, and wrote the manuscript.

FUNDING

These studies were supported by AI123651 and AI137412 (JL) and Baylor College of Medicine Junior Faculty Seed Grant (JL).

REFERENCES

Altschul, S. F., Gish, W., Miller, W., Myers, E. W., and Lipman, D. J. (1990). Basic local alignment search tool. *J. Mol. Biol.* 215, 403–410. doi: 10.1016/S0022-2836(05)80360-2

Assous, M. V., and Wilamowski, A. (2009). Relapsing fever borreliosis in Eurasia–forgotten, but certainly not gone! *Clin. Microbiol. Infect*. 15, 407–414. doi: 10.1111/j.1469-0691.2009.02767.x

Balashov, Y. S. (1972). Bloodsucking ticks (Ixodoidea)- vectors of diseases of man and animals. *Misc. Publ. Entomol. Soc. Am*. 8, 161–376.

Bissett, J. D., Ledet, S., Krishnavajhala, A., Armstrong, B. A., Kliioueva, A., Sexton, C., et al. (2018). Detection of tickborne relapsing fever spirochete, Austin, Texas, USA. *Emerg. Infect. Dis*. 24, 2003–2009. doi: 10.3201/eid2411.172033

Boulanger, N., Bulet, P., and Lowenberger, C. (2006). Antimicrobial peptides in the interactions between insects and flagellate parasites. *Trends Parasitol.* 22, 262–268. doi: 10.1016/j.pt.2006.04.003

Bourret, T. J., Boyle, W. K., Zalud, A. K., Valenzuela, J. G., Oliveira, F., and Lopez, J. E. (2019). The relapsing fever spirochete *Borrelia turicatae* persists in the highly oxidative environment of its soft-bodied tick vector. *Cell Microbiol*. 21:e12987. doi: 10.1111/cmi.12987

Boyle, W. K., Wilder, H. K., Lawrence, A. M., and Lopez, J. E. (2014). Transmission dynamics of Borrelia turicatae from the arthropod vector. *PLoS Negl. Trop. Dis*. 8:e2767. doi: 10.1371/journal.pntd.0002767

Bulet, P., and Stöcklin, R. (2005). Insect antimicrobial peptides structures, properties and gene regulation. *Protein. Pept. Lett*. 12, 3–11. doi: 10.2174/0929866053406011

Christensen, A. M., Pietralczyk, E., Lopez, J. E., Brooks, C., Schriefer, M. E., Wozniak, E., et al. (2017). Diagnosis and management of *Borrelia turicatae* infection in febrile soldier, Texas, USA. *Emerg. Infect. Dis*. 23, 883–884. doi: 10.3201/eid2305.162069

Chrudimska, T., Cerovsky, V., Slaninova, J., Rego, R. O., and Grubhoffer, L. (2014). Defensin from the ornate sheep tick *Dermacentor marginatus* and its effect on Lyme borreliosis spirochetes. *Dev. Comp. Immunol*. 46, 165–170. doi: 10.1016/j.dci.2014.04.005

Chrudimska, T., Chrudimsky, T., Golovchenko, M., Rudenko, N., and Grubhoffer, L. (2010). New defensins from hard and soft ticks: similarities, differences, and phylogenetic analyses. *Vet. Parasitol*. 167, 298–303. doi: 10.1016/j.vetpar.2009.09.032

Cooley, R. A., and Kohls, G. M. (1944). *The Agarasidae of North America, Central America, and Cuba*. Notre Dame, IN: The University Press.

Davis, G. E. (1939). Ornithodoros parkeri: distribution and host data; spontaneous infection with relapsing fever spirochetes. *Pub. Health Rep*. 54, 1345–1349. doi: 10.2307/4582963

Davis, G. E. (1943). Relapsing fever: the tick *Ornithodoros turicata* as a spirochetal reservoir. *Pub. Health Rep*. 58, 839–842. doi: 10.2307/4584474

Donaldson, T. G., Perez De Leon, A. A., Li, A. I., Castro-Arellano, I., Wozniak, E., Boyle, W. K., et al. (2016). Assessment of the geographic distribution of *Ornithodoros turicata* (Argasidae): climate variation and host diversity. *PLoS Negl. Trop. Dis*. 10:e0004383. doi: 10.1371/journal.pntd.0004383

Dress, A. W. M., Flamm, C., Fritzsch, G., Grünewald, S., Kruspe, M., Prohaska, S. J., et al. (2008). Noisy: identification of problematic columns in multiple sequence alignments. *Algorithms Mol. Biol.* 3:7. doi: 10.1186/1748-7188-3-7

Duckert, P., Brunak, S., and Blom, N. (2004). Prediction of proprotein convertase cleavage sites. *Protein Eng. Des. Sel*. 17, 107–112. doi: 10.1093/protein/gzh013

Dworkin, M. S., Schwan, T. G., and Anderson, D. E. (2002). Tick-borne relapsing fever in North America. *Med. Clin. North Amer*. 86, 417–433. doi: 10.1016/S0025-7125(03)00095-6

Edgar, R. C. (2004). MUSCLE: multiple sequence alignment with high accuracy and high throughput. *Nucleic Acids Res*. 32, 1792–1797. doi: 10.1093/nar/gkh340

Fogaça, A. C., Almeida, I. C., Eberlin, M. N., Tanaka, A. S., Bulet, P., and Daffre, S. (2006). Ixodidin, a novel antimicrobial peptide from the hemocytes of the cattle tick *Boophilus microplus* with inhibitory activity against serine proteinases. *Peptides* 27, 667–674. doi: 10.1016/j.peptides.2005.07.013

Grubhoffer, L., Kovár, V., and Rudenko, N. (2004). Tick lectins: structural and functional properties. *Parasitology* 129, S113–S125. doi: 10.1017/S0031182004004858

Grunclová, L., Fouquier, H., Hypša, V., and Kopáček, P. (2003). Lysozyme from the gut of the soft tick *Ornithodoros moubata*: the sequence, phylogeny and post-feeding regulation. *Dev. Comp. Immunol.* 27, 651–660. doi: 10.1016/S0145-305X(03)00052-1

Guex, N., and Peitsch, M. C. (1997). SWISS-MODEL and the Swiss-Pdb Viewer: an environment for comparative protein modeling. *Electrophoresis* 18, 2714–2723. doi: 10.1002/elps.1150181505

Hajdusek, O., Sima, R., Ayllon, N., Jalovecka, M., Perner, J., De La Fuente, J., et al. (2013). Interaction of the tick immune system with transmitted pathogens. *Front. Cell. Infect. Microbiol*. 3:26. doi: 10.3389/fcimb.2013.00026

Hess, W. R., Endris, R. G., Haslett, T. M., Monahan, M. J., and Mccoy, J. P. (1987). Potential arthropod vectors of African swine fever virus in North America and the Caribbean basin. *Vet. Parasitol*. 26, 145–155. doi: 10.1016/0304-4017(87)90084-7

Hosaka, M., Nagahama, M., Kim, W. S., Watanabe, T., Hatsuzawa, K., Ikemizu, J., et al. (1991). Arg-X-Lys/Arg-Arg motif as a signal for precursor cleavage catalyzed by furin within the constitutive secretory pathway. *J. Biol. Chem.* 266, 12127–12130.

Hynes, W. L. (2014). "How ticks control microbes," in *Biology of Ticks*, eds D. E. Sonenshine and R. M. Roe (New York, NY: Oxford University Press), 129–146.

Isogai, E., Isogai, H., Okumura, K., Hori, H., Tsuruta, H., and Kurebayashi, Y. (2011). Tertiary structure-related activity of tick defensin (persulcatusin) in the taiga tick, *Ixodes persulcatus*. *Exp. Appl. Acarol*. 53, 71–77. doi: 10.1007/s10493-010-9379-3

Kim, H. J., Filatov, S., Lopez, J. E., Pérez De León, A. A., and Teel, P. D. (2017). Blood feeding of *Ornithodoros turicata* larvae using an artificial membrane system. *Med. Vet. Entomol*. 31, 230–233. doi: 10.1111/mve.12223

Kopáček, P., Hajdušek, O., Burešová, V., and Daffre, S. (2010). "Tick innate immunity," in *Invertebrate Immunity*, eds K. Söderhäll (Springer Science+Business Media, LLC), 137–162. doi: 10.1007/978-1-4419-8059-5_8

Krishnavajhala, A., Armstrong, B. A., and Lopez, J. E. (2018). Vector competence of geographical populations of *Ornithodoros turicata* for the tick-borne relapsing fever spirochete *Borrelia turicatae*. *Appl. Environ. Microbiol*. 84:18. doi: 10.1128/AEM.01505-18

Krishnavajhala, A., Wilder, H. K., Boyle, W. K., Damania, A., Thornton, J. A., Perez De Leon, A. A., et al. (2017). Imaging of *Borrelia turicatae* producing the green fluorescent protein reveals persistent colonization of the *Ornithodoros turicata* midgut and salivary glands from nymphal acquisition through transmission. *Appl. Environ. Microbiol*. 83:16. doi: 10.1128/AEM.02503-16

Kumar, S., Stecher, G., Li, M., Knyaz, C., and Tamura, K. (2018). MEGA X: molecular evolutionary genetics analysis across computing platforms. *Mol. Biol. Evol*. 35, 1547–1549. doi: 10.1093/molbev/msy096

Lai, R., Takeuchi, H., Lomas, L. O., Jonczy, J., Rigden, D. J., Rees, H. H., et al. (2004). A new type of antimicrobial protein with multiple histidines from the hard tick, *Amblyomma hebraeum*. *Faseb J* 18, 1447–1459. doi: 10.1096/fj.03-1154fje

Lane, R. S., Burgdorfer, W., Hayes, S. F., and Barbour, A. G. (1985). Isolation of a spirochete from the soft tick, *Ornithodoros coriaceus*: a possible agent of epizootic bovine abortion. *Science* 230, 85–87. doi: 10.1126/science.3898367

Lemoine, F., Domelevo Entfellner, J. B., Wilkinson, E., Correia, D., Dávila Felipe, M., De Oliveira, T., et al. (2018). Renewing Felsenstein's phylogenetic bootstrap in the era of big data. *Nature* 556, 452–456. doi: 10.1038/s41586-018-0043-0

Liu, Z., Liu, H., Liu, X., and Wu, X. (2008). Purification and cloning of a novel antimicrobial peptide from salivary glands of the hard tick, *Ixodes*

sinensis. *Comp. Biochem. Physiol. B. Biochem. Mol. Biol.* 149, 557–561. doi: 10.1016/j.cbpb.2007.10.002

Lopez, J. E., Krishnavahjala, A., Garcia, M. N., and Bermudez, S. E. (2016). Tick-borne relapsing fever spirochetes in the Americas. *Vet. Sci.* 3, 1–18. doi: 10.3390/vetsci3030016

Lopez, J. E., Mccoy, B. N., Krajacich, B. J., and Schwan, T. G. (2011). Acquisition and subsequent transmission of *Borrelia hermsii* by the soft tick *Ornithodoros hermsi*. *J. Med. Entomol.* 48, 891–895. doi: 10.1603/ME10283

Lopez, J. E., Wilder, H. K., Hargrove, R., Brooks, C. P., Peterson, K. E., Beare, P. A., et al. (2013). Development of genetic system to inactivate a *Borrelia turicatae* surface protein selectively produced within the salivary glands of the arthropod vector. *PLoS Negl. Trop. Dis.* 7:e2514. doi: 10.1371/journal.pntd.0002514

Malan, M., Serem, J. C., Bester, M. J., Neitz, A. W., and Gaspar, A. R. (2016). Anti-inflammatory and anti-endotoxin properties of peptides derived from the carboxy-terminal region of a defensin from the tick *Ornithodoros savignyi*. *J. Pept. Sci.* 22, 43–51. doi: 10.1002/psc.2838

Nakajima, Y., Ishibashi, J., Yukuhiro, F., Asaoka, A., Taylor, D., and Yamakawa, M. (2003a). Antibacterial activity and mechanism of action of tick defensin against Gram-positive bacteria. *Biochim. Biophys. Acta*. 1624, 125–130. doi: 10.1016/j.bbagen.2003.10.004

Nakajima, Y., Ogihara, K., Taylor, D., and Yamakawa, M. (2003b). Antibacterial hemoglobin fragments from the midgut of the soft tick, *Ornithodoros moubata* (Acari: Argasidae). *J. Med. Entomol.* 40, 78–81. doi: 10.1603/0022-2585-40.1.78

Nakajima, Y., Taylor, D., and Yamakawa, M. (2002a). Involvement of antibacterial peptide defensin in tick midgut defense. *Exp. Appl. Acarol.* 28, 135–140. doi: 10.1023/A:1025399610947

Nakajima, Y., Van Der Goes Van Naters-Yasui, A., Taylor, D., and Yamakawa, M. (2001). Two isoforms of a member of the arthropod defensin family from the soft tick, *Ornithodoros moubata* (Acari: Argasidae). *Insect. Biochem. Mol. Biol.* 31, 747–751. doi: 10.1016/S0965-1748(01)00066-2

Nakajima, Y., Van Der Goes Van Naters-Yasui, A., Taylor, D., and Yamakawa, M. (2002b). Antibacterial peptide defensin is involved in midgut immunity of the soft tick, *Ornithodoros moubata*. *Insect Mol. Biol.* 11, 611–618. doi: 10.1046/j.1365-2583.2002.00372.x

Nieto, N. C., Teglas, M. B., Stewart, K. M., Wasley, T., and Wolff, P. L. (2012). Detection of relapsing fever spirochetes (*Borrelia hermsii* and Borrelia coriaceae) in free-ranging mule deer (*Odocoileus hemionus*) from Nevada, United States. *Vector Borne Zoonotic Dis.* 12, 99–105. doi: 10.1089/vbz.2011.0716

Oliva Chavez, A. S., Shaw, D. K., Munderloh, U. G., and Pedra, J. H. (2017). Tick humoral responses: marching to the beat of a different drummer. *Front. Microbiol.* 8:e223. doi: 10.3389/fmicb.2017.00223

Price, M. N., Dehal, P. S., and Arkin, A. P. (2009). FastTree: computing large minimum evolution trees with profiles instead of a distance matrix. *Mol Biol Evol* 26, 1641–1650. doi: 10.1093/molbev/msp077

Price, M. N., Dehal, P. S., and Arkin, A. P. (2010). FastTree 2–approximately maximum-likelihood trees for large alignments. *PLoS ONE* 5:e9490. doi: 10.1371/journal.pone.0009490

Prinsloo, L., Naidoo, A., Serem, J., Taute, H., Sayed, Y., Bester, M., et al. (2013). Structural and functional characterization of peptides derived from the carboxy-terminal region of a defensin from the tick *Ornithodoros savignyi*. *J. Pept. Sci.* 19, 325–332. doi: 10.1002/psc.2505

Rodríguez-García, M. J., García-Reina, A., Machado, V., and Galián, J. (2016). Identification, structural characterisation and expression analysis of a defensin gene from the tiger beetle *Calomera littoralis* (Coleoptera: Cicindelidae). *Gene* 589:30. doi: 10.1016/j.gene.2016.05.030

Sage, K. M., Johnson, T. L., Teglas, M. B., Nieto, N. C., and Schwan, T. G. (2017). Ecological niche modeling and distribution of *Ornithodoros hermsi* associated with tick-borne relapsing fever in western North America. *PLoS Negl. Trop. Dis.* 11:e6047. doi: 10.1371/journal.pntd.0006047

Schwan, T. G. (1996). Ticks and Borrelia: model systems for investigating pathogen-arthropod interactions. *Infect. Agents Dis.* 5, 167–181.

Schwan, T. G., and Hinnebusch, B. J. (1998). Bloodstream- versus tick-associated variants of a relapsing fever bacterium. *Science* 280, 1938–1940. doi: 10.1126/science.280.5371.1938

Silva, F. D., Rezende, C. A., Rossi, D. C. P., Esteves, E., Dyszy, F. H., Schreier, S., et al. (2009). Structure and mode of action of microplusin, a copper II-chelating antimicrobial peptide from the cattle tick *Rhipicephalus (Boophilus) microplus*. *J. Biol. Chem.* 284, 34735–34746. doi: 10.1074/jbc.M109.016410

Sonenshine, D. E., Ceraul, S. M., Hynes, W. E., Macaluso, K. R., and Azad, A. F. (2002). Expression of defensin-like peptides in tick hemolymph and midgut in response to challenge with *Borrelia burgdorferi*, *Escherichia coli*, and *Bacillus subtilis*. *Exp. Appl. Acarol.* 28, 127–134. doi: 10.1023/A:1025354326877

Sonenshine, D. E., and Hynes, W. L. (2008). Molecular characterization and related aspects of the innate immune response in ticks. *Front. Biosci.* 13, 7046–7063. doi: 10.2741/3209

Sonenshine, D. E., Hynes, W. L., Ceraul, S. M., Mitchell, R., and Benzine, T. (2005). Host blood proteins and peptides in the midgut of the tick *Dermacentor variabilis* contribute to bacterial control. *Exp. Appl. Acarol.* 36, 207–223. doi: 10.1007/s10493-005-2564-0

Sonenshine, D. E., and Macaluso, K. R. (2017). Microbial invasion vs. tick immune regulation. *Front. Cell. Infect. Microbiol.* 7:e390. doi: 10.3389/fcimb.2017.00390

Tonk, M., Cabezas-Cruz, A., Valdés, J. J., Rego, R. O. M., Chrudimská, T., Strnad, M., et al. (2014). Defensins from the tick *Ixodes scapularis* are effective against phytopathogenic fungi and the human bacterial pathogen *Listeria grayi*. *Parasit. Vectors*. 7, 554–554. doi: 10.1186/s13071-014-0554-y

Van Der Goes Van Naters-Yasui, A., Taylor, D., Shono, T., and Yamakawa, M. (1999). "Purification and partial amino acid sequence of antibacterial peptides from the hemolymph of the soft tick, *Ornithodoros moubata*, (Acari: Argasidae)," in *Proceedings of the Third International Conference on Ticks and Tick-borne Pathogens: Into the 21st Century*, eds M. Kazimirova, M. Labuda, and P.A. Nutall (Institute of Zoology, Slovak Academy of Sciences), 189–194.

Webb, B., and Sali, A. (2016). Comparative protein structure modeling using MODELLER. *Curr. Protoc. Protein Sci.* 86, 291–297. doi: 10.1002/cpps.20

Wiederstein, M., and Sippl, M. J. (2007). ProSA-web: interactive web service for the recognition of errors in three-dimensional structures of proteins. *Nucleic Acids Res.* 35, W407–W410. doi: 10.1093/nar/gkm290

Zimmermann, L., Stephens, A., Nam, S.-Z., Rau, D., Kübler, J., Lozajic, M., et al. (2018). A completely reimplemented MPI bioinformatics toolkit with a new HHpred server at its core. *J. Mol. Biol.* 430, 2237–2243. doi: 10.1016/j.jmb.2017.12.007

Conflict of Interest: The authors declare that the research was conducted in the absence of any commercial or financial relationships that could be construed as a potential conflict of interest.

frontiers in Cellular and Infection Microbiology

CORRECTION
published: 02 July 2020
doi: 10.3389/fcimb.2020.00310

Corrigendum: Differential Expression of Putative *Ornithodoros turicata* Defensins Mediated by Tick Feeding

*Brittany A. Armstrong[1,2], Alexander R. Kneubehl[1,2], Robert D. Mitchell III[3], Aparna Krishnavajhala[2], Pete D. Teel[4], Adalberto A. Pérez de León[3] and Job E. Lopez[1,2]**

[1] Department of Molecular Virology and Microbiology, Baylor College of Medicine, Houston, TX, United States, [2] Department of Pediatrics, National School of Tropical Medicine, Baylor College of Medicine, Houston, TX, United States, [3] Knipling-Bushland U.S. Livestock Insects Research Laboratory, Veterinary Pest Genomics Center, Department of Agriculture—Agricultural Research Service, Kerrville, TX, United States, [4] Department of Entomology, Texas A&M AgriLife Research, College Station, TX, United States

Keywords: *Ornithdoros turicata*, antimicrobial peptide (AMP), gene expression, defensins, argasid (soft) ticks, immune response

OPEN ACCESS

Edited and reviewed by:
Emily Derbyshire, Duke University, United States

****Correspondence:***
Job E. Lopez
job.lopez@bcm.edu

Specialty section:
This article was submitted to Parasite and Host, a section of the journal Frontiers in Cellular and Infection Microbiology

Received: *08 May 2020*
Accepted: *22 May 2020*
Published: *02 July 2020*

Citation:
Armstrong BA, Kneubehl AR, Mitchell RD III, Krishnavajhala A, Teel PD, Pérez de León AA and Lopez JE (2020) Corrigendum: Differential Expression of Putative Ornithodoros turicata Defensins Mediated by Tick Feeding. Front. Cell. Infect. Microbiol. 10:310. doi: 10.3389/fcimb.2020.00310

A Corrigendum on

Differential Expression of Putative *Ornithodoros turicata* Defensins Mediated by Tick Feeding
by Armstrong, B. A., Kneubehl, A. R., Mitchell, R. D. III., Krishnavajhala, A., Teel, P. D., Pérez de León, A. A., et al. (2020). Front. Cell. Infect. Microbiol. 10:152. doi: 10.3389/fcimb.2020.00152

The original article stated that "Moreover, *O. turicata, O. coriaceus*, and *O. parkeri* were experimentally shown to be competent vectors of African swine fever virus (ASFV) (Hess et al., 1987), an emerging pathogen in Europe and Asia," which is incorrect. It should read "Moreover, *O. turicata* and *O. coriaceus* were experimentally shown to be competent vectors of African swine fever virus (ASFV) (Hess et al., 1987), an emerging pathogen in Europe and Asia. *O. parkeri* was able to be infected with ASFV, but unable to transmit the pathogen via tick bite (Hess et al., 1987)." A correction has been made to the **Introduction**, first paragraph:

"*Ornithodoros* (argasid) species are vectors of veterinary and medically significant pathogens. The primary species in the United States that transmit pathogens include *Ornithodoros turicata*, *Ornithodoros hermsi*, *Ornithodoros parkeri*, *Ornithodoros talaje*, and *Ornithodoros coriaceus* (Davis, 1939; Cooley and Kohls, 1944; Hess et al., 1987; Donaldson et al., 2016; Lopez et al., 2016; Sage et al., 2017). These species have been implicated in the transmission of tick-borne relapsing fever spirochetes (Lane et al., 1985; Dworkin et al., 2002; Nieto et al., 2012; Lopez et al., 2016; Christensen et al., 2017; Bissett et al., 2018). Moreover, *O. turicata* and *O. coriaceus* were experimentally shown to be competent vectors of African swine fever virus (ASFV) (Hess et al., 1987), an emerging pathogen in Europe and Asia. *O. parkeri* was able to be infected with ASFV, but unable to transmit the pathogen via tick bite (Hess et al., 1987). *Ornithodoros* ticks play a significant role in pathogen maintenance, yet very little is known regarding vector competence."

The authors apologize for the error and state that it does not change the scientific conclusions of the article in any way. The original article has been updated.

REFERENCES

Bissett, J. D., Ledet, S., Krishnavajhala, A., Armstrong, B. A., Kliioueva, A., Sexton, C., et al. (2018). Detection of tickborne relapsing fever spirochete, Austin, Texas, USA. *Emerg. Infect. Dis.* 24, 2003–2009. doi: 10.3201/eid2411.172033

Christensen, A. M., Pietralczyk, E., Lopez, J. E., Brooks, C., Schriefer, M. E., Wozniak, E., et al. (2017). Diagnosis and management of *Borrelia turicatae* infection in febrile soldier, Texas, USA. *Emerg. Infect. Dis.* 23, 883–884. doi: 10.3201/eid2305.162069

Cooley, R. A., and Kohls, G. M. (1944). *The Agarasidae of North America, Central America, and Cuba*. Notre Dame, IN: The University Press.

Davis, G. E. (1939). Ornithodoros parkeri: distribution and host data; spontaneous infection with relapsing fever spirochetes. *Pub. Health Rep.* 54, 1345–1349. doi: 10.2307/4582963

Donaldson, T. G., Perez De Leon, A. A., Li, A. I., Castro-Arellano, I., Wozniak, E., Boyle, W. K., et al. (2016). Assessment of the geographic distribution of *Ornithodoros turicata* (Argasidae): climate variation and host diversity. *PLoS Negl. Trop. Dis.* 10:e0004383. doi: 10.1371/journal.pntd.0004383

Dworkin, M. S., Schwan, T. G., and Anderson, D. E. (2002). Tick-borne relapsing fever in North America. *Med. Clin. North Amer.* 86, 417–433. doi: 10.1016/S0025-71250300095-6

Hess, W. R., Endris, R. G., Haslett, T. M., Monahan, M. J., and Mccoy, J. P. (1987). Potential arthropod vectors of African swine fever virus in North America and the Caribbean basin. *Vet. Parasitol.* 26, 145–155. doi: 10.1016/0304-40178790084-7

Lane, R. S., Burgdorfer, W., Hayes, S. F., and Barbour, A. G. (1985). Isolation of a spirochete from the soft tick, *Ornithodoros coriaceus*: a possible agent of epizootic bovine abortion. *Science* 230, 85–87. doi: 10.1126/science.3898367

Lopez, J. E., Krishnavahjala, A., Garcia, M. N., and Bermudez, S. E. (2016). Tick-borne relapsing fever spirochetes in the Americas. *Vet. Sci.* 3, 1–18. doi: 10.3390/vetsci3030016

Nieto, N. C., Teglas, M. B., Stewart, K. M., Wasley, T., and Wolff, P. L. (2012). Detection of relapsing fever spirochetes (*Borrelia hermsii* and *Borrelia coriaceae*) in free-ranging mule deer (*Odocoileus hemionus*) from Nevada, United States. *Vector Borne Zoonotic Dis.* 12, 99–105. doi: 10.1089/vbz.2011.0716

Sage, K. M., Johnson, T. L., Teglas, M. B., Nieto, N. C., and Schwan, T. G. (2017). Ecological niche modeling and distribution of *Ornithodoros hermsi* associated with tick-borne relapsing fever in western North America. *PLoS Negl. Trop. Dis.* 11:e6047. doi: 10.1371/journal.pntd.0006047

frontiers in Cellular and Infection Microbiology

ORIGINAL RESEARCH
published: 08 May 2020
doi: 10.3389/fcimb.2020.00211

Poor Unstable Midgut Microbiome of Hard Ticks Contrasts With Abundant and Stable Monospecific Microbiome in Ovaries

Melina Garcia Guizzo[1,2], Saraswoti Neupane[3], Matej Kucera[2,4], Jan Perner[2], Helena Frantová[2], Itabajara da Silva Vaz Junior[5,6], Pedro L. de Oliveira[7], Petr Kopacek[2] and Ludek Zurek[1,8]**

[1] Central European Institute of Technology (CEITEC), Center for Zoonoses, University of Veterinary and Pharmaceutical Sciences, Brno, Czechia, [2] Biology Centre, Institute of Parasitology, Czech Academy of Sciences, Ceske Budejovice, Czechia, [3] Department of Entomology, Kansas State University, Manhattan, KS, United States, [4] Faculty of Science, University of South Bohemia, Ceske Budejovice, Czechia, [5] Laboratório de Imunologia Aplicada a Sanidade Animal, Centro de Biotecnologia, Universidade Federal do Rio Grande do Sul, Porto Alegre, Brazil, [6] Faculdade de Veterinária, Universidade Federal do Rio Grande do Sul, Porto Alegre, Brazil, [7] Laboratório de Bioquímica de Artrópodes Hematófagos, Instituto de Bioquímica Médica, Universidade Federal do Rio de Janeiro, Rio de Janeiro, Brazil, [8] Department of Chemistry and Biochemistry, Mendel University, Brno, Czechia

OPEN ACCESS

Edited by:
Alejandro Cabezas-Cruz, Institut National de la Recherche Agronomique (INRA), France

Reviewed by:
Travis Bourret, Creighton University, United States
Davide Sassera, University of Pavia, Italy
Sandra Antunes, New University of Lisbon, Portugal

***Correspondence:**
Melina Garcia Guizzo
melinaguizzo@gmail.com
Ludek Zurek
zureklu@vfu.cz

Specialty section:
This article was submitted to Parasite and Host, a section of the journal Frontiers in Cellular and Infection Microbiology

Received: *28 November 2019*
Accepted: *17 April 2020*
Published: *08 May 2020*

Citation:
Guizzo MG, Neupane S, Kucera M, Perner J, Frantová H, da Silva Vaz I, Oliveira PL, Kopacek P and Zurek L (2020) Poor Unstable Midgut Microbiome of Hard Ticks Contrasts With Abundant and Stable Monospecific Microbiome in Ovaries. Front. Cell. Infect. Microbiol. 10:211. doi: 10.3389/fcimb.2020.00211

Culture-independent metagenomic methodologies have enabled detection and identification of microorganisms in various biological systems and often revealed complex and unknown microbiomes. In many organisms, the microbiome outnumbers the host cells and greatly affects the host biology and fitness. Ticks are hematophagous ectoparasites with a wide host range. They vector a number of human and animal pathogens and also directly cause major economic losses in livestock. Although several reports on a tick midgut microbiota show a diverse bacterial community, in most cases the size of the bacterial population has not been determined. In this study, the microbiome was quantified in the midgut and ovaries of the ticks *Ixodes ricinus* and *Rhipicephalus microplus* before, during, and after blood feeding. Although the size of bacterial community in the midgut fluctuated with blood feeding, it was overall extremely low in comparison to that of other hematophagous arthropods. In addition, the tick ovarian microbiome of both tick species exceeded the midgut 16S rDNA copy numbers by several orders of magnitude. This indicates that the ratio of a tick midgut/ovary microbiome represents an exception to the general biology of other metazoans. In addition to the very low abundance, the tick midgut diversity in *I. ricinus* was variable and that is in contrast to that found in the tick ovary. The ovary of *I. ricinus* had a very low bacterial diversity and a very high and stable bacterial abundance with the dominant endosymbiont, *Midichloria* sp. The elucidation of this aspect of tick biology highlights a unique tissue-specific microbial-invertebrate host interaction.

Keywords: tick, *Ixodes ricinus*, *Rhipicephalus microplus*, midgut microbiome, ovary microbiome, symbiosis, *Midichloria mitochondrii*

INTRODUCTION

Ticks are obligate blood-feeding ectoparasites of a wide range of hosts including wild and domestic animals and people. They transmit a large number of pathogens and also directly cause great economic losses in livestock (Estrada-Peña, 2015). While the majority of studies focused on detection of the pathogens ticks transmit, several studies also explored the overall microbial diversity of ticks, including that of *Ixodes ricinus* and *Rhipicephalus microplus* (Andreotti et al., 2011; Carpi et al., 2011; Greay et al., 2018). However, the identification of the microbial taxa is only the first step toward the understanding of host-microbiota interactions. Till present, the main advance has been made in the functional characterization of endosymbionts housed in the tick ovary. Maternally-inherited bacteria *Coxiella* sp. and *Francisella* sp. were shown to be essential for tick molt and/or survival (Guizzo et al., 2017; Duron et al., 2018). In contrast, little is known about the microbiota residing in the tick midgut, its role in tick physiology and vector competence for pathogens as well as its potential origins (Narasimhan et al., 2014; Narasimhan and Fikrig, 2015; Vayssier-Taussat et al., 2015; Bonnet et al., 2017). In the past decade, several metagenomic studies using next-generation sequencing (NGS) have described the tick midgut as an organ harboring a diverse bacterial community (Moreno et al., 2006; Andreotti et al., 2011; Budachetri et al., 2014; Clayton et al., 2015). However, it is important to point that NGS methods are based on an amplification of the bacterial 16S rDNA gene fragment, allowing the detection of less abundant bacteria, but also potentially introduce false-positive results due to background contamination and also do not distinguish between viable bacteria and pieces of DNA from lysed cells (Goodrich et al., 2014; Huttenhower et al., 2014; Strong et al., 2014). Moreover, it was demonstrated that the sterilization protocols of the tick surface greatly impact results of the microbial diversity (Binetruy et al., 2019).

This study aimed to assess the bacterial diversity in the midgut and ovaries of *I. ricinus*, and to investigate its potential source from the host blood and skin by culture-independent approaches. Moreover, the dynamic of bacterial colonization was elucidated through the absolute quantification of the microbiome in the midgut and ovaries of *I. ricinus* and *R. microplus* during the feeding course on the vertebrate host.

MATERIALS AND METHODS

Tick Rearing

Wild-caught unfed *I. ricinus* females were collected by flagging on grass around Ceske Budejovice, Czech Republic. Ticks were maintained in the rearing facility at the Institute of Parasitology, Biology Centre Czech Academy of Sciences (CAS) under controlled conditions (temperature: 24°C and humidity: 95%). To complete the life cycle, unfed female ticks were allowed to feed on guinea pigs until the natural detachment from the host. All laboratory animals were treated in accordance with the Animal Protection Law of the Czech Republic No. 246/1992 Sb., ethics approval No. 25/2018. The study was approved by the Institute of Parasitology, Biology Centre CAS and Central Committee for Animal Welfare, Czech Republic (Protocol No. 1/2015).

Rhipicephalus microplus (Porto Alegre strain) were maintained on Hereford cattle brought from a naturally tick-free area (Santa Vitória do Palmar, Brazil; 33° 32′2″ S, 53° 20′59″ W) and kept in individual tick-proof pens on a slatted floor at the Faculdade de Veterinária of Universidade Federal do Rio Grande do Sul (Brazil) (Reck et al., 2009). The colony is maintained without the introduction of field ticks. Calves were infested with 15-day-old tick larvae. Partially engorged and fully engorged females were collected directly from the host and after natural detachment, respectively. All animal care and experimental protocols were conducted following the guidelines of the institutional care and use committee (Ethics Committee on Animal Experimentation) and were approved under the registry 14403/protocol 07.

Vertebrate Host and Tick Samples

Ixodes ricinus females were collected at several time points during a blood-feeding course on a guinea pig host. Unfed ticks, ticks on day 1, 3, and 5 during blood feeding, fully fed ticks, and ticks on day 2 and 6 after natural detachment were dissected to remove the midgut. Ovaries were dissected out from fully fed ticks and from ticks on day 2 and 6 after detachment. Similarly, the midgut and ovaries from partially engorged (mean weight 75.0 mg/tick) and fully engorged females were dissected from *R. microplus*. Before dissection, ticks were surface sterilized with 70% ethanol for 1 min, followed by three washes in sterile phosphate buffered saline (PBS) (Sigma, St. Louis, Missouri). *Ixodes ricinus* and *R. microplus* were then subjected to the 16S rDNA gene absolute quantification through qPCR and *I. ricinus* to Illumina sequencing analysis.

Swab skin and blood samples were collected from the vertebrate host (guinea pig). The bacterial recovery from the host skin was performed through the homogenization of the swab skin in 500 μl of sterile PBS. Before blood collection, the host skin was cleaned with 70% ethanol and blood was collected from the jugular vein using a sterile syringe and needle.

Genomic DNA Extraction and Culture-Independent Analysis of the Bacterial Community in the Midgut and Ovaries of *I. ricinus*

The tick genomic DNA was isolated using the PowerSoil DNA isolation kit (MO BIO, Hilden, Germany) according to the manufacturer's instructions. The bacterial community of the midgut and ovary of wild *I. ricinus*, the midgut of laboratory-reared *I. ricinus*, host swab skin, and host blood was investigated by the 16S rDNA sequencing of the total DNA. For the midgut DNA extraction, the whole organ was used, including the lumen content. The protocol was adapted for fully fed females using a double volume of reaction adjusted at the final step. The sequencing library preparation

was done at the Integrated Microbiome Resource (IMR) facility, Dalhousie University, Halifax, Nova Scotia, Canada as described by Comeau et al. (2017). Briefly, a dual-indexing one-step PCR strategy was applied using the extracted total DNA as a template to amplify the V6-V8 16S rDNA region (Comeau et al., 2011) with the Illumina Nextera adaptors plus the indices/barcodes. DNA-free water (Top-Bio, Praha, Czech Republic) was used as a negative control. PCR was performed in duplicates using two template dilutions, combined in one plate and visualized on an Invitrogen 96-well E-gel (Invitrogen, California, USA). Amplicons were cleaned-up and normalized using the high-throughput Invitrogen Sequal-Prep 96-well plate kit (Invitrogen, California, USA). Using the Invitrogen Qubit double-stranded DNA high sensitivity fluorescence-based method (Invitrogen, California, USA), the samples were pooled and quantified before the sequencing on an Illumina MiSeq machine.

The raw paired-end sequence reads obtained from the Illumina MiSeq sequencing platform were analyzed using the Mothur bioinformatic software pipeline (version 1.42.3) (Schloss et al., 2009). In short, primers were removed, and paired-end sequences were assembled into contigs. The quality of each contig (sequence hereafter) was checked. Sequence with low quality ($q < 25$), ambiguous base and ambiguous length (<200 and >450 bp) sequences were removed. High quality sequences were aligned with SSU rRNA SILVA reference alignment (Yilmaz et al., 2014) using Needleman-Wunsch global alignment algorithm (Needleman and Wunsch, 1970). VSEARCH (Rognes et al., 2016) was used to check chimera and removed chimeric sequences if present. High quality, non-chimeric sequences were clustered into operational taxonomic units (OTUs) with 97% sequence similarity using distance-based greedy cluster (DGC) algorithm. The representative sequence for each OTU was used to determine the phylogenetic identification of OTUs. These sequences were compared with SILVA reference datasets (Quast et al., 2013) using basic alignment search tool (BLAST) (Altschul et al., 1997). Erroneous OTUs (<2 sequence reads) were removed from the OTU table. Moreover, OTUs from background bacterial contamination were filtered from OTU table by removing OTUs that were clustered together with OTUs of the DNA-free water sample. The final OTU table was used for further statistical analyses.

Quantification of the Bacterial 16S rDNA and Tick Elongation Factor Genes

The tick genomic DNA was isolated as described above. The single copy gene for tick elongation factor-1α (*ef-1α*) was used as a reference for data normalization (Nijhof et al., 2009). Quantification of the bacterial 16S rDNA gene (Nadkarni et al., 2002) was carried out in a LightCycler® 480 (Roche, Basel, Switzerland) with 50 cycles of 95°C (10 s), 60°C (10 s), and 72°C (10 s) following an initial denaturation of 95°C (10 min). Each 20 μl reaction mixture contained 10 μl of FastStart universal probe master (Rox) (Roche), 10 pmol of each primer, 5 pmol of TaqMan probe (Nadkarni et al., 2002), 2 μl of genomic DNA, and 5 μl of DNA-free water (Top-Bio, Praha, Czech Republic). Quantification of *ef-1α* was performed on the same equipment as described above with 50 cycles of 95°C (10 s), 60°C (10 s) and 72°C (10 s) following an initial denaturation of 95°C (10 min). The amplification was performed with 12.5 μl of FastStart universal SYBR green master (Rox) (Roche), 10 pmol of each primer, 2 μl of genomic DNA, and DNA-free water (Top-Bio). In order to perform the absolute quantification, standard curves were plotted using serial dilutions (10^6-10^2) of a plasmid containing the fragment of a single copy tick specie-specific *ef-1α* gene or the bacterial 16S rDNA gene. The *ef-1α* gene for *I. ricinus* and the bacterial 16S rDNA gene were cloned into TOPO plasmid vector (Invitrogen, California, USA), while the *ef-1α* for *R. microplus* into the pGEM®-T easy (Promega, Wisconsin, USA). Bacterial 16S rDNA counts in DNA-free water (Top-Bio, Praha, Czech Republic) were used as a control for background contamination. Midgut and ovary from seven *I. ricinus* and six *R. microplus* ticks were analyzed at each time-point during a feeding course on a vertebrate host. The total 16S rDNA copy number was represented either by an organ or by the tick elongation factor gene. Primers and probe sequences are listed in **Table 1**.

Statistical Analysis

Statistical analysis of the microbiome quantification data was performed using the GraphPad Prism software (version 8). First, all the data were tested for normality using Shapiro-Wilk test. Differences among three or more groups were determined using Kruskal-Wallis for a non-parametric test. Other comparisons were performed using Mann Whitney test or unpaired *t*-test depending on the Gaussian distribution.

TABLE 1 | List of primers and probe used in this study.

Primer or probe	Sequence	Size of the amplicon	Tm (°C)	References
V6-V8_For (B969F)	A CGC GI-1N RAA CCT TAC C	400 bp	53	Comeau et al., 2011
V6-V8_Rev (BA1406R)	AC GGG CRG TGW GTR CAA		57	
16S_For	TCC TAC GGG AGG CAG CAG T	466 bp	59	Nadkarni et al., 2002
16S_Rev	GGA CTA CCA GGG TAT CTAATC CTG TT		58	
16S_probe	CGT ATT ACC GCG GCT GCT GGC AC		70	
RmEF_For	CGT CTA CAA GAT TGG TGG CAT T	108 bp	60	Nijhof et al., 2009
RmEF_Rev	CTC AGT GGT CAG GTT GGC AG		60	
IREF For	ACG AGG CTC TGA CGG AAG	81 bp	60	Nijhof et al., 2009
IREF Rev	CAC GAC GCA ACT CCT TCA C		60	

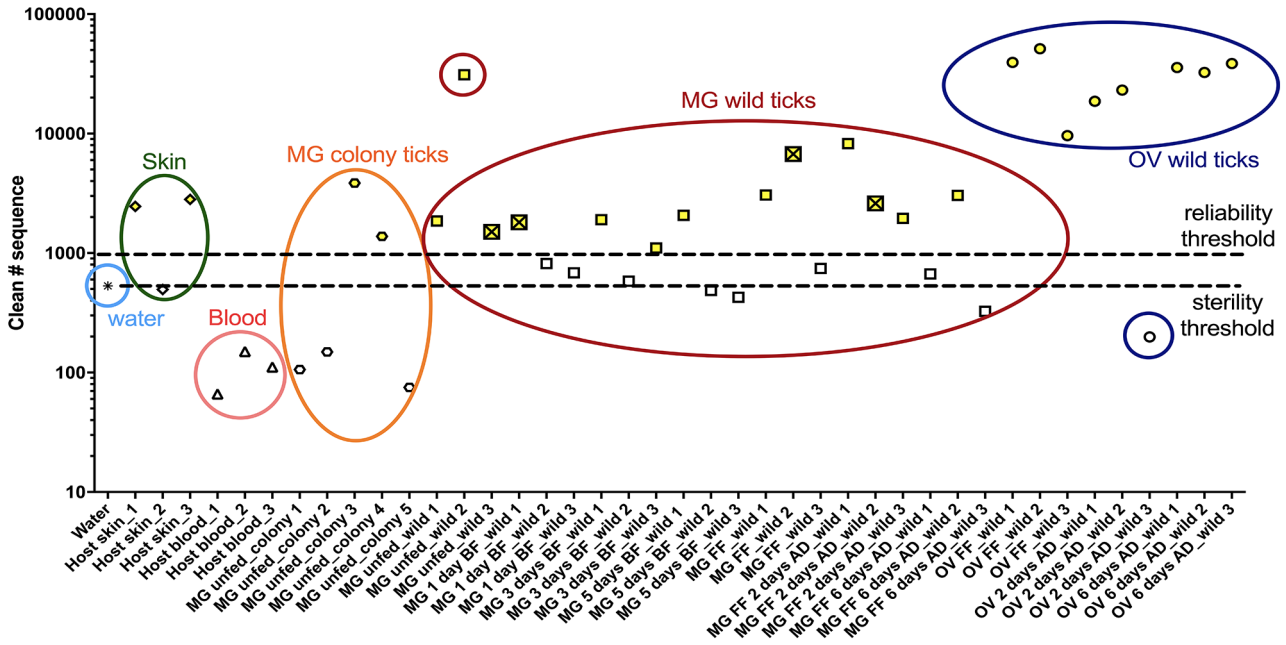

FIGURE 1 | Numbers of good quality 16S rDNA gene sequences obtained through bioinformatic analysis. Samples above both thresholds (yellow) were selected to bacterial diversity analysis. The crossed square represents a tick infected with *Borreliella* sp. MG, midgut; OV, ovary; UF, unfed; 1D, 1-day; 3D, 3-days; 5D, 5-days; FF, fully fed; AD, after detachment.

The values were considered statistically significant with $p < 0.05$. The correlation coefficient was calculated using the Spearman's rank.

Statistical analysis of the microbiome data from 16S rDNA sequencing was performed in R v.3.4.4 (R Core Team, 2018). Alpha diversity (species richness, Shannon diversity index, and Pielou's evenness) were calculated using the vegan package in R (Oksanen et al., 2019). Prevalence of bacterial phyla and genera in individual samples were summarized in a bar plot.

RESULTS

A High Midgut vs. Low Ovary Diversity in *I. ricinus*

In order to characterize the bacterial diversity of the *I. ricinus* midgut and ovary, the microbial community from wild and laboratory-reared ticks was investigated using Illumina sequencing. To elucidate the potential source, the microbiota from the host skin and blood was also assessed. The number of 16S rDNA good quality sequences obtained through bioinformatic analysis was used to determine two thresholds: sterility and reliability. The sterility threshold was used as a control for background contamination based on the bacterial counts obtained from DNA-free water (Top-Bio, Praha, Czech Republic). The reliability threshold was arbitrarily determined based on the number of good quality 16S rDNA sequences >1,000, which is directly related to the target DNA biomass and consequently to the DNA amplification. Only those samples above both thresholds were further analyzed (**Figure 1** and **Table S1**).

A total of 300,206 good quality sequences were obtained and these were clustered into 1,138 OTUs at a similarity level 97% (**Table 2** and **Table S2**). The bacterial diversity in the midgut was higher and variable comparing to that of the ovary, depending on the individual variation and the tick-borne pathogen infection status. Bacteria from the phyla Bacterioidetes and Proteobacteria, *Prevotella* sp., and *Neisseria* sp. respectively, were identified from the host skin (**Figures 2A,D**) as well as from midguts of all blood fed ticks (**Figures 2B,E**). However, any bacterial genus was found in all the midgut samples irrespective of the tick feeding status (**Figure 2E** and **Table S2**). As expected, only wild ticks were infected with tick-borne pathogens. Four out of twelve wild ticks were positive for *Borreliella* sp., the bacterial agent causing Lyme disease. *Spiroplasma* sp. was the dominant bacterial taxon in the midgut of two blood fed females. Other bacterial genera including *Escherichia* sp., *Neisseria* sp. and *Porphyromonas* sp. were found in a high frequency in the tick midgut (**Figure 2E** and **Table S2**). On average, more bacterial genera were found in the midgut of unfed wild ticks in comparison to that of the laboratory-reared ticks (**Figure 2E** and **Table S2**). The dominant bacterial taxon in ovaries was the endosymbiont *Midichloria* sp. (phylum Proteobacteria) regardless of the tick feeding stage (**Figures 2C,F**). These results are also reflected in the alpha diversity indices, including Shannon and Pielou's evenness, which are lower for the ovarian samples (**Table 2**). *Midichloria* sp. was also identified in the midgut from two unfed wild and two colony ticks, as well as in one blood fed tick (**Figure 2E**).

TABLE 2 | Number of good quality sequences and operational taxonomic units (OTUs), and alpha diversity indices of the bacterial community in the ovary and the midgut of *Ixodes ricinus*.

Source	Sample ID	# Sequences	# OTUs	Shannon diversity index	Pielou's evenness
Skin	Host skin_1	2455	223	4.73	0.87
Skin	Host skin_3	2814	223	4.56	0.84
Ovary	OV FF_wild 1	39414	2	0.00	0.00
Ovary	OV FF_wild 2	51300	2	0.00	0.00
Ovary	OV FF_wild 3	9608	8	0.05	0.02
Ovary	OV 2 days AD_wild 1	18633	3	0.00	0.00
Ovary	OV 6 days AD_wild 1	35750	20	0.03	0.01
Ovary	OV 6 days AD_wild 2	32513	17	0.03	0.01
Ovary	OV 6 days AD_wild 3	38563	12	0.01	0.00
Ovary	MG unfed_colony 3	3857	13	0.29	0.11
Ovary	MG unfed_colony 4	1382	55	3.00	0.75
Midgut	MG unfed_wild 1	1855	103	3.74	0.81
Midgut	MG unfed_wild 2	31070	159	1.28	0.25
Midgut	MG unfed_wild 3	1505	29	1.83	0.54
Midgut	MG 1 day BF_wild 1	1808	54	2.12	0.53
Midgut	MG 3 days BF_wild 1	1902	118	3.90	0.82
Midgut	MG 3 days BF_wild 3	1105	93	4.13	0.91
Midgut	MG 5 days BF_wild 1	2068	111	4.14	0.88
Midgut	MG FF_wild 1	3065	16	0.50	0.18
Midgut	MG FF_wild 2	6743	41	0.37	0.10
Midgut	MG FF 2 days AD_wild 1	8245	48	0.79	0.20
Midgut	MG FF 2 days AD_wild 2	2602	79	1.45	0.33
Midgut	MG FF 2 days AD_wild 3	1949	113	4.19	0.89

MG, midgut; OV, ovary; BF, blood fed; FF, fully fed; AD, after detachment.

Hard Ticks Have Very Low Levels of the Midgut Microbiota During Blood Feeding Stage

The size of the bacterial community in the midgut was followed through a feeding time course of *I. ricinus* wild females on guinea pigs. The total 16S rDNA level increased slightly but not significantly ($p > 0.99$) on day 1 of blood feeding and then started decline with statistically significant decreases on day 5 of blood-feeding ($p = 0.03$) and at the full engorgement ($p = 0.009$) (**Figure 3A** and **Figure S1A**). The total 16S rDNA level in the midgut negatively correlated ($r = -0.88$) with the tick weight during the feeding course (**Figure S2**).

Similarly to *I. ricinus*, very low levels of midgut microbiota were found in *R. microplus* revealing that only few bacterial cells were found in the whole digestive tract (∼100 or less cells). However, due to nature of maintenance of this tick species on cattle, only two time points of blood feeding were examined in these ticks (**Figure 3B** and **Figure S1C**). The bacterial 16S rDNA gene copy number in the tick midgut during the blood feeding significantly increased ($p = 0.002$).

Ovarian Microbial Abundance Greatly Exceeds That of the Midgut in Hard Ticks

In view of the low level of the total midgut microbiota in fully fed females of both, *I. ricinus* and *R. microplus*, we were interested in determination of assessment of the total microbial community in tick ovaries. The same fully fed female ticks from which the midguts were used for the total genomic DNA isolation had the ovarian DNA extracted and subjected to the bacterial quantification. For both tick species, *I. ricinus* and *R. microplus,* the 16S rDNA gene copy numbers per ovary or per house keeping gene levels exceeded that of the midgut by several orders of magnitude (**Figures 3A,B** and **Figures S1B,D**). *Ixodes ricinus* had 2–5 times order of magnitude higher levels of the bacterial 16S rDNA copy number in the ovary than in the midgut when expressed per organ (**Figure 3A**) and even higher when expressed per the house keeping gene (**Figure S1B**). The 16S rDNA absolute number in the ovary of *I. ricinus* decreased comparing 2–6 days after tick detachment from the host (**Figure S1B**).

Interestingly, the level of the bacterial 16S rDNA copy number in the ovary of *R. microplus* significantly increased when represented per organ ($p = 0.004$) or the house keeping gene ($p = 0.02$) during the blood feeding (**Figure 3B** and **Figure S1D**).

DISCUSSION

The digestive tract of metazoans is typically colonized by a numerous and diverse microbial community with an important role in the host physiology and overall fitness and survival (Engel and Moran, 2013; Heintz-Buschart and Wilmes, 2018). Several exceptions to this rule have been recently reported including some microbiome-free arthropod taxa (Hammer et al., 2019); however, blood-feeding arthropods generally possess a gut microbiota that affects their vector competence for pathogens (Weiss and Aksoy, 2011; Dennison et al., 2014; Narasimhan et al., 2014; Narasimhan and Fikrig, 2015). For hematophagous arthropods, blood is the main source of nutrients and is essential for embryo development and molting of juvenile stages. The influx of blood into the digestive system typically leads to an expansion of the midgut bacterial community in blood feeding arthropods as shown, for example, for mosquitoes and triatomine bugs (Eichler and Schaub, 2002; Oliveira et al., 2011). In *Aedes aegypti* the blood uptake increased the culturable midgut bacterial population by about three orders of magnitude (from 10^3 to 10^6 per insect) (Oliveira et al., 2011). In the triatomine bug, *Rhodnius prolixus*, the level of the gut bacterial symbiont *Rhodococcus rhodnii* increased 15-fold in the fifth instars after 10 days of blood feeding and resulted in the population of 10^8 bacteria per insect (Eichler and Schaub, 2002).

During the feeding course on a vertebrate host, hard ticks increase their size 100–1,000 times reflecting a great influx of blood which represents a nutritionally rich substrate for ticks, potentially available also for bacteria present in the tick midgut. Nevertheless, unlike reported for other hematophagous arthropods, we showed here that in the hard ticks, *I. ricinus* and *R. microplus,* the blood intake is not associated with bacterial

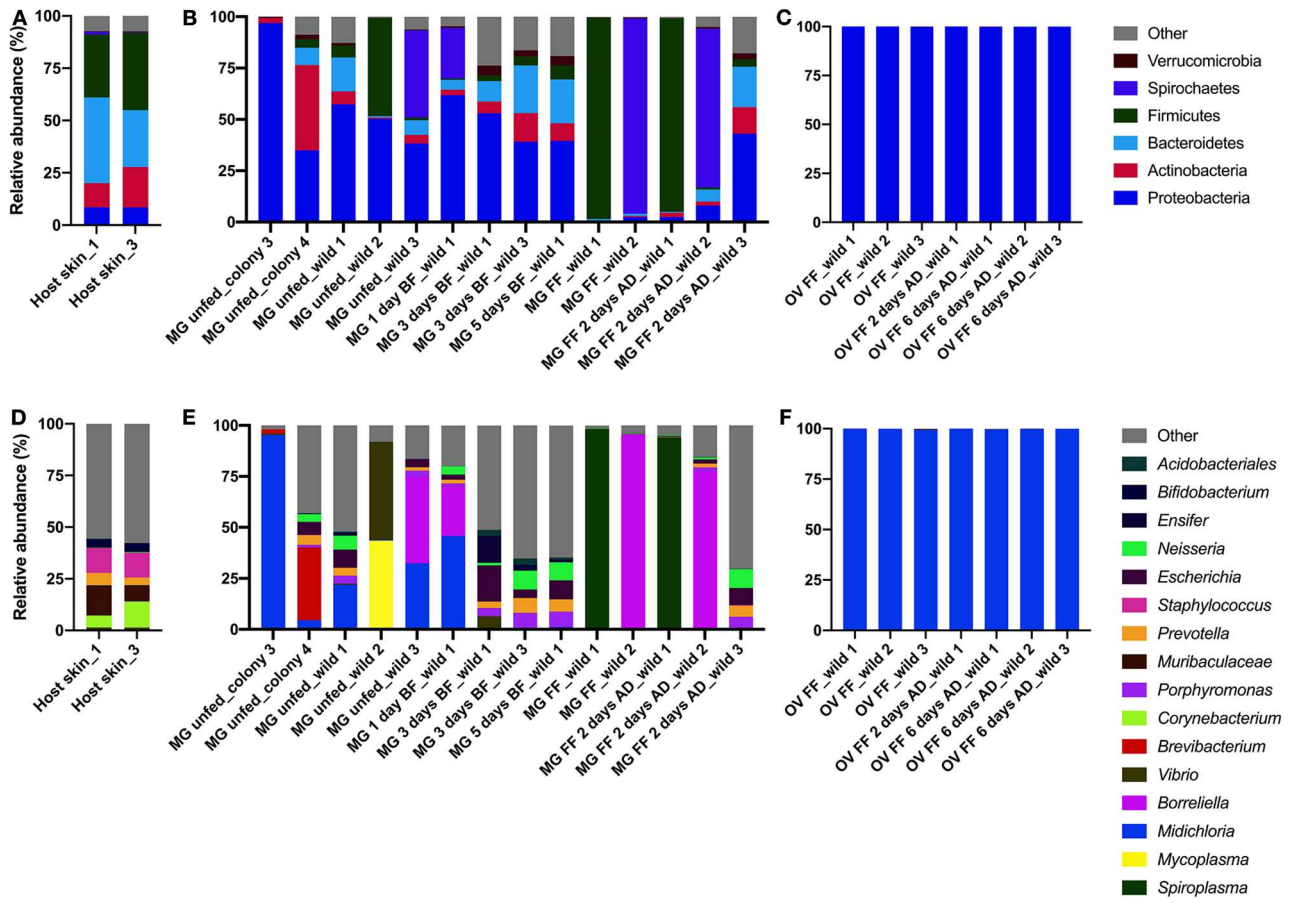

FIGURE 2 | Bacterial diversity in the host skin **(A,D)** and the midgut **(B,E)** and ovary **(C,F)** of *Ixodes ricinus* on phylum **(A–C)** and genus **(D–F)** levels. MG, midgut; OV, ovary; BF, blood fed; FF, fully fed female; AD, after detachment.

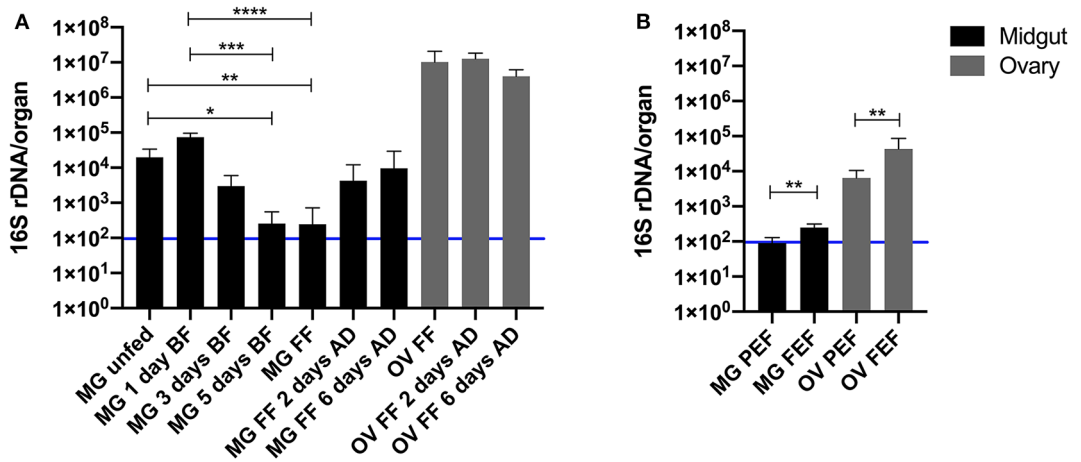

FIGURE 3 | Quantification of the 16S rDNA gene per midgut (black) and ovary (gray) of *Ixodes ricinus* **(A)** and *Rhipicephalus microplus* **(B)** during blood feeding on a vertebrate host. MG, midgut; OV, ovary; BF, blood fed; FF, fully fed; AD, after detachment; PEF, partially engorged female; FEF, fully engorged female. The number of biological replicates analyzed in each time-point was 7 for *I. ricinus* and 6 for *R. microplus*. Error bars indicate standard deviation. The blue line represents the sterility threshold (16S rDNA counts in DNA-free water). Stars indicate statistically significant differences. *$p < 0.05$; **$p < 0.01$; ***$p < 0.001$; and ****$p < 0.0001$.

growth in the midgut. In fact, our results show that there is a negative correlation between the amount of blood consumed and the midgut bacterial level in *I. ricinus*; 16S rDNA levels per organ ranged from 10^4 in unfed females to 10^2 in fully fed females. In *R. microplus*, due the one-host life cycle for all tick stages, the unfed female could not be obtained for analysis. The bacterial levels in this tick species, regardless the blood influx, remained very low with approximately 10^2 16S rDNA copies per midgut in partially and fully engorged females. In both cases, these bacterial levels were close to the sterility technical threshold. Taken together, the numbers do not allow to define if the few bacterial cells found in *I. ricinus* and *R. microplus* midgut are just a transient population or constitute a resident community.

Several hypotheses were formulated for the primary cause of low bacterial levels in the midgut of ticks. First, it is hypothesized that hemoglobin fragments generated during blood digestion and the complement system from the host blood (Fogaça et al., 1999; Nakajima et al., 2009; Kopáček et al., 2010) negatively impact the midgut bacterial community and cause its rapid decline. The second hypothesis is that the epithelial immunity regulates the bacterial population in the tick midgut by antimicrobial peptides and reactive oxygen species (ROS) (Sonenshine and Macaluso, 2017). For example, it was demonstrated in the *I. ricinus* midgut transcriptome that the immune genes such as defensin, lysozyme, and microplusin were substantially upregulated at the end of tick feeding (Perner et al., 2016). Moreover, the capillary feeding of *Dermacentor variabilis* with *Escherichia coli* resulted in expression of defensin-like peptides in tick midgut (Sonenshine et al., 2002). In the majority of hematophagous animals, the digestion is an extracellular process and takes place in the gut lumen. Ticks, however, represent an exception as they digest blood intracellularly in the specialized digestive midgut cells that take up blood components by means of massive endocytosis (Sojka et al., 2013). The third hypothesis is that the midgut microbiota is reduced in part, by the tick digestive cells. Some midgut microbiota might be endocytosed by the tick digestive epithelial cells along with the vertebrate blood components (Lara, 2005) and consequently digested.

Andreotti et al. (2011) reported that the *R. microplus* midgut harbors a highly diverse bacterial community belonging to 11 bacterial genera. Similarly, we showed here that the *I. ricinus* midgut carries a variable bacterial population that differs depending on individual ticks and the tick-borne pathogen infection status. The host skin as a potential source of bacteria in the midgut of *I. ricinus* is indicated by detecting the same bacterial taxa (e.g., *Prevotella* sp. and *Neisseria* sp.) from both, host skin and in the midgut, of blood fed females, regardless the time-point of the blood feeding course. *Prevotella* sp. has been identified as part of the healthy skin microbiome and *Neisseria* sp. is common in the mucosal surface of vertebrate hosts of *I. ricinus* (Elliott et al., 2005; Dimitriu et al., 2019). In contrast to the ovary, the midgut did not show a core microbiome, as we did not detect any common bacterial genera in all midgut samples. It is likely that most of identified bacteria in the midgut originated from the environment; they were accidentally ingested and constitute just a transient population. The hypothesis that the source of the midgut bacteria is the environment is further supported by the finding that wild ticks have a higher bacterial diversity than colony ticks maintained under laboratory-controlled conditions.

Bacterium from the genus *Midichloria* sp. found in the midgut of unfed and in 1-day blood fed *I. ricinus* corroborated the study of Olivieri et al. (2019). *Vibrio* sp. detected in the midgut of five out from fourteen ticks is not usually reported in metagenomic analysis of ticks and it likely represents a bacterium of the environmental origin. *Mycoplasma* sp. found in the midgut of one unfed *I. ricinus* has been reported from ticks previously (Hornok et al., 2019) but its significance in tick biology as well as from the clinical perspective is unknown. The midgut of two blood fed ticks were dominated by *Spiroplasma* sp. Different species in the genus *Spiroplasma* were described in arthropods and plants in commensal, mutualist, and pathogenic associations (Regassa and Gasparich, 2006). In ticks, this taxon was detected in several species and described as a facultative symbiont (Henning et al., 2006; Duron et al., 2017). Four out of twelve wild ticks were infected with a bacterium from the genus *Borreliella,* which make part of a complex of species that are vectored by ticks and cause Lyme disease in humans (Lane et al., 1991). *Borreliella* sp. are acquired by ticks during blood feeding from an infected host at the early tick life-stages and persist in the midgut after tick molting (Benach et al., 1987). Presence of *Borreliella* sp. in *I. ricinus* in some parts of Central Europe can be very high (Strnad et al., 2017) and it is therefore not surprising that it was found in the midgut of 33% of the wild ticks analyzed. It appears that both, *Spiroplasma* sp. and *Borreliella* sp., are capable of outcompeting other bacteria in the midgut during tick blood feeding and blood digestion and become the dominant member of the tick midgut microbiome. However, our data are limited and studies with larger number of specimen are needed to confirm these results.

In contrast to the tick midgut, we found an abundant and stable bacterial community with very low diversity in the ovary of *I. ricinus* with the dominant endosymbiont, *Midichloria* sp. This result corroborates with the finding of high levels of *Midichloria* sp. in fully fed *I. ricinus* females (Sassera et al., 2008). In the *R. microplus* ovary, it was shown that the dominant endosymbiont is *Coxiella* sp. representing 98.2% of the 16S rDNA sequences in fully engorged females (Andreotti et al., 2011). The presence of *Midichloria* sp. and *Coxiella* sp. in tick ovaries and eggs points out to vertical transmission, typical for maternally inherited symbionts (Sassera et al., 2008; Andreotti et al., 2011).

The abundant bacterial population in the tick ovaries and the negligible microbial community in the tick midgut indicate that the physiological role of the gut bacterial community, usually exercised in most metazoan, is accomplished in ticks by the obligate intracellular symbionts housed in the ovary. Indeed, it has been shown that genomes of both, *Midichloria mitochondrii* and *Coxiella* sp., encode genes that participate in the metabolic pathways for the biosynthesis of vitamins and cofactors suggested to be missed in the host blood (Sassera et al., 2011; Guizzo et al., 2017). *Coxiella* sp. in the ovary of *R. microplus* was demonstrated to play an important role in the tick development

and reproductive fitness (Zhong et al., 2007; Guizzo et al., 2017; Zhang et al., 2017). Although the role of *M. mitochondrii* in biology of *I. ricinus* is likely similar to that of *Coxiella* sp. in *R. microplus*, further studies are needed to demonstrate its specific role.

In conclusion, using the quantification of the total 16S rDNA gene, we report here very low levels of the midgut microbiota in *I. ricinus* and *R. microplus,* without a core microbiome in *I. ricinus.* This corroborates the findings of a limited and unstable midgut microbiota in *Ixodes scapularis* (Ross et al., 2018). In contrast, several magnitudes higher levels of 16S rDNA were found in the ovaries of both tick species represented in *I. ricinus* by an endosymbiont *Midichloria* sp. The bacterial distribution in tick internal organs is an exception of the general biology of metazoans, characterized by a high ratio of a tick midgut/ovary microbiome.

DATA AVAILABILITY STATEMENT

Sequenced OTUs were deposited in the Genbank database under accession numbers MT255253- MT256050.

ETHICS STATEMENT

This animal study was reviewed and approved by the Animal Protection Law of the Czech Republic No. 246/1992 Sb., ethics approval No. 25/2018. This study was approved by the Institute of Parasitology, Biology Centre CAS and Central Committee for Animal Welfare, Czech Republic (Protocol No. 1/2015). Ethics Committee on Animal Experimentation and were approved under the registry 14403/protocol 07.

AUTHOR CONTRIBUTIONS

MG conducted the experiments, analyzed the results, and wrote the manuscript. SN analyzed the results of 16S rDNA survey. MK and HF assisted with the experiments. JP, IS, PK, PO, and LZ conceived the experiments and wrote the manuscript. All authors reviewed the manuscript.

FUNDING

This study was mainly funded by the Czech Science Foundation (GACR) Grant No: 19-04301S to LZ and PK; MG, JP, and PK were additionally supported by the Centre for research of pathogenicity and virulence of parasites (No. CZ.02.1.01/0.0/0.0/16_019/0000759) funded by European Regional Development Fund (ERDF) and Ministry of Education, Youth and Sport (MEYS). We would like to acknowledge the support from the Conselho Nacional de Desenvolvimento Científico e Tecnológico CNPq: 573959/2008-0, Coordenação de Aperfeiçoamento de Pessoal de Nível Superior (CAPES: Finance Code 001) and Instituto Nacional de Ciência e Tecnologia em Entomologia Molecular (INCT-EM) to MG, IS, and PO. We are grateful to Radek Sima for the generation of 16S rDNA standard curve and also Jan Erhart and Tereza Hatalová for excellent technical support.

SUPPLEMENTARY MATERIAL

The Supplementary Material for this article can be found online at: https://www.frontiersin.org/articles/10.3389/fcimb.2020.00211/full#supplementary-material

Figure S1 | Quantification of the 16S rDNA gene per the elongation *ef-1α* in the midgut **(A)** and ovary **(B)** of *Ixodes ricinus* and in the midgut **(C)** and ovary **(D)** of *Rhipicephalus microplus* during blood feeding on a vertebrate host. MG, midgut; OV, ovary; BF, blood fed; FF, fully fed; AD, after detachment; PEF, partially engorged female; FEF, fully engorged female. Each time-point represents the median of 7 biological replicates for *I. ricinus* and 6 for *R. microplus.* Error bars indicate standard deviation. Stars indicate statistically significant differences. $*p < 0.05$; $**p < 0.01$; and $****p < 0.0001$.

Figure S2 | Negative correlation between 16S rDNA gene in the midgut per the *ef-1α* and *Ixodes ricinus* weight during blood feeding on a vertebrate host. The results represent the median for 7 organs. Spearman's rank correlation coefficient = −0.88.

Table S1 | Number of good quality 16S rDNA gene sequences obtained through bioinformatic analysis for the analyzed samples. MG, midgut; OV, ovary; BF, blood fed; FF, fully fed; AD, after detachment. Samples in yellow are above both sterility and reliability threshold. Samples in red were removed from the final analysis.

Table S2 | Overview of the identified OTUs, and its classification into bacterial phylum and genera.

REFERENCES

Altschul, S. F., Madden, T. L., Schäffer, A. A., Zhang, J., Zhang, Z., Miller, W., et al. (1997). Gapped BLAST and PSI-BLAST: a new generation of protein database search programs. *Nucleic Acids Res.* 25, 3389–402. doi: 10.1093/nar/25.17.3389

Andreotti, R., Pérez de León, A. A., Dowd, S. E., Guerrero, F. D., Bendele, K. G., and Scoles, G. A. (2011). Assessment of bacterial diversity in the cattle tick *Rhipicephalus (Boophilus) microplus* through tag-encoded pyrosequencing. *BMC Microbiol.* 11:6. doi: 10.1186/1471-2180-11-6

Benach, J. L., Coleman, J. L., Skinner, R. A., and Rosler, E. M. (1987). Adult *ixodes dammini* on rabbits: a hypothesis for the development and transmission of borrelia burgdorferi. *J. Infect. Dis.* 155, 1300–6. doi: 10.1093/infdis/155.6.1300

Binetruy, F., Dupraz, M., Buysse, M., and Duron, O. (2019). Surface sterilization methods impact measures of internal microbial diversity in ticks. *Parasit. Vectors* 12:268. doi: 10.1186/s13071-019-3517-5

Bonnet, S. I., Binetruy, F., Hernández-Jarguín, A. M., and Duron, O. (2017). The tick microbiome: why non-pathogenic microorganisms matter in tick biology and pathogen transmission. *Front. Cell. Infect. Microbiol.* 7:236. doi: 10.3389/fcimb.2017.00236

Budachetri, K., Browning, R. E., Adamson, S. W., Dowd, S. E., Chao, C. C., Ching, W. M., et al. (2014). An insight into the microbiome of the *Amblyomma maculatum* (Acari: Ixodidae). *J. Med. Entomol.* 51, 119–29. doi: 10.1603/me12223

Carpi, G., Cagnacci, F., Wittekindt, N. E., Zhao, F., Qi, J., Tomsho, L. P., et al. (2011). Metagenomic profile of the bacterial communities associated with *Ixodes ricinus* ticks. *PLoS ONE* 6:e25604. doi: 10.1371/journal.pone.0025604

Clayton, K. A., Gall, C. A., Mason, K. L., Scoles, G. A., and Brayton, K. A. (2015). The characterization and manipulation of the bacterial microbiome of the Rocky mountain wood tick, *Dermacentor andersoni*. *Parasit. Vectors* 8:632. doi: 10.1186/s13071-015-1245-z

Comeau, A. M., Douglas, G. M., and Langille, M. G. I. (2017). Microbiome helper: a custom and streamlined workflow for microbiome research. *mSystems* 2:e00127-16. doi: 10.1128/msystems.00127-16

Comeau, A. M., Li, W. K. W., Tremblay, J. É., Carmack, E. C., and Lovejoy, C. (2011). Arctic ocean microbial community structure before

and after the 2007 record sea ice minimum. *PLoS ONE* 6:e27492. doi: 10.1371/journal.pone.0027492

Dennison, N. J., Jupatanakul, N., and Dimopoulos, G. (2014). The mosquito microbiota influences vector competence for human pathogens. *Curr. Opin. Insect Sci.* 3, 6–13. doi: 10.1016/j.cois.2014.07.004

Dimitriu, P. A., Iker, B., Malik, K., Leung, H., Mohn, W. W., and Hillebrand, G. G. (2019). New insights into the intrinsic and extrinsic factors that shape the human skin microbiome. *MBio* 10:e00839-19. doi: 10.1128/mBio.00839-19

Duron, O., Binetruy, F., Noël, V., Cremaschi, J., McCoy, K. D., Arnathau, C., et al. (2017). Evolutionary changes in symbiont community structure in ticks. *Mol. Ecol.* 26, 2905–2921. doi: 10.1111/mec.14094

Duron, O., Morel, O., Noël, V., Buysse, M., Binetruy, F., Lancelot, R., et al. (2018). Tick-bacteria mutualism depends on B vitamin synthesis pathways. *Curr. Biol.* 28, 1896–1902.e5. doi: 10.1016/j.cub.2018.04.038

Eichler, S., and Schaub, G. A. (2002). Development of symbionts in triatomine bugs and the effects of infections with trypanosomatids. *Exp. Parasitol.* 100, 17–27. doi: 10.1006/expr.2001.4653

Elliott, D. R., Wilson, M., Buckley, C. M. F., and Spratt, D. A. (2005). Cultivable oral microbiota of domestic dogs. *J. Clin. Microbiol.* 43, 5470–6. doi: 10.1128/JCM.43.11.5470-5476.2005

Engel, P., and Moran, N. A. (2013). The gut microbiota of insects - diversity in structure and function. *FEMS Microbiol. Rev.* 37, 699–735. doi: 10.1111/1574-6976.12025

Estrada-Peña, A. (2015). Ticks as vectors: taxonomy, biology and ecology. *Rev. Sci. Tech.* 34, 53–65. doi: 10.20506/rst.34.1.2345

Fogaça, A. C., Da Silva, P. I., Miranda, M. T. M., Bianchi, A. G., Miranda, A., Ribolla, P. E. M., et al. (1999). Antimicrobial activity of a bovine hemoglobin fragment in the tick *Boophilus microplus*. *J. Biol. Chem.* 274, 25330–4. doi: 10.1074/jbc.274.36.25330

Goodrich, J. K., Di Rienzi, S. C., Poole, A. C., Koren, O., Walters, W. A., Caporaso, J. G., et al. (2014). Conducting a microbiome study. *Cell* 158, 250–262. doi: 10.1016/j.cell.2014.06.037

Greay, T. L., Gofton, A. W., Paparini, A., Ryan, U. M., Oskam, C. L., and Irwin, P. J. (2018). Recent insights into the tick microbiome gained through next-generation sequencing. *Parasit. Vectors* 11:12. doi: 10.1186/s13071-017-2550-5

Guizzo, M. G., Parizi, L. F., Nunes, R. D., Schama, R., Albano, R. M., Tirloni, L., et al. (2017). A *Coxiella* mutualist symbiont is essential to the development of *Rhipicephalus microplus*. *Sci. Rep.* 7:17554. doi: 10.1038/s41598-017-17309-x

Hammer, T. J., Sanders, J. G., and Fierer, N. (2019). Not all animals need a microbiome. *FEMS Microbiol. Lett.* 366:fnz117. doi: 10.1093/femsle/fnz117

Heintz-Buschart, A., and Wilmes, P. (2018). Human gut microbiome: function matters. *Trends Microbiol.* 26, 563–574. doi: 10.1016/j.tim.2017.11.002

Henning, K., Greiner-Fischer, S., Hotzel, H., Ebsen, M., and Theegarten, D. (2006). Isolation of spiroplasma sp. *from an ixodes tick. Int. J. Med. Microbiol.* 40, 157–61. doi: 10.1016/j.ijmm.2006.01.012

Hornok, S., Szoke, K., Meli, M. L., Sándor, A. D., Görföl, T., Estók, P., et al. (2019). Molecular detection of vector-borne bacteria in bat ticks (acari: ixodidae, argasidae) from eight countries of the old and new worlds 06 biological sciences 0604 genetics. *Parasit. Vectors*. 12:50. doi: 10.1186/s13071-019-3303-4

Huttenhower, C., Knight, R., Brown, C. T., Caporaso, J. G., Clemente, J. C., Gevers, D., et al. (2014). Advancing the microbiome research community. *Cell* 159, 227–30. doi: 10.1016/j.cell.2014.09.022

Kopáček, P., Hajdušek, O., Burešová, V., and Daffre, S. (2010). Tick innate immunity. *Adv. Exp. Med. Biol.* 708, 137–162. doi: 10.1007/978-1-4419-8059-5-8

Lane, R. S., Piesman, J., and Burgdorfer, W. (1991). Lyme borreliosis: relation of its causative agent to its vectors and hosts in North America and Europe. *Annu. Rev. Entomol.* 36, 587–609. doi: 10.1146/annurev.ento.36.1.587

Lara, F. A. (2005). Tracing heme in a living cell: hemoglobin degradation and heme traffic in digest cells of the cattle tick *Boophilus microplus*. *J. Exp. Biol.* 208, 3093–3101. doi: 10.1242/jeb.01749

Moreno, C. X., Moy, F., Daniels, T. J., Godfrey, H. P., and Cabello, F. C. (2006). Molecular analysis of microbial communities identified in different developmental stages of *Ixodes scapularis* ticks from westchester and dutchess counties, New York. *Environ. Microbiol.* 8, 761–72. doi: 10.1111/j.1462-2920.2005.00955.x

Nadkarni, M. A., Martin, F. E., Jacques, N. A., and Hunter, N. (2002). Determination of bacterial load by real-time PCR using a broad-range (universal) probe and primers set. *Microbiology* 148(Pt 1), 257–266. doi: 10.1099/00221287-148-1-257

Nakajima, Y., Ogihara, K., Taylor, D., and Yamakawa, M. (2009). Antibacterial hemoglobin fragments from the midgut of the soft tick, *Ornithodoros moubata* (Acari: Argasidae). *J. Med. Entomol.* 40, 78–81. doi: 10.1603/0022-2585-40.1.78

Narasimhan, S., and Fikrig, E. (2015). Tick microbiome: the force within. *Trends Parasitol.* 31, 315–323. doi: 10.1016/j.pt.2015.03.010

Narasimhan, S., Rajeevan, N., Liu, L., Zhao, Y. O., Heisig, J., Pan, J., et al. (2014). Gut microbiota of the tick vector *Ixodes scapularis* modulate colonization of the Lyme disease spirochete. *Cell Host Microbe* 15, 58–71. doi: 10.1016/j.chom.2013.12.001

Needleman, S. B., and Wunsch, C. D. (1970). A general method applicable to the search for similarities in the amino acid sequence of two proteins. *J. Mol. Biol.* 48, 443–53. doi: 10.1016/0022-2836(70)90057-4

Nijhof, A. M., Balk, J. A., Postigo, M., and Jongejan, F. (2009). Selection of reference genes for quantitative RT-PCR studies in *Rhipicephalus (Boophilus) microplus* and *Rhipicephalus appendiculatus* ticks and determination of the expression profile of Bm86. *BMC Mol. Biol.* 10:112. doi: 10.1186/1471-2199-10-112

Oksanen, J., Blanchet, F. G., Friendly, M., Kindt, R., Legendre, P., McGlinn, D., et al. (2019). *vegan: Community Ecology Package*. R package version 2.5-2. Cran R.

Oliveira, J. H. M., Gonçalves, R. L. S., Lara, F. A., Dias, F. A., Gandara, A. C. P., Menna-Barreto, R. F. S., et al. (2011). Blood meal-derived heme decreases ROS levels in the midgut of *Aedes aegypti* and allows proliferation of intestinal microbiota. *PLoS Pathog.* 7:e1001320. doi: 10.1371/journal.ppat.1001320

Olivieri, E., Epis, S., Castelli, M., Varotto Boccazzi, I., Romeo, C., Desirò, A., et al. (2019). Tissue tropism and metabolic pathways of *Midichloria mitochondrii* suggest tissue-specific functions in the symbiosis with Ixodes ricinus. *Ticks Tick. Borne. Dis.* 10, 1070–1077. doi: 10.1016/j.ttbdis.2019.05.019

Perner, J., Provazník, J., Schrenková, J., Urbanová, V., Ribeiro, J. M. C., and Kopáček, P. (2016). RNA-seq analyses of the midgut from blood- and serum-fed *Ixodes ricinus* ticks. *Sci. Rep.* 6:36695. doi: 10.1038/srep36695

Quast, C., Pruesse, E., Yilmaz, P., Gerken, J., Schweer, T., Yarza, P., et al. (2013). The SILVA ribosomal RNA gene database project: Improved data processing and web-based tools. *Nucleic Acids Res.* 41, D590–D596. doi: 10.1093/nar/gks1219

R Core Team (2018). R: A language and environment for statistical computing. *R Foundation for Statistical Computing*, Vienna. Available online at: https://www.R-project.org/

Reck, J., Berger, M., Terra, R. M. S., Marks, F. S., da Silva Vaz, I., Guimarães, J. A., et al. (2009). Systemic alterations of bovine hemostasis due to *Rhipicephalus (Boophilus) microplus* infestation. *Res. Vet. Sci.* 86, 56–62. doi: 10.1016/j.rvsc.2008.05.007

Regassa, L. B., and Gasparich, G. E. (2006). Spiroplasmas: evolutionary relationships and biodiversity. *Front. Biosci.* 11, 2983–3002. doi: 10.2741/2027

Rognes, T., Flouri, T., Nichols, B., Quince, C., and Mahé, F. (2016). VSEARCH: a versatile open source tool for metagenomics. *PeerJ*. 4:e2584. doi: 10.7717/peerj.2584

Ross, B. D., Hayes, B., Radey, M. C., Lee, X., Josek, T., Bjork, J., et al. (2018). *Ixodes scapularis* does not harbor a stable midgut microbiome. *ISME J.* 12, 2596–2607. doi: 10.1038/s41396-018-0161-6

Sassera, D., Lo, N., Bouman, E. A. P., Epis, S., Mortarino, M., and Bandi, C. (2008). "*Candidatus midichloria*" endosymbionts bloom after the blood meal of the host, the hard tick *Ixodes ricinus*. *Appl. Environ. Microbiol.* 74, 6138–40. doi: 10.1128/AEM.00248-08

Sassera, D., Lo, N., Epis, S., D'Auria, G., Montagna, M., Comandatore, F., et al. (2011). Phylogenomic evidence for the presence of a flagellum and cbb 3 oxidase in the free-living mitochondrial ancestor. *Mol. Biol. Evol.* 28, 3285–96. doi: 10.1093/molbev/msr159

Schloss, P. D., Westcott, S. L., Ryabin, T., Hall, J. R., Hartmann, M., Hollister, E. B., et al. (2009). Introducing mothur: open-source, platform-independent, community-supported software for describing and comparing microbial communities. *Appl. Environ. Microbiol.* 75, 7537–7541. doi: 10.1128/AEM.01541-09

Sojka, D., Franta, Z., Horn, M., Caffrey, C. R., Mareš, M., and Kopáček, P. (2013). New insights into the machinery of blood digestion by ticks. *Trends Parasitol.* 29, 276–285. doi: 10.1016/j.pt.2013.04.002

Sonenshine, D. E., Ceraul, S. M., Hynes, W. E., Macaluso, K. R., and Azad, A. F. (2002). Expression of defensin-like peptides in tick hemolymph and midgut in

response to challenge with *Borrelia burgdorferi*, *Escherichia coli* and *Bacillus subtilis*. *Exp. Appl. Acarol.* 28, 127–34. doi: 10.1023/A:1025354326877

Sonenshine, D. E., and Macaluso, K. R. (2017). Microbial invasion vs. *tick immune regulation*. *Front. Cell. Infect. Microbiol.* 7:390. doi: 10.3389/fcimb.2017.00390

Strnad, M., Hönig, V., RuŽek, D., Grubhoffer, L., and Rego, R. O. M. (2017). Europe-wide meta-analysis of *Borrelia burgdorferi* sensu lato prevalence in questing *Ixodes ricinus* ticks. *Appl. Environ. Microbiol.* 83:e00609-17. doi: 10.1128/AEM.00609-17

Strong, M. J., Xu, G., Morici, L., Splinter Bon-Durant, S., Baddoo, M., Lin, Z., et al. (2014). Microbial contamination in next generation sequencing: implications for sequence-based analysis of clinical samples. *PLoS Pathog.* 10:e1004437. doi: 10.1371/journal.ppat.1004437

Vayssier-Taussat, M., Kazimirova, M., Hubalek, Z., Hornok, S., Farkas, R., Cosson, J. F., et al. (2015). Emerging horizons for tick-borne pathogens: From the "one pathogen-one disease" vision to the pathobiome paradigm. *Future Microbiol.* 10, 2033–43. doi: 10.2217/fmb.15.114

Weiss, B., and Aksoy, S. (2011). Microbiome influences on insect host vector competence. *Trends Parasitol.* 27, 514–22. doi: 10.1016/j.pt.2011.05.001

Yilmaz, P., Parfrey, L. W., Yarza, P., Gerken, J., Pruesse, E., Quast, C., et al. (2014). The SILVA and "all-species living tree project (LTP)" taxonomic frameworks. *Nucleic Acids Res.* 42, D643–D648. doi: 10.1093/nar/gkt1209

Zhang, C. M., Li, N. X., Zhang, T. T., Qiu, Z. X., Li, Y., Li, L. W., et al. (2017). Endosymbiont CLS-HI plays a role in reproduction and development of *Haemaphysalis longicornis*. *Exp. Appl. Acarol.* 73, 429–438. doi: 10.1007/s10493-017-0194-y

Zhong, J., Jasinskas, A., and Barbour, A. G. (2007). Antibiotic treatment of the tick vector *Amblyomma americanum* reduced reproductive fitness. *PLoS ONE* 2:e405. doi: 10.1371/journal.pone.0000405

Conflict of Interest: The authors declare that the research was conducted in the absence of any commercial or financial relationships that could be construed as a potential conflict of interest.

frontiers in Cellular and Infection Microbiology

ORIGINAL RESEARCH
published: 12 June 2020
doi: 10.3389/fcimb.2020.00244

Tick-Borne Flavivirus Inhibits Sphingomyelinase (*Is*SMase), a Venomous Spider Ortholog to Increase Sphingomyelin Lipid Levels for Its Survival in *Ixodes scapularis* Ticks

Pravesh Regmi[1], *Supreet Khanal*[1], *Girish Neelakanta*[1†] *and Hameeda Sultana*[1,2*†]

[1] *Department of Biological Sciences, Old Dominion University, Norfolk, VA, United States,* [2] *Division of Infectious Diseases and International Health, Department of Medicine, University of Virginia School of Medicine, Charlottesville, VA, United States*

OPEN ACCESS

Edited by:
Alejandro Cabezas-Cruz, Institut National de Recherche pour l'Agriculture, l'Alimentation et l'Environnement (INRAE), France

Reviewed by:
Saravanan Thangamani, Upstate Medical University, United States
Maria Kazimirova, Slovak Academy of Sciences, Slovakia

***Correspondence:**
Hameeda Sultana
hsultana@odu.edu

†Present address:
Girish Neelakanta and Hameeda Sultana, Center for Molecular Medicine, Old Dominion University, Norfolk, VA, United States

Specialty section:
This article was submitted to Virus and Host, a section of the journal Frontiers in Cellular and Infection Microbiology

Received: *11 February 2020*
Accepted: *27 April 2020*
Published: *12 June 2020*

Citation:
Regmi P, Khanal S, Neelakanta G and Sultana H (2020) Tick-Borne Flavivirus Inhibits Sphingomyelinase (IsSMase), a Venomous Spider Ortholog to Increase Sphingomyelin Lipid Levels for Its Survival in Ixodes scapularis Ticks. Front. Cell. Infect. Microbiol. 10:244. doi: 10.3389/fcimb.2020.00244

Our previous study showed that cells from medically important arthropods, such as ticks, secrete extracellular vesicles (EVs) including exosomes that mediate transmission of flavivirus RNA and proteins to the human cells. Understanding the molecular determinants and mechanism(s) of arthropod-borne flavivirus transmission via exosome biogenesis is very important. In this current study, we showed that in the presence of tick-borne Langat Virus (LGTV; a member of tick-borne encephalitis virus complex), the expression of arthropod *Is*SMase, a sphingomyelinase D (SMase D) that catalyzes the hydrolytic cleavage of substrates like sphingomyelin (SM) lipids, was significantly reduced in both *Ixodes scapularis* ticks (*in vivo*) and in tick cells (*in vitro*). The *Is*SMase reduced levels correlated with down-regulation of its activity upon LGTV replication in tick cells. Our data show that LGTV-mediated suppression of *Is*SMase allowed accumulation of SM lipid levels that supported membrane-associated viral replication and exosome biogenesis. Inhibition of viral loads and SM lipid built up upon GW4869 inhibitor treatment reversed the *Is*SMase levels and restored its activity. Our results suggest an important role for this spider venomous ortholog *Is*SMase in regulating viral replication associated with membrane-bound SM lipids in ticks. In summary, our study not only suggests a novel role for arthropod *Is*SMase in tick-LGTV interactions but also provides new insights into its important function in vector defense mechanism(s) against tick-borne virus infection and in anti-viral pathway(s).

Keywords: ticks, *Is*SMase, Langat Virus (LGTV), GW4869 inhibitor, sphingomyelinase, sphingomyelin, exosomes

INTRODUCTION

Vector-borne diseases that account for high morbidity and mortality throughout the world have been of major concern (Powell, 2019; Qurollo, 2019; Scalway et al., 2019; Shaw and Catteruccia, 2019; Spence Beaulieu, 2019; Wilke et al., 2019; Wilson et al., 2019). The medically important *Ixodes scapularis* tick transmits a variety of pathogens that cause severe diseases in humans and animals (Labuda et al., 1996; Labuda and Randolph, 1999; Nuttall et al., 2000; Nuttall and Labuda, 2003, 2004; Piesman and Eisen, 2008; Neelakanta and Sultana, 2015; de la Fuente, 2018; Kim, 2019). Some

of the tick-borne pathogens of human health importance are the newly emerging Powassan virus (POWV), tick-borne encephalitis virus (TBEV), Lyme disease agent *Borrelia burgdorferi*, rickettsial pathogens (such as *Rickettsia rickettsii* and *Anaplasma phagocytophilum*), and *Francisella tularensis*, a bacterium causing tularemia (Randolph et al., 1996; Sexton and Kirkland, 1998; Nuttall et al., 2000; Piesman and Eisen, 2008; Sultana et al., 2010; Valarcher et al., 2015; Vora et al., 2017; Zhou et al., 2018; Sekeyova et al., 2019; Zellner and Huntley, 2019). Ticks have evolved a myriad of strategies that allow them to get a blood meal through feeding on a vertebrate host for several days. The presence of pharmacological agents in tick's saliva modulates pain, itch, blood clotting, wound healing, immune responses, and inflammation that allows longer feeding periods and sufficient time for the transmission of pathogens to a variety of vertebrate host (Nuttall et al., 2000; Nuttall and Labuda, 2003, 2004). A study has identified a novel sphingomyelinase-like enzyme (*Is*SMase) in *I. scapularis* tick saliva that modulates the adaptive immune response by inclining the host CD4+ T-cells to result in a shift from a neutralizing Th1 cytokine response toward a Th2-induced cytokine profile response (Alarcon-Chaidez et al., 2009). This Mg^{+2}-dependent, neutral form of *Is*SMase directly (independent of its enzymatic activity) programmed the CD4+ T cells in order to express interleukin 4 (IL-4), which is a hallmark of Th2 effects (Alarcon-Chaidez et al., 2009). *Is*SMase showed high homology to the *Loxosceles* venomous spider's sphingomyelinase D (SMase D) protein (Alarcon-Chaidez et al., 2009). SMase D is also known as phospholipase D (PLD1) or sphingomyelin (SM) phosphodiesterase D that catalyzes the hydrolytic cleavage of substrates like SM or lysophospholipid, such as lysophosphotidylcholine resulting in the formation of choline and ceramide 1-phosphate or choline and lysophosphatidic acid (LPA), respectively (Truett, 1993; Zager et al., 2000; Binford et al., 2009; Zobel-Thropp et al., 2010; Dias-Lopes et al., 2013). SM (with generic name *N*-acyl-sphingosine-L-phosphorylcholine) is a major structural component of the plasma membrane in all eukaryotic cells that performs biological functions together with other phospholipids, glycolipids, cholesterol, and membrane-integrated proteins (Truett, 1993; Zager et al., 2000; Zobel-Thropp et al., 2010; Schneider-Schaulies and Schneider-Schaulies, 2015). By-products of SM such as ceramide, sphingosine, and sphingosine-L-phosphate are essential cellular effectors playing roles in apoptosis, cell development, and survival (Kolesnick and Kronke, 1998; Chmura et al., 2000; Bikman and Summers, 2011; Vijayan and Hahm, 2014; Schneider-Schaulies and Schneider-Schaulies, 2015; Bezgovsek et al., 2018; Soudani et al., 2019). It has been shown that SMase D, the main toxin in the spider venom, causes dermonecrotic lesions on mammalian skin, which are characteristic of envenomation by the *Loxosceles* spiders (Zobel-Thropp et al., 2010). *Loxosceles intermedia* Class 2 venom SMase D has shown to increase the production and secretion of matrix metalloproteinases (MMPs) 2 and 9, whereas the more potent Class 1 SMase D from *L. laeta* induced MMP7 in addition to MMP2 and 9, thereby resulting in keratinocyte death (Paixao-Cavalcante et al., 2007; Correa et al., 2016). It is interesting to note that spider's SMase D is responsible for local skin necrosis in general, and in occasional cases, it also results in severe systemic manifestations, such as acute kidney failure and death (Paixao-Cavalcante et al., 2007; Zobel-Thropp et al., 2010; Correa et al., 2016).

A bioinformatics analysis identified SMase D or proteins with SMase D activity in bacteria (*Corynebacteria* and *Arcanobacterium*), fungi (*Aspergillus* and *Coccidioides*), mites, spiders, and tick saliva (Binford et al., 2009; Zobel-Thropp et al., 2010; Dias-Lopes et al., 2013; Lopes et al., 2013; Pedroso et al., 2015). A common C-terminal similar motif (SMD-tail) at the end of spider's SMase D supported the identification of the broadly conserved glycerophosphoryl-diester phosphodiesterase (GDPD) family in different organisms (Binford et al., 2005). Phylogenetic analysis of spider's SMase D showed a possible convergent evolution that is independent from GDPD ancestor such as fungi and arthropods (Zobel-Thropp et al., 2010; Dias-Lopes et al., 2013). Tick *Is*SMase recombinant protein intradermal injections (at 5 μg) showed no dermonecrotic activity or any detectable cutaneous changes or inflammation (Alarcon-Chaidez et al., 2009). However, in the presence of salivary contents, *Is*SMase may contribute to the feeding lesions at the tick bite site (Alarcon-Chaidez et al., 2009). In addition to *I. scapularis* ticks, SMase D has been identified in other genera of ticks such as *Amblyomma* and *Rhiphicephalus,* where this toxin is shown to be involved in animal ear inflammation and possible necrosis (Binder, 1989; Truett, 1993; Binford et al., 2005, 2009). Our previous study showed that both positive and negative strands of LGTV RNA and viral envelope (E), non-structural 1 (NS1) protein, and perhaps poly-protein were contained inside exosomes derived from ISE6 tick cells (Zhou et al., 2018). These tick cell-derived exosomes were enriched with exosomal marker HSP70 and infection with LGTV induced exosome production and release as a means of induced viral RNA and protein dissemination (Zhou et al., 2018). This study indicates a role for sphingomyelinases in affecting the exosome's biogenesis, viral replication, and dissemination. In this current study, we not only report a novel role for *Is*SMase in tick-LGTV interactions but also delineate its important function in tick anti-viral pathway(s).

MATERIALS AND METHODS

Bioinformatics and Prediction Analysis

The amino acid sequences of *Is*SMase were used from GenBank and analyzed at Prosite website (http://prosite.expasy.org). The deduced *Is*SMase amino acid sequence is aligned (with other orthologs) using ClustalW program in DNASTAR Lasergene. Matching residues are shaded in black color for easy identification. Annotation/prediction analysis performed in CLC Genomics Workbench 20.0 for *Is*SMase protein sequence is shown. Prosite from Expasy (https://prosite.expasy.org/) and NCBI CDD search (https://www.ncbi.nlm.nih.gov/Structure/cdd/wrpsb.cgi) was used for the prediction of glycosylation, myristoylation, protein kinase C (PKC) phosphorylation, casein kinase II phosphorylation,

tyrosine phosphorylation, and cAMP-dependent protein kinase phosphorylation sites in *Is*SMase.

GenBank Accession Numbers

The GenBank accession numbers for the sphingomyelinase sequences used in this study are as follows: *I. scapularis* sphingomyelinase-like enzyme (*Is*SMase; accession number ABD73957), *Rhipicephalus pulchellus* (SM phosphodiesterase; accession number JAA56531), *Amblyomma maculatum* (hypothetical protein; accession number AEO33547), and spider orthologs such as *Scicarius patagonicus* (SMase D; accession number C0JB69), *Hemiscorpius lepturus* (venom toxin; accession number API81381) and *L. similis* (loxtox protein; accession number ANY30961).

Ticks, Synchronous Infections, and Tick Feeding on Mice

Unfed nymphal *I. scapularis* ticks were obtained from BEI resources (ATCC)/Centers for Disease Prevention and Control (CDC) and were maintained in our laboratory. Ticks were kept at room temperature with approximately 98% relative humidity under a photoperiod of 14 h of light and 10 h of darkness. For the expression of *Is*SMase, we used three different developmental stages of ticks: larvae, nymphs, and adults (male or female) obtained from BEI Resources/CDC. For synchronous infection, we followed published protocols (Mitzel et al., 2007; Taank et al., 2018). Unfed nymphs were collected in sterile 1.5-ml Eppendorf tubes. Out of 48 nymphs (used in total), 24 (12 in each tube) were maintained as uninfected controls and 24 (12 in each tube) were synchronously infected with LGTV (LGT-TP21 strain). Briefly, nymphs were infected by immersion into 0.5 ml of complete Dulbecco's modified eagle's medium (DMEM) containing 1×10^7 plaque-forming units (pfu)/ml of LGTV. For the uninfected control group, nymphs were immersed into DMEM without virus. The tubes were incubated for 45 min at 34°C (with tubes being vortexed every 10 min to redistribute ticks in the media). Tubes were then chilled on ice (for 2 min) and centrifuged at 200 × g for 30 s. Nymphs were washed twice with cold 1× PBS by centrifugation. After washing, ticks were dried with Whatman paper and transferred into sterile collection tubes with holed caps covered with nylon mesh cloth. LGTV-infected and uninfected nymphs were kept in separate tubes with proper labels in an environmental chamber maintained at room temperature and a relative humidity of 98% for 17 days. Ticks generated by this synchronous method were used as LGTV-infected unfed ticks. LGTV-infected ticks were partially fed (for 24 h during feeding- DF) on wild-type C57BL/6 mice (purchased from Charles River Laboratories) for 24 h and ticks were pulled with forceps. Uninfected ticks fed on naïve C57BL/6 mice were used as controls. All experiments were conducted in strict accordance with the recommendations in the *Guide for the Care and Use of Laboratory Animals* of the NIH, USA, and using approved protocol from the Institutional Animal Care and Use Committee (IACUC; protocol #18-011).

In vitro Tick Cell Culture, Infections, and Exosome Isolation From Cell Culture Supernatants

We used *I. scapularis* ISE6 tick cell line that is grown and maintained as described in our previous study (Zhou et al., 2018). Wild-type LGTV (LGT-TP21) strain used in this study is maintained in Vero cells as laboratory virus stocks. Briefly, 5×10^5 cells were seeded in 12-well plates and infected with LGTV [with a multiplication of infection (MOI) of 1, for time points 24, 48, and 72 h post-infection (p.i.), or with various MOI doses of 1–3; for dose response collections at 72 h p.i.]. Exosomes were isolated from tick cell culture supernatants by a differential ultracentrifugation method (Vora et al., 2018; Zhou et al., 2018, 2019). Details for these procedures are also schematically shown in our previous study (Zhou et al., 2018). To isolate exosomes, we used concentrated cell culture supernatants. Purified exosome preparations were stored at −80°C and used for further analysis.

RNA Extraction, cDNA Synthesis, and QRT-PCR Analysis

Total RNA was extracted from both uninfected and LGTV-infected nymphal ticks (unfed or 24 h partially fed) or ISE6 tick cells or exosomes derived from tick cells, using Aurum Total RNA Mini kit (Bio-Rad) and following the manufacturer's instruction. RNA samples generated (in our previous studies) from *B. burgdorferi*- or *A. phagocytophilum*-infected unfed nymphs (Khanal et al., 2018; Taank et al., 2018) were used in this study. RNA (1 μg) was converted into cDNA using iScript cDNA synthesis kit (Bio-Rad). The generated cDNA was used as a template to amplify and determine the viral burdens and *Is*SMase levels by performing quantitative real-time PCR (QRT-PCR) using the iQ-SYBR Green Supermix kit (Bio-Rad) and by following the manufacturer's instructions. We used a Bio-Rad CFX96 QPCR machine to perform the QRT-PCR reactions. Published forward and reverse primers were used to detect LGTV-RNA (Zhou et al., 2018). *Is*SMase transcripts were detected using primer pairs 5′ CGCCGCTGGAGTAGA CATC 3′ and 5′ GACCCACATCGAATCCCACA 3′. The *hsp70* transcripts were amplified using published primers (Vora et al., 2017). Tick beta-actin levels were quantified using published primers (Taank et al., 2018; Zhou et al., 2018) and were used to normalize the levels of other transcripts in all analysis. In addition to normalizing with tick actin, LGTV prM-E levels were also normalized to the total RNA levels that are shown on the *Y*-axis. Equal volume of cDNA was used in parallel for LGTV prM-E, beta-actin, *hsp70*, and *issmase* primers. Standard curves were prepared from each gene standard using 10-fold serial dilutions starting from standard 1 as 1 ng to standard 6 as 0.000001 ng of known quantities of *actin*. Untreated samples served as internal controls.

GW4869 Inhibitor Studies

We used GW4869, a cell-permeable, selective inhibitor for neutral sphingomyelinase (N-SMase) (obtained from Santa Cruz Biotechnologies, Inc). Tick cells showed no cytotoxicity with 1 μM of GW4869 inhibitor treatment and hence we considered

this dose in both experiments. DMSO was used as a vehicle control. A similar volume of DMSO that is equal to 1 μM GW4869 was used in our experiments. Tick cells were plated and incubated overnight and then treated with 1 μM GW4869 inhibitor for 4 h, followed by infection with LGTV for 72 h p.i. Before infection, we did not wash cells to remove the inhibitor.

Sphingomyelinase and SM Quantification Assays

We used colorimetric sphingomyelinase or SM quantification assay kits from Sigma-Aldrich (USA) and followed the manufacturer's instructions. Sphingomyelinase assay was performed as described in our recent study (Zhou et al., 2019). Briefly, we plated 5×10^5 tick cells, and after overnight incubation, cells were infected with LGTV (MOI 1) for either 24 or 72 h (p.i.) for both assays. Cell lysates were resuspended in 1× PBS and processed for sphingomyelinase activity or SM lipid levels, immediately. For each time point and reaction well, 50 μl of samples (uninfected or LGTV-infected) was used as six replicates. Zero blank sphingomyelinase/SM standards were considered as background values, respectively, in each assay. Samples from sphingomyelinase or SM assays were measured at 655 or 570 nm absorbance, respectively. Using the standard values, curves were plotted and the amount of enzyme or lipid present in the samples was determined from the standard curve.

Statistics

Statistical differences observed in data sets were analyzed using GraphPad Prism6 software and Microsoft Excel. The non-paired, two-tailed Student's *t*-test was performed (for data to compare two means) for the entire analysis. Each experiment was performed for three independent times and 5–10 replicates were considered in each experiment. Error bars represent mean (±SD) values, and *P*-values of <0.05 were considered significant in all analyses.

RESULTS

Detailed Bioinformatics Analysis Revealed *I. scapularis* Sphingomyelinase (*Is*SMase) as a Potential Venomous Protein Ortholog From Spiders

In this study, we characterized *Is*SMase in detail. Expression of *issmase* gene transcripts was noted in uninfected tick cells, unfed nymphs, and 24 h partially fed nymphs (**Supplementary Figure 1**). We performed bioinformatics, comparative, and prediction analysis on *Is*SMase (accession number ABD73957) and compared its sequence with that of its orthologs from other ticks such as *R. pulchellus* (SM phosphodiesterase; JAA56531), *A. maculatum* (hypothetical protein; AEO33547), and spider orthologs such as *S. patagonicus* (SMase D; C0JB69), *H. lepturus* (venom toxin; API81381), and *L. similis* (loxtox protein; ANY30961). ClustalW alignment of *Is*SMase with *R. pulchellus* or *A. maculatum* ticks showed less degree of conservation (**Figure 1A**), whereas *Is*SMase sequence comparison with *S. patagonicus*, *H. lepturus*, and *L. similis* spider orthologs revealed high conservation in the amino acid sequence (**Figure 1A**). Comparative sequence analysis of *Is*SMase protein with tick or spider orthologs found the conserved motif/domain glycerophosphoryl diester phosphodiesterases (GDPD-like SMase D-PLD) from the SMase D family (**Figure 1A**). This conserved motif/domain sequence is highlighted with a black box and the predicted leader peptide for *Is*SMase is underlined (**Figures 1A,B**). Domain analysis revealed that *Is*SMase shared catalytic sites with other SMase D orthologs. The residues (H34, H70, C76, and C80; highlighted with arrows) important for catalytic activity were conserved among all the analyzed SMases (**Figure 1A**). The catalytic site lies between residues 29 and 65 with two catalytic loops of residues 64–71 and 74–78 (**Figure 1B**). The magnesium binding site that overlapped with the catalytic site lies between residues 49/51 and 109 (**Figure 1B**).

Furthermore, the phylogenetic analysis showed that *Is*SMase is closely related to spider orthologs and forms a clade that clusters with the venomous spider ortholog SMase D (**Figure 2A**). However, both *R. pulchellus* and *A. maculatum* tick orthologs formed separate sub-clades, suggesting differences in SMases from these ticks (**Figure 2A**). Tick SMase D orthologs from *R. pulchellus* and *A. maculatum* also showed high degree of divergence to *Is*SMase and the spider orthologs (**Figure 2B**). *Is*SMase amino acid sequence comparison revealed 43.1 or 40.7% identity to *R. pulchellus* and *A. maculatum* ticks, and it showed 41.1, 39.4, and 37.2% identity with *S. patagonicus*, *H. lepturus*, and *L. similis* spider orthologs, respectively (**Figure 2B**). In addition, protein feature prediction analysis, performed as previously described (Turck et al., 2019), revealed the presence of 12 PKC phospho-sites (with 4 serine and 8 threonine residues), 6 casein kinase II phospho-sites (with 5 serine and 1 threonine residue), 2 cAMP/cGMP-dependent phospho-sites (with 1 each of serine and threonine residues), 3 tyrosine kinase phospho-sites (with 3 tyrosine residues), 2 N-glycosylation sites (with 2 N-linked GlcNAc; asparagine residues), and 3 N-myristoylation sites (with 3 glycine residues), respectively (**Figure 2C**). Presence of several protein modification sites suggests *Is*SMase to be a highly functional enzyme in ticks.

*Is*SMase Is Not Developmentally Regulated in *I. scapularis* Ticks

We analyzed the expression of *Is*SMase in three different stages of ticks: larvae, nymphs, and adults (male or female) to understand the importance of this molecule in tick life cycle and developmental stages. QRT-PCR analysis showed that *Is*SMase is expressed in all three developmental stages of ticks. *Is*SMase mRNA levels appeared to be higher in adult male and female ticks and low level of expression was noted in larval and nymphal ticks (**Figure 3A**). However, the levels of *Is*SMase in the three developmental stages of ticks showed no significant ($P > 0.05$) differences in its expression (**Figure 3A**). These data suggest that *Is*SMase expression is not influenced by developmental changes in ticks.

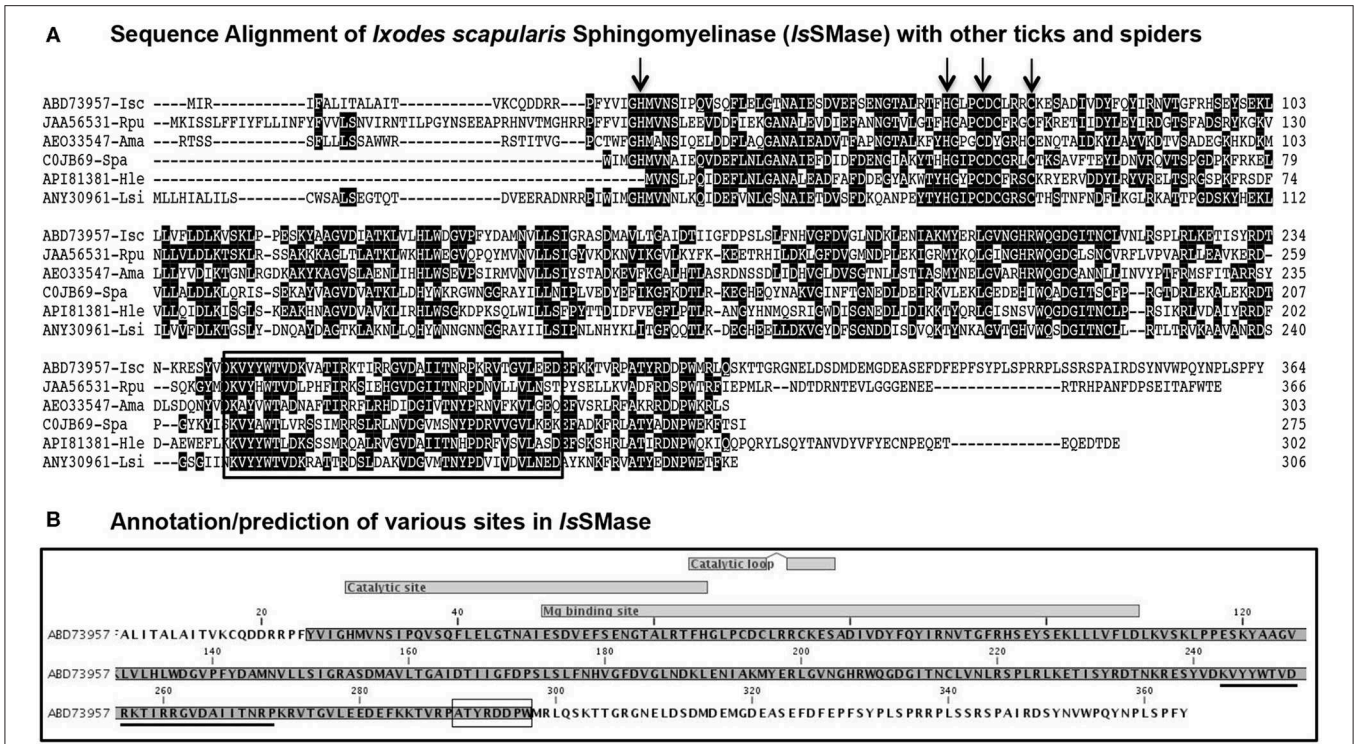

FIGURE 1 | Sequence alignments and prediction analysis of *Is*SMase with tick and spider orthologs. **(A)** The deduced *I. scapularis* (*Isc*) SMase (*Is*SMase) amino acid sequence alignment (with other orthologs) using ClustalW program in DNASTAR Lasergene is shown. Matching residues are shaded in black color. GenBank accession numbers for *R. pulchellus* (*Rpu*) sphingomyelin phosphodiesterase, *A. maculatum* (*Ama*) hypothetical protein, *S. patagonicus* (*Spa*) sphingomyelinase D, *H. lepturus* (*Hle*) venom toxin, and *L. similis* (*Lsi*) loxtox protein sequences are shown. GenBank accession numbers for *Isc*, *Rpu*, and *Ama* are provided. Total length of the amino acid sequence is provided at the right end of each sequence. **(B)** Annotation/prediction analysis performed in CLC Genomics Workbench 20.0 for *Is*SMase protein sequence is shown. The catalytic site and magnesium binding sites and their overlap site are shown. The underlined sequence indicates the glycero-phosphodiester phosphodiesterase-like motif. The SMaseD consensus motif is shown as a boxed amino acid sequence.

*Is*SMase Expression Is Reduced Upon LGTV Infection in Both Unfed/Fed Ticks and in Tick Cells

Our previous study (Zhou et al., 2018) suggests analyzing the importance of *Is*SMase in ticks. Combing of *I. scapularis* genome revealed the presence of several sphingomyelinase-like enzymes of both acidic and basic types; however, we addressed the spider venomous SMase D ortholog *Is*SMase that was previously identified in ticks (Alarcon-Chaidez et al., 2009). QRT-PCR analysis revealed detection of LGTV loads in unfed nymphs that were generated by synchronous viral infection (see section Materials and Methods) (**Figure 3B**). Viral loads were highly detectable in all tested ticks, but the *Is*SMase transcript levels were significantly ($P < 0.05$) reduced in LGTV-infected unfed ticks (**Figure 3C**) in comparison to the uninfected controls. Next, we generated synchronously infected LGTV *I. scapularis* ticks and partially fed them on uninfected mice. Ticks were collected at 24 h during feeding. As expected, we found significantly ($P < 0.05$) higher viral burden determined by LGTV-prM-E transcript levels (**Figure 3D**). Similar to the observation noted with unfed nymphs, LGTV-infected ticks collected during 24 h of partial feeding also showed significantly ($P < 0.05$) reduced *Is*SMase transcript levels in comparison to the levels noted in uninfected controls (**Figure 3E**).

We have previously shown that LGTV readily infected *I. scapularis* ISE6 tick cells, with increased viremia at 72 h p.i. (Zhou et al., 2018). Next, we determined the *Is*SMase levels in ISE6 tick cells. We first performed a time response of LGTV infection (with MOI 1) in tick cells by considering one early (24 h p.i.) and one late time point (72 h p.i.). QRT-PCR analysis showed significant ($P < 0.05$) induction in LGTV infection over the time course of 24 and 72 h p.i. (**Figure 4A**); however, in the same samples, we found that *Is*SMase transcript levels were significantly ($P > 0.05$) reduced at both tested time points in comparison to the respective uninfected controls (**Figure 4B**). In addition, we performed a dose-response experiment by infecting tick cells with various doses of LGTV (MOIs of 1, 2, and 3). We found that tick cells were tolerant for MOI 1 and 2; however, 25–30% of tick cells were susceptible to LGTV infection at MOI 3. QRT-PCR analysis revealed no significant differences in viral loads between tick cells that were infected with MOI 1 and 2 (**Figure 4C**). However, significant ($P < 0.05$) difference in viral loads was evident between tick cells infected with MOI 2 and 3 (**Figure 4C**). We found that *Is*SMase transcript levels were significantly ($P < 0.05$) lower at all tested MOIs in comparison to

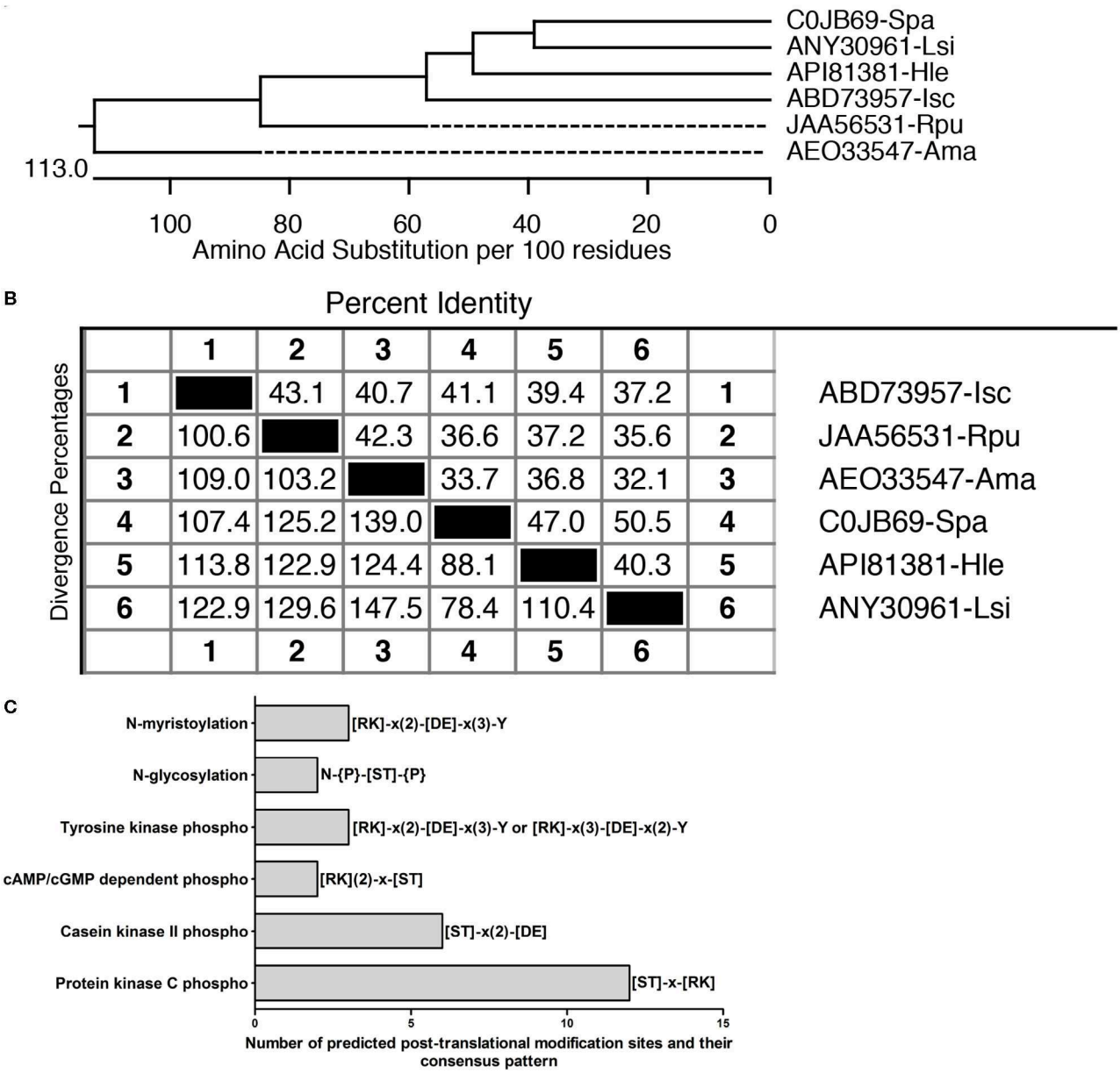

FIGURE 2 | Comparative bioinformatics analysis of *Is*SMase with other orthologs. **(A)** Phylogenetic analysis comparing *Is*SMase and other orthologs was performed in DNASTAR by ClustalW slow/accurate alignment method using Gonnet as default value for protein weight matrix. Scale at the bottom denotes amino acid substitutions per 100 amino acid residues. **(B)** Percent identity (horizontally above black boxed diagonal) and divergence (vertically below black boxed diagonal) of *Is*SMase nucleotide sequence in comparison to *R. pulchellus* (*Rpu*) sphingomyelin phosphodiesterase, *A. maculatum* (*Ama*) hypothetical protein, *S. patagonicus* (*Spa*) sphingomyelinase D, *H. lepturus* (*Hle*) venom toxin, and *L. similis* (*Lsi*) loxtox protein sequence is shown. **(C)** Protein feature prediction analysis showing *Is*SMase protein modification sites and relevant amino acids as functionally active residues in those modifications. *Is*SMase contains 12 protein kinase C (PKC) phospho-sites, 6 casein kinase II phospho-sites, 2 cAMP/cGMP-dependent phospho-sites, 3 tyrosine kinase phospho-sites, 2 N-glycosylation sites, and 3 N-myristoylation sites.

the uninfected control (**Figure 4D**). Reproducible to our previous study, we found that LGTV loads were abundantly present in tick cell-derived exosomes (**Supplementary Figure 2A**). We noticed the exosomal marker HSP70 transcript levels; however, we did not detect *Is*SMase transcript levels in tick cell-derived exosomes (**Supplementary Figures 2B,C**). Overall, these data suggest that LGTV infection reduces the levels of *Is*SMase in unfed nymphs, in partially fed nymphs (collected at 24 h during feeding), and in tick cells (in a time- and dose-dependent response).

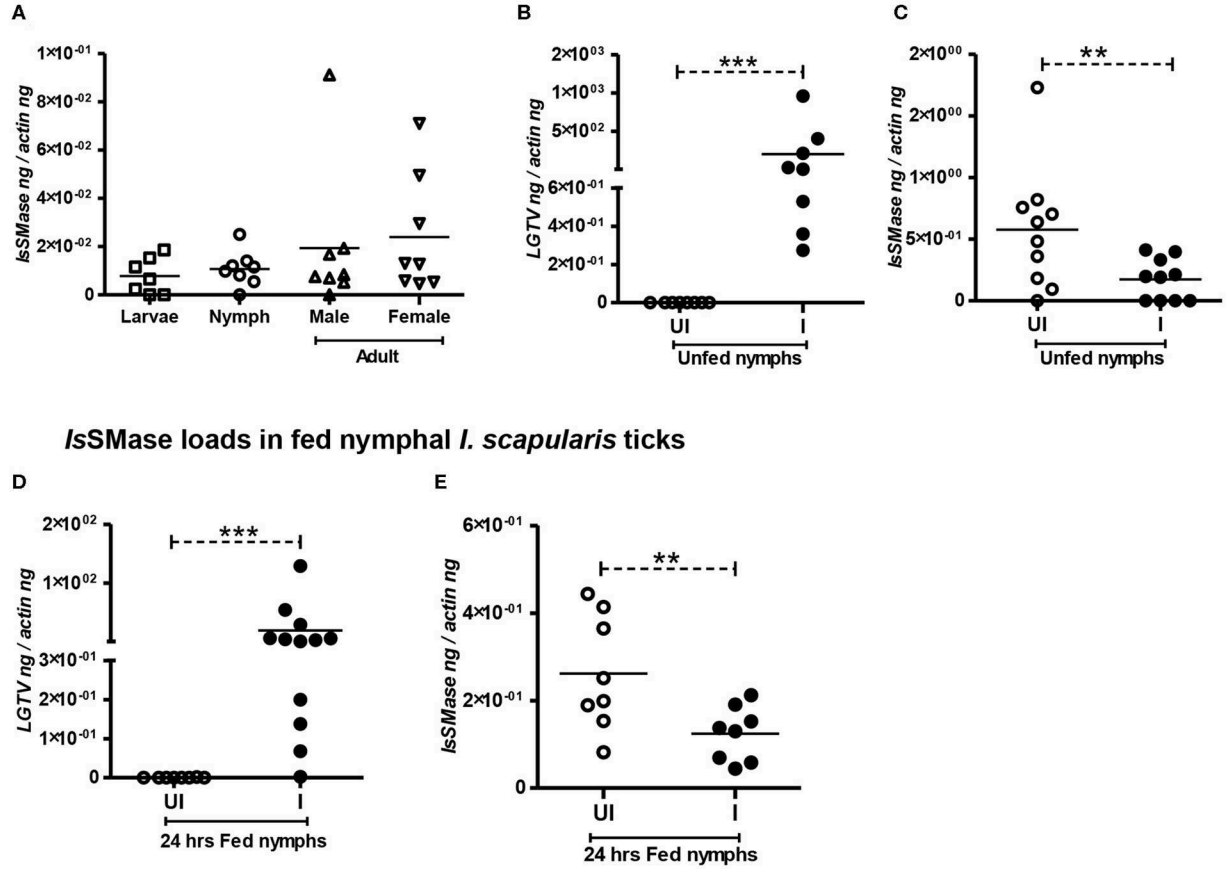

FIGURE 3 | *Is*SMase expression is reduced upon LGTV infection in ticks. QRT-PCR analysis showing *Is*SMase gene expression levels in different developmental/life stages (larvae, nymphs, adult male, and female) of ticks **(A)**. LGTV viral loads **(B)** or *Is*SMase transcript loads **(C)** in unfed nymphs is shown. QRT-PCR showing LGTV viral loads **(D)** or *Is*SMase transcript loads **(E)** in partially fed (24 h) nymphs. UI indicates uninfected or I denotes LGTV-infected nymphs. Each square, circle, triangle, or inverted triangle indicates one tick. Open circles represent uninfected (UI) group, whereas closed circles denote LGTV-infected (I) group. LGTV loads or *Is*SMase mRNA levels were normalized to tick beta-actin levels. *P*-value determined by Student's two-tailed *t*-test is shown. The asterisk indicates significance, and ** or *** denotes a *P*-value of less than 0.01 or 0.001, respectively.

GW4869 Inhibitor Treatment Reduced LGTV Loads and Restored the *Is*SMase Transcript Levels

Dihydrochloride hydrate (GW4869) is a cell-permeable but selective inhibitor for neutral sphingomyelinase(s) that affects the exosome production and release. Our previous study showed that GW4869 inhibitor treatment reduced LGTV loads in exosomes and also inhibited the transmission of LGTV RNA and proteins via infectious exosomes to both tick (5 μM) and vertebrate (1–20 μM) host cells (Zhou et al., 2018). We determined whether GW4869 (1 μM) treatment for either 4 or 24 h also reduced the LGTV loads in tick cells. QRT-PCR analysis revealed that LGTV loads were significantly ($P < 0.05$) reduced at 4 h of GW4869 treatment (**Figure 5A**). The reduction in LGTV replication/loads correlated with significantly ($P < 0.05$) increased expression of *Is*SMase in these tick cells (**Figure 5B**). In addition, higher incubation times (for 24 h) of GW4869 treatment showed significant ($P < 0.05$) reduction of LGTV loads (**Figure 5C**) that significantly ($P < 0.05$) increased expression of *Is*SMase in these tick cells (**Figure 5D**). These data show a direct association of LGTV replication/loads in the suppression of the *Is*SMase levels in tick cells that are restored with GW4869 treatment.

LGTV Reduced *Is*SMase Activity to Induce SM Lipid Accumulation

Since LGTV reduced *Is*SMase expression, we investigated whether the increased replication of LGTV (at time points of 24 and 72 h p.i., with MOI 1) also affects the *Is*SMase enzymatic activity and its function. We performed *Is*SMase activity assay in whole-cell lysates and found that LGTV significantly ($P < 0.05$) reduced *Is*SMase activity at an early time point (24 h p.i.) of infection (**Figure 6A**). However, no difference in the *Is*SMase activity was observed at a later time point (72 h p.i.) of LGTV infection (**Figure 6A**). Reduced activity of *Is*SMase upon LGTV infection suggested accumulating lipid metabolism pathway. Next, we determined the SM levels in whole tick cell

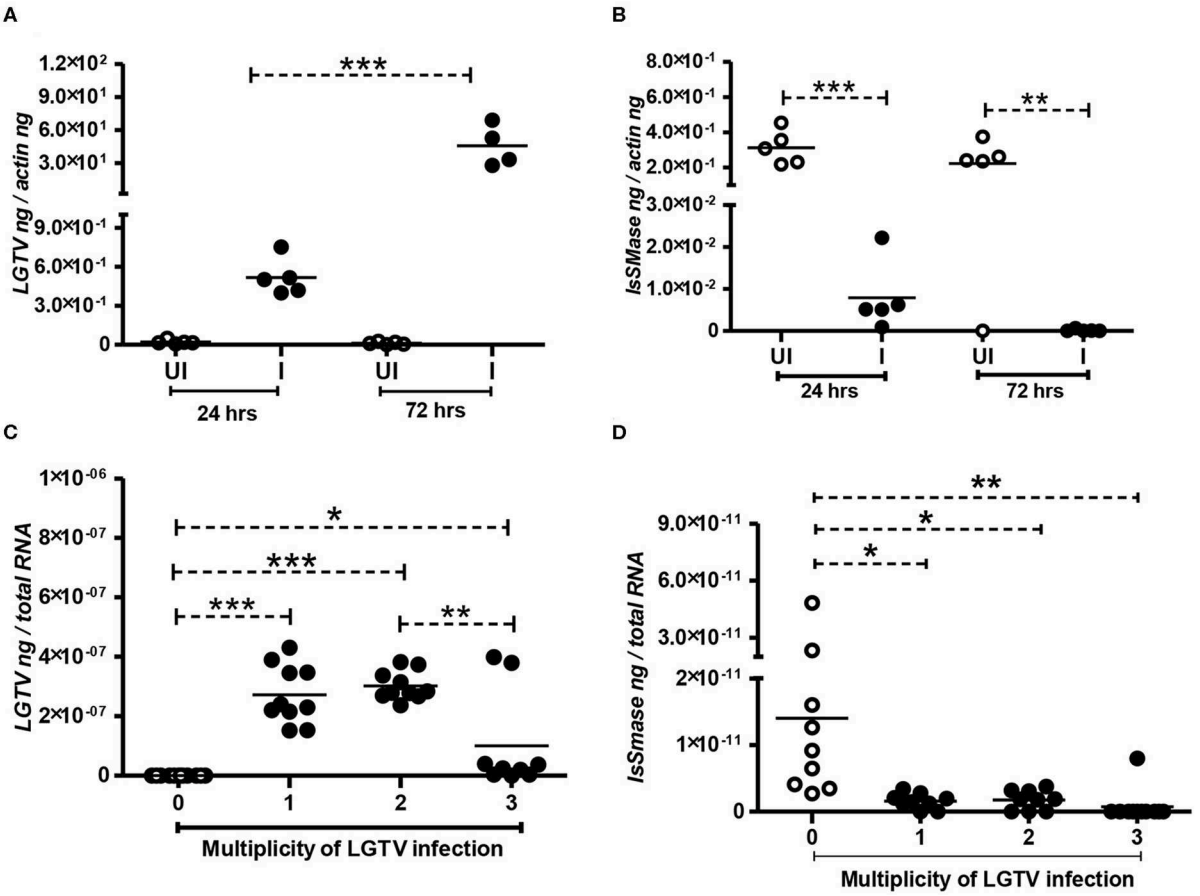

FIGURE 4 | Reduced *Is*SMase expression upon LGTV infection is time and dose dependent. QRT-PCR analysis showing LGTV viral loads **(A,C)** or *Is*SMase gene expression levels **(B,D)** at different time points **(A,B)**, or doses **(C,D)** in tick cells. LGTV loads **(A)** and *Is*SMase transcript levels **(B)** were determined at two different time points of 24 and 72 h p.i. **(C,D)**, numbers (1, 2, 3) indicate multiplication of infection (MOI) corresponding to LGTV loads **(C)** or levels of *Is*SMase transcripts **(D)** in uninfected (0) or LGTV-infected (1, 2, 3 MOI) tick cells. Each circle indicates sample generated from one culture well analyzed as 5–10 replicates. Open circles represent the uninfected (UI or 0) group, whereas closed circles denote the LGTV-infected (1, 2, and 3 in dose or I in time points) group. LGTV loads or *Is*SMase mRNA levels were normalized to tick beta-actin levels. *P*-value determined by Student's two-tailed *t*-test is shown. The asterisk indicates significance, and *, **, or *** denotes a *P*-value of less than 0.05, 0.01, and 0.001, respectively.

lysates at 24 and 72 h post-LGTV infection. Quantification assay showed significantly ($P < 0.05$) increased SM levels upon LGTV infection at both time points of 24 and 72 h p.i., in comparison to the respective uninfected controls (**Figure 6B**). These data suggest that upon LGTV infection of tick cells, the reduced *Is*SMase expression and enzymatic activity/function perhaps lead to accumulation of SM lipid levels upon LGTV infection in ticks.

GW4869 Treatment Restored *Is*SMase Activity by Suppressing LGTV-Induced SM Lipid Levels

Since GW4869 inhibitor treatment (at 1 μM) significantly affected the LGTV loads and restored the *Is*SMase transcript levels, next we analyzed the *Is*SMase enzymatic activity and SM levels. Tick cells treated with GW4869 inhibitor (1 μM for 4 h) followed by LGTV infection (MOI 1; at two different time points of 24 and 72 h p.i.) were analyzed for *Is*SMase activity and SM levels. We found that GW4869 inhibitor treatment restored the reduced *Is*SMase activity (**Figure 6C**). *Is*SMase activity was significantly ($P < 0.05$) increased upon GW4869 treatment and in a specific and early tested time point (24 h p.i.) of LGTV infection, in comparison to the mock control (**Figure 6C**). No further increase was observed at 72 h post LGTV infection in comparison to the mock control suggesting a complete restoration of *Is*SMase activity at an early time point (of 24 h p.i.,) (**Figure 6C**). Furthermore, GW4869 treatment significantly ($P < 0.05$) inhibited LGTV-induced SM lipid buildup at both 24 and 72 h p.i. in comparison to the respective mock LGTV-infected control groups (**Figure 6D**). These data indicate that GW4869 treatment inhibited LGTV loads resulting in increased *Is*SMase expression and activity that subsequently lead to reduction

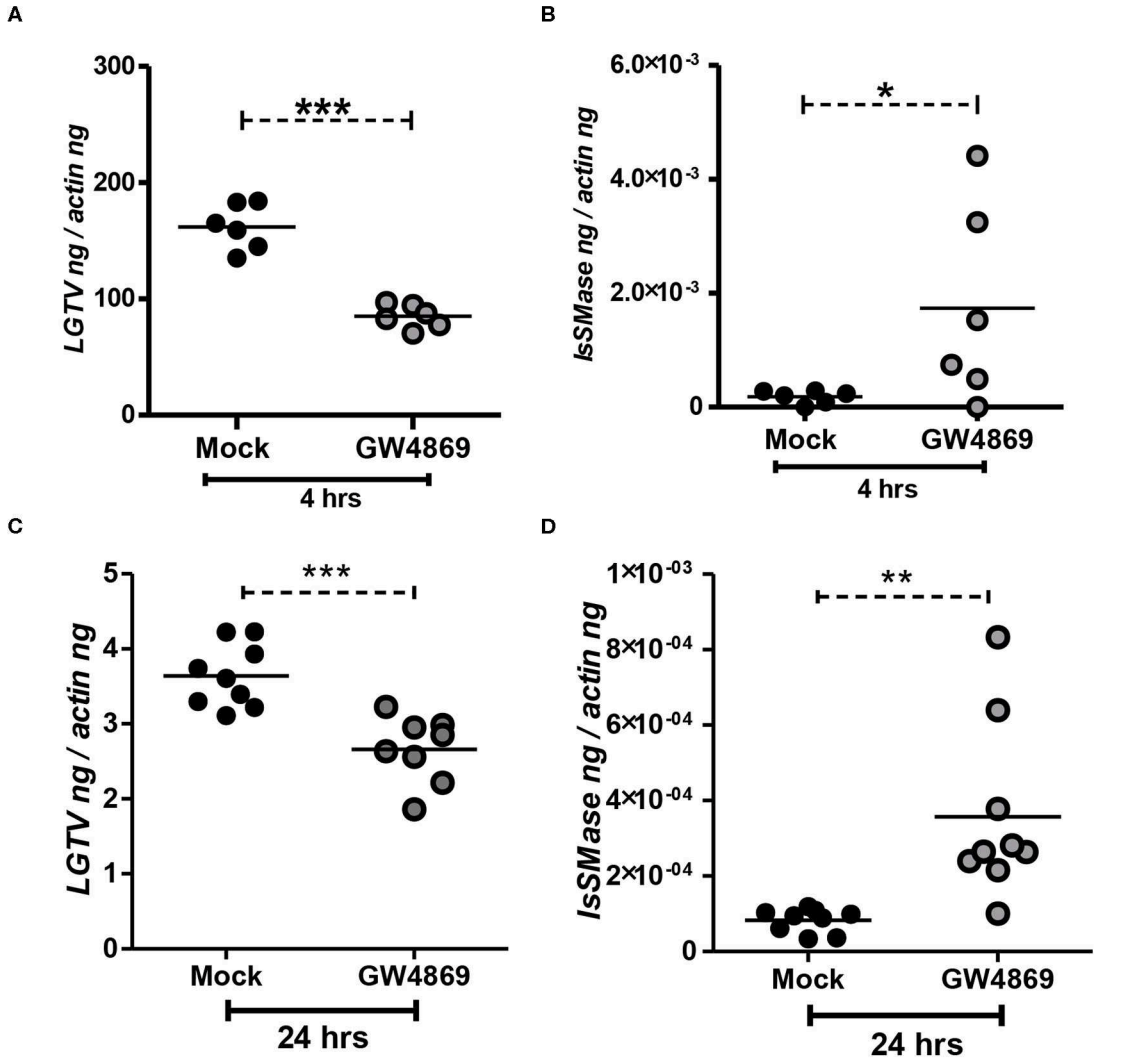

FIGURE 5 | GW4869 treatment restored the *Is*SMase expression by inhibiting LGTV loads in tick cells. **(A)** QRT-PCR analysis showing LGTV loads **(A,C)** or *Is*SMase mRNA levels **(B,D)** upon pre-treatment of ISE6 tick cells with GW4869 (1 μM) for either 4 h **(A,B)** or 24 h **(C,D)** followed by LGTV infection (for 72 h p.i.). Both mock and GW4869 inhibitor-treated groups were infected with 1 MOI of LGTV. Mock represents the group treated with vehicle DMSO. Each circle indicates sample generated from one culture well and analyzed as 6–10 replicates. Black circles represent the LGTV-infected mock group, whereas gray circles denote the LGTV-infected GW4869 inhibitor-treated group. LGTV loads or *Is*SMase mRNA levels were normalized to tick beta-actin levels. *P*-value determined by Student's two-tailed *t*-test is shown. The asterisk indicates significance, and *, **, or *** denotes a *P*-value of less than 0.05, 0.01, and 0.001, respectively.

in SM lipid levels. Overall, these results suggest that a tick-borne flavivirus suppresses *Is*SMase expression and its activity to induce SM lipid levels that perhaps facilitate LGTV replication, packaging of viral RNA genomes and proteins, and budding of these virally activated exosomes.

DISCUSSION

Understanding the persistence, established colonization, and survival of pathogens for an extended period of time in medically important vector has been a topic of interest for several decades. The molecular mechanisms supporting the survival strategies have not been clearly understood for many of the vector-borne pathogens. Our previous study showed in detail how a tick-borne bacterium *A. phagocytophilum* induces the phosphorylation of fundamental molecule actin in order to selectively regulate the gene transcription of a salivary gland protein Salp16 to survive in *I. scapularis* ticks (Sultana et al., 2010). Proteins do phosphorylate and de-phosphorylate in a feedback mechanism, and this bacterium-induced phosphorylation of actin was an extended event that was observed for a lifelong time in ticks (Sultana et al., 2010). Our other important study showed that *A. phagocytophilum* induces anti-freeze glycoprotein (IAFGP) in *I. scapularis* ticks and establishes a beneficial/symbiotic relationship

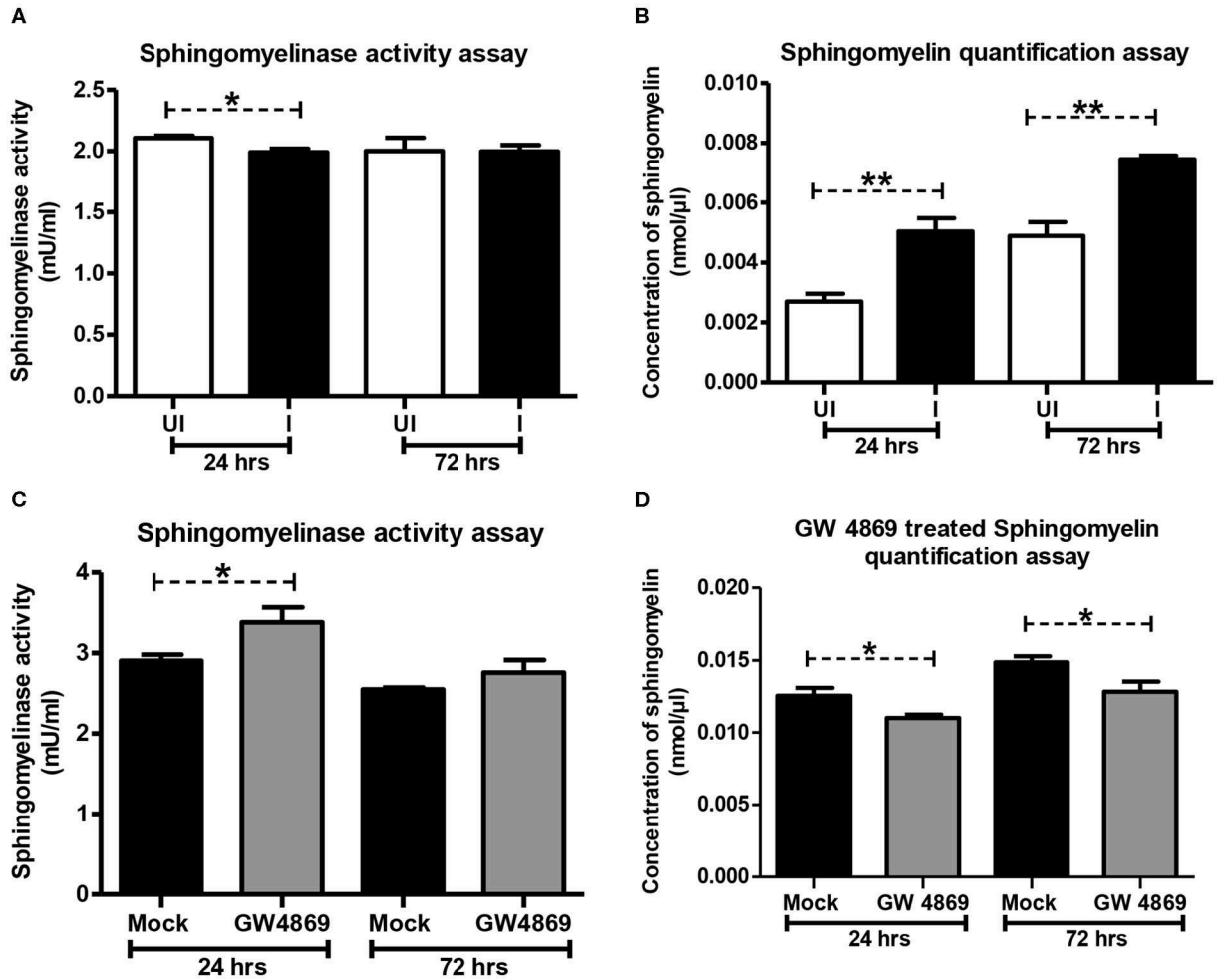

FIGURE 6 | LGTV infection reduced *Is*SMase activity resulting in induced levels of sphingomyelin lipids but GW4869 treatment restored the infection-mediated effects. **(A)** Measurement of sphingomyelinase activity in uninfected or LGTV-infected tick cells **(A)** or mock or GW4869 (1 μM)-treated, LGTV-infected tick cells **(C)** at 24 and 72 h p.i. is shown. **(B)** Sphingomyelin levels in uninfected or LGTV-infected tick cells **(B)** or mock or GW4869 (1 μM)-treated, LGTV-infected tick cells **(D)** at 24 h and 72 h p.i. are shown. White bars represent uninfected (UI) and black bars denote LGTV-infected (I, MOI 1) groups. Mock represents group treated with vehicle DMSO. Both mock and GW4869 inhibitor-treated groups were infected with LGTV (MOI 1) for indicated time points. *Is*SMase activity and SM lipid levels were measured in milliunits/ml. *P*-value determined by Student's two-tailed *t*-test is shown. The asterisk indicates significance, and * or ** denotes a *P*-value of less than 0.05 or 0.01, respectively.

with its vector to survive in the cold (Neelakanta et al., 2010). Several other studies have also implicated molecules in regulating pathogen survival and transmission from the vector (Nuttall et al., 2000; Chambers and Diamond, 2003; Nuttall and Labuda, 2004; Piesman and Eisen, 2008; Kuhn et al., 2015; de la Fuente, 2018; Kim, 2019). An important study from Dr. Wikel's group identified a novel *Is*SMase, a gene with high homology to the *Loxosceles* venomous spider's SMase D protein in *I. scapularis* tick saliva (Alarcon-Chaidez et al., 2009). *Is*SMase regulated the expression and programming of IL-4, and a freeze-thaw stable structure within this molecule was proposed to bind a Toll-like receptor (TLR) or other receptor on antigen-presenting cells (like dendritic cells or monocytes) or innate immune cells that perhaps switches ON the Th2 differentiation (Alarcon-Chaidez et al., 2009).

In the current study, we determined the role of *Is*SMase in tick-borne flaviviral infection. It has been shown that the spider venom enzyme SMase D is in a gene family with multiple members that had variations in functional specificities and activities of this protein (Truett, 1993; Binford et al., 2005, 2009; Murakami et al., 2005; Fry et al., 2009; Pedroso et al., 2015). Several isoforms of SMase D were identified and characterized in different groups of spiders. Other than spiders, SMase D orthologs have also been identified in bacteria, fungi, and ticks (Binford et al., 2005; Dias-Lopes et al., 2013). Alignment of *Is*SMase (Q202J4), a novel sphingomyelinase-like enzyme (also

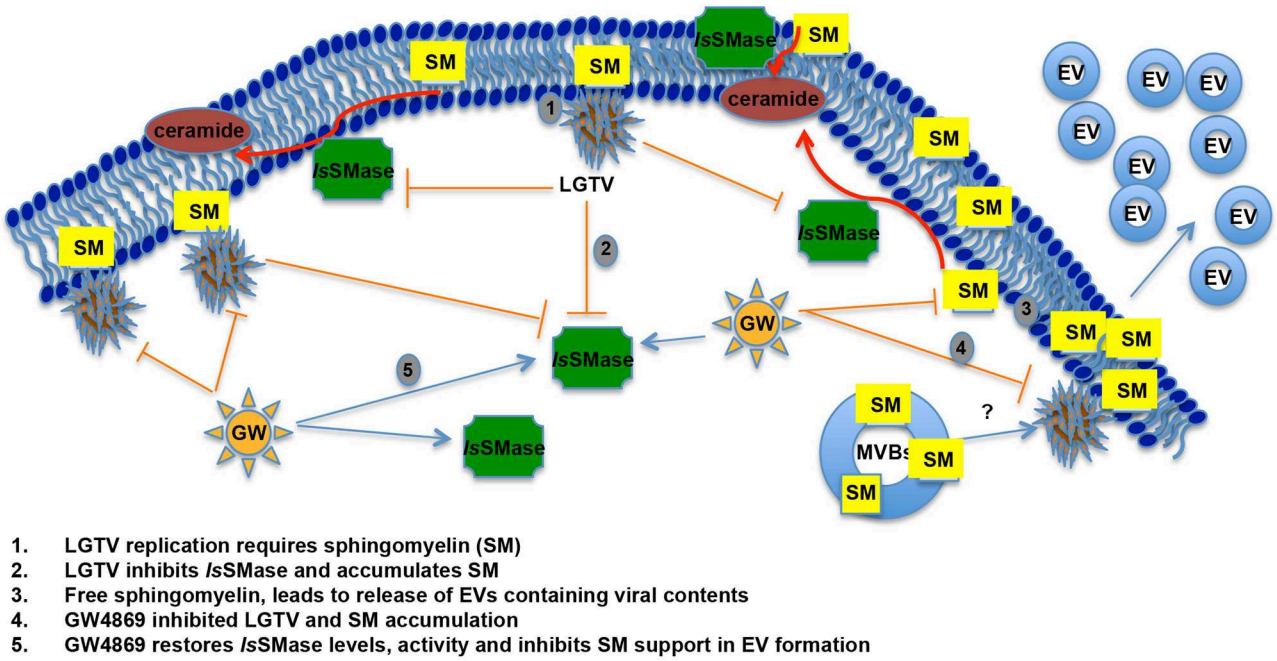

FIGURE 7 | LGTV modulates sphingomyelinase and sphingomyelin lipids for its replication and survival in tick cells. Schematic representation with a proposed model on how LGTV plays a role in the suppression of sphingomyelinase levels and its activity to induce SM lipid levels for its own benefit in membrane association and viral replication processes. Treatment with GW4869 inhibitor reduced LGTV loads to restore the sphingomyelinase levels and activity, thereby inhibiting the buildup of SM lipids. We hypothesize that accumulated amounts of SM lipids not only support membrane-associated viral replication but also aid in the production and release of exosomes/EVs that mediate viral exit and dissemination. SM indicates sphingomyelin, EVs represents extracellular vesicles, and MVBs denotes multi-vesicular bodies.

known as Dermonectrotic toxin SPH; precursor), with SMase D from *Loxosceles* spp. spiders, suggested this tick molecule to be a venomous protein ortholog (Alarcon-Chaidez et al., 2009). Our detailed bioinformatics and comparative analyses further confirmed that *Is*SMase is a spider, SMase D venomous protein ortholog. Several isoforms of SMase D were identified and structurally classified into two groups. Class I SMase D proteins contained a single disulfide bridge and variable loops, whereas Class II proteins presented an additional intra-chain disulfide bridge that connected a flexible loop with a catalytic loop (Binford et al., 2009; Zobel-Thropp et al., 2010; Dias-Lopes et al., 2013; Pedroso et al., 2015). Toxic potential was, however, variable between the two classes, and the class II enzymes were less toxic than the Class I proteins (Binford et al., 2009; Zobel-Thropp et al., 2010; Dias-Lopes et al., 2013). Their phylogenetic data revealed that the Class I SMase D proteins are recent in their evolution driven by natural selection with an increased toxic variation and their origin from a single ancestor (Binford et al., 2009; Zobel-Thropp et al., 2010; Dias-Lopes et al., 2013). The protein structure has been solved for a member of this gene family (PDB 1XX1). This enzyme has a $(\alpha/ß)_8$ barrel structure with active sites that are dependent on binding of a Mg^{2+} ion for catalysis (Binford et al., 2009; Zobel-Thropp et al., 2010). ClustalW alignment of *I. scapularis* SMase D amino acid sequence showed higher identity with *R. pulchellus* or *A. maculatum* ticks. However, the phylogenetic analysis revealed that *Is*SMase formed a clade with spider venom protein orthologs from *S. patagonicus*, *H. lepturus*, and *L. similis*. The protein feature prediction analysis disclosed that *Is*SMase is a multifunctional protein with several active sites or motifs. The presence of several phospho-sites suggests that the process of phosphorylation perhaps regulates *IsSMase*.

The role of *Is*SMase in viral infections and pathogen transmission has not been studied. We have recently shown that medically important arthropods, such as ticks and mosquitoes, secrete extracellular vesicles including exosomes that mediate transmission of flavivirus RNA and proteins to vertebrate cells (Zhou et al., 2018). Our previous work showed that a tick-borne model pathogen LGTV readily infected *I. scapularis* (ISE6) tick cells, with increased viremia at 72 h p.i. and disseminated both positive and negative strands of LGTV RNA and viral proteins via secured exosomes (Zhou et al., 2018). Tick cell-derived exosomes enriched with exosomal marker HSP70 showed higher packaging of viral RNA and proteins. We noted induction in the number of exosome production and release from LGTV-infected tick cells and proposed this observation could result in enhanced viral dissemination (Zhou et al., 2018). Our previous study recommended analyzing the importance of neutral sphingomyelinase(s) in *I. scapularis* ticks

upon LGTV infection. Our finding that LGTV dramatically reduced *Is*SMase levels in LGTV-infected unfed/fed ticks and in tick cells suggests that decrease in sphingomyelinase(s) leads to buildup of SM lipids that in turn may facilitate higher budding and release of exosomes. Furthermore, reversibility seen in restoring the expression of *Is*SMase upon GW4869 treatment suggested an involvement of this molecule in inhibiting LGTV replication and transmission via blocking/inhibition of exosome release and dissemination. We hypothesize that the venomous properties of *Is*SMase perhaps interfere with the viral replication by participating in tick anti-viral pathways. Upregulation of *Is*SMase expression and enzymatic activity upon GW4869 treatment perhaps suggests a negative role for this enzyme in exosome biogenesis. Combing of *I. scapularis* genome showed the presence of several other sphingomyelinases that are currently addressed in tick-LGTV interactions and exosome-mediated transmission of flaviviruses. In all animals, plants, and fungi, and in some of the prokaryotes and viruses, sphingolipids are the ubiquitous constituents of all the membranes, which include plasma membranes and membrane-bound organelles (Raposo and Stoorvogel, 2013; Schneider-Schaulies and Schneider-Schaulies, 2015; Bezgovsek et al., 2018; Shanbhogue and Hannun, 2018). In order to convert SM lipids into phosphocholine and ceramide, SMases have to be active and functional to hydrolyze this process (Clarke et al., 2006; Bartke and Hannun, 2009). SM consisting of phosphocholine and ceramide or a phospho-ethanolamine head group is a type of sphingolipid found in all animal membranes (Hannun and Obeid, 2018; Shanbhogue and Hannun, 2018). It represents 85% of all sphingolipids in human and accounts to 10–20 mol % of the plasma membrane lipids (van Meer and Lisman, 2002; Futerman, 2006; Bartke and Hannun, 2009). SM plays a critical role in signal transduction (van Meer and Lisman, 2002; Futerman, 2006; Bartke and Hannun, 2009). Sphingomyelinases are enzymes that hydrolyze SM to release phosphocholine into the aqueous environment and ceramide that diffuses through the plasma membrane (Clarke et al., 2006; Bartke and Hannun, 2009). Furthermore, there are several reports that are in positive notion that host lipids facilitate the genome replication of positive-strand RNA viruses (Apte-Sengupta et al., 2014; Vijayan and Hahm, 2014; Schneider-Schaulies and Schneider-Schaulies, 2015; Bezgovsek et al., 2018; Hannun and Obeid, 2018; Zhang et al., 2019). SM levels increased West Nile Virus (WNV) infection both *in vivo* and *in vitro* and have been suited as an antiviral target against WNV pathogenesis (Martin-Acebes et al., 2016). Dynamic remodeling of lipids, shown by alteration of the biochemical landscape of the mosquito midgut during dengue virus infection and replication suggested sphingolipids as "choke points" for targeting blocking of virus transmission (Chotiwan et al., 2018). Almost all well-studied positive-strand RNA viruses remodel and reorganize the membrane and lipid metabolism pathways through the coordinated virus-host interactions to create right niche or a suitable microenvironment for their survival and replication (Futerman, 2006; Zhang et al., 2013, 2019; Apte-Sengupta et al., 2014; Martin-Acebes et al., 2016; Chotiwan et al., 2018). Membrane components such as sphingolipids have been shown to participate in all steps of virus life cycles including membrane attachments and fusion, intracellular transport, replication, protein sorting, and budding/exogenesis of viral particles and virions (Futerman, 2006; Bartke and Hannun, 2009; Raposo and Stoorvogel, 2013; Schneider-Schaulies and Schneider-Schaulies, 2015; Hannun and Obeid, 2018). Influenza A virus (IAV) has been shown to activate the sphingosine kinase 1 and the transcription factor NF-kB, to manipulate the cellular signaling and the sphingosine metabolism as a hallmark for viral genome replication (Vijayan and Hahm, 2014; Soudani et al., 2019). In addition, human immunodeficiency virus (HIV) interacts directly with glycosphingolipids, and similar to HIV, hepatitis C virus (HCV) uses the lipid components for viral assembly and budding during viral infection and release (Hirata et al., 2012; Schneider-Schaulies and Schneider-Schaulies, 2015). Rhinoviruses stimulate the ceramide enrichment and endocytosis, whereas measles virus (MV) activates the sphingomyelinases (SMases) (Dreschers et al., 2007; Avota and Schneider-Schaulies, 2014; Schneider-Schaulies and Schneider-Schaulies, 2015). Interestingly, Sindbis viruses have been shown to replicate better in the absence of acid SMases (ASMases) (Jan et al., 2000; Ng and Griffin, 2006; Schneider-Schaulies and Schneider-Schaulies, 2015). Our study suggests that LGTV inhibits the expression and activity of *Is*SMase, in order to induce the production and accumulation of SM lipids (**Figure 7**). However, treatment with GW4869 (at only 1 μM), inhibited viral-induced SM lipid production and restored the *Is*SMase loads and activity as a feedback loop, suggesting a new role for this venomous ortholog in inhibition of tick-borne viral replication (**Figure 7**). Our data also suggest a specific role for *Is*SMase during LGTV infection, as ticks infected with *B. burgdorferi* or *A. phagocytophilum* bacteria did not show any significant difference in expression of *Is*SMase in comparison to levels noted in uninfected ticks (**Supplementary Figure 3**). This specific viral-mediated inhibition of *Is*SMase not only indicates a negative role or function for this enzyme in exosome-mediated transmission of virus but also suggests a new role for this venomous protein ortholog *Is*SMase in tick defense and/or anti-viral mechanism(s).

DATA AVAILABILITY STATEMENT

All datasets generated for this study are included in the article/**Supplementary Material**.

ETHICS STATEMENT

The animal study was reviewed and approved by Institutional Animal Care and Use Committee (IACUC; protocol # 18-011).

AUTHOR CONTRIBUTIONS

PR, SK, GN, and HS performed experiments, and discussed, analyzed, and interpreted the data in several settings. GN generated the 24 h fed *I. scapularis* uninfected and LGTV-infected ticks. PR and SK performed RNA extractions

and QRT-PCR. SK and GN performed bioinformatics analysis. PR and HS performed the quantification assays. All authors read and edited the manuscript. HS collected all required materials and reagents, designed and coordinated the entire study, compiled and organized all the data, supervised overall investigations, and wrote the paper.

FUNDING

This study was supported by funding from National Institute of Allergy and Infectious Diseases (NIAID)/National Institutes of Health (R01 Award number R01AI141790 to HS) and independent start-up funds from Old Dominion University to GN and HS.

ACKNOWLEDGMENTS

We would like to acknowledge the useful resource of ticks (larvae, nymphs, and adults) from BEI resources/CDC. The following reagents were provided by Centers for Disease Control and Prevention for distribution by BEI Resources, NIAID, NIH: *I. scapularis* Larvae (Live), NR-44115; *I. scapularis* Nymph (Live), NR-44116; and *I. scapularis* Adult (Live), NR-42510. We are extremely thankful to Dr. Michael L. Levin and Shelby Ford for help with these ticks rearing and supply.

SUPPLEMENTARY MATERIAL

The Supplementary Material for this article can be found online at: https://www.frontiersin.org/articles/10.3389/fcimb.2020.00244/full#supplementary-material

Supplementary Figure 1 | Amplification of *I. scapularis* sphingomyelinase-like gene fragment (*Is*SMase) from ticks and tick cells. PCR amplification of *Is*SMase gene fragment from *I. scapularis* unfed or post-fed nymphal ticks or uninfected ISE6 tick cell line cDNA is shown. Similar size fragments were amplified from all three tested groups, and band of approximately 194 bp was detected on 1% agarose gel. Marker indicates size of the product amplified and NTC denotes no template control. M represents DNA ladder. Arrows indicate the 200 bp bands on ladder lane.

Supplementary Figure 2 | Exosomes derived from tick cells had low or undetectable levels of *Is*SMase. QRT-PCR analysis showing detectable LGTV loads **(A)**, HSP70 transcript levels **(B)** and low or undetectable levels of *Is*SMase transcripts **(C)** in tick cell-derived exosomes that are uninfected (UI) or LGTV-infected (I) at day 1 and day 3 post infection (p.i.). Each circle, triangle, inverted triangle, or square represent sample generated from one culture well and analyzed in multiple replicate. Open circles indicate uninfected (UI) and closed circles denotes LGTV-infected group. LGTV loads, *hsp70* or *Is*SMase mRNA levels were normalized to tick beta-actin levels. *P*-value determined by Student's two-tail *t*-test is shown. The asterisk * indicates significance, and denotes a *P*-value of less than 0.05.

Supplementary Figure 3 | *Is*SMase expression is unaffected in presence of other pathogens. QRT-PCR analysis showing levels of *Is*SMase transcripts in unfed *I. scapularis* nymphs infected with either extracellular bacterium *B. burgdorferi* or intracellular bacterium *A. phagocytophilum*. Open circles indicate uninfected (UI) and closed circles denote infected (I) groups. *Is*SMase mRNA levels were normalized to tick beta-actin levels. No significant differences were noted between UI and I groups.

REFERENCES

Alarcon-Chaidez, F. J., Boppana, V. D., Hagymasi, A. T., Adler, A. J., and Wikel, S. K. (2009). A novel sphingomyelinase-like enzyme in *Ixodes scapularis* tick saliva drives host CD4 T cells to express IL-4. *Parasite Immunol.* 31, 210–219. doi: 10.1111/j.1365-3024.2009.01095.x

Apte-Sengupta, S., Sirohi, D., and Kuhn, R. J. (2014). Coupling of replication and assembly in flaviviruses. *Curr. Opin. Virol.* 9, 134–142. doi: 10.1016/j.coviro.2014.09.020

Avota, E., and Schneider-Schaulies, S. (2014). The role of sphingomyelin breakdown in measles virus immunmodulation. *Cell. Physiol. Biochem.* 34, 20–26. doi: 10.1159/000362981

Bartke, N., and Hannun, Y. A. (2009). Bioactive sphingolipids: metabolism and function. *J. Lipid Res.* 50(Suppl.), S91–S96. doi: 10.1194/jlr.R800080-JLR200

Bezgovsek, J., Gulbins, E., Friedrich, S. K., Lang, K. S., and Duhan, V. (2018). Sphingolipids in early viral replication and innate immune activation. *Biol. Chem.* 399, 1115–1123. doi: 10.1515/hsz-2018-0181

Bikman, B. T., and Summers, S. A. (2011). Ceramides as modulators of cellular and whole-body metabolism. *J. Clin. Invest.* 121, 4222–4230. doi: 10.1172/JCI57144

Binder, L. S. (1989). Acute arthropod envenomation. Incidence, clinical features and management. *Med. Toxicol. Adverse Drugs Exp.* 4, 163–173. doi: 10.1007/bf03259994

Binford, G. J., Bodner, M. R., Cordes, M. H., Baldwin, K. L., Rynerson, M. R., Burns, S. N., et al. (2009). Molecular evolution, functional variation, and proposed nomenclature of the gene family that includes sphingomyelinase D in *sicariid* spider venoms. *Mol. Biol. Evol.* 26, 547–566. doi: 10.1093/molbev/msn274

Binford, G. J., Cordes, M. H., and Wells, M. A. (2005). Sphingomyelinase D from venoms of *Loxosceles* spiders: evolutionary insights from cDNA sequences and gene structure. *Toxicon* 45, 547–560. doi: 10.1016/j.toxicon.2004.11.011

Chambers, T. J., and Diamond, M. S. (2003). Pathogenesis of flavivirus encephalitis. *Adv. Virus Res.* 60, 273–342. doi: 10.1016/s0065-3527(03)60008-4

Chmura, S. J., Nodzenski, E., Kharbanda, S., Pandey, P., Quintans, J., Kufe, D. W., et al. (2000). Down-regulation of ceramide production abrogates ionizing radiation-induced cytochrome c release and apoptosis. *Mol. Pharmacol.* 57, 792–796. doi: 10.1124/mol.57.4.792

Chotiwan, N., Andre, B. G., Sanchez-Vargas, I., Islam, M. N., Grabowski, J. M., Hopf-Jannasch, A., et al. (2018). Dynamic remodeling of lipids coincides with dengue virus replication in the midgut of *Aedes aegypti* mosquitoes. *PLoS Pathog.* 14:e1006853. doi: 10.1371/journal.ppat.1006853

Clarke, C. J., Snook, C. F., Tani, M., Matmati, N., Marchesini, N., and Hannun, Y. A. (2006). The extended family of neutral sphingomyelinases. *Biochemistry* 45, 11247–11256. doi: 10.1021/bi061307z

Correa, M. A., Okamoto, C. K., Goncalves-de-Andrade, R. M., van den Berg, C. W., and Tambourgi, D. V. (2016). Sphingomyelinase D from *Loxosceles laeta* Venom Induces the Expression of MMP7 in Human Keratinocytes: contribution to Dermonecrosis. *PLoS ONE* 11:e0153090. doi: 10.1371/journal.pone.0153090

de la Fuente, J. (2018). Controlling ticks and tick-borne diseases..looking forward. *Ticks Tick Borne Dis.* 9, 1354–1357. doi: 10.1016/j.ttbdis.2018.04.001

Dias-Lopes, C., Neshich, I. A., Neshich, G., Ortega, J. M., Granier, C., Chavez-Olortegui, C., et al. (2013). Identification of new sphingomyelinases D in pathogenic fungi and other pathogenic organisms. *PLoS ONE* 8:e79240. doi: 10.1371/journal.pone.0079240

Dreschers, S., Franz, P., Dumitru, C., Wilker, B., Jahnke, K., and Gulbins, E. (2007). Infections with human rhinovirus induce the formation of distinct functional membrane domains. *Cell. Physiol. Biochem.* 20, 241–254. doi: 10.1159/000104170

Fry, B. G., Roelants, K., Champagne, D. E., Scheib, H., Tyndall, J. D., King, G. F., et al. (2009). The toxicogenomic multiverse: convergent recruitment of proteins into animal venoms. *Annu. Rev. Genomics Hum Genet.* 10, 483–511. doi: 10.1146/annurev.genom.9.081307.164356

Futerman, A. H. (2006). Intracellular trafficking of sphingolipids: relationship to biosynthesis. *Biochim. Biophys. Acta* 1758, 1885–1892. doi: 10.1016/j.bbamem.2006.08.004

Hannun, Y. A., and Obeid, L. M. (2018). Sphingolipids and their metabolism in physiology and disease. *Nat. Rev. Mol. Cell. Biol.* 19, 175–191. doi: 10.1038/nrm.2017.107

Hirata, Y., Ikeda, K., Sudoh, M., Tokunaga, Y., Suzuki, A., Weng, L., et al. (2012). Self-enhancement of hepatitis C virus replication by promotion of specific sphingolipid biosynthesis. *PLoS Pathog.* 8:e1002860. doi: 10.1371/journal.ppat.1002860

Jan, J. T., Chatterjee, S., and Griffin, D. E. (2000). Sindbis virus entry into cells triggers apoptosis by activating sphingomyelinase, leading to the release of ceramide. *J. Virol.* 74, 6425–6432. doi: 10.1128/jvi.74.14.6425-6432.2000

Khanal, S., Taank, V., Anderson, J. F., Sultana, H., and Neelakanta, G. (2018). Arthropod transcriptional activator protein-1 (AP-1) aids tick-rickettsial pathogen survival in the cold. *Sci. Rep*. 8:11409. doi: 10.1038/s41598-018-29654-6

Kim, K. S. (2019). Current challenges in the development of vaccines and drugs against emerging vector-borne diseases. *Curr. Med. Chem.* 26, 2974–2986. doi: 10.2174/0929867325666181105121146

Kolesnick, R. N., and Kronke, M. (1998). Regulation of ceramide production and apoptosis. *Annu. Rev. Physiol.* 60, 643–665. doi: 10.1146/annurev.physiol.60.1.643

Kuhn, R. J., Dowd, K. A., Beth Post, C., and Pierson, T. C. (2015). Shake, rattle, and roll: impact of the dynamics of flavivirus particles on their interactions with the host. *Virology* 479–480, 508–517. doi: 10.1016/j.virol.2015.03.025

Labuda, M., Austyn, J. M., Zuffova, E., Kozuch, O., Fuchsberger, N., Lysy, J., et al. (1996). Importance of localized skin infection in tick-borne encephalitis virus transmission. *Virology* 219, 357–366. doi: 10.1006/viro.1996.0261

Labuda, M., and Randolph, S. E. (1999). Survival strategy of tick-borne encephalitis virus: cellular basis and environmental determinants. *Zentralbl Bakteriol.* 289, 513–524.

Lopes, P. H., Bertani, R., Goncalves-de-Andrade, R. M., Nagahama, R. H., van den Berg, C. W., and Tambourgi, D. V. (2013). Venom of the Brazilian spider *Sicarius ornatus* (*Araneae, Sicariidae*) contains active sphingomyelinase D: potential for toxicity after envenomation. *PLoS. Negl. Trop. Dis.* 7:e2394. doi: 10.1371/journal.pntd.0002394

Martin-Acebes, M. A., Gabande-Rodriguez, E., Garcia-Cabrero, A. M., Sanchez, M. P., Ledesma, M. D., Sobrino, F., et al. (2016). Host sphingomyelin increases West Nile virus infection *in vivo*. *J. Lipid Res.* 57, 422–432. doi: 10.1194/jlr.M064212

Mitzel, D. N., Wolfinbarger, J. B., Long, R. D., Masnick, M., Best, S. M., and Bloom, M. E. (2007). Tick-borne flavivirus infection in *Ixodes scapularis* larvae: development of a novel method for synchronous viral infection of ticks. *Virology* 365, 410–418. doi: 10.1016/j.virol.2007.03.057

Murakami, M. T., Fernandes-Pedrosa, M. F., Tambourgi, D. V., and Arni, R. K. (2005). Structural basis for metal ion coordination and the catalytic mechanism of sphingomyelinases D. *J. Biol. Chem.* 280, 13658–13664. doi: 10.1074/jbc.M412437200

Neelakanta, G., and Sultana, H. (2015). Transmission-Blocking vaccines: focus on anti-vector vaccines against tick-borne diseases. *Arch. Immunol. Ther. Exp.* 63, 169–179. doi: 10.1007/s00005-014-0324-8

Neelakanta, G., Sultana, H., Fish, D., Anderson, J. F., and Fikrig, E. (2010). *Anaplasma phagocytophilum* induces *Ixodes scapularis* ticks to express an antifreeze glycoprotein gene that enhances their survival in the cold. *J. Clin. Invest.* 120, 3179–3190. doi: 10.1172/JCI42868

Ng, C. G., and Griffin, D. E. (2006). Acid sphingomyelinase deficiency increases susceptibility to fatal alphavirus encephalomyelitis. *J. Virol.* 80, 10989–10999. doi: 10.1128/JVI.01154-06

Nuttall, P. A., and Labuda, M. (2003). Dynamics of infection in tick vectors and at the tick-host interface. *Adv. Virus Res.* 60, 233–272. doi: 10.1016/s0065-3527(03)60007-2

Nuttall, P. A., and Labuda, M. (2004). Tick-host interactions: saliva-activated transmission. *Parasitology* 129(Suppl.), S177–S189. doi: 10.1017/s0031182004005633

Nuttall, P. A., Paesen, G. C., Lawrie, C. H., and Wang, H. (2000). Vector-host interactions in disease transmission. *J. Mol. Microbiol. Biotechnol.* 2, 381–386.

Paixao-Cavalcante, D., van den Berg, C. W., Goncalves-de-Andrade, R. M., Fernandes-Pedrosa Mde, F., Okamoto, C. K., and Tambourgi, D. V. (2007). Tetracycline protects against dermonecrosis induced by *Loxosceles* spider venom. *J. Invest. Dermatol.* 127, 1410–1418. doi: 10.1038/sj.jid.5700688

Pedroso, A., Matioli, S. R., Murakami, M. T., Pidde-Queiroz, G., and Tambourgi, D. V. (2015). Adaptive evolution in the toxicity of a spider's venom enzymes. *BMC. Evol. Biol.* 15:290. doi: 10.1186/s12862-015-0561-4

Piesman, J., and Eisen, L. (2008). Prevention of tick-borne diseases. *Annu. Rev. Entomol.* 53, 323–343. doi: 10.1146/annurev.ento.53.103106.093429

Powell, J. R. (2019). An evolutionary perspective on vector-borne diseases. *Front. Genet.* 10:1266. doi: 10.3389/fgene.2019.01266

Qurollo, B. (2019). Feline vector-borne diseases in North America. *Vet. Clin. North Am. Small Anim. Pract.* 49, 687–702. doi: 10.1016/j.cvsm.2019.02.012

Randolph, S. E., Gern, L., and Nuttall, P. A. (1996). Co-feeding ticks: epidemiological significance for tick-borne pathogen transmission. *Parasitol. Today* 12, 472–479.

Raposo, G., and Stoorvogel, W. (2013). Extracellular vesicles: exosomes, microvesicles, and friends. *J. Cell. Biol.* 200, 373–383. doi: 10.1083/jcb.201211138

Scalway, T., Otmani Del Barrio, M., and Ramirez, B. (2019). Research on vector-borne diseases: implementation of research communication strategies. *Infect. Dis. Poverty* 8, 101. doi: 10.1186/s40249-019-0610-0

Schneider-Schaulies, J., and Schneider-Schaulies, S. (2015). Sphingolipids in viral infection. *Biol. Chem.* 396, 585–595. doi: 10.1515/hsz-2014-0273

Sekeyova, Z., Danchenko, M., Filipcik, P., and Fournier, P. E. (2019). Rickettsial infections of the central nervous system. *PLoS Negl. Trop. Dis.* 13:e0007469. doi: 10.1371/journal.pntd.0007469

Sexton, D. J., and Kirkland, K. B. (1998). Rickettsial infections and the central nervous system. *Clin. Infect. Dis.* 26, 247–248. doi: 10.1086/517043

Shanbhogue, P., and Hannun, Y. A. (2018). Exploring the therapeutic landscape of sphingomyelinases. *Handb. Exp. Pharmacol.* 259, 19–47. doi: 10.1007/164_2018_179

Shaw, W. R., and Catteruccia, F. (2019). Vector biology meets disease control: using basic research to fight vector-borne diseases. *Nat. Microbiol.* 4, 20–34. doi: 10.1038/s41564-018-0214-7

Soudani, N., Hage-Sleiman, R., Karam, W., Dbaibo, G., and Zaraket, H. (2019). Ceramide suppresses Influenza A virus replication *in vitro*. *J. Virol.* 93:e00053–19. doi: 10.1128/JVI.00053-19

Spence Beaulieu, M. R. (2019). The role of parasite manipulation in vector-borne diseases. *Evol. Med. Public Health* 2019, 106–107. doi: 10.1093/emph/eoz019

Sultana, H., Neelakanta, G., Kantor, F. S., Malawista, S. E., Fish, D., Montgomery, R. R., et al. (2010). *Anaplasma phagocytophilum* induces actin phosphorylation to selectively regulate gene transcription in *Ixodes scapularis* ticks. *J. Exp. Med.* 207, 1727–1743. doi: 10.1084/jem.20100276

Taank, V., Zhou, W., Zhuang, X., Anderson, J. F., Pal, U., Sultana, H., et al. (2018). Characterization of tick organic anion transporting polypeptides (OATPs) upon bacterial and viral infections. *Parasite Vectors*11:593. doi: 10.1186/s13071-018-3160-6

Truett, A. P. III, and King, L. E. Jr. (1993). Sphingomyelinase D: a pathogenic agent produced by bacteria and arthropods. *Adv. Lipid Res.* 26, 275–291.

Turck, J. W., Taank, V., Neelakanta, G., and Sultana, H. (2019). *Ixodes scapularis* Src tyrosine kinase facilitates *Anaplasma phagocytophilum* survival in its arthropod vector. *Ticks Tick Borne Dis.* 10, 838–847. doi: 10.1016/j.ttbdis.2019.04.002

Valarcher, J. F., Hagglund, S., Juremalm, M., Blomqvist, G., Renstrom, L., Zohari, S., et al. (2015). Tick-borne encephalitis. *Rev. Sci. Tech.* 34, 453–466. doi: 10.1007/s00115-016-0134-9

van Meer, G., and Lisman, Q. (2002). Sphingolipid transport: rafts and translocators. *J. Biol. Chem.* 277, 25855–25858. doi: 10.1074/jbc.R200010200

Vijayan, M., and Hahm, B. (2014). Influenza viral manipulation of sphingolipid metabolism and signaling to modulate host defense system. *Scientifica* 2014:793815. doi: 10.1155/2014/793815

Vora, A., Taank, V., Dutta, S. M., Anderson, J. F., Fish, D., Sonenshine, D. E., et al. (2017). Ticks elicit variable fibrinogenolytic activities upon feeding on hosts with different immune backgrounds. *Sci. Rep.* 7:44593. doi: 10.1038/srep44593

Vora, A., Zhou, W., Londono-Renteria, B., Woodson, M., Sherman, M. B., Colpitts, T. M., et al. (2018). Arthropod EVs mediate dengue virus transmission through

interaction with a tetraspanin domain containing glycoprotein Tsp29Fb. *Proc. Natl. Acad. Sci. U.S.A.* 115, E6604–E6613. doi: 10.1073/pnas.1720125115

Wilke, A. B. B., Beier, J. C., and Benelli, G. (2019). Complexity of the relationship between global warming and urbanization - an obscure future for predicting increases in vector-borne infectious diseases. *Curr. Opin. Insect Sci.* 35, 1–9. doi: 10.1016/j.cois.2019.06.002

Wilson, A. L., Davies, M., and Lindsay, S. W. (2019). Revisiting an old idea: engineering against vector-borne diseases in the domestic environment. *Trans. R. Soc. Trop. Med. Hyg.* 113, 53–55. doi: 10.1093/trstmh/try103

Zager, R. A., Burkhart, K. M., and Johnson, A. (2000). Sphingomyelinase and membrane sphingomyelin content: determinants of Proximal tubule cell susceptibility to injury. *J. Am. Soc. Nephrol.* 11, 894–902.

Zellner, B., and Huntley, J. F. (2019). Ticks and tularemia: do we know what we don't know? *Front. Cell Infect. Microbiol.* 9:146. doi: 10.3389/fcimb.2019.00146

Zhang, W., Kaufmann, B., Chipman, P. R., Kuhn, R. J., and Rossmann, M. G. (2013). Membrane curvature in flaviviruses. *J. Struct. Biol.* 183, 86–94. doi: 10.1016/j.jsb.2013.04.005

Zhang, Z., He, G., Filipowicz, N. A., Randall, G., Belov, G. A., Kopek, B. G., et al. (2019). Host lipids in positive-strand RNA virus genome replication. *Front. Microbiol.* 10:286. doi: 10.3389/fmicb.2019.00286

Zhou, W., Woodson, M., Neupane, B., Bai, F., Sherman, M. B., Choi, K. H., et al. (2018). Exosomes serve as novel modes of tick-borne flavivirus transmission from arthropod to human cells and facilitates dissemination of viral RNA and proteins to the vertebrate neuronal cells. *PLoS Pathog.* 14:e1006764. doi: 10.1371/journal.ppat.1006764

Zhou, W., Woodson, M., Sherman, M. B., Neelakanta, G., and Sultana, H. (2019). Exosomes mediate Zika virus transmission through SMPD3 neutral Sphingomyelinase in cortical neurons. *Emerg. Microbes Infect.* 8, 307–326. doi: 10.1080/22221751.2019.1578188

Zobel-Thropp, P. A., Bodner, M. R., and Binford, G. J. (2010). Comparative analyses of venoms from American and African *Sicarius* spiders that differ in sphingomyelinase D activity. *Toxicon* 55, 1274–1282. doi: 10.1016/j.toxicon.2010.01.019

Conflict of Interest: The authors declare that the research was conducted in the absence of any commercial or financial relationships that could be construed as a potential conflict of interest.

Advantages of publishing in Frontiers

OPEN ACCESS
Articles are free to read for greatest visibility and readership

FAST PUBLICATION
Around 90 days from submission to decision

HIGH QUALITY PEER-REVIEW
Rigorous, collaborative, and constructive peer-review

TRANSPARENT PEER-REVIEW
Editors and reviewers acknowledged by name on published articles

Frontiers
Avenue du Tribunal-Fédéral 34
1005 Lausanne | Switzerland

Visit us: www.frontiersin.org
Contact us: info@frontiersin.org | +41 21 510 17 00

REPRODUCIBILITY OF RESEARCH
Support open data and methods to enhance research reproducibility

DIGITAL PUBLISHING
Articles designed for optimal readership across devices

FOLLOW US
@frontiersin

IMPACT METRICS
Advanced article metrics track visibility across digital media

EXTENSIVE PROMOTION
Marketing and promotion of impactful research

LOOP RESEARCH NETWORK
Our network increases your article's readership